Contrails

FOREWORD

This summary report was prepared by the Aerojet-General Corporation under Contract AF 33(657)-8740: Project No. 7381, "Materials Application," Task No. 738101, "Exploratory Design and Prototype Development."

The work was administered under the direction of the AF Materials Laboratory Research and Technology Division, with Lts. W. F. Payne and R. M. Dunco acting as project engineers.

The study program at the Aerojet-General Corporation was performed under the management of W. S. Tenner, Manager of the Chamber Materials and Fabrication R & D Department, with Messrs. R. E. Anderson and P. P. Crimmins acting as project engineers. The program was conducted jointly by Messrs. L. Albertin, G. E. Faulkner, R. E. Handley, C. E. Hartbower, G. K. Hickox, J. T. Niemann, and H. R. Smith, all of whom were co-authors of this report.

This report covers the work performed during the period from 31 May 1962 to 31 January 1964.

Approved for Public Release

Contrails

Approved for Public Release

Contrails

ABSTRACT

The tensile, aging response, and fracture toughness properties of seven heats of 18% nickel maraging steel plate and bar stock with yield strength values ranging from 200 to 300 ksi were evaluated during a 20-month study program, and the results of this investigation were correlated with material melting and processing practices. In addition to the basic physical material properties that were studied, metallurgical properties also were studied to determine the grain size, general microstructure, inclusion content and banding characteristics of these heats of material. Relationships between yield strength, fracture toughness, and alloy composition were established. Fracture toughness correlation studies were conducted using the part-through-crack tensile, center-notch tensile, precrack-Charpy and slow-notch-bend test specimens.

TIG, MIG, and submerged-arc welding processes were evaluated using 200- and 250-ksi yield-strength base metals. Weldment tensile, fracture toughness, chemical composition, and metallurgical properties were evaluated and relationships between these properties established.

Based on the results of this program, an optimum 18% nickel maraging steel was selected for the fabrication of large-diameter booster motors and evaluated in the form of 3/4-in.-thick plate and 1 x 4-in. and 4 x 4-in. ring forgings. Tensile, aging response, fracture toughness, and metallurgical properties of the optimum material were evaluated. TIG and MIG welding studies were also conducted using the 3/4-in.-thick plate material and the weldment tensile, fracture toughness, chemical composition, and metallurgical properties were established.

Finally, this study program culminated in the preparation of plate, forging, and filler wire specifications for use in the fabrication of large-diameter solid-rocket motor chambers. These specifications are presented herein.

This technical documentary report has been reviewed and is approved.

FOR THE COMMANDER

W. P. Conrardy

W. P. Conrardy, Chief
Materials Engineering Branch
Materials Applications Division
AF Materials Laboratory

Approved for Public Release

Contrails

TABLE OF CONTENTS

Approved for Public Release

Contrails

TABLE OF CONTENTS (cont'd)

Approved for Public Release

Contrails

TABLE OF CONTENTS (cont'd)

Approved for Public Release

Contrails

ILLUSTRATIONS

Approved for Public Release

Contrails

Approved for Public Release

Contrails

Approved for Public Release

Contrails

Approved for Public Release

Contrails

FIGURE PAGE

Approved for Public Release

Contrails

Approved for Public Release

Contrails

Approved for Public Release

Contrails

Approved for Public Release

Contrails

Approved for Public Release

Contrails

Approved for Public Release

Contrails

TABLES

Approved for Public Release

Contrails

Approved for Public Release

Contrails

Approved for Public Release

Contrails

Approved for Public Release

Contrails

Approved for Public Release

Contrails

Approved for Public Release

Contrails

SECTION 1 - INTRODUCTION*

The design and fabrication of large-diameter solid-rocket motor cases pose a unique problem in material selection. For maximum performance, a high strength-to-weight ratio is essential; however, this must be combined with good fracture toughness. At the same time, the large sizes impose severe limitations on the manufacturing methods that can be used. Welding and heat-treating are particularly important in this respect. Complex pre- and post-weld heat-treatments and conventional quench-and-temper treatments of finished assemblies are undesirable because of the handling problems and the facility limitations. Because of these restrictions, the choice of materials for large motor cases is limited.

Of the materials which meet the requirements for large motor cases, the 18% nickel maraging steels appear especially well suited for such applications. Yield strengths in the 200 to 300 ksi range can be obtained in these steels. At the same time, these alloys exhibit better fracture toughness than other steels in comparable thicknesses heat-treated to the same strength range. Another outstanding advantage is that strengthening occurs through a precipitation phenomenon and maximum strength is not a function of carbon content. Because of this, the high-temperature portion of the heat-treatment, which consists of air-cooling from 1500°F, can be performed as the first step in the processing. In this solution-annealed condition, the 18% nickel maraging steels can be readily machined, formed and welded. Pre- and post-weld heat-treatments are not required to prevent weld cracking. The hardening of finished assemblies is achieved by aging only at the relatively low temperature of 900°F thereby significantly reducing the distortion problems and facility requirements associated with quench-and-temper treatments.

Because of these advantages, considerable interest has been shown in the 18% nickel maraging steels for aerospace applications. This study was undertaken to evaluate their potential for use in large rocket-motor cases. The primary objective of the research was to select and evaluate an optimum 18% nickel maraging steel that would provide the high strength and toughness needed in rocket motor cases. This was done by studying seven selected heats to determine if a relationship exists between strength and fracture toughness, and, if so, how it is affected by factors such as mill-processing variables and chemical composition. Based on this study, an optimum composition was selected, and a heat was evaluated to determine its aging response characteristics and toughness. Also, extensive welding studies were conducted on the selected heats and optimum material. This study included evaluations of welding processes, filler metals and joint properties. Subsequent to these investigations, material and welding filler wire specifications for the optimum material were prepared.

---

*Manuscript released by the authors (March 1964) for publication as an ASD Technical Documentary Report.

Approved for Public Release

Contrails

SECTION 2 - SUMMARY

This report describes a series of investigations which were made to evaluate and select 18% nickel maraging steel alloys intended specifically for use in large-diameter rocket-motor cases.

A. EVALUATION OF SELECTED ALLOYS

The most important material properties needed in rocket motor cases were considered to be strength, fracture toughness and weldability, and an optimum alloy for fabrication of rocket-motor cases was one that would provide the best combination of these properties. Before such an optimum alloy could be selected, it was first necessary to determine the influence of factors such as mill-processing variables, aging treatments and chemical composition on material quality, strength and toughness. This was done by evaluating seven selected heats of 18% nickel maraging steel purchased from six different suppliers. Plate material from each heat and bar stock from two heats were evaluated. Strength levels of 200, 250 and 300 ksi were represented in these selected materials together with three different melting practices: air melting, air melting and vacuum-degassing and air melting followed by vacuum-arc-remelting. The tensile properties, fracture toughness, and weldability of each heat was determined as a function of aging time and temperature.

1. Material Quality, Tensile Properties and Mill Processing

Each of the selected heats was examined metallographically to compare their quality from the standpoint of inclusion content, grain size and banding. Typical sections showed that all the heats had a satisfactory inclusion count and grain size. Existing differences could not be related to mill-processing variables. Banding was present to some extent in all heats, although banding in only one heat was characterized by the presence of retained austenite. The intensity appeared to be a function of ingot size rather than melting or rolling practice.

The evaluation of the seven selected alloys showed that these materials reached their specified yield strengths on aging at 900°F. The required aging time varied from heat to heat, but in no case did the aging time exceed 8 hr. For a given aging time, temperature fluctuations of ± 50°F could result in decreased strength due to either underaging or overaging as evidenced by tests of samples aged at 850°F and 950°F.

The anistropy measured in the plate materials, which was indicated by variations in longitudinal and transverse yield strength, was found to vary from heat to heat and could be related to rolling practice. Although significant differences were found in yield strength, the corresponding changes in ductility were not appreciable in plate material. On the other hand, bar stock showed directionality in ductility but not in yield strength.

The selected heats were received in either the as-rolled or mill-annealed condition. Some of the heats were tested in the as-received and aged condition and also after being solution-annealed at 1500°F for

Approved for Public Release

Contrails

30 min and aged. Generally, the material showed a higher yield strength after solution-annealing. This was true for both as-rolled and mill-annealed materials. The reason for this increase could not be determined within the scope of this program.

Although differences in tensile properties found in the selected heats could be attributed partly to mill practices, it was found that the most important variable in determining these properties was chemical composition. The following equation for predicting 0.2% offset yield st strength on the basis of chemical composition was derived by applying statistical methods in a multiple linear regression analysis.

$$\text{Yield Strength (ksi)} = 38.1 + 8.8\ (\%\ \text{Co}) + 22.6\ (\%\ \text{Mo}) + 87.7\ (\%\ \text{Ti})$$

This analysis showed that 95% of the variations in strength between the heats could be attributed to differences in titanium, molybdenum, and cobalt content. By applying the derived equation, it was found that the variations in these elements required by the steel mills could result in strength differences of 35 ksi for a given nominal strength level. The influence of these material contents overshadowed variations in tensile properties which could be attributed to mill processing.

2. Fracture Toughness Evaluations - Correlation Studies

Tests were conducted using one heat of 1/2-in.-thick 18% nickel maraging steel plate material to determine the relationship between the fracture toughness values obtained from plate-size and subsize part-through-crack tensile, plate-size center-notch tensile, slow-notch-bend and precracked-Charpy test specimens. Agreement was indicated within 10% between the precracked-Charpy W/A and the center-notch-tensile G_c values. Likewise, comparisons between the plane-strain fracture toughness (G_{Ic}, G_{nc}) values determined from 1) the center-notch tensile pop-in tests, 2) the part-through-crack tensile tests using both plate-size and smaller specimens, and 3) two sizes of slow-notch-bend tests indicated that specimen size did not affect the plane-strain fracture toughness measurements in the Grade-250 heat investigated. Also, agreement was indicated within 10% between the fracture toughness values obtained with full thickness, part-through-crack tensile, and slow-notch-bend tests.

3. Fracture Toughness Evaluations of Selected Alloys

Slow-notch-bend and precracked-Charpy-impact tests were used to establish relationships between fracture toughness, tensile properties, melting practice, and mill-processing variables that were investigated during the program. Grade 200 alloys generally were found to exhibit higher fracture toughness than either Grades 250 or 300 materials. Two heats of Grade 200 alloy were investigated; both had a plane-strain fracture toughness of approximately 300 in.-lb/in.^{2} (K_{Ic} = 95 ksi $\sqrt{\text{in.}}$) as measured in slow-notch-bend tests. Two of three heats of Grade 250 material developed plane-strain fracture toughness of approximately 200 in.-lb/in.^{2} (K_{Ic} = 78 ksi $\sqrt{\text{in.}}$) and the third heat had a fracture toughness below 100 in.-lb/in.^{2} (K_{Ic} = 55 ksi $\sqrt{\text{in.}}$). However, both the chemistry and

Approved for Public Release

Contrails

strength level of the third Grade 250 heat closely approximated a Grade 300 alloy. The one heat of Grade-300 alloy investigated exhibited plane-strain fracture toughness values of approximately 100 in.-lb/in.^{2}. In general, the transverse specimen orientation resulted in lower toughness values in comparison to the longitudinal specimen orientation.

Through these tests, the plane-strain fracture toughness was found to be controlled primarily by yield strength, with rolling practice and banding, also affecting fracture toughness. The relationship between yield strength and fracture toughness overshadowed almost all other variables investigated in the program. Aging treatments and melting practices also were found to produce minor effects. Mill-processing procedures appeared to affect toughness as evidenced by directionality in fracture toughness measurements, but these effects did not significantly alter the inverse relationship that was established between tensile strength and toughness. Also, solution-annealing treatments appeared to be desirable as a method for reducing directionality in fracture toughness. Based on these results, the procedure of cross-rolling plate material to reduce it approximately the same degree in both directions during final rolling followed by solution-annealing appeared to be the most desirable mill-processing procedure.

The plane-strain fracture toughness data were used to estimate the critical-defect size for the various grades of 18% nickel maraging steel plate. Assuming a design fracture stress equivalent to the nominal 0.2% offset yield strength of the material and a surface defect configuration ($a/2c = 0.1$), the following critical-defect sizes were calculated:

	G_{nc} (in.-lb/in.^{2})		Crack Length (in.)	
Fracture Stress, (ksi)	min	max	min	max
200	290	440	0.53	0.68
235	230	390	0.32	0.51
250	170	350	0.20	0.40
275	100	275	0.09	0.26

Based on these critical-defect sizes and nondestructive testing considerations, the use of 18% nickel maraging steel alloys at the 200-235 ksi stress level appears to be desirable for section thicknesses of 0.5-0.75 in. in large-diameter rocket-motor-case applications. This strength level was selected for the optimum alloy that was evaluated in the program.

4. Welding Evaluations of Selected Alloys

A welding program was conducted on 1/2-in.-thick, Grades 200 and 250 selected alloys to evaluate the weldability of 18% nickel maraging steel plate, to select filler wire compositions for welding this material and to develop reliable procedures that are applicable to the fabrication of

Approved for Public Release

Contrails

large-rocket motor chambers. The 18% nickel maraging steel plate was found to be readily adaptable to welding with the inert-gas-shielded tungsten-arc (TIG) and metal-arc (MIG) processes and with the submerged-arc process provided that proper welding filler metal compositions, inert-gas shielding procedures and flux compositions were used. Weld cracking problems were not encountered and preheating and postheating were found to be unnecessary in welding 1/2-in.-thick plate.

The composition of the weld filler wire was found to be an important variable. Through variations in filler wire composition, it was possible to match the tensile strength of weld metals with that of Grades 200 and 250 plate materials. The important strengthening elements in the weld filler wire were cobalt, molybdenum, and titanium. Slightly higher amounts of these elements were required in weld filler wires than in the wrought base metal to achieve a given strength; otherwise, the compositions of the base metals and filler wires were essentially the same. Alloy segregation in weld-fusion-zones, with or without a loss of alloy content in transfer across the arc, may account for the need to increase the alloy content slightly in weld filler wires.

The tensile and notch tensile properties of seven filler wires were evaluated as welded and aged at 900°F for 4 hr. Based on these tests, a filler wire composition was selected for aging response tests. This filler wire composition matched the base metal yield strength (250 ksi) most closely and was accompanied by high notch-tensile strength. These studies showed that the general relationships between weld-metal tensile strength and aging temperatures and time were similar to those of the base metal. Thus, simple aging treatments after welding may be used to age-harden the welded joints simultaneously with plate aging.

Fracture toughness evaluations of weldments in the selected alloys indicated that precracked-Charpy-impact fracture toughness (W/A) values and a notched/unnotched tensile ratio (K_t = 10) approaching that of the base metal was possible in weldments of Grade 200 plate. However, based on notched-tensile tests, low fracture toughness would be expected in Grade 250 weldments.

The effects of multiple-weld thermal cycles on the microstructure and hardness of weld metals and weld heat-affected zones were established. In the as-deposited condition, coarse columnar weld metal grains were found, but when these structures were subjected to the high temperature thermal cycles of subsequent weld passes, the grains were somewhat refined and equiaxed. Although these equiaxed weld-metal grain structures were coarser than the fine-grained wrought material, they were considered to be more desirable than the large columnar grains that were found in the as-deposited weld metal.

Weld metal and heat-affected zone hardness was affected by the thermal cycles of welding. When subjected to only high temperature thermal cycles, low hardness similar to that of solution-treated plate was found in the weld zones. When subjected to low temperature thermal cycles, increased hardness was found which indicated that partial age hardening occurred during welding. This partial aging during welding resulted in slightly reduced hardness after aging.

Approved for Public Release

Contrails

Three heat-treated sequences were investigated on the basis of tensile properties. Simultaneous aging of the base metal and joints after welding was found to be comparable to aging the base metal prior to welding and locally aging the welded joint after welding. However, fracture toughness tests would be necessary to fully evaluate these heat-treating sequences. Also, solution-annealing the welded joints at 1500°F for 1 hr and aging appeared to be comparable to simple aging treatments.

High-temperature, solution-annealing treatments were investigated as a method for reducing alloy segregation in weld-fusion-zones. Post-welding solution-annealing at 2000°F was required to produce any significant evidence of weld metal homogenization, but excessive grain growth occurred in the adjacent base plate.

B. EVALUATION OF THE OPTIMUM MATERIAL

Evaluation of the selected heats permitted the selection of a strength level and chemical composition for the optimum material, and a tentative material specification was prepared and used in the procurement of a heat of the optimum material. A maximum 0.2% offset yield strength of 235 ksi was selected for the optimum material on the basis of the strength-fracture toughness relationship established during the evaluation of the selected heats. By applying the equation which expressed the relationship between composition and yield strength, it was determined that a fluctuation of about 30 ksi could be expected within the steel producers ability to control the amount of critical alloying elements. A composition to provide a minimum yield strength of 200 ksi was selected using the regression analysis equation, and a material specification was prepared for the procurement of a heat of the optimum material in the form of 3/4-in.-thick plate and 1 x 4-in. and 4 x 4-in. ring forgings.

1. Material Quality and Tensile Properties

Metallographic examination showed that the optimum material plate and forgings were satisfactory from the standpoint of inclusion content. The plate material had a satisfactory grain size but the forgings were coarse-grained and did not meet the specification regarding grain size. There was no evidence of banding in the microstructure (Marbles Etchant - 100X magnification) of either the plate or forgings.

Tension tests, which were conducted to determine the aging response characteristics of the plate material, showed that the optimum material did not meet the specification requirements for 0.2% offset yield strength. A minimum yield strength of 200 ksi after aging at 900°F for 4 or 8 hr was required. The optimum plate material met the 200 ksi requirement with only one aging condition; namely, 850°F for 16 hr. Failure to meet the yield strength requirements was attributed to the molybdenum content, which was about 1% below the specified minimum.

2. Fracture Toughness Evaluations

The fracture toughness of the optimum alloy plate and forgings was comparable to that of the Grade 200 selected alloys which were investigated earlier in the program. The plane-strain fracture toughness of the optimum plate material ranged from 270 to 470 in.-lb/in.^{2}, while the yield

Approved for Public Release

Contrails

strength ranged from 193 to 200 ksi. In comparison, the plane-strain fracture toughness of the selected Grade 200 alloys ranged from 290 to 430 in.-lb/in.^{2} at 195 ksi yield strength and from 280 to 425 in.-lb/in.^{2} at 205 ksi yield strength. These results indicate that little difference existed in the plane-strain fracture toughness between the selected alloys and optimum plate material at the same strength level. In the mandrel-forged rings of the optimum material, values as low as 230 in.-lb/in.^{2} were measured in the transverse specimen orientation. However, these lower values were associated with the relatively low degree of working received in these components in the transverse orientation.

In general, the precracked-Charpy fracture-toughness data also showed the same trends as the test results previously obtained in evaluating the selected alloys. The fracture toughness of the optimum plate material in the longitudinal orientation was higher thn the values obtained with the selected alloys at the same strength level; however, the fracture toughness of the 4 x 4-in. mandrel-forged section in the transverse and short-transverse orientation was lower than the toughness of the selected alloys. Also, the transverse fracture toughness values in the plate material was lower than the plate longitudinal properties. These effects indicated that both the plate and the ring forgings received insufficient cross-working either during rolling, forging, or both.

3. Welding Evaluations

The welding characteristics of the optimum alloy were evaluated using the TIG and MIG welding processes. Three filler wires were selected; a Grade 200 filler wire for TIG welding, a Grade 200 filler wire with slightly higher titanium content for MIG welding, and a Grade 250 filler wire for both TIG and MIG welding. The Grade 200 filler wires were selected to provide maximum weld-metal fracture toughness. The Grade 250 filler wire was selected to provide additional data concerning the relationship between the tensile strength and fracture toughness of weld metals. In addition, the heat-treating sequence in which the parent metal and welded joints are aged simultaneously was selected for evaluation of the optimum alloy.

The optimum material was selected to provide the best combination of tensile properties and fracture toughness. The welding studies on this plate verified that comparable tensile and fracture toughness properties were achieved in TIG-welded joints when filler wires that produced weld metals with a tensile strength only slightly higher than the minimum yield strength of Grade 200 plate were used. However, MIG weld metals had significantly lower fracture toughness than comparable TIG weld metals. These studies also showed that fracture toughness was sacrificed whenever filler wires were used to greatly overmatch the tensile strength of the base metal. In this regard, it was also shown that the fracture toughness of Grade 250 TIG weldments were comparable to Grade 250 base metal and that the toughness of both were significantly lower than the Grade 200 base metal and weldments.

Based on this evaluation, a specification for the composition of Grade 200 filler wire has been proposed. The composition was formulated to obtain weld metal with a 215 ksi nominal 0.2% offset yield strength. The potential yield strength of the proposed weld filler wire composition ranges from 203 to 225 ksi depending on the cobalt, molybdenum, and titanium content. This composition range was selected to obtain weld metals that have yield strengths only slightly higher than the minimum yield strength of Grade 200 plate so that maximum fracture toughness in the weld metal can be achieved.

Approved for Public Release

Contrails

SECTION 3 - EVALUATION OF COMMERCIAL ALLOYS

Several commercial heats of 18% nickel maraging steel were evaluated as part of the over-all program to select an optimum material. This evaluation had a twofold purpose, namely: 1) to study the effects of mill processing so that the best melting and processing practice consistent with cost and volume production could be chosen, and 2) to select a material chemical composition that would provide the highest strength consistent with good fracture toughness under aging conditions compatible with production requirements. These objectives were achieved by selecting different alloy compositions produced by several manufacturers and comparing these alloys on the basis of quality and mechanical and metallurgical properties.

A. ALLOY SELECTION

The 18% nickel maraging steels are produced in Grades 200, 250 and 300, and these grades are classified by yield strength. Different strength levels are obtained primarily by varying the molybdenum, cobalt and titanium content. Nominal chemical compositions of the three grades are listed in Table 1. One of the primary objectives in evaluating commercial alloys was to select an 18% nickel maraging steel composition that would provide an optimum combination of yield-strength and fracture toughness. Therefore, compositions representing each grade were obtained for evaluation. In selecting these alloys, mill-processing variables that possibly could influence final properties also were considered. Among the most important of these variables are melting practice and the method of working the metal to obtain the final product.

The three melting practices used to produce the 18% nickel maraging-steels are air melting, air melting followed by vacuum-degassing during pouring, and air melting followed by consummable-electrode remelting in a vacuum. Vacuum processes are claimed to be superior; particularly vacuum-arc remelting. Reported advantages of this method are minimum segregation, low gas content, and improved cleanliness with better ductility, fatigue strength, and toughness properties. Alloys were selected for this program so that the three processes could be compared to determine if one is markedly superior to the others for fabrication of large-diameter rocket-motor cases. For this comparison, heats of the same strength level, Grade 250, produced by each method were procured. These heats were manufactured by three different steel mills.

The metal-working practices evaluated were rolling and forging. Material from all heats was rolled to 1/2-in.-thick plate. In addition, part of the ingots from a Grade 200 and Grade 300 heat were forged into 4 x 4-in. bar stock to permit a comparison of the extent of anisotropy produced in plate and bar stock and the effects of the varying degrees of working on the resultant material properties. Also, the selection afforded an opportunity to determine the variations from mill to mill because several different producers were represented.

The first stage in the heat treatment of the 18% nickel maraging steels consists of solution-annealing and is accomplished by air cooling from approximately 1500°F or above. The purpose of this step is to produce

Approved for Public Release

Contrails

a martensitic microstructure with the hardening agents retained in solution. The possibility of accomplishing this effect by air cooling from the finish-working temperature was considered in this program. To check this possibility, some heats were obtained in the as-rolled condition. These heats were tested after aging only and also after solution-annealing at 1500°F for 30 min and then aging.

Before selecting the commercial heats for evaluation, the steel industry was surveyed to determine the state-of-the-art which existed at that time (August 1962). The results of this survey are discussed in Appendix I. As a result of the survey, seven heats were selected as being representative of the mill practices observed at that time. The information obtained from the producers concerning the processing of each heat is described below and summarized in Table 2. These heats represent the melting practices of five different producers. Both of the Grade 200 heats were melted by the same producer, but one of these was rolled by a different mill. Two of the Grade 250 heats were melted and rolled by the same producer.

1. Grade 200, Heat 10675

This material was air-induction-melted and yielded a 750 lb 9 x 9-in. ingot. The ingot was soaked at 2300°F for 3 hr and then press-forged to form a 6 x 6-in. bar. No reheating was required during this operation. After conditioning, the 6 x 6-in. bar was cut into two pieces, one of which was used to produce plate and the other was used for bar stock.

The bar stock was produced by hammer-forging at 2150°F. Reheating was required in the reduction to 4 x 4-in. final size. The finished bar was supplied in the mill-annealed condition (1500°F from 7-10 hr).

The second 6 x 6-in. bar obtained from the bottom portion of the ingot, was hammer-forged to a 2-in.-thick, 10-in.-wide slab preparatory to rolling. During the first rolling operation which was started at 1850°F, the slab was cross-rolled to spread the transverse width from 10 in. to 20 in. and to reduce the thickness to 1 in. Rolling was completed by turning the slab 90-deg and straight-away rolling it to 1/2-in.-thick plate. Rolling was completed below 1400°F, and no reheating was done during the rolling operations. This material was furnished in a mill-annealed condition, which consisted of reheating to 1500°F, holding for 1/2 hr, and then air cooling. No mechanical property data for either the bar or plate were provided by the supplier.

2. Grade 200, Heat 28889

This heat was air melted and vacuum-degassed in the ingot mold. The yield was a 17 x 42-in. rectangular ingot which was upset-forged to form a 6600 lb, 6 x 47 x 85-in. slab. This slab was cut in two, and a 6 x 47 x 42-in. section was sent to another mill for rolling to 1/2-in.-thick plate. During the first rolling operation, the 42-in. length was increased to 65 in., and the slab was trimmed to 3 x 54 x 65-in. After conditioning, the slab was reheated to 2000°F and the thickness reduced to approximately 2 in. During the final rolling operation, which was started at 1750°F, the slab was turned 90-deg and cross-rolled in 6 passes to 0.517 x 87 x 190-in., finishing at 1620°F. The plate was annealed at 1500°F for 1 hr and trimmed to the final size of 0.517 x 83 x 160-in. No mechanical property data were supplied by the producer.

Approved for Public Release

Contrails

3. Grade 250, Heat 120D163

This heat was produced by air melting followed by vacuum-degassing during pouring. The yield was a 7 ton, 32-in.-dia corrugated ingot. The first step in the reducing operation consisted of block-forging parallel to the original ingot axis to form a round that was 28 in. in diameter and 72 in. long. Forging was started between 2250°F and 2300°F and finished at 1880°F. The ingot then was reheated and upset to a round 40 in. in diameter and 38 in. long, finishing at 1880°F. After reheating, the round was upset to form a slab 21-3/4 x 38 x 49-in., again finishing at 1880°F. Next, the slab was cross-forged to spread the transverse axis from 38 to 45-in., with the slab dimensions 18 x 45 x 49 in. This operation was finished at 1750°F. Again starting at 2250°F, the cross-forging was continued to form a slab 9-1/2 x 70 x 44-in. This slab was ground and trimmed to 9 x 70 x 44-in. prior to rolling.

The first rolling operations were carried out in a three-high reversing mill. Each operation began at 2300°F. In the first step, the 9 x 70 x 44-in. slab was reduced to 5 x 128 x 44-in. in 8 passes each with a draft of 1/2 in. The slab then was rotated 90-deg and straight-away rolled to 4-1/2 in. thick x 128 in. wide in two passes. After reheating, the slab was reduced to 3-1/2 x 128 in. in 2 passes.

The final rolling was done in a four-high mill, with reheating to 2300°F after each step. In the first two steps, the thickness was reduced to 3-1/4 in. and then to 3 in. with one pass for each reduction. The final reduction to 1/2-in.-thick plate was accomplished in 15 passes without reheating and finished at approximately 1500°F. The plate was supplied in the as-rolled condition. Mechanical property data furnished by the producer are as follows:

As Rolled and Aged at 900°F for 3 Hours

	0.2% Offset Yield Strength (ksi)	Tensile Strength (ksi)	Elongation in 1 In. (%)	Reduction of Area (%)	Hardness (R_c)
Longitudinal	264.6	270.6	9.2	44.1	51
Transverse	267.5	276.5	8.1	38.9	51
Solution-Annealed at 1500°F for 1 Hour					
Longitudinal	115.0	155.0	16.2	65.6	32
Transverse	123.2	159.5	15.4	63.5	32
Solution-Annealed and Aged at 900°F for 3 Hours					
Longitudinal	260.6	269.5	10.0	44.6	51
Transverse	267.6	277.6	9.0	42.8	51

Approved for Public Release

Contrails

4. Grade 250, Heats 3888471, 3888472 and 3888473

All three of these heats were processed in the same manner. A 450 lb ingot, 7 in. square was produced by air melting, and then press-forged to a 5-1/2 in. round. This round was used as the electrode in a consummable-electrode vacuum remelt. The remelt yield was a 400 lb, 8-1/2 in.-dia ingot, which was press-forged to form a 3 x 9-in. slab. After reconditioning and cropping to a length of 18 in., the slab was heated to 2000°F, cross-rolled to a width of 14 in., turned, and straight-away rolled to 1/2-in.-thick x 14-in.-wide plate. No reheating was required during rolling. The finishing temperature is not known, but the mill practice at the time was to complete the final 25% reduction between 1700°F and 1800°F. This material was supplied in an as-rolled condition.

Tensile data supplied by the producer are:

As-Rolled Plate

	0.2 Offset Yield Strength (ksi)	Tensile Strength (ksi)	Elongation in 1 In. (%)	Reduction of Area (%)
3888472	124	158	14	45
3888473	126	158	13	57
As-Rolled Plate Aged at 900°F for 3 Hours				
3888472	278	286	6	28
3888473	287	293	4	20

Early in the program at Aerojet, it was found that heat 3888471 would not respond to aging. The highest yield strength attained was approximately 200 ksi, well below the expected minimum of 250 ksi. A check of the chemical composition showed that the material was similar to 3888472 and 3888473, which met the expected minimum strength. Metallographic examination of the low-strength heat showed that massive inclusions were present as seen in Figure 1. These inclusions are believed to be complex titanium-molybdenum sulfides. In this case the critical hardening elements may have been incapable of going into solution and, consequently, they were not available for strengthening during aging. Because this heat did not meet strength requirements, it was not considered further during this program.

5. Grade 250, Heat 13371

This 22-ton heat was air melted and yielded a 32 x 60-in. ingot. The ingot was heated to 2275°F and forged to a 6-in.-thick x 55-in.-wide slab. Intermediate reheating was used and the ingot was worked parallel to its original axis during forging. After conditioning, the slab was reheated to 2275°F and cross-rolled to a thickness of 1/2 in. This was the only heat

Approved for Public Release

Contrails

in which the direction of rolling (longitudinal) was not parallel to the original ingot axis. The finishing temperature was below 1750°F, and was estimated to be between 1500°F and 1600°F. The material was supplied in the as-rolled condition. No mechanical property data were supplied by the producer.

6. Grade 300, Heat 07148

This heat was produced by air-induction-melting followed by consummable-electrode vacuum remelting. A 9-in.-dia, 1000 lb ingot was produced and cut in half. The bottom half of the ingot was press-forged at 2300°F to a 4 in., round-cornered bar. No reheating was required. The pressing operation was finished below 1500°F. This bar was supplied in a mill-annealed condition (1500°F for 4 hr).

The top half of the original ingot was heated to 2275°F and pressed to a 3-in.-thick x 10-in.-wide slab. This slab was conditioned, heated to 2050°F and rolled to 1/2-in.-thick plate; 50% of the reduction was made in the transverse direction. Rolling was finished between 1600°F and 1700°F. The final step in the processing was annealing at 1500°F for 30 min.

Property data furnished by the producer are as follows:

Mill-Annealed Plate, Aged at 900°F for 3 Hours*

Location	0.2% Offset Yield Strength (ksi)	Tensile Strength (ksi)	Elongation in 1 In. (%)	Reduction of Area (%)
1/2 In. Plate				
Top of Ingot	300.2	307.4	6.0	34.4
Middle of Ingot	297.5	304.3	6.0	39.2
4 x 4-In. Bar				
Middle of Ingot	293.5	304.8	4.0	20.4
Bottom of Ingot	294.8	304.2	3.5	17.9

* .250-in.-Dia Button-Head Specimen, 1 in. Gage Length, Longitudinal in Bar, Transverse in Plate

B. MATERIAL QUALITY

Each commercial heat was examined metallographically as it was received to evaluate its quality. The factors considered were cleanliness, degree of banding and grain size. For this purpose, the specimens were examined both as-polished and as-etched. Two different etchants, marbles

Approved for Public Release

Contrails

reagent and a 5% chromic acid electrolytic technique, were used. The first of these was used to indicate the presence of the martensitic structure and banding, and the second was used to show the prior austenitic-grain size. Similar studies were made after solution-annealing the as-received material at 1500°F to determine the effect of this operation on microstructure.

Photomicrographs of the seven heats are shown in Figure 2,and rated according to inclusion content in Table 3. This table also lists tentative specification limits on inclusions for ready comparison. These limits were established as the result of this program and were also specified for the optimum material. With the exception of heat 120D163, all the commercial heats were within the specification limit. Although the heats differed in inclusion content, these differences do not appear to be related to melting practice because, in some instances, there was as great a difference in quality between heats produced by the same process as between those produced by different processes. This can be seen by comparing vacuum-arc-remelted heats 07148 and 3888472 and air-melted heat 13371.

Heat 120D163 did not fall within the inclusion limits shown in Table 3 because of excessive Type B inclusions. This section was not representative of the entire plate, however, and was selected as a result of ultrasonic inspection. An 18 x 24-in. section of plate was inspected by both ultrasonic and penetrant methods. No defects were located by penetrant inspection, but several questionable areas were located by ultrasonic inspection. The technique used is described in Appendix II. Three areas, which appeared to contain the worst defects, were sectioned and found to contain aluminate stringers as shown in Figure 2. With the exception of these three areas, the material met the inclusion requirements shown in Table 3.

Grain sizes of the commercial heats in both the as-received and solution-annealed conditions are shown in Figures 3, 4, and 5. In all cases, the grain size was finer than that required by the tentative specification, but the size varied from heat to heat. However, these differences cannot be related to any single processing variable. Although final grain size is a function of working temperature, amount of working, and finishing temperature, it was not possible to definitely establish the effects of each of these variables on the properties of the plate from information supplied for the processing of each heat of material. Also, solution-annealing of the as-received material at 1500°F for 30 min did not have a significant effect on grain size, as illustrated in Figure 4 for the Grade 250 alloys.

In heat 10675 (mill-annealed condition) with grain size as shown in Figure 3, an appreciable difference was observed in grain sizes between the rolled plate and the center of the forged bar. The photomicrograph of the bar in the re-solution-treated condition shows that the grain structure is finer than that of the plate. However, this finer structure reflects the difference between the center and surface of the bar rather than refinement caused by re-annealing. Such a difference would be expected in hammer-forging where working is concentrated on the surface. A significant grain-size change from center to surface was not encountered in press-forging, where working is distributed throughout the bar thickness. This is shown in Figure 5. Again, the mill-annealed condition represents the center of the bar and the re-solution-annealed specimen was taken near the surface. However, a preference for press-forging cannot be justified on the basis of this study since the metallurgical properties produced by each technique depends on many variables

Approved for Public Release

Contrails

which could differ significantly from vendor to vendor and between different component configurations.

The banded areas shown in Figures 6, 7 and 8 are caused by composition variations within the structure that alter its etching characteristics. The dark areas are believed to be high in nickel, molybdenum, and titanium content. These enriched areas are attributed to segregation which occurs during solidification of the ingot. Banding was present to some extent in all the heats evaluated. In all heats but one, the variations in composition were not drastic enough to change the basic microstructure but only its etching characteristics. In heats such as 120D163, both the light and dark areas were martensitic. However, in heat 13371, the composition gradients caused by segregation were more pronounced and austenite bands were found in the structure. The solution-annealed sample shown in Figure 7 contains one of these bands. This latter type of banding is considered the most severe.

The different degrees of banding noted in the seven heats appeared to be related to ingot size rather than to melting practice. With the exception of heat 3888473, banding appeared to be most pronounced in the three heats that yielded the largest ingots; namely, 13371, 120D163 and 28889. Also, ingots of the same size, such as 3888472 and 10675, were comparable from the standpoint of banding even though they were prepared using different melting practices.

C. TENSILE PROPERTIES

The tensile properties of all the commercial heats, both plate and bar stock, were determined as functions of the aging treatment. Standard tensile specimens with a 1/4-in.-dia x 1-1/4 in. long reduced section (1 in. long gage length) were tested. Specimens were machined from as-received or solution-annealed blanks as indicated in Figures 9 and 10 and then aged. During the aging treatment, the furnace was maintained within $\pm$ 5°F of the desired temperature. The thin oxide film that formed during aging was removed by abrading with emery paper before testing. Results of the tension tests are summarized in Table 4, and are shown graphically as functions of aging time and temperature in Figures 11 through 16. These values are averages; data for the individual tests are tabulated in Appendix III. Data obtained from notched-tensile-specimens are included in the Appendix III tabulation for some heats. The notch severity (K_t) of these specimens was 10. In all cases, the notch tensile-strength was well above the ultimate strength, and followed the same general trends. Because the notched specimens did not provide any significant additional information regarding the effects of aging cycle, specimen orientation, etc., their use was discontinued early in the program.

1. Aging Response Characteristics

One of the objectives in the study of tensile properties was the determination of the aging response characteristics of the individual grades. In either screening, acceptance testing, or both, all grades of the 18% nickel maraging steel normally are aged at 900°F for approximately 3 hr. However, in the production of large-rocket motor cases, temperature variations of 50°F can be expected during aging. Thus, it became necessary to determine whether temperature variations of this magnitude would affect properties significantly and if time at temperature was critical.

Approved for Public Release

Contrails

The aging response characteristics of one heat from each grade are shown in Figure 17. At 850°F, overaging as evidenced by reduced strength was not found in any of the alloys at aging times up to 16 hr. In most cases, this also was true at 900°F; however, some heats, such as Grade 250 heat 120D163, showed a loss of strength after aging for 8 hr. At 950°F, some heats were overaged after only 2 hr. These data show that yield strength can vary appreciably with the aging conditions selected and illustrate the desirability of establishing aging response curves for each heat of material used in fabrication. Generally, however, 900°F appears to be the most satisfactory aging temperature. In all cases, aging at 900°F for 4 or 8 hr was sufficient to meet the yield strength minimum.

Even though the yield strength was influenced greatly by aging conditions, ductility was not. As would be expected, both elongation and reduction of area tended to vary inversely with strength changes. However, the changes were not appreciable. The changes in ductility and strength are compared in the following tabulation:

	0.2% Offset Yield Strength (ksi)		Elongation in 1 In. (%)		Reduction of Area (%)	
Heat	Max	Min	Max	Min	Max	Min
10675	240	205	12.9	9.2	58.9	49.4
28889	213	185	13.2	9.8	61.6	54.8
120D163	267	241	10.5	6.8	47.5	38.4
13371	286	252	9.1	7.1	47.0	38.5
3888472	284	268	9.7	8.4	43.4	38.0
3888473	279	268	9.2	8.2	43.7	38.6
01748	306	285	9.4	7.1	43.2	37.5

2. Effects of Mill-Processing Variables

Tensile specimens were taken in both the longitudinal and transverse directions as indicated in Figures 9 and 10 to determine the degree of anisotropy in each alloy composition. In most heats, there was little difference between the strength in each orientation. The difference was most pronounced in heats 120D163 and 13371; the extent of the difference is shown in Figure 18.

The differences found in each heat are summarized in the following table. These values were selected to show maximum differences for a specific aging treatment of each heat. However, the data do not represent a comparable aging treatment for all heats.

Approved for Public Release

Contrails

Heat	Increase in Yield Strength, Transverse (%)	Elongation (%) Long.	Elongation (%) Trans	Reduction of Area (%) Long.	Reduction of Area (%) Trans
13371	+6.8	9.5	7.6	42.9	38.6
120D163	+5.3	8.8	6.3	41.3	28.9
28889	+3.0	12.0	10.7	55.4	49.8
07148 Plate	-1.1	7.9	6.4	42.4	34.1
07148 Bar	-1.7	7.7	3.2	42.5	16.9
10675 Plate	+4.5	12.9	11.4	57.2	52.3
10675 Bar	-2.0	10.2	7.9	53.4	41.3
3888472	+2.6	9.6	8.6	42.0	40.5
3888473	+1.9	8.9	8.2	43.7	39.3

Some degree of anisotropy was noted in each heat. However, the tendency for the transverse and longitudinal yield strengths to differ after all aging treatments was found only in heats 13371, 120D163 and 28889. These heats also showed the greatest strength difference. (The maximum difference of 4.5% for heat 10675 given in the table above was not typical.) Processing of each of these heats included a final rolling operation with a heavy reduction of 75% or more in the longitudinal direction. Also, the photomicrographs presented in Figures 3 and 4 show these heats to have an elongated grain structure. Directionality in properties would be expected because of the heavy reduction during final rolling. The remaining heats were worked more uniformly in both directions and the final rolling operation did not exceed a 50% reduction. These heats were characterized by an equiaxed grain structure, which also are shown in Figures 3, 4 and 5.

It also may be significant that heats 13371, 120D163 and 28889, which showed the greatest degree of anisotropy, were produced from the largest ingots. The photomicrographs in Figures 6 and 7 show that these heats were heavily banded. The banding may also have influenced the differences in transverse and longitudinal yield strength observed.

Although the plate stock showed directionality in yield strength, a corresponding significant change in ductility did not occur. This situation was reversed in the bar stock from heat 01748. In this heat, the ductility varied from 7.7% elongation and 42.5% reduction of area in the longitudinal direction to 3.2% elongation and 16.9% reduction of area in the short transverse direction. This difference could not be explained and was not observed in bar stock from heat 10675. The two heats used for bar stock differed in melting practice, working procedure, and strength level. The Grade 300 Heat 01748 was vacuum-arc-remelted and press-forged while the Grade 200 Heat 10675 was air melted and hammer-forged. However, based on the processing history supplied by the producers, the causes of these effects could not definitely be established.

Approved for Public Release

Contrails

None of the variations in strength or ductility noted in the study of tensile properties could be attributed to melting practice, which was the other major mill-processing variable studied. If one of the three processes is superior to the others, its advantages were overshadowed by other factors such as rolling practice or chemical composition.

3. Effects of Solution-Annealing

The tensile properties of four of the commercial heats were determined in both the as-received (eighter as-rolled or mill-annealed) and aged condition and after solution-annealing at 1500°F for 1/2 hr and aging. The change in 0.2% offset yield strength produced by solution-annealing before aging is summarized in the following table for 1/2-in.-thick plate from these four heats:

Aging Cycle (°F - hr)	Change in Yield Strength, (ksi)			
	10675	13371	120D163	01748
850 - 4	+11.0	+6.6	+5.3	--
850 - 8	+5.0	+7.9	+5.2	+3.3
850 - 16	+7.4	--	+1.7	+2.2
900 - 2	+21.0	--	+15.1	-0.3
900 - 4	+14.9	+10.0	+13.6	-0.5
900 - 8	+9.1	+3.8	+10.0	+1.4
900 - 16	+5.0	--	+2.5	-2.7
950 - 2	+13.0	-3.5	-1.5	+4.3
950 - 4	+6.2	+3.0	--	0.0
950 - 16	--	--	+3.8	--

In heats 10675, 13371 and 120D163, solution-annealing of the as-received material before aging produced significant changes in the yield strength. In all but two of the aging conditions checked for these heats, the yield strength increased. Also, the magnitude of the change encountered appeared to be a function of both aging temperature and time. The greatest increases were found at 850°F and 900°F at aging times up to 8 hr. The aging condition which produced the greatest change varied from heat to heat.

Two of the heats that showed increased strength as the result of solution annealing prior to aging were received in the as-rolled condition. These heats were 13371 and 120D163. Heat 10675, which showed the greatest change in strength, as a result of solution-annealing at 1500°F for 30 min at Aerojet-General, was received in the mill-annealed condition (1500°F for 1/2 hr). Re-solution annealing would not be expected to improve the strength. On the contrary, a strength loss might be caused by relief of residual working effects. However, a possible explanation for the observed trend may be that during solution annealing, molybdenum, cobalt, or titanium compounds formed during rolling are dissolved thereby increasing the amount of hardener in solution and resulting in the increased

Approved for Public Release

Contrails

strength levels noted after aging. It is significant to note that the bar stock from the same heat did not behave in the same manner as the plate, but showed a loss of strength after re-solution annealing before aging. In the mill-annealed and aged condition, the bar stock had a yield strength of 235 ksi compared with a yield strength of 226 ksi for the plate. After re-solution annealing and aging, the strengths were 228 ksi for the bar stock and 235 ksi for the plate. The bar stock in the mill-annealed and aged condition had approximately the same strength as the plate in the re-solution annealed and aged conditions. The mill-annealing treatment for the bar differed from that of the plate in that it was held at temperature for 7 to 10 hr. It is not known if this difference in treatments influenced the behavior of the two products after re-solution annealing, although solution annealing for 7 to 10 hr may have resulted in the additional solutioning of molybdenum, cobalt, or titanium compounds precipitated during the processing of the bar products. More research should be done to determine why re-solution annealing of mill-annealed material should improve strength after aging. Metallographic studies did not show structural changes that satisfactorily explain this phenomenon. Also, the increased strength may be a function of the processing or composition. Heat 01748 in the mill-annealed form, for example, did not show a significant change after re-annealing in plate form, although re-annealing in bar form did result in an increase of 11 ksi.

4. Effects of Variations in Chemical Composition

Tension test data show that considerable variations in maximum strength were measured in heats of the same nominal strength level. These variations are attributed primarily to differences in chemical composition. The elements considered especially important are titanium, cobalt, and molybdenum. The strengths and compositions of the various alloys investigated are compared in the following tabulation:

	Heat	Maximum Yield Strength (ksi)	Ti %	Co %	Mo %
Grade 200	28889	231	0.19	8.52	3.30
	10675	240	0.42	8.50	3.26
Grade 250	120D163	267	0.48	8.00	4.95
	13371	273	0.52	8.05	4.90
	3888472	284	0.62	9.10	5.10
	3888473	289	0.65	8.82	4.85
Grade 300	01748	304	0.65	9.30	5.12

These data indicate that the maximum strength is related to the titanium, cobalt, and molybdenum content. A further study was made by applying statistical techniques to determine the functional relationship between the yield strength of 18% nickel maraging steels and the amounts of certain key constituents. The critical elements were considered to be titanium,

Approved for Public Release

Contrails

cobalt, molybdenum, and aluminum. The initial analysis was based on the yield strength data from 13 heats of 18% nickel maraging steel sheet stock, aged at 900°F for 4 hr. Initially this relationship was assumed to be linear, which resulted in an equation of the type:

$$\text{Yield Strength (ksi)} = A + B\,(\%Co) + C\,(\%Mo) + D\,(\%Ti) + E\,(\%Al) \quad (1)$$

A multiple linear regression technique incorporating a least-squares fit was used to determine the numerical values of the constants A, B, C, D and E. The coefficients were determined using an IBM 7094 digital computer. Analysis of the results indicated that the initial assumption of linearity between the yield strength and the alloy composition was valid. The value of the regression coefficient, E, for the aluminum content was found to be insignificant and was discarded in the final equation. Thus, the final linear relationship between the yield strength and key constituents became:

$$\text{Yield Strength (ksi)} = 15.1 + 9.1\,(\%Co) + 28.3\,(\%Mo) + 80.1\,(\%Ti) \quad (2)$$

A second analysis was made incorporating data from additional heats including those studied in this investigation. The following equation was obtained from this second analysis:

$$\text{Yield Strength (ksi)} = 38.1 + 8.8\,(\%Co) + 22.6\,(\%Mo) + 87.7\,(\%Ti) \quad (3)$$

The coefficients of the two equations appear quite different, but similar values are obtained for a given composition. Heat 28889, for instance, had an actual yield strength of 196.7 ksi after aging at 900°F for 4 hr. The predicted yield strengths are 193.2 ksi using Equation 2 and 196 ksi using Equation 3. The tabulation below compares the actual yield strengths of each heat with values calculated using Equation 3:

	Heat	Yield Strength After Aging at 900°F for 4 Hours (ksi)	Predicted Yield Strength (ksi)	Difference (ksi)
Grade 200	28889	196.7	204.5	-7.8
	10675	217.5	223.6	-6.1
Grade 250	13371	274.7	265.5	+9.1
	120D163	257.8	262.8	-5.0
	3888472	277.5	288.1	-10.6
	3888473	277.4	282.6	-5.2
Grade 300	01748	292.2	293.0	-0.8

The standard error of estimate for all 23 heats was 7.28 ksi.

Approved for Public Release

Contrails

Analysis of the computer evaluation shows that the derived equation represents an accurate analytical expression of the yield strength. The validity of the equation was verified using the "F" test (Reference 1). In this test, numerical F-values greater than 4 indicate, to some extent, the effectiveness of the regression analysis. In this application, the F-value was found to be 125, which indicated that the analysis was extremely good.

The coefficient of determination was another significant quantity that was computed. The significance of this quantity, which had a numerical value of 0.952, indicated that 95% of the variation in the yield strength of the different heats can be explained by changes in the cobalt, molybdenum, and titanium content.

The derived equation also can be used to indicate the relative influence of the individual alloying elements. For example, a 0.5% increase in molybdenum, which is permissible within the nominal grade composition, would produce a strength increase of 11 ksi. Similarily, an increase in the titanium content from the minimum to the maximum allowable value would increase the strength about 9 ksi or more. In the Grade 250 compositions, allowable cobalt, molybdenum, and titanium composition variations could produce strength differences of 34.3 ksi. Strength variations of this magnitude are far greater than those which could be attributed to mill-processing variables.

D. FRACTURE TOUGHNESS OF 18% NICKEL MARAGING STEEL PLATE

1. General

Fracture toughness or "crack toughness" is that characteristic of a material which defines its resistance to crack growth. The technology of fracture testing is based on the concept of a pre-existing flaw which, under increasing load or a repetitive load cycle, grows to critical dimensions and then propagates catastrophically under constant load. In simplest terms, the length of crack that will cause catastrophic propagation is calculated from the relation:

$$A = 2G_c E/\pi F^2, \qquad (4)$$

where A is the critical crack length, G_c is the fracture toughness under plane-stress conditions, E is the modulus of elasticity, and F is the applied stress. Equation 4 indicates that the critical flaw size varies directly as the fracture toughness of the material and inversely as the square of the applied stress. In other words, an increase in the working stress necessitates a substantially greater toughness to avoid crack propagation. Unfortunately, a higher working stress usually requires that a higher strength material be used which, in turn, may possibly result in lower toughness. Thus, if a material is strengthened to withstand the higher working stresses, the critical-defect size may fall below that which can be detected using practical nondestructive test procedures.

Initial crack growth or "pop-in" occurs under plane-strain conditions and is characterized by flat fracture as opposed to oblique shear under plane-stress conditions. The stress necessary to cause pop-in of a given defect size is generally low under plane-strain (G_{Ic}) conditions compared with the stress that causes crack propagation under plane-stress (G_c) conditions. In sheet thicknesses, if the pop-in crack does not reach critical size for

Approved for Public Release

Contrails

plane-stress propagation, slow crack growth will follow the initial crack growth and, in some instances, slow growth may even be arrested. In plate thicknesses, on the other hand, both the initial pop-in and subsequent propagation occur predominately under plane-strain conditions; consequently, pop-in and catastrophic propagation tend to occur in immediate sequence. Thus, resistance to pop-in is the prime consideration for materials of plate thickness.

The fatigue-cracked, circumferentially-notched tensile test is generally accepted as a quantitative measure of plane-strain fracture toughness (K_{Ic}) provided that the specimen is sufficiently large and that the net-section stress at fracture does not exceed 1.1 times the 0.2% offset yield stress. Although this test is generally recognized as quantitative, relatively few data have been collected with notched, round tensile-specimens because valid measurements require large-diameter specimens.

For purposes of this investigation, the tests that were considered are the center-notch tensile, the part-through-crack (PTC) tensile, the slow-notch-bend (SNB), and the fatigue-precracked Charpy.

The fatigue-cracked, center-notch tensile test offers the advantage of measuring both plane-stress and plain-strain fracture toughness in a single test, provided pop-in occurs and is detectable. However, these specimens are inconveniently large both from the standpoint of machining and testing when plate thicknesses are being tested. For valid plane-stress (G_c) measurements using the center-notch tensile specimen, the ASTM Fracture Testing Committee has recommended the following dimensions for specimens up to 1/4-in.-thick:

Thickness Range (in.)	Test Section Width (in.)	Length Minimum (in.)
0.044 to 0.125	2	8
0.088 to 0.250	4	16

For the evaluation of 0.5-in.-thick plate, a specimen with a cross-section of 0.5 x 8-in. and 32 in. long was deemed necessary. A smaller test specimen would have required testing of a lesser thickness machined from the 0.5 in. plate.

The part-through-crack (PTC) tensile test includes a flaw-type that is known to be the origin of some service failures. The test can be performed simply because slow crack growth is assumed to be negligible. Likewise, analysis of the test results is relatively simple using Irwin's equation

$$K_{Ic}^2 = 1.21\pi\,(a/Q)F^2, \qquad (5)$$

where K_{Ic} is the stress intensity factor (a fracture-toughness parameter), a is the depth of the surface flaw, Q is a flaw-shape parameter which is calculated from an elliptic integral function of the ratio of crack depth to half length (see p. 339) or is obtained from a graphical solution (Figure 19), and F is the gross fracture stress as measured in the PTC tensile test. In terms

Approved for Public Release

Contrails

of strain-energy release rate,

$$K_{Ic}^2 = G_{Ic}E/(1-\nu^2). \quad (6)$$

Substituting the above for K_{Ic}^2 in Equation 5, using published values of $E = 27 \times 10^6$ and Poisson's ratio $\nu = 0.33$;

$$G_{Ic} = 1.24 \times 10^{-7} (a/Q)F^2 \quad (7)$$

The PTC tensile test specimen generally is used in testing to determine the effect of defects in the plate surface. Flaws also may be embedded in the plate causing pop-in and propagation in a lateral direction and, therefore, fracture testing with the notch perpendicular to the plate surface, through the thickness, also may be necessary. Such tests are not usually conducted by PTC tensile test because the plate may not be thick enough to provide the width of specimen necessary for a valid fracture toughness (G_{Ic}) measurement. For this reason, other test methods such as the slow-notch-bend test are used.

The slow-notch-bend test has been used during the evaluation of plate materials to measure plane-strain fracture toughness. The procedural details of this application are presented in Appendix IV. For the general case in which the crack depth is a and the bar width is b, the expression for determining plane-strain fracture toughness from the slow-notch-bend test is

$$G_{nc} = 1/2(L/b)^2 \, d(b/M)/da, \quad (8)$$

where L/b is the bending load per unit width of bar, and b/M is the reciprocal of the spring constant for the notch depth, a, as determined from calibration data. Thus, a series of calibration bars is required in this method to obtain a relationship between the spring constant and notch depth.

In that plane-strain fracture toughness is concerned with initial crack growth, the load, L, used in Equation 8 should correspond to a value which produces pop-in. However, one of the difficulties in making quantitative plane-strain fracture toughness measurements is that often there is no positive indication of initial crack extension or pop-in. This problem was discussed but not resolved, at the 20th meeting of the ASTM Fracture Testing Committee (Washington, D.C., 17 December 1963) both in connection with notched-tensile and notched-slow-bend testing.

Autographically recorded load-deflection diagrams of slow-bend tests consist of two general types. The first of these is the type-1 diagram, in which failure of the test specimen occurs before the proportional-limit load is reached. The second is the type-2 diagram, in which failure of the test specimen occurs after plastic-deformation work is done in bending; that is, failure beyond the proportional limit. These diagram types are illustrated in Figure 20. When a material fails and a type-1 load-deflection diagram is recorded, maximum load is used to calculate fracture toughness without problem. On the other hand, when a material failure produces a type-2 load deflection diagram, initial deviation from the straight-line portion of

Approved for Public Release

Contrails

the load-deflection diagram may be attributed either to the formation of a plastic zone at the tip of the fatigue crack or to initial crack extension. Preliminary ink-staining experiments indicate that pop-in occurs at or just beyond the proportional limit. These results are illustrated in Figure 21, which shows a typical type-2 load-deflection curve obtained for a Grade-200 18% nickel maraging steel and the extent of crack growth associated with various points along the curve.* In calculating the plane-strain fracture toughness, the load associated with the initial deviation from a straight line is used (point X). From the fracture surfaces shown in Figure 21, the crack propagation, as outlined by the ink staining, that occurred at point X on the load-deflection curve apparently was associated entirely with the flat fracture surface. Consequently, fracture-toughness values calculated using the load and deflection associated with the first deviation from linearity in the load-deflection curve should provide an accurate measurement of plane-strain fracture toughness.

Whenever the load-deflection diagram indicates that pop-in occurs, it may be associated with secondary rather than initial crack extension. Thus, for a type-2 load-deflection diagram, the calculation of plane-strain fracture toughness based on pop-in indications from the load-deflection diagram generally involves loads above the proportional-limit load. Thus, use of the proportional-limit load is a conservative approach.

An additional approach has been investigated for calculating fracture toughness from slow-notch-bend tests. Based on Bueckner's work, Winne and Wundt (Reference 2) of the Turbine Division of General Electric Company, Schenectady, New York, have developed an analytical expression for the strain-energy release rate, G, for notched beams in 3-point loading; viz.,

$$G_{Ic} = \left[(1-\nu^2)/E \right] F^2 h\, f(a/d), \qquad (9)$$

where F is the nominal bending stress at the notched section, h is the beam depth after notching and fatigue cracking, and the function a/d is determined graphically from Figure 22. Bueckner (Reference 3) has reported that the function (a/d) can be applied to beams with notches up to 50% of the depth of the beam and span-to-width ratios of 4:1 or higher. Using the graphical relationship between a/d and f(a/d), Equation 9 requires only a measurement of the appropriate notch-plus-crack depth, and specimen dimensions b and d. The nominal bending stress at the notched section is computed from the equation:

$$F = 3/2 \frac{Ll}{bh^2}, \qquad (10)$$

where l is the beam span and L is the maximum load or proportional-limit load, whichever occurs first.

*The extent of crack growth associated with this point and at other locations along the load-deflection curve, were determined by means of a series of 0.5-in.-thick 18% nickel maraging steel bend-test-specimens that were loaded to various points along this curve. Then, ink was introduced in the crack and the specimen unloaded and allowed to dry. Next, the specimens were fractured and photographs were taken of the fracture surface to show the extent of crack propagation that occurred during the loading.

Approved for Public Release

Contrails

Use of Equation 9 and Bueckner's a/d function permits verification of the fracture-toughness values calculated from Equation 8. Both solutions are obtained using an IBM computer.

Although many fracture tests have been used since 1900 to evaluate the notch sensitivity of plates, the V-notch-Charpy-impact test has been used more than all other fracture tests combined. Hartbower and Orner (Reference 4) have demonstrated that the V-notch-Charpy-impact test can be used to determine a crack-arrest transition temperature for constructional metals in section thicknesses ranging from 0.030 to 0.800-in. or larger. This is accomplished by introducing a crack at the root of the V-notch before testing to provide the pre-existing flaw that is necessary when the Griffith equation is used to calculate critical flaw size.

In the precracked condition, the Charpy-impact-test has been shown to correlate with other larger, more costly tests (see Reference 5). For example, the V-notch-Charpy test, precracked by a preliminary low-energy blow, has been shown to provide a 1-to-1 prediction of the Naval Research Laboratory drop-weight nil-ductility-transition (NDT) temperature. Likewise, the precrack-Charpy has been shown to provide a 1-to-1 prediction of the crack-arrest temperature in 60-in.-wide plate tensile specimens. It is worth noting when comparing the results of center-notch tensile and precrack-Charpy-impact tests, that both tests involve a measure of the resistance of a material to a propagating crack. Plane-strain fracture toughness measurements, on the other hand, are concerned with initial crack growth or pop-in.

In reporting fracture toughness data from the various tests, individual values of G_{Ic} are tabulated; whereas, in general, the corresponding average value of K_{Ic} are tabulated as calculated from equation 6.

2. Fracture-Testing Objectives

The fracture toughness evaluations in this program were conducted to determine: 1) the toughness of each heat and grade of 18% nickel maraging steel investigated, 2) whether a correlation existed between various fracture toughness test specimens, and 3) if subscale test specimens could be used to quantitatively evaluate either the plane-stress, plane-strain fracture toughness, or both of the maraging steel alloys in plate thicknesses. The materials evaluated included plate and bar stock ranging in tensile yield strength from 200 to 300 ksi. Both plane-strain and plane-stress fracture toughness were evaluated. The general objective of this program was to obtain fracture toughness data on which material comparisons and material acceptance testing could be based, and to determine the limiting flaw sizes that can be tolerated in 18% nickel maraging steel.

3. Correlation Test Specimens and Procedures

Various specimen types and sizes were investigated in a single heat (120D163) of 18% nickel maraging steel to determine whether a correlation existed between various fracture toughness test specimens and to establish if subscale test specimens could be used to measure the fracture toughness of these maraging steel alloys in plate thicknesses. The various specimen types and the procedures that were evaluated are discussed briefly in the following paragraphs and in detail in Appendices IV and V.

Approved for Public Release

Contrails

a. Slow-Notch-Bend Test

Two sizes of fatigue-precrack slow-notch-bend (SNB) specimens were investigated. The first of these specimen sizes was 0.50 in. wide, 0.75 in. deep, and 4 in. long, and the second specimen size was 0.50 in. wide, 0.50 in. deep, and 4 in. long. The first size is a specimen configuration that has been used extensively at Aerojet to evaluate plate materials. The 0.5 x 0.5-in. specimen was important to this investigation because it allowed testing 0.5-in.-thick plate in two notch orientations with respect to thickness as indicated in Figure 23. Specifically, these orientations are 1) with the notch perpendicular to the as-rolled plate surface (notch through the thickness) and 2) with the notch parallel to the as-rolled plate surface (notch in the as-rolled surface).

An electrodynamic vibration system was used to fatigue-crack the SNB specimens. The specimens were subjected to vibration at resonant frequencies (approximately 5-600 cps) until a crack approximately 0.1 in. deep was produced at the apex of the machined notch. The input intensity level during vibration was 45-50 g peak. The desired crack was produced in 2-3 min. India ink was used to facilitate detection and measurement of fatigue-crack growth. After the ink was dry, the specimens were fractured using conventional tensile machine and a 3-point loading system with a 3 in. span. Data for fracture toughness calculations were obtained from load-deflection curves, and the notch depth was determined both from calibration curves and from measurement of the actual notch plus fatigue-crack depth. The detailed procedure for SNB testing is outlined in Appendix IV, together with illustrations showing the test specimens and the setup for fatigue cracking and bending.

b. Part-Through-Crack Tensile Test

Two sizes of part-through-crack (PTC) tensile specimens were investigated. These were 0.50 in. thick, 4 in. wide, and 26 in. long and 0.125 in. thick, 0.50 in. wide, and 8 in. long. The larger specimen was selected to test the full thickness of plate. Use of the smaller specimen permitted testing of 0.5-in.-thick plate in two notch orientations with respect to thickness as indicated in Figure 24, which allowed notches through the thickness and notches in the as-rolled plate surface. The smaller specimens were cut from the broken halves of the larger specimens to assure metallurgically replicate specimens.

The initial surface notch was induced by an "arc-strike" from an electrical-discharge machine (EDM) at the center of gage area of the test specimen. In both the plate-size and subscale specimens, fatigue-cracking was induced at the EDM notch by cyclic bending using a maximum bending stress of less than 50% of the yield strength of the material. Details of this testing procedure are presented in Appendix V, together with illustrations showing the test specimens and the setup for fatigue cracking.

c. Center-Notch Tensile Test

A specimen 0.5 in. thick, 8 in. wide, and 32 in. long was used for center-notch tensile testing of 0.5-in.-thick plate. The center

Approved for Public Release

Contrails

notch was machined by the electrical arc discharge technique. Fatigue-cracking was induced by cyclic bending on a hydraulically-operated fatigue machine, producing a crack extension of approximately 0.070 in. at each end of the machined notch. The specimens were tensile-tested in a 4-million lb Southwark Emery Testing Machine, located at the Engineering Materials Laboratory of the University of California, Berkeley. Ink stains were used to establish the length of crack at the onset of fast fracture. It should be noted that the ASTM Fracture Testing Committee no longer recommends the use of ink because of two complications. First, although "fast" fracture is of interest, concern should be directed primarily to the onset of unstable crack growth. Secondly, ink has an environmental effect on some metals, resulting in crack growth at lower stress than with a dry environment and, consequently, with ink, longer cracks develop before the onset of fast fracture. The load corresponding to audible crack pop-in was noted for the calculation of G_{Ic}. The details of this testing procedure also are presented in Appendix V, together with illustrations showing the specimen and setup for testing.

d. Precrack-Charpy-Impact Test

Precrack-Charpy-impact test specimens 0.394 x 0.394 x 2-in. were cut from the broken halves of the large tensile specimens to assure metallurgically replicate specimens. The V-notched specimens were fatigue-precracked and impact-tested at ManLabs Inc., Cambridge, Mass., over a range of test temperatures. The details of this testing procedure also are presented in Appendix V, together with illustrations showing the specimen and the impact-testing machine.

4. Correlation Test Results

The objectives of this phase were 1) to determine whether a correlation existed between various fracture-toughness tests, 2) to establish if subscale test specimens could be used to measure the fracture toughness of 18% nickel maraging steel alloys in plate thicknesses, and 3) to provide baseline data for comparing the various heats and grades of 18% nickel maraging steel in subsequent phases of the investigation.

A single material was used for all of these evaluations: 1/2-in.-thick, 18% nickel maraging steel plate, heat 120D163, solution-annealed at 1500°F for 30 min and aged at 900°F for 4 hr. This treatment produced an average 0.2% offset yield strength of 258 ksi in the longitudinal rolling direction and 265 ksi in the transverse direction.

Fracture-toughness data from the various specimen configurations and sizes are presented in Tables 5 and 10 and summarized on the following page for the individual test specimens evaluated. The test data presented in the following table are categorized according to notch orientation either perpendicular or parallel to the plate surface. Comparison between the precrack-Charpy-impact test values and the center-notch-tensile test data indicated agreement within 10% of G_c despite the difference in specimen sizes. Likewise, comparisons between the plane-strain fracture toughness (G_{Ic}, G_{nc}) values determined from 1) the center-notch tensile pop-in tests, 2) the part-through-crack tensile tests using both plate-sized and smaller specimens, and 3) the two sizes of slow-notch-bend tests indicated that specimen size at the

Approved for Public Release

Contrails

strength and toughness level investigated (Grade 250) did not appreciably affect the plane-strain fracture toughness measurements. Also a comparison between the full-thickness part-through-crack (PTC) tensile and slow-notch-bend test results indicated agreement within 10% between the plane-strain fracture toughness valves obtained from the two tests.

The difference in toughness values between the longitudinally- and transversely-oriented test specimens was neither consistent from specimen to specimen nor sufficiently large to be significant. However, anisotropy was indicated in the thickness direction, with somewhat lower toughness when the specimens were notched through the thickness. Such a difference can be caused by the mechanical effect of laminar defects or the metallurgical effect of material inhomogeneity in the thickness direction. When both factors are present, the interpretation of data is complicated by the possible interaction of the mechanical and metallurgical effects.

NOTCHED PERPENDICULAR TO THE PLATE SURFACE

Specimen Orientation	Precrack Charpy Impact W/A (1)	Fatigue-Cracked Center-Notch Tensile G_c (2)	Fatigue-Cracked Center-Notch Tensile G_{Ic} (2)	Part Through Crack Tensile G_{Ic} (3)	Slow-Notch-Bend G_{nc} (4)	Slow-Notch-Bend G_{nc} (5)
Longitudinal	329-392	---	---	246-265	184-239	185-220
	Avg(3)366			Avg(3)257	Avg(5)213	Avg(5)205
Transverse	342-364	344-438	205-218	231-246	223-266	209-257
	Avg(2)358	Avg(2)391	Avg(2)211	Avg(2)238	Avg(5)246	Avg(5)240

NOTCH IN THE PLATE SURFACE

Specimen Orientation	PTC Tensile Test G_{Ic} (6)	PTC Tensile Test G_{Ic} (3)	Slow-Notch-Bend G_{nc} (5)
Longitudinal	208-339	259-266	201-295
	Avg(5)278(7)	Avg(3)262	Avg(5)246
Transverse	211-326	269-293	237-289
	Avg(5)275	Avg(3)284	Avg(5)263

(1) Specimen 0.394 x 0.394 x 2-in.
(2) Specimen 0.5 x 8 x 32-in.
(3) Specimen 0.125 x 0.5 x 8-in.
(4) Specimen 0.5 x 0.75 x 4-in.
(5) Specimen 0.5 x 0.5 x 4-in.
(6) Specimen 0.5 x 4 x 25-in.
(7) Number of tests included in the average are shown in parentheses.

Approved for Public Release

Contrails

5. Plane-Strain Toughness by Slow-Notch-Bend Test

Plane-strain fracture toughness was measured by the slow-notch-bend (SNB) test using test specimens obtained from each of the selected heats of 1/2-in.-thick 18% nickel maraging steel. All data pertain to a notch oriented perpendicular to the plate surface (notched through the thickness). Data for individual test specimens are reported in sufficient detail in Appendix IV to permit recalculation if desired. The average test values are summarized and discussed in the following paragraphs for each heat of material evaluated. Aging cycles were selected in most cases to represent maximum strength at each aging temperature based on the aging response data and tensile properties previously discussed for each heat of material.

a. Grade 200, Air Melted, Vacuum-Degassed, 1/2 In. Plate, Heat 28889

The plane-strain fracture toughness values for this material as determined by the SNB test are presented in Table 6. Two aging treatments were investigated: 900°F for 4 and 8 hr for both longitudinal and transverse specimen orientations.

Material Condition	Aging Cycle (°F-hr)	Yield Strength (ksi) Longitudinal	Yield Strength (ksi) Transverse	G_{nc} (in.-lb/in.^{2}) Longitudinal	G_{nc} (in.-lb/in.^{2}) Transverse
Re-Solution Treated*	900-4	197	202	310-480 Avg(5)382	254-390 Avg(5)303
	900-8	211	217	386-432 Avg(5)407	214-323 Avg(5)261

* Mill-annealed plate was re-solution treated at 1500°F for 30 min.

Although tensile tests of this heat showed an increase in yield strength of approximately 15,000 psi (from 197 to 211 ksi) on increasing the aging time from 4 to 8 hr at 900°F, the plane-strain fracture toughness was approximately constant at 400 in.-lb/in.^{2} in the longitudinal and 300 in.-lb/in.^{2} in the transverse specimen orientation for both aging times investigated.

b. Grade 200, Air Melted, 1/2 In. Plate, Heat 10675

Plane-strain fracture toughness values for heat 10675 as determined from the SNB test are presented in Table 7 and are summarized in the next page. Two aging treatments (900°F for 4 and 8 hr) were investigated in the mill-annealed condition, and three aging treatments (850°F for 8 hr and 900°F for 4 and 8 hr) were investigated in the re-solution-treated condition for both longitudinal and transverse specimen orientations. Despite the generally increasing yield strength with increasing aging time, the plane-strain fracture toughness appeared to increase slightly in the mill-annealed condition

Approved for Public Release

Contrails

as aging time was increased. In the re-solution-treated condition, the toughness was constant at approximately 300 in.-lb/in.^{2}, although the yield strength increased as the aging temperature or time increased. A comparison between vacuum-degassed heat 28889 and air-melted heat 10675 after aging to approximately the same strength level indicated that heat 28889 was the tougher of the two heats in the longitudinal specimen orientation; however, there was little or no difference between the two heats in the transverse specimen orientation. Fracture toughness values for heat 10675 computed from Bueckner's equation indicated higher toughness than the spring-constant method.

Material Condition	Aging Cycle (°F-hr)	Yield Strength (ksi) Longitudinal	Yield Strength (ksi) Transverse	G_{nc} (in.-lb/in.^{2}) Longitudinal	G_{nc} (in.-lb/in.^{2}) Transverse
Mill-Annealed	900-4	218	214	252-300 Avg(5)283	263-400 Avg(5)316
				271-335 Avg(5)304(1)	281-530 Avg(5)375(1)
	900-8	226	228	195-316 Avg(4)248	289-382 Avg(5)337
				242-372 Avg(4)322(1)	396-495 Avg(5)459(1)
Re-Solution Treated(2)	850-8	222	224	233-316 Avg(3)288	280-339 Avg(3)311
	900-4	232	225	299-386 Avg(4)329	292-332 Avg(4)313
	900-8	235	245	277-346 Avg(3)315	285-322 Avg(3)298

(1) These values were calculated using Bueckner's equation based on the proportional-limit load.

(2) Mill-annealed plate was re-solution treated at 1500°F for 30 min.

c. Grade 200, Air Melted, 4 x 4-In. Bar Stock, Heat 10675

The plane-strain fracture toughness values for the bar stock as determined from the SNB test are presented in Table 8 and are summarized on the following page. Two aging treatments (850°F for 16 hr and 900°F for 8 hr) were investigated in the re-solution-treated condition, for both longitudinal and transverse specimen orientations. Little or no difference in toughness was observed in the longitudinal specimen orientations between plate and bar stock or between aging treatments. In the transverse specimen orientation

Approved for Public Release

Contrails

Material Condition	Aging Cycle (°F-hr)	Yield Strength (ksi) Longitudinal	Yield Strength (ksi) Transverse	G_{nc} (in.-lb/in.^{2}) Longitudinal	G_{nc} (in.-lb/in.^{2}) Transverse
Re-Solution Treated*	850-16	-	-	258-355 Avg(5)305	215-384 Avg(5)235
	900-8	228	229	255-336 Avg(5)307	187-226 Avg(5)211

*Mill-annealed product was cut into specimen blanks and re-solution-treated at 1500°F for 30 min.

(fracture propagating longitudinally in the billet), the fracture toughness was approximately 100 in.-lb/in.^{2} lower for the bar stock than for the plate material at approximately the same strength level. This same difference was also noted for the longitudinal and transverse bar stock test data and results from the differences in working between the two products. The bar stock was produced by hammer-forging in which the metal working was entirely unidirectional (longitudinal). The plate, on the other hand, had approximately 50% of its working done in the form of cross-rolling. In the mill-annealed condition, both the spring constant and Bueckner's equation showed the plate to have lower toughness in the longitudinal specimen orientation; whereas, after re-solution treatment, the plate showed little or no anisotropy (approximately 300 in.-lb/in.^{2} for both specimen orinetations).

d. Grade 250, Air Melted, 1/2 In. Plate, Heat 13371

The plane-strain fracture toughness values as determined from the slow-notch-bend test are presented in Table 9 and are summarized on the following page. Three aging cycles were investigated in the as-rolled condition: 850°F for 8 hr, 900°F for 4 hr, and 950°F for 2 hr for both the longitudinal and transverse specimen orientations. In the solution-treated condition, two aging cycles were investigated, namely, 900°F for 4 and 8 hr for both the longitudinal and transverse specimen orientations. In the as-rolled condition, increased aging temperature (with decreased aging time) was attended by a slight increase in both strength and toughness. Solution-treatment and aging at 900°F for 4 hr increased the strength approximately 10 ksi over that in the as-rolled and aged condition and, at the same time, produced a slight increase in toughness. Overall, however, this heat at the higher strength level was not as tough as either of the Grade 200 heats investigated. Furthermore, as a result of severe banding shown in Figure 25, and the resultant lamination-like splitting of the fracture surfaces as shown in Figure 26, the longitudinal specimen orientation generally indicated higher toughness than the transverse specimen orientation.

Approved for Public Release

Contrails

Material Condition	Aging Cycle (°F-hr)	Yield Strength (ksi) Longitudinal	Yield Strength (ksi) Transverse	G_{nc} (in.-lb/in.^{2}) Longitudinal	G_{nc} (in.-lb/in.^{2}) Transverse
As-Rolled	850-8	-	260	159-196 Avg(5)171(1)	158-216 Avg(5)189(1)
	900-4	243	265	187-245 Avg(5)220(1)	148-230 Avg(5)174(1)
	950-2	-	264	235-305 Avg(4)266(1)	214-233 Avg(2)223(1)
Solution Treated(2)	900-4	259	275	285-349 Avg(5)317	154-213 Avg(5)172
				209-320 Avg(3)273(1)	206-282 Avg(4)238(1)
	900-8	273	286	201-235 Avg(5)227	156-237 Avg(5)187
				203-289 Avg(5)236	175-211 Avg(5)191

(1) These values were calculated using Bueckner's equation.

(2) The as-rolled plate was solution-treated at 1500°F for 30 min.

e. Grade 250, Air Melted, Vacuum-Degassed, 1/2 In. Plate, Heat 120D163

The plane-strain fracture toughness values determined from the SNB test are presented in Table 10 and summarized on the following page. Four aging cycles (850°F for 8 hr, 900°F for 4 and 8 hr, and 950°F for 2 hr) were investigated in the solution-treated condition. Based on the values calculated using Bueckner's equation, a slight increase in toughness occurred with increased aging temperature but little or no difference resulted from an increase in aging time from 4 to 8 hr at 900°F (despite a 10 ksi increase in yield strength with increased aging time). There was also little difference in toughness as a function of specimen orientation in respect to the plate rolling direction. A comparison between solution-treated, vacuum-degassed heat 120D163 and air-melted heat 13371 after aging at 900°F for 4 hr indicated that heat 13371 had a greater toughness than heat 120D163 at the same strength level in the longitudinal specimen orientation and, after aging at 900°F for 8 hr, heat 13371 had greater strength and toughness in both specimen orientations. The data upon which these comparisons were based are summarized in the second table on the following page.

Approved for Public Release

Contrails

Material Condition	Cycle (°F-hr)	Yield Strength (ksi) Longitudinal	Yield Strength (ksi) Transverse	G_{nc} (in.-lb/in.^{2}) Longitudinal	G_{nc} (in.-lb/in.^{2}) Transverse
Solution Treated(4)	850-8	254	-	121-161 Avg(5)136(1)	-
	900-4	258	265	126-226 Avg(5)157(1)	139-163 Avg(4)149(1)
				184-239 Avg(10)208(2)	209-266 Avg(10)243(2)
				201-295 Avg(5)246(3)	237-289 Avg(5)263(3)
	900-8	267	275	140-167 Avg(3)156(1)	127-150 Avg(5)141(1)
	950-2	-	-	175-210 Avg(4)198(1)	-

(1) Values were calculated using Bueckner's equation - notched through the thickness.
(2) Values were calculated using the spring-constant calibration - notched through the thickness.
(3) Values were calculated using the spring-constant calibration - notched in the plate surface.
(4) As-rolled plate was solution treated at 1500°F for 30 min.

Heat No.	Aging Cycle (°F-hr)	Yield Strength (ksi) Longitudinal	Yield Strength (ksi) Transverse	G_{nc} (in.-lb/in.^{2}) Longitudinal	G_{nc} (in.-lb/in.^{2}) Transverse
120D163	900-4	258	265	126-226 Avg(5)157	139-163 Avg(4)149
	900-8	267	275	140-167 Avg(3)156	127-150 Avg(5)141
13371	900-4	259	275	285-349 Avg(5)317	154-213 Avg(5)172
	900-8	273	286	203-289 Avg(5)236	175-211 Avg(5)191

Approved for Public Release

Contrails

f. Grade 250, Vacuum-Arc-Remelt, 1/2 In. Plate, Heat 3888472

The plane-strain fracture-toughness values for heat 3888472 are presented in Table 11 and summarized below. Both the as-rolled and solution-treated material were evaluated after aging at 900°F for 4 and 8 hr.

Material Condition	Aging Cycle (°F-hr)	Yield Strength (ksi) Longitudinal	Yield Strength (ksi) Transverse	G_{nc} (in.-lb/in.^{2}) Longitudinal	G_{nc} (in.-lb/in.^{2}) Transverse
As-Rolled	900-4	269	285	41-55 Avg(2)48	45-81 Avg(3)65
	900-8	-	-	50-69 Avg(2)60	47-56 Avg(2)52
Solution-Treated*	900-4	278	274	56-106 Avg(2)81	46-95 Avg(5)60
	900-8	279	286	51-60 Avg(4)56	50-65 Avg(5)58

*As-rolled plate was solution-treated at 1500°F for 30 min.

The fracture toughness was extremely low regardless of material condition, aging time, or specimen orientation. Air-melted, vacuum-degassed heat 120D163 and air-melted heat 13371 both developed greater toughness than vacuum-arc-remelt heat 3888472. For example, heat 13371 in the transverse specimen orientation (the orientation with the least toughness) aged at 900°F for 4 hr had a toughness of 172 in.-lb/in.^{2} compared with 60 in.-lb/in.^{2} for heat 3888472 (both heats at approximately 275 ksi yield strength). After aging at 900°F for 8 hr, heat 13371 developed 191 in.-lb/in.^{2} compared with 58 in.-lb/in.^{2} for heat 3888472 (both heats at 286 ksi yield strength). The relative toughness of these three heats, all Grade 250, was confirmed by precrack-Charpy-impact tests which are described later.

g. Grade 300, Vacuum-Arc-Remelt, 1/2 In. Plate and Bar Stock, Heat 07148

The plane-strain fracture toughness values for the Grade 300 heat are presented in Table 12 and are summarized on the following page. Mill-annealed and re-solution-treated material was evaluated after aging at 850 and 900°F up to 8 hr. As indicated by these data, the fracture toughness of both the plate and bar stock was extremely low regardless of material condition, aging cycle or specimen orientation. Also, the values were of about the same magnitude as those obtained in the vacuum-arc-remelted, Grade 250 laboratory heat 3888472. Again, the extremely low toughness of the material was confirmed by the precracked-Charpy-impact test.

Approved for Public Release

Contrails

Material Condition	Aging Cycle (°F-hr)	Yield Strength (ksi) Longitudinal	Yield Strength (ksi) Transverse	G_{nc} (in.-lb/in.^{2}) Longitudinal	G_{nc} (in.-lb/in.^{2}) Transverse
Mill-Annealed Plate	850-8	294	-	55-59 Avg(3)58	59-70 Avg(5)60
	900-4	292	302	63-81 Avg(5)73	54-71 Avg(4)60
Re-Solution Treated*	850-8	298	-	52-74 Avg(4)62	63-84 Avg(4)69
	900-8	302	299	55-58 Avg(4)56	55-61 Avg(5)57
4 x 4-In. Bar Stock Re-Solution Treated*	850-8	-	-	62-69 Avg(4)65	64-77 Avg(4)71
	900-8	309	308	73-94 Avg(3)82	71-75 Avg(4)72

*Mill-annealed material was re-solution treated at 1500°F for 30 min.

6. Precrack-Charpy-Impact Tests of Selected Heats of 18% Nickel Maraging Steel

The fracture toughness measured in the precracked-Charpy-impact test (W/A) was investigated for selected heats of the 18% Nickel maraging steel studied during the basic program. Aging treatment, specimen orientation, and test temperature were among the variables investigated. The effects of varying test temperature (-100, RT, 200, 400°F) were investigated to determine if a fracture toughness-transition temperature occurred in the region of room temperature and if slight variations in test temperature would result in a large difference in fracture toughness. The results of the individual tests are presented as Tables 13-20, and summary tabulations of these tables based on average values are presented in subsequent paragraphs to facilitate discussion of the various heats.

a. Grade 200, Air Melted, Vacuum-Degassed, 1/2 In. Plate, Heat 28889

The W/A values for 200 ksi air melted and vacuum-degassed heat 28889 are presented in Table 13 and summarized on the following page. Two aging treatments and four test temperatures were investigated.

Approved for Public Release

Contrails

Material Condition	Specimen Orientation	Aging Cycle (°F-hr)	Yield (ksi)	W/A (in.-lb/in.^{2}) Test Temperature (°F) -100	RT	200	400
Re-Solution Treated	Longitudinal	900-4	197	956	946	1100	1384
	Transverse	900-4	202	631	650	701	710
	Longitudinal	900-8	211	771	893	962	1185
	Transverse	900-8	217	574	555	609	644

The effects of aging treatment and test temperature are shown in Figure 27 for longitudinal and transverse specimen orientations. The figure shows that fracture toughness increased as the test temperature increased with the longitudinal specimen orientation affected by test temperature to a greater extent than the transverse orientation. Aging for 8 hr at 900°F produced lower toughness and somewhat greater strength than did aging at 900°F for 4 hr regardless of specimen orientation. In slow-notch-bend testing,the difference in plane-strain fracture toughness between 4 and 8 hr aging at 900°F was neither consistent nor marked in the longitudinal and transverse specimen orientations. Anisotropy was rather marked in this heat of material with the longitudinal Charpy specimen appreciably more resistant to fracture than the transverse specimen. Similar results were observed in the slow-bend test, with higher plane-strain toughness values in the longitudinal specimen orientation than in the transverse specimen.

b. Grade 200, Air Melted, 1/2 In. Plate and 4 x 4-In. Bar, Heat 10675

The W/A values are presented in Table 14 and summarized below for 1/2-in.-thick plate as received from the supplier in the mill-annealed condition and after re-solution (1500°F-30 min) treatment.

Material Condition	Specimen Orientation	Aging Cycle (°F-hr)	Yield (ksi)	W/A (in.-lb/in.^{2}) Test Temperature (°F) -100	RT	200	400
Mill-Annealed Plate	Longitudinal	900-4	218	764	1346	1454	1724
	Transverse		214	845	1019	1274	1332
Re-Solution Treated Plate	Longitudinal	900-4	232	902	1225	1291	1470
	Transverse		225	757	1060	1165	1162
	Longitudinal	900-8	235	634	1002	1274	1310
	Transverse		245	703	830	909	1210
Re-Solution Treated Bar Stock	Longitudinal	900-4		814	--	1208	1576
	Transverse			592	--	817	--
	Longitudinal	900-8	228	.645	1120	1368	1093
	Transverse		229	512	--	--	--

Approved for Public Release

Contrails

These data indicate the two aging treatments and four test temperatures that were investigated. The effects of these variables on the fracture toughness of the plate material are plotted in Figure 28 for the longitudinal specimen orientation and Figure 29 for the transverse specimen. These data show that the fracture toughness increased as the test temperature increased. At room temperature and above, the mill-annealed plate material was somewhat tougher than the re-solution-treated material; this may be associated with the 14 ksi increase in yield strength resulting from re-solution treating before aging. The W/A values indicated higher toughness values after aging for 4 hr at 900°F for both specimen orientations than after aging for 8 hr at 900°F. The slow-notch-bend test data showed no significant difference in toughness between the mill-annealed and the re-solution-treated materials after aging for 4 and 8 hr at 900°F. Although the W/A values showed the material to be tougher with the fracture propagating transverse to the final rolling direction (longitudinal Charpy-impact test specimen), anisotropy was not as great in the 1/2 in. plate of heat 10675 as it was in heat 28889. Also, based on the results of the slow-notch-bend test, the difference between the two orientations in heat 10675 plate did not appear to be significant.

The W/A values obtained from the re-solution-treated 4 x 4-in. bar stock from heat 10675 are presented in Table 15 but were widely scattered and prevented the plotting of W/A vs temperature. Nevertheless, the tabulated values show greater toughness in the longitudinal specimen orientation with fracture propagating transverse to the axis of the bar than in the transverse orientation. The slow-bend test also indicated a somewhat greater toughness with the longitudinal specimen orientation and as indicated previously probably resulted from the different degrees of working present between the two orientations.

c. Grade 250, Air Melted, 1/2 In. Plate, Heat 13371

The W/A values for air-melted heat 13371 in the as-rolled and solution-treated conditions are presented in Table 16 and summarized below:

Heat No.	Material Condition	Specimen Orientation	Aging Cycle (°F-hr)	Yield (ksi)	W/A (in.-lb/in.^{2}) Test Temperature (°F) -100	RT	200	400
13371	As-Rolled	Longitudinal	900-8		--	440	489	--
		Transverse			177	--	271	320
	Solution-Treated	Longitudinal	900-4	259	412	--	598	707
		Transverse		275	280	336	357	420
		Longitudinal	900-8	273	--	--	--	606
		Transverse		286	226	346	346	381
120D163	Solution-Treated	Longitudinal	900-4	258	90	366	460	58
		Transverse		265	123	353	401	51

Approved for Public Release

Contrails

These data indicate that two treatments and four test temperatures were investigated and the effects of these variables are shown graphically in Figure 30. The figure shows that the solution-treated material was somewhat tougher under impact loading than the as-rolled material, and that the transversely-oriented specimens produced values that were lower than those obtained in testing the longitudinal specimens. Also metallographic examination of this material revealed severe banding which resulted in lamination-like defects in the fracture surfaces of the specimens. This effect is shown in Figure 31. Specimens notched parallel to the as-rolled plate surface indicated consistently higher W/A values than those notched perpendicular to the as-rolled surface (Figure 32). Also, the specimens notched parallel to the surface developed much higher W/A values after solution treating than were developed by the same notch orientation in the as-rolled plate. This suggests that the strength of the bands, the toughness of the bands, or both was altered by solution treatment.

d. Grade 250, Air Melted, Vacuum-Degassed, 1/2 In. Plate, Heat 120D163

The W/A values for heat 120D163 in the solution-treated condition are presented in Table 17 and summarized on the preceding page. One aging treatment and five test temperatures were investigated. Figure 33 shows an increase in toughness as the test temperature increased with slightly greater toughness in the longitudinal specimen orientation. A comparison between Grade 250 air-melted heat 13371 and vacuum-degassed heat 120D163 showed that, although heat 13371 was appreciably tougher at -100°F, both heats had about the same toughness at room temperature and above.

e. Grade 300, Vacuum-Arc-Remelt, 1/2 In. Plate, Heats 3888472 and 3888473

The impact values for heats 388472 and 3888473 are presented in Tables 18 and 19 and summarized below.

Heat No.	Material Condition	Specimen Orientation	Aging Cycle (°F-hr)	Yield (ksi)	W/A (in.-lb/in.^{2}) Test Temperature (°F) -100	RT	200	400
3888472	As-Rolled	Longitudinal	900-8		87	108	114	168
		Transverse			106	137	164	169
	Solution-Treated	Longitudinal	850-8	274	90	134	146	285
		Transverse		273	96	130	138	205
		Longitudinal	900-8	279	111	141	150	212
		Transverse		286	117	140	151	208
3888473	As-Rolled	Longitudinal	900-8		106	190	172	238
		Transverse			155	149	162	135
	Solution-Treated	Longitudinal	900-8	289	128	216	215	312
		Transverse		294	161	208	180	257
		Longitudinal	850-8	280	118	163	179	272
		Transverse		281	128	137	191	243

Approved for Public Release

Contrails

Two aging treatments and four test temperatures were investigated. The summary presents average values without regard to notch orientation because little, if any, difference was observed between the W/A values for notches oriented parallel with and perpendicular to the plate surface of test specimens from these heats. The effects of aging and test temperature are shown in Figure 34 for the longitudinal test specimen orientation. Only a slight increase in toughness occurred with increased test temperature, little difference was noted between the two specimen orientations, and little or no difference in toughness occurred after aging at 850 and 900°F for 8 hr. Likewise, little or no difference in toughness is noted between the as-rolled and solution-treated conditions. The slow-bend plane-strain fracture toughness tests indicated the same trends as the precrack-Charpy-impact tests; little or no difference in toughness occurred between 1) the as-rolled and solution-treated condition, 2) the aging cycles that were investigated, or 3) the longitudinal and transverse specimen orientations.

f. Grade 200, Vacuum-Arc-Remelt, 1/2 In. Plate and 4 x 4-In. Bar, Heat 07148

The W/A values are presented in Tables 20 and 21 and summarized below.

Material Condition	Specimen Orientation	Aging Cycle (°F-hr)	Yield (ksi)	W/A (in.-lb/in.^{2}) Test Temperature (°F) -100	RT	200	400
Mill-Annealed	Longitudinal	900-8	300	90	112	154	205
	Transverse		294	84	133	124	209
Re-Solution Treated Plate	Longitudinal	900-8	302	96	136	169	231
	Transverse		299	102	127	169	208
	Longitudinal	850-8	298	78	116	153	270
	Transverse			75	101	157	226
Re-Solution Treated Bar Stock	Longitudinal	900-8	309	85	127	168	223
	Transverse		308	83	126	146	--
	Longitudinal	850-8		78	105	176	272
	Transverse			79	112	138	246

Data were obtained for 4 x 4-in. bar stock after re-solution treatment and for 1/2-in.-thick plate as received from the supplier in the mill-annealed condition and after re-solution treatment. Two aging treatments and four test temperatures were investigated. The effects of these variables are shown in Figure 35 for the longitudinal orientation of test specimens. As indicated by these data, the toughness of this heat of material was found to be extremely low, with little or no difference between 1) the mill-annealed and re-solution treated conditions, 2) the aging cycles that were investigated, 3) the notch and specimen orientations investigated, or 4) the plate and billet materials.

Approved for Public Release

Contrails

7. Discussion

The plane-strain fracture toughness values from the slow-notch-bend test are presented graphically in Figure 36. The bars shown in the figure represent average values for longitudinal and transverse specimen orientations (shaded portions are transverse orientations). To facilitate comparisons between the various grades, the 0.2% offset yield strength is typed above the bars for each heat-treat condition tested. To judge the significance of the differences in average toughness values from bar to bar, the scatter involved in the individual test data is represented by a line through the top of each bar (in the high-strength low-toughness materials for which scatter was consistently small, the lines have been omitted). Those bars designated by the letter B in Figure 36 represent values that were obtained using Bueckner's equation (Equation 9) and the unmarked bars represent values that were obtained using the spring-constant equation. Only Bueckner's equation was used for heat 13371 in the as-rolled condition because the testing done early in the program involved inaccurate deflection measurements and, therefore, could not be used to determine toughness by the spring-constant method. However, where test data could be obtained using both Bueckner's equation and the spring-constant method, similar trends were indicated. Based on the comparison of results from both methods in such cases, Bueckner's equation appears suitable for calculating slow-notch-bend fracture toughness values and offers a greatly simplified approach compared with the spring-constant calculation.

Data shown in Figure 36 indicate that the Grade 200 alloys generally exhibited higher fracture-toughness than either the Grade 250 or the Grade 300 materials. Also, the toughness measured in the Grade 200 material by the spring-constant equation indicated that the aging treatments used had little or no effect and that both of the Grade 200 heats investigated had a toughness of approximately 300 in.-lb/in.^{2} (K_{Ic} = 95 ksi $\sqrt{\text{in.}}$). Two of the three heats investigated for the Grade 250 material developed a toughness of approximately 200 in.-lb/in.^{2} (K_{Ic} = 78 ksi $\sqrt{\text{in.}}$), and the third heat (a vacuum-arc-remelt laboratory heat) was below the 100 in.-lb/in.^{2} level (K_{Ic} = 55 ksi $\sqrt{\text{in.}}$). However, both the chemistry and the strength level of the third heat material more closely approximated a Grade 300 alloy, which also had a toughness at the 100 in.-lb/in.^{2} level.

Some directionality in fracture toughness was noted, and probably related to the rolling practice. This effect can be seen by referring to the data from heats 28889 and 13371. Both of these heats exhibited higher toughness and lower strength in the longitudinal orientation, and both received a large degree of reduction in the longitudinal orientation in the last rolling passes. These effects also were noted in evaluating heat 10675 bar stock where higher toughness was obtained in the longitudinal orientation; i.e. fracture propagating perpendicular to the direction of major working (the bar stock was a forging involving 100% unidirectional metal working). Solution annealing before aging tended to reduce toughness anisotropy in some heats such as heat 10675. Solution-annealing at 1500°F for 30 min prior to aging in most instances also resulted in an increased yield strength without a significant reduction in fracture toughness. This effect can be noted by referring to the data shown in Figure 36 for heats 10675 and 13371.

Based on these data, it appears desirable to use cross-rolled plate material reduced approximately the same degree in both directions during

Approved for Public Release

Contrails

final rolling, followed by a solution-annealing although additional work remains to be done to establish the best solution-annealing cycle for each grade of material and mill processing.

The data shown in Figure 36 do not indicate a preference of melting technique in that the plane-strain fracture toughness values at any given strength level are comparable regardless of the melting method. This effect can be seen by comparing the data for heats 28889 (air melted and vacuum-degassed) and 10675 (air melted) at the 200-225 ksi yield strength level, and heats 13371 (air melted) and 120D163 (air melted and vacuum-degassed) in the 250-275 ksi yield strength range. Grade 250 vacuum-arc-remelted heat 3888472, which had significantly lower toughness than heats 13371 and 120D163, was found to have chemistry comparable to a Grade 300 material.

When making comparisons of the plane-strain fracture toughness for different heats, heat-treatments, and specimen orientations, it is desirable to relate the fracture toughness to surface-defect size and to relate the critical-defect-size to non-destructive-testing (NDT) capability under production conditions. Although the slow-notch-bend test does not utilize a surface defect, configuration (a/2c) can be assumed and appropriate equations used to calculate the size defect that would be critical based on slow-notch-bend plane-strain fracture toughness data. Such a calculation has been performed and is indicated by dash lines in Figure 37, which summarizes all of the slow-notch-bend test data plotted as a function of 0.2% offset yield strength (data for the plate are indicated by scatter band). In addition, Figure 38 graphically presents a general solution for Equation 7 relating gross fracture-stress, F, plane-strain fracture toughness, G_{Ic} and G_{nc}, and the surface crack depth, a, for the 18% nickel maraging steel alloys. The flaw shape, a/2c, has been assumed equal to 0.1 to simulate a surface-flaw configuration which approaches the most dangerous condition normally encountered in service. The data in Figure 37 show a decided trend toward decreased toughness with increased yield strength, regardless of specimen orientation, with values of 240 in.-lb/in.^{2} (K_{Ic} = 86 ksi $\sqrt{\text{in.}}$) or less at yield strengths above approximately 235 ksi. With a plane-strain fracture-toughness level of 240 in.-lb/in.^{2} and a stress of 235 ksi, a defect with a depth approximately 1/32-in. is calculated to be critical using Equation 7 and assuming an a/2c ratio of 0.1. At a stress of 200 ksi and a typical toughness of 350 in.-lb/in.^{2} (K_{Ic} = 103 ksi $\sqrt{\text{in.}}$), the critical-defect size would increase to approximately 1/16 in. Using a surface-flaw configuration of a/2c = 0.1, the 1/32 in. and 1/16 in. flaw depths are equivalent to surface lengths of approximately 0.3 in. and 0.6 in., respectively. Although these flaw lengths both appear to be of sufficient size to be detected by NDT techniques in production, a flaw only 1/32 in. deep could be masked by surface roughness.

Additional flaw lengths have been calculated (a/2c = 0.1) using Figure 38 and are tabulated on the following page. These surface crack lengths are representative of values associated with selected yield strengths and plane strain fracture toughness values obtained from Figure 37 as being representative of 200 and 250 grade alloys. From these data it can be seen that surface-flaw lengths associated with the 200-235 grade alloy can vary between approximately 0.3 to 0.7 in. whereas values approximating .09 to .4 are associated with the 235-275 grade materials depending on the actual material plane-strain fracture toughness and the applied stress level.

Approved for Public Release

Contrails

Fracture Stress (ksi)	G_{nc} (in.-lb/in.^{2}) min	G_{nc} (in.-lb/in.^{2}) max	Crack Length (in.) min	Crack Length (in.) max
200	290	440	.53	.68
235	230	390	.32	.51
250	170	350	.20	.40
275	100	275	.09	.26

Based on these critical-defect sizes, it appears highly desirable to use the 18% nickel maraging steel alloys at the 200-235 ksi yield strength level for section thicknesses of 0.5 to 0.75 in. This selection of material yield-strength level was further verified by the weldment fracture-toughness tests discussed in Section 3, Paragraph 4.d. of this report.

Figure 39 is a replot of those data in Figure 37 which represent 900°F aging for 4 and 8 hr. From this plot, the relationship between strength and toughness discussed previously appears to be independent of aging time at 900°F. The curves outlining the scatter band are the same as those used in Figure 37 where all aging treatments were plotted.

Figure 40 is a plot of all the room-temperature precrack-Charpy-impact data (specimen notched through the thickness) for heats 28889, 10675, 13317, 120D163, 3888473, and 07148. The slow-notch-bend data of Figure 37 have been repeated in Figure 40 and are shown as shaded areas. Again, a decided loss of toughness was indicated with increased yield strength. Above approximately 250 ksi yield strength, the precrack-Charpy-impact W/A values approached or even overlapped the plane-strain fracture-toughness values measured in the slow-notch-bend test.* As in the slow-notch-bend test, the relationship between yield strength and toughness appeared to be independent of specimen orientation.

Figure 41 summarizes the precrack-Charpy-impact data, with the corresponding slow-notch-bend plane-strain fracture toughness values shown as shaded bars and included for comparison. Note that, with one significant exception, the two tests indicated the same trends regarding relative toughness, the effect of specimen orientation, and heat treatment. The only noteworthy exception was the difference between air melted, vacuum-degassed heat 28889 and air-melted heat 10675, in which the precrack-Charpy W/A values indicated heat 10675 to be decidedly the tougher of the two heats despite its having a 20-30 ksi higher yield strength. The reason for this effect was not established, although it may have been related to variations in the mill processing of the

* The precrack Charpy W/A value integrates the plane-strain (flat fracture associated with the start of fracture, and crack propagation at mid-thickness of the 0.394-in.-square test piece) and the plane-stress (oblique shear at the free surfaces of the test piece) fracture toughness. In materials of low toughness, the shear lips in the Charpy fractures were a small percentage of the fracture surface and, thus, approached the plane-strain fracture toughness value.

Approved for Public Release

Contrails

two heats. The fact that both the slow-notch-bend and the precracked-Charpy tests generally showed the same relative toughness trends indicates that either test can be used for a qualitative evaluation of fracture toughness, although for quantitative plane-strain fracture toughness measurements, it is necessary to use the slow-notch-bend test or some other type of plane-strain fracture toughness test such as the part-through-crack tensile test.

E. WELDING DEVELOPMENT STUDIES

1. Objectives

The principal objectives of the welding studies were to evaluate the weldability of 18% nickel maraging steel plate, to select filler wire compositions for welding this material, and to develop reliable welding procedures that are adaptable to the fabrication of large rocket-motor chambers. To achieve these objectives, weldments in 1/2 and 3/4-in.-thick Grades 200 and 250, 18% nickel maraging steel plate were prepared with the TIG, MIG and submerged-arc welding processes and evaluated on the basis of nondestructive examinations, mechanical property tests, metallographic examinations and hardness tests. The purpose of these tests and procedures was to investigate:

a. the adaptability of the three basic welding processes (TIG, MIG and submerged-arc) to the fabrication of 18% nickel maraging steel plate and to select two processes for the welding of the optimum material determined during this program,

b. the effect of filler wire composition on the tensile properties of weldments,

c. the aging response of weld metals deposited with selected filler wires,

d. the plane-strain and plane-stress fracture toughness properties of weldments produced with selected filler wires,

e. the microstructure of welded joints in 18% nickel maraging steel plate, and

f. the effect of multiple-weld thermal-cycles on the hardness and aging response of welds in 18% nickel maraging steel plate.

The initial welding studies were conducted utilizing two selected alloys. The information obtained from these studies was used to aid in the preparation of specifications for the optimum material and in the selection of welding procedures and filler wire compositions for welding this optimum material. The selected welding procedures and filler wire compositions then were used to evaluate the weldability of the optimum material. The information obtained in welding the selected and optimum alloys are described in subsequent sections.

2. Welding Studies of Selected Alloys

Selected Grade 250 (heat 120D163) and 200 (heat 10675) alloys were welded to develop procedures for welding 1/2-in.-thick plate with the

Approved for Public Release

Contrails

three basic welding processes and to determine the effects of filler wire composition on the tensile and fracture-toughness properties of 18% nickel maraging steel weldments.

a. Welding Procedures

Weldments in 18% nickel maraging steel plate were made using the TIG, MIG and submerged-arc welding processes to evaluate the adaptability of these processes to the welding of 18% nickel maraging steel and to select two processes for welding the optimum material. The weldments were 12 in. long, 8 in. wide, and 1/2 to 3/4-in.-thick. This specimen size was selected to provide sufficient material for preparation of the various test specimens that would be used in the program. Weld test plates were machine-cut and all plate edges were prepared for welding so that the plate edges would not be subjected to thermal cycles such as those that are encountered in flame or powder cutting, which might affect the mechanical properties and metallurgical characteristics of welded joints. After machining, the plates were degreased and the plate surfaces were ground to remove oxide scale. Immediately before welding, the joint edges were wiped with acetone to remove oil film and other foreign materials.

The weld-test plates were clamped to a rigid, water-cooled, copper backup-bar that also aligned the plates during welding. The backup-bar was water-cooled to increase the weld cooling rates and to eliminate copper pickup during welding. The backup-bar also was grooved to control weld penetration and to provide a means for introducing the inert gas which was used to shield the root of the weld. A sketch of this component showing the groove dimensions and the method for supplying shielding gas to the root of the weld is shown in Figure 42.

Precautions were taken during welding operations to obtain fast weld-cooling rates and to minimize the size of weld heat-affected zones. Pre- and post-heating were not used. Also, the weldments were allowed to cool between passes so that the interpass temperature did not exceed 200°F. These are standard precautions taken in welding 18% nickel maraging steel plate to minimize austenite reversion in the weld heat-affected and weld-fusion-zones during welding.

The procedures that were developed for each of the welding processes are described in detail below.

(1) Inert-Gas-Shielded Tungsten-Arc Welding

The inert-gas-shielded tungsten-arc welding (TIG) process was used extensively to prepare weldments for an evaluation of metallurgical characteristics and for tensile and fracture toughness tests of welded joints in Grades 200 and 250 18% nickel maraging steel plate. This process was selected for the majority of the study because of its ease of welding, weld quality, and for the minimum of development work that would be required to prepare weldments for evaluation of the weldability, welding filler wires, and the tensile and fracture toughness properties of welded joints.

Approved for Public Release

Contrails

A HWM-2 automatic welding head, equipped with a HW-13 welding torch; an EG103 governor-controlled cold-wire feeder; and a 400 amp dc welding-power-source were used to prepare the TIG welds. Two weld-joint configurations and welding schedules were developed as shown in Figures 43 and 44 for the welding of 1/2 and 3/4-in.-thick plate, respectively. A single-U joint configuration was used with both welding schedules to provide a sufficient volume of weld metal to evaluate the properties of the weld metal in either longitudinal weld-metal specimens or transverse weld-joint specimens. The root-land dimension of the joints was adjusted to assure complete penetration of the root pass without a root gap. The welding and shielding conditions were adjusted to provide sound welds using the TIG process.

Preheating was not used in preparation of the weldments and interpass temperatures were maintained below 200°F. Also, the welding conditions were adjusted to obtain relatively low heat input when making the welds. All of these procedures were used to obtain rapid weld cooling-rates to minimize overaging and austenite reversion in the weld zones.

(2) Inert-Gas-Shielded Metal-Arc Welding

Weld porosity was the major problem encountered in adapting inert-gas-shielded metal-arc (MIG) welding to the fabrication of 18% nickel maraging steel plate. Many welding variable combinations were evaluated before this problem was eliminated. The important welding variables that were investigated to reduce porosity are

(a) Joint configuration - single-and double-V joint, single- and double-U joint.

(b) Shielding methods - cup sizes ranging from 1/2 to 1-in.-dia and trailing shields.

(c) Shielding gas mixtures - argon, argon plus 2% oxygen, and argon plus helium.

(d) Welding conditions - travel speeds from 10-30 ipm, arc voltages from 25-35v, welding currents from 300-400 amp, and contact tube-to-work distances from 3/8 to 3/4 in.

(e) Filler wire composition - 0.42 to 1.65% titanium.

The most important relationship between welding conditions and porosity appeared to be associated with weld shielding. By the use of TIG welding to deposit the root passes and a small cup size (1/2 in.) on the MIG torch for initial weld passes in a single-U joint, the majority of weld porosity previously encountered could be eliminated, although some scattered porosity was still encountered. This small nozzle was placed down into the joint to reduce the distance between the nozzle and the work when depositing the initial MIG weld passes. Even with this improved shielding method, however, the weld beads had to be ground to remove oxide scale between weld passes.

An SEH-2 welding head, equipped with a type SCC-6 governor welding control and a constant potential 400-amp welding-power-source,

Approved for Public Release

Contrails

was used to prepare MIG welds. The joint configuration and MIG welding procedures that were developed for 3/4-in.-thick plate are shown in Figure 45. The single-U joint configuration was chosen because it would provide sufficient weld metal volume for preparation of longitudinal and transverse tensile specimens. The other welding conditions were developed to obtain good arc characteristics and to deposit sound welds.

Preheating and post heating were not used in preparing the welds. Also, the interpass temperatures were maintained below 200°F. These precautions were taken as they also were for TIG welds, to minimize austenite reversion in the welded joints.

Comparisons between the TIG and MIG welding procedures indicate the advantages of using the MIG process for welding 1/2 and 3/4-in.-thick plate. Less weld passes and higher welding speeds were achieved with the MIG process, which reduced the welding costs. However, the higher incidence of weld porosity that was found in the MIG welds and the probability that increased weld repair would be required if this process were used to weld large-diameter rocket-motor cases also must be carefully considered in the final selection of a welding process.

(3) Submerged-Arc Welding

The state-of-the-art of submerged-arc welding 18% nickel maraging steel plate has advanced greatly during the performance of this program. During this period, several new submerged-arc welding fluxes were developed for welding this material.

Submerged-arc welds were prepared at Aerojet-General and the Linde Company. The initial welds were made using L709-5 flux, which was originally recommended for processing this material. The initial submerged-arc welds were essentially free from porosity, but they were characterized by low elongation and reduction of area values and inconsistent tensile properties. These inconsistent tensile properties generally were attributed to inconsistent loss of titanium and silicon pickup in the weld-fusion-zone during welding, but a definite cause was not established.

During the last quarter of the program the Linde Company prepared welds with a special flux composition for evaluation using the three welding schedules shown in Figures 46, 47, and 48. Preheating and postheating were not used and the weldments were cooled to room temperature between weld passes. One of these submerged-arc welding schedules included the use of the MIG short-arc welding process to prepare the root pass welds. With the short-arc process, argon and carbon-dioxide mixtures were used to shield the weld.

Welding conditions used to prepare submerged-arc welds show the potential advantages of this process for welding plate. Only a few weld passes were required compared with the TIG welding, and high welding speeds were used. However, difficulties were encountered in the initial submerged-arc welding studies that were performed at Aerojet and, as a result, extensive studies were not performed on submerged-arc welds during this program.

Approved for Public Release

Contrails

b. Weld Inspection

Various methods used to determine the quality of completed weldments included visual and radiographic examinations and dye-penetrant, magnetic-particle, and ultrasonic inspections. Except for the magnetic-particle inspection, all inspection techniques were readily adapted to the 18% nickel maraging steel weldments. During the establishment of TIG welding schedules when defective welds were produced in the early phases of the program, ultrasonic inspection techniques were not used. However, in later phases of the program both ultrasonic and x-ray inspection techniques were employed and when defects such as weld porosity were encountered, both techniques indicated the presence of these defects. Interpretation of magnetic-particle inspections was complicated by the presence of a zone alongside the weld-fusion-zone, where austenite reversion apparently occurred during welding. The presence of this zone resulted in a buildup of particles along the weld bead that could mask small heat-affected zone defects. Because of this effect, carful interpretation is necessary to successfully adapt magnetic-particle inspection to weldments in 18% nickel maraging steel plate.

c. Weld-Cracking Susceptibility

Weld-restraint tests were planned in the program to evaluate the susceptibility to cracking of weldments in 18% nickel maraging steel plate. To carry out these tests, a U-bar fixture shown in Figure 49 was designed to measure the general weld-restraint level at which cracking would occur in the weld and heat-affected zone of 18% nickel maraging steel weldments. Originally, these tests were predicted on the expectation that weld cracking would be encountered when the 18% nickel maraging steel plate was fusion-welded. The intent of these tests was to evaluate the effects of different base-plate and weld wire compositions on weld-cracking sensitivity. However, weld cracking did not occur in any of the weld samples produced, and the weld-restraint tests did not appear to be necessary. Because of the lack of weld-cracking problems, weld-restraint testing of the 18% nickel maraging steels in general and specifically the use of the U-bar fixture was discussed with Professor M. E. Adams of the Massachusetts Institute of Technology, who developed the test and who is a recognized authority in the field of welding. Professor Adams generally agreed that the results obtained using the U-bar restraint test would be of marginal value. He also agreed that weld-restraint tests made in the evaluation of 18% nickel maraging steels probably would be of little value since weld cracking has not been a problem in the processing of these materials. Based on these discussions and on the results of extensive studies made both at Aerojet-General and by other investigators which have indicated that weld cracking is not a problem with the 18% nickel steels, the ASD Contracting Officer approved that further efforts on weld-restraint testing be eliminated from this program. Consequently, the efforts that had been planned for restrained-weld tests were diverted to additional wrought plate evaluations and to fracture toughness tests of welded joints.

The conclusion that weld cracking was not a serious problem was verified during a program in which two 36-in.-dia pressure vessels were fabricated at the Sun Shipbuilding and Drydock Corporation, Chester,

Approved for Public Release

Contrails

Pennsylvania under subcontract to Aerojet-General. These pressure vessels were fabricated from 0.6-in.-thick, Grade 250, 18% nickel maraging steel plate and contained many TIG welded joints that had been made under conditions of high weld restraint. Weld cracking was not encountered in preparing any of the welded joints in these vessels. The lack of weld cracking during the fabrication of these chambers provided evidence even more significant than the planned restraint tests that weld cracking was not a problem in welding 18% nickel maraging steel plate.

d. Tensile Properties of Weldments in 18% Nickel Maraging Steel Plate

Two types of weld-joint tensile specimens were used to evaluate the tensile properties of weldments as shown in Figure 50. The transverse tensile-specimens were used to determine the ultimate tensile strength and location of tensile fractures in weld-joint specimens. Yield strength, elongation, and reduction-of-area measurements were made on the transverse tensile-specimens, but these data must be interpreted cautiously because transverse-weld tensile-specimens vary in thermal history and composition along the specimen gage length due to the presence of the welded joint. The longitudinal tensile specimens were prepared to determine the yield strength and ductility of the weld metals. The combined data from transverse and longitudinal tensile specimens provided a good evaluation of the tensile properties of the weldments.

Notched tensile specimens (K_t = 10) also were used to evaluate weld metals. The notched tensile specimens were prepared as transverse tensile specimens with the notch located in the weld metal.

(1) Effects of Filler Wire Composition

It was shown in the parent metal evaluation that the effects of composition on the tensile and fracture toughness properties of 18% nickel maraging wrought steel plate overshadowed the effects of practically all other variables investigated. Because of the important effects of base metal composition, the effects of filler wire composition on weldability and the tensile and fracture toughness properties of weldments were evaluated. As part of these studies, seven filler wires were used to prepare welds in 1/2-in.-thick, Grade 250 air melted, vacuum-degassed maraging steel plate (heat 120D163) to study the effects of filler wire composition on the properties of weldments. One of the seven filler wires also was used to weld Grade 200, 1/2-in.-thick plate (heat 10675).

The compositions of all of the seven filler wires investigated are listed in Table 22. This table indicates that these filler wires had low carbon, manganese, phosphorous, silicon, and aluminum content as required for 18% nickel maraging steel base metals and filler wires. The nickel content of all the filler wires was comparable, ranging in values from 17.7% to 18.5%.

The most significant differences in composition between the filler wires were the titanium, molybdenum, and cobalt content.

Approved for Public Release

Contrails

As described earlier during the parent metal plate evaluation, the tensile properties of wrought 18% nickel maraging steel plate can be related to the amounts of these elements that are present, and small variations in these elements were found to cause significant changes in the tensile properties of wrought plate. The following ranges in alloy content were present in the filler wires that were investigated.

Titanium	- 0.42 to 1.65%
Molybdenum	- 4.0 to 5.1%
Cobalt	- 7.9 to 12.1%

(a) TIG-Welded Joints

A series of weldments was prepared to evaluate the effects of filler wire composition on the tensile properties of TIG-welded joints. The weldments were prepared with the seven filler wires listed in Table 22 and with the welding conditions and joint configurations shown in steel plate (heat 120D163). The welded joints were evaluated after aging at 900°F for 4 hr. This aging treatment was selected because it is commonly used for heat-treating 18% nickel maraging steel plate and one aging treatment was sufficient to evaluate the effects of filler wire chemistry. Subsequently, aging response studies using a selected filler wire composition were conducted to determine the effects of aging times and temperature on the tensile properties of the weldment.

The average cobalt, molybdenum, and titanium content of the weld metals, obtained when seven filler wires were used to prepare TIG weldments in Grade 250 material (heat 120D163), are listed in Table 23. The alloy contents of the welding filler wires and base metals also are included for comparison. The cobalt, molybdenum, and titanium content of the weld metals varied over a smaller range than that of the filler wires due to dilution with the base metal and losses in welding as indicated in the following tabulation:

	Range in Composition (%)	
	Filler Wire	Weld Metal
Titanium	0.42 - 1.65	0.41 - 0.94
Molybdenum	4.0 - 5.1	4.2 - 4.9
Cobalt	7.9 - 12.1	7.2 - 9.1

Relationships between the composition of the filler wire and the weld metal were compared to determine the extent of alloying element transfer from the filler wire to the weld deposit. For this evaluation, a dilution of 30% - base metal - 70% filler wire was assumed to be representative of the average dilution that occurred, although the dilution varied from the root of the weld to the final passes. Assuming a dilution of 30%, a theoretical value for weld metal alloy content was calculated. These calculated values compared with the actual analytical results as shown on the following page.

Approved for Public Release

Contrails

Filler Wire Heat	Weld Metal Alloy Content (Wt %) Cobalt Calculated	Cobalt Actual	Cobalt Loss or Gain	Molybdenum Calculated	Molybdenum Actual	Molybdenum Loss or Gain	Titanium Calculated	Titanium Actual	Titanium Loss or Gain
7C-092	7.2	6.8	-0.4	5.0	4.9	-0.1	0.81	0.80	-0.01
7C-091	8.2	7.2	-1.0	4.3	4.5	+0.2	1.3	0.94	-0.36
7C-094	9.3	8.8	-0.5	4.7	4.3	-0.4	0.99	0.81	-0.18
7C-093	8.0	8.2	+0.2	4.8	4.6	-0.2	0.60	0.64	+0.04
7C-090	10.8	9.1	-1.7	4.3	4.2	+0.1	0.73	0.65	-0.08
34312	7.9	7.8	-0.1	4.6	4.5	+0.1	0.56	0.57	+0.01
IW450	8.2	8.3	+0.1	4.6	4.3	-0.3	0.43	0.41	-0.02

Molybdenum is easily transferred across an arc and the calculated and actual molybdenum contents of the weld metals were comparable with the exception of filler wire 7C-094. Some loss in cobalt and titanium content was noted. The loss in titanium content was most pronounced when high titanium contents (greater than 1%) were present in the filler wires (7C-091 and 7C-094). Part of this titanium content loss may be accounted for by the presence of a glassy slag that was found intermittently along the weld bead. A semiquantiative analysis of this slag deposit showed that it was high in titanium content with about 10% iron and 10% aluminum and low in cobalt ($<0.1\%$) and nickel (0.2%).

To establish a method for rating the filler wires based on composition, the relationship that was developed between the yield strength and the composition of wrought plate was used to calculate the potential yield strength of the weld metals. This relationship is Yield Strength (Ksi) = 38.1 + 8.8 (% Co) + 22.6 (% Mo) + 87.7 (% Ti). The filler wires and the calculated potential yield strengths of the weld metals are listed below in order of decreasing yield strength.

Filler Wire	Potential Yield Strength of Weld Metal* (ksi)
7C-092	288
7C-091	286
7C-094	283
7C-093	270
7C-090	270
34312	258
IW-450	244

*Based on the composition of the weld deposit (Table 23)

Approved for Public Release

Contrails

The transverse tensile properties of the series of weldments (aged 900°F/4 hr) are listed in Table 24 and are shown in Figure 51 with the longitudinal and transverse tensile properties of the as-received (as-rolled) and aged (900°F for 4 hr) base-metal plate (heat 120D163) for comparison. The tensile results are summarized as:

Filler Wire Heat	Potential Weld Metal Yield Strength (ksi)	Weld Deposit Ultimate Tensile Strength (ksi)	Location of Failure
7C-092	288	251	WM, HAZ
7C-091	286	256	WM, HAZ
7C-094	283	253	WM, HAZ
7C-093	270	247	WM, HAZ
7C-090	270	258	WM, HAZ
34312	258	236	WM
IW450	244	240	WM

The transverse tensile properties of the welded joints varied with the composition of the weld metals. Tensile specimens prepared from welded joints in which the weld metals had the highest potential strengths failed in both the weld heat-affected and fusion-zones. The ultimate tensile strength of these weld metals was comparable to or exceeded that of the weld heat-affected zones and ranged from 0-11 ksi less than that of the base metal. Tensile specimens prepared from welded joints in which the weld metals had the lowest potential strengths failed in the weld metal with ultimate tensile strengths 18-24 ksi lower than that of the base metal. Typical examples of heat-affected zone and weld metal failures are shown in Figure 52. The ultimate tensile strengths of these weld metals were less than expected on the basis of weld-metal composition in that they failed at stresses less than the calculated yield strength of the weld metal. Also, the weld metal obtained with filler wire 34312 had a lower ultimate tensile strength than that obtained with filler wire IW-450, even though the latter weld metal had the lowest alloy content rating based on potential strength.

Notched-tensile tests (K_t=10) also were conducted on the series of TIG-welded joints to study the notch tensile properties of weld metals deposited by the seven filler wires. These tests were conducted to screen and select filler wires for additional evaluations.

The notched-tensile strength and ratio of notched-to-unnotched-tensile strengths of the weld metals are shown in Table 25 and Figure 53. This table also includes the ultimate tensile strengths of transverse tensile specimens prepared with the same filler metals, the location of tensile failures, and the notched-tensile strength of the base metal after solution-annealing at 1500°F for 30 min and aging at 900°F for 4 hr. The ultimate tensile strength of the welded joint was used to calculate the ratio of notched-to-unnotched-tensile strengths. This ratio is not completely valid for the tensile specimens that failed in the heat-affected zones because the

Approved for Public Release

Contrails

specimens were notched in the weld metal. However, the ratios were satisfactory for defining the trends that were observed.

The notched-tensile strength data in Table 25 are summarized below to show the important trends that were observed:

Filler Wire Heat	Notched Tensile Strength (ksi)	Ultimate Tensile Strength (ksi)	Location of Failure	Notched-to-Unnotched Ratio
7C-092	245	251	WM, HAZ	0.98
7C-091	185	256	WM, HAZ	0.72
7C-094	231	253	WM, HAZ	0.91
7C-093	298	247	WM, HAZ	1.2
7C-090	229	258	WM, HAZ	0.89
34312	333	236	WM	1.4
IW-450	380	240	WM	1.6
Base Metal	361	258	--	1.4

As shown in the tabulation, the notched-to-unnotched ratio varied inversely with the alloy content as rated on the basis of potential weld-metal yield strength. In the joints in which the tensile strength of the weld metals were comparable to or exceeded that of the heat-affected zones, notched-to-unnotched-tensile strength ratios were less than 1.0 with only one exception. The weld metals with ratios less than 1.0 are considered to be notch-sensitive. With the lower strength weld metals, notched-to-unnotched ratios of over 1.4 were observed, while the notched tensile strength of the weld metal obtained with IW-450 filler wire exceeded that of the base metal.

Based on the unnotched-tensile properties and on the notched-tensile tests, the high strength filler wire 7C-093 and the low strength filler wire IW450 were selected for additional evaluation. Filler wire 7C-093 was considered applicable for welding Grade 250 plate and filler wire IW-450 appeared the best of the wires evaluated for the welding of Grade 200 plate. Longitudinal tensile tests were conducted to evaluate the tensile properties of weld metals prepared with the two selected filler wires. The longitudinal tensile specimens were prepared from TIG weldments in Grade 250, 1/2-in.-thick plate (heat 120D163) made with the same joint configuration and conditions that were used to prepare weldments for the transverse tensile tests. The tensile specimens were aged at 900°F for 4 hr after welding. The longitudinal tensile properties of the weld metals are listed in Table 26 and are summarized as:

Filler Wire Heat	0.2% Offset Yield Strength (ksi)	Ultimate Tensile Strength (ksi)	Elongation in 1 In. (%)	Reduction of Area (%)
7C-093	229	248	7.7	33
IW-450	222	235	10.7	45

Approved for Public Release

Contrails

As shown above, the longitudinal tensile strength of weld metal specimens obtained with filler wire 7C-093 exceeded that of weld-metal specimens obtained with IW-450 filler wire, which was expected, and the ultimate tensile strengths obtained with the longitudinal specimens were comparable to those obtained from transverse specimens. However, the differences in tensile properties between the two weld metals were less than the expected based on the potential weld-metal yield strength.

Longitudinal tensile test results obtained with filler metal IW-450 indicated that this filler wire was very promising for welding Grade 200, 18% nickel maraging steel plate. To verify this observation, the IW-450 filler metal was used to weld 1/2-in.-thick, Grade 200, 18% nickel maraging steel plate (heat 10675). The longitudinal tensile properties of these weldments were evaluated after aging at 900°F for 4 and 8 hr. The results of the longitudinal tensile tests are listed in Table 27 and are summarized as:

Filler Wire Heat	Aging Cycle (°F-hr)	0.2% Offset Yield Strength (ksi)	Ultimate Tensile Strength (ksi)	Elongation in 1 In. (%)	Reduction of Area (%)
IW-450	900-4	212	225	12.1	58.1
IW-450	900-8	223	235	11.4	55.8

These data show that the weld metal tensile properties obtained in welding Grade 200 plate (heat 10675) with IW-450 filler wire after aging at 900°F for 4 hr were 10 ksi lower than those of weld metals deposited with the same filler wire in Grade 250 (heat 120D163) plate material and aged using the same treatment. Comparisons between the compositions and tensile properties of weld metals in the two base metals provide additional information regarding the effects of composition on the tensile properties of the weld metals as indicated by the following data:

Filler Wire Heat	Base Metal	Weld Metal Alloy Content (wt %)			Potential Weld Metal Yield Strength (ksi)	Actual 0.2% Offset Yield Strength (ksi)
		Co	Mo	Ti		
IW-450	120D163	8.3	4.3	0.41	244	222
IW-450	10675	8.1	3.4	0.42	223	212

The weld metal compositions differed primarily in molybdenum content and correlated with the alloy content of the base metals as shown in the following data:

Base Metal	Alloy Content (wt %)		
	Co	Mo	Ti
120D163	8.0	4.9	0.48
10675	8.5	3.2	0.42

Approved for Public Release

Contrails

(b) MIG-Welded Joints

Welds also were prepared to evaluate the tensile properties of MIG-welded joints in Grade 250, 1/2-in.-thick 18% nickel maraging steel plate (heat 120D163). The weld metal composition and transverse tensile properties of MIG welds made with 7C-094 and 7C-093 filler wires after aging at 900°F for 4 hr are listed in Tables 28 and 29, respectively. Also included for comparison purposes are the compositions and tensile properties of comparable TIG welds.

The data presented in Tables 28 and 29 are summarized below:

Filler Wire Heat	Weld Metal Alloy Content (wt %) Co	Mo	Ti	Ultimate Tensile Strength (ksi)	Failure Location
			MIG Welds		
7C-094	8.7	4.4	0.60	267	WM
7C-093	8.0	4.3	0.63	249	WM
			TIG Welds		
7C-094	8.8	4.3	0.81	253	WM, HAZ
7C-093	8.2	4.6	0.64	247	WM, HAZ

These data show that the ultimate tensile strength of the MIG and TIG weldments were comparable. Also, the MIG weld-metal composition obtained with filler wire 7C-093 was comparable to that of TIG-welded joints. However, the titanium content of the MIG weld metal obtained with filler wire 7C-094 was significantly lower than that of TIG-welded joints, which indicated that a considerable amount of titanium was lost during transfer across the arc. The titanium content of filler wires 7C-094 and 7C-093 were 1.22 and 0.67%, respectively, but the titanium content of the MIG weld metals obtained with these filler wires were comparable, thus indicating that a pronounced amount of titanium was lost in the high titanium-content filler wire. This same trend also occurred in TIG welds. However, when these MIG welds were made, weld porosity was a major problem in preparing MIG-welded joints, and it is possible that the loss of titanium experienced with filler wire 7C-094 was the result of the weld porosity problems that were encountered at that time.

(c) Submerged-Arc Welded Joints

A number of submerged-arc welded joints were evaluated during the program. Many of these welds were prepared using an available commercial welding flux (L709-5). The tensile test results obtained from these initial weldments were inconsistent and exhibited extremely low elongation and reduction-of-area values. As the program progressed, major advances were made in flux development for submerged-arc welding of 18% nickel maraging steel; consequently, the initial evaluations in this program are not considered to be representative of the welds that could be made with the submerged-arc welding process.

Approved for Public Release

Contrails

In 1963, the Linde Corporation used the submerged-arc welding process to weld Grade-250, 1/2-in.-thick, 18% nickel maraging steel plate (heat 120D163) with 7C-090 filler wire for evaluation during this program. These welds were made with an advanced welding flux composition developed for maraging steel.

The weld-metal compositions and tensile properties of the submerged-arc welded joints, which were prepared by Linde and aged at 900°F for 4 hr after welding, are listed in Tables 30 and 31, respectively. The tensile properties and weld-metal compositions of comparable TIG-welded joints also have been included for comparison.

The weld-metal compositions obtained with the submerged-arc process differed from those obtained in making TIG welds primarily in titanium content. Beginning with a titanium content of 0.83% in the filler wire, the submerged-arc weld metals contained 0.33 to 0.40% titanium. In contrast, the TIG weld metal contained 0.65% titanium, which indicated that a significant amount of titanium was lost during welding with the submerged-arc process. Also, a slight increase in silicon content was found in the submerged-arc weldments: from 0.017% in the weld filler-wire to 0.06 to 0.11% silicon in the weld metals. However, this increase in silicon content is not considered to be significant.

The loss of titanium in submerged-arc welding, was not reflected by the transverse tensile properties of the welded joints. In fact, the average ultimate tensile strengths of the submerged-arc welds ranged from 256 to 262 ksi compared with an average ultimate tensile strength of 258 ksi for comparable TIG welds. The reduction-of-area values for submerged-arc welds (7.7-20.5%) were lower than those of TIG-welded joints (25%).

Comparison between submerged-arc and TIG weldments also indicated that variations in welding heat input did not affect the ultimate tensile strength of weldments in 18% nickel maraging steel plate. The TIG weldments were prepared with welding heat inputs ranging from 15,000 to 18,000 joules/in. compared with heat inputs of 21,000 to 46,000 joules/in. for submerged-arc weldments. Despite this difference in heat input, the ultimate tensile strengths of weldments made with the two processes were comparable.

A complete evaluation of submerged-arc welded joints was not performed during the program. Additional tensile tests and fracture toughness tests would be required to evaluate this process fully for the welding of 18% nickel maraging steel plate.

(2) Aging Response

Tests also were conducted during the program to study the aging response of welded joints. A complete aging response curve was established for TIG weldments prepared with filler wire 7C-093 in Grade 250 plate (heat 120D163). This filler wire was selected because it provided the best combination of tensile weld-joint strength and notched-tensile strength for welding this grade of material. The aging response evaluation of the weldments was based on transverse tensile specimens that failed in the weld metal, thus showing the effects of aging temperature and time on the ultimate

Approved for Public Release

Contrails

tensile strength of the weld metals. The aging response data are presented in Table 32 and Figure 54. The results from the aging response tests are summarized below:

Aging Cycle (°F-hr)	Ultimate Tensile Strength (ksi)	
	Weld Metal	Base Metal*
850- 4	234	256
850- 8	246	264
850-16	254	273
900- 2	247	255
900- 4	250	258
900- 8	251	268
900-16	252	270
950- 2	248	264
950- 4	241	266
950- 8	245	255
950-16	242	255

* Base material as rolled and aged.

This tabulation indicates that the general relationships that were established between weld-metal tensile strength and aging temperatures and time were similar to those of the base metal. At 850°F and 900°F. the tensile strength of the weld metal and base metal increased as the aging time increased and indicated that overaging did not occur. At 950°F, some overaging was evident in both the weld metal and base metal, but the effects of overaging were not great. Similar relationships between aging time and temperature also were observed when the yield strengths of the base metal and the weld joint were compared. However, the yield strength values obtained for the welded joint do not represent the actual 0.2% offset yield strength of the weld metal.

Similar trends between the aging response of weld metals and base metals also were observed in comparisons between the base metal and longitudinal weld metal tensile properties obtained after welding Grade 200 plate (heat 10675) with IW-450 filler wire. These tensile properties are listed in Table 27 and are summarized below:

	Aging Cycle (°F-hr)	0.2% Offset Yield Strength (ksi)	Ultimate Tensile Strength (ksi)	Elongation in 1 In. (%)	Reduction of Area (%)
Weld Metal	900-4	212	225	12.1	58.1
	900-8	223	235	11.4	55.8
Base Metal	900-4	218	226	11.0	57.2
	900-8	226	235	10.7	50.9

Approved for Public Release

Contrails

The data on the preceding page show that the tensile properties of the weld metal and base metal were essentially the same after the same aging cycles.

The aging response tests show that the aging response of welded joints in 18% nickel maraging steel plate is compatible with that of the base metal. Thus, unwelded plate and weldments may be aged simultaneously with similar strengthening effects; localized and special aging treatments are not necessary to obtain the desired match between the tensile properties of the plate and weldments.

(3) Effects of Heat-Treating Sequence

All data concerning the tensile properties of welded joints presented thus far were obtained by welding plate material in the as-rolled or mill-annealed condition and aging after welding without intermediate solution annealing. This heat-treating sequence was evaluated because it was considered to be practical for large-diameter rocket-motor cases.

Another heat-treating sequence, however, that might be used in the fabrication of large-diameter rocket-motor cases is one in which the plates are aged prior to welding and the welded joints are aged locally after welding is completed. With this procedure, the plates would be subjected to two aging treatments and weld heat-affected zones would be located in previously aged material. The base metal aging response tests showed that the extra 4 hr required for the double aging treatment of the base metal did not seriously reduce base metal tensile strength at aging temperatures of 900°F. Therefore, weldments were prepared to evaluate the tensile properties of weldments made in plates that were aged in this manner prior to welding and then aged again after welding was completed.

A third heat-treating sequence that possibly might apply to the fabrication of large-diameter rocket-motor cases is the process of solution-annealing and aging after welding. This treatment would eliminate overaging in the weldment and provide a more uniform thermal history for the weldments. This heat-treating sequence also was evaluated.

The effects of heat-treating sequence on the tensile properties to TIG weldments in Grade 250, 1/2-in.-thick maraging steel plate (heat 120D163) made with filler wire 7C-093 are shown by the data in Table 33. These data are summarized on the following page.

In the comparison of the two sequences in which only aging treatments were used after welding, the ultimate tensile strength of transverse tensile specimens is most significant because the weld metals have undergone the same thermal cycles while the heat-affected zones have different thermal histories. Based on data from the transverse specimens, welding of aged material did not decrease the weld-joint strength. This would be expected if a significant amount of overaging occurred in the heat-affected zone. Consequently, it appears that the base metals may be aged before welding and the joints aged after welding, or the base metals may be annealed before welding and the weldments aged after welding to obtain comparable tensile properties. However, many of the transverse tensile specimens failed in the weld metal and additional tests with predominating heat-affected zone failures are needed to verify this observation. Also, fracture toughness tests of weld

Approved for Public Release

Contrails

Heat-Treating Sequence	Longitudinal Weld Tensile Properties				Transverse Weld Tensile Properties
	0.2% Offset Yield Strength (ksi)	Ultimate Tensile Strength (ksi)	Elongation in 1 In. (%)	Reduction of Area (%)	Ultimate Tensile Strength (ksi)
Base metal aged aged at (900°F) for 4 hr before welding, and weldments aged at 900°F for 4 hr.	239	253	6.2	34	255
Base metal as rolled prior to welding, and weldment aged at 900°F for 4 hr.	229	248	7.7	33	247
Weldment solution-annealed at 1500°F for 1/2 hr and aged at 900°F for 4 hr.	226	243	8.5	38.2	247
Base metal as rolled and aged at 900°F for 4 hr.	244	258	9.3	42.3	258

heat-affected zones would be required to fully evaluate welding and heat-treating sequences. When the weldments were solution-annealed and aged after welding, the weld-metal elongation and reduction-of-area properties improved somewhat and these improvements were accompanied by a small reduction in weld tensile strength, although the improved elongation and reduction-of-area does not appear sufficient to justify the solution-annealing treatment of welded joint.

Approved for Public Release

Contrails

e. Fracture Toughness Properties of Weldments in 18% Nickel Maraging Steel Plates

Fracture toughness was considered to be an important criteria in evaluating weldments in the 18% nickel maraging steel alloy. Consequently, for screening purposes, the precracked-Charpy-impact fracture toughness (W/A) of weldments in a Grade 200 selected alloy was evaluated. The specimens were notched through the thickness of the weld (Figure 50) to evaluate the fracture toughness of the weld metal and weld heat-affected zones. The individual fracture toughness specimens were etched with Marble's Reagent before notching to define the weld metal and heat-affected zones and to locate the positions for machining the notches.

The notches were located in two positions to evaluate the fracture toughness of the weld heat-affected zones. One notch location extended slightly into the weld-fusion-zone of the specimen as Figure 55 indicates. With this location, the notches extended from the fusion zone through high and low temperature portions of the heat-affected zones, and the second notch location extended from the center of the heat-affected zone at the face of the weld into the parent metalaat the root of the weld, which was practically unaffected by the welding. Because the notches in the weld heat-affected zone could not be located to conform exactly to any one thermal cycle, the values obtained for weld heat-affected zones represent a composite of weld metal, high and low temperature heat-affected zones and unaffected base metal. Therefore, these evaluations were not made to obtain an absolute value for fracture toughness of weld heat-affected zones, but were used to compare the fracture toughness of heat-affected zones with the unaffected wrought plate.

TIG weldments were prepared in Grade 200, 1/2-in.-thick, 18% nickel maraging steel plate (heat 10675) to evaluate the fracture toughness of weldments. These weldments were prepared with IW 450 filler wire, which was shown by the tensile properties to be well suited to this base plate. The room-temperature precracked-Charpy-impact fracture toughness of these weldments is listed in Table 34 and summarized below:

		Aging Cycle			
		900°F for 4 hr		900°F for 8 hr	
Filler Wire and Base Metal	Notch Location	0.2% Offset Yield Strength (ksi)	W/A (in.-lb/in.^{2})	0.2% Offset Yield Strength (ksi)	W/A (in.-lb/in.^{2})
IW 450	Weld Metal	212	1109	223	953
	HAZ-1	-	1177	-	1116
	HAZ-2	-	1240	-	996
Heat 10675	Longitudinal	218	1225	226	1002
	Transverse	214	1060	228	830

Approved for Public Release

Contrails

As indicated by this summary, the fracture toughness (W/A) of the weldments was comparable to that of the base metal and varied with aging time in the same manner as the base metal. The fracture toughness of weld metal and heat-affected zones exceeded that of the base metal in the transverse orientation for all aging conditions and was almost equal to that of the base metal in the longitudinal orientation. Also, the fracture toughness of the weldments and base metals were lower after aging for 8 hr than aging for 4 hr. This variation in toughness with aging time may be associated with the increase in strength that accompanied the longer aging time.

f. Metallurgical Characteristics of Weldments in 18% Nickel Maraging Steel Plate

Metallographic examinations and microhardness tests were conducted to evaluate the metallurgical characteristics of welded joints in 18% nickel maraging steel plate and to study the effects of multiple-weld thermal cycles on the grain size and aging response of weld metals and weld heat-affected zones. For the metallographic examinations, step-welds were prepared to isolate the effects of multiple thermal cycles on weld-joint microstructures. The step-weld technique is illustrated in Figure 56. When step-weld specimens were prepared, the root pass was deposited the full length of the weld test-plate. The second weld pass was started about 1 in. from the starting end of the first weld pass and was continued to the end of the plate. The third weld pass was started about 1 in. from the start of the second weld pass and was continued to the end of the plate. This same procedure was followed with each weld pass until all passes were completed.

The step-weld specimens then were sectioned to show the cross section of the welded joint at various stages of completion. By Examining these cross sections, each weld pass could be studied as it was deposited and after subsequent weld passes were made. These examinations were used to study the microstructure, grain size, and hardness of weld metal and weld heat-affected zones.

(1) Microstructure

The microstructure of welded joints in 18% nickel maraging steel was characterized by martensitic structures and by dendritic structures which were present in the weld-fusion-zones. Typical photomicrographs illustrating the martensitic structures and dendritic patterns are shown in Figures 57 and 58. Presence of the dendritic structures in the weld-fusion-zones is evidence of the freezing segregation that occurred in these zones when the weld metals solidified.

Based on phase diagrams (Fe-Ni, Fe-Mo, Fe-Co, and Fe-Ti) the dendrites should contain a lower alloy content than the average composition of the weld-fusion-zone. Similarly, the interdendritic material should contain a higher alloy content than the average composition of the weld metal. In addition, an interdendritic phase was observed which had the appearance of retained austenite. This phase is more clearly defined in Figure 59, which was deeply etched and photographed at a high

Approved for Public Release

Contrails

magnification to emphasize the interdendritic phase. Only a small amount of nickel segregation is required to cause austenite stabilization in 18% nickel maraging steel weldments. This interdendritic phase also may contain greater amounts of cobalt, molybdenum, and titanium in comparison to the surrounding matrix.

Alloy segregation undoubtedly affects the tensile and fracture toughness properties of the weld metal. The evaluating weld metals, the tensile properties were lower than expected on the basis of composition. Segregation of the hardening elements to the interdendritic phase might be responsible for these reduced tensile properties.

(a) Effects of Multiple-Weld Thermal Cycles

Figures 60 through 64 show a series of step-weld cross sections in 18% nickel maraging steel plate. These cross sections were examined in the as-welded condition to emphasize the temperature distribution as a result of the various weld passes. Each figure contains a photomacrograph showing the complete cross section and one or more photomicrographs showing the weld-metal structures at various positions in the joint.

The photomacrographs showing the entire weld cross sections indicate the thermal cycles that the weld zones undergo. In each of these cross sections, the high temperature zone of the last weld pass is evident as a light etching area that surrounds the weld-metal deposited during the last weld pass. The darker etching area adjacent to the light etching area is the low temperature area of the weld heat-affected zone. Figures 60, 61, and 62 show that the high temperature zone extends to the bottom surface of the plate through the fifth weld pass. In making the sixth weld pass, however, (Figure 63) the temperature distribution in the joint changes significantly and the high temperature zone extends only a short distance below the bottom edge of the fusion-zone, although the remainder of the joint was subjected to a low temperature cycle that caused the structure to etch darker than before.

The photomicrographs show the effects of the weld thermal cycles on weld joint microstructures. Either in the as-deposited condition or when subjected only to high temperature thermal cycles, the dendritic structure of the weld metals is not readily apparent, and no evidence of the dendritic structure is seen in Figures 60, 61, and 62. After the sixth weld pass was completed (Figure 63), however, the appearance of weld metal subjected to the low temperature thermal cycle changed and the dendritic structure of the weld metal became evident. This effect also is shown in the completed weld shown in Figure 64, where the dendritic structure is clearly evident in the weld metal that was subjected only to high temperature thermal cycles. The appearance of the dendritic structure after the low temperature thermal cycle is believed to be evidence of aging that occurs during the welding operation.

All of the specimens described thus far were prepared with Marbles etchant to emphasize the martensitic and dendritic structure of the weld zones. A 10% chromic acid electrolytic etch also was used to study the effects of weld thermal cycles on the austenitic grain size of weld metals and weld heat-affected zones.

Approved for Public Release

Contrails

Variations in the austenitic grain size of weld metal and weld heat-affected zones are shown in the step-weld cross sections in Figures 65 to 67. In the weld cross section with only one weld pass, the weld metal had a large prior austenitic grain size and dendritic segregation also was evident. In the weld cross section containing three weld passes, the prior-austenitic grains in the first weld pass were refined and equiaxed, but the third weld pass had the characteristic columnar structure of the as-deposited weld pass. In the complete weld shown in Figure 67, the last weld pass has the characteristic columnar as-deposited structure, whereas the weld metals that were subjected to both high- and low-temperature thermal cycles have refined, equiaxed, prior-austenitic grains and show evidence of a dendritic structure.

The heat-affected zone structures show less change due to multiple thermal cycles than the weld metals as shown in Figures 65, 66, and 68. These figures show that the heat-affected zone grain becomes coarser from grain sizes of 7-8 in the parent metal to a size of about 4-5 adjacent to the weld-fusion-zone, but that this coarser grain extended only a short distance from the weld-fusion-zone.

(b) Effects of High Temperature Solution-Annealing Treatments

Several weld sections were solution-annealed at high temperatures to determine the effects of these treatments on alloy segregation in the weld-fusion-zones. The solution-annealing treatments were performed on the step-welds described earlier. These step-weld specimens were heated to temperatures of 1600, 1800, and 2000°F, held for 1 hr, air-cooled to room temperature and aged at 900°F for 4 hr. A 10% chromic acid electrolytic etch was used to show base metal grain size, and Marbles etch was used to show the dendritic structure of the weld-fusion-zone. As seen in Figure 69, little change in general micro-structure and grain size (grain size of 7-8) occurred with the 1600°F treatment. After the 1800°F treatment, the grain size grew slightly (grain size 7) in the base metal but the dendritic structure of the weld metal was still apparent. After 2000°F treatment, grain growth in the base metal (grain size 2) was extensive and the dendritic structure was less readily apparent than for the other treatments. The results of these treatments indicate that very high-temperature solution-annealing treatments are required to effect a change in alloy segregation in weld-fusion-zones, and that these treatments may cause excessive grain growth in the adjacent base metal. Although these treatments are not considered practical for the heat-treatment of welded structures, they may facilitate study of the effects of alloy segregation on weld-metal tensile and fracture toughness properties.

(2) Hardness

Microhardness test results for step-welds made in 18% nickel maraging steel plate are shown in Figures 70 to 79. During these hardness tests, readings were taken through the weld metal and heat-affected zones at the root of the weld to study the effects of subsequent weld thermal cycles on hardness. More extensive tests were made in completed welds to determine the hardness distribution. Knoop hardness measurements were made with a 500 kg load and converted to R_c values for these figures.

Approved for Public Release

Contrails

Figures 70 and 75 show hardness variations in the as-welded joints. Although the hardness values were scattered considerably, several trends were observed. In the as-welded joints which contained one, three and five weld-passes, the weld-metal hardness values of the as-deposited last weld pass were similar to those found at the root of the weld. Such similarities were found because these weld metals were subjected to high temperature thermal cycles---actually solution-annealing temperatures---with each weld pass. As the sixth weld pass was made (Figure 73) and in the completed weld (Figure 74), however, the weld metal hardness at the root of the weld was higher than that of the weld metal in the as-deposited weld pass. In these latter two weld cross sections, weld metal at the root of the weld was subjected to low temperature thermal cycles by subsequent weld passes, and the increased hardness in this area indicated that partial aging occurred during these low temperature thermal cycles.

Similar hardening due to partial aging also was observed in the heat-affected zones of the as-welded joints. Hardening was observed in the low temperature portions of the heat-affected zones at the root of the weld and as-deposited weld pass as shown in Figures 70, 71, and 72. However, in the weld cross section containing the sixth weld pass (Figure 73), and also in the completed weld (Figure 74), the complete heat-affected zone at the root of the weld was partially hardened. In both of these weld cross sections, the complete heat-affected zone had been subjected to low-temperature thermal cycles. These low-temperature thermal cycles were accompanied by partial age-hardening in the entire weld heat-affected zone at the root of the weld.

The effects of multiple-weld thermal cycles on the hardness of the completed, as-welded joint are shown in Figure 75. Areas of the joint having similar hardness values are outlined in the figure for clarity. In general, the hardness in the weld metal and high temperature heat-affected zones decreased from the bottom to the top of the joint as the result of the partial aging effects produced by successive low-temperature thermal cycles. On the other hand, the hardness of the low-temperature heat-affected zones located in the base metal was relatively constant through the thickness. Apparently the temperatures that were reached in these areas were low enough and the times at temperature were short enough to limit the affects of low-temperature thermal cycles that occurred in these areas, and the hardness was not affected significantly.

Hardness tests also were conducted on weldments aged at 900°F for 8 hr to determine if the aging that occurred during welding affected the hardness after aging. Results from weld-joint hardness tests after aging are shown in Figures 76 to 79. Variations in hardness that could be attributed to multiple-weld thermal cycles were less apparent after the joints were aged. However, two trends were observed. First, the hardness of the weld metal and heat-affected zones of the initial weld-pass were slightly lower than those of the last weld pass. The slight reduction in hardness in these areas indicates that some overaging or austenite reversion may have occurred during welding. Second, areas of slightly reduced hardness were observed in several of the heat-affected zones. This reduced hardness also may be due to overaging with or without austenite reversion that occurred during welding. Likewise, this slightly reduced hardness correlates with heat-affected zone failures in transverse-weld tension-tests.

Approved for Public Release

Contrails

3. Discussion

Considerable information was obtained regarding the weldability of 18% nickel maraging steel plate and the tensile and fracture toughness properties of weldments. This information and its relationship to the fabrication of large-diameter rocket-motor cases is discussed in this section of the report.

Extensive welding operations are required in the fabrication of large-diameter rocket-motor chambers. In such chambers, sound weldments capable of withstanding service conditions are necessary to assure reliable performance in the chambers. The success achieved in adapting welding operations to the fabrication of chambers depends on the welding characteristics of the materials that are used and the tensile and fracture toughness properties of the weldments.

The 18% nickel maraging steel plate was found to be readily adaptable to welding. Weld cracking problems were not encountered in welding 1/2 and 3/4-in.-thick plate, and preheating and postheating were not necessary. These desirable welding characteristics are attributed to the metallurgical characteristics of the alloy. When welded, these alloys are subjected to thermal cycles that effectively simulate solution-annealing treatments and the weldments are ductile in the as-welded condition. In addition, some zones of the weld are subjected to low-temperature thermal cycles that simulate aging treatments. However, the times at temperature are short in such zones and only a slight amount of age-hardening occurs.

Although the TIG, MIG, and submerged-arc welding processes were found to be adaptable to the fabrication of 18% nickel maraging steel plate, some precautions were required to obtain sound, high-strength weldments. With the inert-gas-processes, good shielding procedures were necessary to minimize porosity. If shielding was not adequate, oxide scale formed on the weld beads and had to be removed to prevent porosity in subsequent weld deposits. In all other respects, these welding processes were readily adapted to this material. With submerged-arc welding, fluxes that minimize silicon and hydrogen pickup were found to be necessary to obtain satisfactory weld ductility. Even with these precautions, however, weld ductility was slightly lower than with the inert-gas-shielded processes. With all processes, proper filler wire compositions were required to achieve the desired tensile and fracture toughness properties of the welded joints.

The aging response of the weldments was comparable to that of the wrought plate. With proper filler wire compositions, simple aging treatments at temperatures of 900-950°F for 4-8 hr may be used to age-harden the welded joints simultaneously with plate aging. On the basis of tensile properties it also appears possible to age-harden the plate prior to welding and to locally age the welded joint, although fracture toughness studies must be conducted to verify this approach. When the strength of the weld metals matched that of the base metal, the ultimate tensile strengths of weldments were only slightly lower than that of the base metal.

Weld-filler-wire composition was found to be an important welding variable. Through variations in filler wire composition, it was possible to match the tensile strength of weldments with that of Grade 200 and 250

Approved for Public Release

Contrails

plate material. The important strengthening elements in the weld-filler-wire were cobalt, molybdenum, and titanium. Slightly higher amounts of these elements than those of the wrought base metals were required in weld-filler-wires to achieve a given strength level. Otherwise the composition of the filler wires were essentially the same as those of the base metals.

The need for a slightly higher alloy content in the weld-filler-wires may be due to alloy segregation, which was observed in the weld-fusion-zones. Although the extent to which alloy segregation occurred was not determined, it is known that only a small amount of titanium, cobalt, and molybdenum segregation would reduce the tensile properties of the weldments. The slight overaging of areas of the weld deposit which were subjected to low-temperature (1100-1300°F) thermal cycles during welding also may account for some of the need for higher alloy content in weld-filler-wires. However, the effects of overaging were not great based on the high ultimate strength values achieved in transverse-weld tension tests.

The fracture toughness testing of weldments in the selected alloys was limited, but indicated that fracture toughness under impact loading approaching that of the base metal was possible in weldments of Grade 200 plate. On the basis of notched tensile tests (K_t=10), low fracture toughness would be expected in weldments that match the strength of Grade 250 plate.

The effects of multiple-weld thermal cycles on the microstructure of weldments were well defined. In the as-deposited condition, large columnar prior-austenite grains were present in weld-fusion-zones. When these grain structures were subjected to the high-temperature thermal cycles of subsequent weld passes, the grains were refined and equiaxed. Although these refined grains were coarser than the fine-grained wrought metals, they were considered to be much more desirable than the large columnar grains that were found in the original as-deposited weld bead. When extra weld passes or other special procedures are used in finishing welds, it should be possible to refine all weld passes that fall within the thickness of the plate.

Grain growth was found not to be a significant problem in weld heat-affected zones because such grain growth was limited and occurred over only an extremely narrow zone. It was not possible to relate this increased grain size to the tensile failures that were observed in the transverse tensile tests.

High-temperature solution-annealing treatments were investigated as a method for reducing alloy segregation in weld-fusion-zones. Post-welding solution-annealing of weld specimens at a temperature of 2000°F for 1 hr may have resulted in some homogenization of the weld metal, but excessive grain growth occurred in the adjacent base plate and the treatment was not considered practical for large rocket-motor cases.

The evaluation of the selected alloys provided a basis for evaluating the welding characteristics of the optimum alloy. On the basis of this evaluation, the TIG and MIG welding processes were selected in preference to submerged-arc welding to eliminate the need for an evaluation of fluxes. Also, three filler wires were selected. One of these was a Grade 200 filler wire for TIG welding and another was a Grade 200 filler wire with slightly higher titanium content for MIG welding. The third was a Grade 250 filler wire

Approved for Public Release

Contrails

for both TIG and MIG welding. The two Grade 200 filler wires were selected to provide maximum weld-metal fracture toughness. The Grade 250 filler wire was selected expressly to provide additional data concerning the relationship between the tensile strength and fracture toughness of weld metals. In addition, the heat-treating sequence in which the parent metal and welded joints are aged simultaneously was selected for the optimum alloy based on this study.

Approved for Public Release

Contrails

SECTION 4 - SELECTION AND EVALUATION OF OPTIMUM MATERIAL

The object of this phase of the investigation was to select and evaluate an "optimum" 18% nickel maraging steel that would provide the highest strength attainable consistent with good fracture toughness. This selection was based on the results of the selected alloy investigation which also provided the background needed to prepare a tentative material specification. The specification, which is presented in Appendix VI, was used to procure a heat of the optimum material which was evaluated after it had been received to determine its aging characteristics, quality and fracture toughness. This material was also employed in weldment tensile and fracture toughness evaluations.

A. ALLOY PREPARATION

1. Selection of Composition

Two major factors that were established during the evaluation of seven commercial heats were used to select the optimum material. These factors were the inverse relationship between strength and fracture toughness, and the importance of the hardening elements cobalt, titanium, and molybdenum in determining strength after aging. A yield strength of 235 ksi was selected as the highest strength that would provide the level of fracture toughness considered necessary for fabrication of rocket-motor cases.

A mathematical analysis of the effects of variation in chemical composition resulted in an expression to predict yield strength. This expression is:

$$0.2\%\ \text{Offset Yield Strength (ksi)} = 38.1 + 8.8\ (\%\ \text{Co}) + 22.6\ (\%\ \text{Mo}) + 87.7\ (\%\ \text{Ti})$$

According to this equation, the composition variations that may occur within the producer's ability to control alloy content could produce strength variations of at least 30 ksi within a nominal grade. This possible fluctuation of 30 ksi, coupled with an upper yield strength level of approximately 235 ksi based on fracture toughness, fixed the minimum yield strength at about 200 ksi. Further analysis showed that a nominal Grade 200 would not necessarily meet the strength requirements established for the optimum material. According to the equation developed through the regression analysis, the strength of a nominal Grade 200 composition could vary from 189 ksi to 218 ksi after aging at 900°F for 4 hr. The calculated lower limit of 189 ksi, however, was considered unsatisfactory and a new composition was selected using the equation from the regression analysis. A minimum yield strength of 208 ksi was selected as a starting point to allow for inaccuracies in the equation and to ensure that the minimum yield strength would not fall below 200 ksi. A final composition was selected to have a yield strength between 208 ksi and 232 ksi after aging at 900°F for 4 hr. This composition had a titanium range of 0.15 to 0.25%. However, the steel mills could not guarantee that the titanium content could be controlled within this narrow range; consequently, it was necessary to widen the titanium range to 0.05 to 0.25%. The final composition of the selected optimum material is listed in Table 35 and in Appendix VI.

Requests for the optimum alloy in 3/4-in.-thick plate and in 1-in. and 4-in.-thick ring forgings were forwarded to ten steel producers for

Approved for Public Release

Contrails

price quotations. The study of the commerical alloys indicated that the processing procedures, which included melting practice, breakdown procedures, and rolling and finishing temperatures, normally used in the production of 18% nickel maraging steel varied from producer to producer. However, these differences did not affect the final properties appreciably. Therefore, when the optimum material was processed, no attempt was made to control the melting or rolling practices or to introduce special processes and control procedures.

Of the ten steel producers contacted, five declined to quote because of the small quantity requested. Three others responded, but only for the production of either the plate or the forgings. These were not considered because it was desired that both plate and forgings be produced by the same company. The remaining two mills quoted on both plate and forgings, and the lowest bid was accepted.

2. Mill Processing

A 10-ton heat of the optimum material, Heat 24158, was prepared by the vacuum-arc-remelting process which yielded a 20-in.-dia ingot. The first step in working the ingot was press-forging, in which the ingot cross-section was reduced to a 13-in.-square. Forging was started at 2100°F after soaking for 3 hr at 2300°F. After the first forging operation, the ingot was allowed to cool to 1500°F. Then, it was reheated to 2300°F, soaked for 4 hr, cooled to 2100°F and press-forged to a 9-in.-square slab. At this stage, the slab was cut into three parts; two sections were used to produce ring forgings and the third section was rolled to 3/4-in.-thick plate.

In the first plate rolling operation, the 9-in.-square slab was rolled at 2075°F along the original ingot axis (longitudinally) to a 2-3/4-in. thick x 10-in.-wide slab. After cooling to room temperature, the slab was inspected ultrasonically. No defects were found, and cross rolling was resumed at 1850°F to increase the slab width from 10 to 22 in. Without reheating, the slab was turned 90-deg. and straight-away rolled to a 3/4-in. final thickness. Rolling was finished below 1400°F. The finished plate was mill-annealed at 1500°F for 1 hr and air cooled. Ultrasonic and magnetic particle techniques were used to inspect the plate. No defects were found. The procedures used for ultrasonic inspection and equipment sensitivity are described in Appendix II.

Mandrel ring forgings were produced from sections cut from the ingot after it had been press-forged to a 9-in.-square slab. A 22-in.-long section was heated to 2150°F, upset to form a disc approximately 17-in.-dia x 6-in.-thick, and then pierced and hot sheared to remove a 4-1/2-in.-dia piece from the center. After reheating to 1850°F, forging was resumed on a 4-in.-dia mandrel to expand the inside diameter to 6 in. Forging to the final size of 26-in. OD x 18-in. ID x 4-in. face width was completed on a 6-in.-dia mandrel. Two reheating operations were required, and the finishing temperature was between 1400°F and 1500°F. The forging was cooled to room temperature and then mill-annealed at 1500°F for 4 hr followed by air cooling to room temperature.

The second 9-in.-square ingot section, 6 in. long, was heated to 2150°F, forged to a 5 in. square, and then upset to form a disc 8-3/4-in.-dia x 6-in.-thick. This disc was processed to a final ring forging 20-in. OD x 18-in. ID x 4-in. face width in the manner described above, and mill-annealed at 1500°F for 2 hr.

Approved for Public Release

Contrails

3. Material Quality

Tests were made by the steel producer to determine if the plate met composition, strength, and cleanliness requirements. Chemical analyses were made on both the forged slab and finish-rolled plate. The compositions are shown in Table 35. This heat did not meet the composition requirements specified for the optimum material because the molybdenum content was too low.

Tensile tests were made by the vendor on both slab and plate material. Specimens were cut from the 2-3/4 x 10-in. slab, annealed at 1500°F for 1 hr and aged at 900°F for 3 hr. The tests results are summarized below:

	0.2% Offset Yield Strength (ksi)	Tensile Strength (ksi)	Elongation in 1 In. (%)	Reduction of Area (%)
Transverse	190	200	14.0	46.0
Short Transverse	191	199	11.0	50.0

Specimens cut from the 3/4 in. plate were tested in the mill-annealed and aged condition. The following results were obtained:

Aging Cycle (°F-hr)	0.2% Offset Yield Strength (ksi)	Tensile Strength (ksi)	Elongation in 1 In. (%)	Reduction of Area (%)
850- 3	185.5	189.7	13.0	59.3
850- 4	185.7	191.7	14.0	60.0
850- 8	198.9	203.4	12.0	54.4
900- 3	189.8	198.8	12.5	54.0
900- 6	199.6	207.1	12.9	52.8
900-10	206.8	212.8	15.7	49.6
900-16	212.1	215.1	10.1	50.7
950- 3	196.8	205.3	12.9	50.2
950- 6	196.8	204.3	11.4	53.4

These properties did not meet the specified strength requirements. Another set of specimens from the plate material was tested after re-solution annealing at 1500°F for 1 hr and aging. The strength was improved by the re-solution treatment as shown on the following page.

Metallographic studies were made of the material in both mill-annealed and re-solution annealed conditions. Little difference was found in the microstructure between specimens representing the two conditions as shown in Figure 80. The only apparent difference is that the mill-annealed specimen showed some evidence of residual working in the form of deformed grains that did not recrystallize.

Approved for Public Release

Contrails

Aging Cycle (°F-hr)	0.2% Offset Yield Strength (ksi)	Tensile Strength (ksi)	Elongation in 1 In. (%)	Reduction of Area (%)
850-4	199.0	200.5	12.9	52.3
850-8	208.0	209.1	12.9	52.3
900-3	199.7	205.7	12.0	54.2
900-6	205.7	210.9	12.0	54.2
900-8	215.1	217.1	12.9	49.9
950-4	205.0	207.0	10.0	50.7
950-8	207.1	208.1	10.0	54.3

The possibility that austenite was retained in the mill-annealed material also was investigated. However, evidence of this constituent could not be found in the microstructure and X-ray diffraction studies did not indicate its presence in excess of 1%.

Microcleanliness inspection was conducted by the producer on the finished plate and the following ratings were obtained. These ratings were verified by subsequent evaluation at Aerojet-General. The inclusions rated as B or D type were titanium compounds, either as stringers or randomly-dispersed particles.

	A		B		C		D	
	T	H	T	H	T	H	T	H
Longitudinal								
Worst Field	0	0	2	0	0	0	2	1
Average Field	0	0	1	0	0	0	2	1
Transverse								
Worst Field	0	0	1½	0	0	0	2	2
Average Field	0	0	0	0	0	0	2	2

The ultrasonic, magnetic particle, and metallographic inspections showed the material to be acceptable from the standpoint of specified limits. Despite the low molybdenum content, the producer's evaluation indicated that strength requirements could be met by re-solution annealing prior to aging. Because of this, the material was accepted for further study. The Air Force project engineer also concurred with this approach, which was considered desirable in that it permitted an evaluation of an 18% nickel maraging steel alloy at the 200 ksi yield strength level.

Additional inspections were conducted upon receipt of the plate and forgings at Aerojet-General. Ultrasonic (Refer to Appendix II) and metallographic methods showed that both the plate and forgings were free from defects The photomicrographs in Figure 81 show the inclusions in typical sections of

Approved for Public Release

Contrails

each product. The grain size of the plate and forgings are compared in Figure 82. As indicated by this figure, a typical grain size of 9 was observed in the plate while the prior-austenite grain size approximating 2 was obtained for the 1-in. and 4-in.-thick forgings. Figure 83 shows that banding was not present in samples taken from the plate and both forgings.

B. AGING RESPONSE CHARACTERISTICS

The aging characteristics of the optimum material were established on the basis of tensile properties. Tensile specimens with a 1/4-in.-dia x 1-in. gage length were machined from the 3/4-in.-thick plate and forgings as shown in Figures 84 and 85. The re-solution annealed (1500°F for 1 hr) specimens from the plate material were aged at 850, 900, and 950°F for intervals between 2 and 16 hr. The results of the tension tests are summarized in Table 36. These data are average values; the results of individual tests are tabulated in Appendix III.

Figure 86 shows the aging response characteristic of the optimum plate material. These curves show the usual trend of increased strength with increased aging time. However, overaging did not occur under any aging condition evaluated. The aging response differs from the alloys evaluated earlier in the program in the effect of aging temperature on strength. During the previous investigation, alloys generally showed improved strengths as the aging temperature was increased and overaging occurred at longer aging times at aging temperatures of 900 and 950°F. In the optimum material, this trend was reversed at aging times of 8 hr or more, with the lowest aging temperature providing the highest strength. The target yield strength of 200 ksi was reached through only one aging condition: 850°F for 16 hr. These strength values differ from those reported by the producer; however, the reason for this difference is unknown.

Figure 87 shows that ductility in the plate material was not influenced greatly by aging time or temperature. The elongation ranged from a low of 10.7% to a high of 12.4% and the reduction-of-area varied from 56.7% to 68.3%. There was no appreciable anisotropy. The greatest variations were a 1-1/2% increase in yield strength accompanied by a drop in elongation from 11.4% to 10.1%. The greatest difference in reduction-of-area occurred between 59.2% and 52.5%.

The tensile properties of the forgings were evaluated after aging cycles of 850, 900, and 950°F for 8 hr. These data are shown in Figure 88. The target yield strength was not reached in the 4 x 4-in. section, whereas the 1 x 4-in. forging did exceed 200 ksi after aging at 900°F or 950°F for 8 hr.

For each aging condition, the 1 x 4-in. forging showed a higher yield strength than the 4 x 4-in. forging in both transverse and longitudinal directions. The greatest difference in strength between the two forgings, which was less than 4%, occurred after aging at 950°F. The 1 x 4-in. forging showed little change in ductility with aging temperature. The elongation varied from 9.5% to 11.6% and the reduction-of-area from 49.9% to 54.5%. No difference was observed between the transverse and longitudinal properties. In contrast to these properties, the 4 x 4-in. forging showed a more pronounced difference in reduction-of-area between the transverse and longitudinal directions.

Approved for Public Release

Contrails

The greatest difference, from 51.2% to 29.7%, occurred at 950°F in the short transverse direction. However, after aging treatments at 850°F and 900°F, the greatest anisotropy was in the transverse orientation.

The evaluation of the aging characteristics of the optimum material showed that the desired yield strength level of 200 ksi after aging for 4 to 8 hr at 900°F was not realized. Failure to attain this yield strength level is attributed to the less-than-minimum specified molybdenum content. The influence of the low molybdenum content can be demonstrated by applying the equation derived to show yield strength as a function of composition.

$$\text{Yield Strength} = 38.1 + 8.8\ (\%\ \text{Co}) + 22.6\ (\%\ \text{Mo}) + 87.7\ (\%\ \text{Ti})$$

When this equation is used with the reduced molybdenum content, the predicted yield strength after aging for 4 hr at 900°F is 199 ksi, below the 200 ksi minimum. The actual strength was 194.2 ksi. This difference is within the accuracy expected of the equation. If the minimum specified molybdenum content of 4% had been met, the final product would have been within the desired yield strength range with a predicted yield strength of 218 ksi.

C. FRACTURE TOUGHNESS OF THE OPTIMUM MATERIAL

1. Precrack-Charpy-Impact W/A Toughness

a. Mandrel-Forged 4 x 4-In. Section

The W/A values for the 4 x 4-in. mandrel-forged Grade 200 vacuum-arc-remelt optimum material, (heat 24158) are presented in Table 37 and summarized below. Three specimen orientations, three aging treatments and four test temperatures were investigated. The data are plotted in Figure 89. Figure 90 is a schematic showing the layout of specimens in the part. Aging at 850 and 950°F for 8 hr consistently improved the toughness over an aging treatment at 900°F for 8 hr. Lower toughness in the material aged at 900°F for 8 hr was consistent with higher tensile strength after this aging treatment in comparison with the material aged at 850 and 950°F for 8 hr.

Aging Cycle (°F-hr)	Specimen Orientation	0.2% Offset Yield Strength (ksi)	W/A (in.-lb/in.^{2}) Test Temperature (°F) -100	RT	200	400
950-8	Longitudinal	191.5	884	1136	1498	1401
	Transverse	192.0	420	574	609	656
	Short Trans	193.5	510	719	791	956
900-8	Longitudinal	199.3	713	876	1350	1136
	Transverse	197.5	364	500	537	580
	Short Trans	198.8	439	630	644	678
850-8	Longitudinal	182.5	707	1024	1307	1306
	Transverse	184.6	413	656	650	819
	Short Trans	182.0	513	731	874	986

Approved for Public Release

Contrails

Anisotropy was evident, with the longitudinally oriented specimen (fracture propagating perpendicular to metal flow in the forged part) indicating appreciably higher toughness than the transverse specimen orientations. The fact that the transverse specimen orientation in the finished part resulted in lower toughness values than the short-transverse orientation suggests that fracture toughness in this specimen orientation was controlled by the upsetting operation (the transverse specimen in the mandrel-forged part was short transverse in the upsetting operation - See Figure 90).

b. Mandrel-Forged 1 x 4-In. Section

The W/A values for the 1 x 4-in. mandrel-forged cross section are presented in Table 38 and summarized below. Three aging treatments and four testing temperatures were investigated. The data are plotted in Figure 91.

Aging Cycle (°F-hr)	Specimen Orientation	0.2% Offset Yield Strength (ksi)	W/A (in.-lb/in.^{2}) Test Temperature (°F)			
			-100	RT	200	400
950-8	Longitudinal	197.1	759	1068	1152	1219
900-8	Longitudinal	203.6	676	972	1164	1268
850-8	Longitudinal	187.5	627	965	1044	1050
	Transverse		--	882	--	1079

Little difference was observed in W/A values between the 1 x 4-in. and 4 x 4-in. cross sections at room temperature and below. However, at the elevated test temperatures, the 1 x 4-in. material was not as tough as the 4 x 4-in. material after aging at 850 and 950°F, but it was tougher after aging at 900°F. A comparison between the longitudinal and transverse specimen orientations indicated relatively little anisotropy in the 1 x 4-in. mandrel-forging.

c. 3/4-In.-Thick Plate

The W/A values for plate are presented in Table 39 and summarized below. Two specimen orientations, three aging treatments and four test temperatures were investigated. The data are plotted in Figure 92.

Aging Cycle (°F-hr)	Specimen Orientation	0.2% Offset Yield Strength (ksi)	W/A (in.-lb/in.^{2}) Test Temperature (°F)			
			-100	RT	200	400
950-8	Longitudinal	193.4	1172	1605	2094	2307
	Transverse	196.0	749	1008	1143	1346
900-8	Longitudinal	196.8	910	1273	1499	1509
	Transverse	199.5	611	888	907	1102
850-8	Longitudinal	197.5	1218	1566	1916	2017
	Transverse	196.1	696	1134	1077	1278

Approved for Public Release

Contrails

As in the case of the 4 x 4-in. forging, aging at 850 and 950°F for 8 hr produced a consistent and marked improvement in toughness over the treatment at 900°F for 8 hr. Again, this trend was consistent with slightly higher strength after aging at 900°F for 8 hr. The transverse specimen orientation in the plate (fracture parallel with the final rolling operation) produced decidedly lower W/A values than the longitudinal specimen. A comparison between the 1 x 4-in. forging, the 4 x 4-in. forging and the plate material indicated significantly greater toughness in the plate longitudinal-specimen orientation (See Figure 91). However, the plate transverse-specimen orientation indicated approximately the same toughness as the longitudinal specimen orientation in the mandrel forgings. This suggests that the increased amount of working involved in straight-away rolling the 9 x 9-in. press-forging to 3/4-in.-thick plate (See Figure 93) was effective in increasing the toughness of the plate in the longitudinal orientation, over that of the mandrel forgins; whereas the relatively small amount of cross-rolling that was necessary to spread the 2-3/4-in.-thick x 10-in.-wide slab to a 22 in. width resulted in approximately the same toughness in the plate transverse-specimen orientation as that in the mandrel-forged longitudinal-specimen orientation. The very coarse grain size in the forged material also may have contributed to the lower toughness in the forgings as compared with the relatively fine-grain plate material although the results obtained indicate that the effects of working over-shadowed any effects of grain size.

2. Plane-Strain Fracture Toughness

a. Mandrel-Forged 4 x 4-In. Section

The slow-notch-bend test results are detailed in Table 41 and summarized below:

Aging Cycle (°F-hr)	0.2% Offset Yield Strength (ksi)			G_{nc} (in.-lb/in.^{2})		
	Long.	Trans.	Short Trans	Longitudinal	Transverse	Short Transverse
850-8	182	185	182	286-387 Avg(4) 327	214-334 Avg(5) 277	154-365 Avg(5) 269
				221-354 Avg(4) 308*	269-331 Avg(5) 304*	256-290 Avg(5) 283*
900-8	199	198	199	304-472 Avg(5)	179-317 Avg(5) 243	268-329 Avg(4) 297
				354-438 Avg(5) 397*	178-282 Avg(5) 229*	253-379 Avg(4) 295*
950-8	192	192	194	370-496 Avg(5) 411	169-379 Avg(5) 245	250-390 Avg(3) 339
				445-499 Avg(5) 467*	170-302 Avg(5) 237*	366-407 Avg(3) 390*

*G_{Ic} values were calculated using Bueckner's method.

Approved for Public Release

Contrails

Figure 94 permits a comparison of G_{nc} as calculated from the spring-constant method, G_{Ic} as calculated from Bueckner's equation, and W/A as calculated from the Charpy-impact test, as well as the scatter in test results. The slow-notch-bend test data represent averages of 3 to 5 tests. Although the scatter in slow-notch-bend test results was much greater than in the precrack-Charpy-impact test, the same trends were indicated by the two tests. Furthermore, the values calculated from the spring-constant method and the values calculated from Bueckner's equation showed the same trends, with appreciably less scatter in the values obtained from Bueckner's equation. The slow-notch-bend test results showed: 1) little or no difference between the longitudinal, transverse, and short-transverse specimen orientations after aging at 850°F for 8 hr; 2) lower toughness in the transverse and short-transverse specimen orientations after aging at 900 and 950°F (as compared with the longitudinal specimen orientation); 3) greater toughness in the short-transverse specimen orientation after aging at 900 and 950°F (as compared with the transverse specimen orientation); and 4) somewhat lower toughness in both the longitudinal and transverse specimen orientations after aging at 900°F for 8 hr (as compared with the material aged at 950°F for 8 hr).

b. Mandrel-Forged 1 x 4-In. Section

The slow-notch-bend test results are detailed in Table 42 and summarized below. Figure 95 compares the toughness as measured by the precrack-Charpy-impact test with the plane-strain fracture toughness calculated by the spring-constant method and from Bueckner's equation.

Aging Cycle (°F-hr)	0.2% Offset Yield Strength (ksi)	G_{nc} (in.-lb/in.^{2}) Longitudinal	G_{nc} (in.-lb/in.^{2}) Transverse
850-8	Longitudinal 188	408-555 Avg(5) 484	152-457 Avg(5) 342
	Transverse 189	290-372 Avg(5) 324*	154-333 Avg(5) 254*
900-8	Longitudinal 204	427-531 Avg(4) 477	444-542 Avg(5) 493
	Transverse 202	301-397 Avg(4) 367*	373-486 Avg(5) 430*
950-8	Longitudinal 197	428-530 Avg(5) 518	443-599 Avg(4) 521
	Transverse 199	370-530 Avg(5) 446*	393-484 Avg(4) 430*

* G_{Ic} values were calculated using Bueckner's method.

Approved for Public Release

Contrails

The slow-notch-bend test results as obtained by the spring-constant method were widely scattered (five replicate tests for each of three aging cycles and two specimen orientations). Nevertheless, the trends in fracture toughness values calculated from both the spring-constant and Bueckner's equation were the same, indicating that the toughness increased with increased aging temperature, and that little or no significant difference occurred between the fracture toughness of the longitudinal and transverse specimen orientations. A comparison between the 1 x 4 and 4 x 4-in. mandrel-forged sections indicated the plane-strain fracture toughness of the two forgings as calculated from Bueckner's equation to be approximately the same in the longitudinal specimen orientation after a given aging treatment whereas, in the transverse specimen orientation, the 4 x 4-in. forging had appreciably lower toughness. The precrack-Charpy-impact test showed the same trend. As discussed in connection with the Charpy test, these trends regarding specimen orientation appear to be related to the relative amounts of metal working in the two forgings.

c. 3/4-In.-Thick Plate

The slow-notch-bend test results for the 3/4-in.-thick plate are detailed in Table 43 and summarized below. Both 0.5 and 0.75-in.-thick specimens were tested. Figure 96 permits a comparison between the results obtained from two sizes of slow-notch-bend test specimen, and a comparison of G_{nc} as calculated from the spring-constant, G_{Ic} as calculated from Bueckner's equation, and the effect of different aging temperatures. As demonstrated in the correlation study (Table 5), little or no difference occurred between the test results obtained from the two sizes of SNB test specimen. Consequently, both sets of data may be considered in comparing the fracture toughness values with those previously obtained in evaluating the selected alloys.

Aging Cycle (°F-hr)	0.2% Offset Yield Strength (ksi)	3/4 x 3/4-in. SNB Specimen G_{nc} (in.-lb/in.^{2})		1/2 x 3/4-in. SNB Specimen G_{nc} (in.-lb/in.^{2})	
		Longitudinal	Transverse	Longitudinal	Transverse
850-8	Longitudinal 198	353-469 Avg(5) 415	333-447 Avg(4) 394	344-498 Avg(4) 443	288-338 Avg(5) 317
	Transverse 196	208-521 Avg(5) 338*	315-340 Avg(4) 324*	394-492 Avg(4) 453*	330-406 Avg(5) 350*
900-8	Longitudinal 197	303-483 Avg(4) 417	287-299 Avg(2) 293	358-540 Avg(5) 461	269-339 Avg(5) 300
	Transverse 200	297-485 Avg(4) 362*	310-341 Avg(2) 325*	362-458 Avg(5) 422*	206-304 Avg(5) 270*
950-8	Longitudinal 193	392-606 Avg(5) 496	279-484 Avg(5) 359	271-474 Avg(5) 363	262-496 Avg(4) 365
	Transverse 196	313-510 Avg(5) 430*	338-427 Avg(5) 380*	370-451 Avg(5) 411*	423-479 Avg(4) 445*

* G_{Ic} values were calculated using Bueckner's method.

Approved for Public Release

Contrails

In contrast to the precrack-Charpy test, the SNB test did not show a consistent difference between the two specimen orientations. However, the scatter in data from replicate tests was great, particularly in the longitudinal specimen orientation, and this may have overshadowed the anisotropy effect. In the longitudinal specimen orientation, aging treatment had little or no effect on the fracture toughness values; however, in the transverse specimen orientation, both the spring-constant method and Bueckner's equation indicated that there was somewhat greater toughness after aging at 950°F for 8 hr than after aging at 850° and 900°F for 8 hr.

3. Discussion

The plane-strain fracture toughness values from the slow-notch-bend tests of the optimum material are presented graphically in Figure 97. The bars represent average values for longitudinal and transverse specimen orientations with the transverse orientations shaded. To judge the significance of the variation in average values from bar to bar, the scatter in replicate test data is represented as a line through the top of each bar. The scatter in the SNB tests of the optimum heat was troublesome (4 to 5 replicate tests for each aging cycle and each specimen orientation) particularly when toughness was determined by the spring-constant method, and the scatter could not be explained. The coarse grain size in the mandrel-forged rings may have been a contributing factor, but this was not conclusive because the fine-grained plate material also involved scattered data from replicate test specimens. In this regard, it is significant to note that the Charpy-test, which is normally affected adversely by coarse grain size, showed relatively little scatter in the mandrel-forged ring materials.

For the over-all comparison between the plate and mandrel-forged rings in Figure 97, the plate data including those from two specimen sizes were averaged and plotted with the mandrel-forging data (each section size separately averaged). Because the fracture toughness values from replicate test specimens as computed using Bueckner's method generally involved somewhat less scatter than those computed from the spring-constant equation, only Bueckner's values were used in Figure 97. Furthermore, it was observed (from Figure 96) that the fracture toughness values computed by Bueckner's method were generally somewhat lower than those computed from the spring-constant equation. Nevertheless, both methods generally showed the same trends. Figure 97 indicates that, after aging the mandrel-forged rings at 850°F for 8 hr, the material had appreciably lower toughness than after aging at 950°F for 8 hr. The toughness appeared to be at an intermediate level after aging the mandrel-forged rings at 900°F; however, the trend was not consistent for both specimen orientations. Generally, the longitudinal specimen orientation appeared to give higher toughness values than the transverse or short transverse, although the trend was neither consistent from one aging-cycle to another nor was it always significant because of the scatter in the test results. Otherwise, comparisons at the various aging temperatures and in the two specimen orientations indicated no significant difference in fracture toughness between the plate and mandrel forgings.

Figure 98 permits a comparison between the plane-strain fracture toughness in the optimum heat and the selected heats investigated during the first phase of the program. The average values from 3 to 5 replicate test specimens are plotted as a function of the 0.2% offset yield strength,

Approved for Public Release

Contrails

where the shaded area is the band indicated in Figure 37. The data plotted in Figure 98 include only the toughness values computed by Bueckner's method. The toughness in the various material conditions of the optimum plate material ranged from 270 to 450 in.-lb/in.^{2}, while the yield strength ranged from 193 to 200 ksi. Data from Figure 37 indicate that the selected plate materials investigated during the evaluation phase of the study ranged in toughness from 290 to 430 in.-lb/in.^{2} at 195 ksi yield strength and from 280 to 425 in.-lb/in.^{2} at 205 ksi yield strength. These results also indicate that little difference existed in the plane-strain fracture toughness between the selected alloys and optimum plate material at the same strength level. In the mandrel-forged rings of the optimum material, values as low as 230 in.-lb/in.^{2} were measured in the transverse specimen orientation. However, as indicated previously, these lower values were associated with the relatively low degree of working received in these components in the transverse orientation.

The precrack-Charpy-test results for the optimum material generally involved less scatter than the slow-notch-bend test data. Figure 99 permits a comparison between the room temperature W/A values for the optimum plate material and the mandrel forgings. Three trends consistently were observed from one aging treatment to another and from one material condition to another. First, the transverse specimen orientation resulted in lower fracture toughness values, indicating insufficient cross-working in both the mandrel forgings and the plate. Second, the 900°F for 8 hr aging cycle developed lower toughness than either the 850°F or the 950°F cycles for 8 hr (this observation was consistent with slightly higher yield strength after aging at 900°F for 8 hr as compared with 850 and 950°F for 8 hr). Third, the short-transverse specimen orientation in the 4 x 4-in. mandrel-forged cross-section gave higher toughness values than the transverse. In connection with the latter observation, it should be noted that the short-transverse specimen orientation was longitudinal in the upset forging operation whereas the transverse specimen orientation (which consistently gave the lowest toughness in the 4 x 4-in. forging) was short-transverse in the upset-forging operations. The lower toughness in the transverse specimen orientation indicated that the work done in upset-forging the 9 x 9-in. square controlled the fracture-toughness anisotropy in the finished component. The plate anisotropy was likewise explained by the relatively small amount of cross-rolling done in producing the 3/4-in.-thick plate. (See Figure 93.)

Figure 100 compares the precrack-Charpy-impact W/A values as measured in the optimum material and in the selected heats investigated during the evaluation phase. As in the SNB test results, the transverse and short-transverse specimen orientations in the mandrel-forged 4 x 4-in. section gave lower toughness values than any of the plate materials investigated, whereas, the longitudinal specimen orientation in the plate gave values on the high side of the range established during the evaluation phase of the program. The transverse orientation test results were in the center of the W/A fracture toughness range previously established.

D. WELDING EVALUATION OF THE OPTIMUM ALLOY

The objective of the welding evaluation was to determine the weldability of the optimum plate and the tensile and fracture toughness properties of weldments in this material.

Approved for Public Release

Contrails

1. Welding Procedures

The welding studies of the selected alloys showed TIG, MIG and submerged-arc processes were adaptable to 18% nickel maraging steel plate on the basis of weld quality and weld-joint tensile properties. Of these processes, TIG and MIG were selected for use in the program to evaluate the optimum material. The procedures used with each of these processes were described in detail earlier during the evaluation of the selected alloys. The joint designs and the welding schedules that were used to weld the 3/4-in.-thick optimum plate are shown in Figures 44 and 45.

2. Filler Wire Composition

Welding-filler-wire composition was shown to be an important variable in the welding of the selected alloys. Further, it was shown that the filler wire composition could be varied to match the tensile strength of the weld metal with that of the base metal for both Grades 200 and 250 plate. Three filler wires were selected for welding the optimum plate material. One filler wire, heat 34482, was selected to obtain a low-strength weld deposit during the TIG welding process to achieve maximum fracture toughness in the weldment. A second filler wire, heat 34428-.38 Ti, with lower cobalt and molybdenum content but a higher titanium content, was selected for MIG welding to obtain a low-strength weld deposit which exhibited maximum fracture toughness. These two filler wires were expected to match the tensile properties of Grade 200 optimum plate. The third filler wire was selected for TIG and MIG welding to overmatch the strength of the base plate and to obtain additional data concerning the fracture toughness properties of high-strength weld deposits. This latter weld-filler-wire was expected to match the tensile properties of Grade 250 plate. The composition of these filler wires are listed in Table 46, and their cobalt, molybdenum and titanium content are as follows:

Filler Wire Heat	Alloy Content (Wt %)		
	Co	Mo	Ti
34482	7.8	4.1	0.24
34428-.38 Ti	7.5	3.9	0.38
24589	9.3	5.1	0.65

3. Tensile Properties

The tensile properties of TIG and MIG welds made with the selected filler wires were evaluated on the basis of transverse and longitudinal weld tensile properties.

a. TIG-Welded Joints

The transverse and longitudinal tensile properties of TIG welds in the optimum plate material are listed in Tables 47 and 48. The weldments were aged at 900 and 950°F for 8 hr after welding. These aging

Approved for Public Release

Contrails

cycles were selected on the basis of previous tests of weldments in the selected alloys to provide good combinations of strength and fracture toughness in the optimum plate material weldments.

The average longitudinal tensile properties of the weldments are summarized below:

Filler Wire Heat	Aging Cycle (°F-hr)	0.2% Offset Yield Strength (ksi)	Ultimate Tensile Strength (ksi)	Elongation in 1 In. (%)	Reduction of Area (%)
24589	900-8	247	269	8.6	37.8
34482	900-8	214	219	12.3	57.0
24589	950-8	232	250	11.0	44.0
34482	950-8	209	216	14.5	58.5

The composition of the weld metals are listed in Table 49 and the cobalt, molybdenum and titanium contents and potential yield strengths of the weld metal are listed below:

Filler Wire Heat	Potential Yield Strength (ksi)	Alloy Content (Wt %)		
		Co	Mo	Ti
34482	204	7.8	3.5	0.22
24589	269	9.3	4.5	0.54

The weld metal deposited by the Grade 250 filler wire was found to have higher cobalt, molybdenum, and titanium contents than weld metal deposited with the Grade 200 filler wire. The higher alloy content was indicated by an increase in yield strength of 23 to 33 ksi for the Grade 250 weld metal over that of the Grade 200 weld metal. However, the tensile yield strength of the weld metal obtained with the Grade 200 filler wire exceeded the minimum specified yield strength of Grade 200 plate. Also, the yield strength of the Grade 200 weld metal exceeded the calculated potential yield strength based on the following relationship, which was developed for the wrought plate:

$$\text{Yield Strength, (ksi)} = 38.1 \times 8.8\ (\%\ \text{Co}) + 22.6\ (\%\ \text{Mo}) + 87.7\ (\%\ \text{Ti})$$

This is the only weld metal in which the actual yield strength of the weld metal exceeded the calculated value. However, the calculated potential yield strength was based on an aging cycle of 900°F for 4 hr and the actual yield strength of the weld metal was determined after an 8 hr aging cycle and may have been lower if a 4 hr aging cycle had been used. If so, the difference in aging time might account for the fact that the actual yield strength of the Grade 200 weld metal exceeded the calculated value. The high-strength weld metal followed the trend established earlier in the

Approved for Public Release

Contrails

program in that the actual yield strength was significantly lower than the calculated value even though it also was aged at 900°F for 8 hr. The lower tensile strength of filler wire 34482 weld metal was accompanied by higher ductility than that of the Grade 200 weld metal. The reduced tensile strength that was observed in both weld metals during the 950°F aging treatments indicated that slight overaging occurred.

The transverse tensile properties of weldments in the optimum plate material are summarized below:

Filler Wire Heat	Aging Cycle (°F-hr)	Ultimate Tensile Strength (ksi)	Location of Failure
24589	900-8	217	HAZ
34482	900-8	213	HAZ
24589	950-8	203	HAZ
34482	950-8	207	HAZ

This summary indicates that the transverse tensile specimens failed in the heat-affected zones for both the Grade 250 and Grade 200 filler wires at stress levels comparable to or greater than the ultimate tensile strength of the base metal. This indicates that use of the high-strength filler wire did not offer an advantage over the use of the low-strength filler wire for the Grade 200 optimum plate. For welding Grade 250 plate, however, the high-strength filler wire would be required to match the tensile strength of the base metal.

b. MIG-Welded Joints

The longitudinal and transverse tensile properties of MIG welds in the optimum plate material are listed in Tables 50 and 51. These weldments were aged at 900 and 950°F for 8 hr after welding in accordance with the aging cycles used for TIG-welded joints.

The average longitudinal tensile properties of the MIG weld-metals are summarized below.

Filler Wire Heat	Aging Cycle (°F-hr)	0.2% Offset Yield Strength (ksi)	Ultimate Tensile Strength (ksi)	Elongation in 1 In. (%)	Reduction of Area (%)
24589	900-8	228	246	7.7	32.7
34428-.38 Ti	900-8	215	224	6.7	26.7
24589	950-8	217	239	5.9	19.1
34428-.38 Ti	950-8	202	214	9.5	32.5

Filler wire 24589 was selected for the program to represent a Grade 250 filler wire. The yield strength of the weld metal obtained with this filler wire, however, was lower than that required to match the yield strength of Grade 250 wrought plate. Filler wire 34428-.38 Ti was

Approved for Public Release

Contrails

selected to represent a Grade 200 filler wire. The yield strength of the weld metal obtained with the Grade 200 filler wire exceeded the minimum yield strength of Grade 200 wrought plate.

The composition of the weld metals is listed in Table 52 and the cobalt, molybdenum, and titanium contents and the potential yield strengths of the weld metals are:

Filler Wire Heat	Potential Yield Strength (ksi)	Alloy Content, Wt % Co	Mo	Ti
24589	264	9.1	4.5	0.50
34428-.38 Ti	213.6	7.8	3.8	0.24

The weld metal deposited with the Grade 250, heat 24589, filler wire had higher cobalt, molybdenum, and titanium content than the weld metal deposited with the Grade 200, heat 34428-.38 Ti filler wire. This higher alloy content was accompanied by higher yield strength of the weld metal deposited with the Grade 250 filler wire, which exceeded that of weld metal deposited with the Grade 200 filler wire by about 14 ksi after both aging treatments.

After aging at 900°F for 8 hr, the elongation and reduction of area of the Grade 250 weld deposit were slightly higher than those of the Grade 200 weld deposits although this difference may not be significant. After aging at 950°F for 8 hr, however, the normal trend was observed in that the Grade 200 weld deposit had the highest values of elongation and reduction of area. The observed reduction in tensile strength that accompanied the aging cycle of 950°F for 8 hr is indicative that slight overaging occurred in both weld metals with this aging treatment.

Compared with TIG weld metal, the MIG weld metal obtained with filler-wire heat 24589 had lower yield and ultimate strengths than expected on the basis of composition. Also, the reduced tensile strength was accompanied by slightly reduced values of elongation and reduction of area, which is not normally expected. This combination of reduced strength and ductility in the MIG weld metal indicates that a difference in the alloy segregation occurs in the weld fusion-zone of MIG and TIG welds or a difference in the microstructure of the weld metals; however, such a difference could not be established conclusively in metallographic studies that were conducted on the MIG welds. In most areas of the MIG weld-metals, the structures were typical of those found in TIG welds described earlier. A slightly greater amount of retained austenite appeared in the MIG weld metal over the amount found in the TIG weld metal and the retained austenite phase was more continuous between the dendrites. Extensive studies would be required to conclusively establish that a higher retained austenite content is characteristic of MIG welds.

The MIG weld-metal deposited with filler wire heat 34478-.38 Ti also had lower elongation and reduction of area values than expected based on the TIG weld-metal obtained with filler wire heat 34482.

Approved for Public Release

Contrails

This difference can not be explained on the basis of alloy content because the composition of the two weld metals were very similar. However, alloy segregation and microstructure might account for the difference, although extensive studies would be required to conclusively establish that significant differences exist between the two types of weldments.

Vacuum fusion analyses also were conducted to determine if the oxygen or hydrogen content of the TIG- and MIG-welds differed. The oxygen content of TIG-welds made with filler wires 24589 and 34483 varied from 16-94 ppm and 4-96 ppm respectively, compared with an oxygen content of 71 ppm for the MIG-weld made with filler wire 24589. These results do not indicate whether oxygen content accounts for the difference between the welds, but they do indicate that additional studies are needed.

The transverse tensile properties of MIG weldments in the optimum plate material are summarized below:

Filler Wire Heat	Aging Cycle (°F-hr)	Ultimate Tensile Strength, (ksi)	Location of Failure
24589	900-8	214	HAZ
34428-.38 Ti	900-8	220	HAZ
24589	950-8	210	HAZ
34428-.38 Ti	950-8	209	HAZ

With the exception of one transverse tensile specimen, which failed at a lack of fusion defect in the joint, all of the transverse specimens failed in the weld heat-affected zone at stress levels comparable to or greater than the ultimate tensile strength of the wrought base metal. The transverse tensile properties of the MIG weldments were comparable to those of the TIG weldments as expected.

4. Fracture Toughness of Weldments

The plane-stress and plane-strain fracture toughness of TIG and MIG weldments made with the selected filler wires were evaluated by precracked-Charpy-impact and slow-notch-bend tests. The notches were located through the thickness in the weld metal and in two locations in the weld heat-affected zones. Full thickness (0.7 in.) precracked-Charpy-impact specimens were prepared from weldments in the optimum plate, whereas standard size specimens (0.394 x 0.394-in.) were prepared in the welding studies on selected alloys. Because of the larger size of the optimum plate weldment specimens, the notches in the heat-affected zones were located further from the weld-fusion-line at the center and root of the weldment than similar notches made in weldments from the selected alloys. For this reason, the notch location in heat-affected zone 1 (HAZ-1) included some unaffected base metal as well as weld metal, and high and low temperature heat-affected zone and notch location 2 (HAZ-2) was located primarily in unaffected base metal as indicated in Figure 101.

Approved for Public Release

Contrails

a. TIG-Welded Joints

The W/A fracture toughness of TIG weldments in the optimum plate is shown in Table 53 and Figures 102 and 103 and summarized as follows:

Filler Wire Heat	Aging Cycle (°F-hr)	Notch Location	0.2% Offset Yield Strength (ksi)	W/A (in.-lb/in.^{2})*			
				-100	RT	200	400
24589	900-8	WM	247	196	388	345	267
34482	900-8	WM	214	735	1157	1217	1544
---	900-8	HAZ-1	-	1104	1164	1259	1434
---	900-8	HAZ-2	-	967	1189	1271	1154
---	900-8	Base Metal					
		Long.	196.8	1025	1214	1584	1354
		Trans	199.5	628	800	854	722
24589	950-8	WM	232	287	303	370	315
34482	950-8	WM	209	739	1125	1515	1328
---	950-8	HAZ-1		1350	1662	1597	1781
---	950-8	HAZ-2		964	1454	1438	1649
---	950-8	Base Metal					
		Long.	193.4	-	1315	-	2354
		Trans	196.0	695	831	911	877

*Specimen size was 0.7 x 0.394-in. for WM and HAZ, and 0.75 x 0.394-in. for the base metal.

The precracked-Charpy-impact fracture toughness (W/A) of the Grade 200 weld metal (filler wire 34482) exceeded that of the base metal in the transverse orientation after both aging treatments and was comparable to that of the base metal in the longitudinal orientation after the 900°F aging cycle. After the 950°F aging cycle, the weld metal fracture toughness was lower than that of the base metal in the longitudinal direction because the increase in aging temperature had only a slight effect on weld metal fracture toughness although it improved the fracture toughness of the base metal in the longitudinal orientation.

The fracture toughness of the heat-affected zones was comparable to that of the base metal in the longitudinal orientation at most test temperatures and exceeded that of the base metal in the

Approved for Public Release

Contrails

transverse orientation at all test temperatures and for both aging cycles. These heat-affected zone specimens were tested in the longitudinal orientation with respect to the plate to simulate structures in which the rolling direction of the plate would be oriented parallel to the maximum stresses in the structure. Such an orientation simulates longitudinal welds in large-diameter rocket-motor cases.

The W/A fracture toughness of the Grade 250 weld metal (filler wire 24589) was much lower than that of Grade 200 weld metal base metal and weld heat-affected zones. The low fracture toughness of this weld metal, however, is attributed to its high strength, which is comparable to that of Grade 250 plate. The fracture toughness of the high-strength weld metal is compared with that of Grade 250 plate in the following tabulation:

Material	Aging Cycle (°F-hr)	0.2% Offset Yield Strength (ksi)	W/A (in.-lb/in.^{2})			
			-100	RT	200	400
24589 Weld Metal	900-8	247	196	388	345	267
Heat 120D163 Plate*	900-8	257	90	366	460	584

*Longitudinal orientation and re-solution annealed before aging.

This summary indicates that the fracture toughness of the high-strength weld metal was comparable to that of the Grade 250 plate at room temperature and below. At temperatures of 200 and 400°F, the base metal fracture toughness was higher than that of the weld metal.

The plane-strain fracture toughness of TIG weldments in the optimum plate is listed in Table 54 and summarized in the tabulation at the top of the following page. This table summarization indicates that the plane-strain fracture toughness of the Grade 200 weld metal (filler wire 34482) exceeded that of the base metal and weld heat-affected zones after both aging treatments. Also, the plane-strain fracture toughness of the weld heat-affected zones was comparable to that of the base metal after both aging treatments.

Approved for Public Release

Contrails

Filler Wire Heat	Aging Cycle (°F-hr)	Notch Location	0.2% Offset Yield Strength (ksi)	G_{Ic},(1) (in.-lb/in.^{2})
24589	900-8	WM	247	146(2)
34482	900-8	WM	214	538
---	900-8	HAZ-1		348
---	900-8	HAZ-2		332
---	900-8	Base Metal		
		Long.	196.8	362
		Trans	199.5	325
24589	950-8	WM	232	246(2)
34482	950-8	WM	209	561
---	950-8	HAZ-1		410
---	950-8	HAZ-2		400
	950-8	Base Metal		
		Long.	193.4	430
		Trans	196.0	380

(1) These values are based on Bueckner's equation.
(2) These values are based on calibration curves.

The plane-strain fracture-toughness of the Grade 250 weld metal (filler wire 24589) was lower than that of the Grade 200 weld metal, base plate and heat-affected zones but was comparable to that of Grade 250 plate as shown below.

Material	0.2% Offset Yield Strength (ksi)	G_{nc}(in.-lb/in.^{2})
24589 Weld Metal	247	146
	232	246
Heat 120D163 Plate	254	136
	258	157--246

It is also desirable to rate the Grade 200 and the Grade 250 weldments in regard to critical-surface-flaw length. Using the data shown in Figure 38 and $a/2c = 0.1$, critical-surface-flaw length of 0.82 to 0.9 in. are obtained for the Grade 200 weldment and 0.17 to 0.33 in. for the Grade 250 weldment. In these calculations, the fracture stress is assumed equal to the weld deposit 0.2% offset yield strength shown above. When compared on this basis, the Grade 200 weld deposit is significantly superior to the Grade 250 weldment and is recommended for application in the fabrication of large-diameter solid-rocket motors.

Approved for Public Release

Contrails

b. MIG-Welded Joints

The W/A fracture toughness of MIG weldments in the optimum plate material is listed in Table 55 and summarized below:

Filler Wire Heat	Aging Cycle (°F-hr)	Notch Location	0.2% Offset Yield Strength (ksi)	W/A (in.-lb/in.^{2})* -100	RT	200	400
24589	900-8	WM	228	220	269	257	235
34428-.38 Ti	900-8	WM	215	303	308	408	459
--	900-8	HAZ-1	-	911	1103	1235	1085
--	900-8	HAZ-2	-	871	1395	1130	1690
--	900-8	Base Metal					
		Longitudinal	196.8	1025	1214	1584	1359
		Transverse	199.5	628	800	854	722
24589	950-8	WM	217	236	346	300	294
34428-.38 Ti	950-8	WM	202	-	474	502	519
--	950-8	HAZ-1	-	-	1317	1429	1503
	950-8	HAZ-2	-	1125	1433	1422	-
--	950-8	Base Metal					
		Longitudinal	193.4	-	1315	-	2354
		Transverse	196.0	695	831	911	877

* Specimen Sizes were 0.7 x 0.394-in. for WM and HAZ, and 0.75 x 0.394-in. for the base metal.

The W/A fracture toughness of Grades 250 and 200 MIG weld-metals was lower than that of the base metal in both the longitudinal and transverse orientations. However, the fracture toughness of the Grade 200 weld metal was slightly higher than that of the Grade 250 weld metal at testing temperatures of 200 and 400°F, after aging at 900°F for 8 hr and at all test temperatures after aging at 950°F for 8 hr. The higher fracture toughness of the Grade 200 weld metal may be associated with its slightly lower yield strength, but the differences in yield strength and fracture toughness of the two heats are not great.

The fracture toughness of the heat-affected zones was comparable to that of the base metal in the longitudinal orientation for most test temperatures and exceeded that of the base metal in the transverse orientation at all test temperature for both aging cycles. These

Approved for Public Release

Contrails

heat-affected zone specimens were tested in the longitudinal orientation with respect to the plate to simulate large-diameter rocket-motor cases in which the rolling direction of the plate would be oriented parallel to the maximum stresses in the structure and normal to the longitudinal welds.

The W/A fracture toughness of the MIG weld-metals is compared with that of TIG weld metals and wrought base metals on the basis of yield strength in Figure 104. Based on yield strength, the MIG weld-metals have lower fracture toughness values than the TIG weld metals and the difference between the MIG and TIG weld-metals is most pronounced for the Grade 200 filler wires. An additional comparison between the fracture toughness of Grade 200 TIG weld metals and the MIG weld data discussed above is obtained from the data in Table 34, which shows the fracture toughness of the weld metal obtained in TIG welding Grade 200 (heat 10675) plate with Grade 200 (IW450) filler wire. These data indicate that the W/A values obtained with TIG weld-metals deposited using the IW450 filler wire are comparable to those obtained with the 34482 filler wire and greatly exceed those obtained with MIG weld metals of comparable yield strength. The fracture toughness of weld metals deposited with IW450 filler metal in heat 10675 plate cannot be compared directly with those obtained in the optimum material because standard 0.394 x 0.394-in. pre-cracked-Charpy-impact specimens were used for the former evaluations and 0.7 x 0.394-in. specimens were used to evaluate the optimum plate weldments. However, the trend that MIG weld metals have lower fracture toughness than TIG weld metals is considered valid. Also, the lower than expected elongation and reduction of area values obtained in tensile tests on the MIG weld metals support this observation.

The MIG weld-metals also appeared to have lower fracture toughness than wrought plate based on yield strength. The fracture toughness of TIG weld metals, on the other hand, was comparable to that of the base metal on this same basis.

The W/A fracture toughness of MIG-weld heat-affected zones is compared with that of TIG-weld heat-affected zones and the optimum plate material in Figure 105. For most test temperatures, the fracture toughness of the weld heat-affected zones obtained with the two processes were comparable.

The plane-strain fracture toughness of MIG weldments in the optimum plate material is listed in Table 56 and summarized as follows:

Approved for Public Release

Contrails

Filler Wire Heat	Aging Cycle (°F-hr)	Notch Location	0.2 Offset Yield Strength (ksi)	G_{Ic} (in.-lb/in.^{2})*
24589	900-8	WM	228	121
34428-.38 Ti	900-8	WM	215	189
--	900-8	HAZ-1	-	409
--	900-8	HAZ-2	-	430
--	900-8	Base Metal		
		Longitudinal	196.8	362
		Transverse	199.5	325
24589	950-8	WM	217	64
34428-.38 Ti	950-8	WM	202	200
--	950-8	HAZ-1	-	491
--	950-8	HAZ-2	-	452
--	950-8	Base Metal		
		Longitudinal	193.4	430
		Transverse	196.0	380

* These values are based on calculations using Bueckner's equation.

The plane-strain fracture toughness of the Grade 250 and 200 MIG weld-metals was lower than that of the base metal after both aging cycles, but the fracture toughness of the weld heat-affected zones was comparable to that of the base metal.

The plane-strain fracture toughness of the MIG weld metals is compared with that of TIG weld metals and wrought base metals in Figure 106. The trends are similar to those observed with W/A fracture toughness in that the fracture toughness of the MIG weld-metals appears low when compared with that of TIG weld-metals and wrought base metals on the basis of yield strength, and the difference between weld metals is most pronounced for the Grade 200 weld deposits.

5. Discussion

Modified Grade 200 18% nickel maraging steel was selected as the optimum material because it provided the best combination of tensile properties and fracture toughness. To realize the full potential of this material in the fabrication of large-diameter rocket-motor cases, the same desirable combination of tensile properties and fracture toughness also should be obtained in the weldments. The welding studies on the optimum plate material verified that such a combination of properties could be achieved for TIG-welded joints when filler wires that produced weld metal

Approved for Public Release

Contrails

with a tensile yield strength only slightly higher than the minimum yield strength of Grade 200 plate were used. However, this same desirable combination of tensile strength and fracture toughness was not obtained for MIG-welded joints. Further studies are needed to compare the properties of MIG- and TIG-welds to determine the cause of the differences observed and to develop methods for improving the fracture toughness of MIG-deposited weld metals. The studies also showed that fracture toughness was sacrificed whenever filler wires were used to greatly overmatch the tensile strength of the base metal.

Based on the data obtained during the welding evaluation of the optimum material, a specification for Grade 200 weld filler wire composition has been proposed and is presented in Appendix VI. The composition of this proposed weld filler wire, which is to be used with the inert-gas-shielded tungsten-arc welding process (TIG), is:

Element	Wt %
Carbon	0.03 max
Manganese	0.10 max
Silicon	0.01 max
Sulphur	0.01 max
Phosphorus	0.01 max
Aluminum	0.01 max
Nickel	17.5-18.5
Cobalt	8.0-8.5
Molybdenum	3.6-3.8
Titanium	0.26-0.30

This composition is formulated at a nominal weld metal 0.2% offset yield strength value of 215 ksi. The potential yield strength of the proposed weld filler wire composition ranges from 203 to 225 ksi, depending on the cobalt, molybdenum, and titanium contents. The molybdenum content is lower than that specified for the optimum alloy and the titanium content is higher because dilution with the base metal during welding tends to raise the molybdenum content and reduce the titanium content of the weld deposit. Although the specified composition range for the weld filler wires are more restricted than those specified for wrought plate, these compositions can be met consistently during the production of small heats (1000 lb) of weld-filler-wire.

Additional effort will be required to verify the proposed composition specification for Grade 200 filler wire. Many heats of filler wire will have to be procured and used to weld a variety of Grade 200 plate before the proposed composition can be considered adequate. As such experience is gained, the composition ranges may have to be altered to meet all of the requirements of welding Grade 200, 18% nickel maraging steel plate. Factors such as plate thickness and the welding processes that affect dilution in the joint and alloy transfer must be considered as this experience is gained.

Approved for Public Release

Contrails

SECTION 5 -- CONCLUSIONS

During the investigation, seven selected commercial heats and an optimum composition heat of 18% nickel maraging steel were evaluated to determine their tensile properties, fracture toughness, and weldability. The test results were compared to determine the effects of such factors as mill-processing variables, heat-treatment, and chemical composition. On the basis of these comparisons, the following observations and conclusions were made:

1. The most important factor in determining the strength of 18% nickel maraging steel is the chemical composition, and the most important alloying elements are titanium, molybdenum, and cobalt. Variations of these elements within the nominal composition range required by the steel mills for a given grade can produce yield strength variations of 30 ksi or more. The 0.2% offset yield strength after aging at 900°F for 4 hr can be predicted according to the equation,

$$\text{Yield Strength (ksi)} = 38.1 + 8.8\ (\%\ \text{Co}) + 22.6\ (\%\ \text{Mo}) + 87.7\ (\%\ \text{Ti})$$

2. Rolling practice can produce differences in yield strength between transverse and longitudinal directions. The greatest differences occurred when the final rolling operation consisted of a reduction of 75% or more in one direction. Rolling practice did not appear to have a significant effect on ductility. In the bar stock tested, the transverse and short-transverse ductility were lower than in the longitudinal direction with no significant difference in strength.

3. There was no evidence that the melting process influenced the strength, ductility or cleanliness of the materials studied. Differences in the amount of banding was attributed to ingot size rather than to melting practice.

4. All of the 18% maraging steel heats, with the exception of the optimum material which was low in molybdenum content, reached their nominal yield strength on aging at 900°F for 8 hr or less. In some heats, aging for this length of time at 850 or 950°F produced a lower strength due to under-aging or overaging. Consequently, it may be necessary to determine the aging characteristics of the heats being used and their sensitivity to variation for a selected aging condition.

5. Aging the selected commercial 18% nickel maraging steels in either the as-rolled or mill-annealed condition produced strengths above the nominal grade level. The strength was increased when the as-rolled plate material was solution-annealed at 1500°F for 30 min before aging. The same tendency was observed when the mill-annealed (1500°F) plate was re-solution annealed at 1500°F for 30 min before aging.

Approved for Public Release

Contrails

6. Bueckner's solution for use in the slow-notch-bend test generally resulted in a more conservative and a more accurate measurement of plane-strain fracture toughness than Rawe's solution which uses the spring-constant technique (See Appendix IV).

7. If the spring-constant solution is used in the slow-notch-bend tests, a computer should be used in each step to eliminate the need for determining the coefficients to the equation relating b/M to the variable a. Thus, the computer would be used to:

a. obtain a least-squares best fit of the calibration data, plotting b/M vs a,

b. obtain the first derivative with respect to crack depth at any given experimental value of b/M and a, and

c. solve Irwin's equation

$$G_{Ic} = 1/2 \left(\frac{L}{b}\right)^2 d(b/M)da$$

by a direct substitution of d(b/M)da (obtained by computer during step 7b), proportional-limit load, L, and specimen width, b. Thus, the input to the computer would be the data from the initial calibration experiment, and the proportional-limit load, deflection at the proportional-limit load, and specimen width from the individual SNB test.

8. Plane-strain fracture toughness of the 18% nickel maraging steel alloys was found to be controlled primarily by yield strength, with rolling practice and banding (listed in the order of descending importance) also affecting fracture toughness. An increase in the 0.2% offset yield strength from 200 ksi to 300 ksi reduced the plane-strain fracture toughness from approximately 300 in.-lb/in.^{2} to less than 100 in.-lb/in.^{2} The relationship between strength and toughness overshadowed all other variables. The effects of steel-mill processing and banding on fracture toughness are interrelated; both had a marked effect by producing anistropy. Examination of these variables indicated that, when the material is rolled from slab to plate, the straight-away and cross-rolling passes should be balanced.

9. The effect of melting practice on fracture toughness was over-shadowed by the dominating effects of strength and rolling practice. There was no conclusive evidence of a difference in fracture toughness between air-melt, vacuum-degassed and vacuum-arc-remelted steel.

10. The 18% nickel maraging steel alloys are readily adapted to welding operations. These materials can be welded with TIG, MIG or submerged-arc welding processes without preheating or postheating provided that proper weld shielding procedures, flux, and filler wire compositions are used.

11. TIG weldments with tensile and fracture toughness properties comparable to those of the base metal can be achieved in Grades 200 and 250 plate material through proper selection of weld-filler-wire composition.

Approved for Public Release

Contrails

12. Weld-Filler-wires that produce weld metals with tensile yield strengths only slightly higher than the minimum yield strength of the base plate should be used to obtain maximum fracture toughness. The use of weld-filler-wires that greatly overmatch the tensile strength of the base plate should be avoided from the standpoint of fracture toughness.

13. The aging response characteristics of weldments are comparable to those of wrought base plate. Heat-treating sequences in which the base metals and welded joints were aged simultaneously developed comparable tensile and fracture toughness in both the base metals and weldments. Also, on the basis of tensile properties, similar results are obtained by aging the base metals prior to welding and locally aging the weldments.

14. Additional fracture toughness data on welded joints are needed to compare the TIG, MIG, and submerged-arc welding processes and to fully evaluate the effects of weldment heat-treating sequence.

Approved for Public Release

Contrails

SECTION 6 - RECOMMENDATIONS

The results of this program reveal several areas in which either test data, knowledge, or both, are lacking and which require further investigation. These areas are described specifically in the following paragraphs.

A. Studies should be performed to accurately determine the effects of various solution-annealing treatments on the tensile, fracture toughness, and metallurgical properties of 18% nickel maraging steel alloys and to relate these effects to variations in mill-processing variables.

B. The relationship developed in this program between strength and chemical composition should be verified and similar studies relating composition to fracture toughness should be conducted. These studies should utilize the results of this program as a starting basis and include the production and evaluation of additional heats of material in order to establish ratios of cobalt, molybdenum, and titanium that provide optimum combinations of strength and toughness.

C. Overaging and underaging should be evaluated as a means of improving fracture toughness.

D. The transformation kinetics of the 18% nickel maraging steel alloys should be determined and studies should be undertaken to determine how these kinetics are affected by the alloying element (cobalt, molybdenum, titanium and nickel) content, cooling rate from the solution-treating temperature, and section size.

E. Evaluation of MIG and submerged-arc welding processes for the fabrication of large-diameter, solid-rocket motor chambers should be continued.

F. The effects of composition and multiple thermal-cycles on weld-metal transformation kinetics and on tensile, fracture toughness, and metallurgical properties should be evaluated.

G. The effects of residual stresses on weldment tensile and fracture toughness properties should be evaluated.

H. Techniques for the reduction or elimination of banding and weld-zone segregation should be developed and evaluated.

Approved for Public Release

Contrails

SECTION 7 - REFERENCES

1. E. C. Bryant, Statistical Analysis, New York, McGraw-Hill, 1960.

2. D. H. Winne and B. M. Wundt, "Application of the Griffith-Irwin Theory of Crack Propagation to the Bursting Behavior of Disks, Including Analytical and Experimental Studies," Trans. ASME, Vol. 80, pp. 1643-1658 (1958); also, B. M Wundt, A Unified Interpretation of Room-Temperature Strength of Notched Specimens as Influenced by Their Size, ASME Paper 59-MET-9, 1959.

3. H. F. Bueckner, The Stress Concentration of a Notched Bar in Bending, Large Steam Turbine-Generator Department, General Electric Company, Data Folder, 28 June 1957; also, H. F. Bueckner, On the 3-Point Bar Bending Test, Large Steam Turbine-Generator Department, General Electric Company, Data Folder, 14 June 1957.

4. G. M. Orner and C. E. Hartbower, "The Low-Blow Transition Temperature," ASTM Proc., Vol. 58, p. 623 (1958); also, G. M. Orner and C. E. Hartbower, "Sheet Fracture Toughness Evaluated by Charpy Impact and Slow Bend," The Welding Journal, Vol. 40, No. 9 (Sep 1961), p. 405-s.

5. G. M. Orner and C. E. Hartbower, "Transition-Temperature Correlations in Contructional Alloy Steels," The Welding Journal, Vol. 40, No. 9 (Sep 1961), p. 459-s.

Approved for Public Release

Contrails

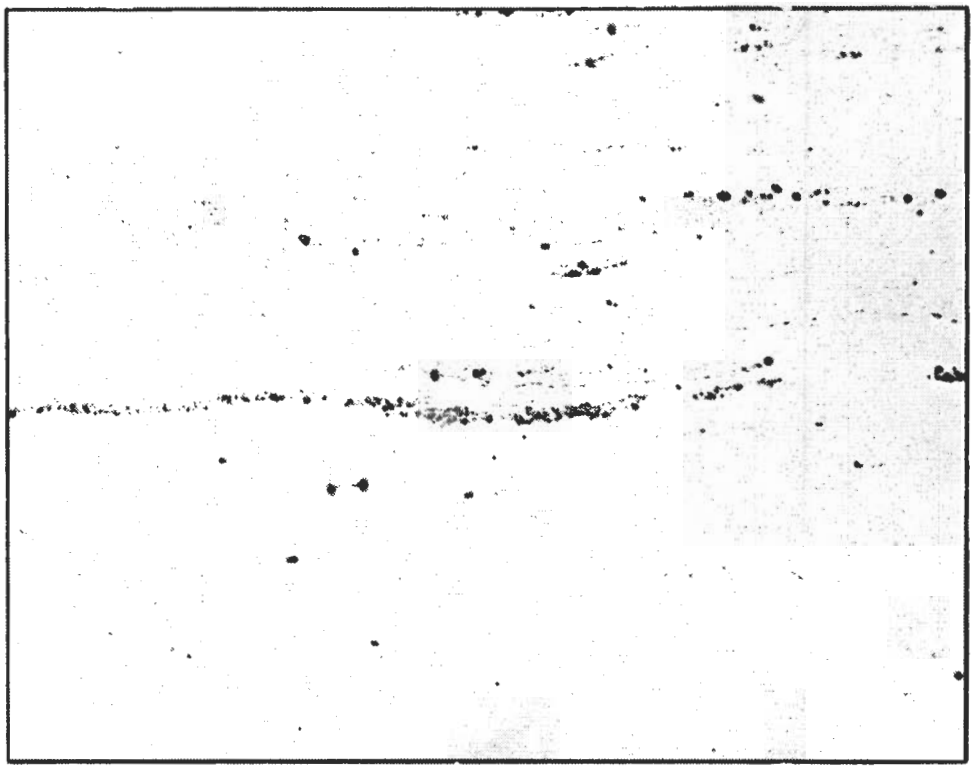

As Polished Magnification: 100X

Figure 1. Inclusion Content of Grade 250, Vacuum-Arc-Remelted 18% Nickel Maraging Steel, Heat 3888471

Approved for Public Release

Contrails

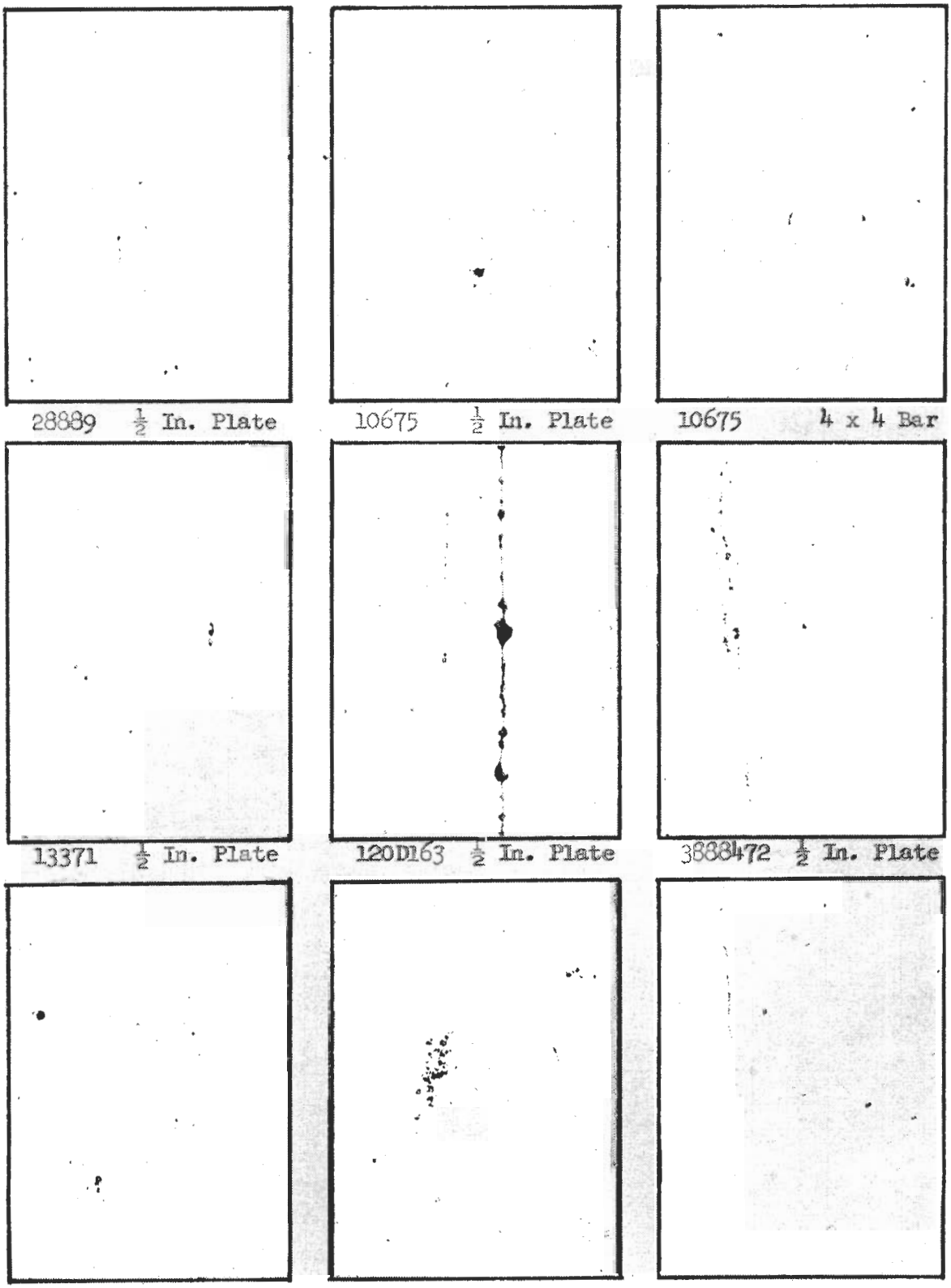

Figure 2. Comparison of Microcleanliness of Seven Commercial Heats of 18% Nickel Maraging Steel

Approved for Public Release

Contrails

Mill Annealed

Re-Solution Annealed at 1500°F for 30 Minutes

Etchant - 5% Chromic Acid Electrolytic

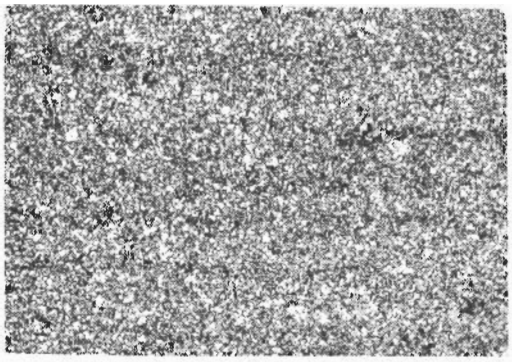

10675 ½ In. Plate

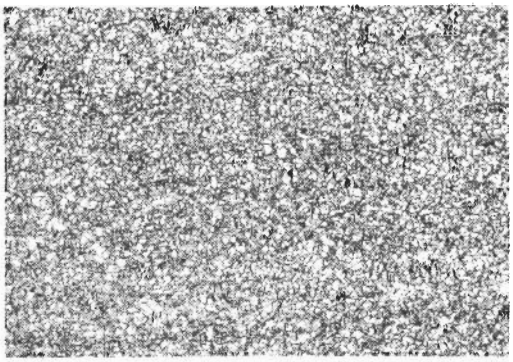

10675 ½ In. Plate

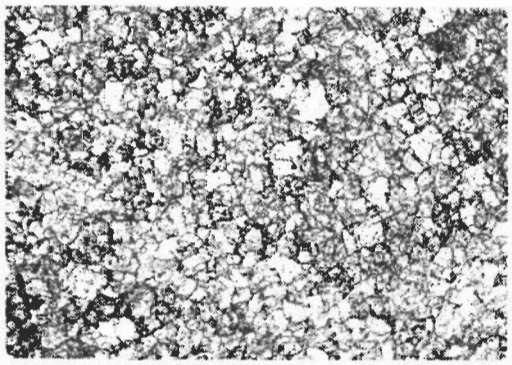

10675 4 x 4 Bar

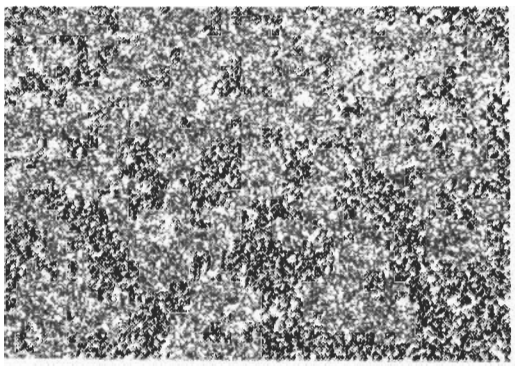

10675 4 x 4 Bar

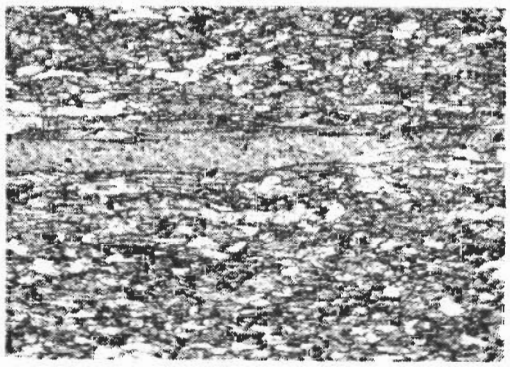

28889 ½ In. Plate

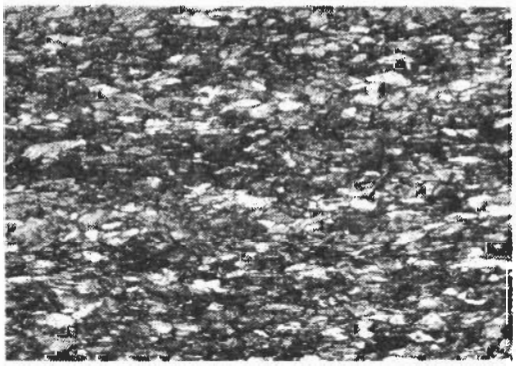

28889 ½ In. Plate

Magnification 100X

All Specimens Aged at 900°F for 8 Hours

Figure 3. Comparison of Typical Grain Size in Commercial Heats of Grade 200, 18% Nickel Maraging Steel

Approved for Public Release

Contrails

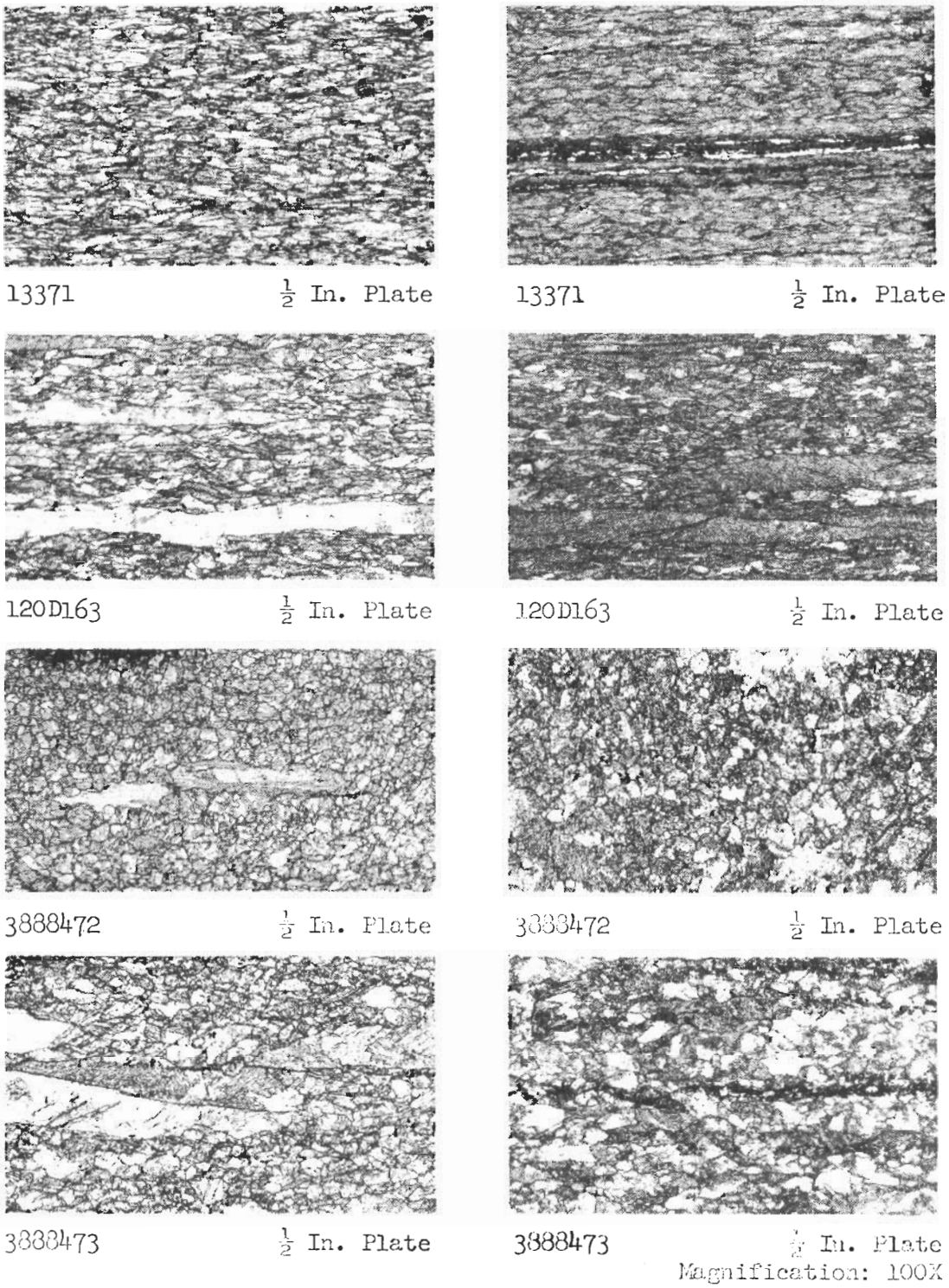

All Specimens Aged at 900°F for 8 Hours

Figure 4. Comparison of Typical Grain Size in Commercial Heats of Grade 250, 18% Nickel Maraging Steel

Approved for Public Release

Contrails

Mill Annealed

Re-Solution Annealed at 1500°F for 30 Minutes

Etchant: - 5% Chromic Acid Electrolytic

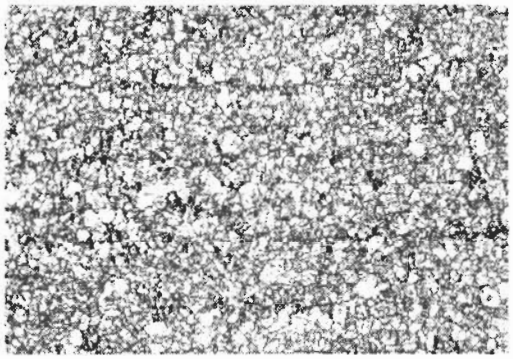

07148 ½ In. Plate

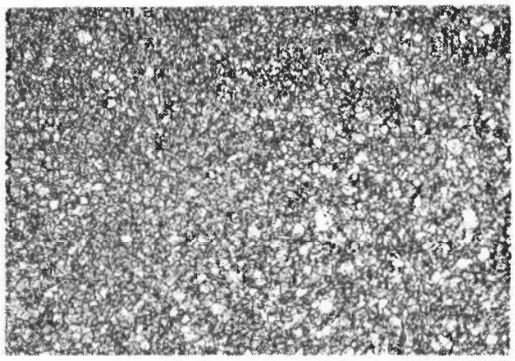

07148 ½ In. Plate

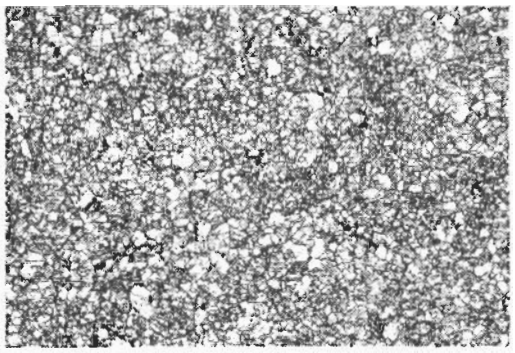

07148 4 x 4 Bar

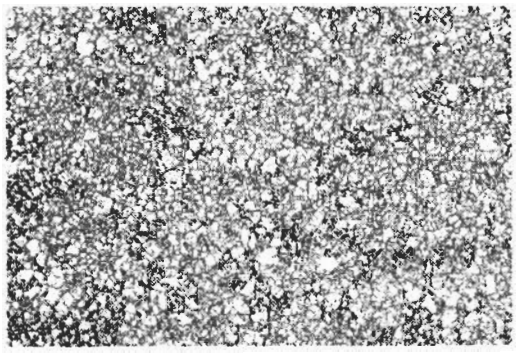

07148 4 x 4 Bar

Magnification: 100X

All Specimens Aged at 900°F for 8 Hours

Figure 5. Typical Grain Size of Commercial Heat of Grade 300, 18% Nickel Maraging Steel

Approved for Public Release

Contrails

Mill Annealed

Re-Solution Annealed at 1500°F for 30 Minutes

Etchant - Marbles Reagent

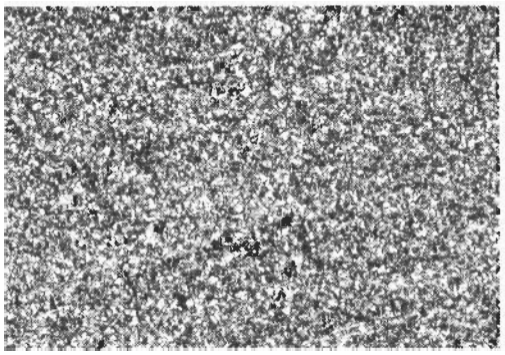

10675 ½ In. Plate

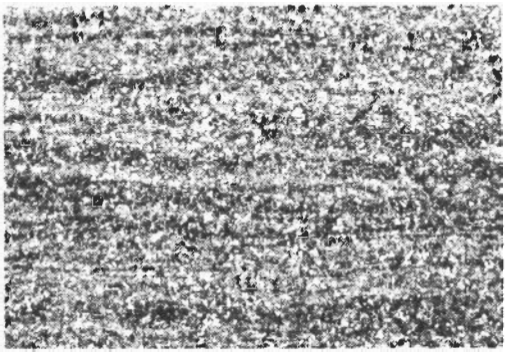

10675 ½ In. Plate

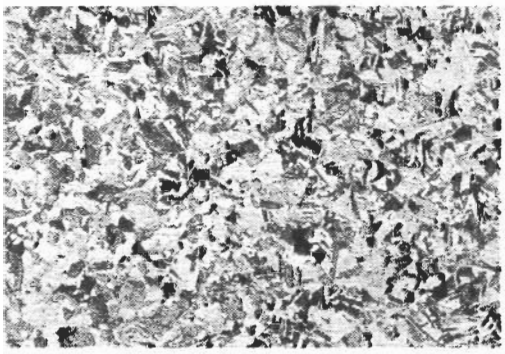

10675 4 x 4 Bar

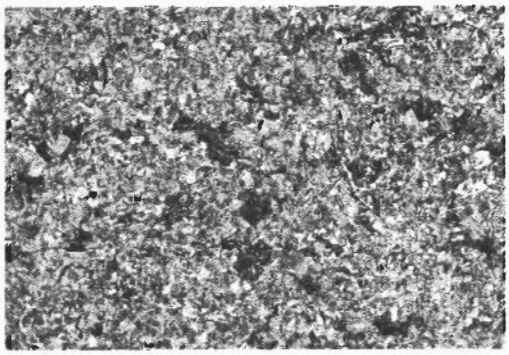

10675 4 x 4 Bar

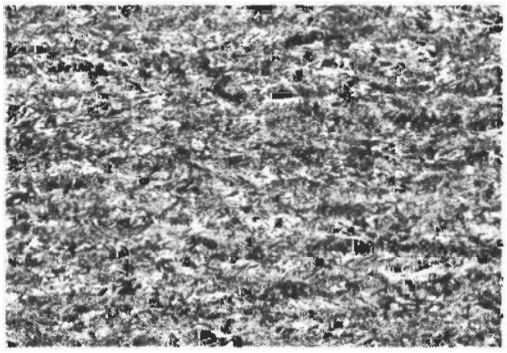

23839 ½ In. Plate

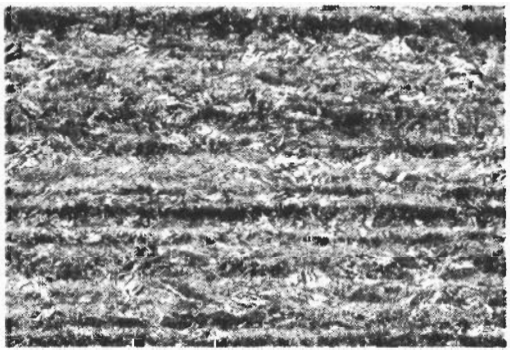

23839 ½ In. Plate

Magnification: 100X

All Specimens Aged at 900°F for 8 Hours

Figure 6. Comparison of Typical Banding in Commercial Heats of Grade 200, 18% Nickel Maraging Steel

Approved for Public Release

Contrails

As Rolled

Solution Annealed at 1500° F for 30 Minutes

Etchant - Marbles Reagent

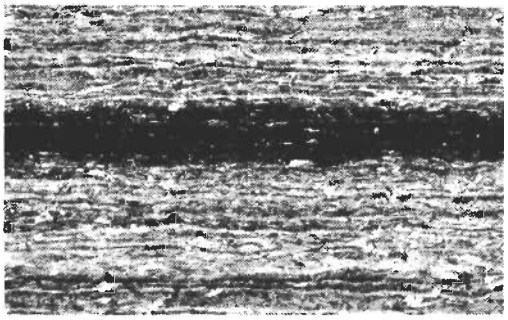

13371 ½ In. Plate

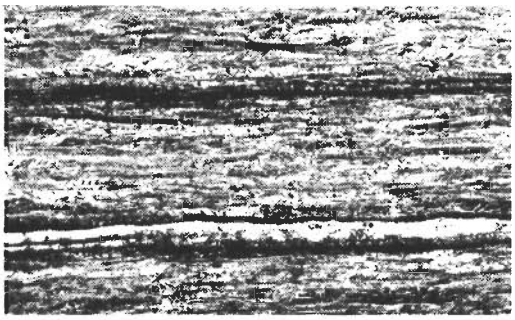

13371 ½ In. Plate

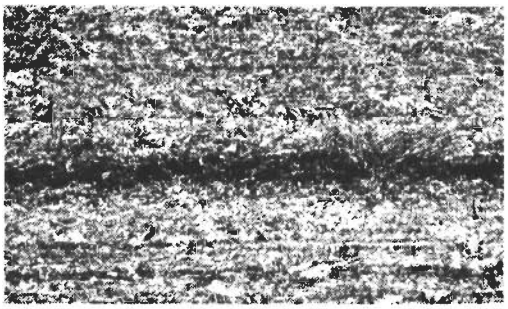

120D163 ½ In. Plate

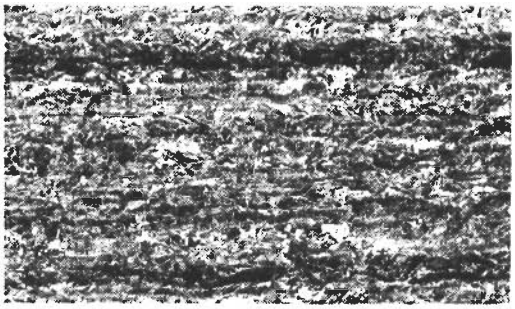

120D163 ½ In. Plate

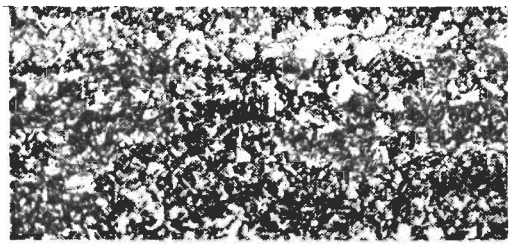

3888472 ½ In. Plate

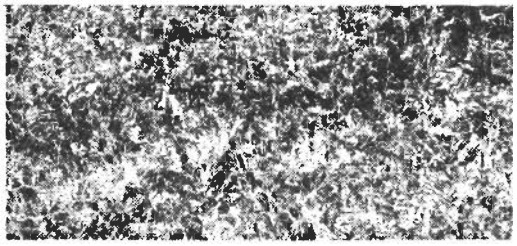

3888472 ½ In. Plate

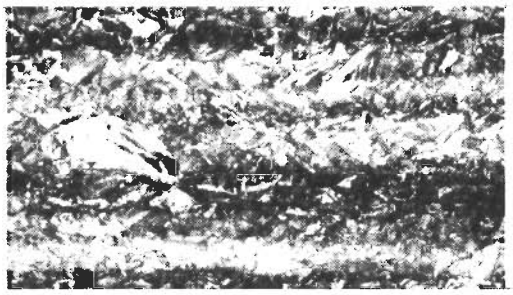

3888473 ½ In. Plate

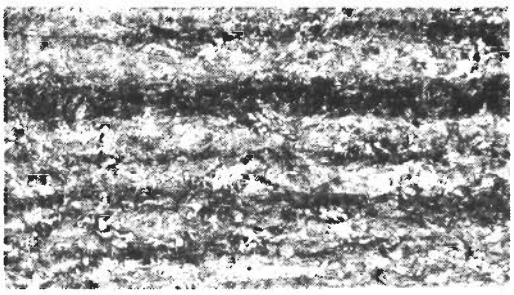

3888473 ½ In. Plate

Magnification: 100X

All Specimens Aged at 900° F for 8 Hours

Figure 7. Comparison of Typical Banding in Commercial Heats of Grade 250, 18% Nickel Maraging Steel

Approved for Public Release

Contrails

Mill Annealed

Re-Solution Annealed at 1500°F for 30 Minutes

Etchant: Marbles Reagent

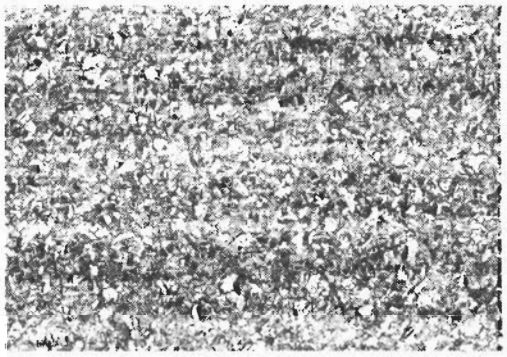

07148 ½ In. Plate

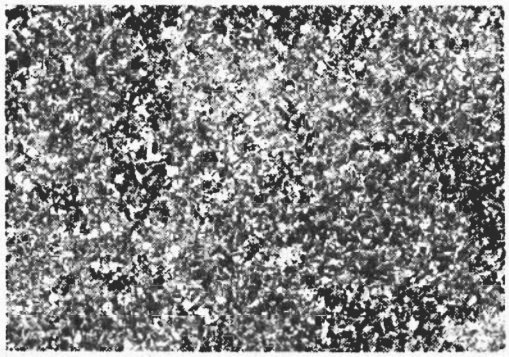

07148 ½ In. Plate

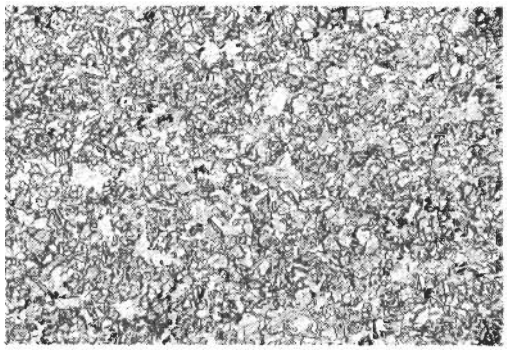

07148 4 x 4 Bar

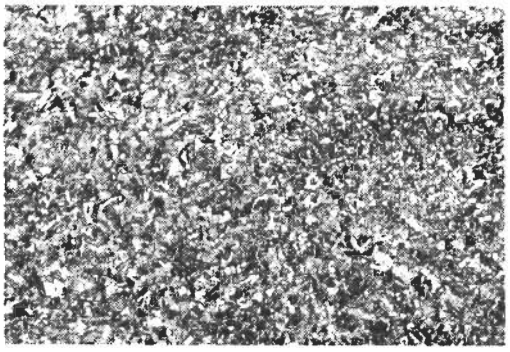

07148 4 x 4 Bar

Magnification: 100X

All Specimens Aged at 900°F for 8 Hours

Figure 8. Typical Banding in Commercial Heat of Grade 300, 18% Nickel Maraging Steel

Approved for Public Release

Approved for Public Release

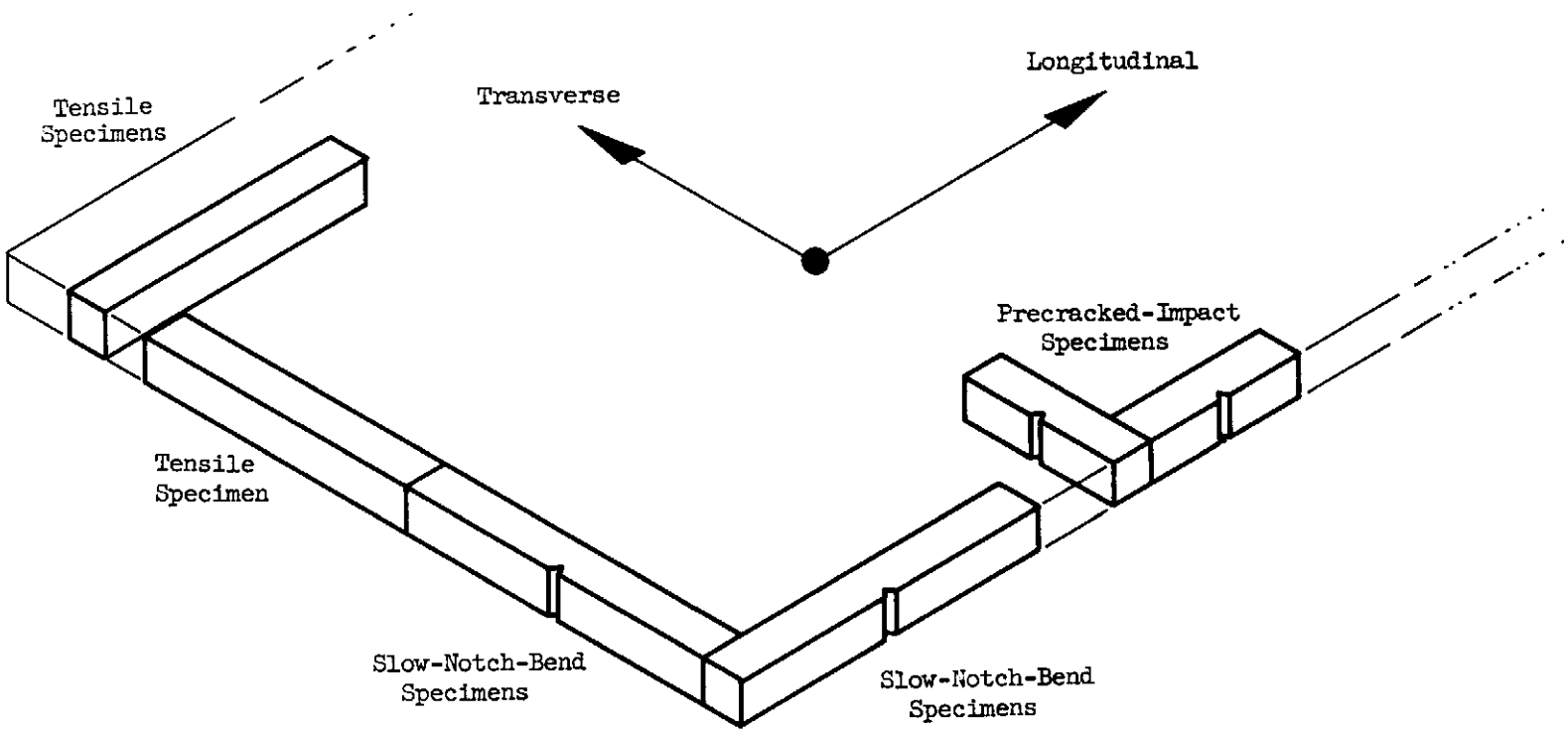

Figure 9. Typical Orientation of Test Specimens in $\frac{1}{2}$-In.-Thick Plate

Contrails

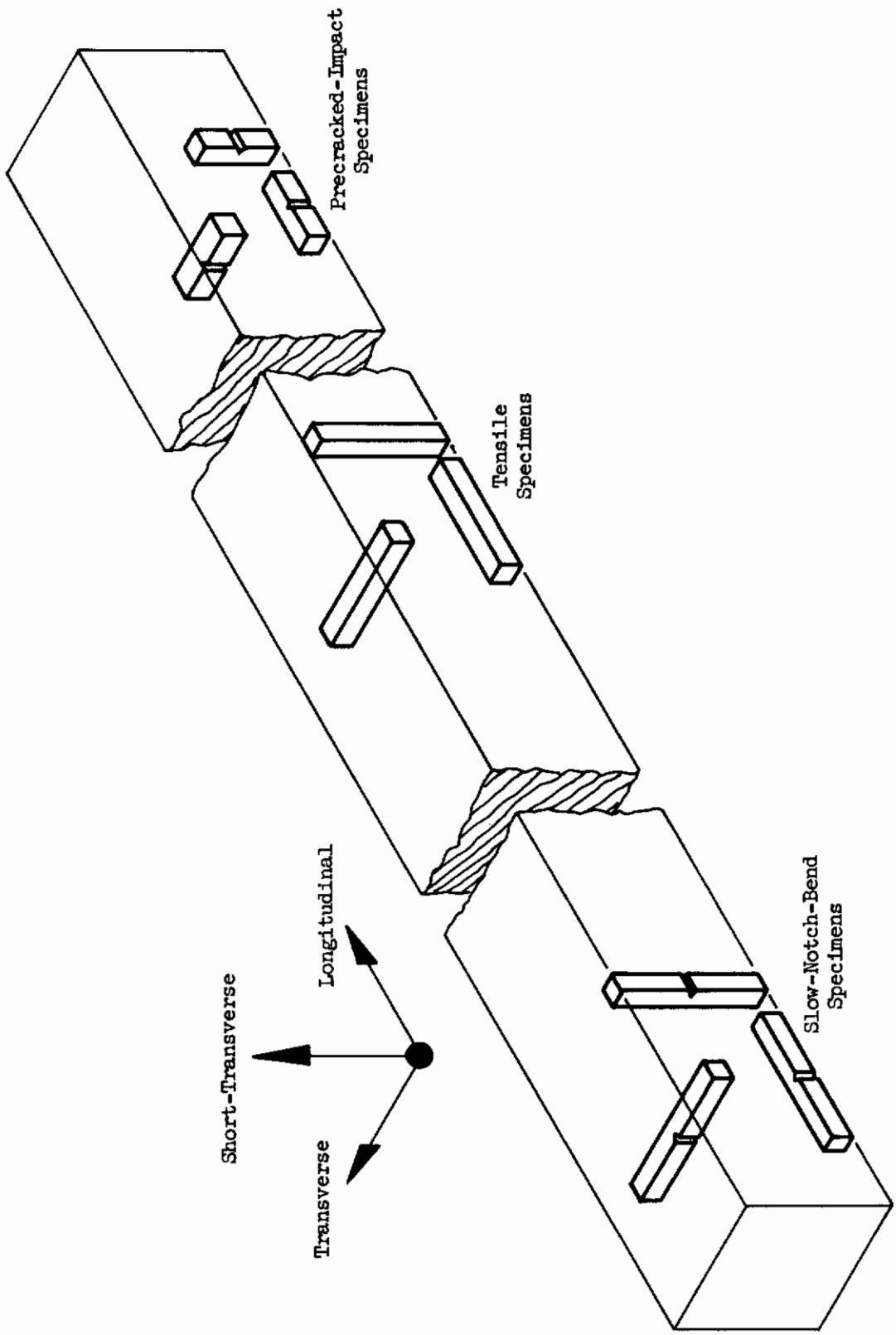

Figure 10. Typical Orientation of Test Specimens in 4 x 4-In. Bar Stock

Approved for Public Release

Contrails

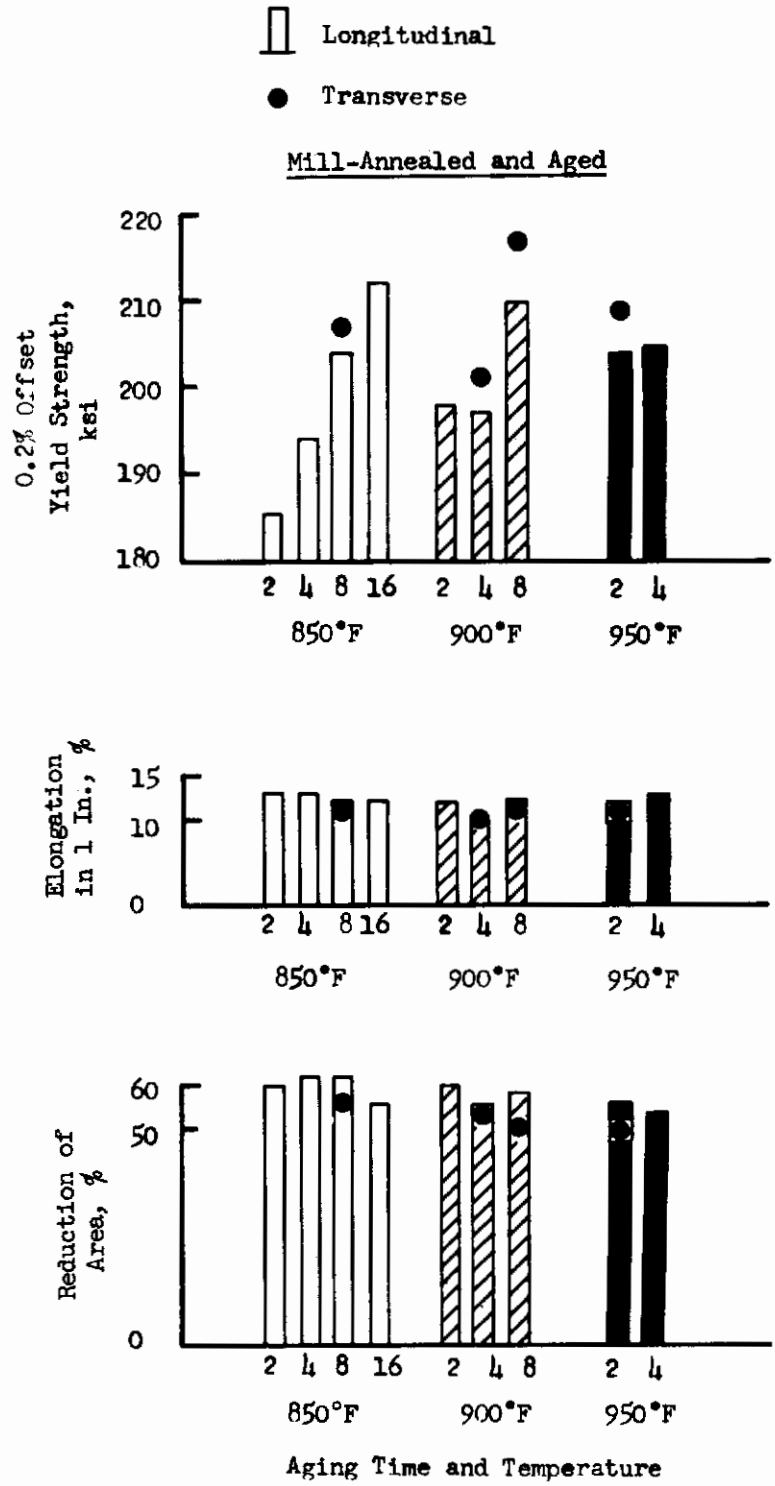

Figure 11. Effects of Aging Time and Temperature on Tensile Properties of Grade 200, 18% Nickel Maraging Steel, ½-In.-Thick Plate Material, Heat 28889

Approved for Public Release

Contrails

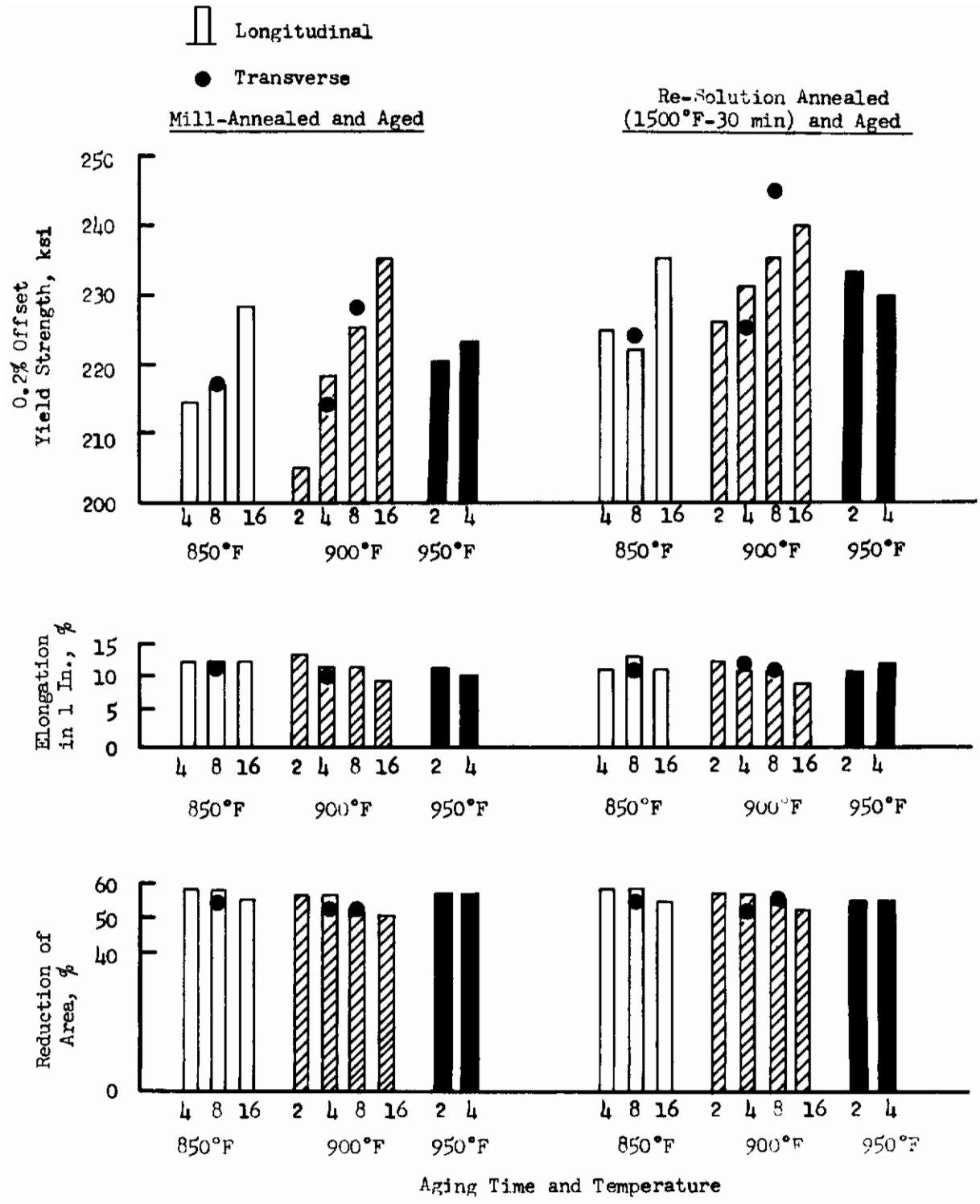

Figure 12. Effect of Aging Time and Temperature on Tensile Properties of Grade 200, 18% Nickel Maraging Steel, $\frac{1}{2}$-In.-Thick Plate Material, Heat 10675

Approved for Public Release

Contrails

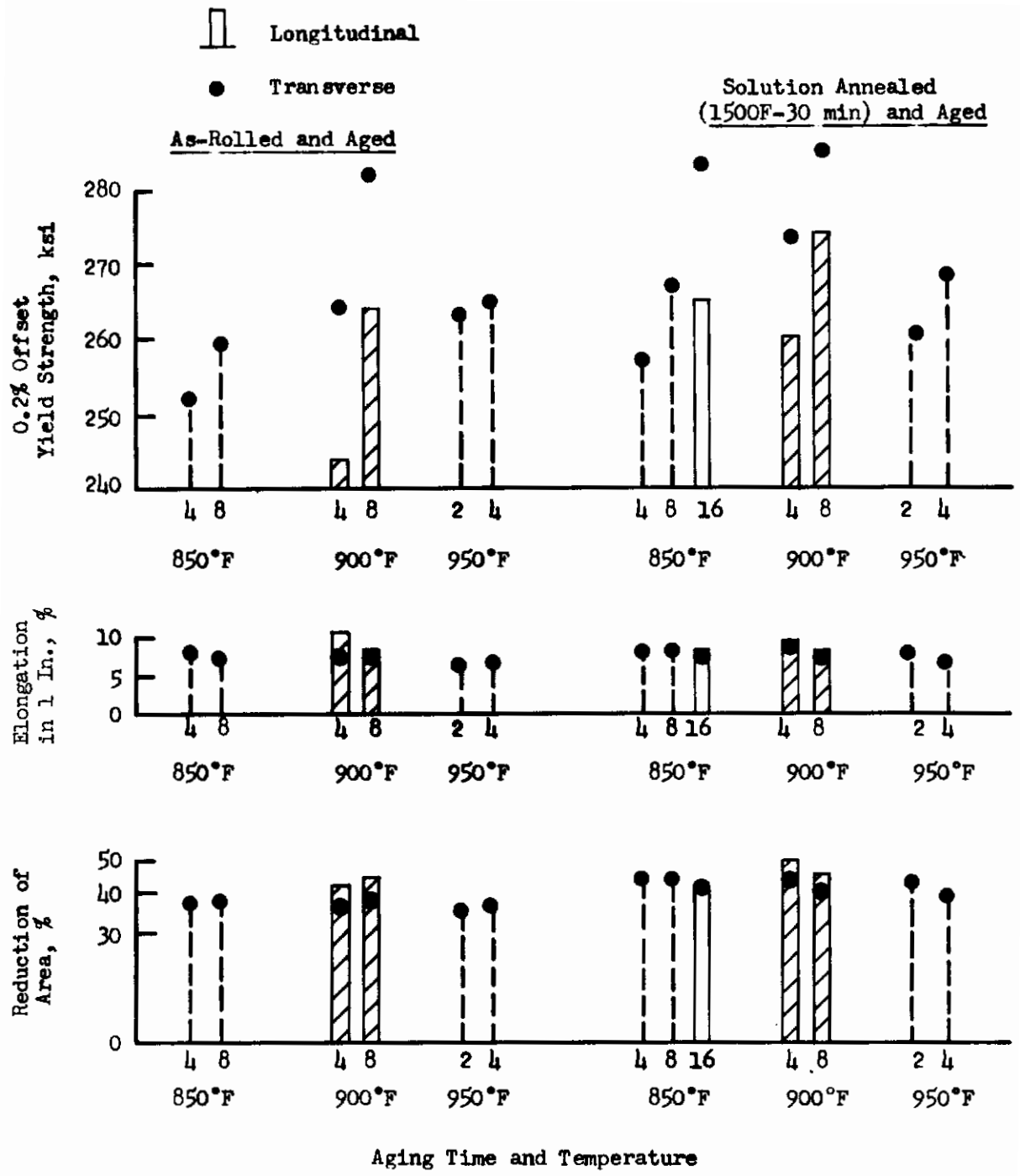

Figure 13. Effect of Aging Time and Temperature on Tensile Properties of Grade 250, 18% Nickel Maraging Steel, $\frac{1}{2}$-In.-Thick Plate Material, Heat 13371

Approved for Public Release

Contrails

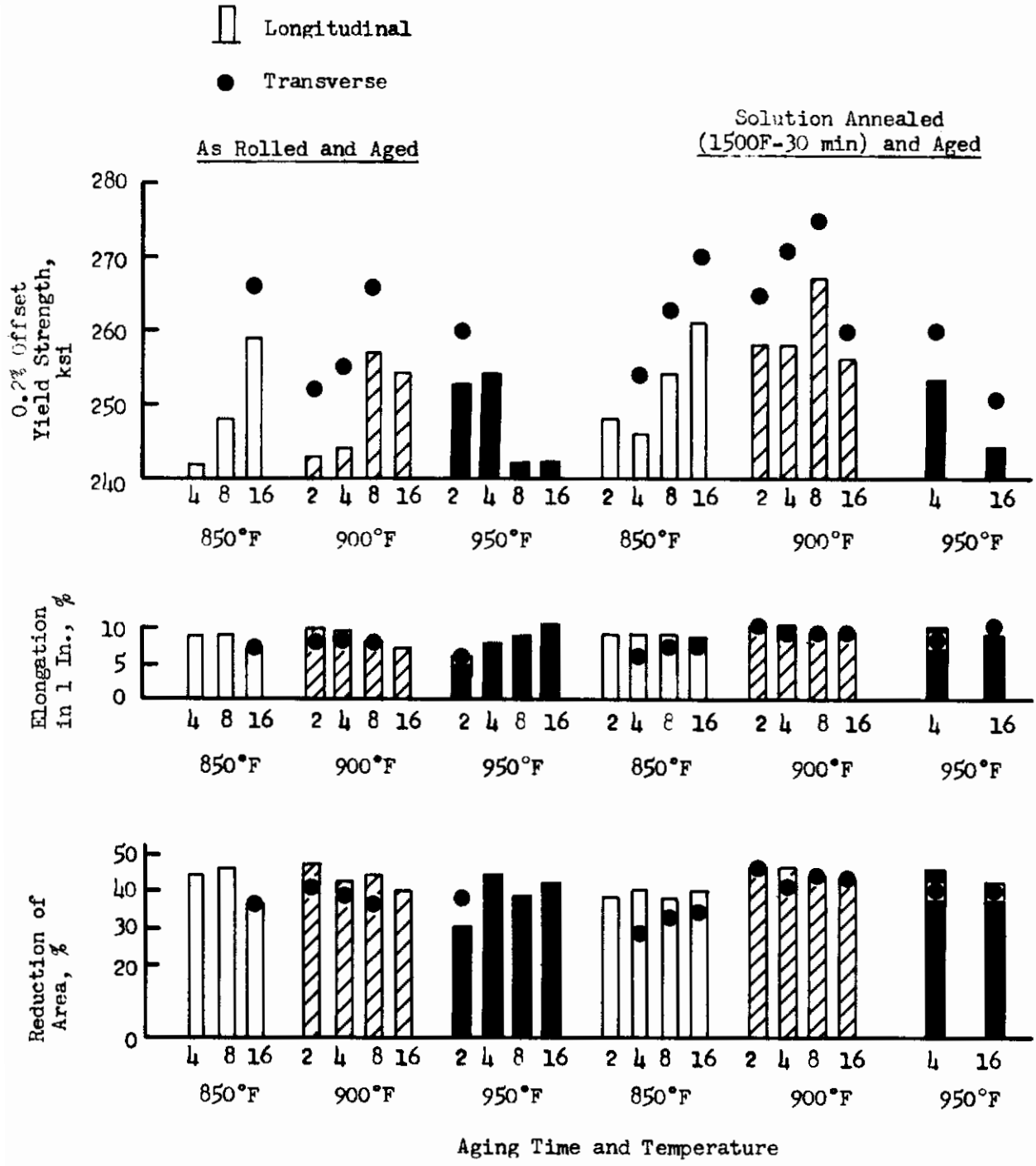

Figure 14. Effect of Aging Time and Temperature on Tensile Properties of Grade 250, 18% Nickel Maraging Steel, $\frac{1}{2}$-In.-Thick Plate Material, Heat 120D163

Approved for Public Release

Contrails

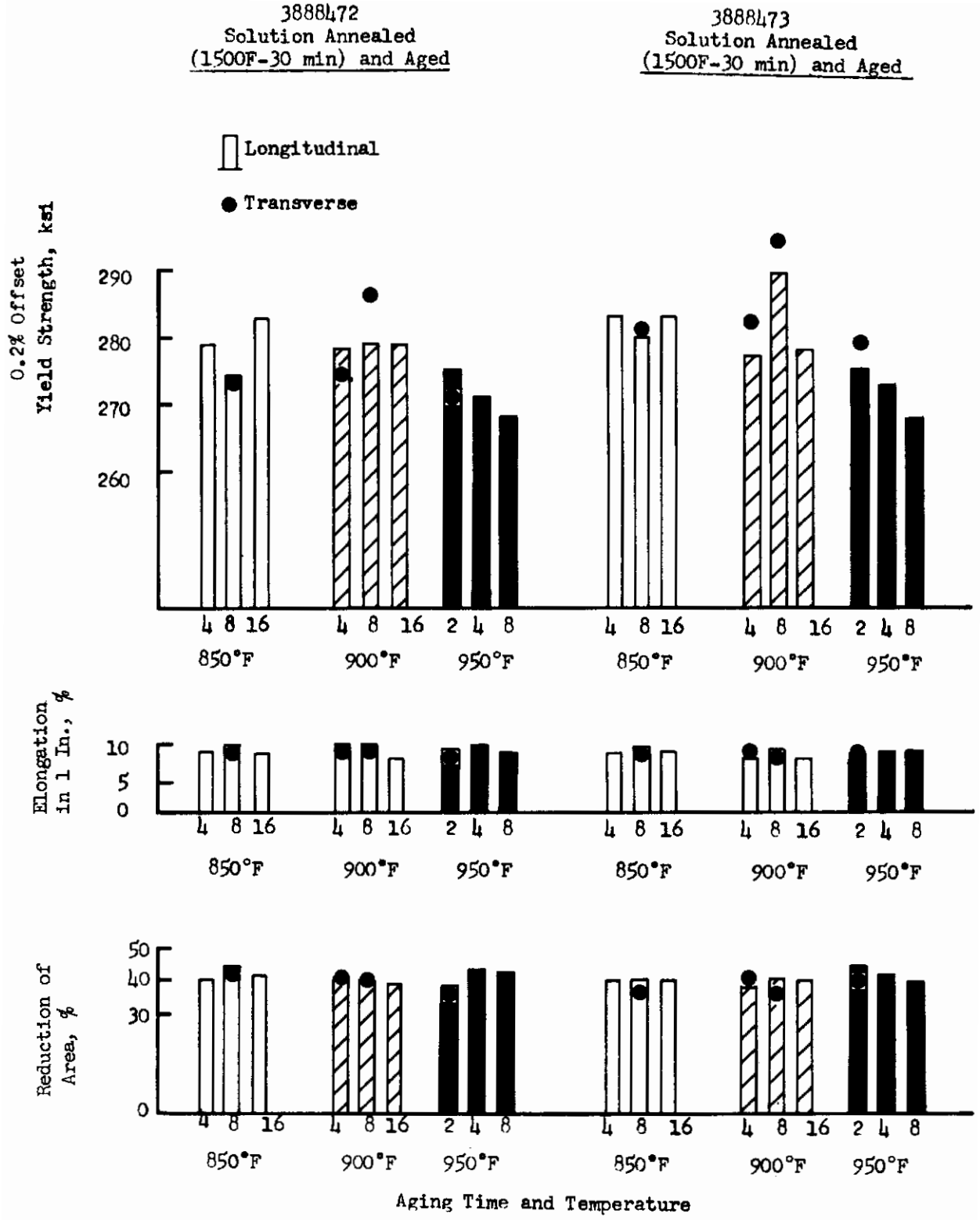

Figure 15. Effect of Aging Time and Temperature on Tensile Properties of Grade 250, 18% Nickel Maraging Steel, 1/2-In.-Thick Plate Material Heats 3888472 and 3888473

Approved for Public Release

Contrails

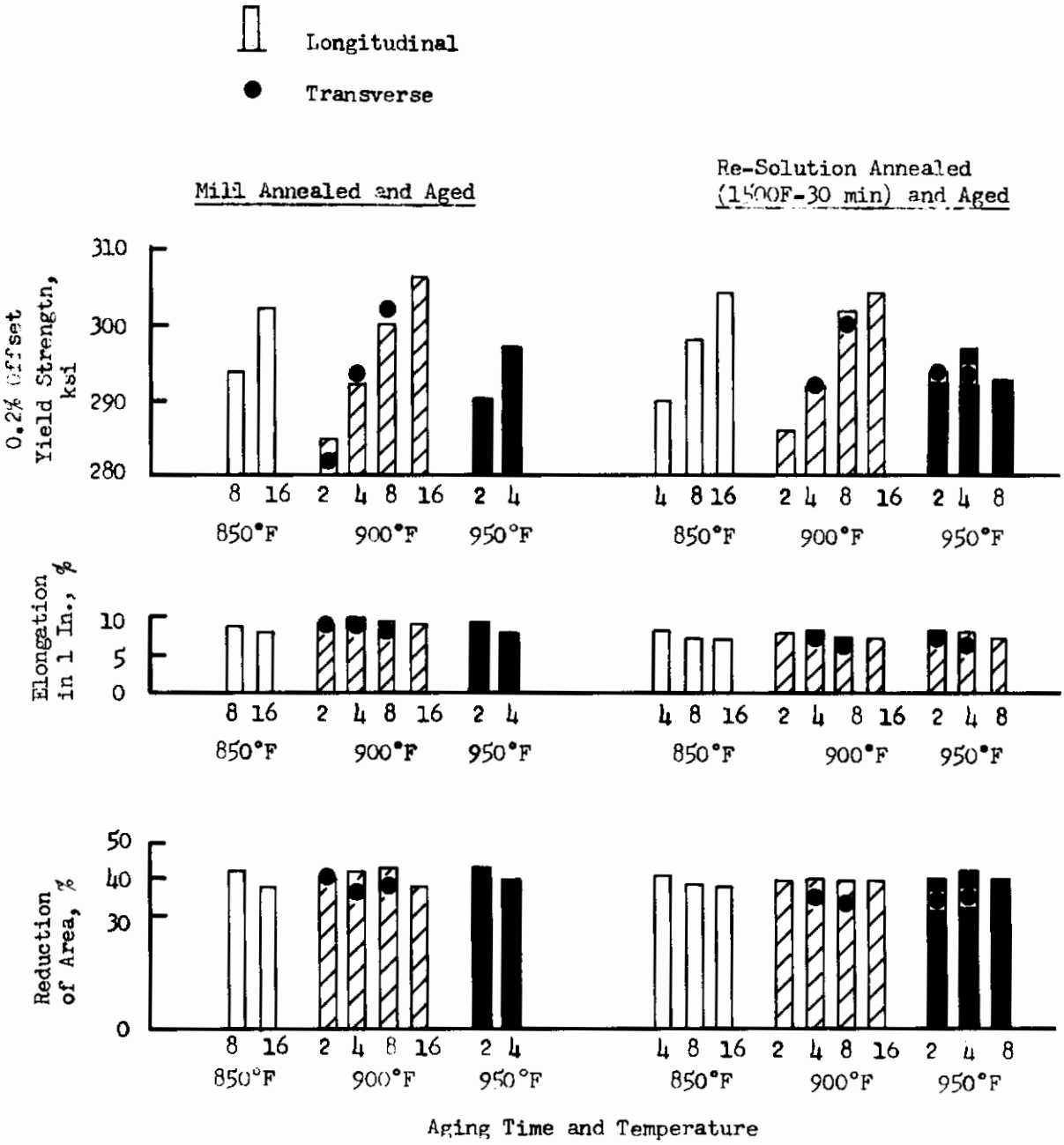

Figure 16. Effect of Aging Time and Temperature on Tensile Properties of Grade 300, 18% Nickel Maraging Steel, 1/2-In.-Thick Plate Material, Heat 07148

Approved for Public Release

Contrails

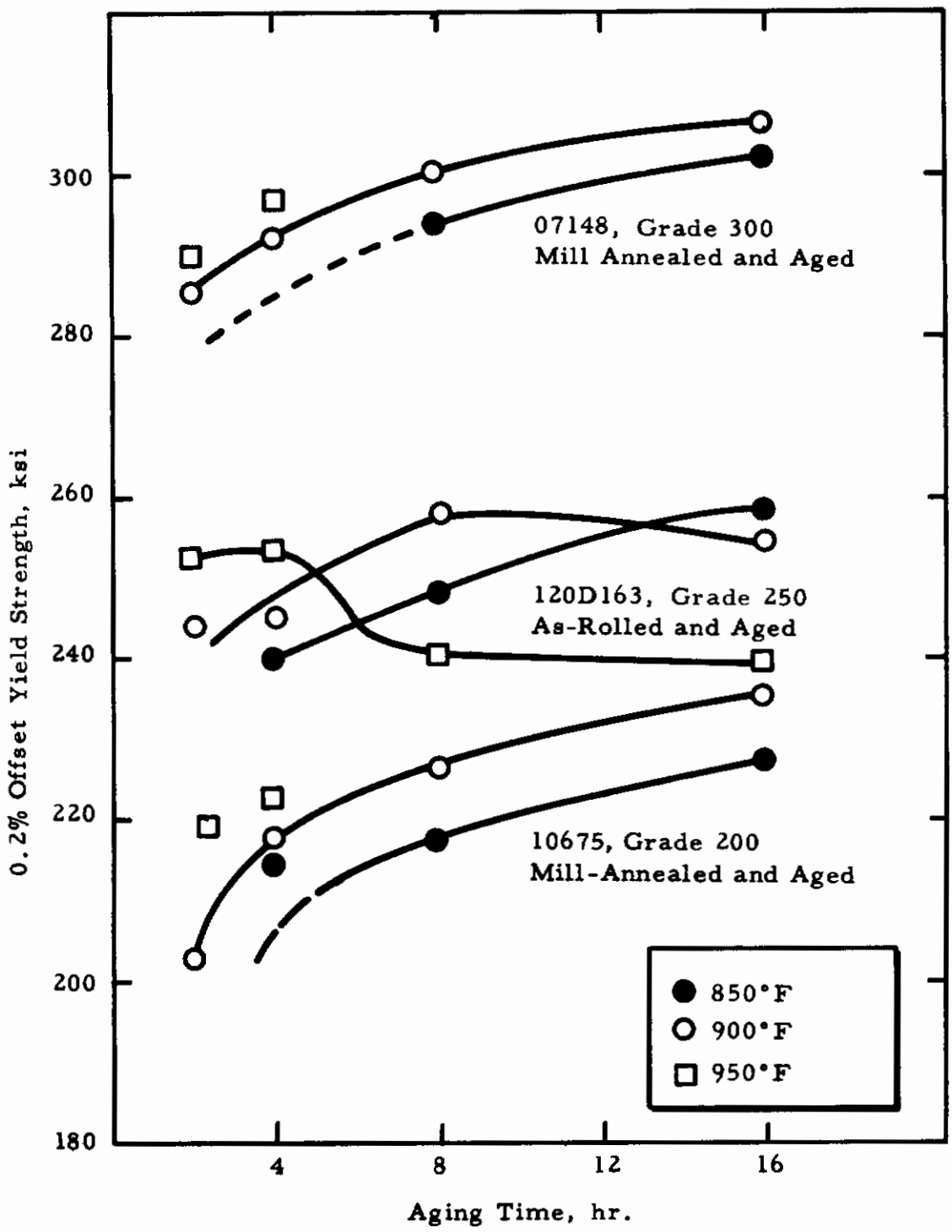

Figure 17. Typical Aging Response Characteristics of Three Heats of 18% Nickel Maraging Steel, 1/2-In.-Thick Plate

Approved for Public Release

Contrails

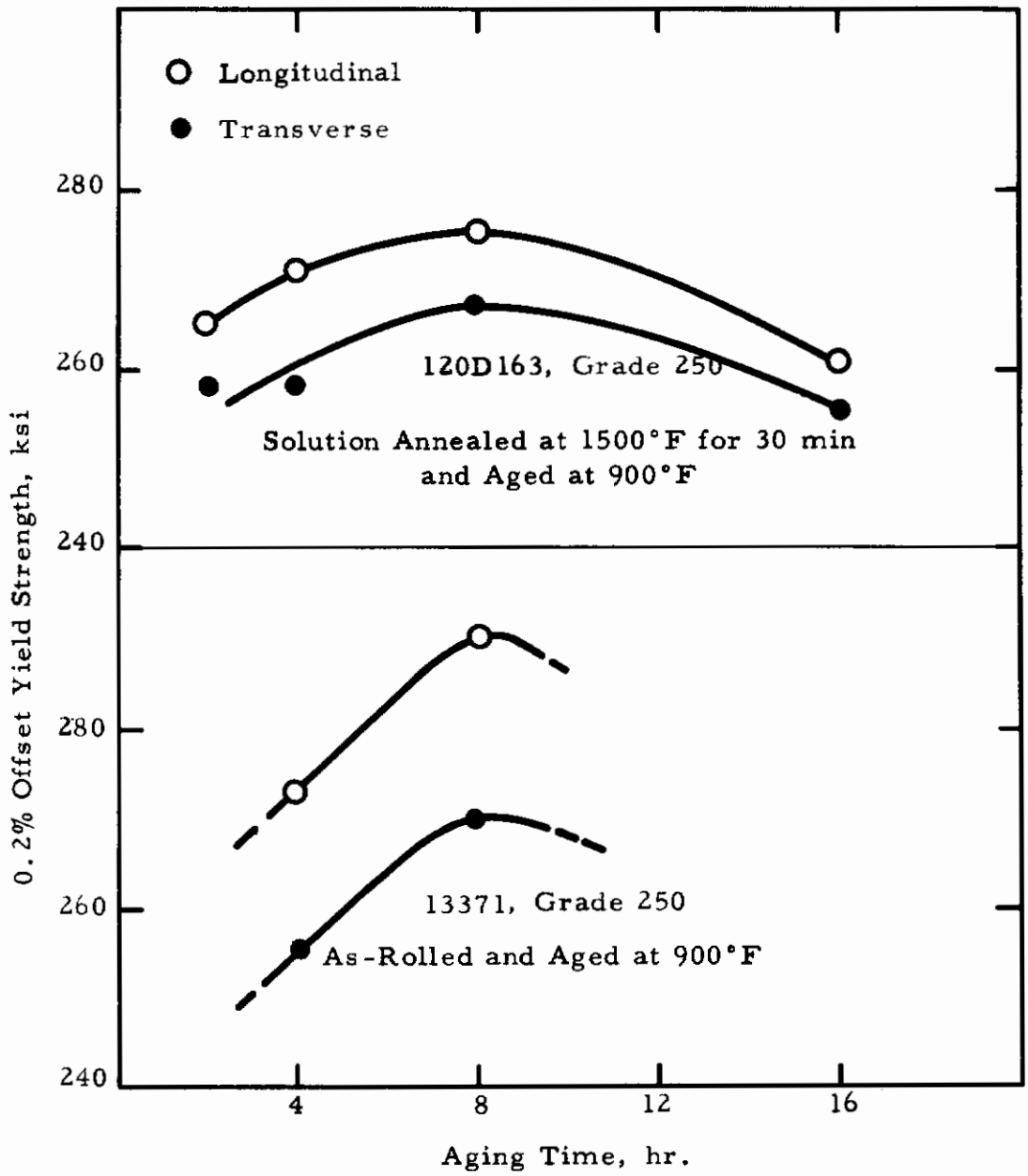

Figure 18. Comparison of Directional Properties in Two Heats of 18% Nickel Maraging Steel, 1/2-In.-Thick Plate

Approved for Public Release

Contrails

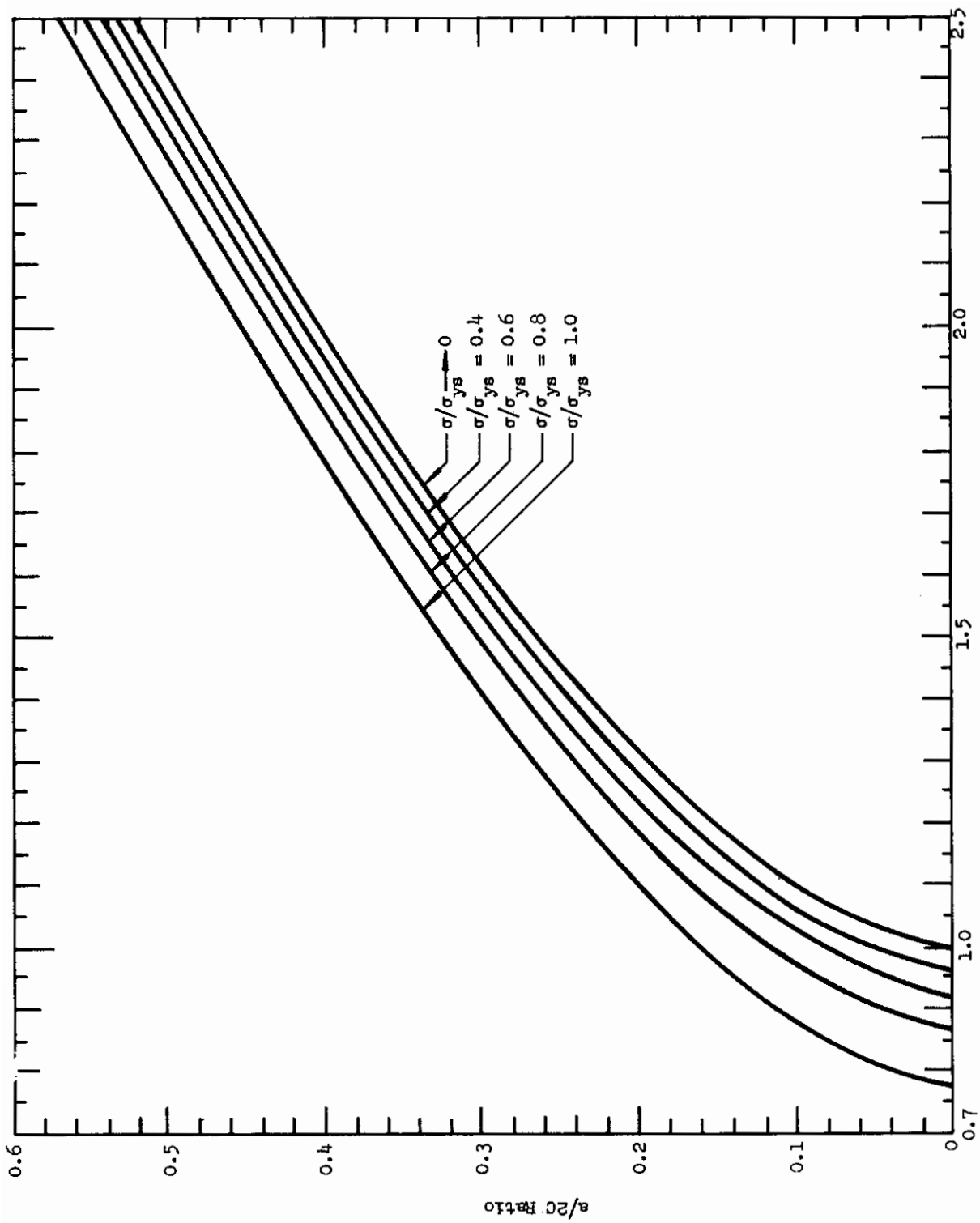

Figure 19. Flaw-Shape Parameter for Surface and Embedded Flaws

Approved for Public Release

Contrails

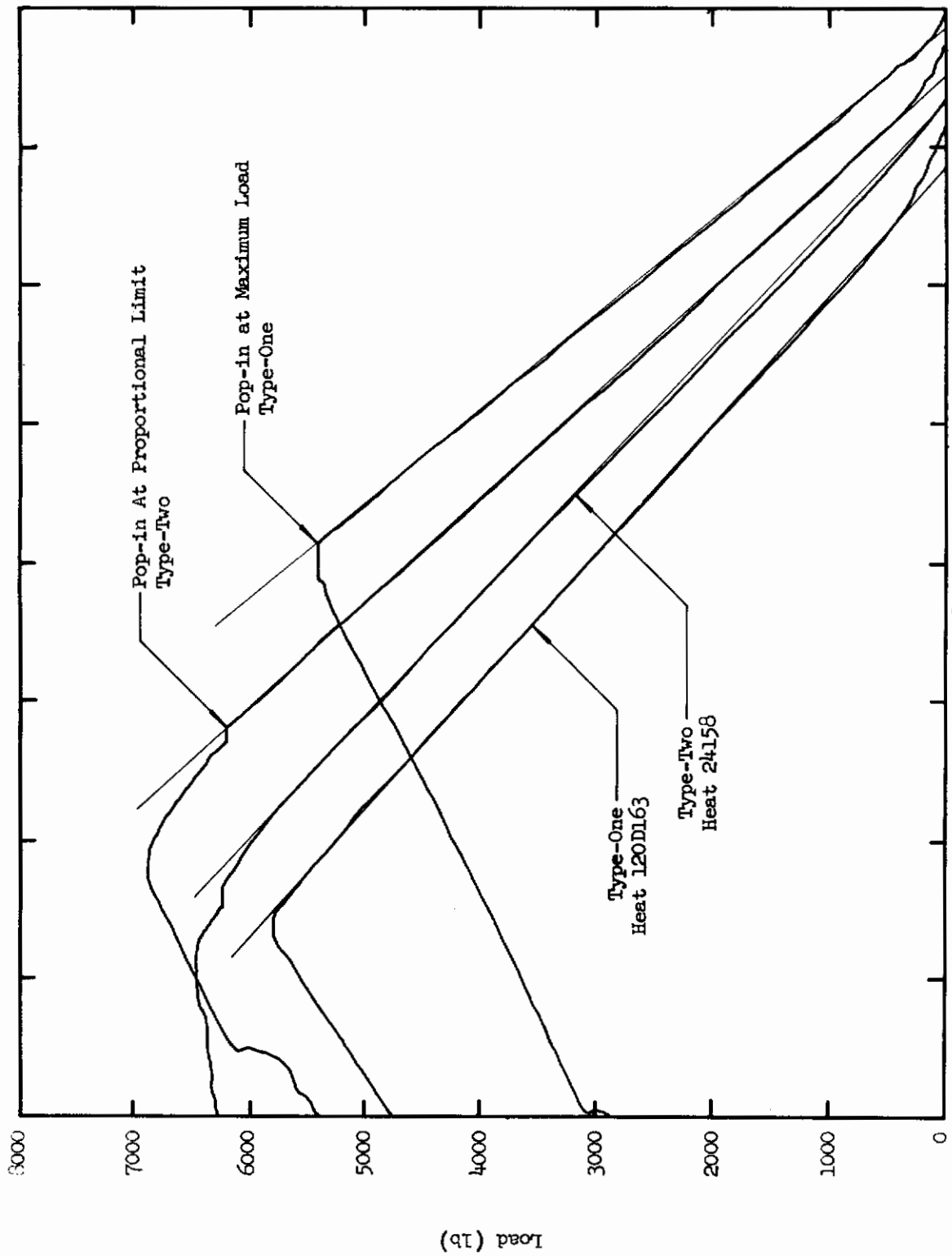

Figure 20. Typical Load-Deflection Diagrams in the Slow-Notch-Bend Test

Approved for Public Release

Contrails

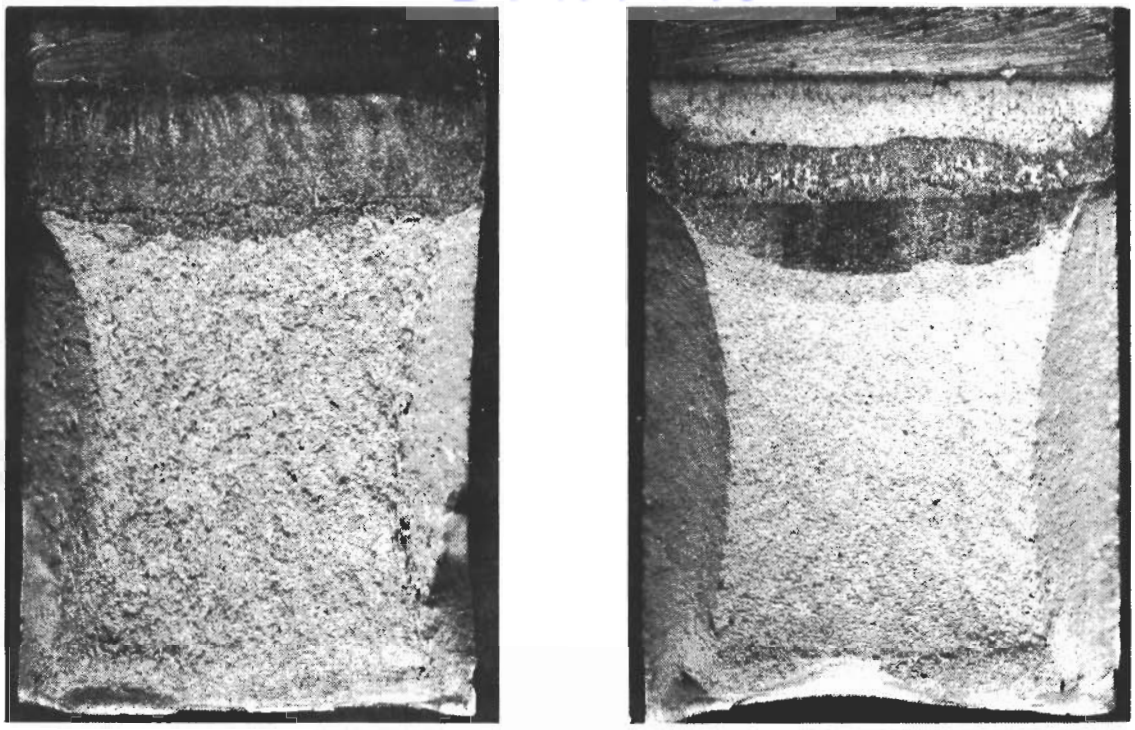

Point A

Point B

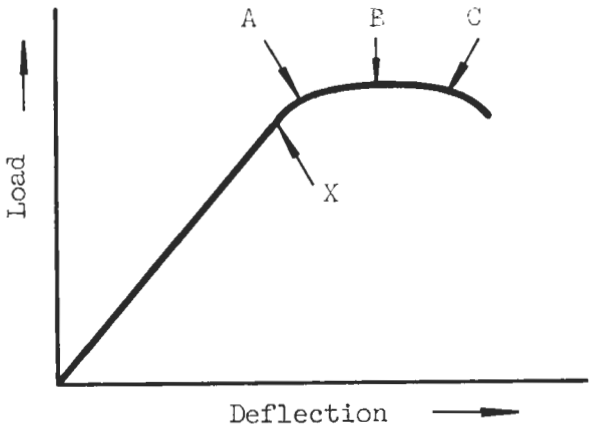

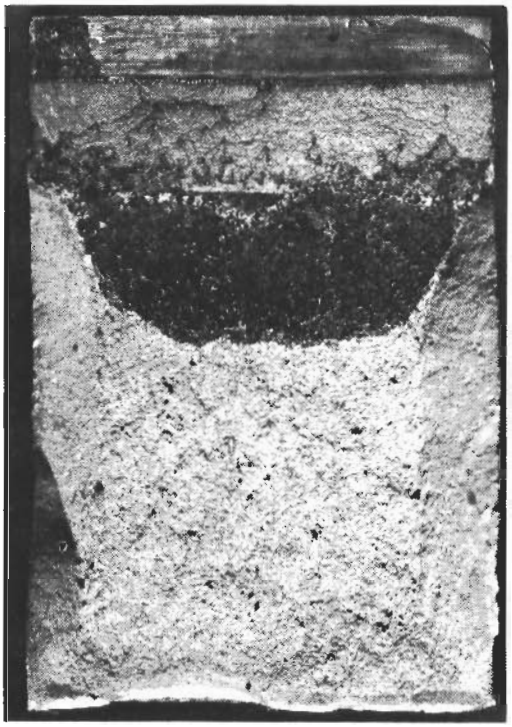

Point C

Figure 21. Relationship Between Crack Growth and Load-Deflection. Point X (Proportional-Limit Load) Indicates Load and Deflection Values Used in Calculating Fracture Toughness

Approved for Public Release

Contrails

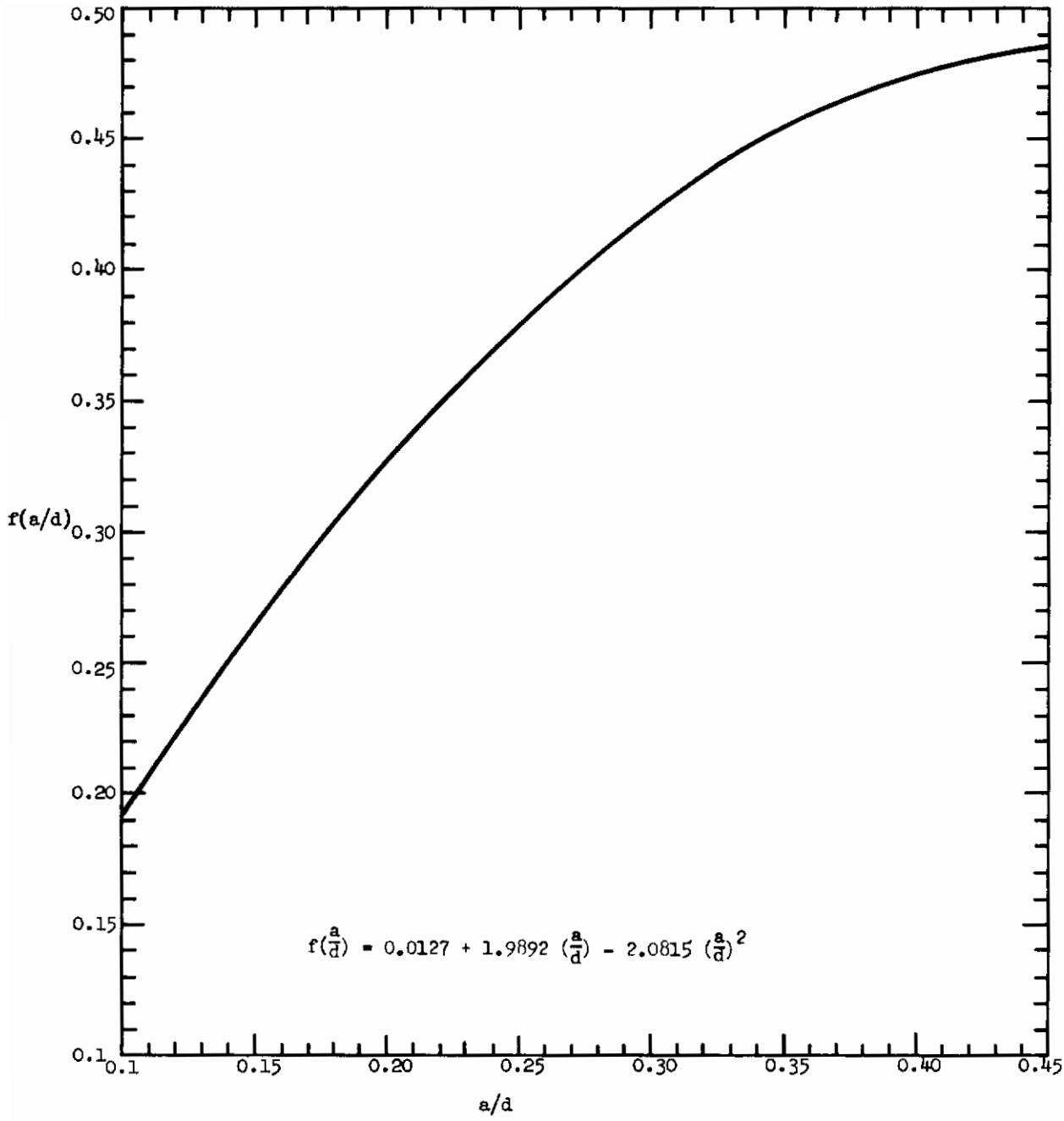

Figure 22. Strain-Energy Release Rate for Notched Beams in Three-Point Loading (after Bueckner)

Approved for Public Release

Contrails

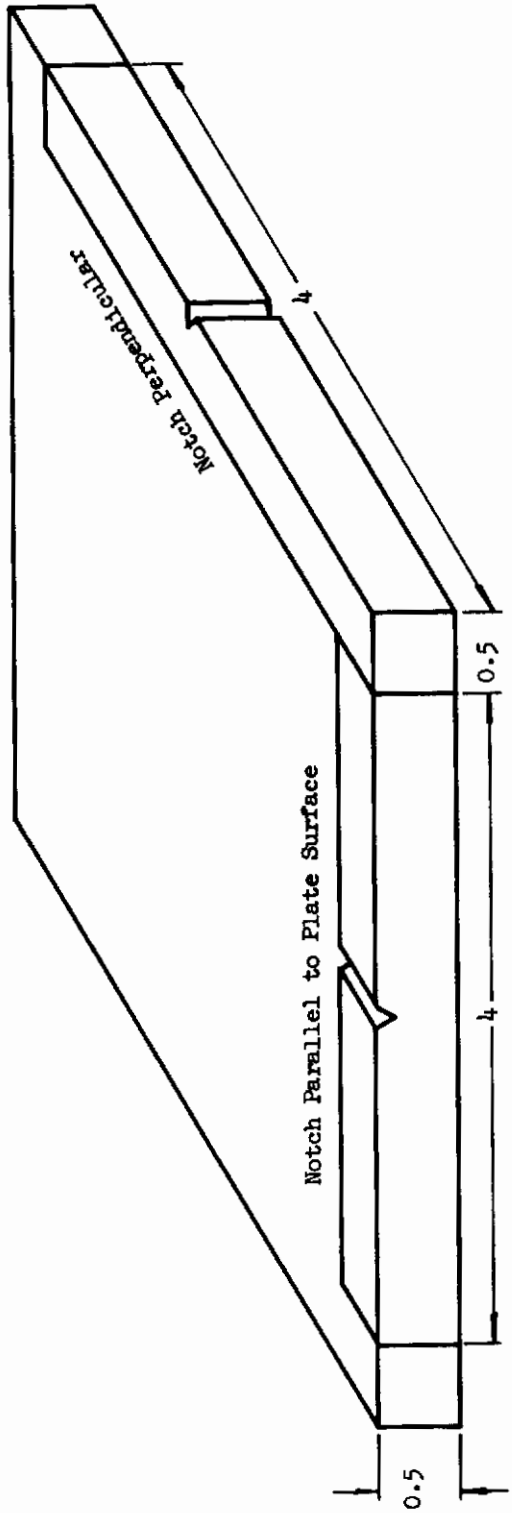

Figure 23. Schematic of Slow-Notch-Bend Test Specimen in Two Orientations

Approved for Public Release

Contrails

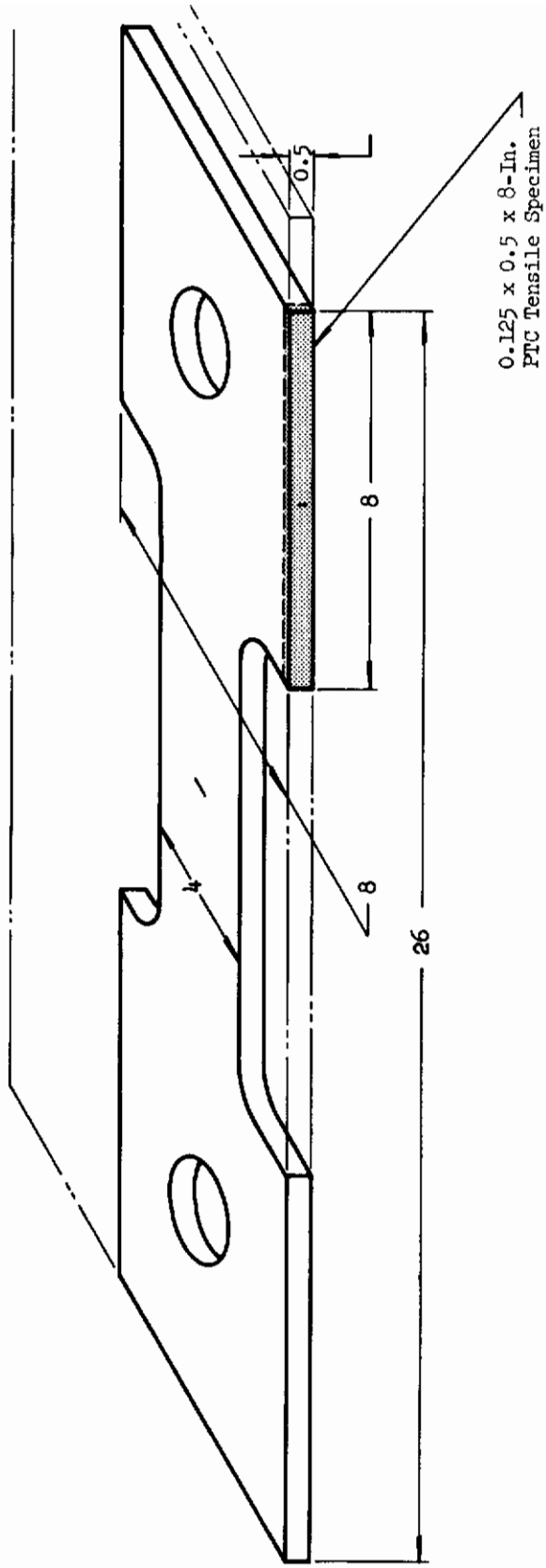

Figure 24. Schematic of Part-Through-Crack Tensile Test in Two Orientations

Approved for Public Release

Contrails

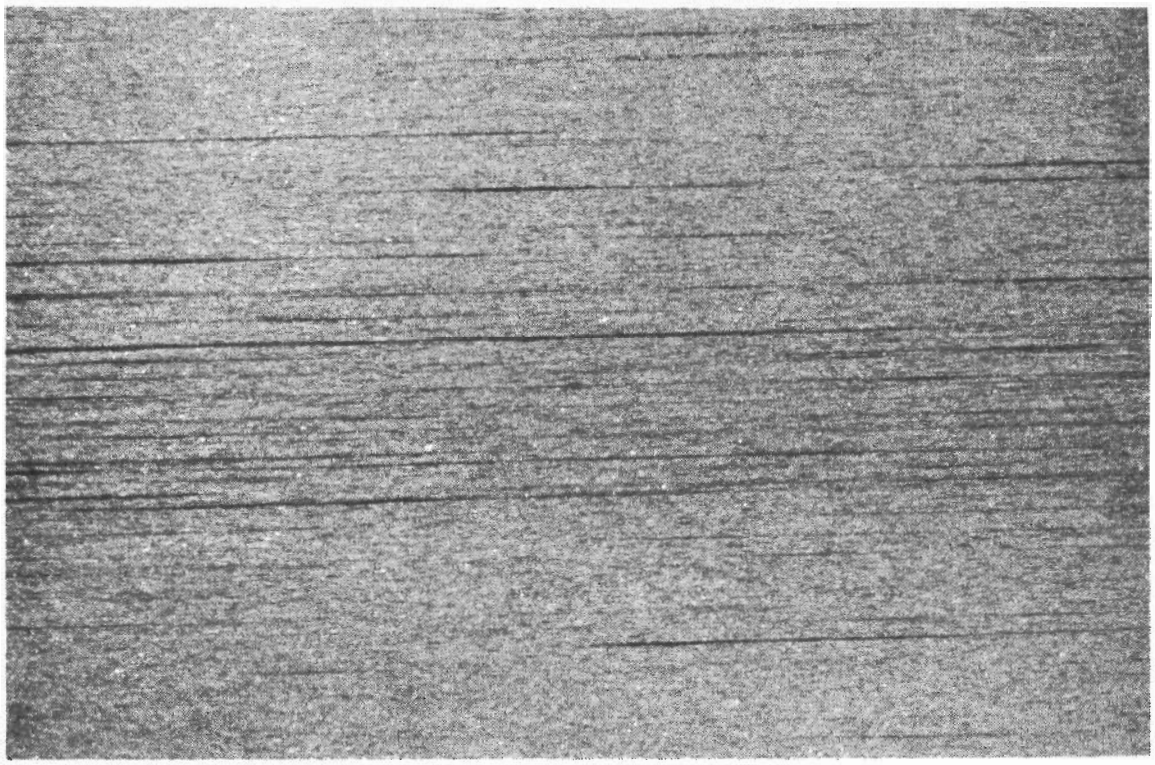

Marbles Etch Magnification: 10X

Figure 25. Typical Banding Found in Slow-Notch-Bend Test Specimens of 18% Nickel Maraging Steel, Heat 13371

Approved for Public Release

Approved for Public Release

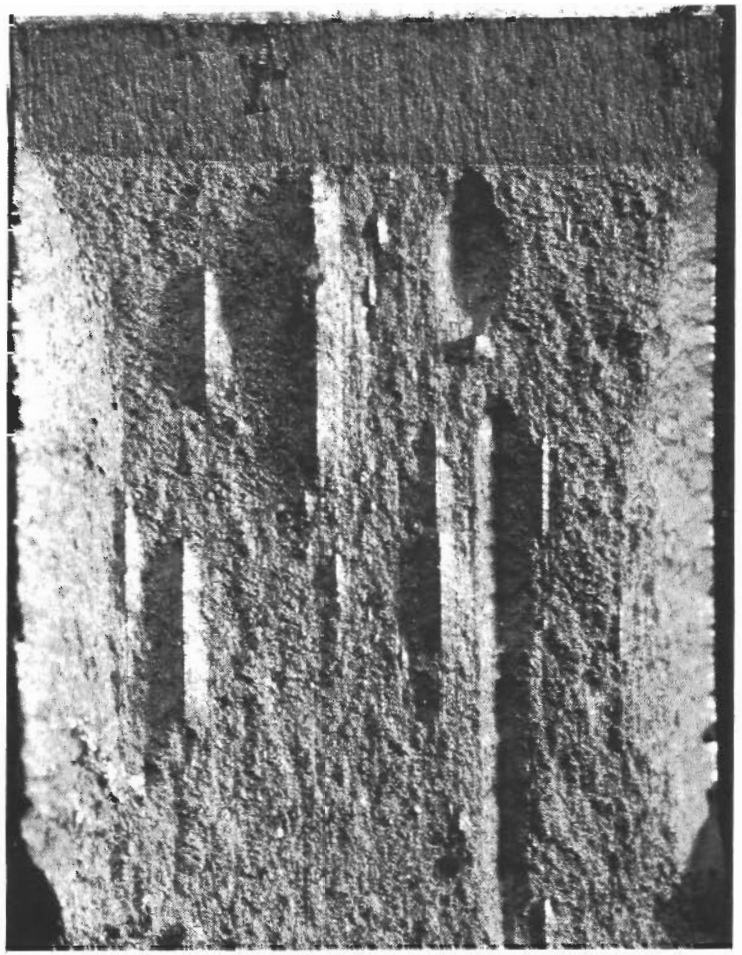

a. Transverse, G_{nc} = 154 in. lb/in.^{2}

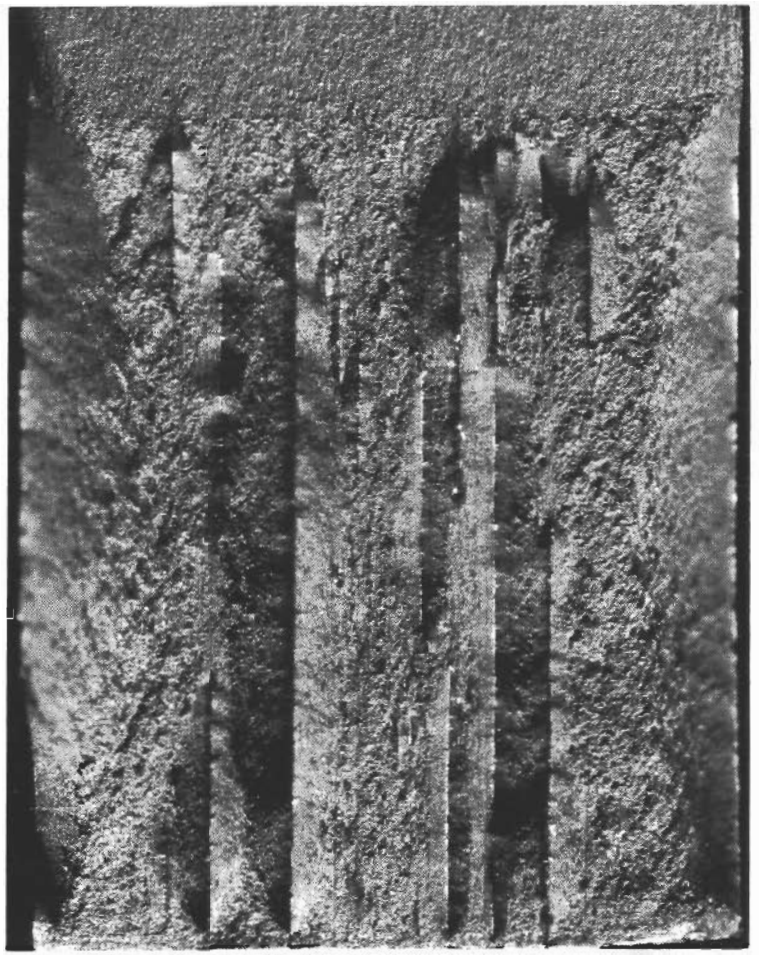

b. Longitudinal, G_{nc} = 327 in. lb/in.^{2}

Figure 26. Typical Slow-Notch-Bend Fracture Surfaces in Two Specimen Orientations Showing the Effect of Severe Banding in 18% Nickel Maraging Steel Heat 13371

Confidential

Contrails

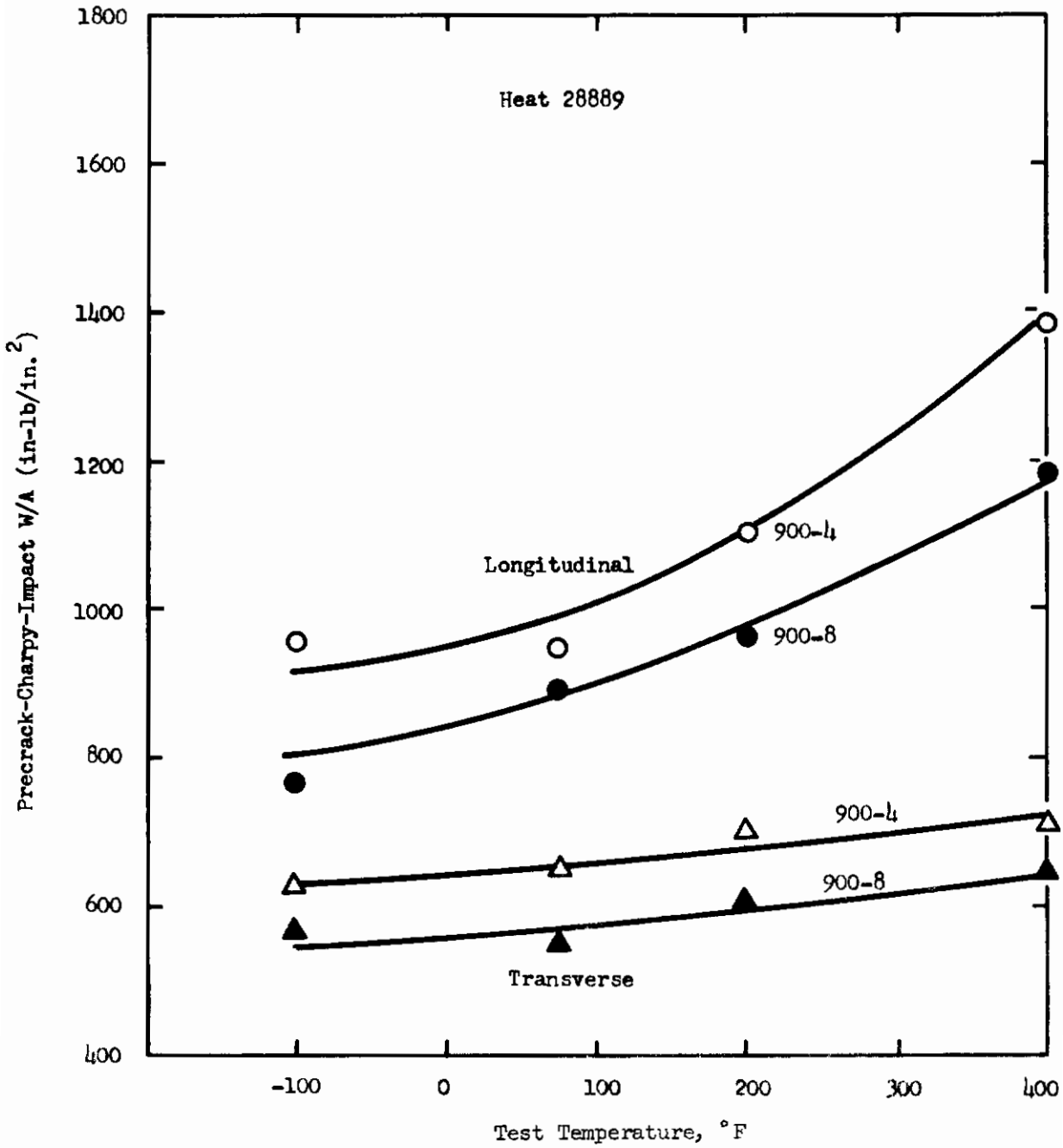

Figure 27. Effect of Heat Treatment, Specimen Orientation and Test Temperature on Toughness (W/A) in 1/2-In.-Thick, Vacuum-Degassed, Grade 200, 18% Nickel Maraging Steel Plate, Heat 28889

Approved for Public Release

Contrails

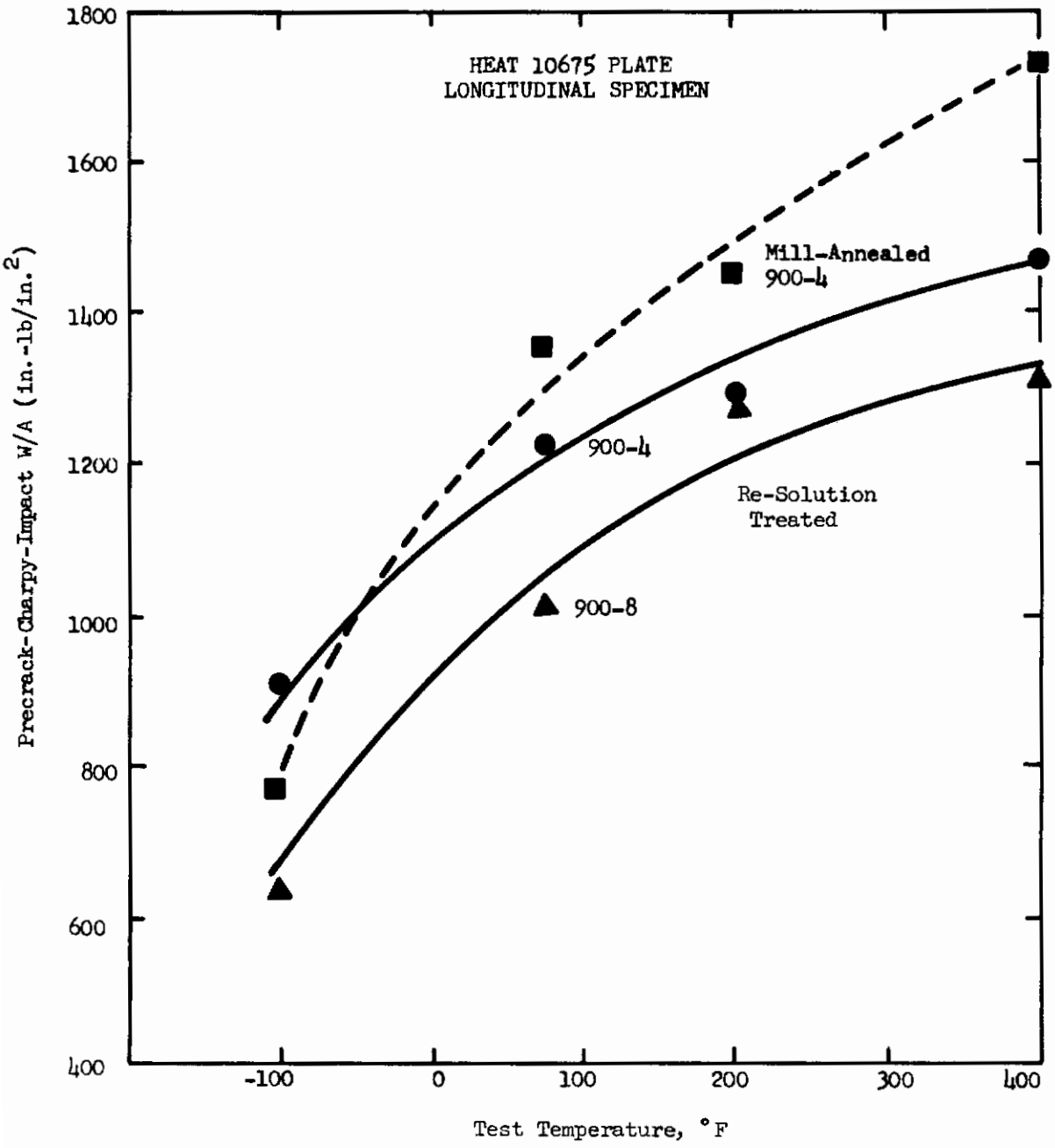

Figure 28. Effect of Heat Treatment and Test Temperature on Toughness (W/A) in 1/2-In.-Thick, Air Melted, Grade 200, 18% Nickel Maraging Steel Plate, Heat 10675

Approved for Public Release

Contrails

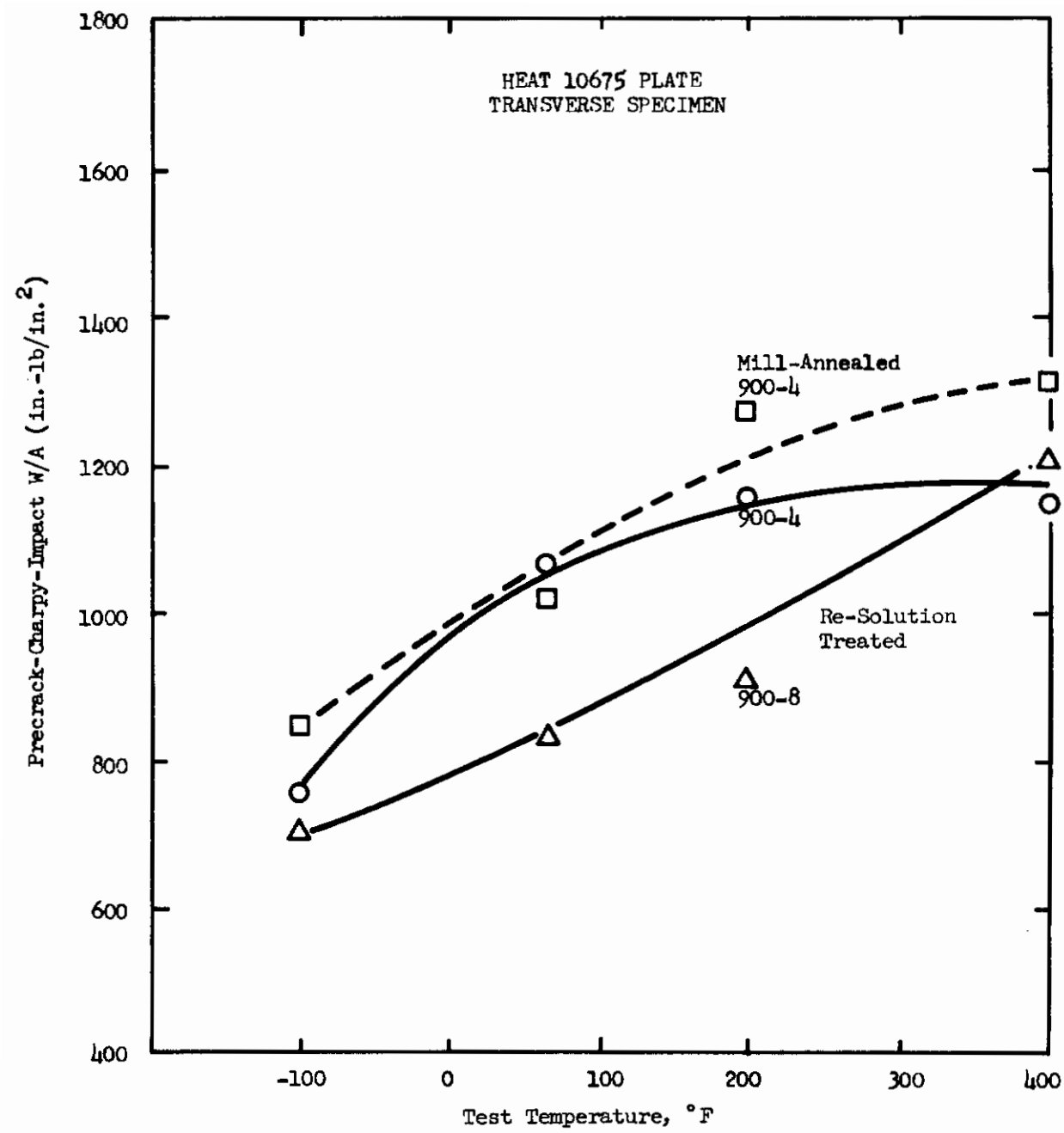

Figure 29. Effect of Heat Treatment and Test Temperature on Toughness (W/A) in 1/2-In.-Thick, Air Melted, Grade 200, 18% Nickel Maraging Steel Plate, Heat 10675

Approved for Public Release

Contrails

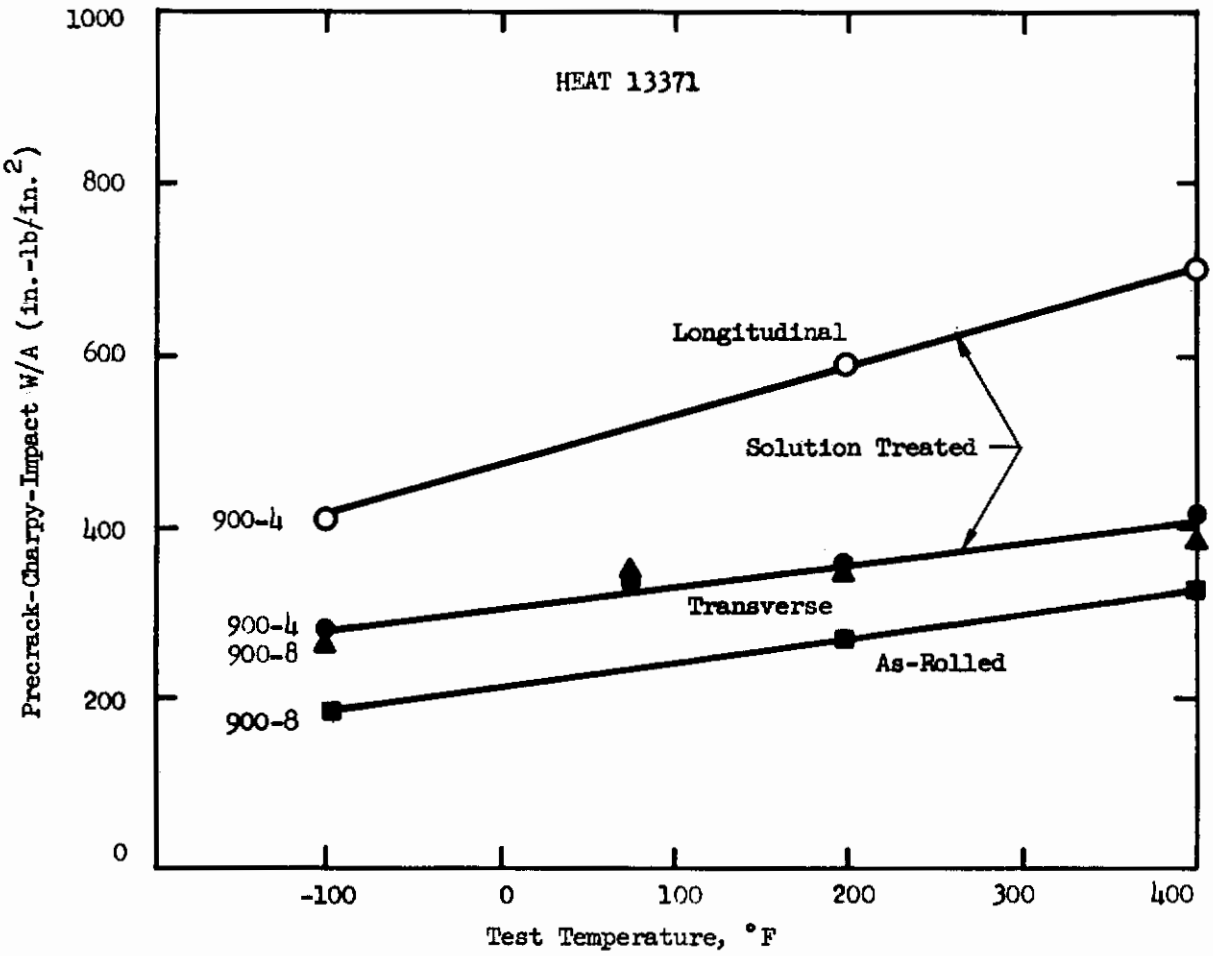

Figure 30. Effect of Heat Treatment, Specimen Orientation, and Test Temperature on Toughness (W/A) in 1/2-In.-Thick, Air Melted, Grade 250, 18% Nickel Maraging Steel Plate, Heat 13371

Approved for Public Release

Contrails

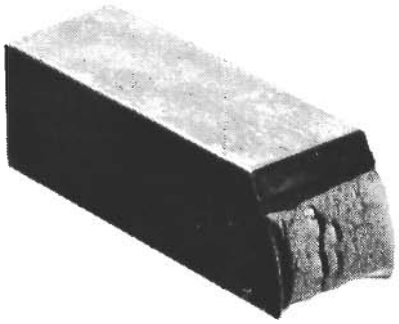

Notch Perpendicular to the Plate Surface

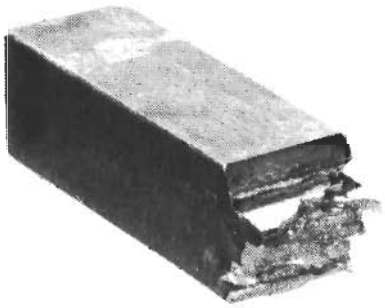

Notch Parallel to the Plate Surface

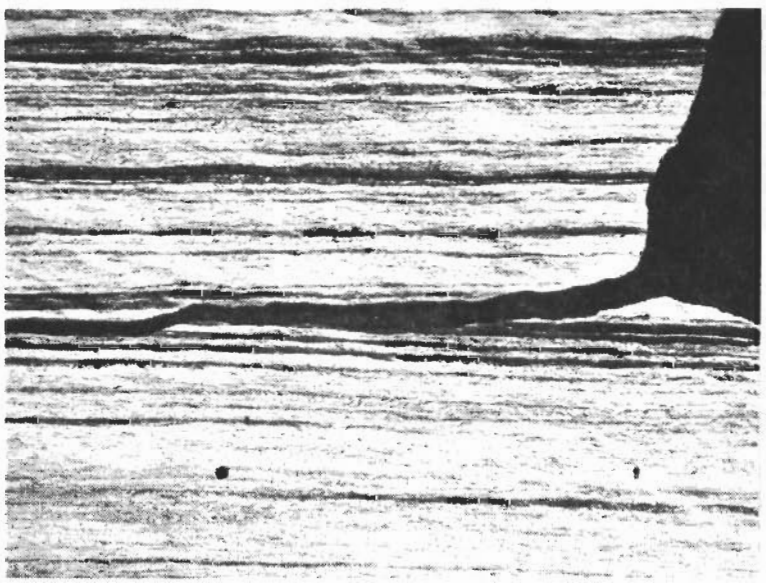

Splitting Along Bands Perpendicular to the Fracture Path

Figure 31. Typical Precrack-Charpy-Impact Fracture Surfaces in Transverse Specimens with Two Orientations of Notch, 18% Nickel Maraging Steel, Heat 13371

Approved for Public Release

Contrails

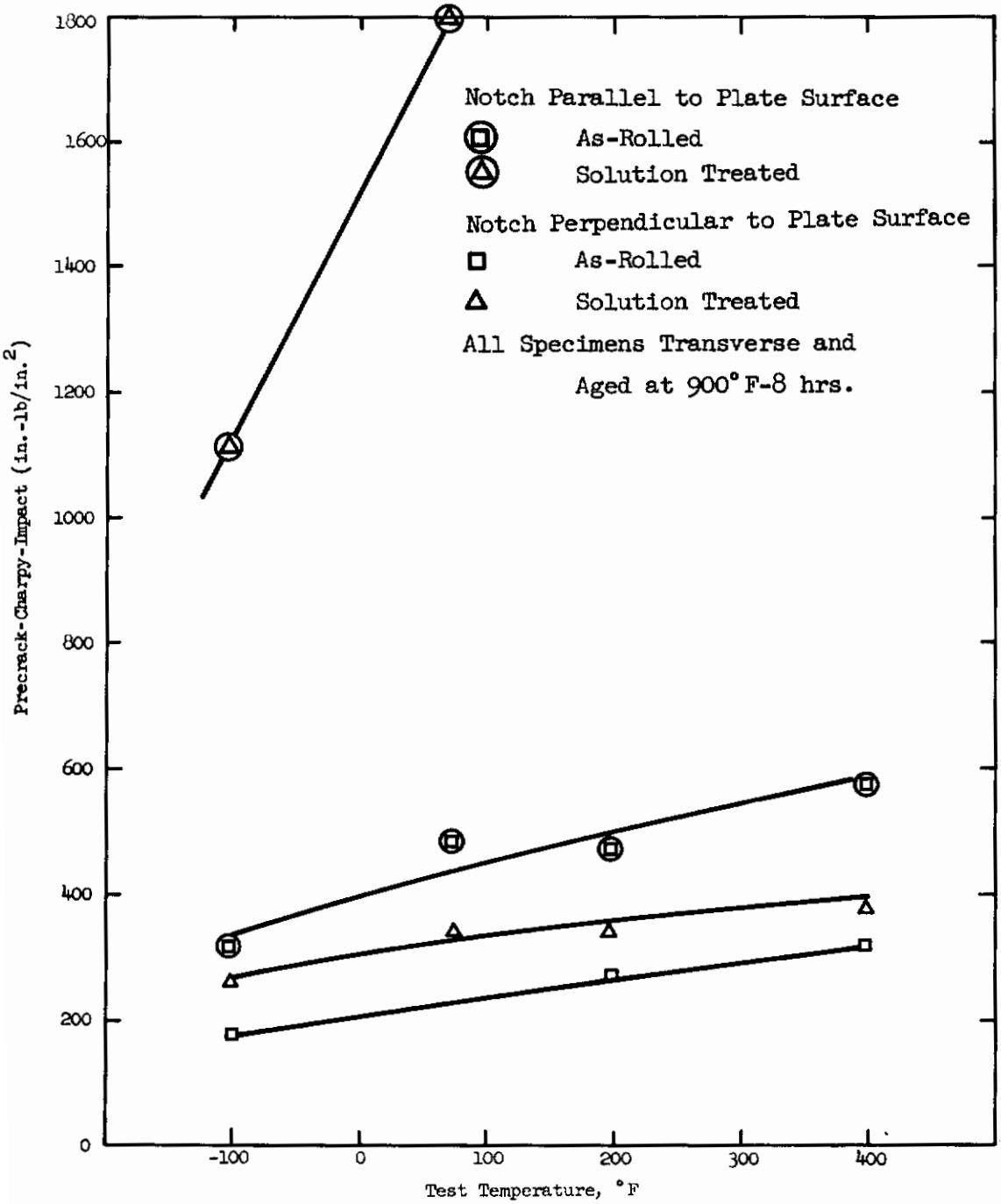

Figure 32. Effect of Heat Treatment, Notch Orientation, and Test Temperature on Toughness (W/A) in 1/2-In.-Thick, Air Melted, Grade 250, 18% Nickel Maraging Steel Plate, Heat 13371

Approved for Public Release

Contrails

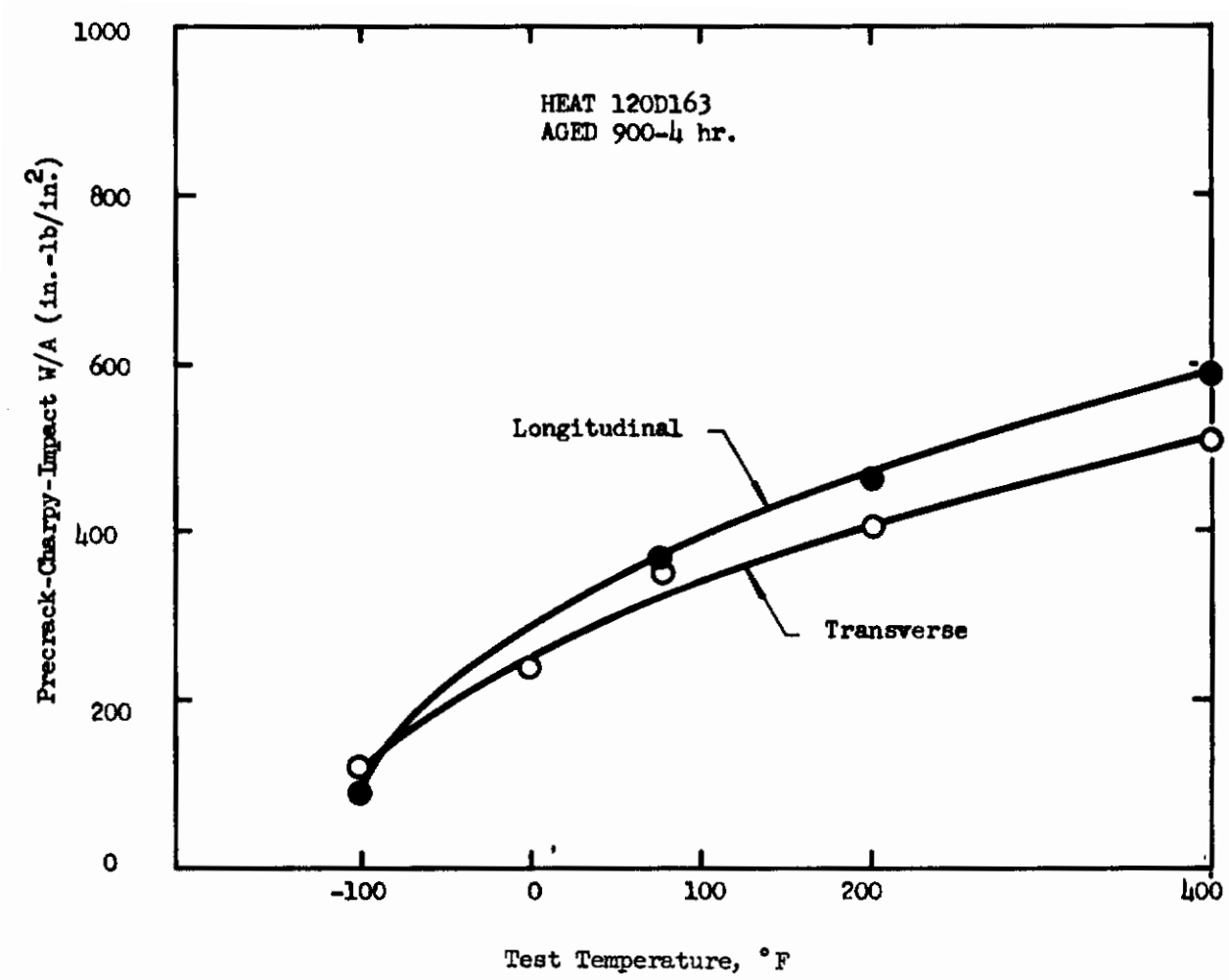

Figure 33. Effect of Specimen Orientation and Test Temperature on Toughness (W/A) in 1/2-In.-Thick, Vacuum-Degassed, Grade 250, 18% Nickel Maraging Steel Plate, Heat 120D163

Approved for Public Release

Contrails

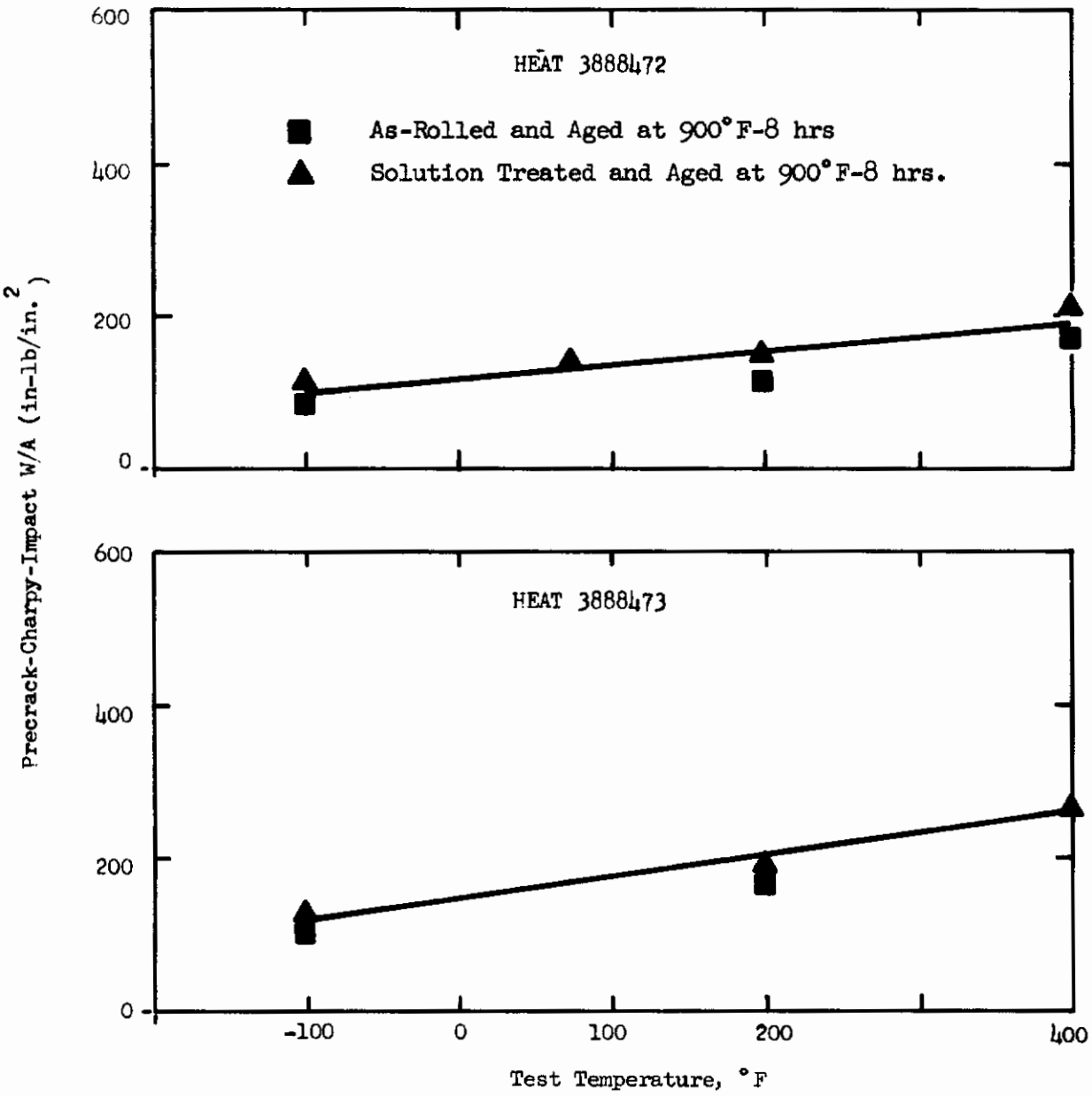

Figure 34. Effect of Heat Treatment and Test Temperature on Toughness (W/A) in 1/2-In.-Thick, Vacuum-Arc-Remelt, Heats 3888472 and 3888473, Longitudinal Specimen Orientation

Approved for Public Release

Contrails

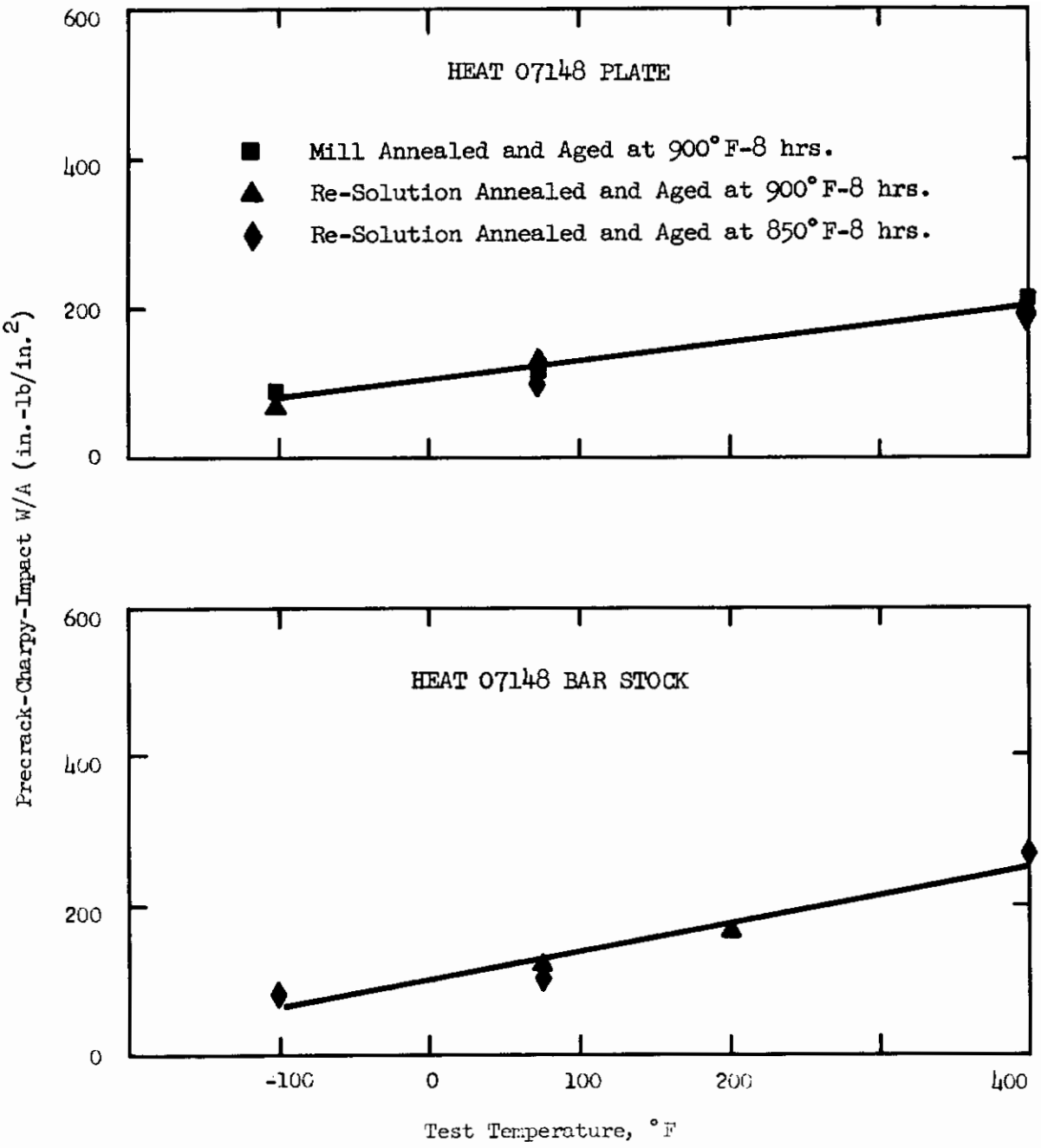

Figure 35. Effect of Heat Treatment and Test Temperature on Toughness (W/A) in Vacuum-Arc-Remelt, Grade 300, 18% Nickel Maraging Steel Plate and Bar Stock, Heat 07148, Longitudinal Specimen Orientation

Approved for Public Release

Contrails

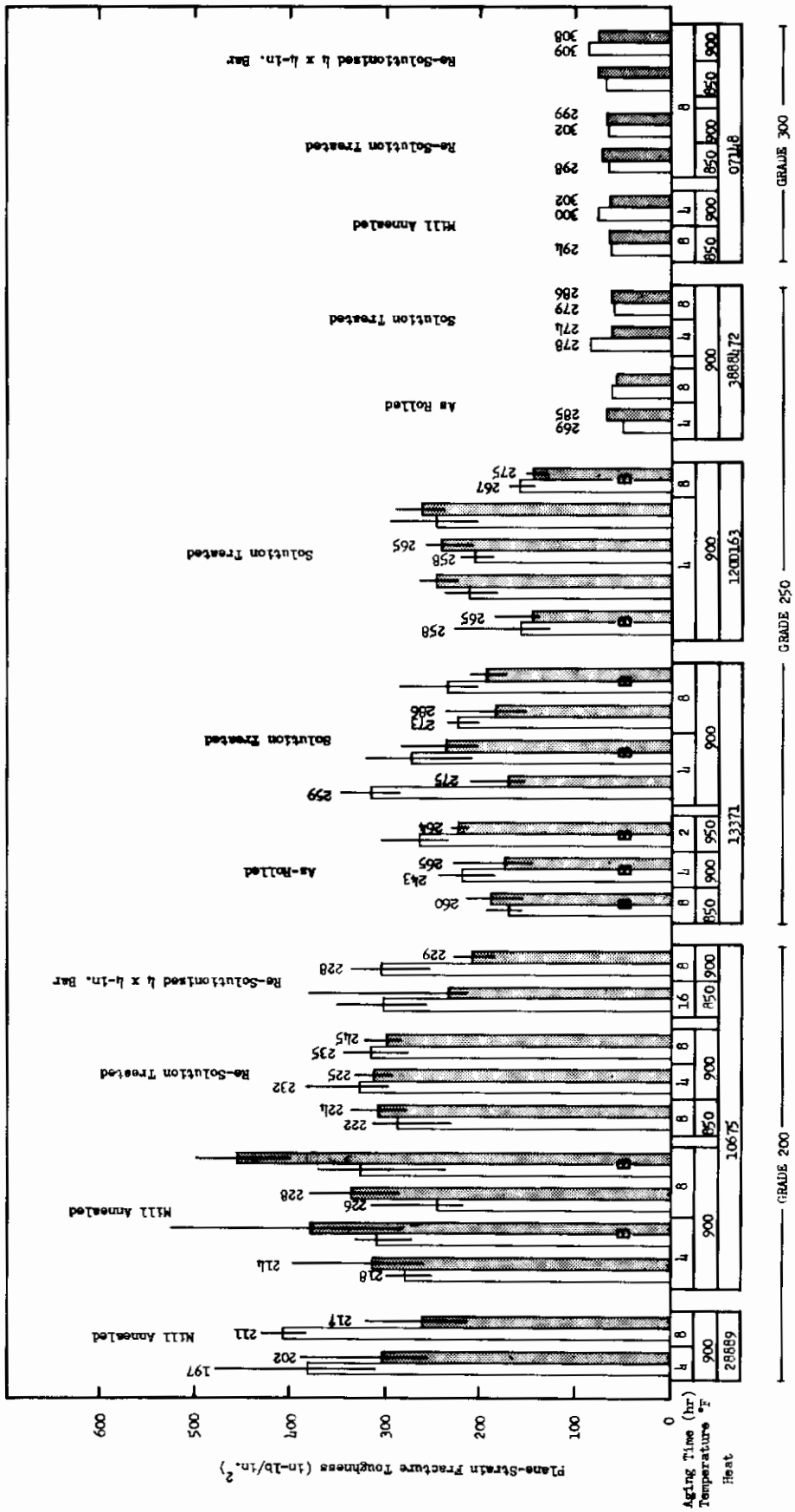

Figure 36. Comparison of Plane-Strain Fracture Toughness in Several Heats of 18% Nickel Maraging Steel (Bars, left-to-right are for longitudinal and transverse (shaded) specimens; lines show the scatter from replicate test specimens; B indicates Bueckner's value; numbers above each bar represent 0.2% offset yield strength, ksi.)

Approved for Public Release

Contrails

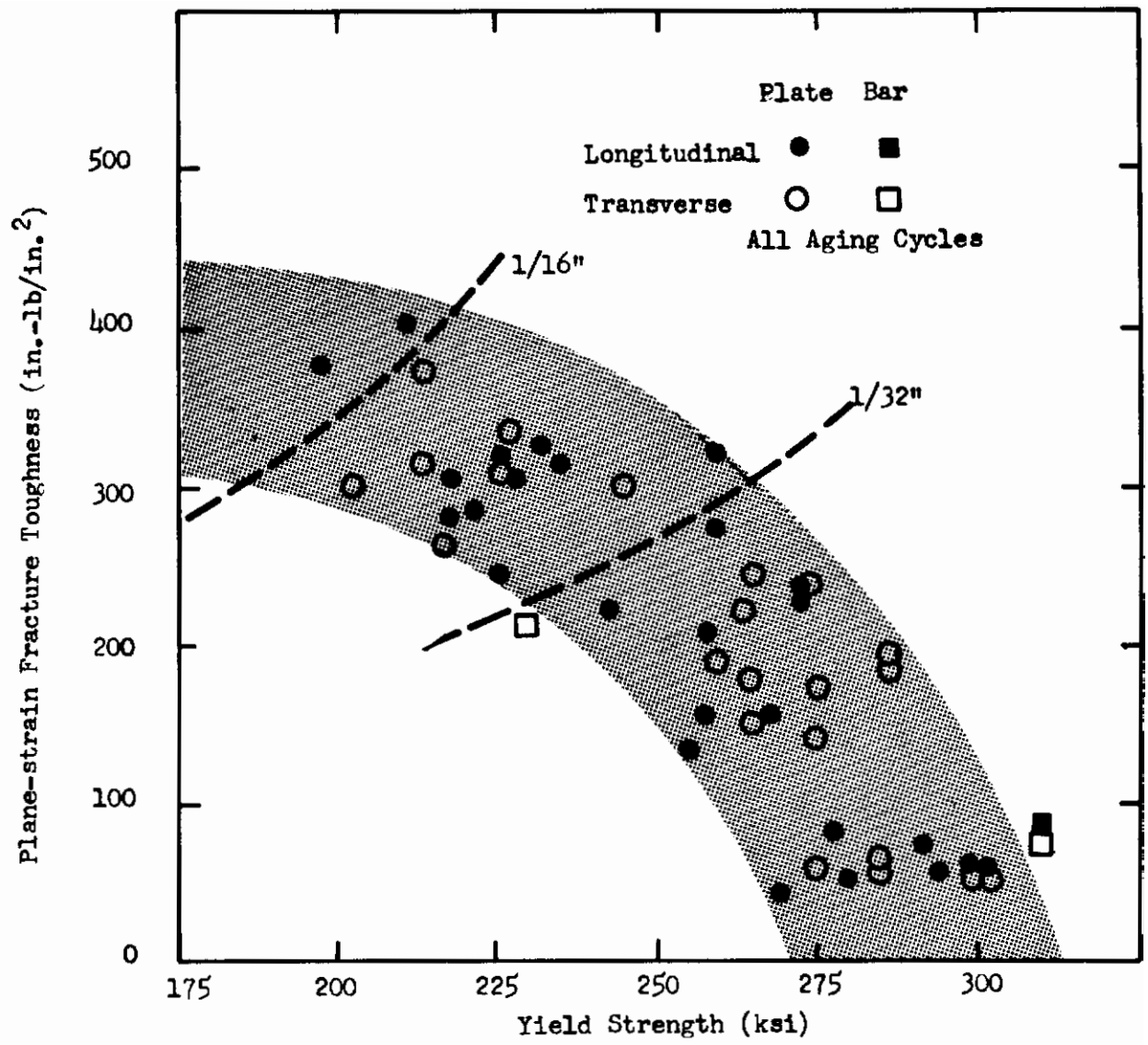

Figure 37. Relationship Between Plane-Strain Fracture Toughness and Yield Strength in Six Heats of 18% Nickel Maraging Steel (dash lines represent the limits for critical surface flaws 1/16 and 1/32 in. deep) Data for the Plate are indicated by the Scatter band.

Approved for Public Release

Contrails

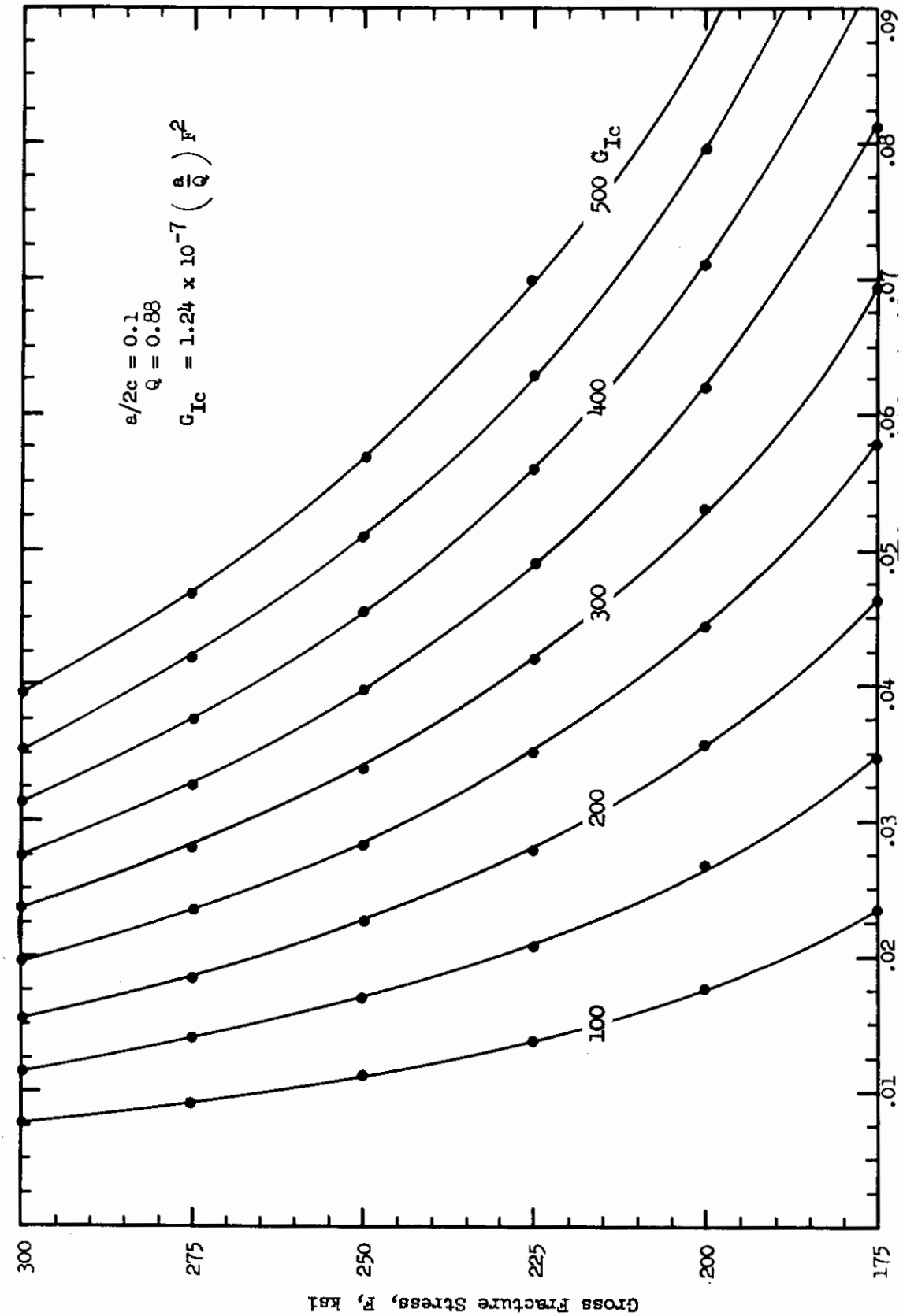

Figure 38. Graphical Solution Relating Gross Fracture Stress (F), Plane-Strain Fracture Toughness (G_{Ic}) and Surface Crack Depth (a). (a/2c = .1)

Approved for Public Release

Contrails

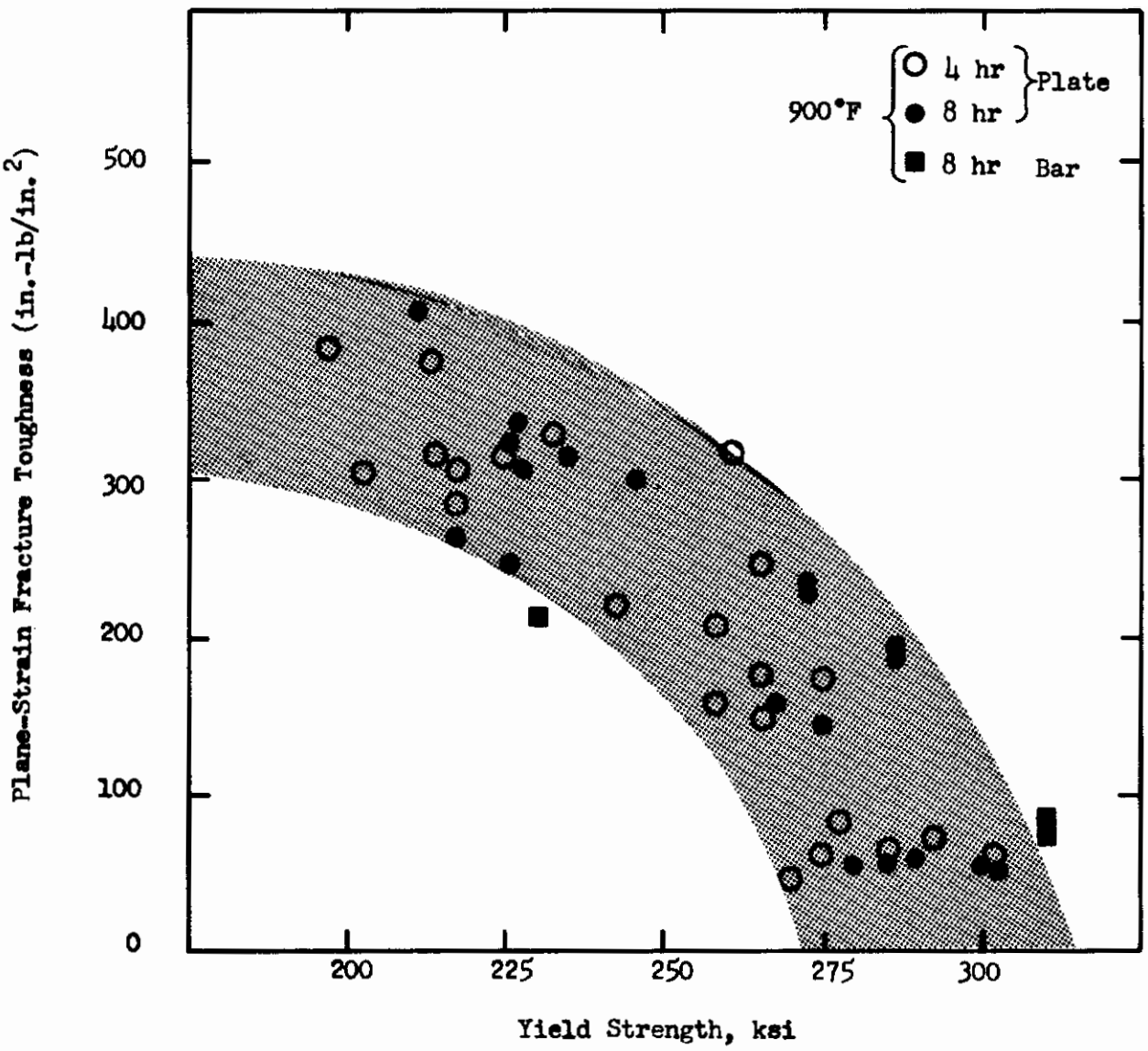

Figure 39. Relationship Between Plane-Strain Fracture Toughness and Yield Strength in Six Heats of 18% Nickel Maraging Steel, Solution-Treated at 1500°F and Aged at 900°F for 4 and 8 Hours

Approved for Public Release

Contrails

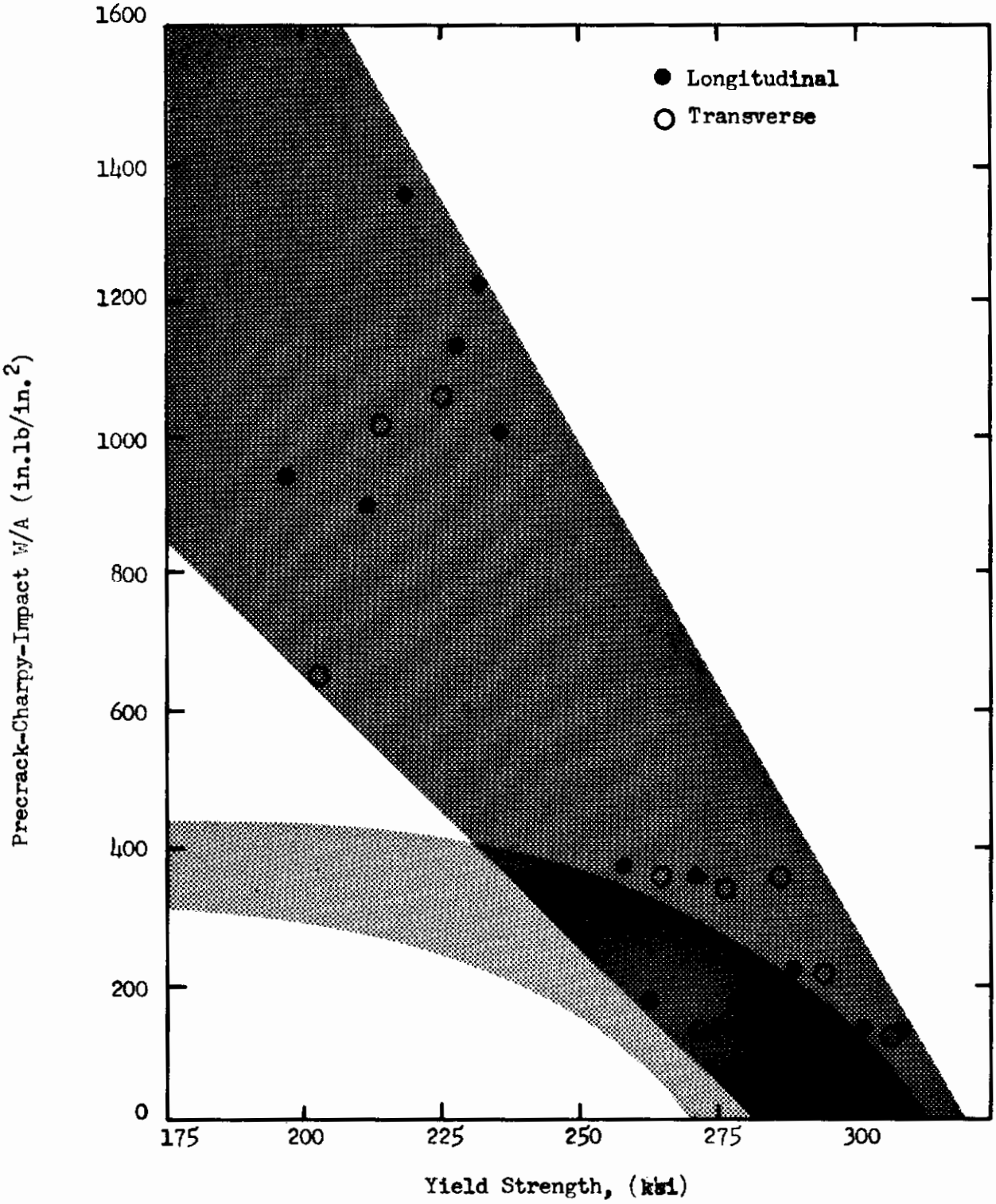

Figure 40. Toughness (W/A) in Seven Heats of 18% Nickel Maraging Steel as a Function of Yield Strength (the lower shaded area is the plane-strain fracture toughness from Figure 37).

Approved for Public Release

Contrails

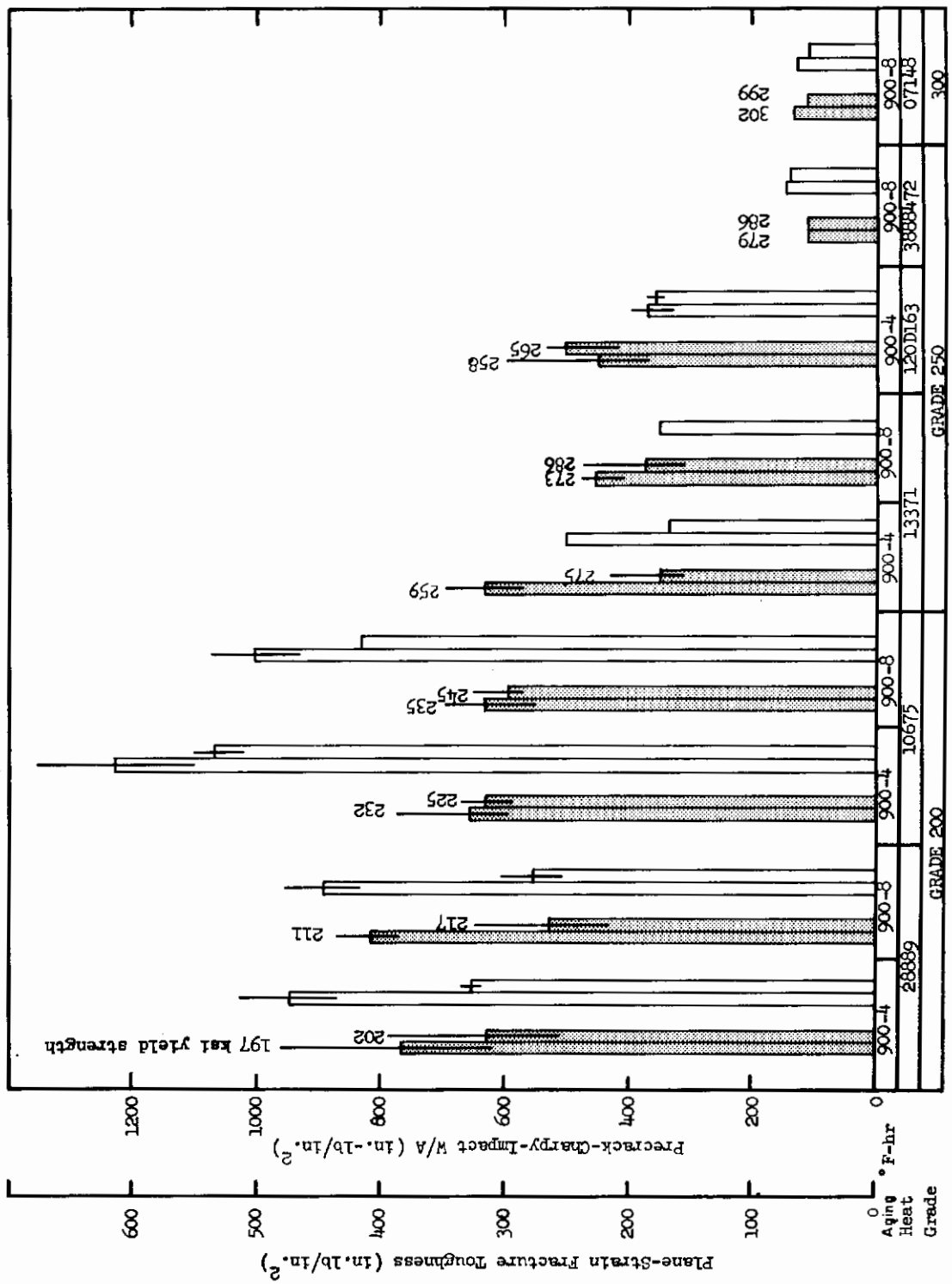

Figure 41. Comparison of G_{nc} (shaded) and (W/A) Fracture Toughness Values in Six Heats of 18% Nickel Maraging Steel (bars left-to-right are for longitudinal and transverse specimens; lines show the scatter in replicate test specimens).

Approved for Public Release

Contrails

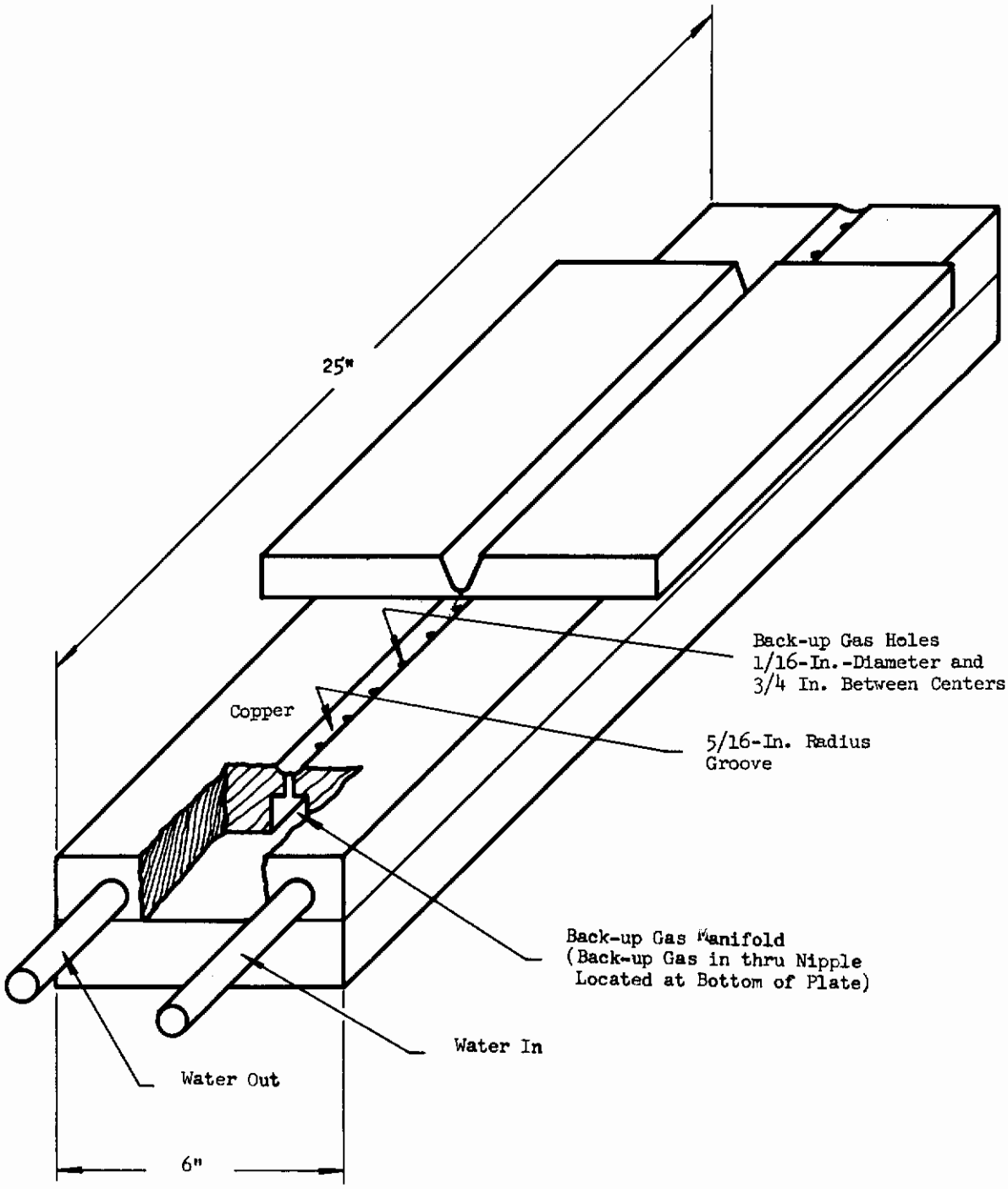

Figure 42. Weld Backing-Bar

Approved for Public Release

Contrails

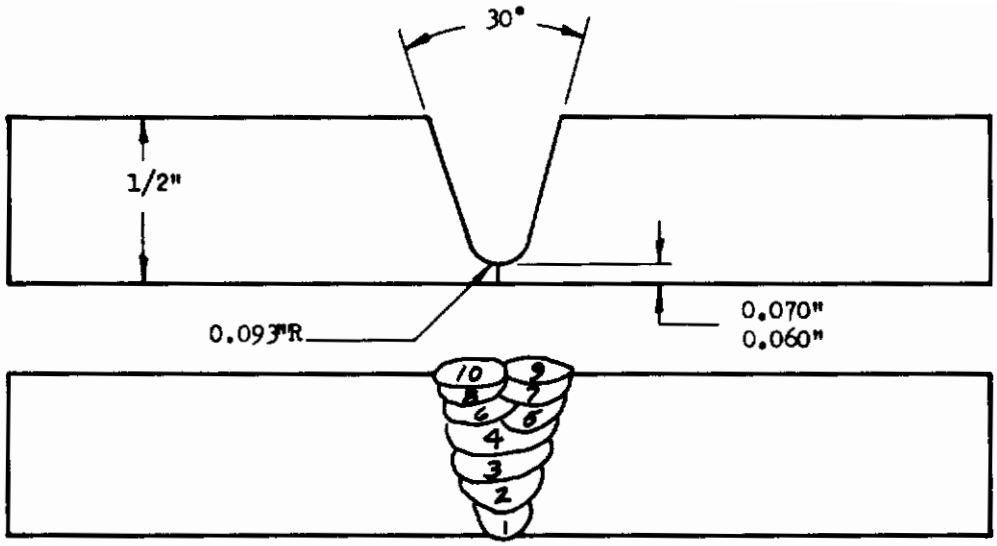

Weld(1) Pass	Amps(2)	Volts	Travel ipm	Wire(3) Feed, ipm	Torch Gas Argon, cfh	Backup Gas cfh
1	150	10	6	18	25	10
2	150	8.5	6	18		
3	160	10	6	24		
4	160		6			
5	180		6			
6			6			
7			7			
8			7			
9			7			
10			10			

(1) Electrode was thoriated tungsten with a 1/8 in. diameter.
(2) Direct current, straight polarity.
(3) Filler wire diameter was 1/16 in.

Figure 43. TIG Welding Conditions for 1/2-In. Plate

Approved for Public Release

Contrails

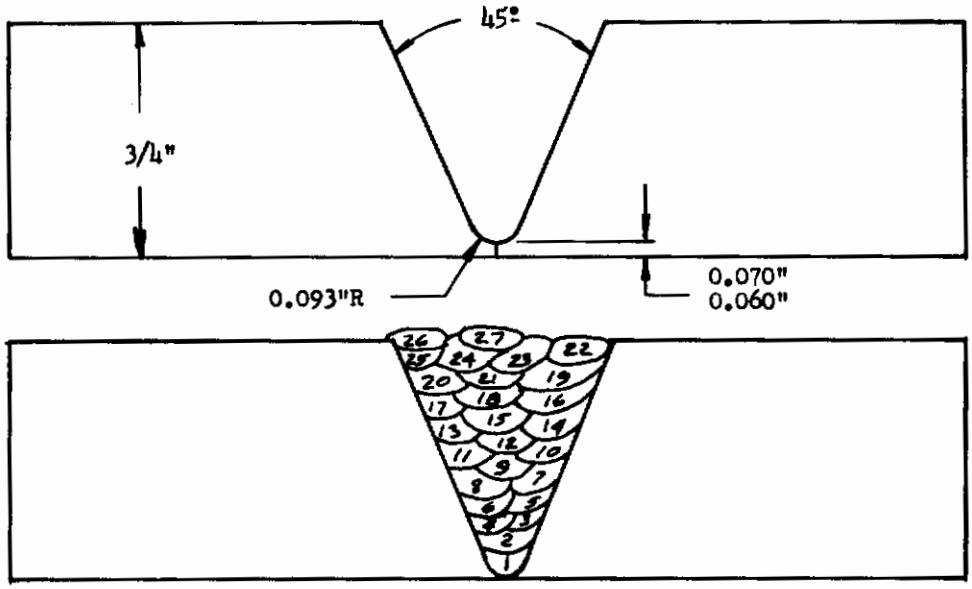

Weld(1) Pass	Amps(2)	Volts	Travel ipm	Wire(3) Feed ipm	Torch Gas, cfh	Backup Gas, cfh
1	135	8	6	15	30	10
2	175	10	6	15		
3	170	9	6	25		
4	200	10	6	25		
5	195	10	6	25		
6-9	200	10	6	30		
10-21	175	10	8	20		
22	175	10	8	15		
23-25	175	11	8	15		
26	175	10	8	15		
27	175	10	8	15		

(1) Electrode was thoriated tungsten with a 1/8-in. diameter
(2) Direct current, straight polarity
(3) Filler Wire diameter was 1/16 in.

Figure 44. TIG Welding Conditions for 3/4-In. Plate

Approved for Public Release

Contrails

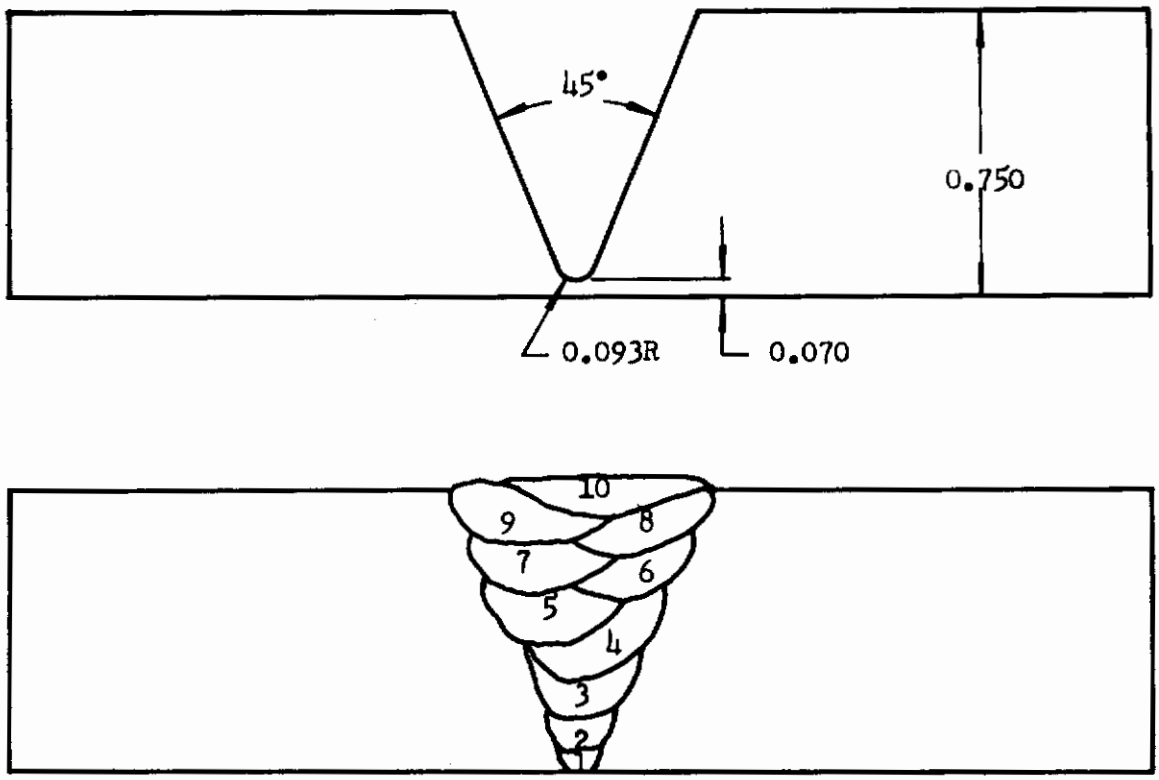

Pass No.	Amperage (1)	Voltage	Travel, ipm	Gas Flow (2) cfh
1 (TIG)	160	8	6	30
2 (TIG)	175	10	4	30
3 (MIG)	350-375	28	20	45
4			15	
5				
6				
7				
8				
9				
10				

(1) TIG passes were made using direct current with straight polarity, and MIG passes were made using direct current and reversed polarity.
(2) TIG passes were made with argon only; MIG passes were made using argon and 2% oxygen.

Figure 45. MIG Welding Conditions for 3/4-In. Plate

Approved for Public Release

Contrails

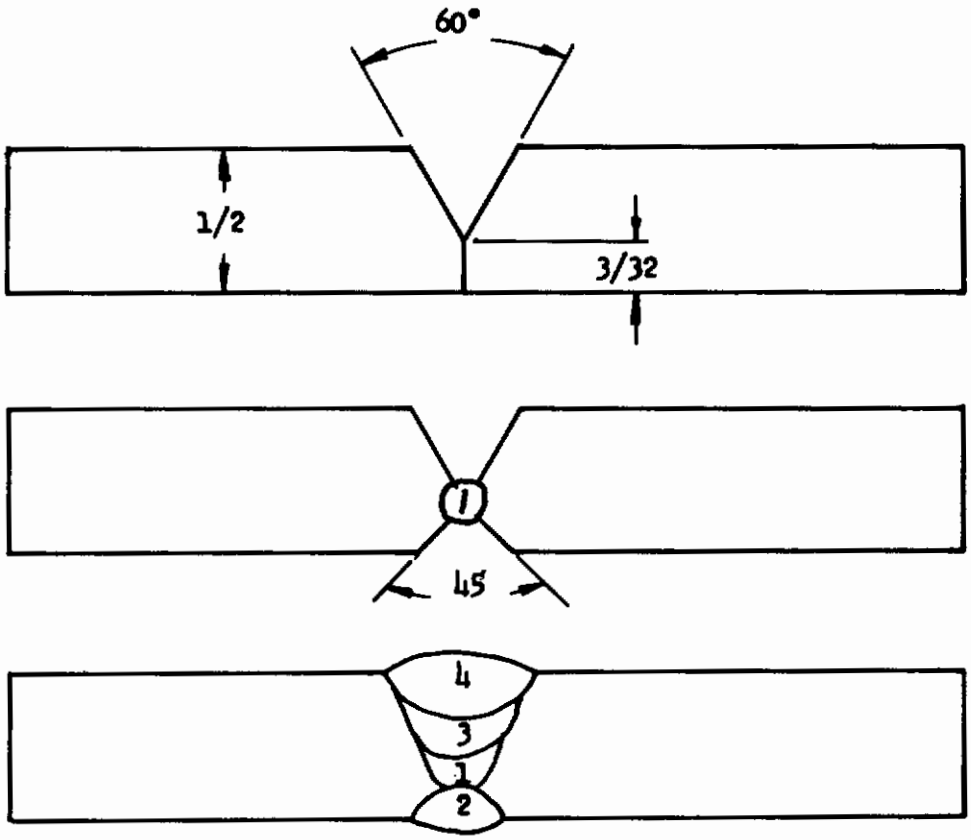

Weld(1) Pass	Amps(2)	Volts	Travel ipm
1	240	26	18
2	230	27	18
3	230	28	11
4	230	28	10

(1) Filler wire diameter was 1/16 in. and Unionmelt flux composition 898-37A was used.
(2) Direct current, reversed polarity.

Figure 46. Submerged-Arc Welding Conditions for Joint A

Approved for Public Release

Contrails

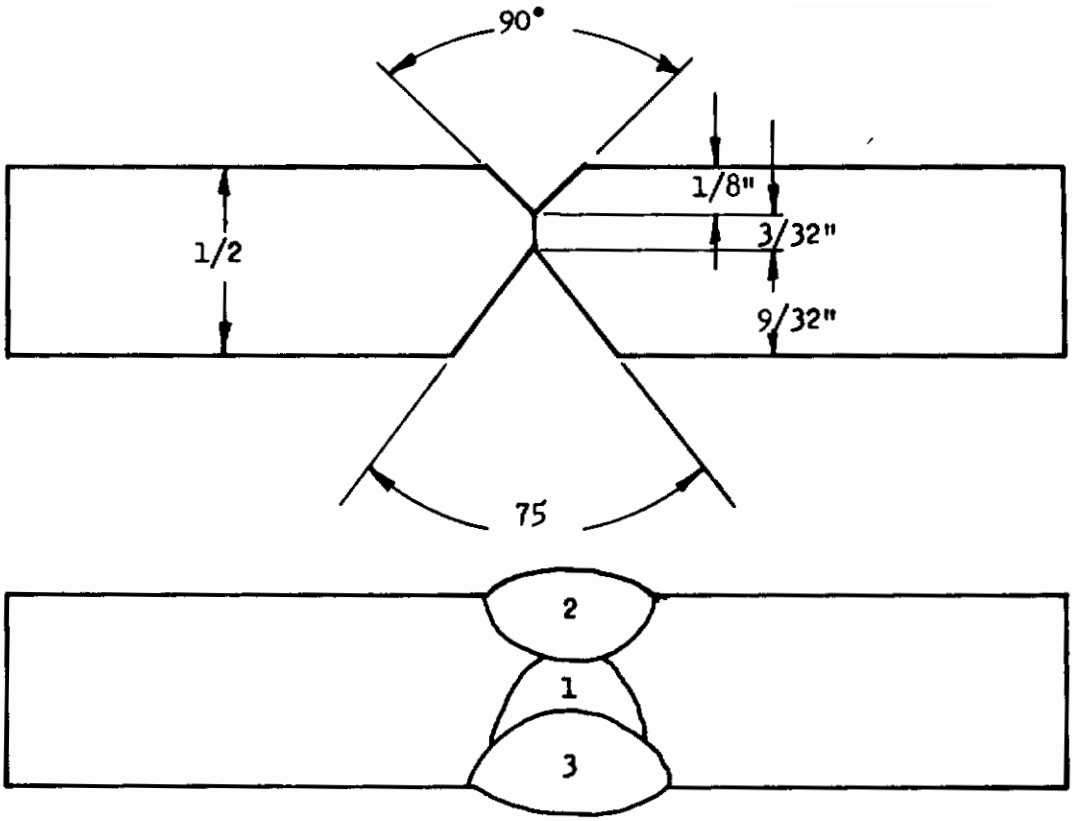

Weld Pass (1)	Amps (2)	Volts	Travel ipm
1	240	26	10
2	240	28	10
3	230	28	11

(1) Filler wire diameter was 1/16 in. and Unionmelt flux composition 898-37A was used.
(2) Direct current, reverse polarity.

Figure 47. Submerged-Arc Welding Conditions for Joint B

Approved for Public Release

Contrails

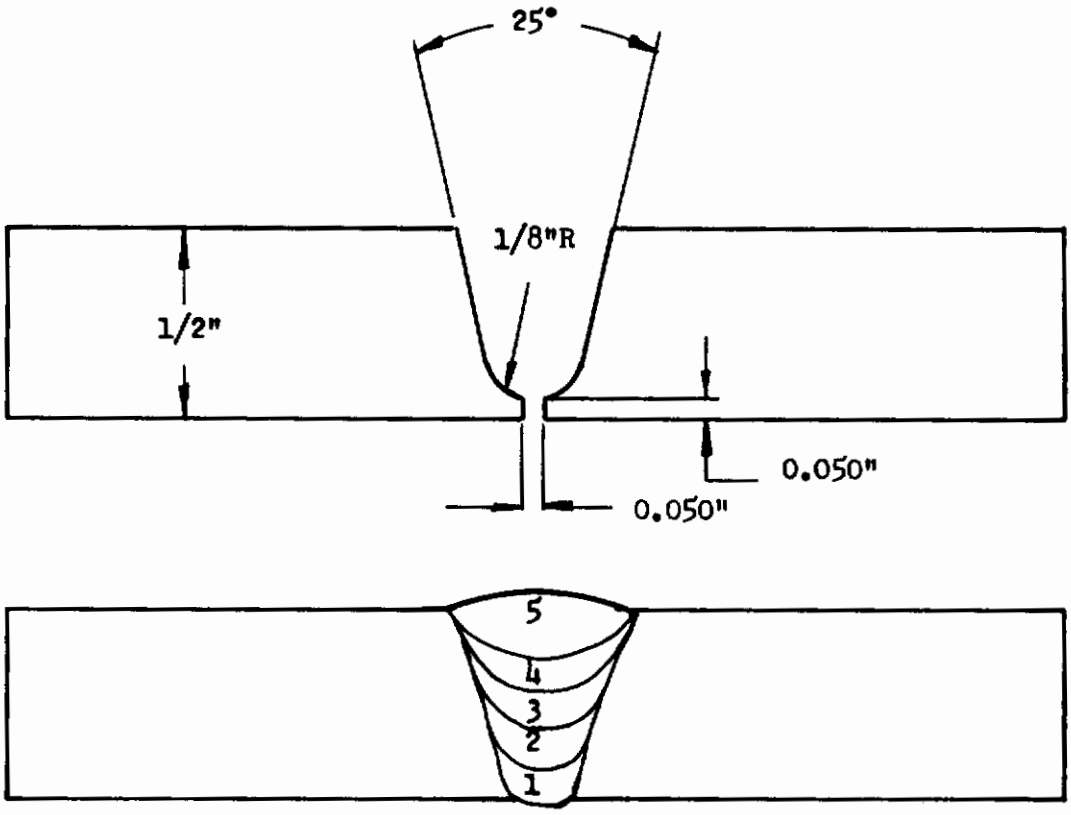

Weld(1) Pass	Amps(2)	Volts	Travel ipm	Process
1	75	19.5	12-14	Short arc
2	90	20	8	Short arc
3	220	30	12	Submerged Arc
4	220	30	8	
5	210	32	12	

(1) Electrode diameter was 1/16 in.
(2) Direct current, reverse polarity.

Figure 48. Combined Short-Arc and Submerged-Arc Welding Conditions for Joint C

Approved for Public Release

Contrails

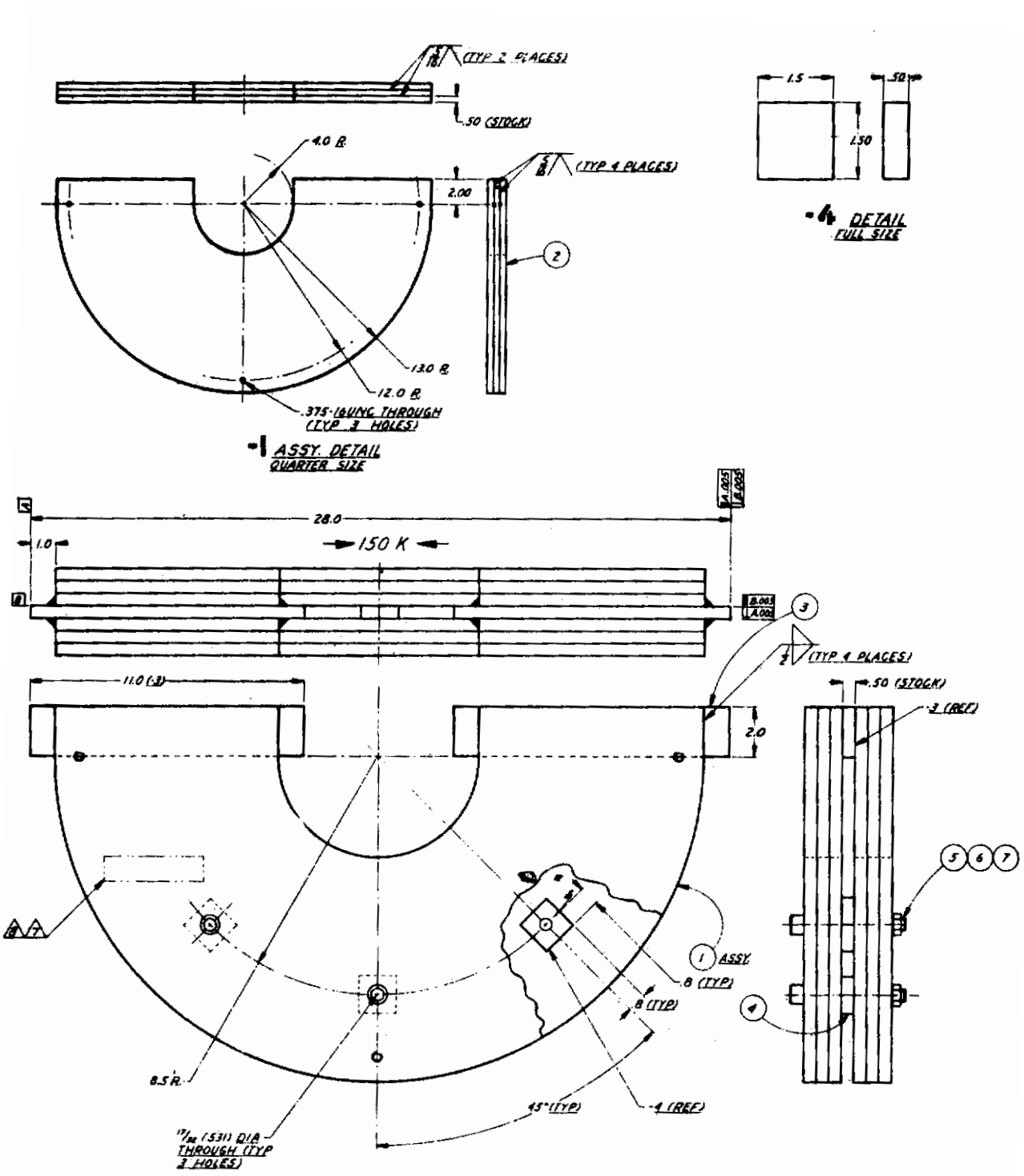

Figure 49. U-Bar Weld-Restraint Fixture

Approved for Public Release

Contrails

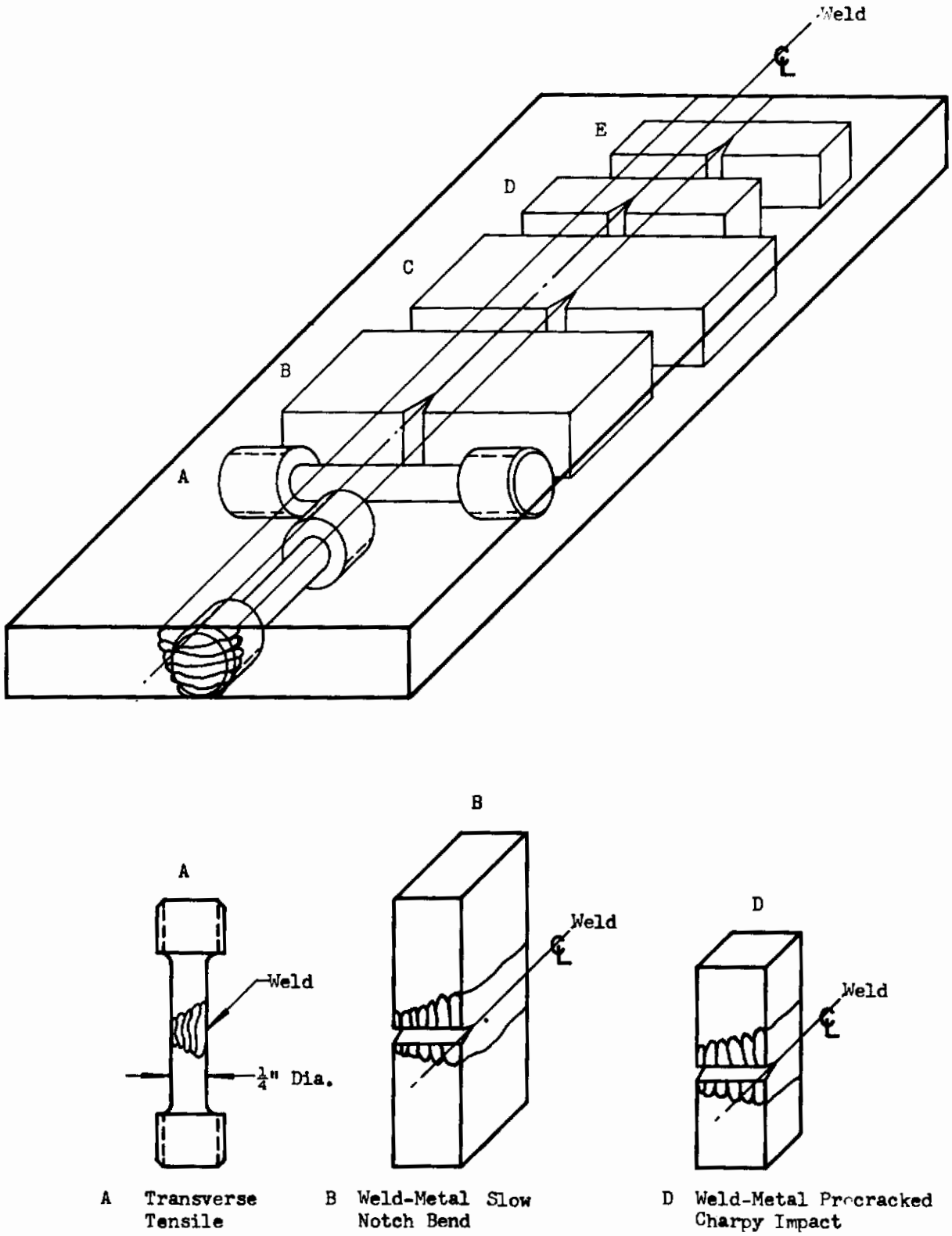

Figure 50. Orientation of Weld-Joint Test Specimens

Approved for Public Release

Contrails

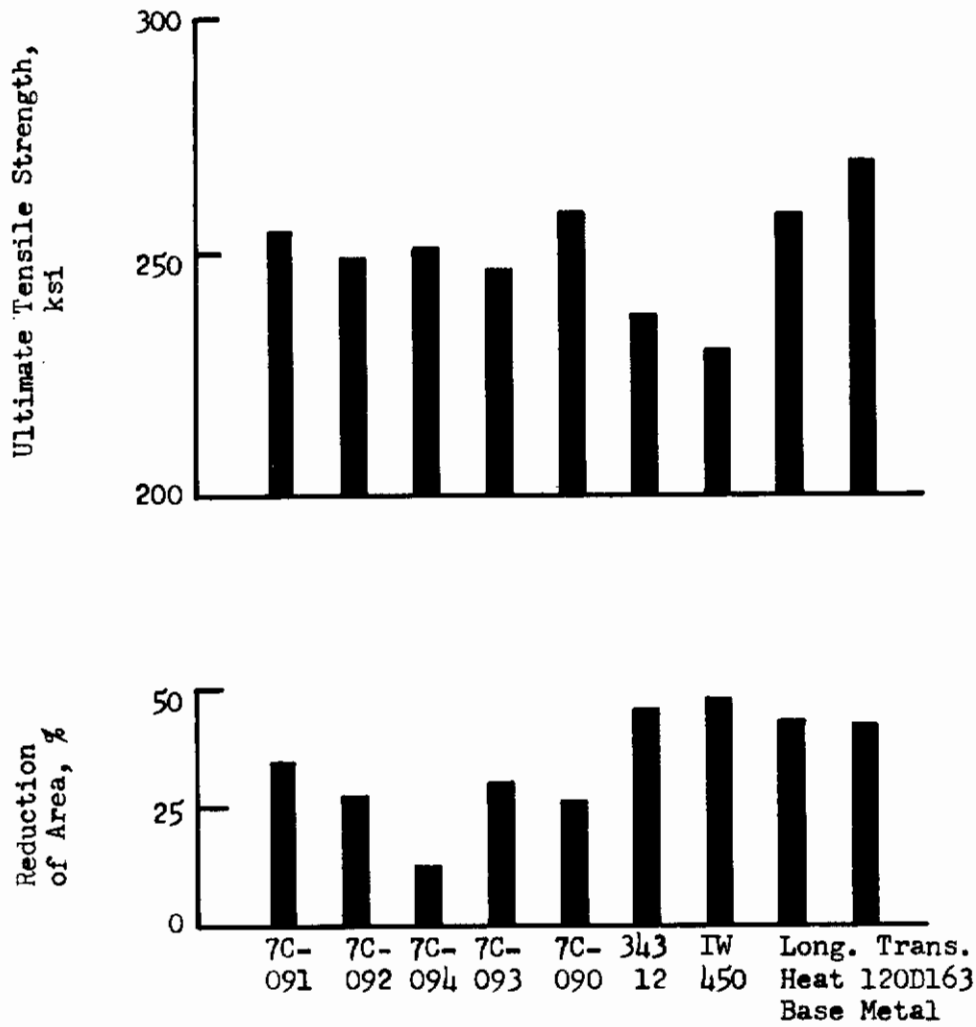

Figure 51. Transverse Tensile Properties of TIG Weldments Made with Various Filler Wires in Grade 250, 1/2-In.-Thick, 18% Nickel Maraging Steel Plate, Heat 120D163, Aged at 900°F for 4 Hours After Welding

Approved for Public Release

Contrails

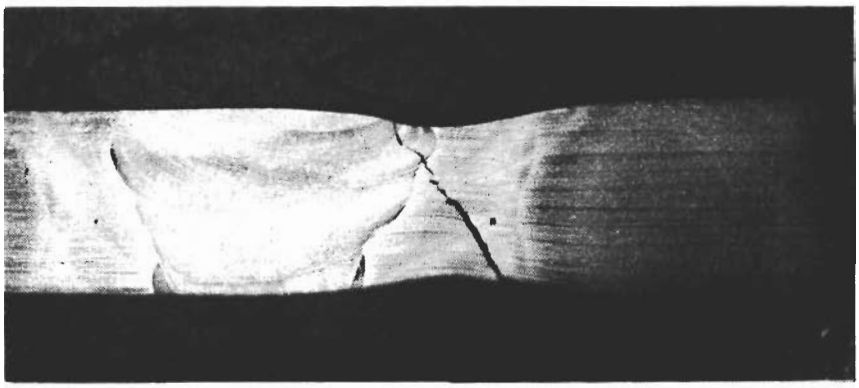

Marbles Etch Magnification: 5X

Filler Wire 7C-091

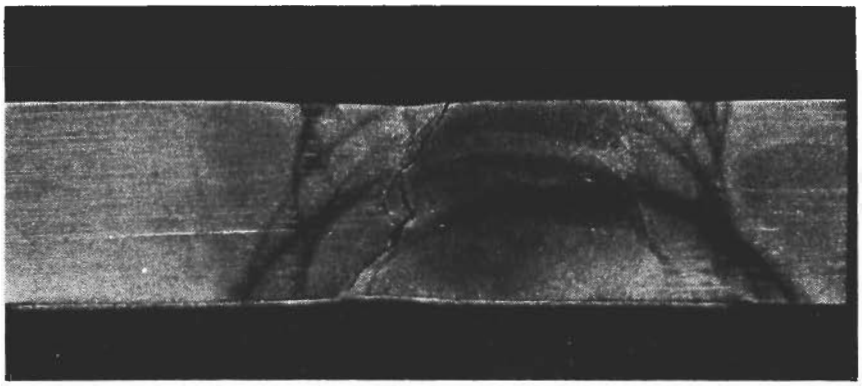

Marbles Etch Magnification: 5X

Filler-Wire 7C-094

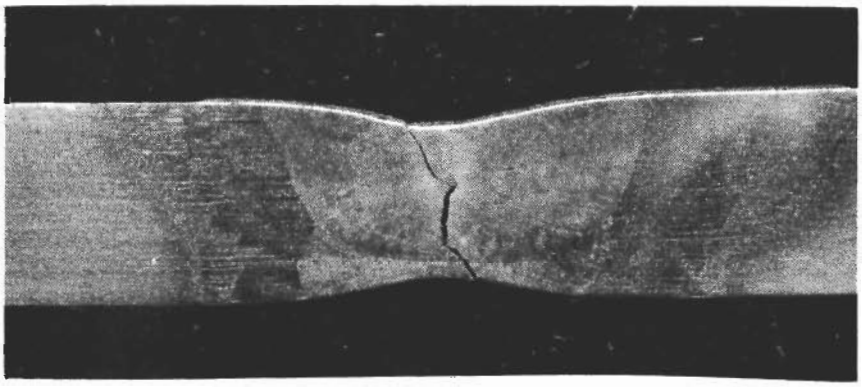

Marbles Etch Magnification: 5X

Filler Wire 7C-093

Figure 52. Typical Locations of Tensile Test Failures in Zones of TIG Weldments of Grade 250, 1/2-In.-Thick, 18% Nickel Maraging Steel Plate, Heat 120D163

Approved for Public Release

Contrails

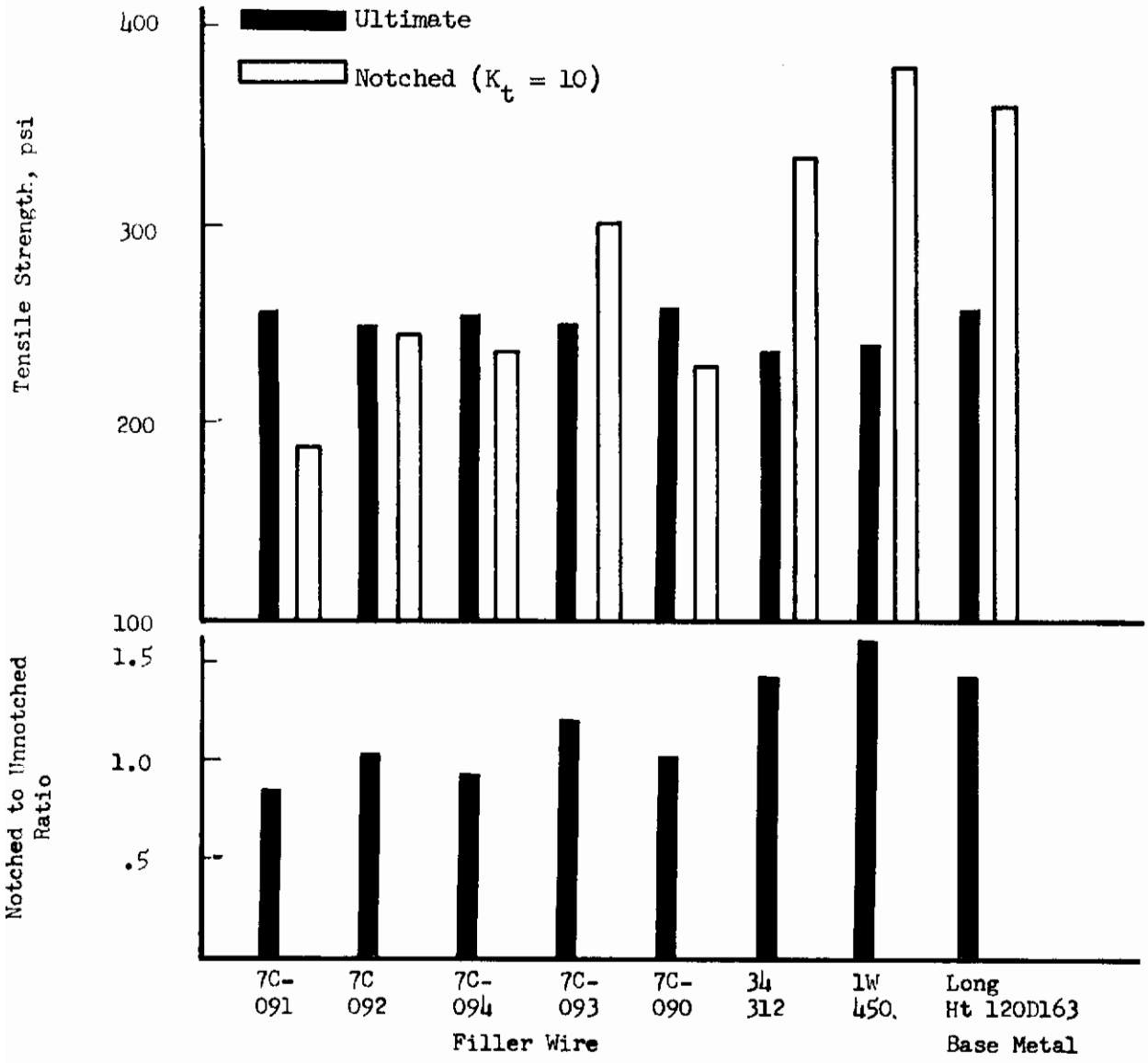

Figure 53. Notched Tensile Properties of TIG Weld Metals Deposited with Various Filler Wires in Grade 250, 1/2-In.-Thick, 18% Nickel Maraging Steel Plate, Heat 120D163, Aged at 900°F for 4 Hours after Welding

Approved for Public Release

Contrails

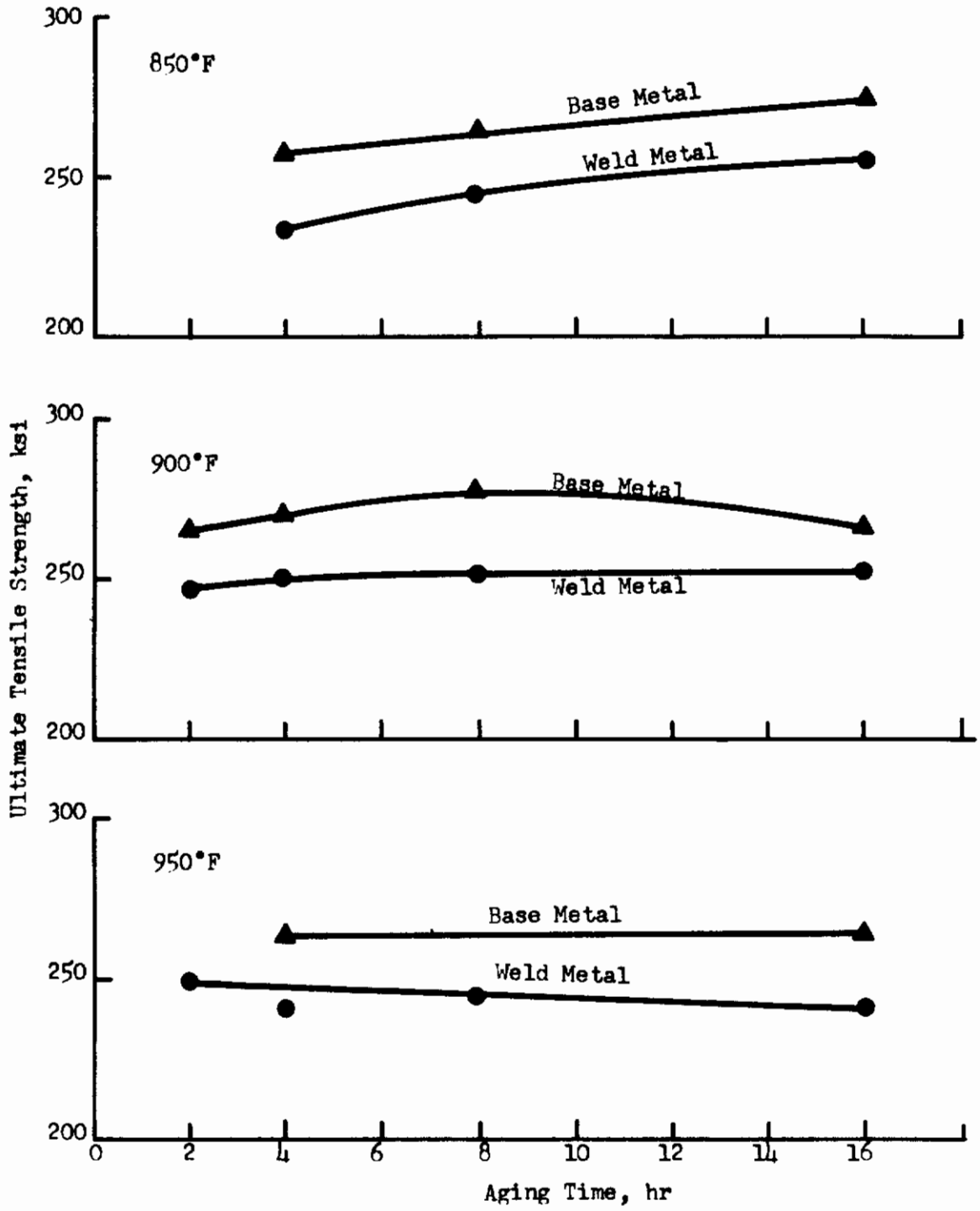

Figure 54. Effects of Aging Time and Temperature on the Ultimate Tensile Strength of TIG Weldments made with Filler Wire 7C-093 in Grade 250, 1/2-In.-Thick, 18% Nickel Maraging Steel Plate, Heat 120D163

Approved for Public Release

Contrails

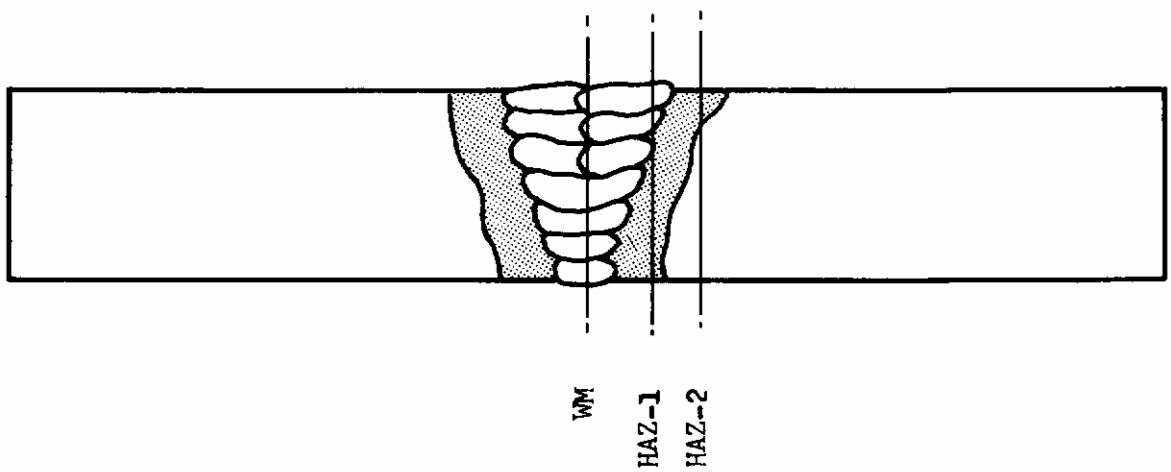

Figure 55. Schematic Diagram Showing Notch Location for Precracked-Charpy-Impact Specimens Prepared from Weldments in Grade 200, 1/2-In.-Thick, 18% Nickel Maraging Steel Plate, Heat 10675

Approved for Public Release

Contrails

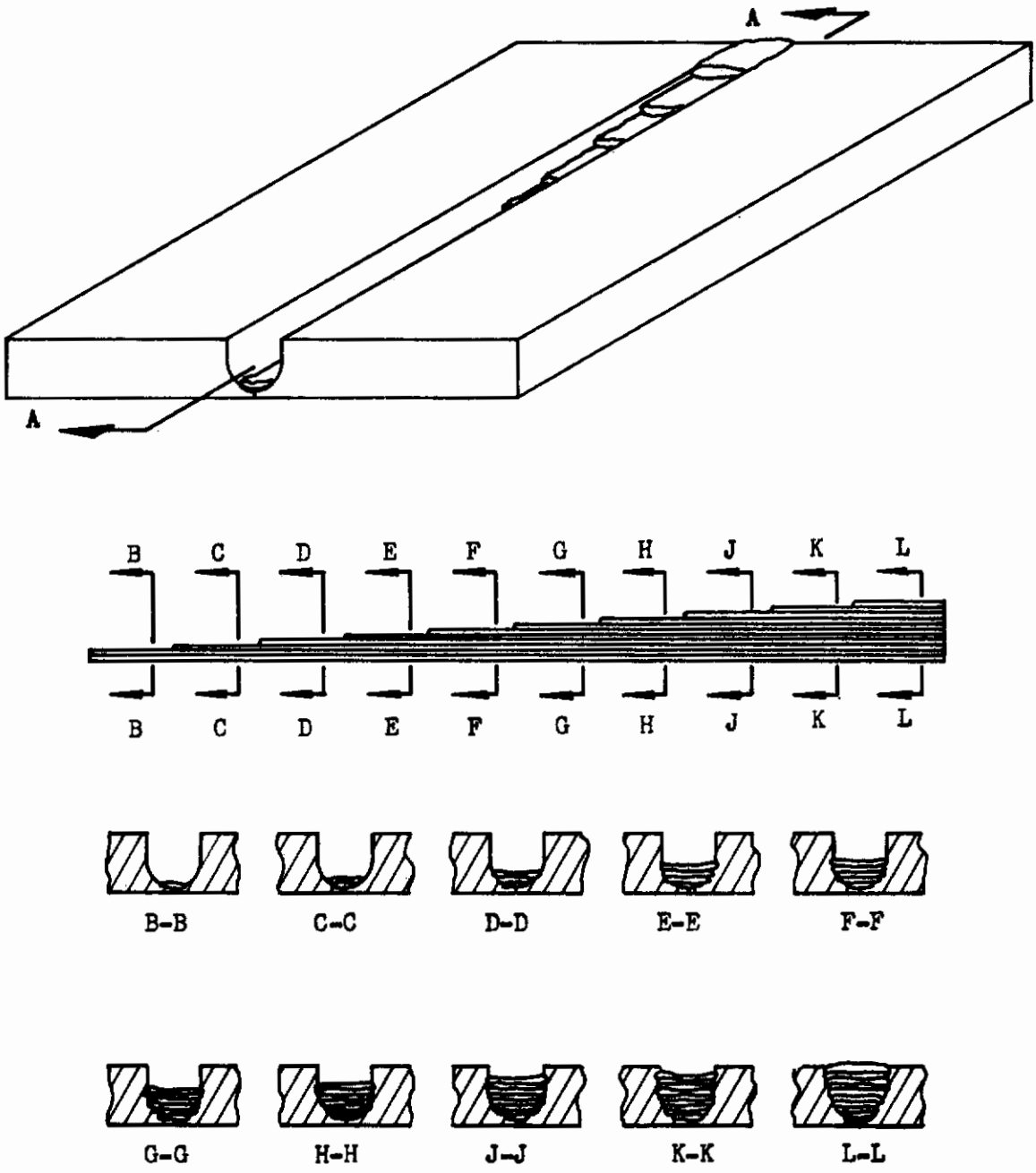

Figure 56. Schematic Diagram Illustrating the Processing of Weld Test Plates for Step-Weld Studies to Evaluate the Metallurgical Properties of Multipass Weldments in 18% Nickel Maraging Steel Plate

Approved for Public Release

Contrails

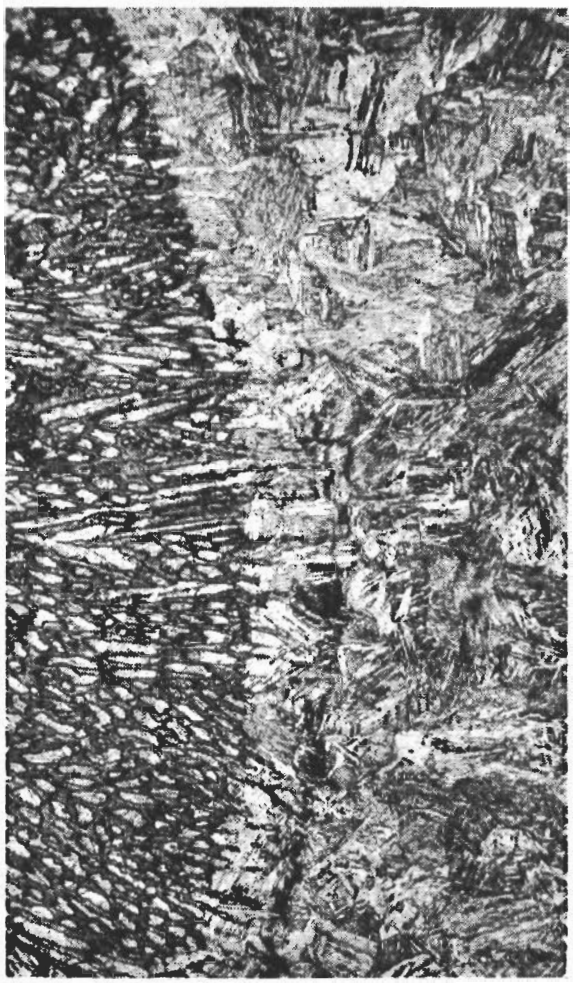

Marbles Etch Magnification: 250X

WM HAZ

Marbles Etch Magnification: 250X

WM HAZ

Figure 57. Typical Weld Metal and Heat-Affected Zone Microstructures in 18% Nickel Maraging Steel Plate

Approved for Public Release

Contrails

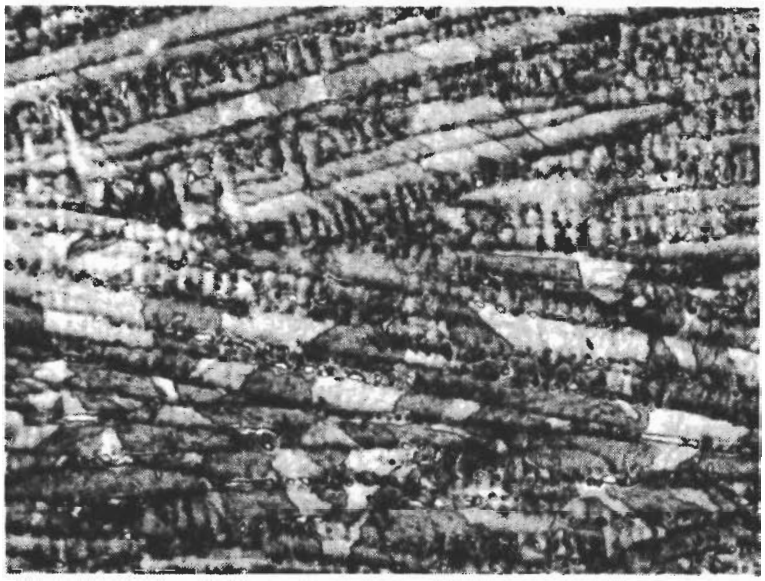

Marbles Etch Magnification: 250X

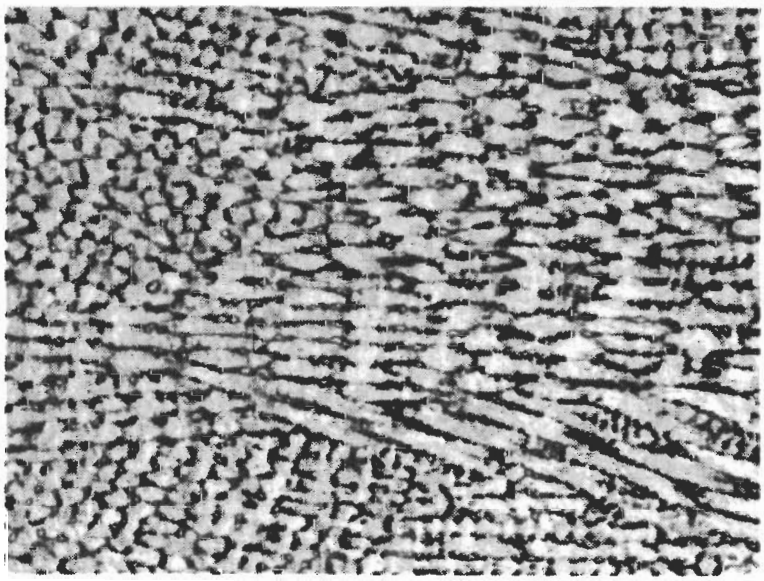

Marbles Etch Magnification: 250X

Figure 58. Typical Dendrite Segregation Found in Weld-Fusion-Zones of Weldments in 18% Nickel Maraging Steel Plate

Approved for Public Release

Contrails

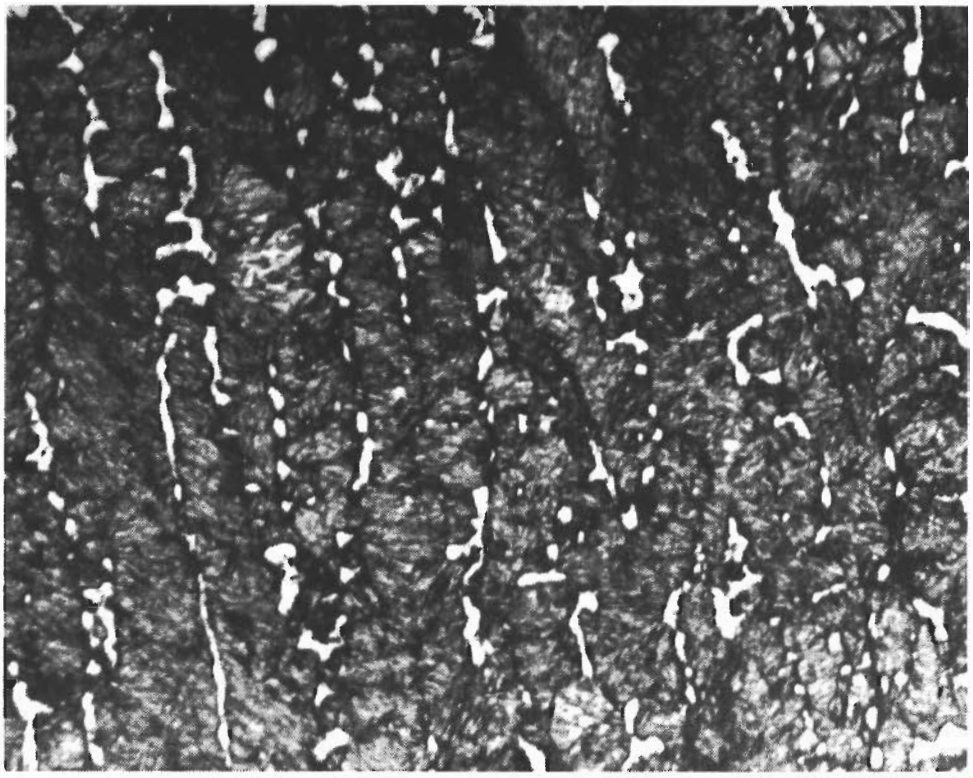

Marbles Etch Magnification: 530X

Figure 59. Interdendritic Phase in Weld-Fusion-Zones in 18% Nickel Maraging Steel Plate

Approved for Public Release

Contrails

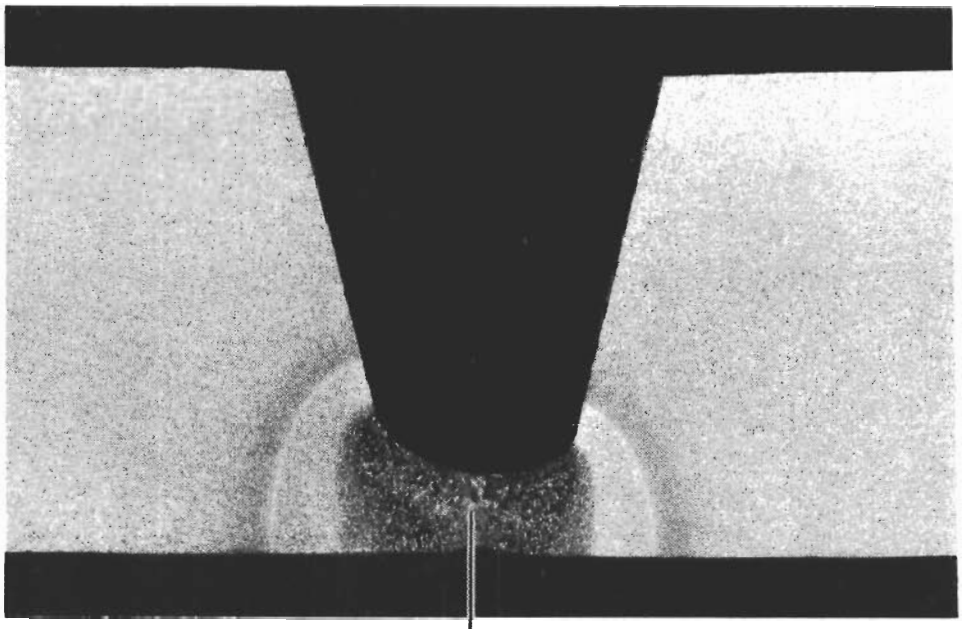

Marbles Etch Magnification: 5X

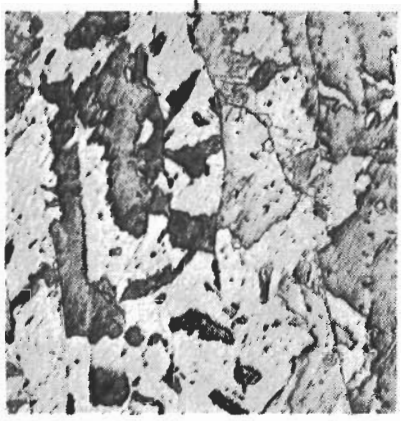

Marbles Etch Magnification: 250X

Figure 60. Weld-Metal Microstructure-As Welded. One TIG Weld Pass in Grade 250, 1/2-In.-Thick, 18% Nickel Maraging Steel Plate, Heat 120D163, Filler Wire 7C-093

Approved for Public Release

Contrails

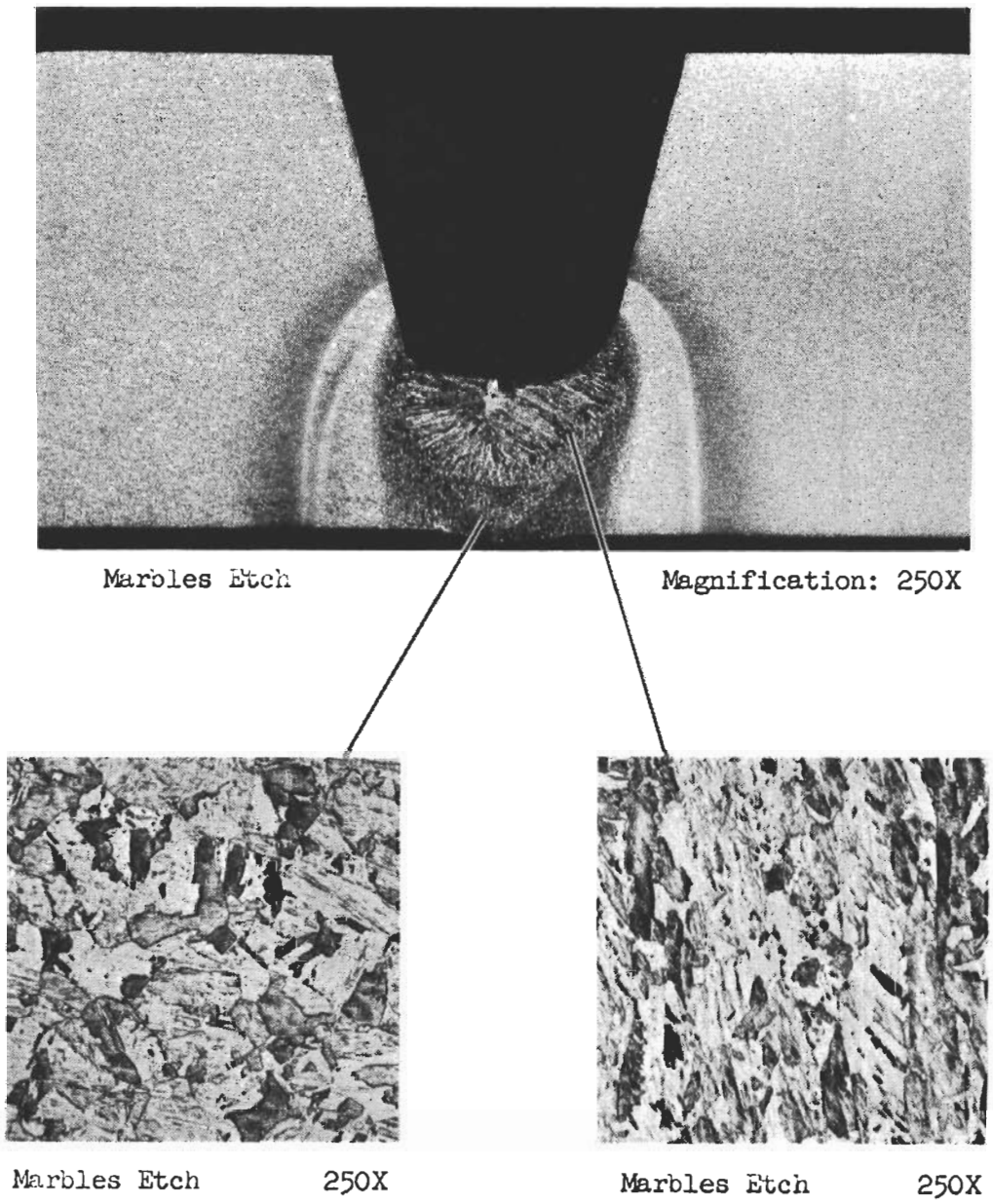

Figure 61. Weld-Metal Microstructure-As Welded. Three TIG Weld-Passes in Grade 250, 1/2-In.-Thick, 18% Nickel Maraging Steel Plate, Heat 120D163, Filler Wire 7C-093

Approved for Public Release

Contrails

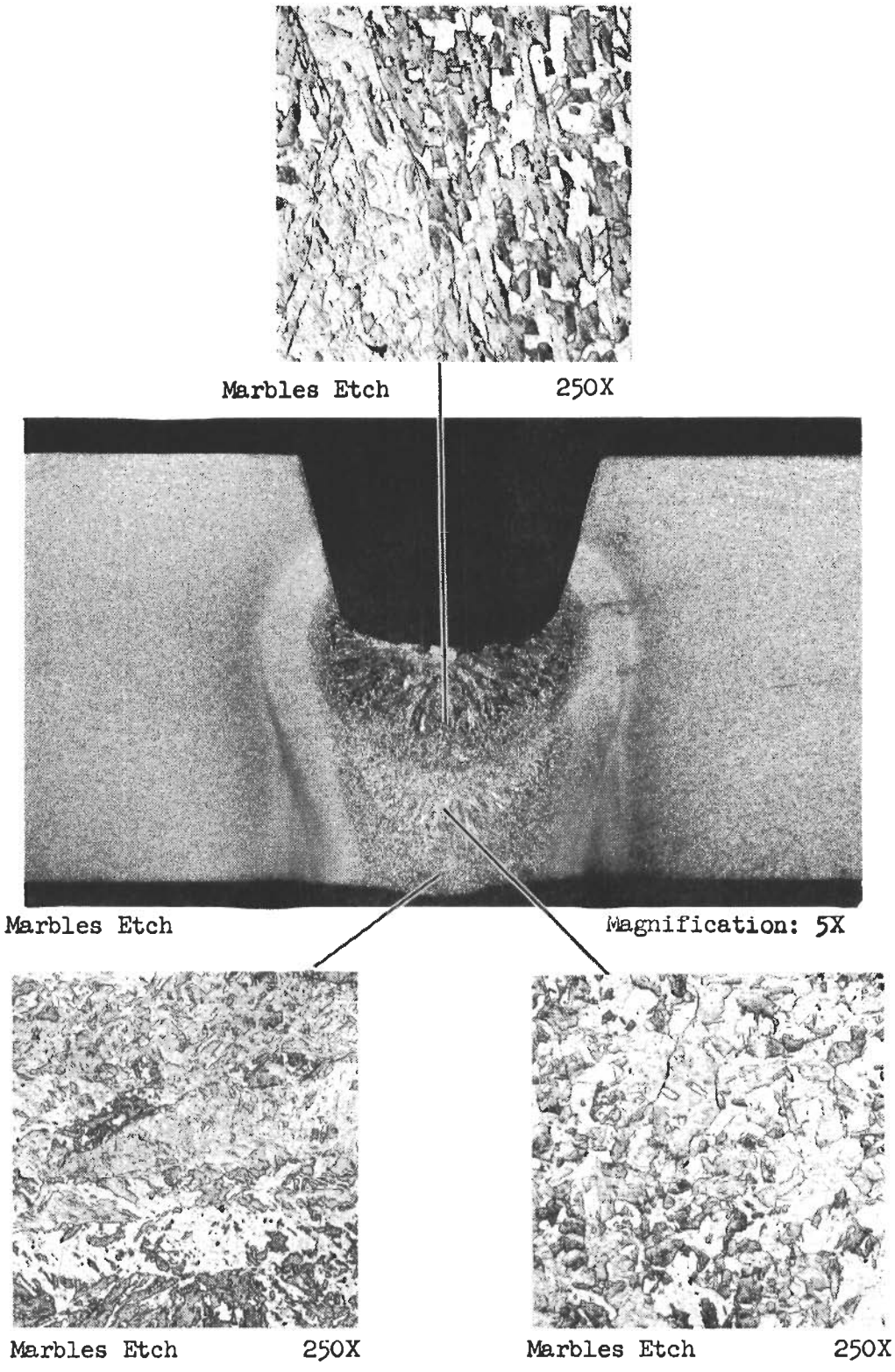

Figure 62. Weld-Metal Microstructure-As Welded. Five TIG Weld Passes in Grade 250, 1/2-In.-Thick, 18% Nickel Maraging Steel Plate, Heat 120D163, Filler Wire 7C-093

Approved for Public Release

Contrails

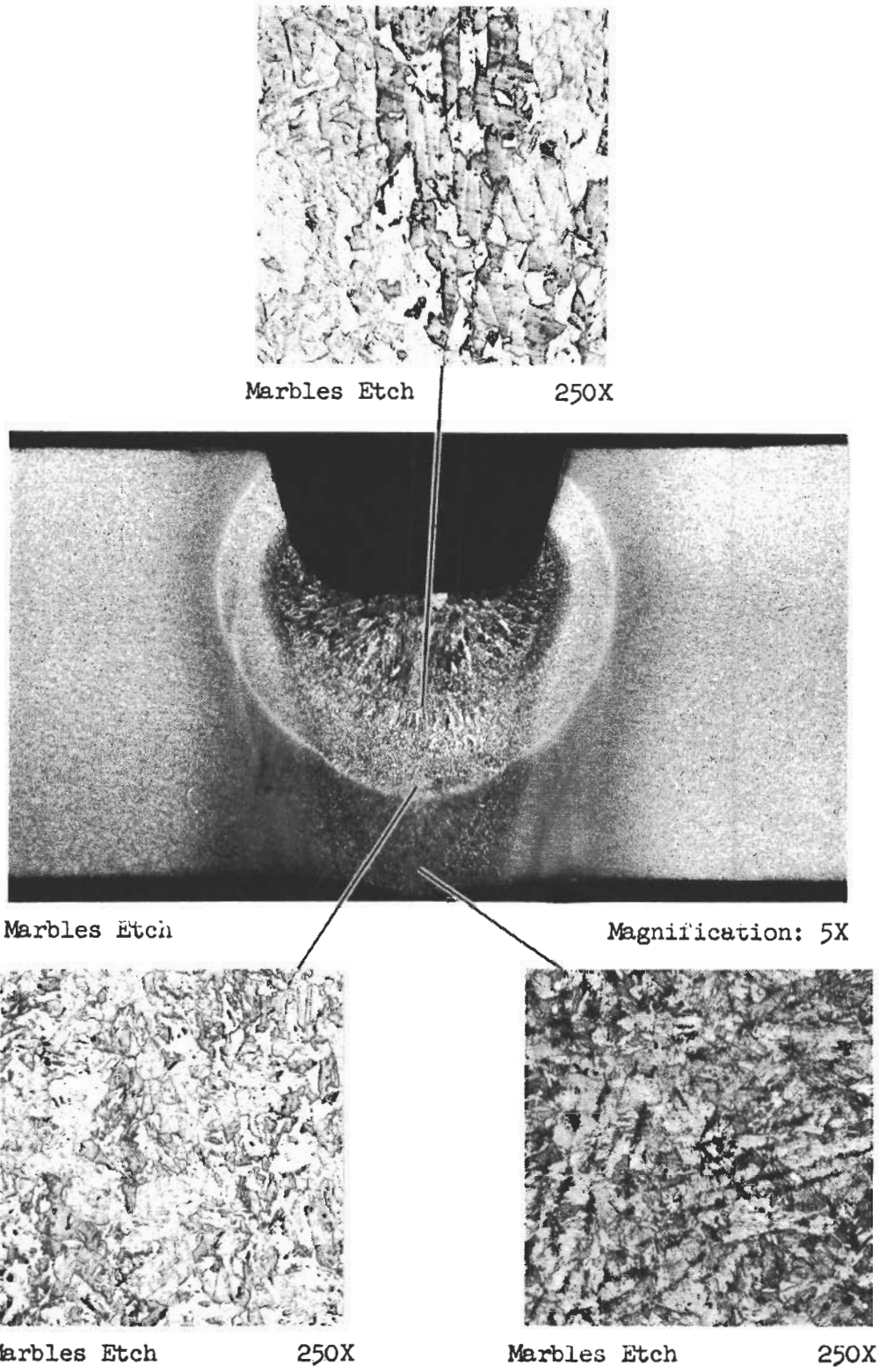

Figure 63. Weld-Metal Microstructure-As Welded. Six TIG Weld Passes in Grade 250, 1/2-In.-Thick, 18% Nickel Maraging Steel Plate, Heat 120D163, Filler Wire 7C-093

Approved for Public Release

Contrails

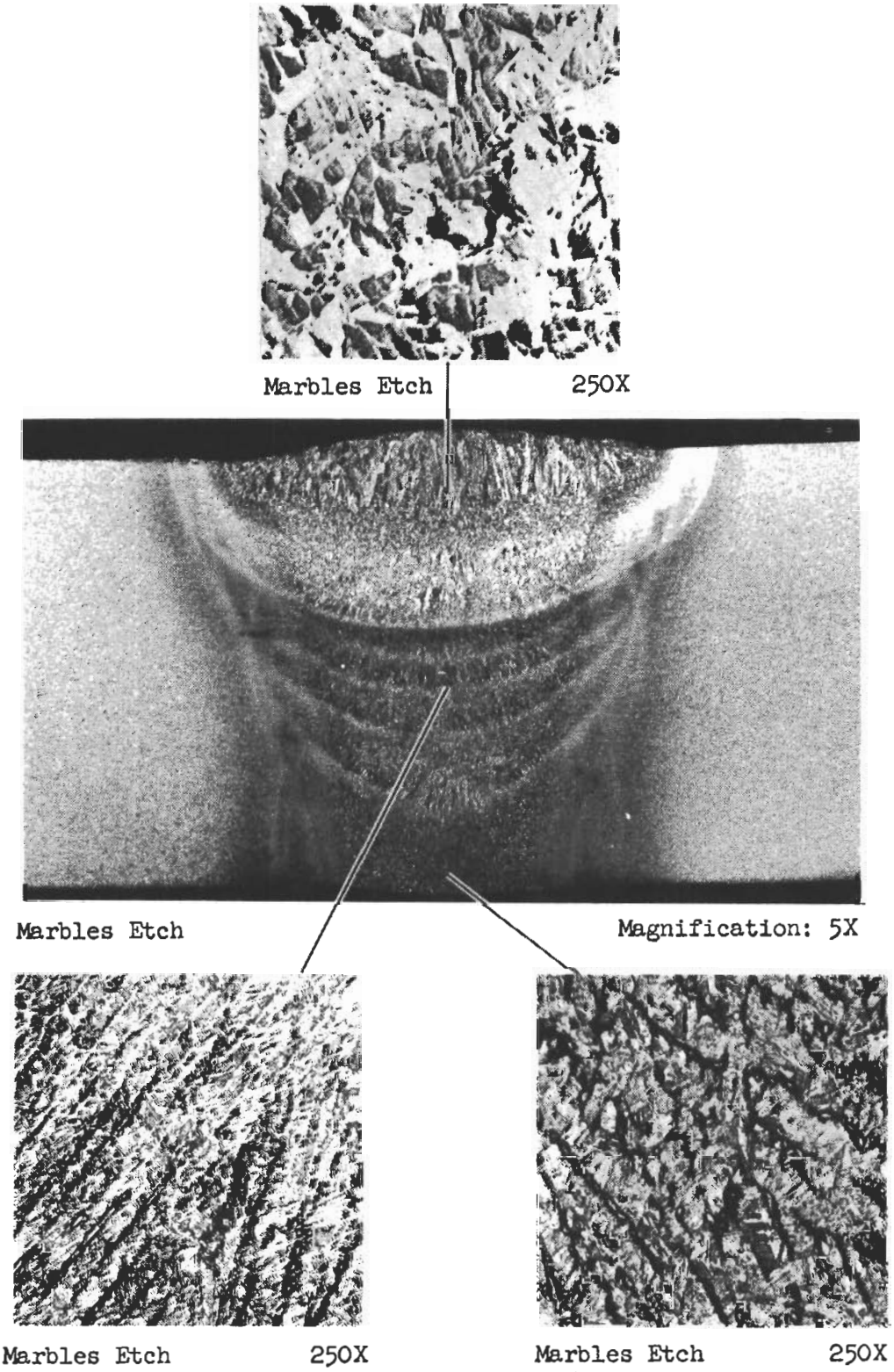

Figure 64. Weld-Metal Microstructure-As Welded. Complete TIG Weld in Grade 250, 1/2-In.-Thick, 18% Nickel Maraging Steel Plate, Heat 120D163, Filler Wire 7C-093

Approved for Public Release

Contrails

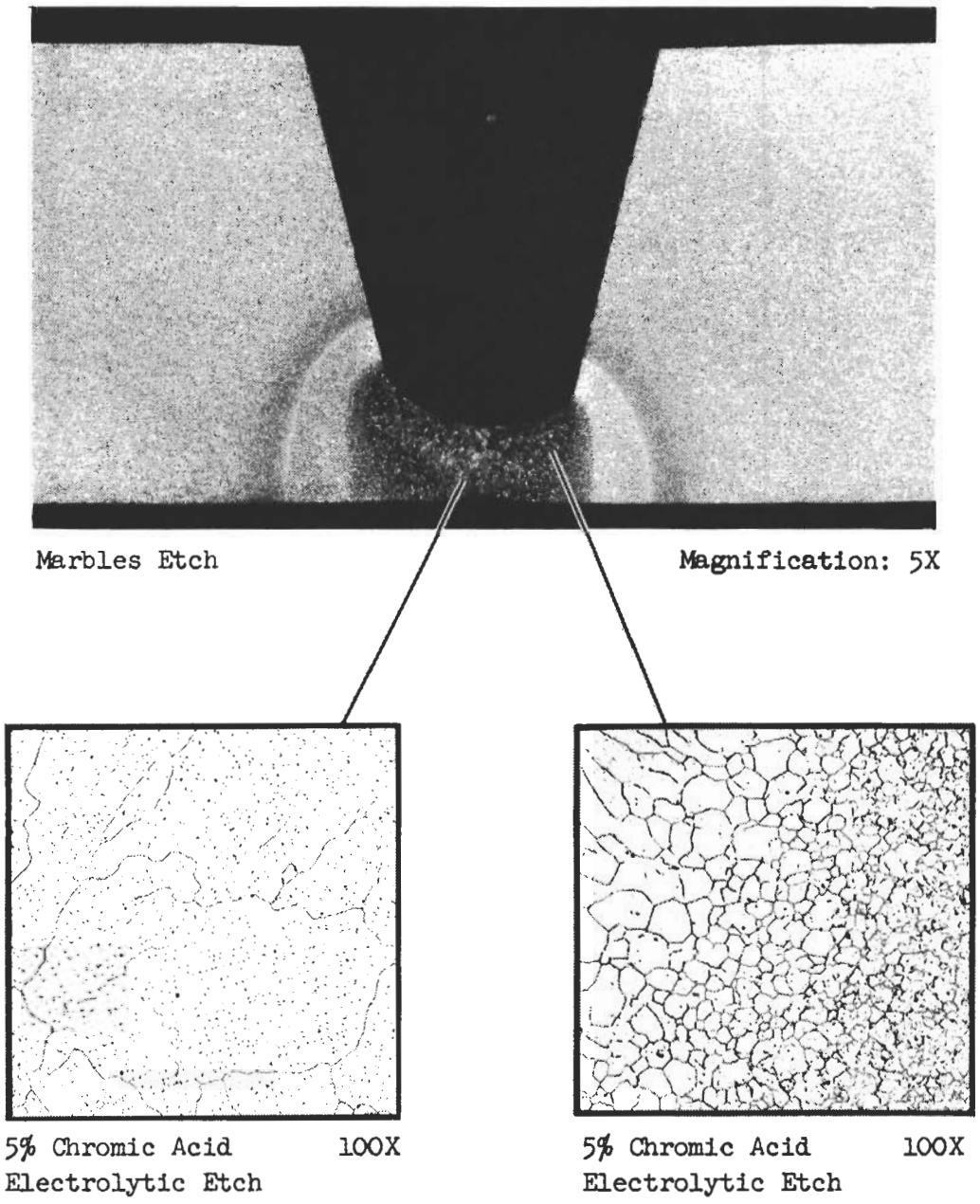

Figure 65. Weld Metal and Heat-Affected Zone Grain Size After One TIG Weld-Pass in Grade 250, 1/2-In.-Thick, 18% Nickel Maraging Steel Plate, Heat 120D163, Filler Wire 7C-093

Approved for Public Release

Contrails

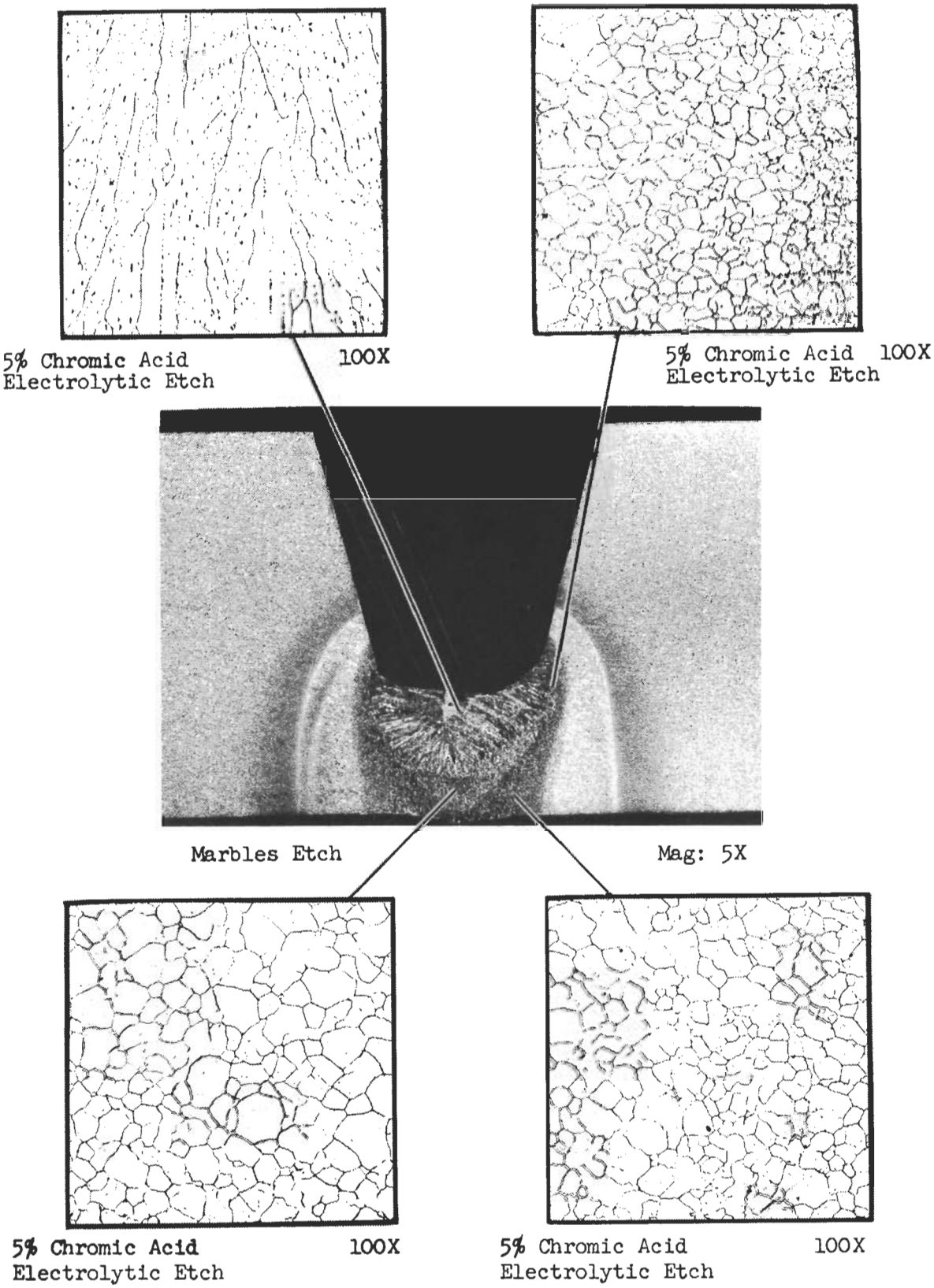

Figure 66. Weld Metal and Heat-Affected Zone Grain Size, After Three TIG Weld Passes in Grade 250, 1/2-In.-Thick, 18% Nickel Maraging Steel Plate, Heat 120D163, Filler Wire 7C-093

Approved for Public Release

Contrails

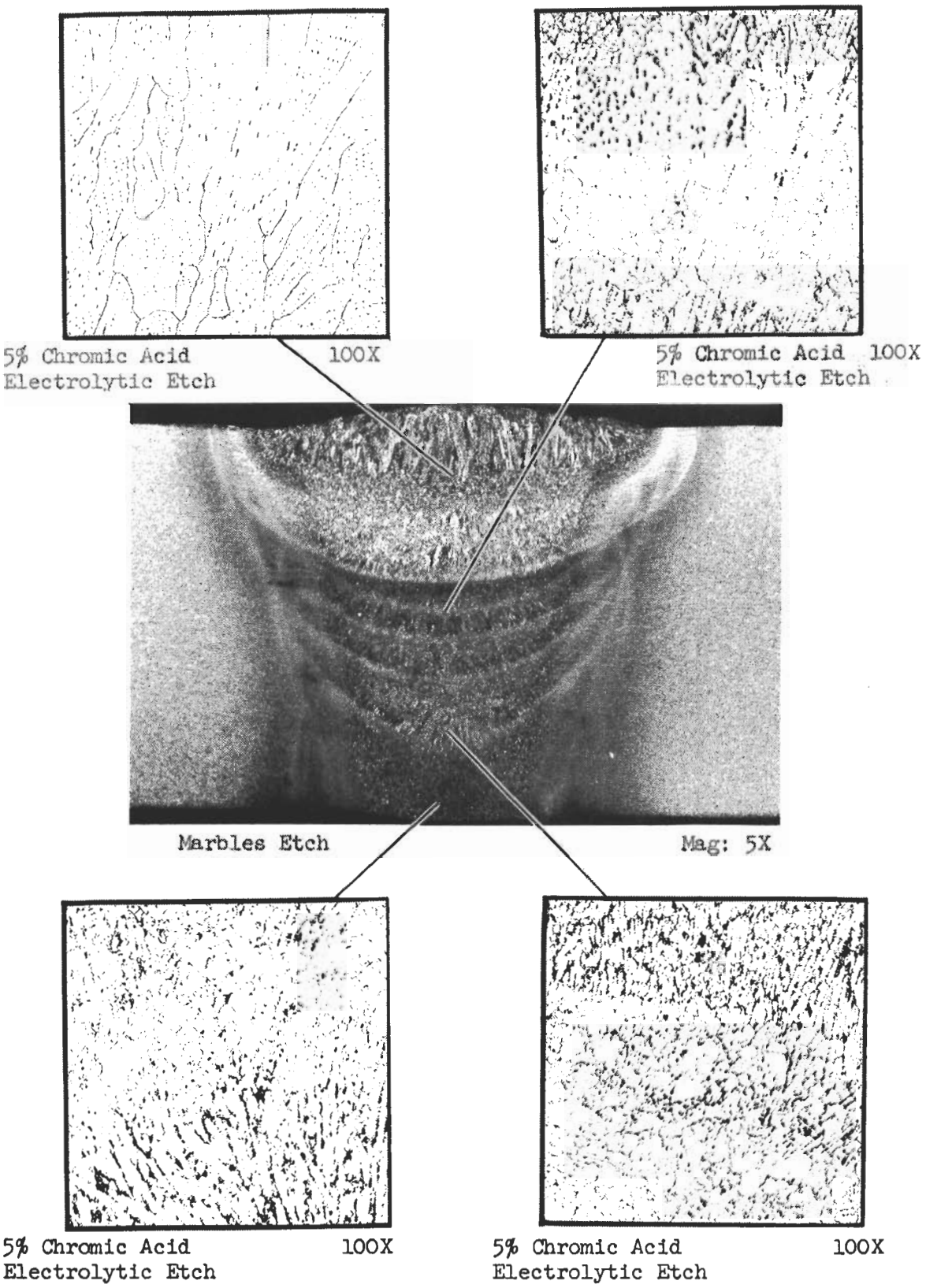

Figure 67: Weld-Metal Grain Size, After Completed TIG Weld in Grade 250, 1/2-In.-Thick, 18% Nickel Maraging Steel Plate, Heat 120D163, Filler Wire 7C-093

Approved for Public Release

Contrails

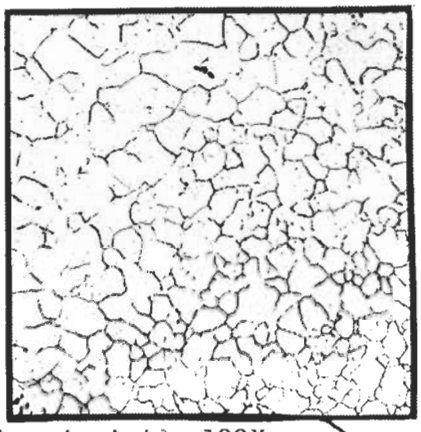

5% Chromic Acid 100X
Electrolytic Etch

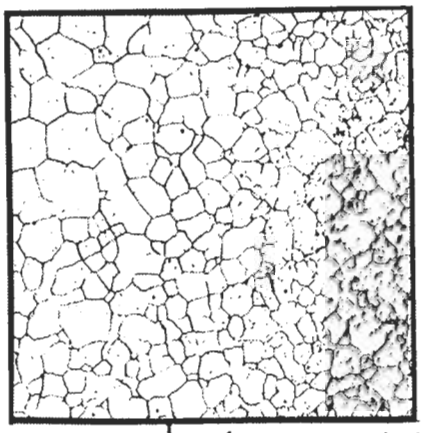

5% Chromic Acid 100X
Electrolytic Etch

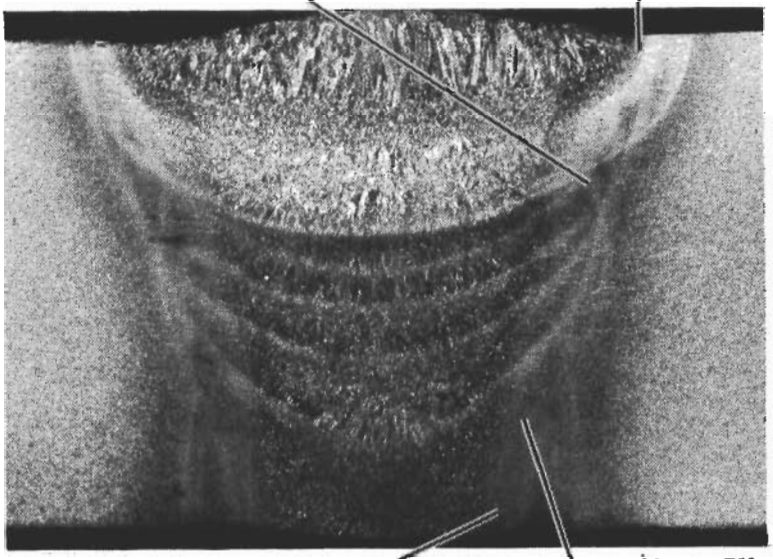

Marbles Etch

Mag: 5X

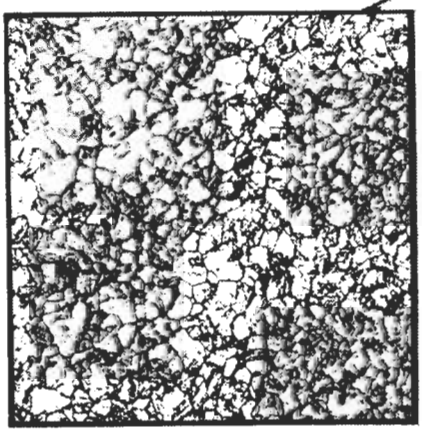

5% Chromic Acid 100X
Electrolytic Etch

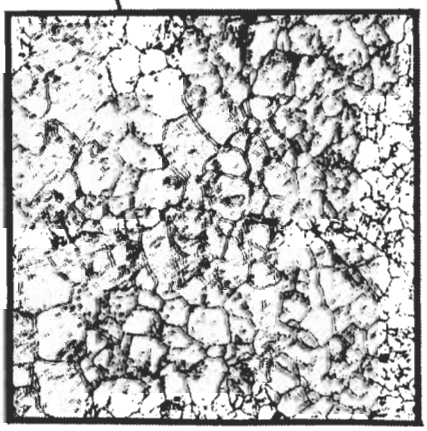

5% Chromic Acid 100X
Electrolytic Etch

Figure 68. Heat-Affected Zone Grain Size After Completed TIG Weld in Grade 250, 1/2-In.-Thick, 18% Nickel Maraging Steel Plate, Heat 120D163, Filler Wire 7C-093

Approved for Public Release

Contrails

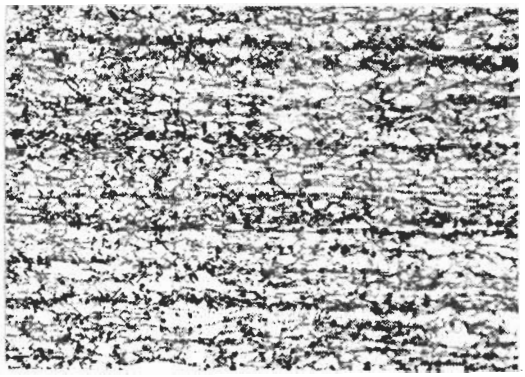

10% Chromic Acid Electrolytic Etch 250X

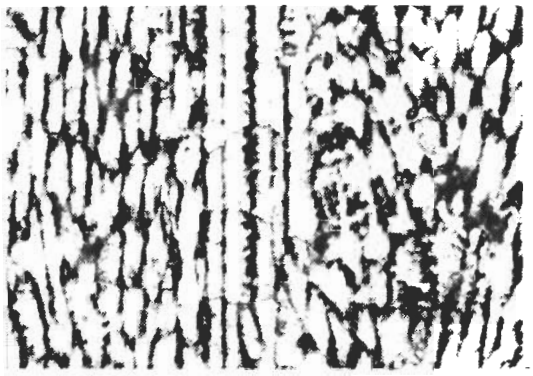

Marbles Etch 250X

1600°F for 1 Hour

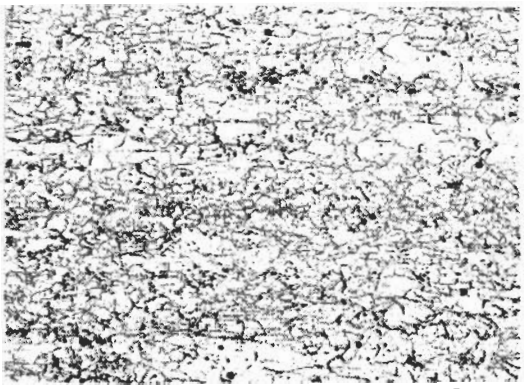

10% Chromic Acid Electrolytic Etch 250X

Marbles Etch 250X

1800°F for 1 Hour

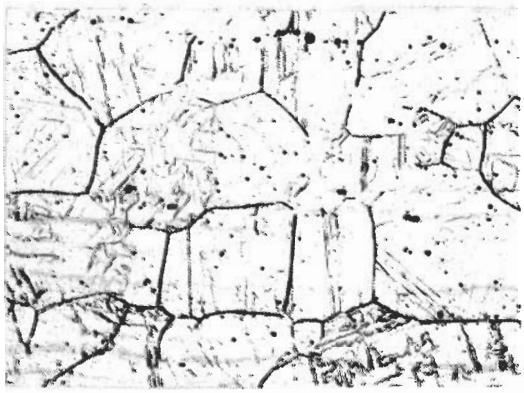

10% Chromic Acid Electrolytic Etch 250X

Marbles Etch 250X

2000°F for 1 Hour

Base Metal Weld Metal

Figure 69. Effects of Solution-Annealing Treatments on the Microstructure of Grade 250, 18% Nickel Maraging Steel Plate, Heat 120D163, Filler Wire 7C-093

Approved for Public Release

Contrails

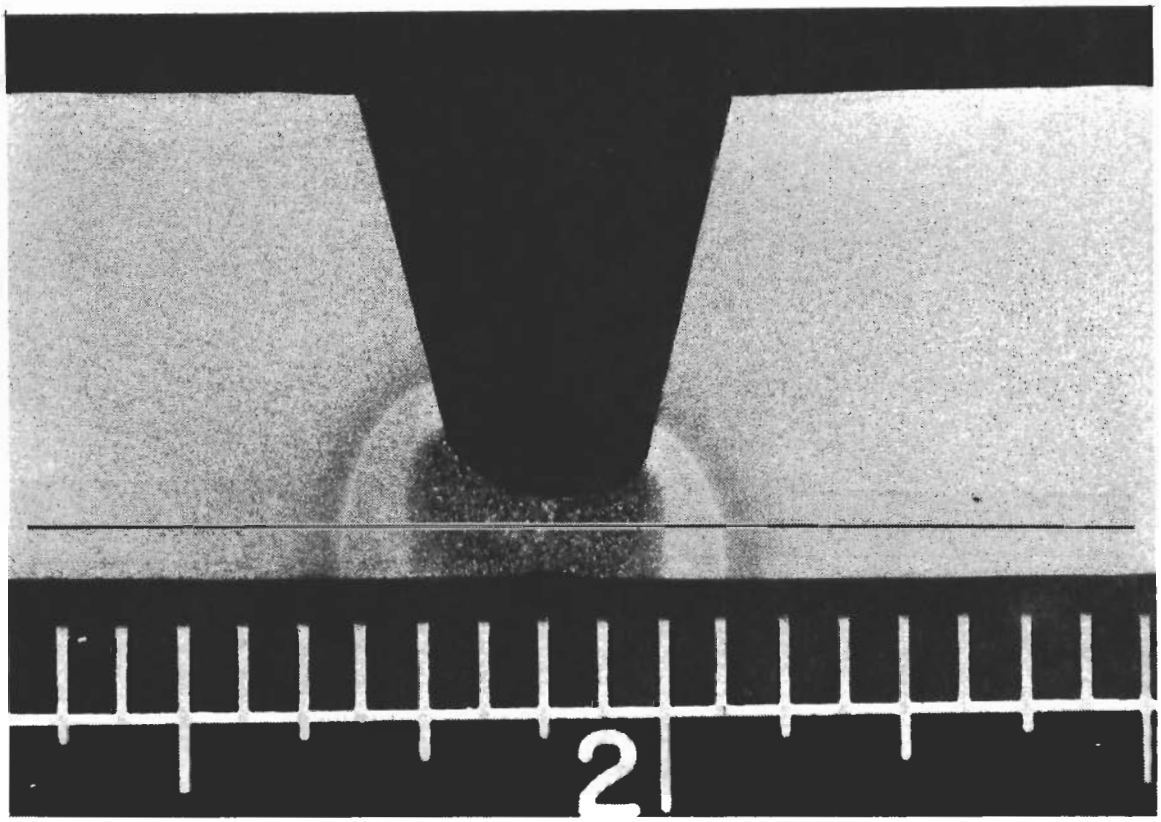

Marbles Etch

Magnification: 5X

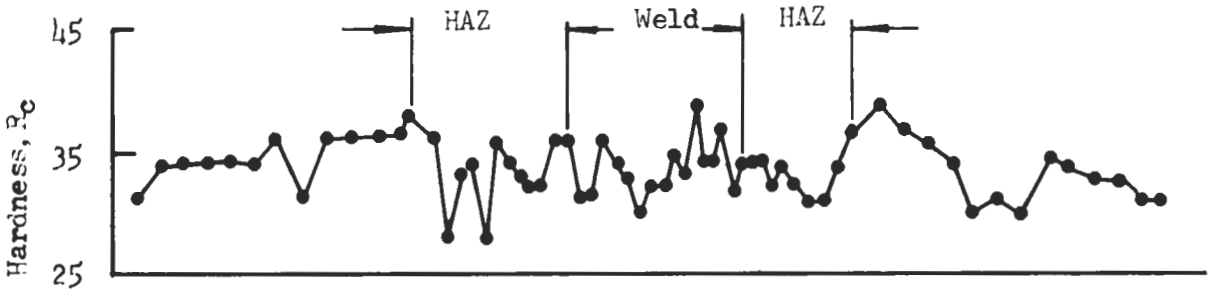

Figure 70. Typical Results of Microhardness Evaluations of Grade 250, 1/2-In.-Thick, 18% Nickel Maraging Steel Plate Weldments Using TIG Process, As Welded with One Weld Pass, Heat 120D163, Filler Wire 7C-093

Approved for Public Release

Contrails

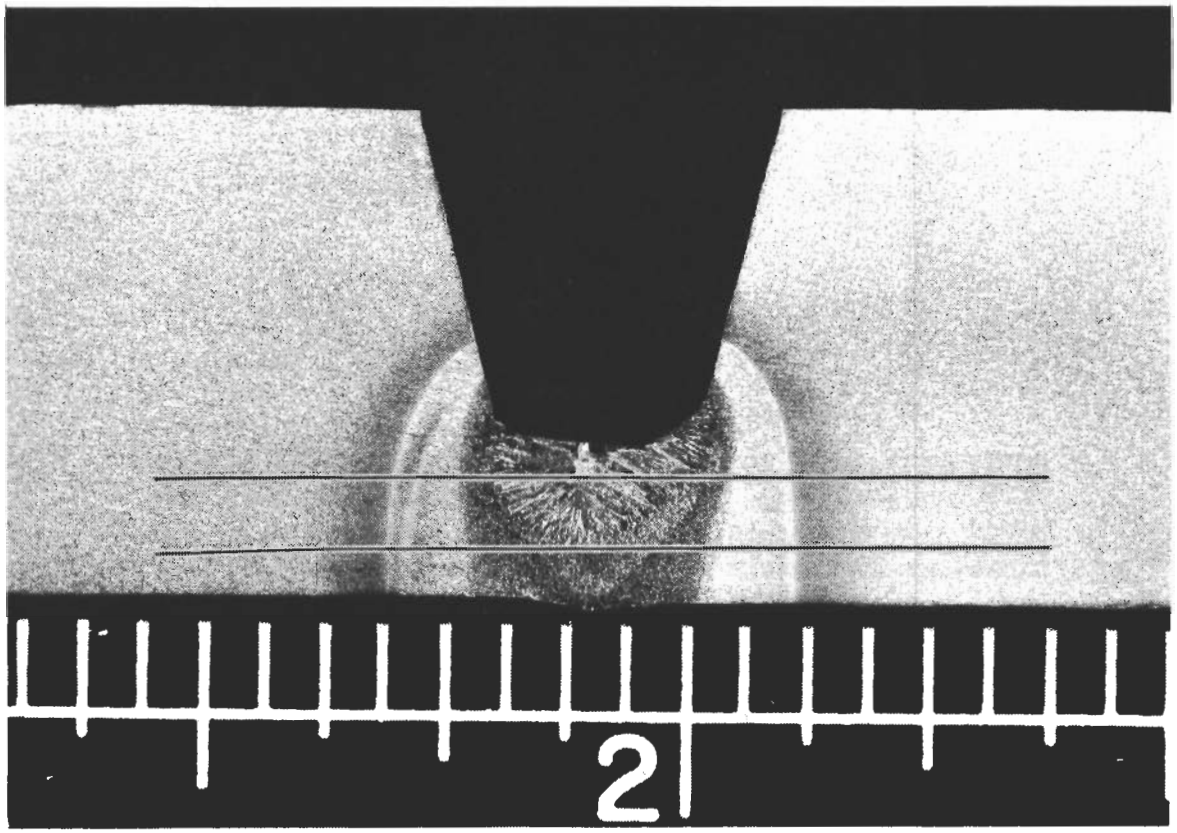

Marbles Etch

Magnification: 5X

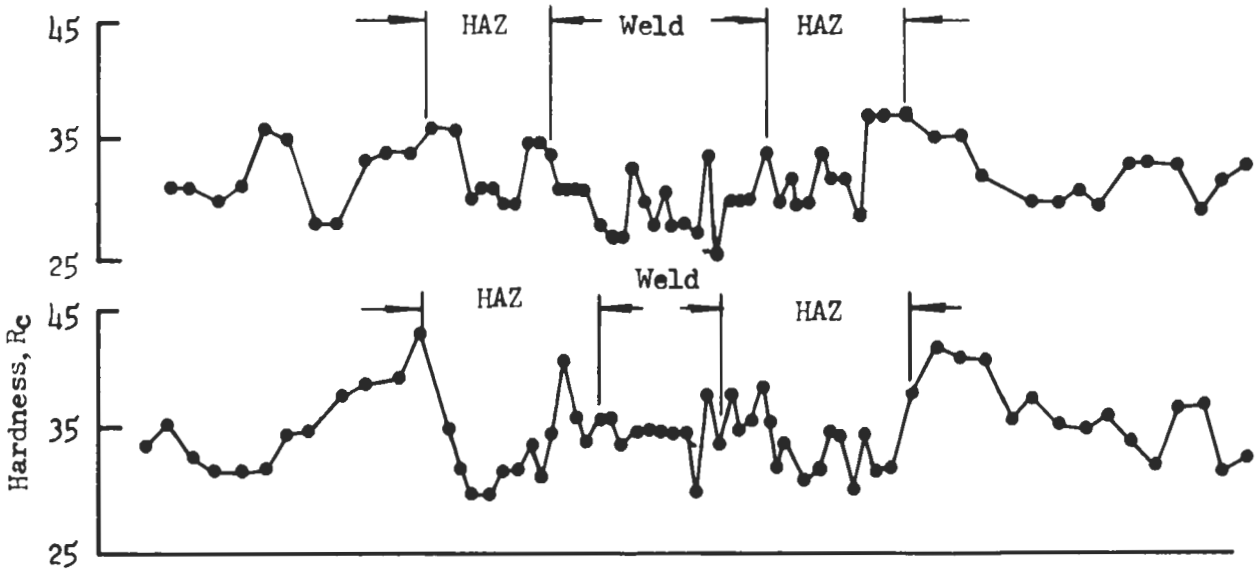

Figure 71. Typical Results of Microhardness Evaluations of Grade 250, 1/2-In.-Thick, 18% Nickel Maraging Steel Plate Weldments Using TIG Process, As Welded with Three Weld Passes, Heat 120D163, Filler Wire 7C-093

Approved for Public Release

Contrails

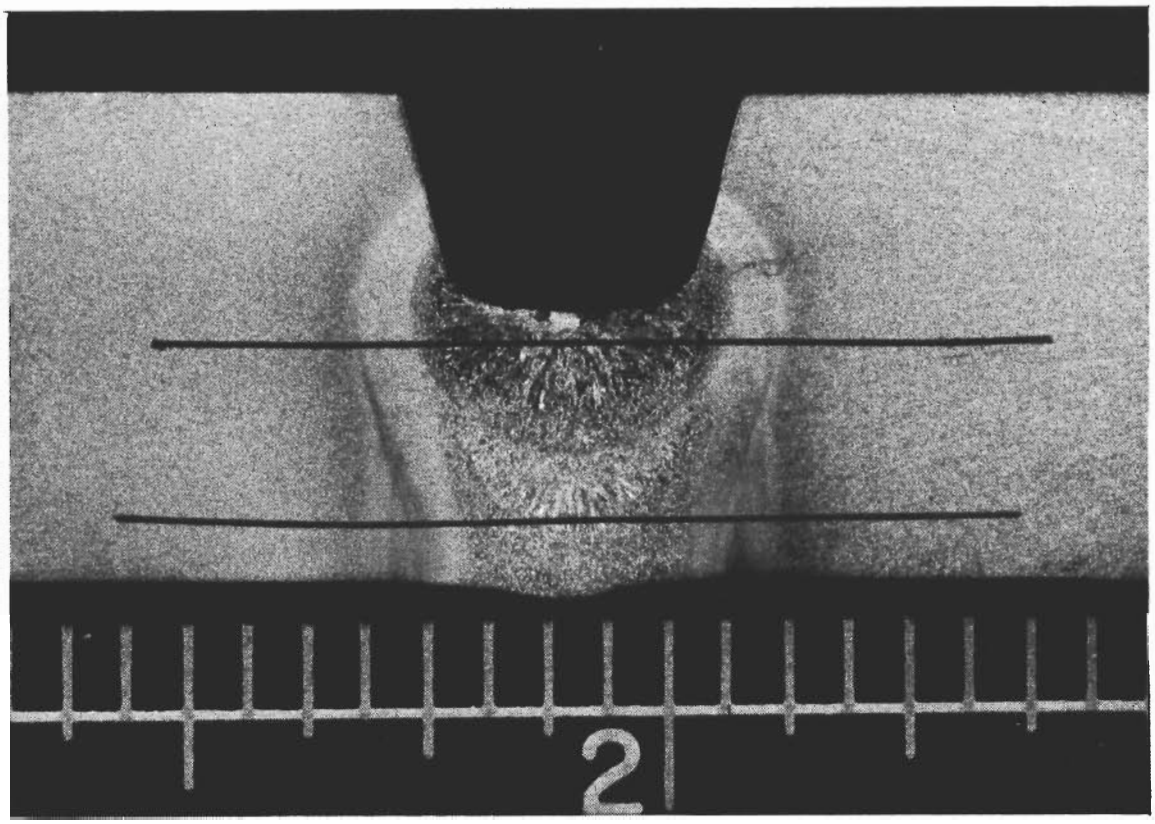

Marbles Etch Magnification: 5X

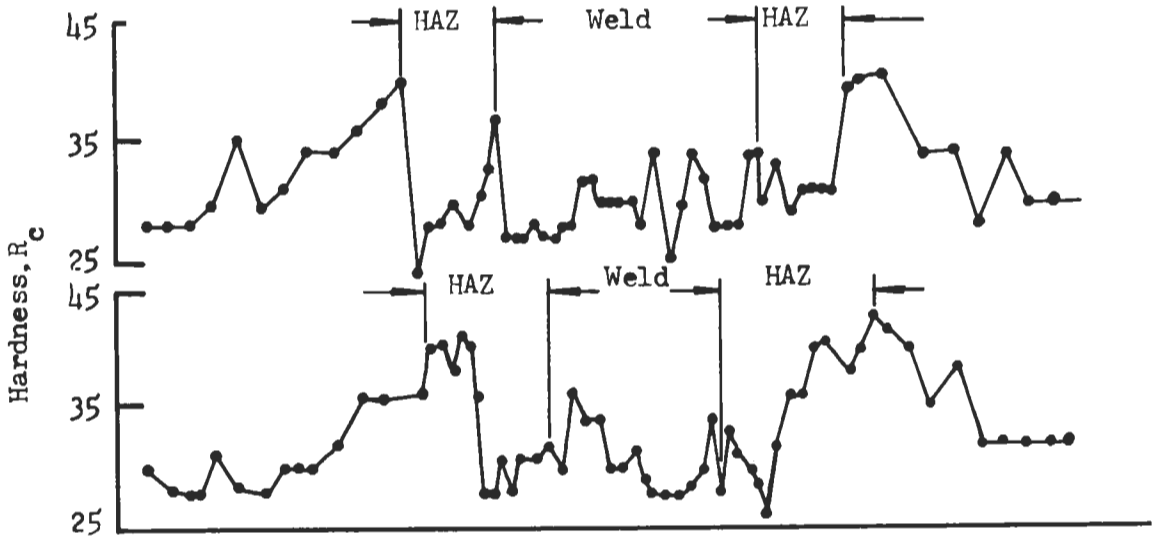

Figure 72. Typical Results of Microhardness Evaluations of Grade 250, 1/2-In.-Thick, 18% Nickel Maraging Steel Plate Weldments Using TIG Process, As Welded with Five Weld Passes, Heat 120D163, Filler Wire 7C-093

Approved for Public Release

Contrails

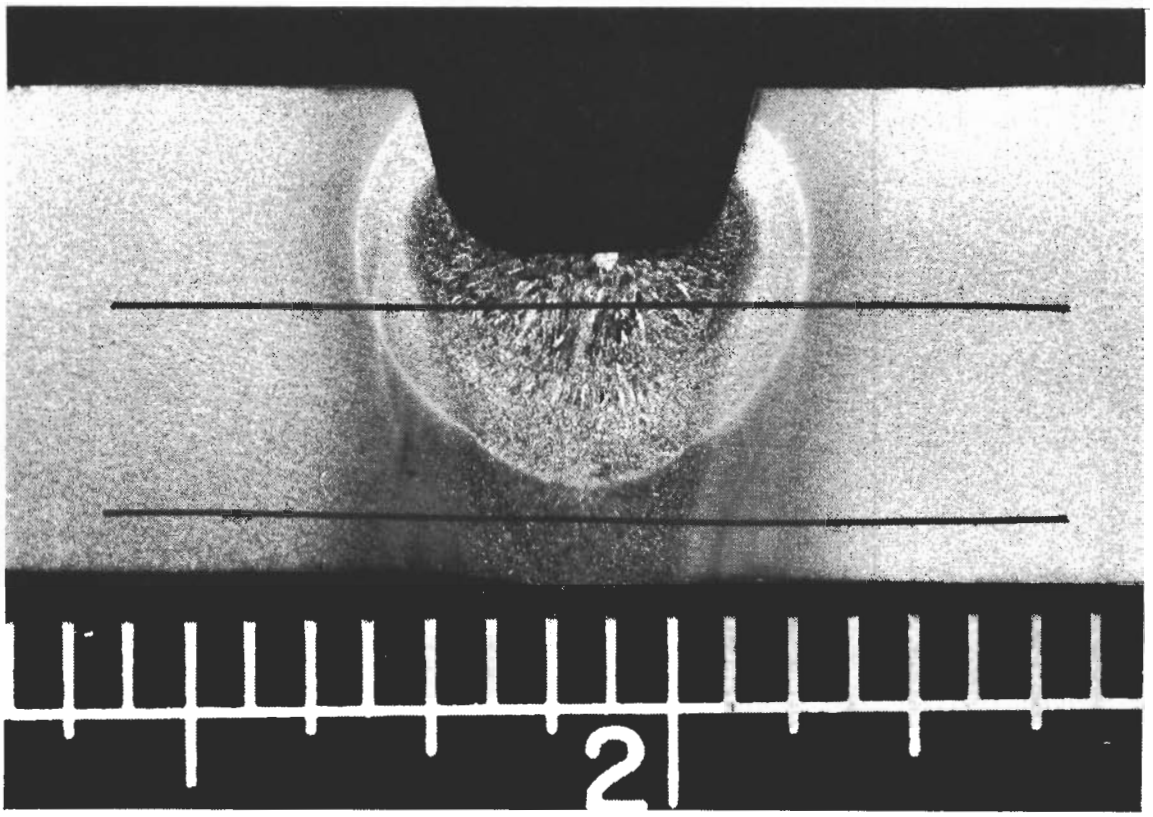

Marbles Etch Magnification: 5X

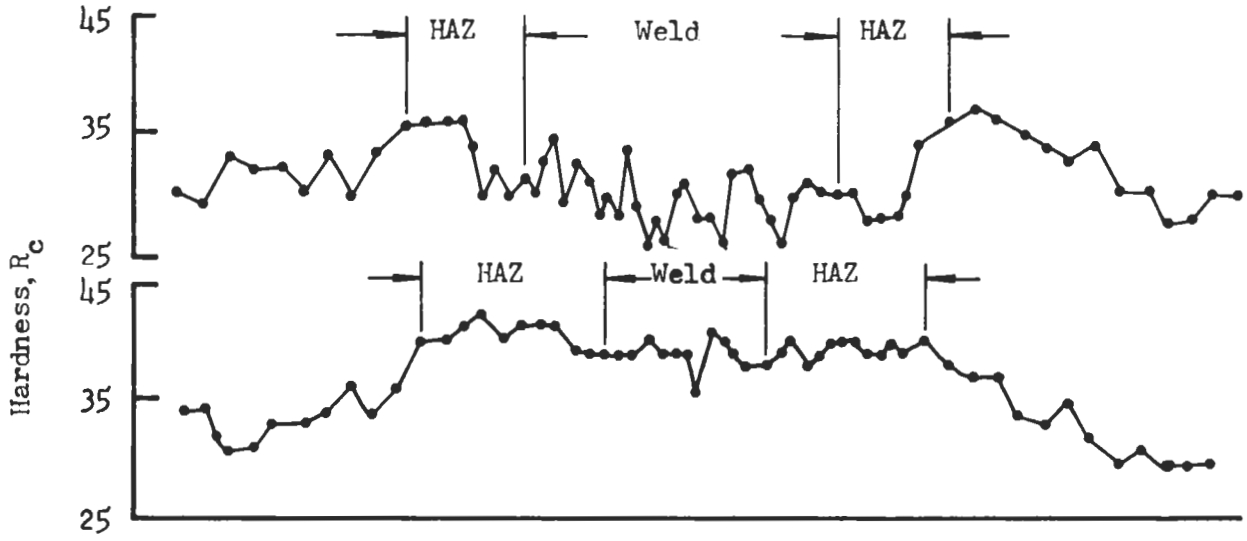

Figure 73. Typical Results of Microhardness Evaluations of Grade 250, 1/2-In.-Thick, 18% Maraging Steel Plate Weldments Using TIG Process, As Welded with Six Weld Passes Heat 120D163, Filler Wire 7C-093

Approved for Public Release

Contrails

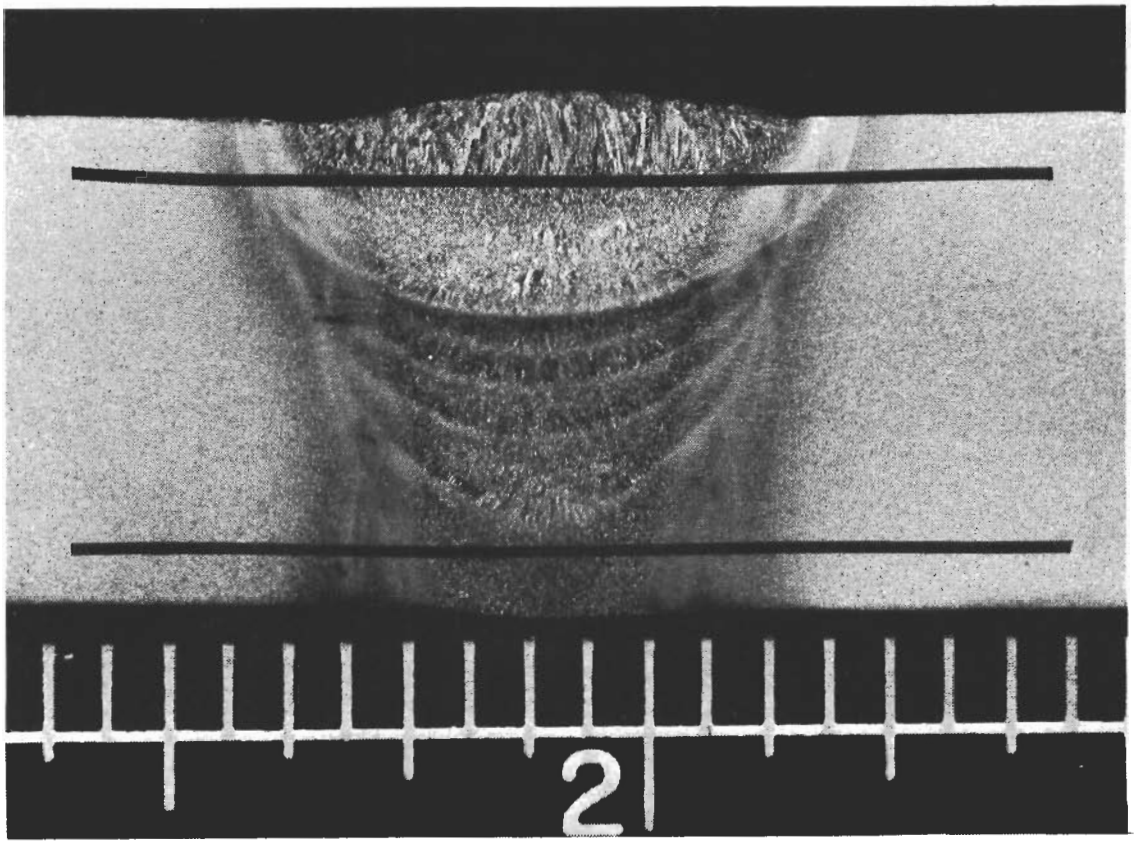

Marbles Etch

Magnification: 5X

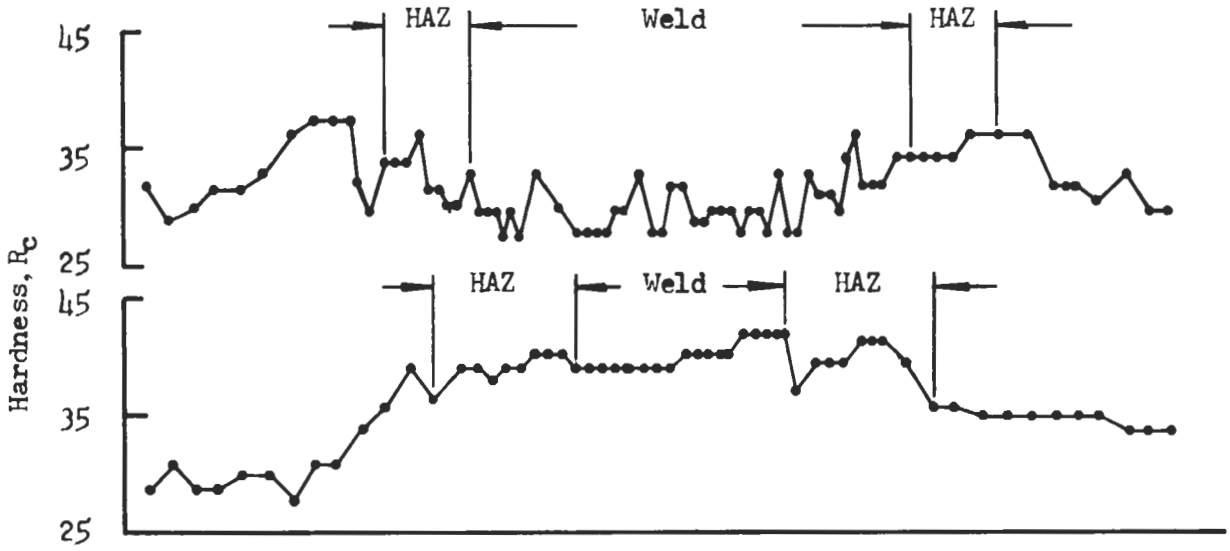

Figure 74. Typical Results of Macrostructure and Microhardness Evaluations of Grade 250, 1/2-In.-Thick, 18% Nickel Maraging Steel Plate Weldments Using TIG Process, As Welded, Complete Weld, Heat 120D163, Filler Wire 7C-093

Approved for Public Release

Contrails

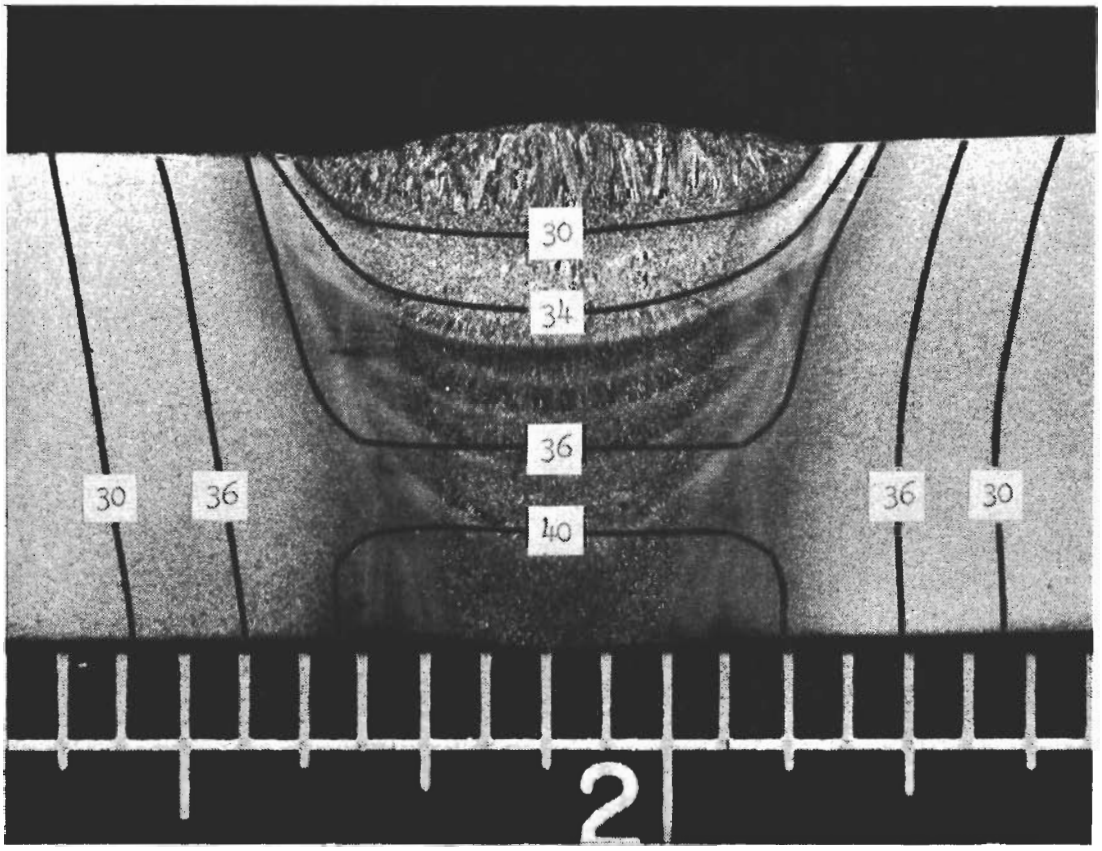

Marbles Etch Magnification: 5X

Figure 75. Typical Results of Microhardness Evaluations of Grade 250, 1/2-In.-Thick, 18% Nickel Maraging Steel Plate Weldments Using TIG Process, As Welded, Complete Weld, Heat 120D163, Filler Wire 7C-093

Approved for Public Release

Contrails

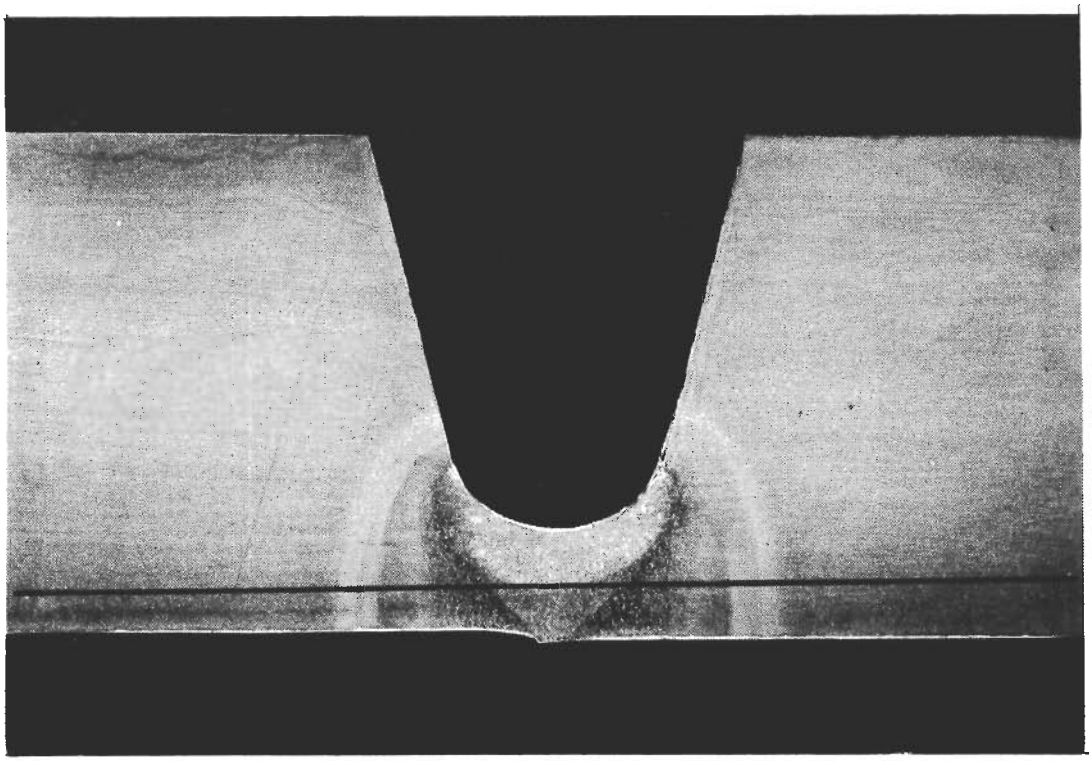

Marbles Etch

Magnification: 5X

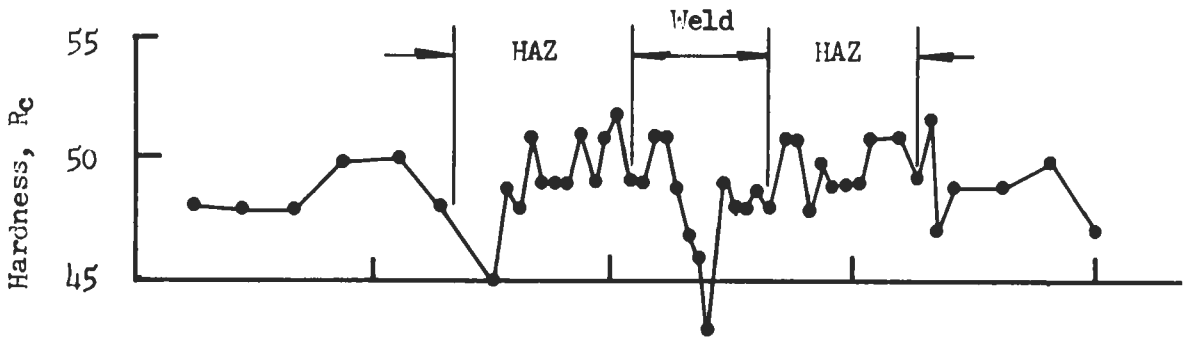

Figure 76. Typical Results of Microhardness Evaluations of Grade 250, 1/2-In.-Thick, 18% Nickel Maraging Steel Plate Weldments Using TIG Process, Welded with Two Weld Passes and Aged at 900°F for 8 Hours, Heat 120D163, Filler Wire 7C-093

Approved for Public Release

Contrails

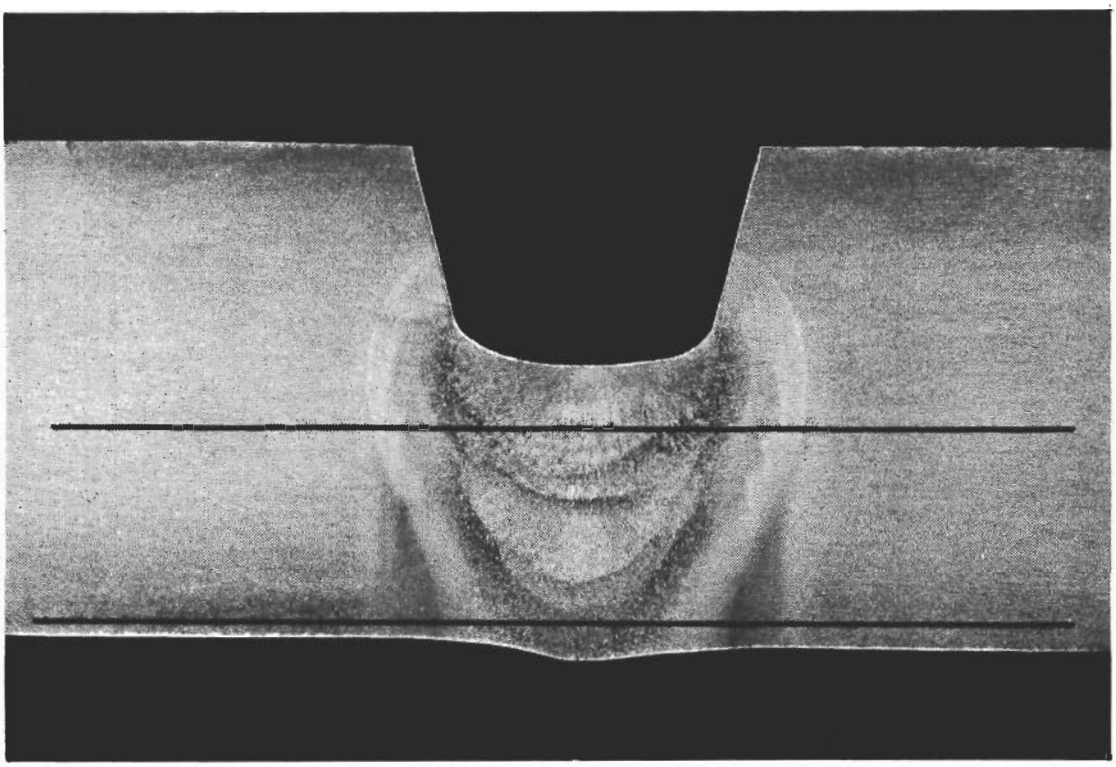

Marbles Etch

Magnification: 5X

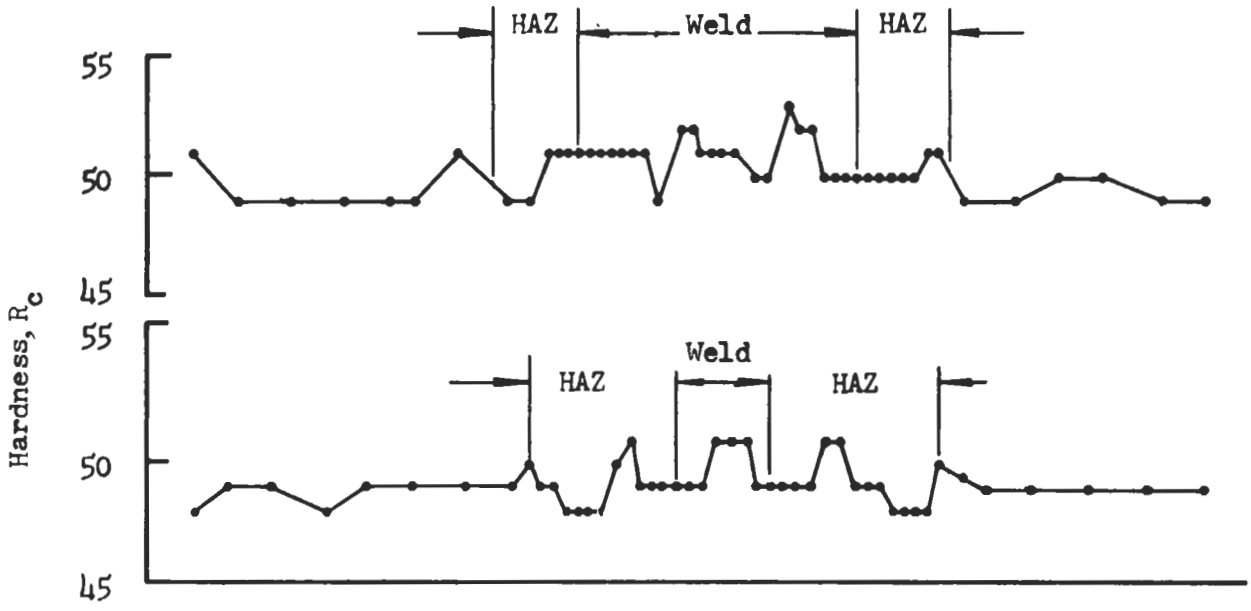

Figure 77. Typical Results of Microhardness Evaluations of Grade 250, 1/2-In.-Thick, 18% Maraging Steel Plate Weldments Using TIG Process, Welded With Five Weld Passes and Aged at 900°F for 8 Hours, Heat 120D163, Filler Wire 7C-093

Approved for Public Release

Contrails

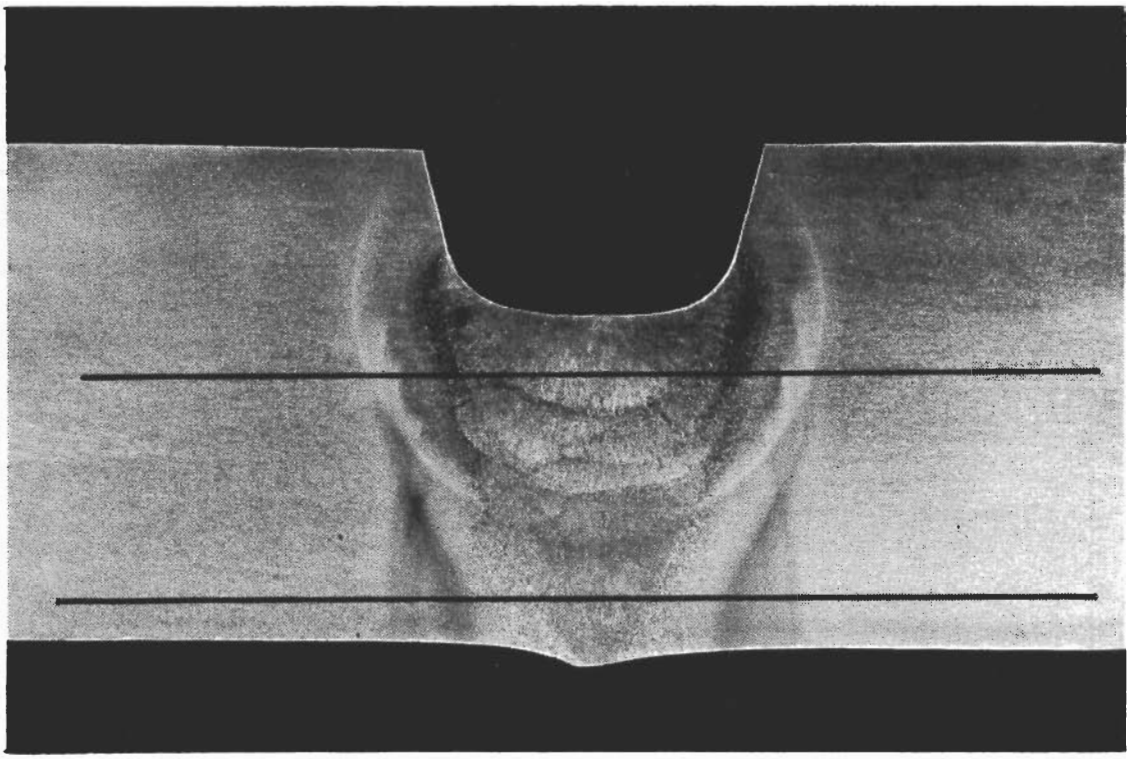

Marbles Etch Magnification: 5X

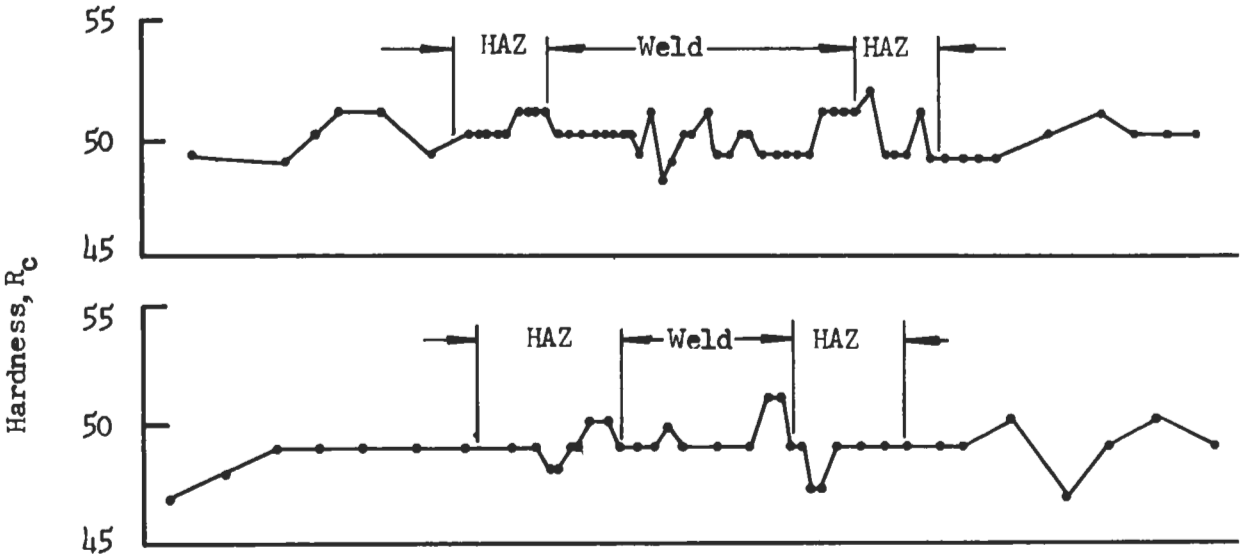

Figure 78. Typical Results of Macrostructure and Microhardness Evaluations of Grade 250, 1/2-In.-Thick, 18% Nickel Maraging Steel Plate Weldments Using TIG Process, Welded With Six Weld Passes and Aged at 900°F for 8 Hours, Heat 120D163 Filler Wire 7C-093

Approved for Public Release

Contrails

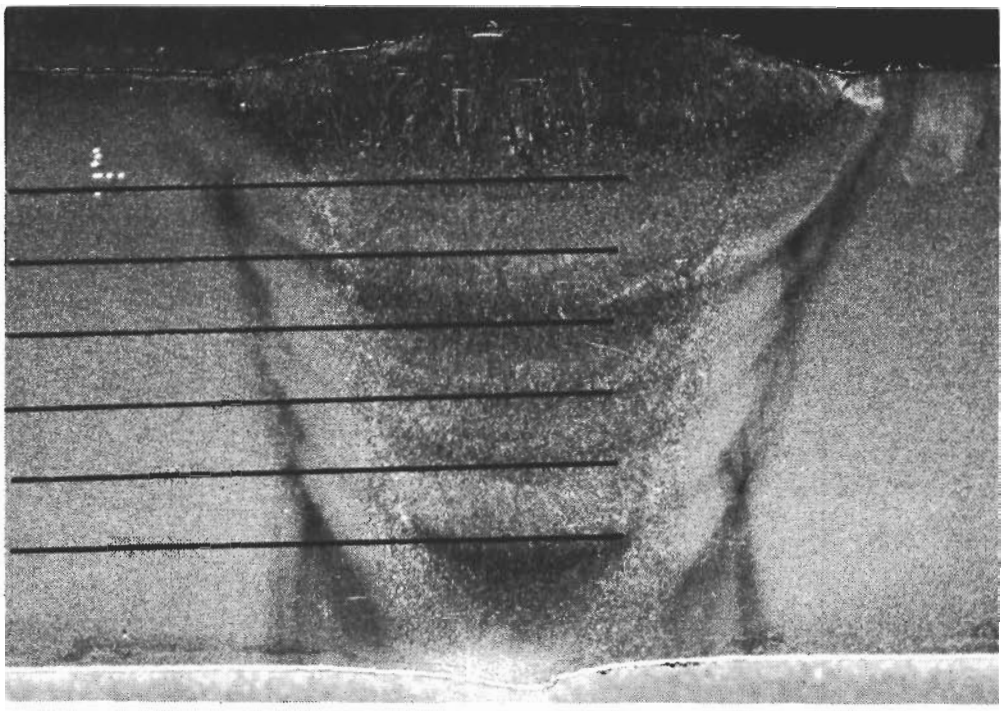

Marbles Etch Magnification: 5X

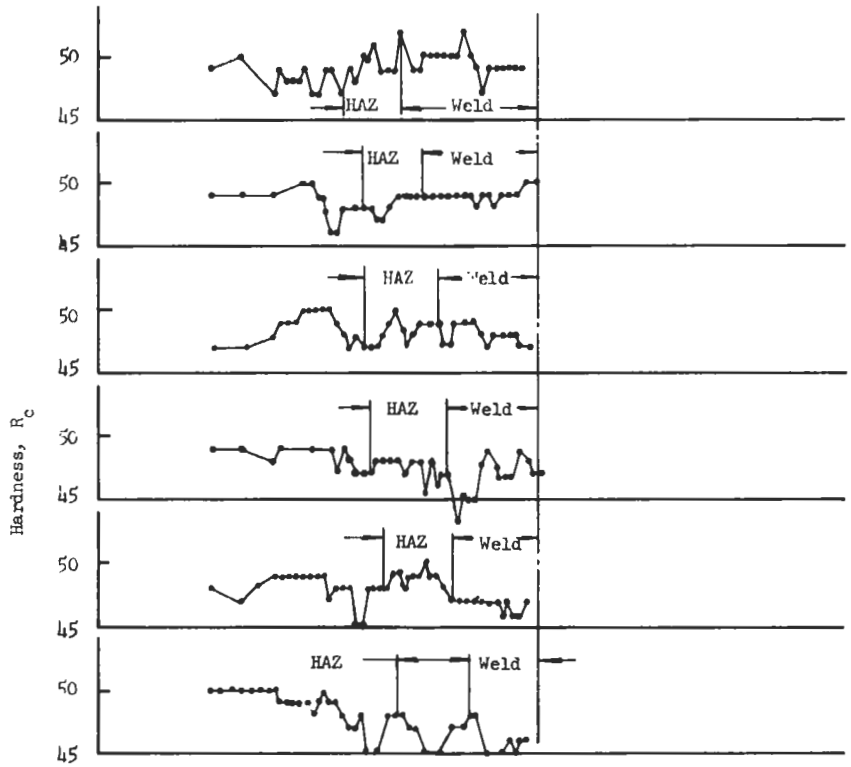

Figure 79. Typical Results of Microhardness Evaluations of Grade 250, 1/2-In.-Thick, 18% Nickel Maraging Steel Plate Weldments Using TIG Process, Welded and Aged at 900° F for 8 Hours, Heat 120D163, Filler Wire 7C-093

Approved for Public Release

Contrails

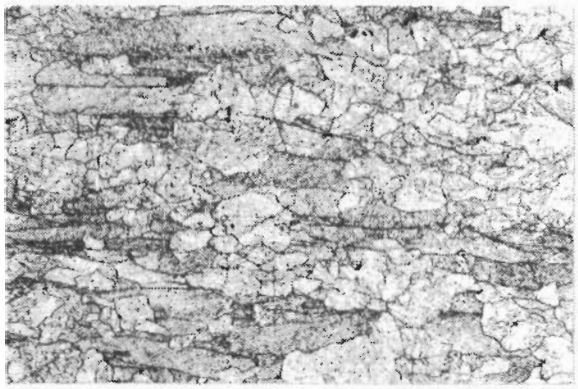

Magnification: 250X

Mill-Annealed at 1500° F for 1 Hour
and Aged at 900° F for 3 Hours

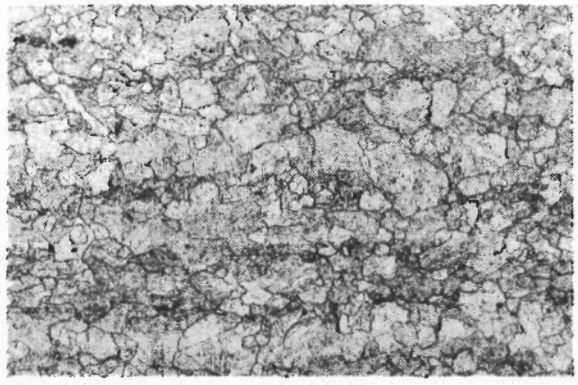

Magnification: 250X

Mill-Annealed at 1500° F for 3 Hours
and Re-Solution Annealed at 1500° F
for 1 Hour, and Aged at 900° F for
3 Hours

Marbles Etch

Figure 80. Comparison of Mill-Annealed, Aged, and Re-Solution Annealed and Aged Microstructures in 3/4-In.-Thick, 18% Nickel Maraging Steel Plate, Heat 24158

Approved for Public Release

Contrails

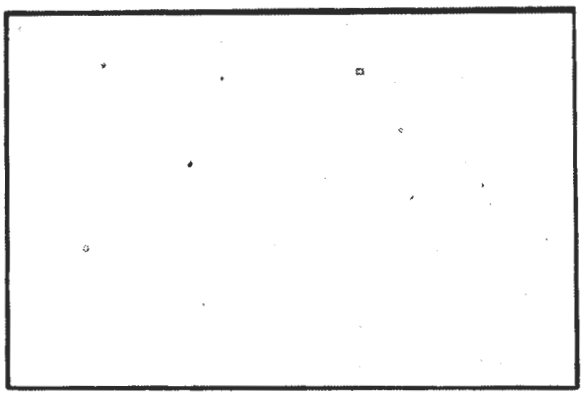

3/4 In. Plate

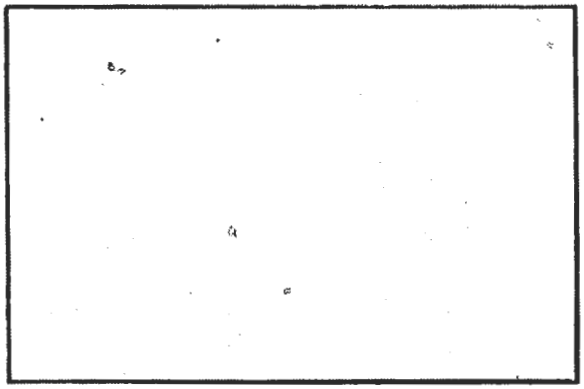

1 x 4 In. Forging

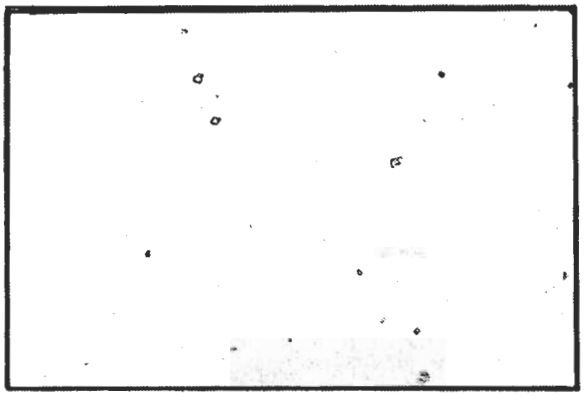

4 x 4 In. Forging

As Polished Magnification: 100X

Figure 81. Typical Inclusion Content of 18% Nickel Maraging Steel, Heat 24158

Approved for Public Release

Contrails

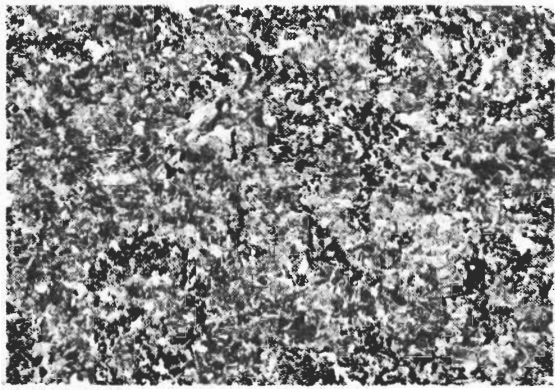

3/4 In. Plate

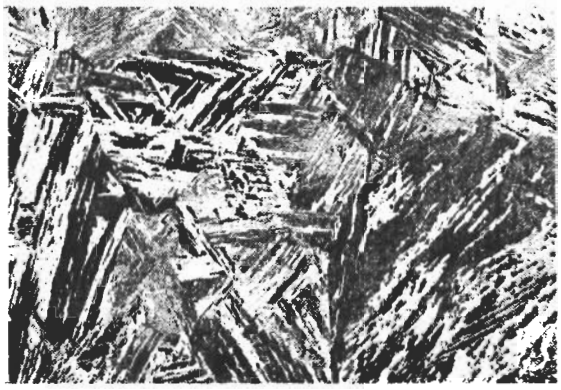

1 x 4 In. Forging

4 x 4 In. Forging

5% Chromic Acid Electrolytic Etch Magnification: 100X

Figure 82. Typical Grain Size of 18% Nickel Maraging Steel, Heat 24158

Approved for Public Release

Contrails

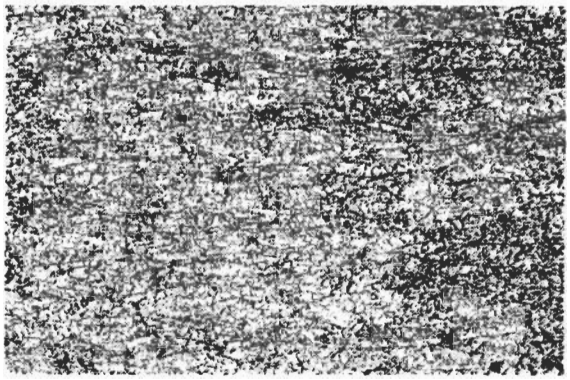

3/4 In. Plate

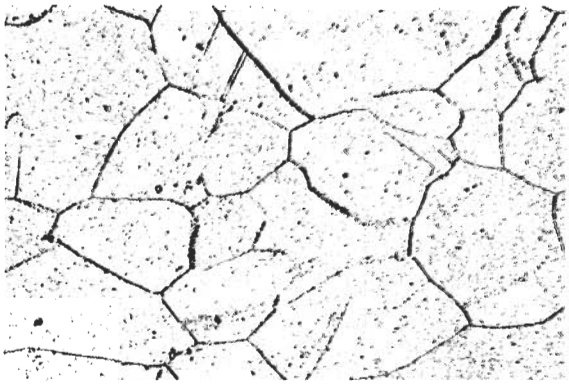

1 x 4 In. Forging

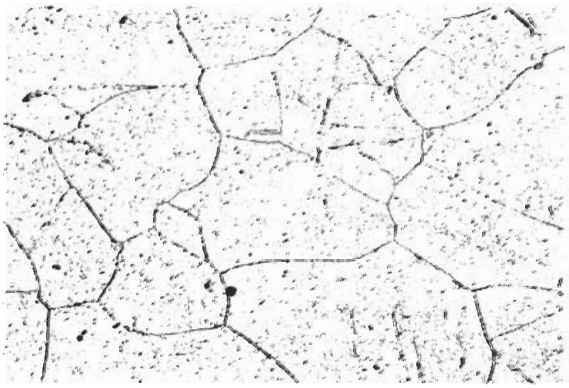

4 x 4 In. Forging

Marbles Etch Magnification: 100X

Figure 83. Typical Microstructure of 18% Nickel Maraging Steel, Heat 24158

Approved for Public Release

Contrails

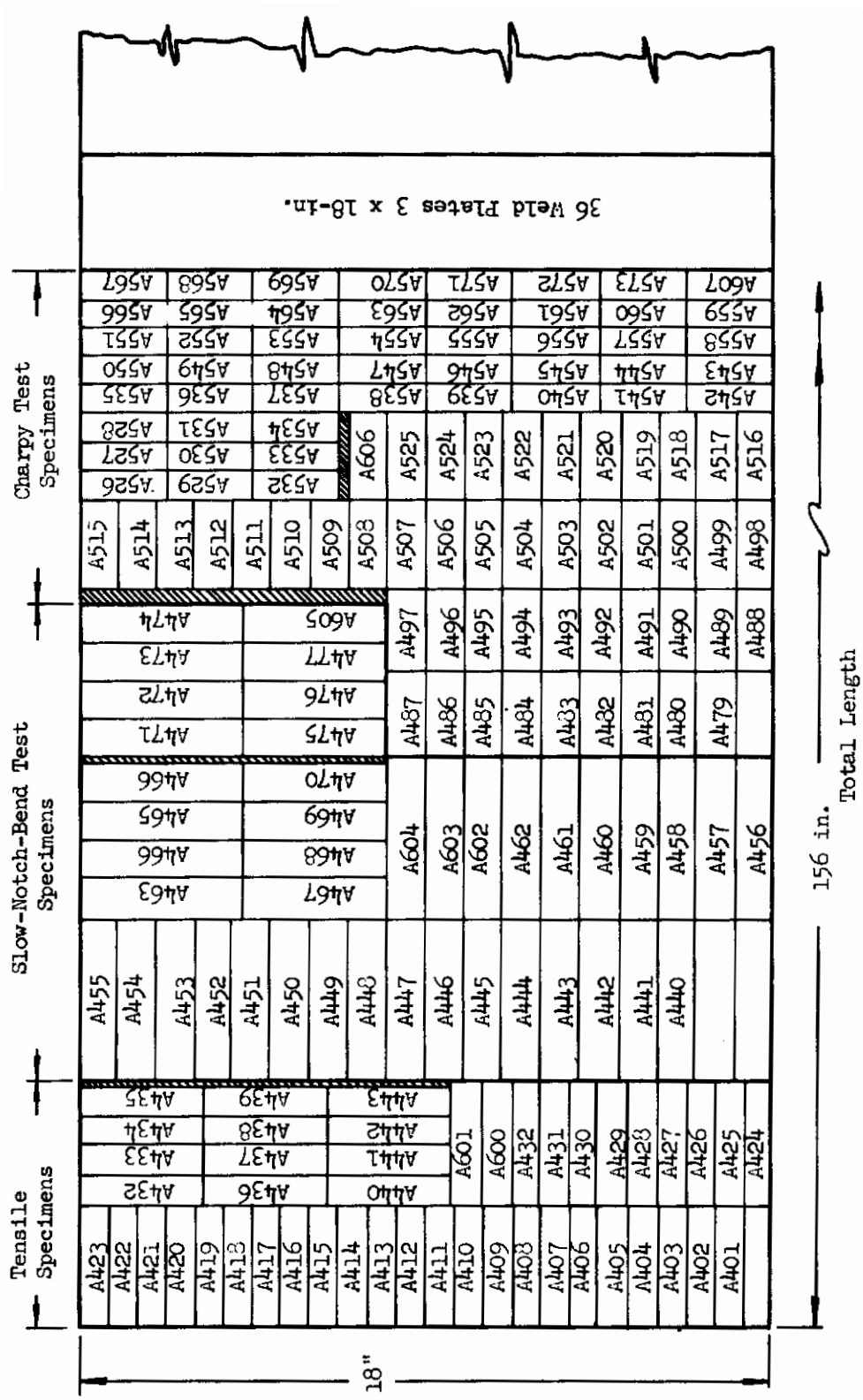

Figure 84. Location of Test Specimens in 3/4-In.-Thick 18% Nickel Maraging Steel Plate, Heat 24158

Approved for Public Release

Contrails

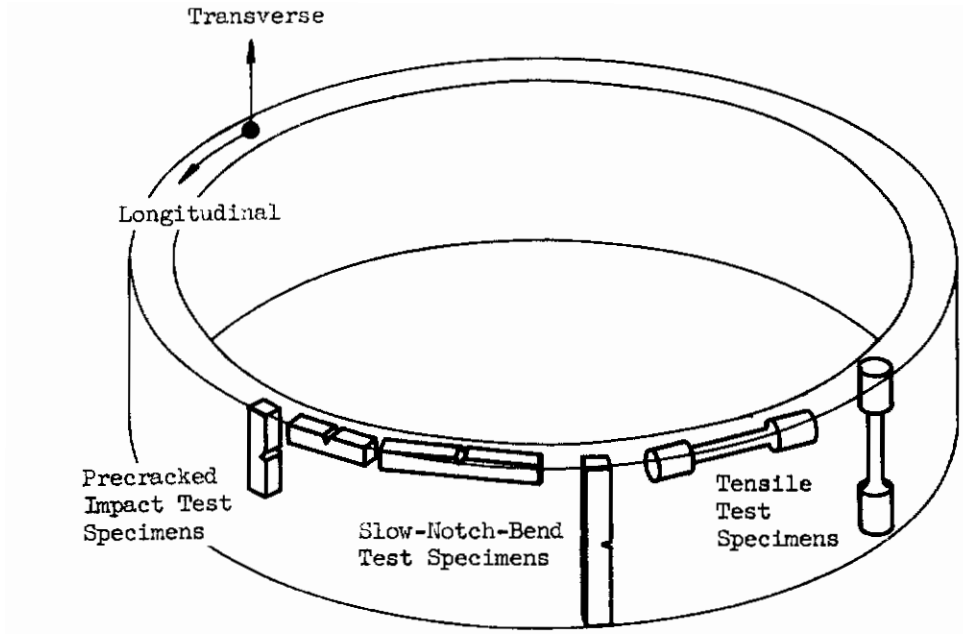

1 x 4-In. Ring-Rolled Forging

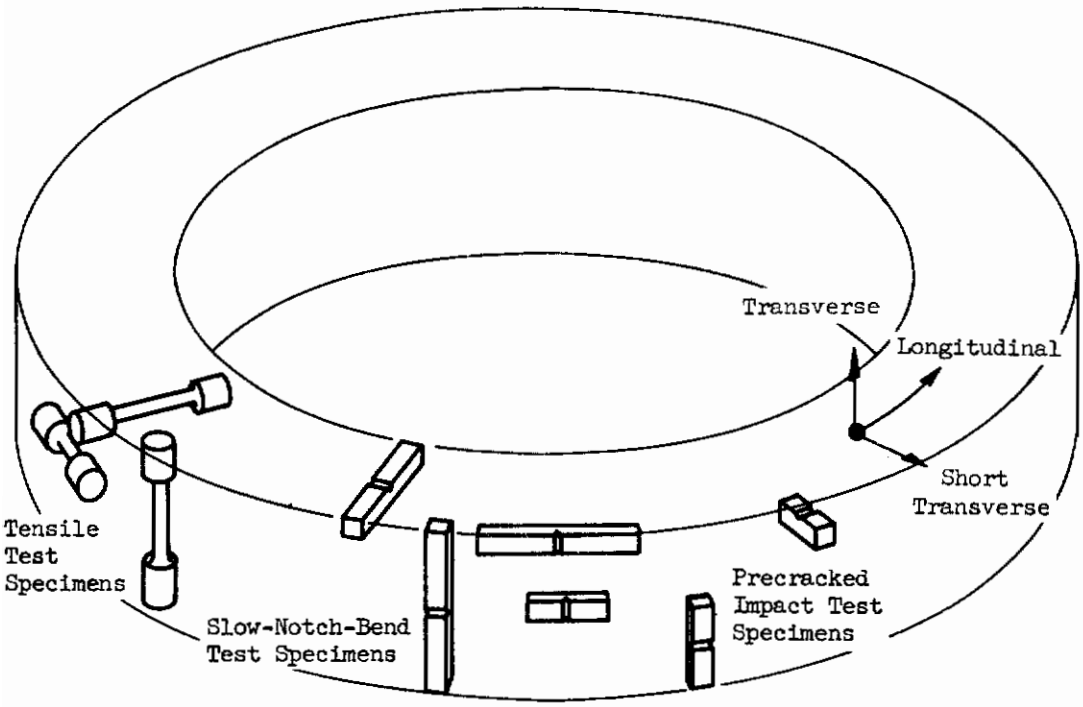

4 x 4-In. Ring-Rolled Forging

Figure 85. Location of Test Specimens in 18% Nickel Maraging Steel Forgings, Heat 24158

Approved for Public Release

Contrails

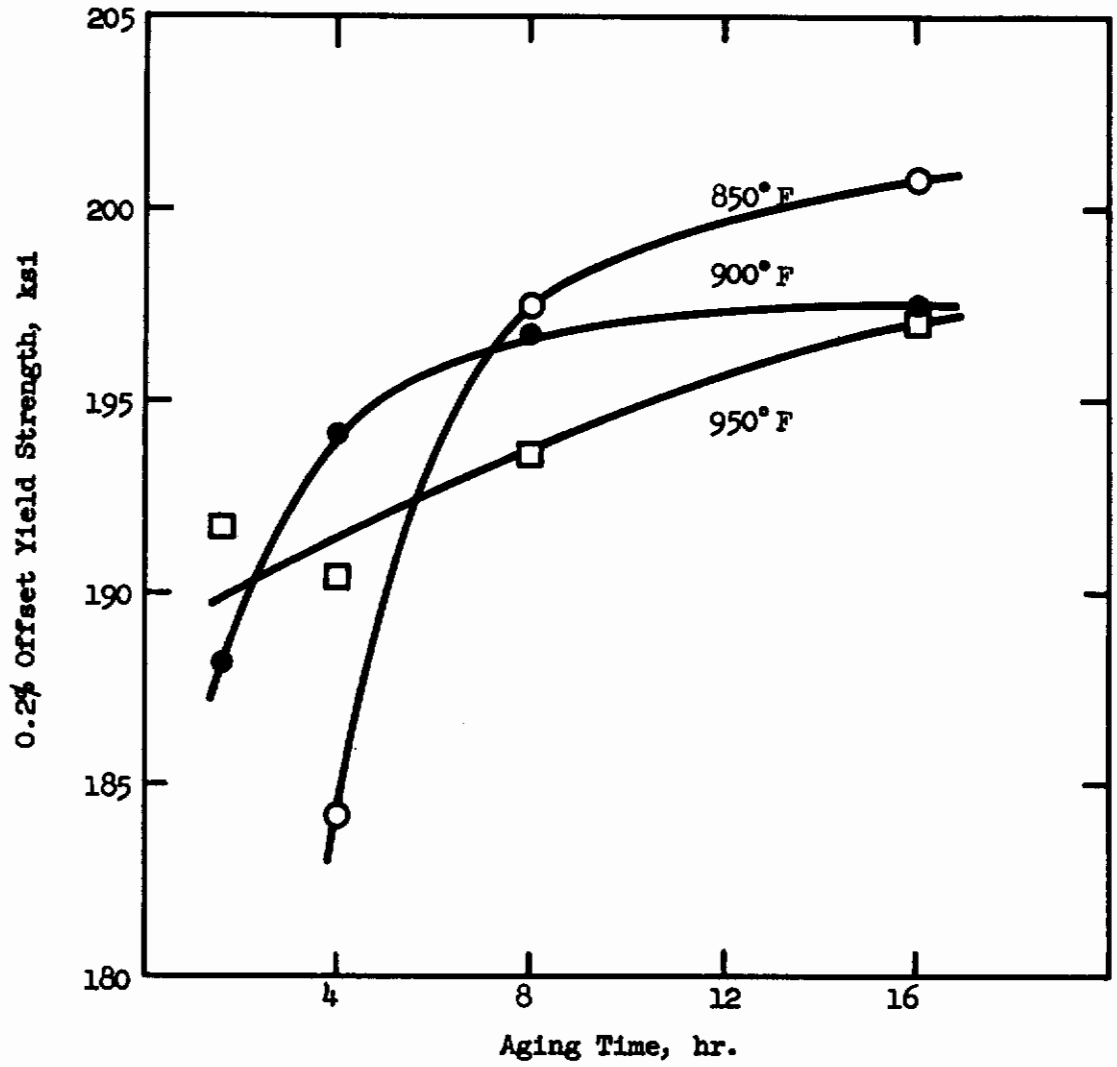

Figure 86. Aging Response Characteristics of 3/4-In.-Thick, Maraging Steel Plate, Heat 24158, Re-Solution Annealed at 1500° F for 30 Minutes

Approved for Public Release

Contrails

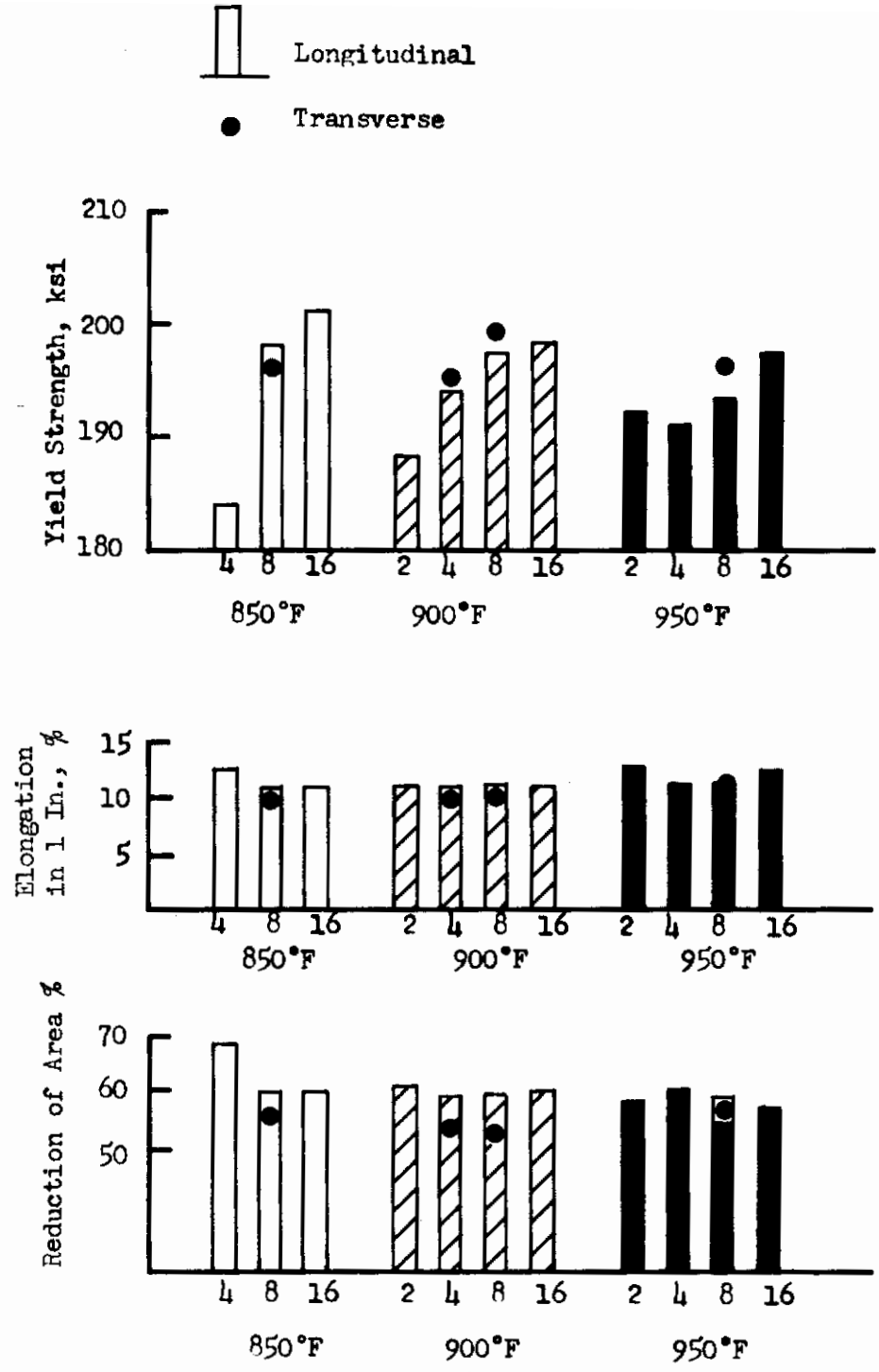

Figure 87. Effect of Aging Time and Temperature on Tensile Properties of 3/4-In.-Thick, 18% Nickel Maraging Steel Plate, Heat 24158

Approved for Public Release

Contrails

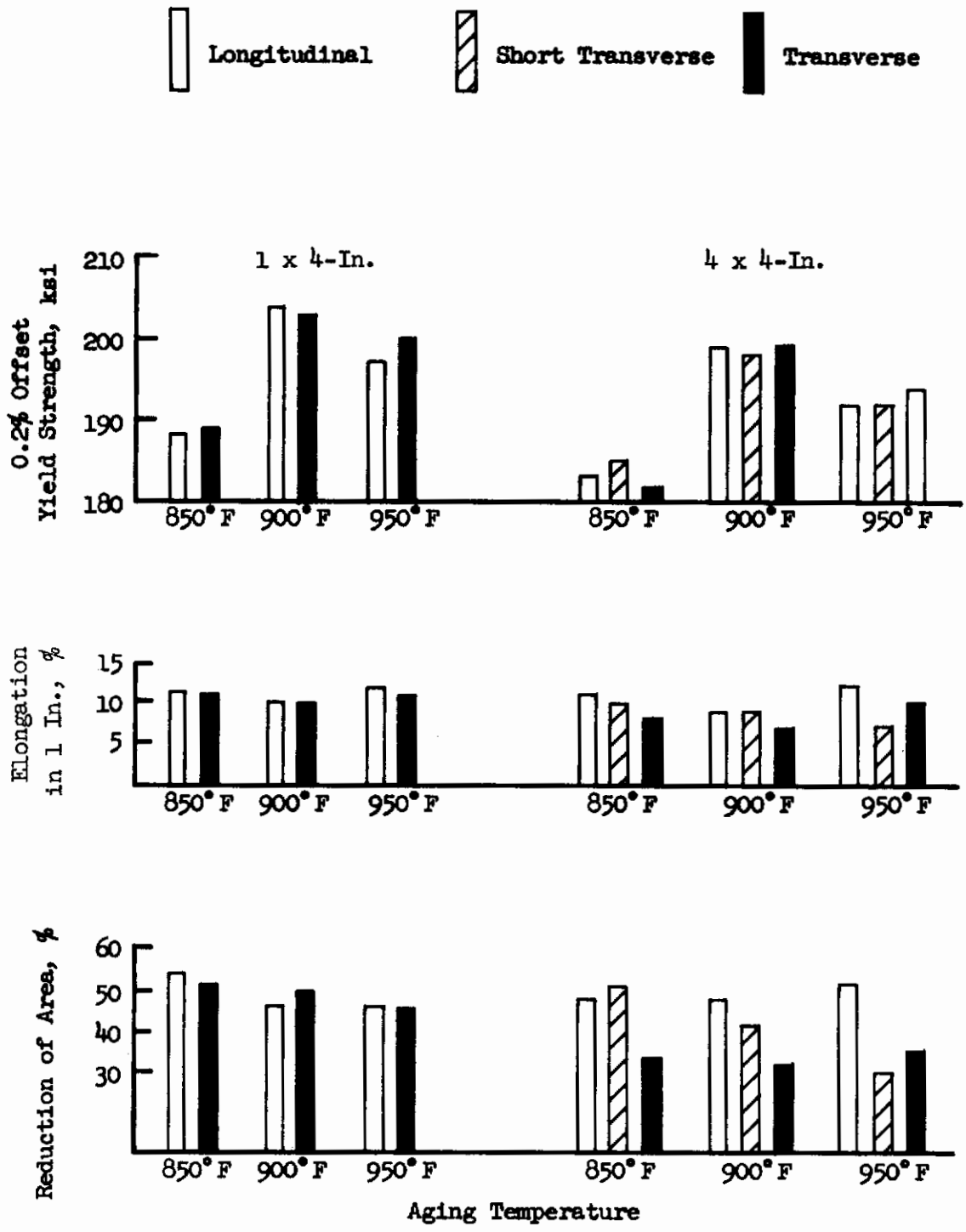

Figure 88. Tensile Properties of 18% Nickel Maraging Steel Mandrel-Forgings, Heat 24158, After Re-Solution Annealing at 1500° F for 30 Minutes and Aging for 8 Hours

Approved for Public Release

Contrails

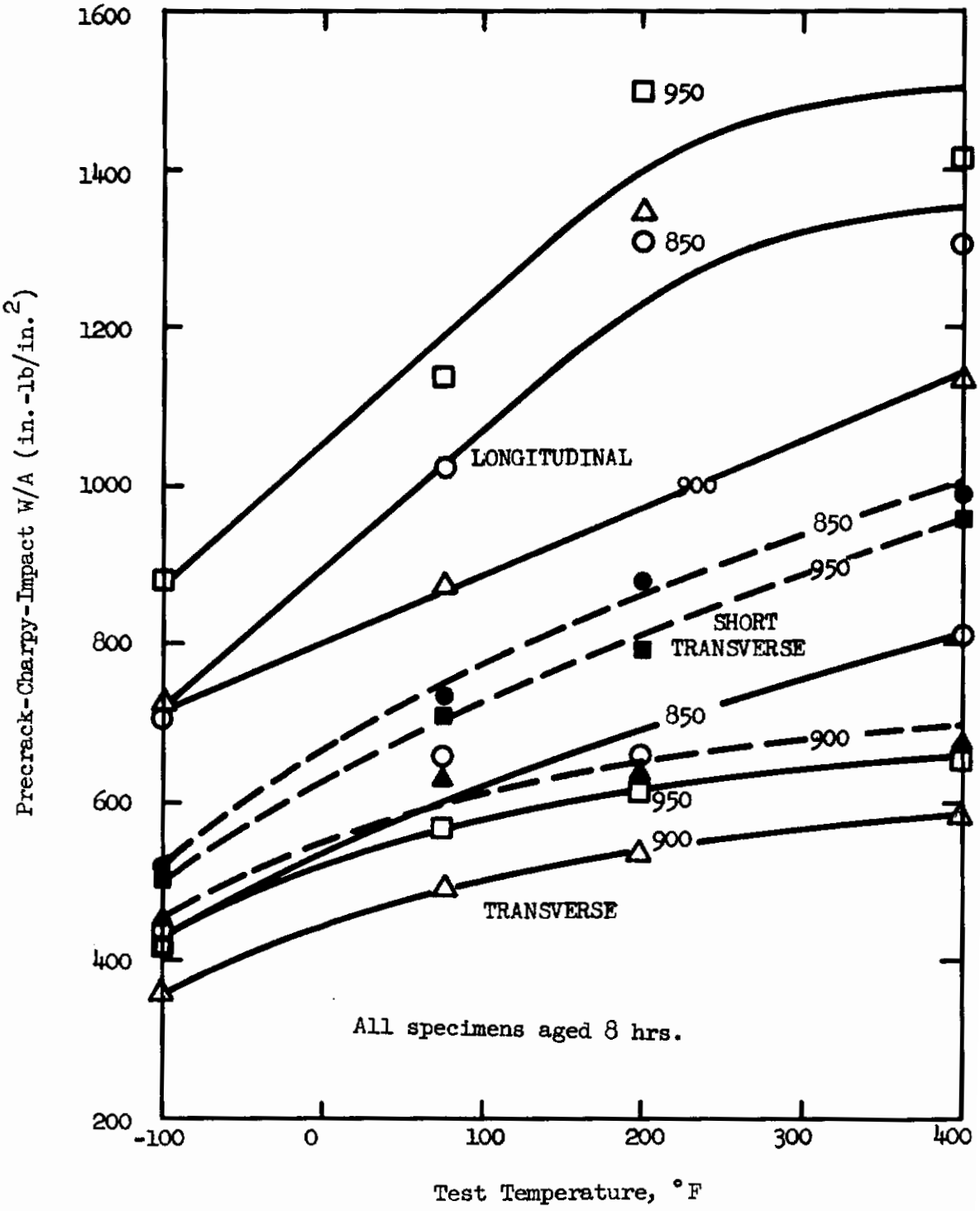

Figure 89. Effect of Heat Treatment, Specimen Orientation and Test Temperature on Toughness (W/A) in a 4 x 4-In. Mandrel-Forged Section of Vacuum-Arc-Remelt, Grade 200, 18% Nickel Maraging Steel, Heat 24158. (Dash curves indicate short-transverse specimen orientation - see Figure 90.)

Approved for Public Release

Contrails

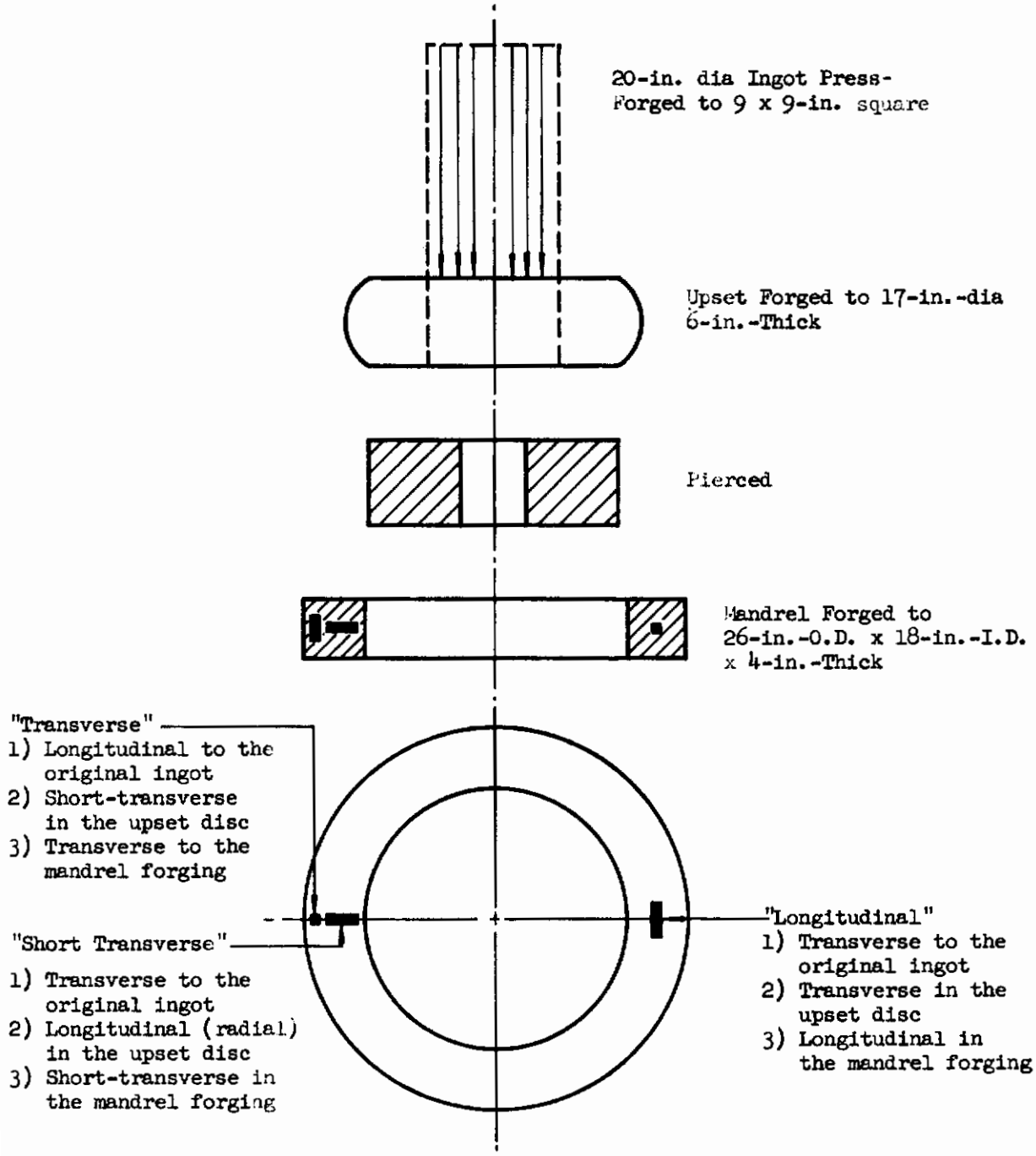

Figure 90. Schematic of Forging Practice and Specimen Orientation in the 4 x 4-In. Mandrel-Forged Ring

Approved for Public Release

Contrails

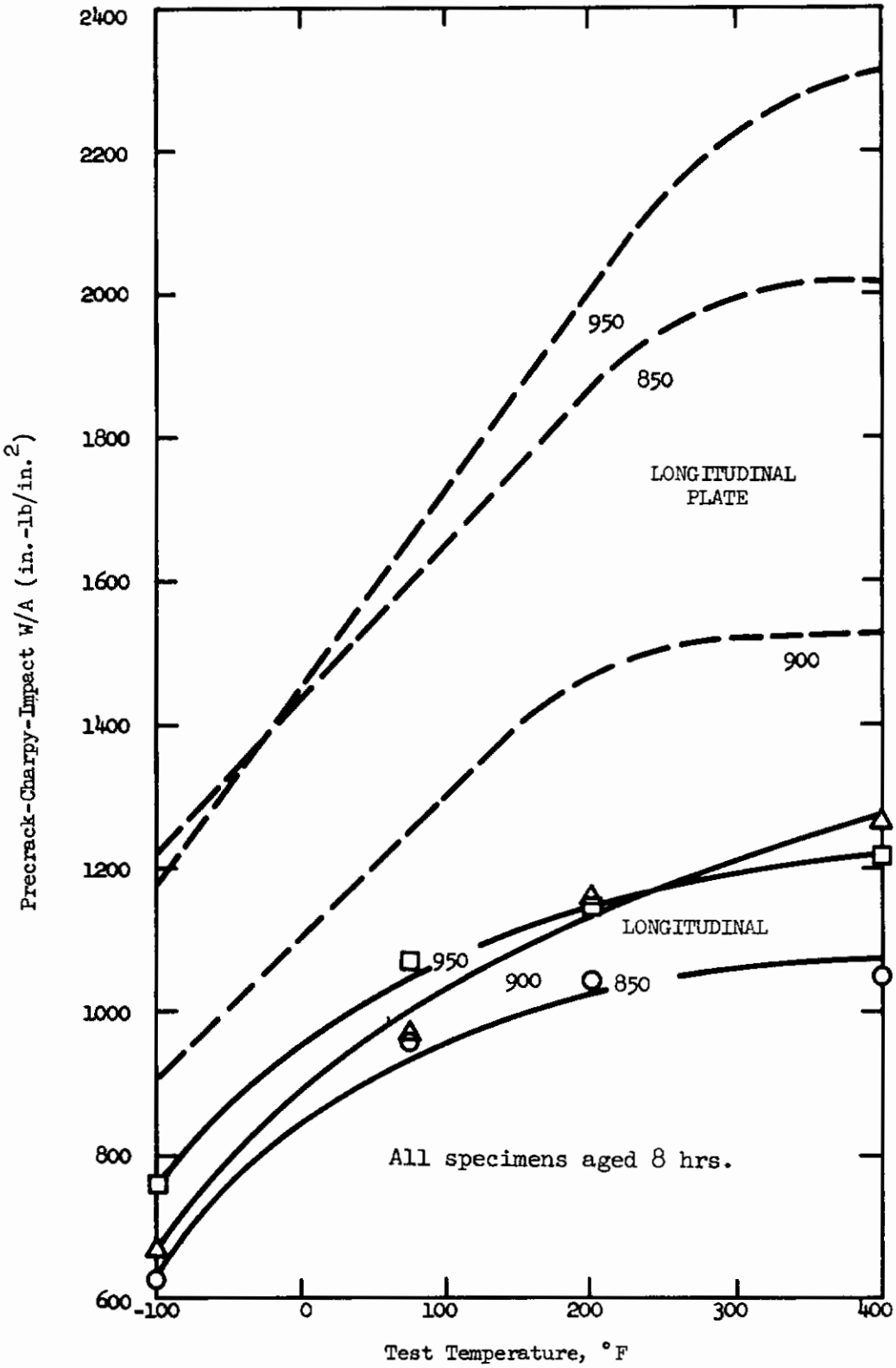

Figure 91. Effect of Heat Treatment and Test Temperature on Toughness (W/A) in a 1 x 4-In. Mandrel-Forged Section of Vacuum-Arc-Remelt, Grade 200, 18% Nickel, Maraging Steel, Heat 24158 (Dash curves indicate plate material, from Figure 92.)

Approved for Public Release

Contrails

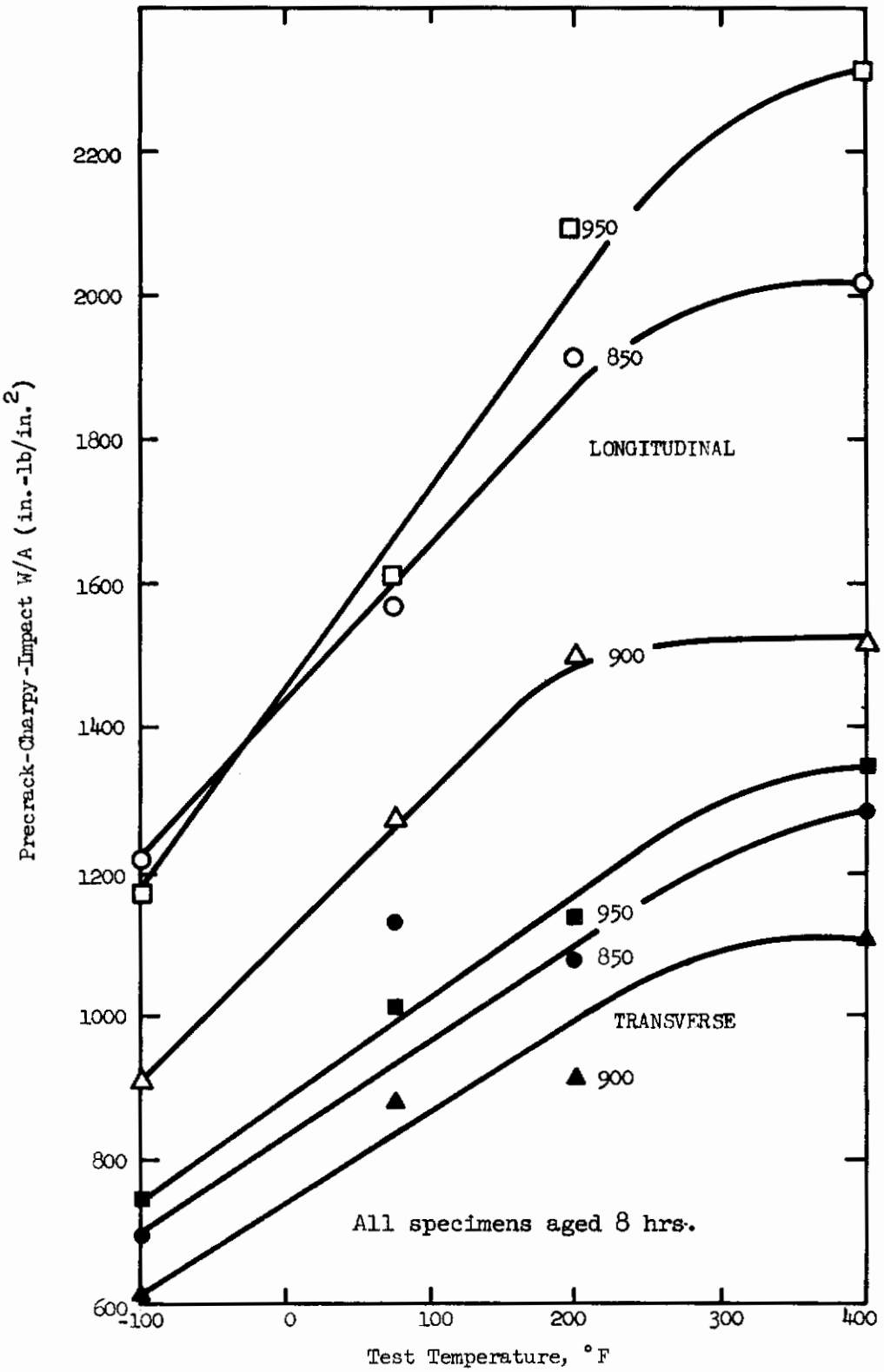

Figure 92. Effect of Heat Treatment, Specimen Orientation and Test Temperature on Toughness (W/A) in 3/4-In.-Thick, Vacuum-Arc-Remelt, Grade 200, 18% Nickel Maraging Steel Plate, Heat 24158

Approved for Public Release

Contrails

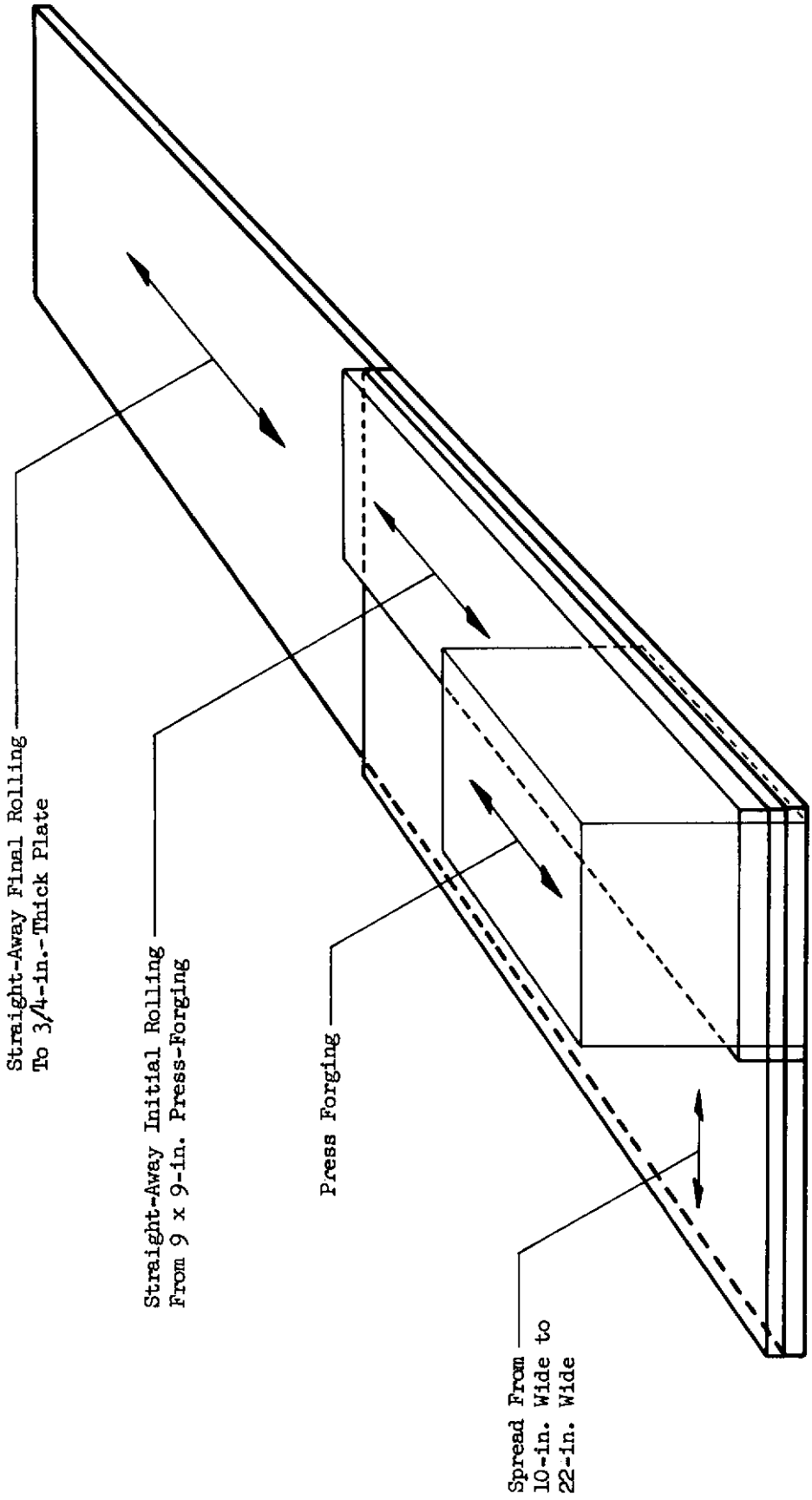

Figure 93. Schematic of Forging and Rolling Practice for Producing 3/4-In.-Thick Plate, Heat 24158

Approved for Public Release

Contrails

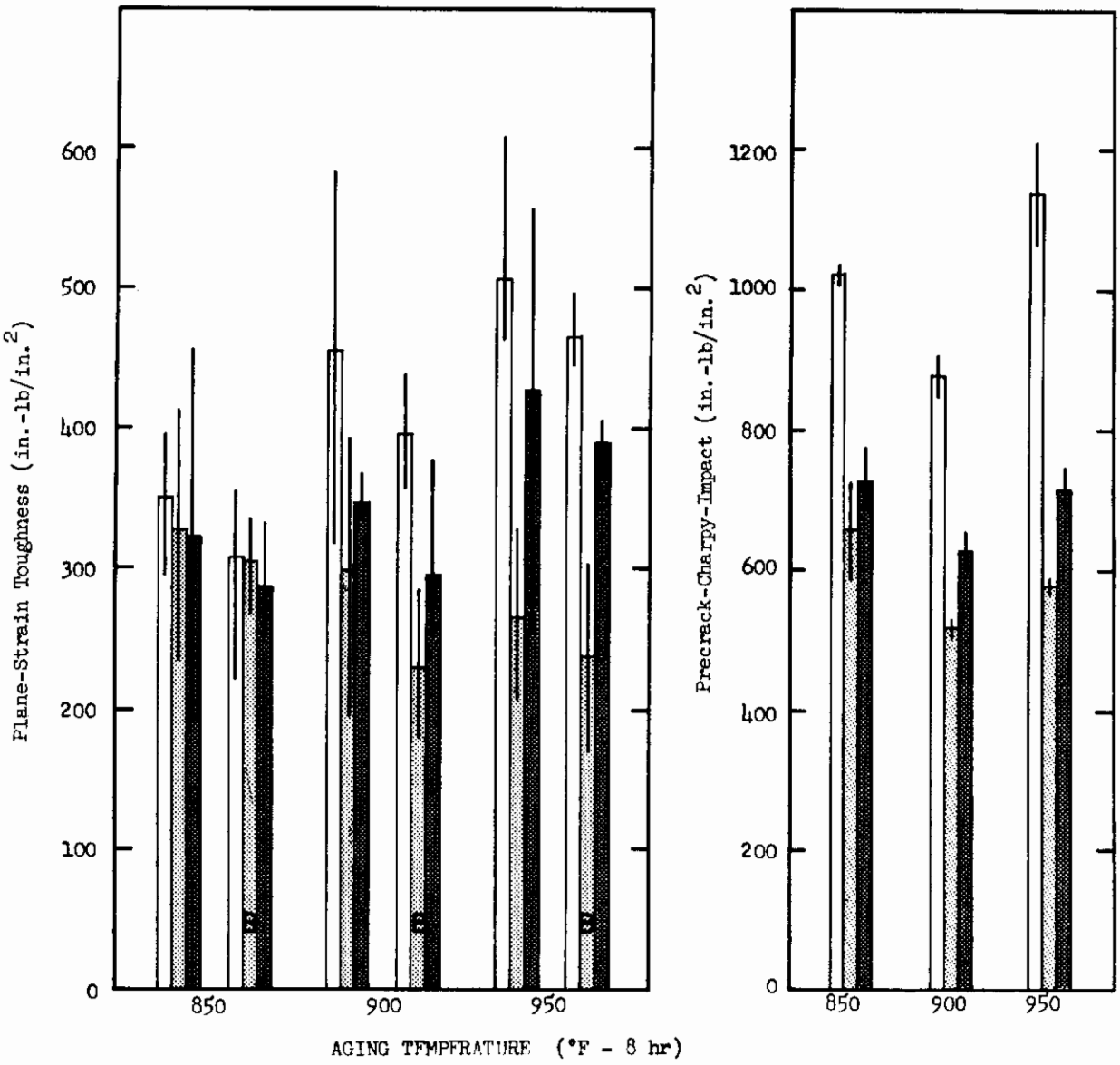

Figure 94. Effect of Heat Treatment and Specimen Orientation on Toughness in Mandrel-Forged 4 x 4-In. Section of Vacuum-Arc-Remelt, Grade 200, 18% Nickel Maraging Steel, Heat 24158. (Bars left-to-right indicate longitudinal, transverse and short-transverse specimens; lines show the extent of scatter in replicate test specimens; B indicates Bueckner's value.)

Approved for Public Release

Contrails

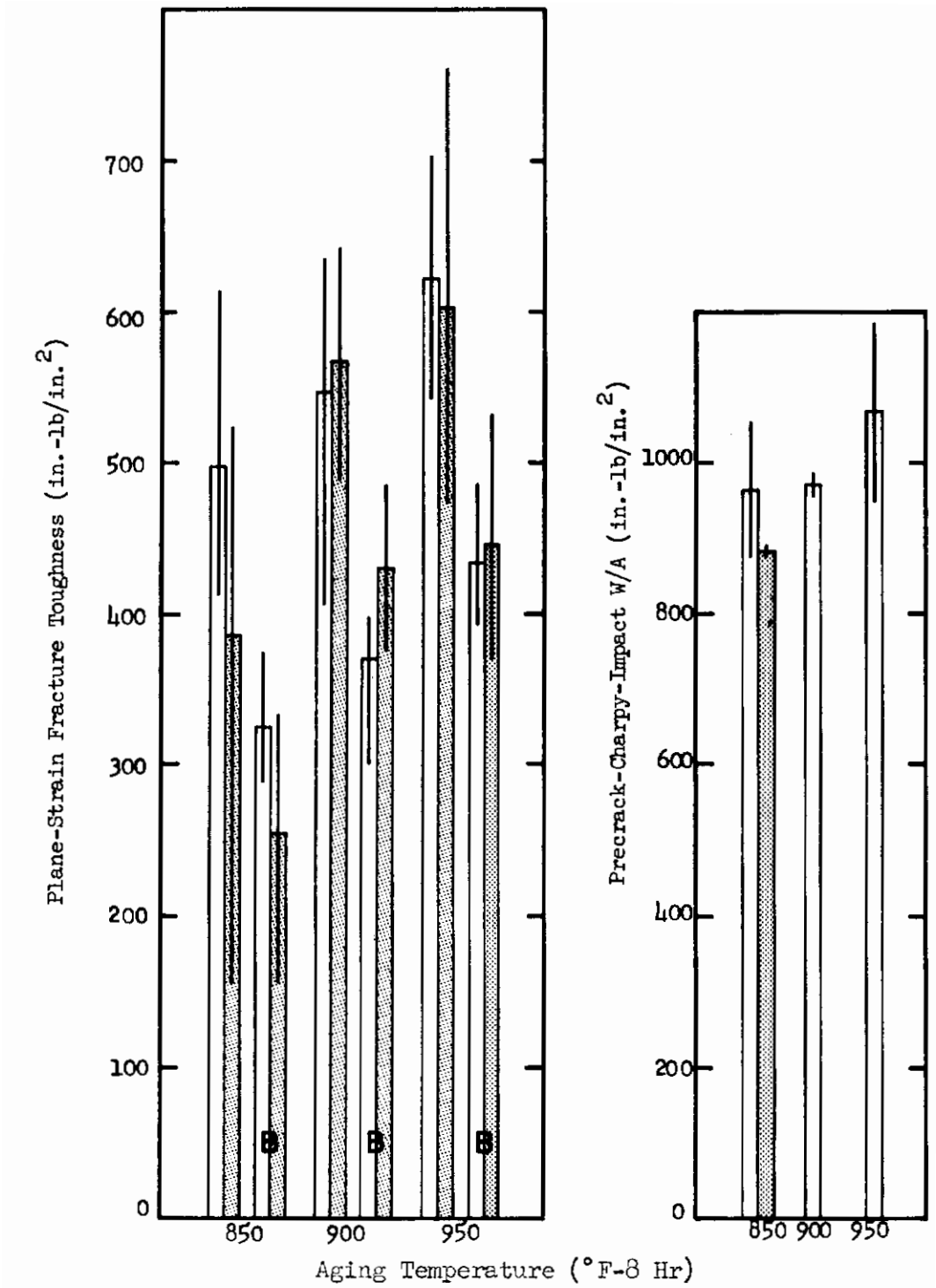

Figure 95. Effect of Heat Treatment and Specimen Orientation on Toughness in Mandrel-Forged 1 x 4-In. Section of Vacuum-Arc-Remelt, Grade 200, 18% Maraging Steel, Heat 24158. (Bars left-to-right indicate longitudinal and transverse specimens; lines show the extent of scatter in replicate test specimens; B indicates Bueckner's value.)

Approved for Public Release

Contrails

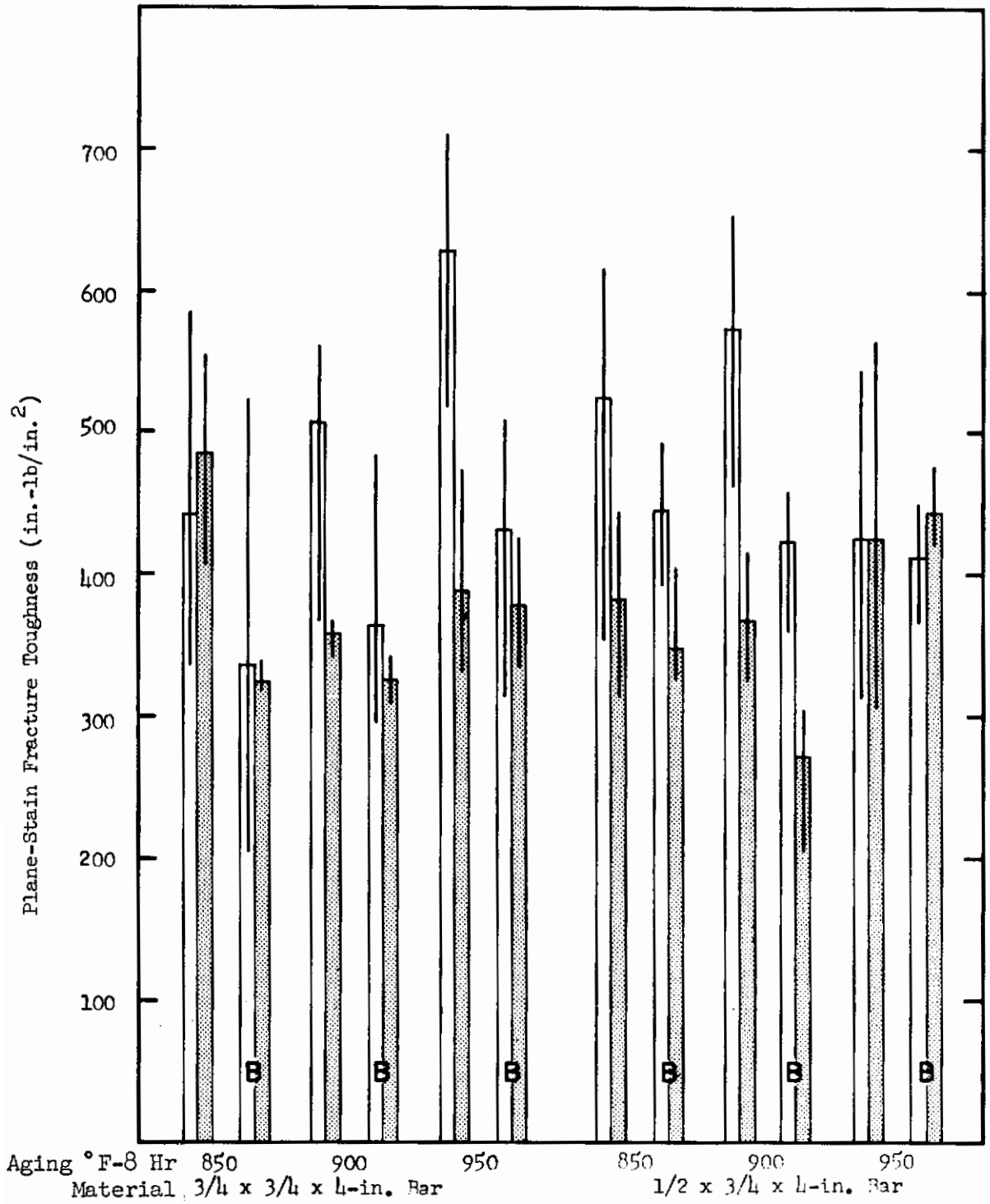

Figure 96. Effect of Heat Treatment and Specimen Orientation on Toughness in 3/4-In.-Thick, Vacuum-Arc-Remelt, Grade 200, 18% Nickel Maraging Steel Plate, Heat 24158. (Bars left-to-right indicate longitudinal and transverse specimens; lines show the extent of scatter in replicate test specimens; B indicates Bueckner's value.)

Approved for Public Release

Contrails

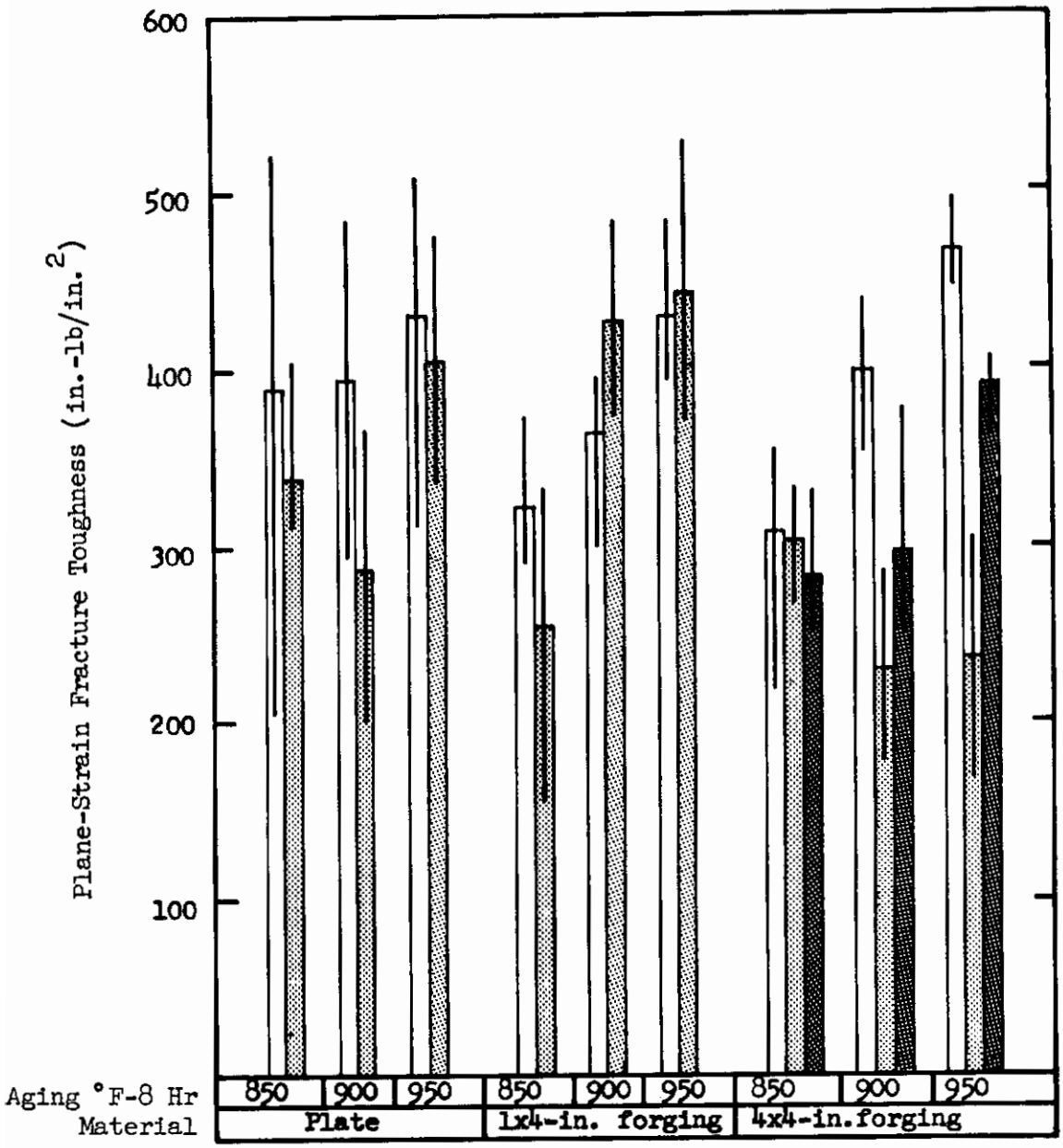

Figure 97. Effect of Mill Processing on Toughness (Bueckner) in Vacuum-Arc-Remelt, Heat 24158. (Bars left-to-right indicate longitudinal, transverse and short transverse specimens; lines show extent of scatter in replicate test specimens; Plate values are averages involving two specimen widths.)

Approved for Public Release

Contrails

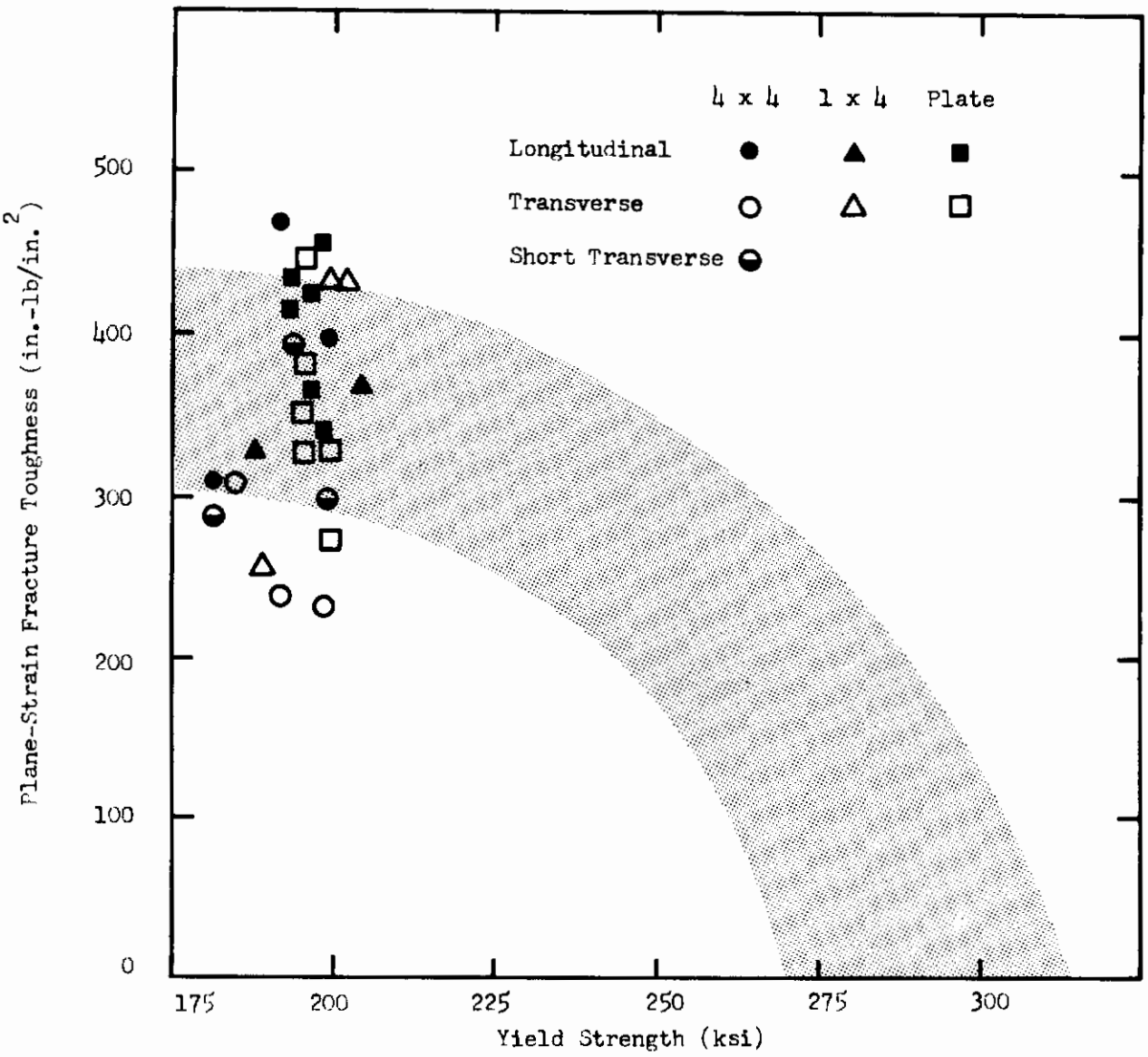

Figure 98. Plane-Strain Fracture Toughness in the Mill Products of Heat 24158 Superimposed on the Strength-Toughness Band of Figure 37

Approved for Public Release

Contrails

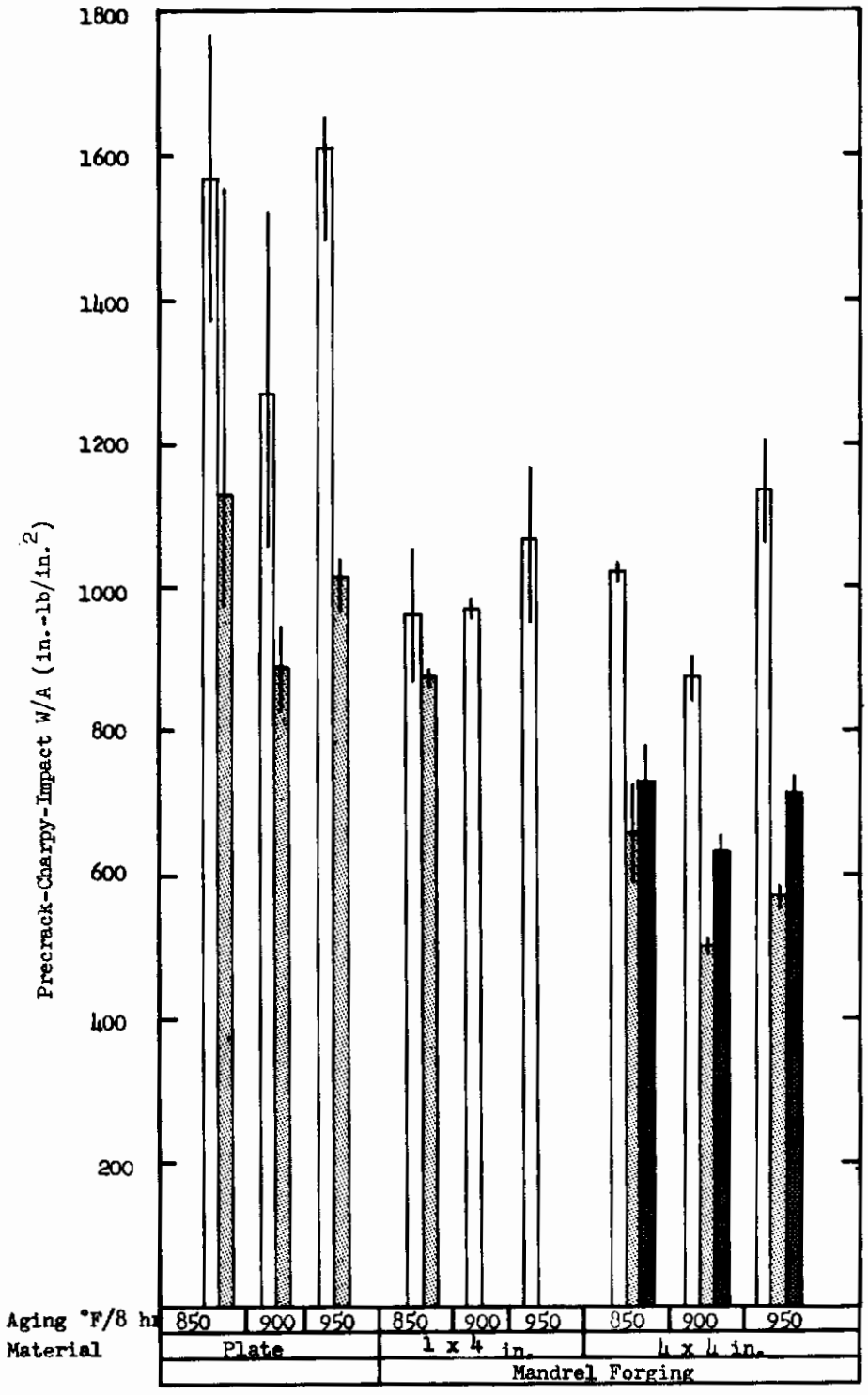

Figure 99. Effect of Heat Treatment Specimen Orientation and Mill Processing on Toughness (W/A) in Vacuum-Arc-Remelt, Heat 24158 (Bars left-to-right indicate longitudinal, transverse and short transverse specimens; lines show the extent of scatter in replicate test specimens.)

Approved for Public Release

Contrails

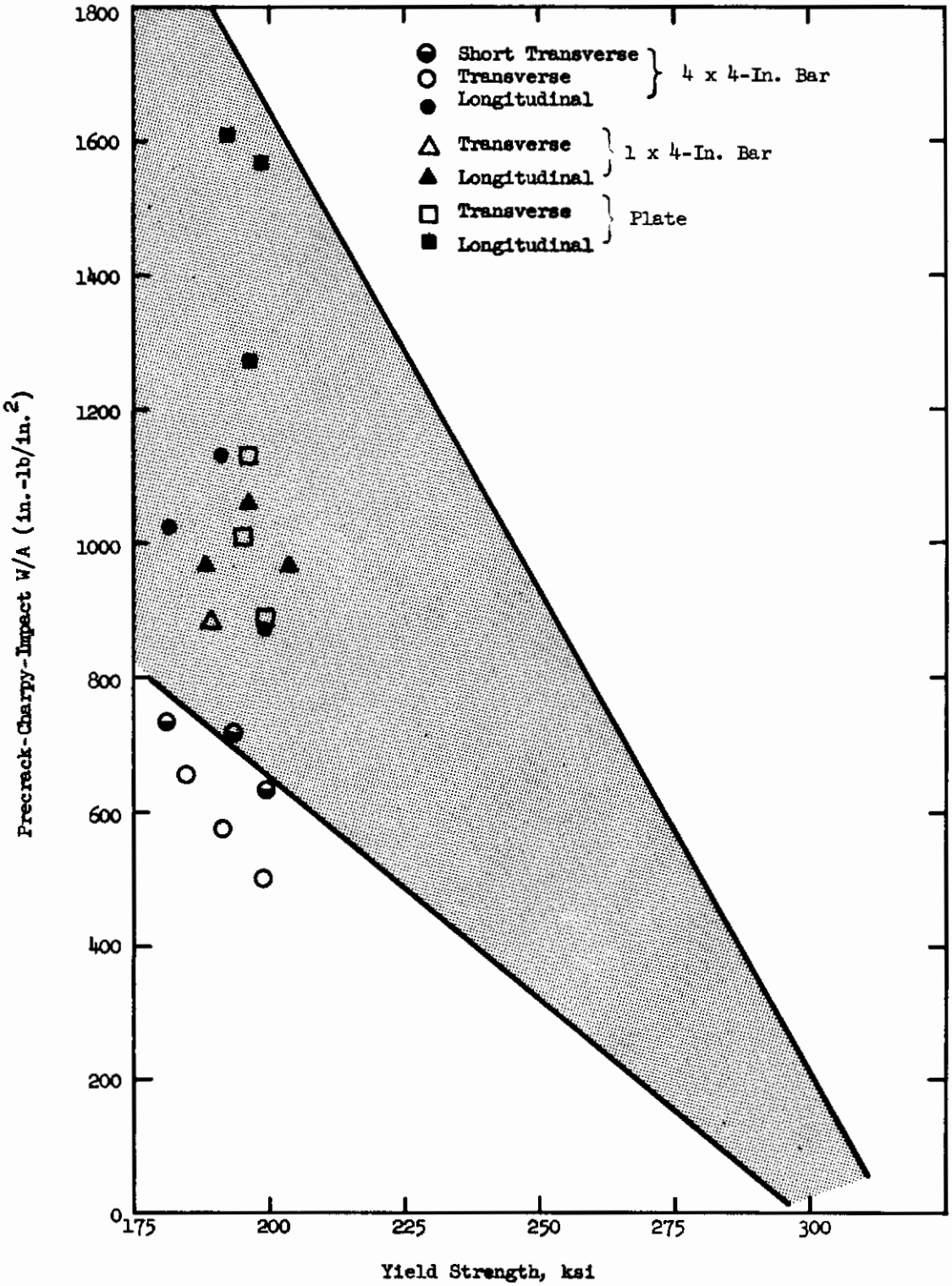

Figure 100. Comparison of Toughness (W/A) in Optimum Heat 24158 and Phase I Heats (shaded area from Figure 40) as a Function of Yield Strength

Approved for Public Release

Contrails

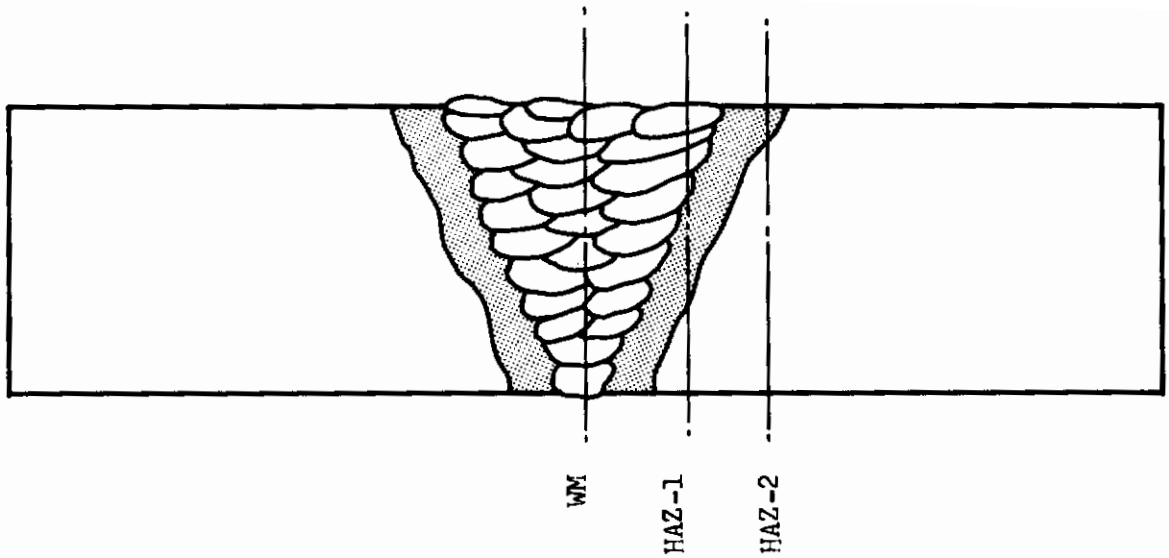

Figure 101. Schematic Diagram Showing Notch Locations for Precracked-Charpy-Impact and Slow-Notch-Bend Test Specimens Prepared from Weldments in Grade 200, 3/4-In.-Thick, 18% Maraging Steel Plate, Heat 24158

Approved for Public Release

Contrails

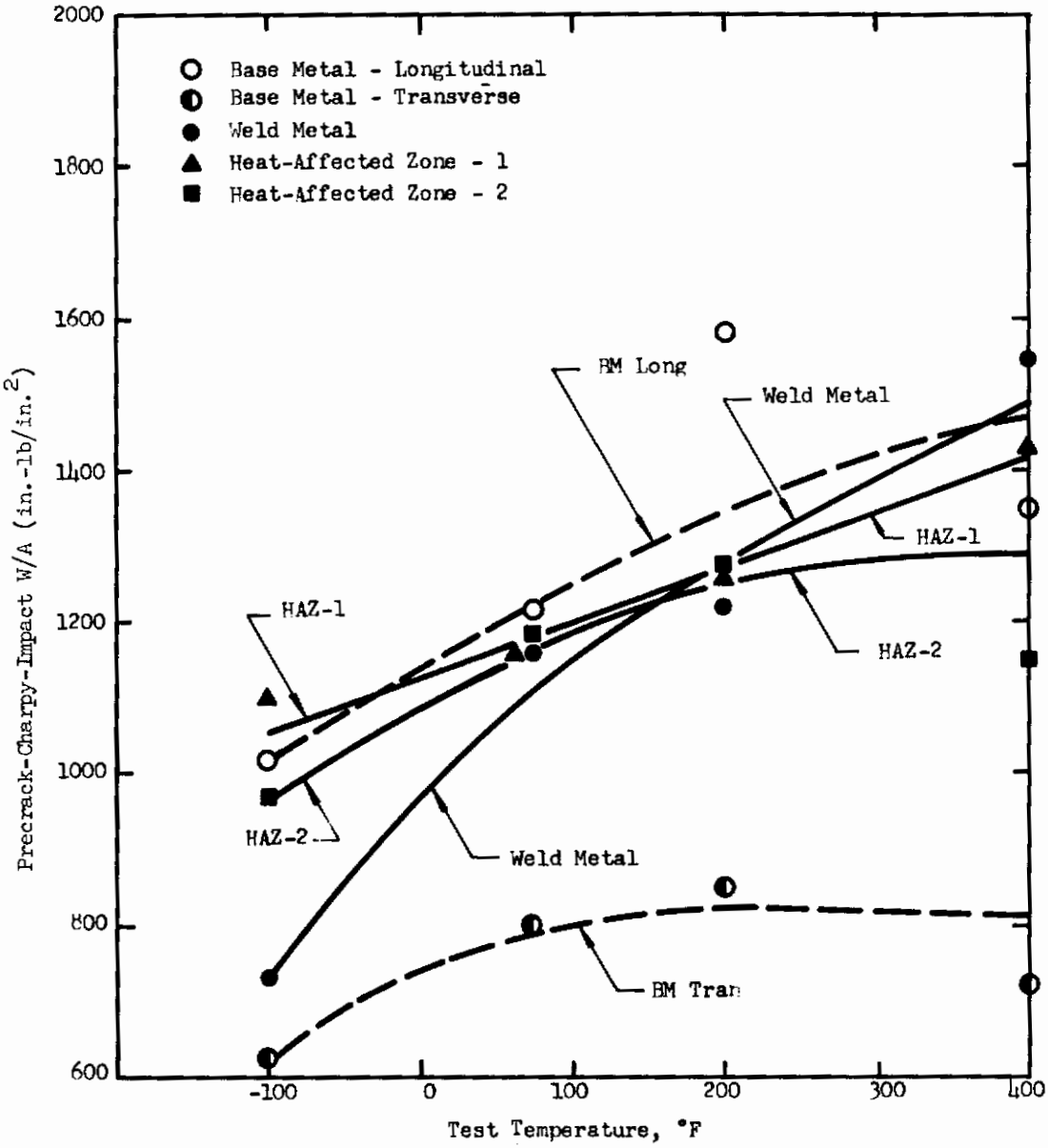

Figure 102. Precracked-Charpy-Impact (W/A) Fracture Toughness of TIG Weldments Made with Filler Wire 34482 in Grade 200, 3/4-In.-Thick, 18% Nickel Maraging Steel Plate, Heat 24158, and Aged at 900°F for 8 Hours (Specimen Size - 0.7 x 0.394-In.)

Approved for Public Release

Contrails

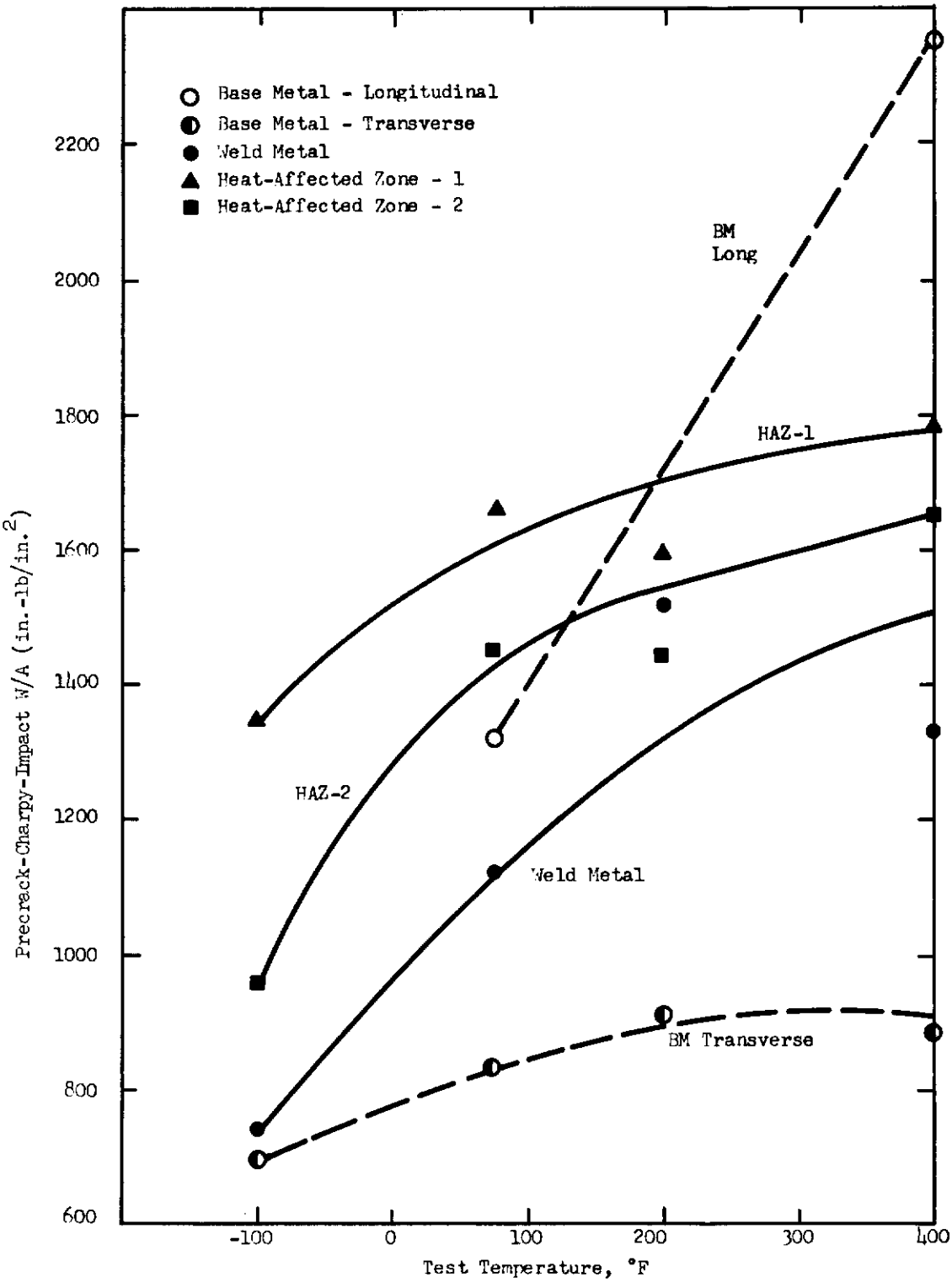

Figure 103. Precracked-Charpy-Impact Fracture Toughness (W/A) of TIG Weldments Made with Filler Wire 34482 in Grade 200, 3/4-In.-Thick, 18% Nickel Maraging Steel Plate, Heat 24158, and Aged at 950°F for 8 Hours (Specimen Sizes are 0.7 x 0.394-in. for WM and HAZ, and 0.75 x 0.394-in. for the base metal.)

Approved for Public Release

Contrails

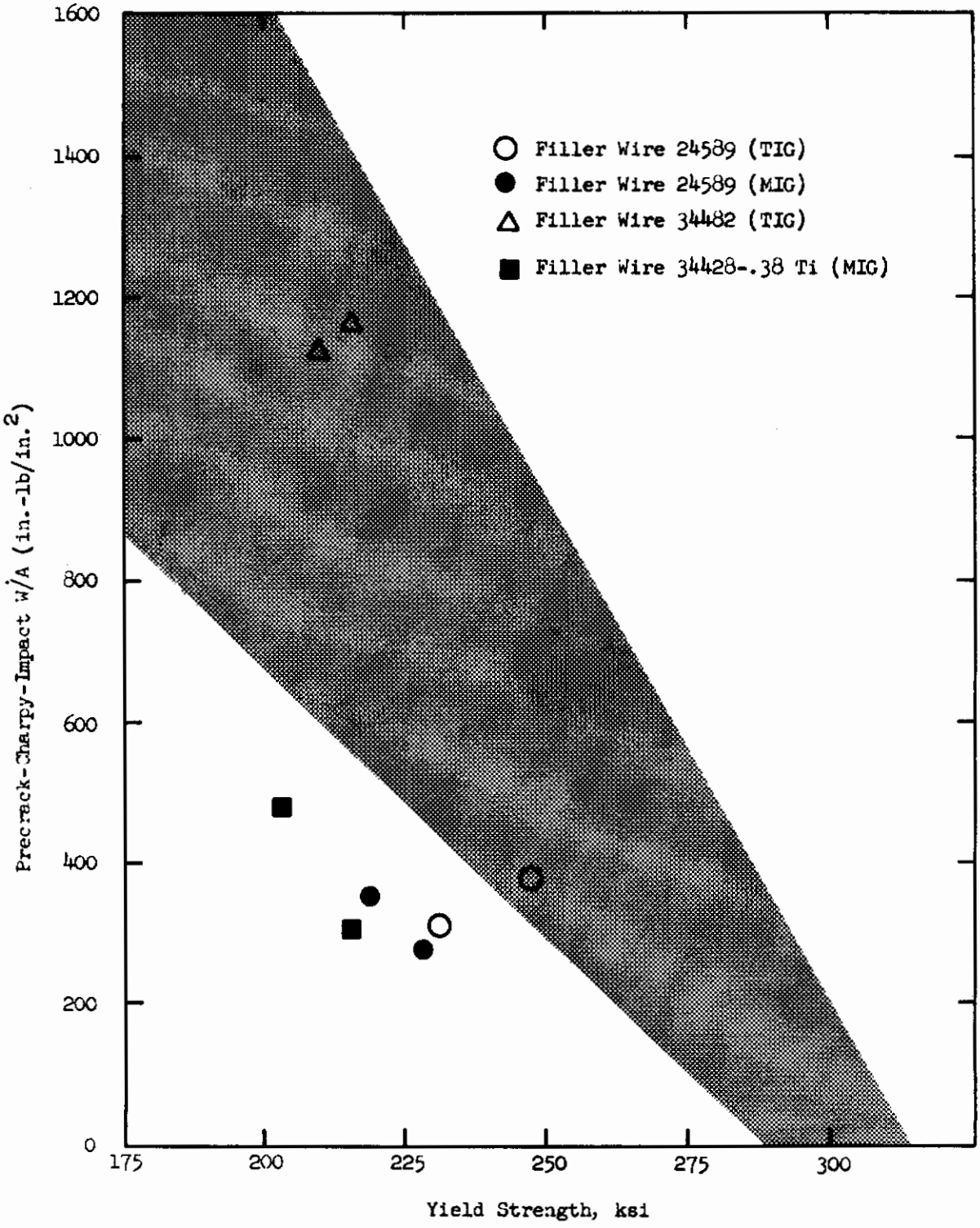

Figure 104. Precracked-Charpy-Impact Fracture Toughness (W/A) of TIG and MIG Weld Metals in Grade 200, 18% Nickel Maraging Steel Plate, Heat 24158, Compared with That of Wrought Base Metals from Figure 40. (Specimen Sizes were 0.7 x 0.394-in. for the weld metal and 0.394 x 0.394-in. for the base metal.)

Approved for Public Release

Contrails

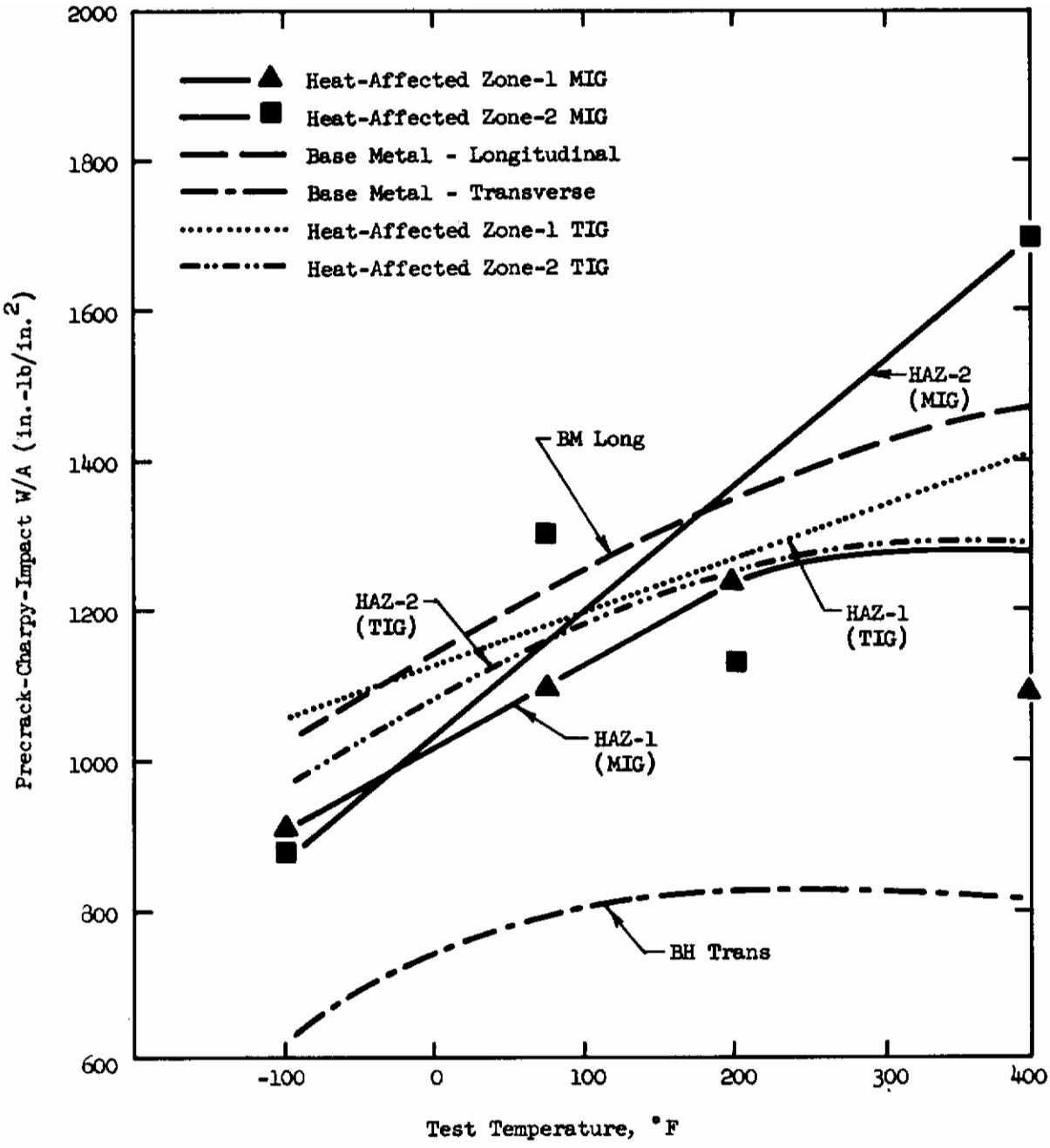

Figure 105. Precracked-Charpy-Impact Fracture Toughness (W/A) of MIG and TIG Weld Heat-Affected Zones and Unaffected Base Metal in Grade 200, 3/4-In.-Thick, 18% Nickel Maraging Steel Plate, Heat 24158, Aged at 900°F for 8 Hours. (Specimen sizes were 0.7 x 0.394-in. for the HAZ and 0.75 x 0.394-in. for the base metal.)

Approved for Public Release

Contrails

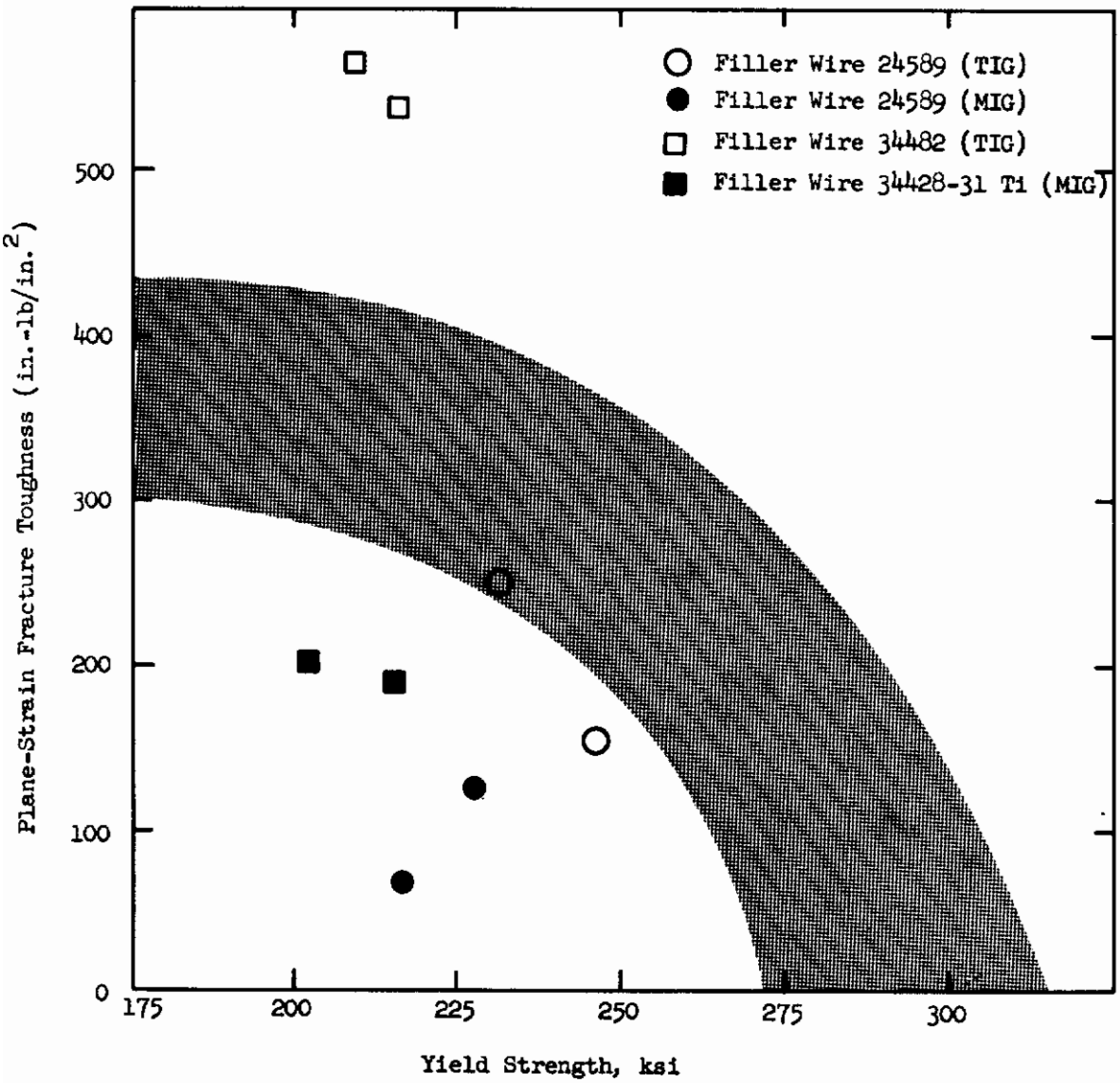

Figure 106. Plane-Strain Fracture Toughness of TIG and MIG Weld Metals in Grade 200, 18% Nickel Maraging Steel Plate, Heat 24158, Compared with That of Wrought Base Metals from Figure 39.

Approved for Public Release

Approved for Public Release

TABLE 1

COMPOSITION OF SEVEN COMMERCIAL 18% NICKEL MARAGING STEEL HEATS SELECTED FOR EVALUATION

				Composition, Wt %											
Grade	Melting Practice	Heat		C	Mn	P	S	Si	Ni	Co	Mo	Ti	Al	Zr	B
200	Nominal Composition*, Grade 200			.03 max	.10 max	.01 max	.01 max	-	17.00 19.00	8.00 9.00	3.00 3.50	.15 .25	.05 .15	.02	.003
	Air Melted	10675	Mill Analysis	.008	.04	.001	.003	.02	17.69	8.60	3.16	.44	.17	-	-
			AGC Analysis	.020	.028	.006	.003	.09	17.40	8.50	3.26	.42	.30	-	-
	Air Melted and Vacuum Degassed	28889	Mill Analysis	.026	.03	.005	.010	.08	17.89	8.52	3.30	.09	.012	-	-
			AGC Analysis	.020	.02	.005	.008	.07	18.00	8.51	3.30	.19	.07	-	-
250	Nominal Composition*, Grade 250			.03 max	.10 max	.01 max	.01 max	-	17.00 19.00	7.00 8.50	4.60 5.20	.30 .50	.05 .15	.02	.003
	Air Melted	13371	Mill Analysis	.02	.04	.004	.009	.08	17.83	7.41	4.70	.46	.11	-	-
			AGC Analysis	.023	-	.003	.009	.06	18.65	8.05	4.90	.52	.05	-	-
	Air Melted and Vacuum Degassed	120D163	Mill Analysis	.017	.06	.005	.004	.18	17.84	8.25	4.80	.55	.12	-	-
			AGC Analysis	.016	-	.005	.003	-	18.60	8.00	4.95	.48	.06	-	-
	Vacuum Arc Remelted	3888472	Mill Analysis	.026	.11	.006	.006	.07	18.46	8.82	4.80	.62	.08	-	-
			AGC Analysis	.019	.025	.006	.003	.08	18.60	9.10	5.10	.62	.07	-	-
	Vacuum Arc Remelted	3888473	Mill Analysis	.026	.08	.006	.007	.05	18.38	8.68	4.80	.67	.07	-	-
			AGC Analysis	.020	.03	.005	.003	.07	18.80	8.82	4.85	.65	.07	-	-
300	Nominal Composition*, Grade 300			.03 max	.10 max	.01 max	.01 max	-	18.00 19.00	8.50 9.50	4.60 5.20	.50 .80	.05 .15	.02	.003
	Vacuum Arc Remelted	07148	Certified	.02	.04	.005	.007	.04	19.00	9.28	5.00	.68	.24	-	-
			Mill Analysis	.018	.03	.006	.003	.09	18.70	9.30	5.12	.65	.39	-	-

*Nominal compositions taken from steel producers' published literature.

TABLE 2

PROCESSING CONDITIONS FOR SELECTED HEATS OF 18% NICKEL MARAGING STEEL

Grade	Melting Process	Heat	Ingot Size	Reduction Practice		Product Form	Finishing Temp., °F	As-Received Condition
				Long., %	Trans., %			
200	Air Melted	10675	9 in. x 9 in. x 750 lb.	50	50	1/2 in. Plate	1400	1500F/30 min
				Hammer-Forged		4 x 4 Bar		1500F/7-10 hr
	Air Melted Vacuum Degassed	28889	17 in. x 42 in. x 3 ton	88	75	1/2 in. Plate	1620	1500F/60 min
250	Air Melted Vacuum Degassed	120D163	32-in.-dia. x 7 ton	90	76	1/2 in. Plate	1500	As-Rolled
	Air Melted	13371	32 in. x 60 in. x 22 ton	80	90	1/2 in. Plate	1500-1600	As-Rolled
	Vacuum Arc Remelted	3888472 and 3888473	8 1/2-in.-dia. x 400 lb	65	50	1/2 in. Plate	1700-1800	As-Rolled
300	Vacuum Arc Remelted	07148	9-in.-dia. x 1000 lb	1/1 ratio		1/2 in. Plate	1600-1700	1500F/30 min
				Press-Forged		4 x 4 Bar	1500	1500F/4 hr

Approved for Public Release

TABLE 3

MATERIAL QUALITY EVALUATION FOR SELECTED HEATS OF 18% NICKEL MARAGING STEEL

Grade	Heat	Melting Process	Ingot Size	Product Form	Finishing Temperature, °F	As-Received Condition	Inclusion Rating								ASTM Grain Size	
							A		B		C		D			
							Thin	Heavy	Thin	Heavy	Thin	Heavy	Thin	Heavy	As Received	Solution-Annealed
200	28889	Air Melted and Vacuum Degassed	17 x 42 x 3 ton	1/2 in. plate	1620	1500°F/ 60 min.	1/2	1/2	1/2	1/2	1/2	1/2	1	1	8-9	7-8
	10675	Air Melted	9 x 9 x 750 lb.	1/2 in. plate	1400	1500°F/ 30 min.	1/2	1/2	1/2	1/2	1/2	1/2	1/2	1/2	< 12	11-12
				4 x 4 bar		1500°F/ 7 to 10 hr.	1/2	1/2	1/2	1/2	1/2	1/2	2	2	> 7	-
250	120D163	Air Melted and Vacuum Degassed	32-in.-dia. x 7 ton	1/2 in. plate	1500	As-Rolled	1/2	1/2	4	4	1/2	1/2	1/2	1/2	7-8	8
	3888472	Vacuum-Arc-Remelted	8 1/2-in.-dia. x 400 lb.	1/2 in. plate.	1700 to 1800	As-Rolled	1/2	1/2	1 1/2	1 1/2	1/2	1/2	1/2	1/2	8-9	7-8
	3888473	Vacuum-Arc-Remelted	8 1/2-in.-dia. x 400 lb.	1/2 in. plate	1700 to 1800	As-Rolled	1/2	1/2	1/2	1/2	1/2	1/2	1/2	1/2	7-8	6-7
	13371	Air Melted	32 x 60 x 22 ton	1/2 in. plate	1500 to 1600	As-Rolled	1/2	1/2	1/2	1/2	1/2	1/2	1/2	1/2	8-9	7-8
300	07148	Vacuum-Arc Remelted	9-in.-dia. x 1000 lb.	1/2 in. plate	1600 to 1700	1500°F/ 30 min.	1/2	1/2	2	2	1/2	1/2	1/2	1/2	10-11	10-11
				4 x 4 bar	<1500	1500°F/ 4 hrs.	1/2	1/2	1/2	1/2	1/2	1/2	1/2	1/2	10-11	10-11
Tentative Specification							2	1 1/2	2 1/2	1 1/2	2	1 1/2	2 1/2	2	5 or finer	5 or finer

Approved for Public Release

Contrails

TABLE 4 (SHEET 1 OF 2 SHEETS)

SUMMARY OF AVERAGE TENSILE PROPERTIES OF SEVEN HEATS OF 18% NICKEL MARAGING STEEL

		AS-ROLLED AND AGED																							
		Longitudinal Direction												Transverse Direction											
		850°F				900°F				950°F				850°F				900°F				950°F			
		2	4	8	16	2	4	8	16	2	4	8	16	2	4	8	16	2	4	8	16	2	4	8	16
Grade 200 Air Melted and Vacuum Degassed 1/2 In. Plate Heat 28869 Received Mill-Annealed	0.2% Offset Yield Strength, ksi	185.3	193.7	204.3	212.7	198.2	196.7	210.5	-	204.4	204.9	-	-	-	-	207.0	-	-	201.5	218.7	-	209.3	-	-	-
	Tensile Strength, ksi	186.5	196.9	205.1	213.6	199.1	203.8	211.6	-	205.3	207.5	-	-	-	-	208.6	-	-	210.7	218.1	-	210.3	-	-	-
	Elongation in 1 in., %	13.2	13.2	11.7	11.5	11.9	9.8	12.0	-	11.8	13.0	-	-	-	-	11.4	-	-	9.8	10.7	-	11.4	-	-	-
	Reduction of Area, %	60.4	61.6	61.4	56.2	60.1	55.5	54.8	-	55.4	58.1	-	-	-	-	55.2	-	-	53.3	50.0	-	49.8	-	-	-
Grade 200 Air Melted 1/2 In. Plate Heat 10675 Received Mill-Annealed	0.2% Offset Yield Strength, ksi	-	214.0	217.1	227.8	204.8	217.5	225.6	234.6	220.1	222.9	-	-	-	-	217.2	-	-	214.3	228.2	-	-	-	-	-
	Tensile Strength, ksi	-	220.0	224.8	237.0	217.4	226.1	234.8	243.4	226.9	231.0	-	-	-	-	226.8	-	-	228.3	237.4	-	-	-	-	-
	Elongation in 1 in., %	-	11.6	11.5	11.6	12.6	11.0	10.7	9.2	11.2	10.3	-	-	-	-	10.9	-	-	10.3	11.2	-	-	-	-	-
	Reduction of Area, %	-	58.5	56.1	53.8	57.2	57.2	50.9	49.4	56.6	56.4	-	-	-	-	53.8	-	-	52.3	52.8	-	-	-	-	-
Grade 200 Air Melted 4 In. x 4 In. Bar* Heat 10675 Received Mill-Annealed	0.2% Offset Yield Strength, ksi	-	-	-	-	-	-	235.1	-	-	-	-	-	-	-	-	-	-	-	231.0 231.7	-	-	-	-	-
	Tensile Strength, ksi	-	-	-	-	-	-	241.2	-	-	-	-	-	-	-	-	-	-	-	241.5 242.5	-	-	-	-	-
	Elongation in 1 in., %	-	-	-	-	-	-	10.2	-	-	-	-	-	-	-	-	-	-	-	7.9 9.0	-	-	-	-	-
	Reduction of Area, %	-	-	-	-	-	-	53.4	-	-	-	-	-	-	-	-	-	-	-	41.3 44.9	-	-	-	-	-
Grade 250 Air Melted 1/2 In. Plate Heat 13371 Received As Rolled	0.2% Offset Yield Strength, ksi	-	-	-	-	-	243.4	266.9	-	-	-	-	-	-	251.7	260.1	-	-	264.7	283.0	-	264.3	266.2	-	-
	Tensile Strength, ksi	-	-	-	-	-	265.3	272.1	-	-	-	-	-	-	262.9	271.6	-	-	272.6	289.2	-	272.0	276.3	-	-
	Elongation in 1 in., %	-	-	-	-	-	9.5	8.0	-	-	-	-	-	-	9.0	8.6	-	-	7.6	7.1	-	7.7	7.6	-	-
	Reduction of Area, %	-	-	-	-	-	40.7	42.9	-	-	-	-	-	-	39.6	38.9	-	-	37.2	38.6	-	38.5	39.2	-	-
Grade 250 Air Melted and Vacuum Degassed 1/2 In. Plate Heat 120D163 Received As Rolled	0.2% Offset Yield Strength, ksi	-	240.7	248.5	259.0	242.5	244.2	257.4	253.6	252.8	253.7	241.1	240.6	-	-	-	266.4	252.1	255.5	265.5	-	259.9	-	-	-
	Tensile Strength, ksi	-	255.7	264.2	272.8	255.1	258.0	268.5	269.8	264.4	265.7	255.0	254.7	-	-	-	280.0	264.3	269.2	277.6	-	272.7	-	-	-
	Elongation in 1 in., %	-	9.1	9.0	7.9	9.7	9.3	8.3	7.2	6.2	8.1	9.0	10.5	-	-	-	7.2	8.2	7.9	7.8	-	6.8	-	-	-
	Reduction of Area, %	-	44.8	46.3	35.5	47.1	42.3	43.9	40.6	31.1	43.8	38.0	42.5	-	-	-	35.9	40.9	39.4	36.6	-	38.4	-	-	-
Grade 250 Vacuum Arc Remelted 1/2 In. Plate Heat 3888472 Received As Rolled	0.2% Offset Yield Strength, ksi	-	-	-	-	-	-	-	-	-	-	-	-	-	-	-	-	-	-	-	-	-	-	-	-
	Tensile Strength, ksi	-	-	-	-	-	-	-	-	-	-	-	-	-	-	-	-	-	-	-	-	-	-	-	-
	Elongation in 1 in., %	-	-	-	-	-	-	-	-	-	-	-	-	-	-	-	-	-	-	-	-	-	-	-	-
	Reduction of Area, %	-	-	-	-	-	-	-	-	-	-	-	-	-	-	-	-	-	-	-	-	-	-	-	-
Grade 250 Vacuum Arc Remelted 1/2 In. Plate Heat 3888473 Received As Rolled	0.2% Offset Yield Strength, ksi	-	-	-	-	-	-	-	-	-	-	-	-	-	-	-	-	-	-	-	-	-	-	-	-
	Tensile Strength, ksi	-	-	-	-	-	-	-	-	-	-	-	-	-	-	-	-	-	-	-	-	-	-	-	-
	Elongation in 1 in., %	-	-	-	-	-	-	-	-	-	-	-	-	-	-	-	-	-	-	-	-	-	-	-	-
	Reduction of Area, %	-	-	-	-	-	-	-	-	-	-	-	-	-	-	-	-	-	-	-	-	-	-	-	-
Grade 300 Vacuum Arc Remelted 1/2 In. Plate Heat 01748 Received Mill-Annealed	0.2% Offset Yield Strength, ksi	-	-	294.4	302.0	285.2	292.2	300.4	306.3	289.9	295.6	-	-	-	-	-	-	282.0	293.6	301.9	-	-	-	-	-
	Tensile Strength, ksi	-	-	304.8	313.4	293.0	302.9	310.1	315.3	301.2	306.6	-	-	-	-	-	-	296.1	302.9	310.1	-	-	-	-	-
	Elongation in 1 in., %	-	-	8.4	7.9	8.8	9.4	9.0	8.5	9.3	8.2	-	-	-	-	-	-	8.6	8.1	8.1	-	-	-	-	-
	Reduction of Area, %	-	-	42.2	37.5	41.1	42.3	42.2	37.9	41.2	38.8	-	-	-	-	-	-	40.5	36.9	38.0	-	-	-	-	-
Grade 300 Vacuum Arc Remelted 4 In. x 4 In. Bar* Heat 01748 Received Mill-Annealed	0.2% Offset Yield Strength, ksi	-	-	-	-	-	-	298.3	-	-	-	-	-	-	-	-	-	-	-	297.8 298.3	-	-	-	-	-
	Tensile Strength, ksi	-	-	-	-	-	-	310.9	-	-	-	-	-	-	-	-	-	-	-	311.5 311.1	-	-	-	-	-
	Elongation in 1 in., %	-	-	-	-	-	-	6.4	-	-	-	-	-	-	-	-	-	-	-	3.6 4.9	-	-	-	-	-
	Reduction of Area, %	-	-	-	-	-	-	32.9	-	-	-	-	-	-	-	-	-	-	-	12.8 28.4	-	-	-	-	-

*Upper values are transverse direction, lower values pertain to short-transverse direction.

Approved for Public Release

Contrails

TABLE 4 (SHEET 2 OF 2 SHEETS)

SUMMARY OF AVERAGE TENSILE PROPERTIES OF SEVEN HEATS OF 18% NICKEL MARAGING STEEL

		SOLUTION-ANNEALED AT 1500°F FOR 30 MIN AND AGED																							
		Longitudinal Direction												Transverse Direction											
		850°F				900°F				950°F				850°F				900°F				950°F			
		Z	4	8	16	Z	4	8	16	Z	4	8	16	Z	4	8	16	Z	4	8	16	Z	4	8	16
Grade 200 Air Melted and Vacuum Degassed 1/2 In. Plate Heat 26889 Received Mill-Annealed	0.2% Offset Yield Strength, ksi	-	-	-	-	-	-	-	-	-	-	-	-	-	-	-	-	-	-	-	-	-	-	-	-
	Tensile Strength, ksi	-	-	-	-	-	-	-	-	-	-	-	-	-	-	-	-	-	-	-	-	-	-	-	-
	Elongation in 1-in., %	-	-	-	-	-	-	-	-	-	-	-	-	-	-	-	-	-	-	-	-	-	-	-	-
	Reduction of Area, %	-	-	-	-	-	-	-	-	-	-	-	-	-	-	-	-	-	-	-	-	-	-	-	-
Grade 200 Air Melted 1/2 In. Plate Heat 10675 Received Mill-Annealed	0.2% Offset Yield Strength, ksi	-	226.0	222.0	235.2	225.8	232.4	234.7	239.6	233.0	229.1	-	-	-	-	224.3	-	-	225.1	245.2	-	-	-	-	-
	Tensile Strength, ksi	-	231.6	235.3	241.8	230.5	238.3	242.1	247.8	236.7	237.4	-	-	-	-	231.9	-	-	235.5	250.8	-	-	-	-	-
	Elongation in 1-in., %	-	10.9	12.9	10.6	12.3	10.8	11.4	9.2	10.6	11.7	-	-	-	-	11.4	-	-	12.2	11.5	-	-	-	-	-
	Reduction of Area, %	-	58.9	58.2	55.4	57.6	57.1	54.3	52.6	56.0	55.7	-	-	-	-	54.3	-	-	55.4	55.4	-	-	-	-	-
Grade 200 Air Melted 4 In. x 4 In. Bar* Heat 10675 Received Mill-Annealed	0.2% Offset Yield Strength, ksi	-	-	220.5	-	-	-	227.5	-	-	-	-	-	-	-	222.3 221.7	-	-	-	229.0 230.4	-	-	-	-	-
	Tensile Strength, ksi	-	-	230.7	-	-	-	237.1	-	-	-	-	-	-	-	235.1 233.1	-	-	-	238.5 237.8	-	-	-	-	-
	Elongation in 1 in., %	-	-	12.2	-	-	-	11.7	-	-	-	-	-	-	-	10.6 9.9	-	-	-	10.9 11.3	-	-	-	-	-
	Reduction of Area, %	-	-	59.4	-	-	-	58.1	-	-	-	-	-	-	-	50.3 47.3	-	-	-	47.9 55.0	-	-	-	-	-
Grade 250 Air Melted 1/2 In. Plate Heat 13371 Received As Rolled	0.2% Offset Yield Strength, ksi	-	-	-	264.3	-	259.3	273.3	-	-	-	-	-	-	258.3	268.0	283.7	-	274.7	285.8	-	260.8	269.3	-	-
	Tensile Strength, ksi	-	-	-	276.4	-	267.7	279.3	-	-	-	-	-	-	266.0	276.0	290.9	-	280.6	292.2	-	267.1	277.9	-	-
	Elongation in 1 in., %	-	-	-	8.1	-	8.8	7.5	-	-	-	-	-	-	9.1	8.8	7.7	-	7.9	7.6	-	8.9	7.9	-	-
	Reduction of Area, %	-	-	-	42.4	-	46.7	42.9	-	-	-	-	-	-	47.0	46.5	42.1	-	43.5	40.3	-	46.5	41.6	-	-
Grade 250 Air Melted and Vacuum Degassed 1/2 In. Plate Heat 120D163 Received As Rolled	0.2% Offset Yield Strength, ksi	248.1	246.0	253.5	260.7	257.6	257.8	267.4	256.1	-	252.5	-	244.4	-	254.2	263.2	270.3	264.7	271.4	274.6	260.4	-	259.5	-	251.0
	Tensile Strength, ksi	256.7	256.2	265.7	272.6	265.1	269.6	277.1	265.2	-	263.8	-	255.4	-	266.6	274.7	282.2	272.9	279.7	284.3	269.9	-	271.7	-	263.6
	Elongation in 1 in., %	8.5	6.5	6.8	8.3	9.3	9.5	9.3	8.9	-	9.5	-	9.6	-	6.3	6.9	7.4	9.9	8.8	8.7	9.3	-	7.5	-	9.5
	Reduction of Area, %	38.2	41.3	38.6	39.8	47.5	45.9	44.8	45.3	-	46.5	-	41.7	-	28.9	32.6	33.9	46.5	41.4	45.7	46.0	-	40.6	-	39.0
Grade 250 Vacuum Arc Remelted 1/2 In. Plate Heat 3888472 Received As Rolled	0.2% Offset Yield Strength, ksi	-	278.7	274.0	283.8	-	277.5	278.8	279.0	275.0	270.8	268.4	-	-	-	272.5	-	-	273.7	286.0	-	271.0	-	-	-
	Tensile Strength, ksi	-	287.4	287.2	292.7	-	287.7	290.2	289.5	282.4	282.7	281.7	-	-	-	284.7	-	-	283.0	293.4	-	286.5	-	-	-
	Elongation in 1 in., %	-	9.0	9.6	9.3	-	9.7	8.5	8.4	8.8	9.6	9.1	-	-	-	8.6	-	-	9.0	8.6	-	8.1	-	-	-
	Reduction of Area, %	-	40.1	43.0	41.0	-	42.0	39.9	38.5	38.0	43.4	42.6	-	-	-	41.9	-	-	40.5	39.9	-	36.9	-	-	-
Grade 250 Vacuum Arc Remelted 1/2 In. Plate Heat 3888473 Received As Rolled	0.2% Offset Yield Strength, ksi	-	282.7	280.0	281.1	-	277.4	289.0	278.8	274.9	273.3	268.3	-	-	-	281.3	-	-	282.1	294.5	-	279.3	-	-	-
	Tensile Strength, ksi	-	291.5	291.4	298.5	-	286.5	296.7	291.3	284.5	284.9	281.8	-	-	-	293.6	-	-	291.4	301.7	-	289.5	-	-	-
	Elongation in 1 in., %	-	8.9	8.9	8.6	-	8.2	8.6	8.4	8.9	9.2	8.7	-	-	-	8.2	-	-	8.8	8.1	-	8.5	-	-	-
	Reduction of Area, %	-	40.5	40.7	39.3	-	38.6	40.4	40.2	43.7	41.7	39.4	-	-	-	38.6	-	-	39.3	36.8	-	39.3	-	-	-
Grade 300 Vacuum Arc Remelted 1/2 In. Plate Heat 01746 Received Mill-Annealed	0.2% Offset Yield Strength, ksi	-	288.3	297.7	304.4	295.7	291.7	301.8	301.6	294.2	296.6	292.9	-	-	-	-	-	-	291.5	299.1	-	293.7	294.2	-	-
	Tensile Strength, ksi	-	303.8	306.2	311.6	294.9	300.8	310.4	314.2	303.0	304.5	304.6	-	-	-	-	-	-	301.0	309.3	-	302.8	304.5	-	-
	Elongation in 1 in., %	-	7.9	6.9	6.4	7.5	7.5	7.2	7.1	7.9	7.9	7.3	-	-	-	-	-	-	7.2	6.3	-	6.9	6.4	-	-
	Reduction of Area, %	-	41.2	38.3	37.9	38.9	39.6	39.1	39.0	40.0	42.4	39.2	-	-	-	-	-	-	36.7	33.4	-	34.0	35.1	-	-
Grade 300 Vacuum Arc Remelted 4 In. x 4 In. Bar* Heat 01746 Received Mill-Annealed	0.2% Offset Yield Strength, ksi	-	-	-	-	-	300.3	309.4	-	-	-	-	-	-	-	-	-	-	295.3 300.5	307.5 307.7	-	-	-	-	-
	Tensile Strength, ksi	-	-	-	-	-	307.0	316.1	-	-	-	-	-	-	-	-	-	-	305.3 307.3	315.1 315.5	-	-	-	-	-
	Elongation in 1 in., %	-	-	-	-	-	5.6	7.7	-	-	-	-	-	-	-	-	-	-	3.5 3.5	4.7 3.2	-	-	-	-	-
	Reduction of Area, %	-	-	-	-	-	28.3	42.5	-	-	-	-	-	-	-	-	-	-	16.7 16.7	23.5 16.9	-	-	-	-	-

*Upper values are transverse direction; lower values pertain to short-transverse direction.

Approved for Public Release

TABLE 5 (SHEET 1 OF 3 SHEETS)
SLOW-NOTCH-BEND TEST FOR HEAT 120D163
Effect of Heat Treatment and Specimen Orientation in
Air Melted, Vacuum Degassed, 1/2-In.-Thick, Grade 250, 18% Nickel Maraging Steel

Specimen Number	Material Condition	Aging Cycle °F - hr	Specimen Orientation	.2% Offset Yield (ksi)	Width b (in.)	Depth d (in.)	Proportional Limit Load(L) (lb)	Proportional Limit Deflec.(e) (in.)	Maximum Load (2) Load(L) (lb)	Maximum Load (2) Deflec.(e) (in.)	eb/L (in.²/lb)x10⁻⁸	Notch+Crack Depth Effective a (in.)	Notch+Crack Depth Measured a (in.)	PLANE-STRAIN FRACTURE TOUGHNESS(1) G_{nc}	K_{nc}	G_{Ic}	K_{Ic}
			(0.5 x 0.5 x 4.0)														
2L1	Solution	900 - 4	Longitudinal	258	.492	.500	Failure occurred		3395	(3)	329	.113	(3)	258	(3)	(3)	(3)
2L2	Treated		(Notch in		.492	.500	before proportional		3052		340	.123		234			
2L3			Surface)		.492	.500	limit load		2680		354	.134		201			
2L4					.492	.500			2870		362	.140		243			
2L5					.492	.500			3620		329	.113		295			
													Avg	246			
2LF1	Solution	900 - 4	Transverse	271	.492	.500			3520		332	.116		289			
2LF2	Treated		(Notch in		.492	.500			3415		331	.115		269			
2LF3			Surface)		.492	.500			3360		332	.116		263			
2LF4					.492	.500			3310		333	.117		259			
2LF5					.492	.500			3010		345	.127		237			
													Avg	263			
2T1	Solution	900 - 4	Longitudinal	258	.492	.500			2450		345	.145		185			
2T2	Treated		(Notch thru		.492	.500			2660		358	.138		203			
2T3			Thickness)		.492	.500			2590		370	.145		206			
2T4					.492	.500			2680		362	.140		212			
2T5					.492	.500			2790		355	.135		220			
													Avg	205			
2TF1	Solution	900 - 4	Transverse	271	.492	.500			2940		349	.130		233			
2TF2	Treated		(Notch thru		.492	.500			3050		349	.130		250			
2TF3			Thickness)		.492	.500			3130		342	.125		251			
2TF4					.492	.500			3130		345	.127		257			
2TF5					.492	.500			2720		355	.135		209			
													Avg	240			

Calibration Curve Constants: Q = 14.44 x 10^{-6}
R = 306.67 x 10^{-6}
S = -711.11 x 10^{-6}

			(0.5 x 0.75 x 4.0)														
3L1	Solution	900 - 4	Longitudinal	258	.493	.751	Failure occurred		5580	(3)	134	.175	(3)	216	(3)	(3)	(3)
3L2	Treated		Notch thru		.493	.751	before the pro-		5460		138	.185		184			
3L3			thickness		.493	.751	portional limit		5570		142	.195		204			
3L4					.493	.751	load		4940		150	.215		239			
3L5					.493	.751			5815		134	.175		215			
													Avg	213			
3T1	Solution	900 - 4	Transverse	271	.493	.751			6470		126	.150		258			
3T2	Treated		Notch thru		.493	.751			5670		136	.180		223			
3T3			thickness		.493	.751			5875		134	.175		243			
3T4					.493	.751			5240		148	.210		240			
3T5					.493	.751			6600		123	.150		266			
													Avg	246			

Calibration Curve Constants: Q = 17.19 x 10^{-6}
R = -51.67 x 10^{-6}
S = 97.22 x 10^{-6}

(1) G_{nc} (in.-lb/in.^{2}) and K_{nc} (ksi$\sqrt{\text{in.}}$) are based on the proportional-limit load and the effective-crack depth (a) determined from spring-constant-calibration curve
G_{Ic} (in.-lb/in.^{2}) and K_{Ic} (ksi$\sqrt{\text{in.}}$) are based on the proportional-limit load and the measured crack depth (a) using Bueckner's equation.

(2) Failure occurred within the proportional-limit.

(3) Data were not recorded.

Approved for Public Release

Confidential

TABLE 5 (SHEET 2 OF 3 SHEETS)

PART-THROUGH-CRACK TENSILE TEST FOR HEAT 120D163

Grade 250, Air Melted, Vacuum Degassed, 18% Nickel Maraging Steel, Solution-Annealed at 1500°F For 30 min, and Aged at 900°F for 4 Hours. 0.2% Offset Yield Strength, ksi: Longitudinal-258; Transverse-265

Specimen No.	Rolling Direction	Thickness, (in.)	Width, (in.)	Max Load (lb x 10^3)	Gross Stress, (ksi)	Type Notch	Notch Depth, b, (in.)	Notch Length, 2a, (in.)	$\frac{b}{a}$	ϕ^2	PLANE-STRAIN FRACTURE TOUGHNESS K_{Ic} (1) (ksi $\sqrt{in.}$)	PLANE-STRAIN FRACTURE TOUGHNESS G_{Ic} (in.-lb/in.^{2})
1-2 (2)	Longitudinal	0.497	4.00	252	126.7	Surface	0.21	0.76	.552	1.47	95	308
5-3	Longitudinal	0.502	4.00	362	180.0	Notch	0.14	0.36	.778	1.85	99	339
1-3	Longitudinal	0.502	4.00	302	150.8		0.13	0.54	.482	1.42	91	287
2-3	Longitudinal	0.498	4.00	242	121.4		0.18	0.72	.500	1.44	85	249
3-3	Longitudinal	0.497	4.00	314	157.5		0.12	0.40	.600	1.63	79	208
2-1 (2)	Transverse	0.510	3.99	312	153.3		0.16	0.44	.682	1.78	91	287
1-1	Transverse	0.503	4.00	423	210.0		0.10	0.24	.835	2.02	93	297
4-1	Transverse	0.497	4.00	412	207.0		0.10	0.27	.741	1.85	96	326
5-1	Transverse	0.509	3.99	340	167.5		0.13	0.33	.788	1.90	87	253
6-1	Transverse	0.508	4.00	232	114.5		0.16	0.75	.427	1.35	79	211
2L1 (3)	Longitudinal	0.125	0.498	13.90	223.5	Surface	0.059	0.199	.595	1.60	87.6	266
2L2	Longitudinal	0.125	0.497	13.65	219.5	Notch	0.068	0.200	.680	1.78	87.0	261
2L3	Longitudinal	0.125	0.498	15.05	241.0		0.055	0.160	.687	1.79	86.5	259
2T1	Transverse	0.125	0.497	15.25	245.0		0.059	0.180	.738	1.76	92.0	293
2T2	Transverse	0.125	0.497	14.10	227.0		0.065	0.192	.679	1.78	88.0	269
2T3	Transverse	0.125	0.497	15.55	250.0		0.058	0.162	.727	1.82	91.9	291
2ST1A (3)	Longitudinal	0.125	0.495	14.65	236.0	Through-	0.060	0.163	.732	1.85	87.0	260
2ST2B	Longitudinal	0.125	0.495	15.00	241.0	Thickness	0.063	0.157	.798	1.98	87.5	265
2ST3B	Longitudinal	0.125	0.495	14.50	233.0	Notch	0.060	0.159	.760	1.90	84.5	246
2ST2A	Transverse	0.125	0.497	13.25	213.3		0.066	0.185	.710	1.80	81.7	231
2ST1B	Transverse	0.125	0.497	14.25	229.0		0.059	0.174	.703	1.80	84.5	246

(1) Values of K_{Ic} were calculated from the equation: $K^2 = 3.77\ \sigma^2 b/(\phi^2 - 0.212\ \sigma^2/\sigma_{YS}^2)$, where ϕ^2 was obtained from a plot of ϕ^2 vs b/a shown in ASTM Bulletin, (May 1961), p. 390.

(2) Specimen Size was 0.5 x 4 x 26-in.

(3) Specimen Size was 0.125 x 0.5 x 8-in.

Approved for Public Release

TABLE 5 (SHEET 3 OF 3 SHEETS)

CENTER-NOTCH TENSILE TEST FOR HEAT 120D163

Grade 250, Air Melted, Vacuum Degassed, 18% Nickel Maraging Steel, 0.5 x 8 x 32-In. Specimen, Solution-Annealed at 1500°F for 30 min, and Aged at 900°F for 4 Hours. 0.2% Offset Yield Strength, ksi: Longitudinal-258; Transverse-265

Specimen No.	Rolling Direction	Width, (in.)	Thickness, (in.)	Notch Length, 2a, (in.)[1]	Load (lb x 10^3)	Gross Stress, (ksi)	FRACTURE TOUGHNESS G_c (in.-lb/in.^{2})	FRACTURE TOUGHNESS G_{Ic} (in.-lb/in.^{2})	Shear, (%)
2-1	Longitudinal	8.00	0.51	4.16	178	44.5	646[2]		47
2-2	Longitudinal	8.00	0.51	4.56	176	44.0	745[2]		39
2-3	Longitudinal	8.00	0.51	3.86	296	74.0	1582[2]		45
4-1	Transverse	8.00	0.51	3.74	208	52.0	746[2]		33
4-2	Transverse	8.00	0.51	3.20	157	39.3	344		37
4-2	Transverse	8.00	0.51	2.88	130	32.3		205[3]	
4-3	Transverse	7.98	0.51	3.74	158	39.5	438		38
4-3	Transverse	7.98	0.51	2.90	132	33.0		218[3]	

(1) Original Notch length was 2.75 in.

(2) Improper or no fatigue crack.

(3) Crack initiation (pop-in) values were obtained by acoustical means.

Approved for Public Release

TABLE 6

SLOW-NOTCH-BEND TEST FOR HEAT 28889

Effect of Heat Treatment and Specimen Orientation in Air Melted, Vacuum-Degassed, 1/2-In.-Thick, Grade 200, 18% Nickel Maraging Steel

Specimen Number	Material Condition	Aging Cycle °F - hr	Specimen Orientation	.2% Offset Yield (2) (ksi)	Width b (in.)	Depth d (in.)	Proportional Limit Load(L) (lb)	Proportional Limit Deflec.(e) (in.)	Maximum Load Load(L) (lb)	Maximum Load Deflec.(e) (in.)	eb/L (in.²/lb)x10⁻⁸	Notch+Crack Depth Effective a (in.)	Notch+Crack Depth Measured a (in.)	PLANE-STRAIN FRACTURE TOUGHNESS(1) G_{nc}	K_{nc}	G_{Ic}	K_{Ic}
L13	Re-Solution Treated	900 – 4	Longitudinal	197	.489	.751	7700	(3)	8380	(3)	125	.220	(3)	365	101	(3)	(3)
L14					.490	.751	5600		6440		144	.268		315	94		
L15					.489	.751	6100		6830		136	.250		310	93		
L25					.497	.750	7350		7730		137	.252		442	113		
L26					.496	.748	6450		6610		152	.284		480	118		
													Avg	382	104		
L19	Re-Solution Treated	900 – 4	Transverse	202	.490	.751	7400		7470		124	.215		321	95		
L20					.490	.751	6500		6630		141	.260		390	103		
L21					.490	.751	5650		5750		135	.246		254	85		
L29					.497	.748	5500		5710		140	.258		264	86		
L30					.496	.749	6000		6180		136	.249		286	91		
													Avg	303	92		
L16	Re-Solution Treated	900 – 8	Longitudinal	211	.490	.751	6600		6950		141	.260		402	105		
L17					.490	.751	7500		7660		130	.234		396	104		
L18					.490	.751	7250		7520		135	.246		418	108		
L27					.498	.750	6800		7160		138	.254		386	103		
L28					.498	.750	7500		7740		135	.246		432	110		
													Avg	407	106		
L22	Re-Solution Treated	900 – 8	Transverse	217	.490	.751	5550		5820		136	.250		256	85		
L23					.489	.751	4300		4620		167	.320		323	95		
L24					.490	.751	5700		6080		133	.240		243	84		
L31					.497	.750	5300		5400		144	.267		269	86		
L32					.498	.750	6220		6280		123	.213		214	77		
													Avg	261	89		

Calibration Curve Constants: $Q = 1.371 \times 10^{-5}$
$R = -6.5 \times 10^{-5}$
$S = 1.4917 \times 10^{-4}$

Span of the beam = 3 in.

(1) G_{nc} (in.-lb/in.^{2}) and K_{nc} (ksi$\sqrt{\text{in.}}$) are based on the proportional-limit load and the effective-crack depth (a) determined from spring-constant-calibration curve
G_{Ic} (in.-lb/in.^{2}) and K_{Ic} (ksi$\sqrt{\text{in.}}$) are based on the proportional-limit load and the measured crack depth (a) using Bueckner's equation.

(2) These are mill-annealed data.

(3) Data were not recorded.

Approved for Public Release

Approved for Public Release

TABLE 7 (SHEET 1 OF 2 SHEETS)

SLOW-NOTCH-BEND TEST FOR HEAT 10675, 1/2 IN. PLATE

Effect of Heat Treatment and Specimen Orientation in Air Melted, Grade 200, 1/2-In. Plate, 18% Nickel Maraging Steel

Specimen Number	Material Condition	Aging Cycle °F - hr	Specimen Orientation	.2% Offse Yield (ksi)	Width b (in.)	Depth d (in.)	Proportional Limit Load(L) (lb)	Proportional Limit Deflec.(e) (in.)	Maximum Load (2) Load(L) (lb)	Maximum Load (2) Deflec.(e) (in.)	eb/L (in.²/lb)x10⁻⁸	Notch+Crack Depth Effective a (in.)	Notch+Crack Depth Measured a (in.)	PLANE-STRAIN FRACTURE TOUGHNESS(1) G_{nc}	K_{nc}	G_{Ic}	K_{Ic}
200L	Mill-	900 - 4	Longitudinal	218	.4922	.751	6500		7080		128	.190	.210	282		304	
201L	Annealed				.4930	.751	7200		7870		120	.158	.185	297		300	
202L					.4938	.751	6300		7230		126	.180	.205	252		271	
203L					.4940	.751	6700		7300		126	.180	.207	285		312	
204L					.4942	.751	7000		7550		124	.172	.205	300		335	
													Avg	283	Avg 91	Avg 304	Avg 96
210T	Mill-	900 - 4	Transverse	214	.4922	.751	6400		7205		127	.182	.205	265		282	
211T	Annealed				.4932	.751	6400		7200		127	.182	.205	263		281	
212T					.4961	.751	7100		7460		139	.220	.260	369		530	
213T					.4983	.751	8100		8340		124	.175	.220	400		499	
214T					.4989	.751	7100		7780		121	.160	.185	285		285	
													Avg	316	Avg 96	Avg 375	Avg 107
205L	Mill-	900 - 8	Longitudinal	226	.4934	.751	5800		6150		149	.248	.265	270		372	
206L	Annealed				.4965	.751	5400		5980		137	.214	.230	209		242	
207L					.4989	.751	4750		5210		170	.298	.295	195		306	
208L					.4995	.751	7600		7880		119	.154	.200	316		370	
													Avg	248	Avg 85	Avg 322	Avg 99
215T	Mill-	900 - 8	Transverse	228	.4992	.751	7000		7010		148	.246	.260	382		478	
216T	Annealed				.5006	.751	6600		6690		147	.242	.280	334		495	
217T					.5014	.751	7500		7600		128	.186	.240	356		466	
218T					.5014	.751	6450		6505		150	.250		325			
219T					.5008	.751	6400		6540		137	.214	.260	289		396	
													Avg	337	Avg 99	Avg 459	Avg 118

Calibration Curve Constants: $Q = 9.83 \times 10^{-6}$
$R = -2.50 \times 10^{-6}$
$S = -8.33 \times 10^{-6}$

(1) G_{nc} (in.-lb/in.^{2}) and K_{nc} (ksi$\sqrt{\text{in.}}$) are based on the proportional-limit load and the effective-crack depth (a) determined from spring-constant-calibration curve
G_{Ic} (in.-lb/in.^{2}) and K_{Ic} (ksi$\sqrt{\text{in.}}$) are based on the proportional-limit load and the measured crack depth (a) using Bueckner's equation.

(2) Data not recorded.

TABLE 7 (SHEET 2 OF 2 SHEETS)

SLOW-NOTCH-BEND TEST FOR HEAT 10675 PLATE

Effect of Heat Treatment and Specimen Orientation in Air Melted, 1/2-In.-Thick, Grade 200, 18% Nickel Maraging Steel

Specimen Number	Material Condition	Aging Cycle °F - hr	Specimen Orientation	.2% Offset Yield (ksi)	Width b (in.)	Depth d (in.)	Proportional Limit Load(L) (lb)	Proportional Limit Deflec.(e) (in.)	Maximum Load Load(L) (lb)	Maximum Load Deflec.(e) (in.)	eb/L (in.²/lb)x10⁻⁸	Notch+Crack Depth Effective a (in.)	Notch+Crack Depth Measured a (in.)	PLANE-STRAIN FRACTURE TOUGHNESS(1) G_{nc}	K_{nc}	G_{Ic}	K_{Ic}
LA90	Re-Solution	850 - 8	Longitudinal	222	.507	.751	6600	(2)	7050	(2)	141	.225	(2)	315	94	(2)	(2)
LA91	Treated				.504	.751	6500		7170		144	.235		316	94		
LA92					.501	.751	5300		5880		163	.280		233	81		
													Avg	288	89		
TA100	Re-Solution		Transverse	224	.505	.751	6900		7160		132	.198		314	94		
TA101	Treated				.500	.751	7100		7610		133	.200		339	97		
TA102					.501	.751	6200		6920		140	.224		280	88		
													Avg	311	93		
LA93	Re-Solution	900 - 4	Longitudinal	232	.506	.751	6000		6160		164	.283		299	91		
LA94	Treated				.505	.751	6300		6520		158	.272		223	95		
LA95					.505	.751	9070		9070		114	.135		386	104		
LA96					.502	.751	6700		7960		135	.206		308	93		
													Avg	329	96		
TA103	Re-Solution		Transverse	225	.503	.751	8600		9520		111	.120		323	95		
TA104	Treated				.502	.751	5810		5810		174	.303		292	90		
TA105					.504	.751	5980		5980		169	.293		304	92		
TA106					.505	.751	6400		6760		157	.268		332	96		
													Avg	313	94		
LA97	Re-Solution	900 - 8	Longitudinal	235	.498	.751	6200		6680		139	.219		277	88		
LA98	Treated				.497	.751	7100		7350		134	.204		346	99		
LA99					.503	.751	6700		7130		138	.218		320	95		
													Avg	315	94		
TA107	Re-Solution		Transverse	245	.505	.751	6300		6360		157	.268		322	95		
TA108	Treated				.505	.751	6100		6440		145	.238		285	89		
TA109					.507	.751	6100		6220		150	.250		288	90		
													Avg	298	91		

Calibration Curve Constants: $Q = 9.83 \times 10^{-6}$
$R = -2.50 \times 10^{-6}$
$S = -8.33 \times 10^{-6}$

Bar Bending-Length: 3 in.

(1) G_{nc} (in.-lb/in.²) and K_{nc} (ksi$\sqrt{\text{in.}}$) are based on the proportional-limit load and the effective-crack depth (a) determined from spring-constant-calibration curve
G_{Ic} (in.-lb/in.²) and K_{Ic} (ksi$\sqrt{\text{in.}}$) are based on the proportional-limit load and the measured crack depth (a) using Bueckner's equation.

(2) Data were not recorded.

Approved for Public Release

TABLE 8

SLOW-NOTCH-BEND TEST FOR HEAT 10675 BAR STOCK

Effect of Heat Treatment and Specimen Orientation in Air Melted, Grade 200, 18% Nickel Maraging Steel 4 x 4-In. Bar Stock

Specimen Number	Material Condition	Aging Cycle °F - hr	Specimen Orientation	.2% Offset Yield (ksi)	Width b (in.)	Depth d (in.)	Proportional Limit Load(L) (lb)	Proportional Limit Deflec.(e) (in.)	Maximum Load Load(L) (lb)	Maximum Load Deflec.(e) (in.)	eb/L $(in.^2/lb) \times 10^{-8}$	Notch+Crack Depth Effective a (in.)	Notch+Crack Depth Measured s (in.)	PLANE-STRAIN FRACTURE TOUGHNESS(1) G_{nc}	K_{nc}	G_{Ic}	K_{Ic}
A65	Re-Solution Treated	850 - 16	Longitudinal	---	.500	.750	7750	(2)	8080	(2)	122	.164	(2)	345	98	(2)	(2)
A66					.500	.751	7700		8050		124	.172		355	99		
A67					.500	.750	6700		6750		127	.182		281	89		
A68					.498	.750	6650		6920		129	.190		287	90		
A69					.499	.750	7300		7580		114	.134		258	85		
													Avg	305	92		
A75	Re-Solution Treated	850 - 16	Transverse	---	.499	.750	6950		6980		123	.168		284	89		
A76					.498	.750	6400		6465		117	.148		217	78		
A77					.499	.750	6600		6650		119	.151		234	81		
A78					.499	.750	5600		5820		134	.205		215	76		
A79					.500	.751	7500		7130		108	.108		224	79		
													Avg	235	81		
A70L	Re-Solution Treated	900 - 8	Longitudinal	228	.4995	.750	6300		6320		165	.286		336	97		
A71L					.500	.750	7900		8000		117	.146		325	95		
A72L					.500	.750	6920		7020		131	.194		315	94		
A73L					.500	.750	6050		6450		136	.210		255	85		
A74L					.4995	.750	6710		6810		132	.198		301	92		
													Avg	307	92		
A80T	Re-Solution Treated	900 - 8	Transverse	229	.499	.751	5050		5065		155	.264		207	76		
A81T					.499	.750	5050		5235		141	.225		187	72		
A82T					.500	.751	5715		5715		134	.204		223	79		
A83T					.500	.751	5790		5790		133	.200		226	79		
A84T					.500	.752	5325		5430		141	.225		208	76		
													Avg	211	77		

Calibration Curve Constants: $Q = 9.83 \times 10^{-6}$
$R = -2.50 \times 10^{-6}$
$S = -8.33 \times 10^{-6}$

Bar Bending-Length = 3 in.

(1) G_{nc} (in.-lb/in.^{2}) and K_{nc} (ksi$\sqrt{in.}$) are based on the proportional-limit load and the effective-crack depth (a) determined from spring-constant-calibration curve
G_{Ic} (in.-lb/in.^{2}) and K_{Ic} (ksi$\sqrt{in.}$) are based on the proportional-limit load and the measured crack depth (a) using Bueckner's equation.

(2) Data were not recorded.

Approved for Public Release

TABLE 9 (SHEET 1 OF 2 SHEETS)

SLOW-NOTCH-BEND TEST FOR HEAT 13371

Effect of Heat Treatment and Specimen Orientation in Air Melted, 1/2-In.-Thick, Grade 250, 18% Nickel Maraging Steel

Specimen Number	Material Condition	Aging Cycle °F - hr	Specimen Orientation	.2% Offset Yield (ksi)	Width b (in.)	Depth d (in.)	Proportional Limit Load(L) (lb)	Proportional Limit Deflec.(e) (in.)	Maximum Load (2) Load(L) (lb)	Maximum Load (2) Deflec.(e) (in.)	eb/L (in.²/lb)x10⁻⁸	Notch+Crack Depth Effective a (in.)	Notch+Crack Depth Measured a (in.)	PLANE-STRAIN FRACTURE TOUGHNESS(1) G_{nc}	K_{nc}	G_{Ic}	K_{Ic}
U16	As Rolled	850 - 8	Longitudinal	260	.4988	.750	(3)	(3)	1700	(3)	(3)	(2)	.470	(3)	(3)	158	68
U17					.4910	.750			4400				.255			201	77
U18					.4910	.750			4280				.245			176	72
U19					.4910	.750			4300				.270			216	79
U20					.4910	.750			4200				.265			198	76
																Avg 189	Avg 74
U21	As Rolled	850 - 8	Transverse	---	.4905	.750			6400				.140			159	68
U22					.4910	.750			5775				.185			196	76
U23					.490	.750			5650				.170			165	69
U24					.491	.750			4700				.220			174	71
U25					.4910	.750			5750				.165			162	69
																Avg 171	Avg 71
U1	As Rolled	900 - 4	Longitudinal	265	.4992	.750			4650				.230			179	72
U2					.4991	.750			6120				.155			162	69
U3					.4989	.750			5780				.160			152	67
U4					.4989	.750			6130				.145			148	66
U6					.4920	.750			6700				.170			230	82
																Avg 174	Avg 71
U26	As Rolled	900 - 4	Transverse	243	.4996	.750			6740				.150			187	74
U27					.4995	.750			5350				.235			245	85
U28					.4995	.750			5800				.200			217	80
U29					.4994	.750			7270				.150			217	80
U30					.4995	.750			6180				.195			236	83
																Avg 220	Avg 80
U32	As Rolled	950 - 2	Longitudinal	264	.4903	.750			6150				.190			233	83
U35					.4900	.750			6300				.175			214	79
																Avg 223	Avg 81
U36	As Rolled	950 - 2	Transverse	---	.4900	.750			5510				.250			305	94
U37					.4905	.750			2550				.430			262	88
U38					.4905	.750			6760				.170			235	83
U40					.4900	.750			2490				.435			261	87
																Avg 266	Avg 88

(1) G_{nc} (in.-lb/in.^{2}) and K_{nc} (ksi$\sqrt{\text{in.}}$) are based on the proportional-limit load and the effective-crack depth (a) determined from spring-constant-calibration curve
G_{Ic} (in.-lb/in.^{2}) and K_{Ic} (ksi$\sqrt{\text{in.}}$) are based on the proportional-limit load and the measured crack depth (a) using Bueckner's equation.

(2) Failure occurred within the proportional limit.

(3) Data were not recorded.

Approved for Public Release

TABLE 9 (SHEET 2 OF 2 SHEETS)

SLOW-NOTCH-BEND TEST FOR HEAT 13371

Effect of Heat Treatment and Specimen Orientation in Air Melted, 1/2-In.-Thick, Grade 250, 18% Nickel Maraging Steel

Specimen Number	Material Condition	Aging Cycle °F - hr	Specimen Orientation	.2% Offset Yield (ksi)	Width b (in.)	Depth d (in.)	Proportional Limit Load(L) (lb)	Proportional Limit Deflec.(e) (in.)	Maximum Load Load(L) (lb)	Maximum Load Deflec.(e) (in.)	eb/L (in.²/lb)x10⁻⁸	Notch+Crack Depth Effective a (in.)	Notch+Crack Depth Measured a (in.)	PLANE-STRAIN FRACTURE TOUGHNESS(1) G_{nc}	K_{nc}	G_{Ic}	K_{Ic}
U41	Solution	900 - 4	Longitudinal	275	.499	.750	5500	(2)	5525	(2)	132	.238	.245	213	77	282	96
U42	Treated				.499	.750	5800		5875		118	.198	.195	161	67	206	82
U43					.500	.750	6250		6275		117	.172		154	65		
U44					.499	.750	6800		6970		114	.156	.170	166	68	230	87
U45					.499	.750	6150		6210		116	.188	.195	167	69	235	88
													Avg	172	Avg 71	Avg 238	Avg 88
U51	Solution	900 - 4	Transverse	259	.499	.750	7300		7790		126	.222	.145	318	94	209	83
U52	Treated				.499	.749	7250		8320		128	.226		327	96		
U53					.499	.750	6850		7515		129	.231	.195	307	91	291	98
U54					.499	.750	6800		7635		127	.225		285	89		
U55					.499	.750	6100		6305		143	.265	.235	349	99	320	103
													Avg	317	Avg 94	Avg 273	Avg 96
U46	Solution	900 - 8	Longitudinal	286	.500	.750	5450		5570		126	.222	.200	237	81	192	80
U47	Treated				.499	.750	6300		6470		126	.222	.170	156	65	198	81
U48					.499	.750	7400		7540		102	.100	.125	180	71	175	76
U49					.499	.750	5600		5620		125	.218	.205	177	70	211	83
U50					.499	.750	5500		5780		127	.224	.190	184	72	180	77
													Avg	187	Avg 72	Avg 191	Avg 79
U56	Solution	900 - 8	Transverse	273	.499	.750	5700		6050		133	.240	.215	233	81	238	89
U57	Treated				.499	.750	6250		6650		126	.220	.175	229	80	203	82
U58					.499	.750	6000		6200		124	.215	.205	201	77	243	90
U59					.499	.750	6150		6420		128	.226	.220	235	81	289	98
U60					.499	.750	6150		6475		128	.226	.180	235	81	206	93
													Avg	227	Avg 80	Avg 236	Avg 88

Calibration Curve Constants: $Q = 14.42 \times 10^{-6}$
$R = -70.00 \times 10^{-6}$
$S = 158.33 \times 10^{-6}$

Note: Republic Steel Heat 3888472 Calibration Curve was used.

(1) G_{nc} (in.-lb/in.^{2}) and K_{nc} (ksi$\sqrt{\text{in.}}$) are based on the proportional-limit load and the effective-crack depth (a) determined from spring-constant-calibration curve
G_{Ic} (in.-lb/in.^{2}) and K_{Ic} (ksi$\sqrt{\text{in.}}$) are based on the proportional-limit load and the measured crack depth (a) using Bueckner's equation.

(2) Data were not recorded.

Approved for Public Release

TABLE 10

SLOW-NOTCH-BEND TEST FOR HEAT 120D163

Effect of Heat Treatment and Specimen Orientation in Air Melted, Vacuum Degassed, 1/2-In.-Thick, Grade 250, 18% Nickel Maraging Steel

Specimen Number	Material Condition	Aging Cycle °F - hr	Specimen Orientation	.2% Offset Yield (ksi)	Width b (in.)	Depth d (in.)	Proportional Limit Load(L) (lb)	Proportional Limit Deflec.(e) (in.)	Maximum Load (2) Load(L)	Maximum Load (2) Deflec.(e)	eb/L $(in.^2/lb)\times10^{-8}$	Notch+Crack Depth Effective a (in.)	Notch+Crack Depth Measured a (in.)	PLANE-STRAIN FRACTURE TOUGHNESS(1) G_{nc}	K_{nc}	G_{Ic}	K_{Ic}
1	Solution Treated	850 8	Longitudinal	254	0.4930	0.750	(2)	(2)	3425	(3)	(3)	(3)	0.272	(3)	(3)	138	64
2					0.4932	0.750			5090				0.162			123	61
3					0.4935	0.750			4110				0.210			121	60
4					0.4930	0.750			3700				0.250			136	64
5					0.4932	0.750			2700				0.355			161	69
																Avg 136	Avg 64
6	Solution Treated	900 4	Longitudinal	258	0.4868	0.750			6450				0.130			147	66
7					0.4865	0.750			2300				0.435			226	82
8					0.4930	0.750			6000				0.145			145	66
9					0.4930	0.750			5500				0.162			143	65
10					0.4930	0.750			6300				0.122			126	61
																Avg 157	Avg 72
21	Solution Treated	900 4	Transverse	271	0.4910	0.750			5210				0.170			139	64
23					0.4912	0.750			6425				0.130			144	66
24					0.4910	0.750			4000				0.252			163	70
25					0.4910	0.750			4550				0.210			150	67
																Avg 149	Avg 67
11	Solution Treated	900 8	Longitudinal	267	0.4987	0.750			4150				0.250			167	71
12					0.4930	0.750			4900				0.185			140	65
15					0.4860	0.750			4460				0.220			160	69
																Avg 156	Avg 68
26	Solution Treated	900 8	Transverse	275	0.4910	0.750			2300				0.382			145	66
27					0.4910	0.750			2115				0.405			147	66
28					0.4914	0.750			2430				0.372			150	67
29					0.4913	0.750			3400				0.272			137	64
30					0.4915	0.750			4360				0.200			127	62
																Avg 141	Avg 65
16	Solution Treated	950 2	Longitudinal	---	0.4930	0.750			4190				0.270			203	78
17					0.4905	0.750			6280				0.170			203	78
18					0.4910	0.750			3640				0.310			210	77
19					0.4880	0.750			6025				0.162			175	72
																Avg 198	Avg 76

(1) G_{nc} (in.-lb/in.^{2}) and K_{nc} (ksi$\sqrt{in.}$) are based on the proportional-limit load and the effective-crack depth (a) determined from spring-constant-calibration curve
G_{Ic} (in.-lb/in.^{2}) and K_{Ic} (ksi$\sqrt{in.}$) are based on the proportional-limit load and the measured crack depth (a) using Bueckner's equation.

(2) Failure occurred within the proportional limit.

(3) Data were not recorded.

Approved for Public Release

TABLE 11

SLOW-NOTCH-BEND-TEST FOR HEAT 3888472

Effect of Heat Treatment and Specimen Orientation in Air Melted, 1/2-In.-Thick, Grade 250, 18% Nickel Maraging Steel

Specimen Number	Material Condition	Aging Cycle °F - hr	Specimen Orientation	.2% Offset Yield (ksi)	Width b (in.)	Depth d (in.)	Proportional Limit Load(L) (lb)	Proportional Limit Deflec.(e) (in.)	Maximum Load (2) Load(L) (lb)	Maximum Load (2) Deflec.(e) (in.)	eb/L (in.²/lb)x10⁻⁸	Notch+Crack Depth Effective a (in.)	Notch+Crack Depth Measured a (in.)	PLANE-STRAIN FRACTURE TOUGHNESS(1) G_{nc}	K_{nc}	G_{Ic}	K_{Ic}
CONDITION: AS-ROLLED																	
R75L	As Rolled	900 - 4	Longitudinal		.499	.750	(3)	(3)	2770	(3)	118	.194	(3)	41	34	(3)	(3)
R76L					.500	.750			2925		129	.230		55	40		
														Avg 48	Avg 37		
R82T	As Rolled	900 - 4	Transverse		.499	.750			3320		128	.226		68	44		
R83T					.500	.750			3050		141	.258		81	47		
R86T					.500	.750			3450		111	.165		45	36		
														Avg 65	Avg 43		
R77L	As Rolled	900 - 8	Longitudinal	--	.500	.751			3760		111	.155		50	38		
R81L					.500	.751			2130		160	.310		69	45		
														Avg 60	Avg 42		
R89T	As Rolled	900 - 8	Transverse	--	.499	.751			3360		114	.180		47	37		
R90T					.499	.751			4060		107	.145		56	41		
														Avg 52	Avg 39		
CONDITION: SOLUTION-TREATED 1500°F 30 MINUTES																	
R93L	Re-Solution Treated	900 - 4	Longitudinal	278	.498	.748			4550		121	.205		106	55		
R96L					.500	.750			2880		131	.234		56	40		
														Avg 81	Avg 46		
R102T	Re-Solution Treated	900 - 4	Transverse	274	.498	.750			3770		106	.135		46	37		
R103T					.499	.751			4000		104	.120		49	38		
R104T					.498	.750			3820		108	.150		51	38		
R105T					.499	.751			3180		144	.265		95	52		
R106T					.499	.750			3200		123	.212		56	40		
														Avg 60	Avg 43		
R98L	Re-Solution Treated	900 - 8	Longitudinal	279	.499	.751			3880		112	.168		58	41		
R99L					.499	.751			3840		109	.155		53	38		
R100L					.499	.751			3980		111	.165		60	42		
R101L					.499	.751			3240		119	.200		51	39		
														Avg 56	Avg 41		
R107T	Re-Solution Treated	900 - 8	Transverse	286	.499	.751			4390		107	.140		64	43		
R108T					.499	.751			3720		112	.170		54	40		
R109T					.499	.751			2690		142	.260		65	44		
R110T					.499	.751			3670		115	.185		58	41		
R111T					.499	.751			3510		113	.175		50	38		
														Avg 58	Avg 41		

(1) G_{nc} (in.-lb/in.²) and K_{nc} (ksi$\sqrt{in.}$) are based on the proportional-limit load and the effective-crack depth (a) determined from spring-constant-calibration curve
G_{Ic} (in.-lb/in.²) and K_{Ic} (ksi$\sqrt{in.}$) are based on the proportional-limit load and the measured crack depth (a) using Bueckner's equation.

(2) Failure occurred within the proportional limit.

(3) Data were not recorded.

Approved for Public Release

Approved for Public Release

TABLE 12 (SHEET 1 OF 2 SHEETS)

SLOW-NOTCH-BEND TEST FOR HEAT 07148

Effect of Heat Treatment and Specimen Orientation in Vacuum-Arc-Remelt, Grade 300, 18% Nickel Maraging Steel Plate and Bar Stock

Specimen Number	Material Condition	Aging Cycle °F - hr	Specimen Orientation	.2% Offset Yield (ksi)	Width b (in.)	Depth d (in.)	Proportional Limit Load(L) (lb)	Proportional Limit Deflec.(e) (in.)	Maximum Load (2) Load(L)	Maximum Load (2) Deflec.(e)	eb/L (in./lb)x 10^{-8}	Notch+Crack Depth Effective a (in.)	Notch+Crack Depth Measured a (in.)	PLANE-STRAIN FRACTURE TOUGHNESS(1) G_{nc}	K_{nc}	G_{Ic}	K_{Ic}
201	Mill-	850 - 8	Longitudinal	294	.499	.751	(3)	(3)	3950	(3)	107	.138	(3)	55	40	(3)	(3)
200	Annealed				.499	.751			3620		116	.183		59	42		
204					.499	.751			3890		111	.158		59	42		
													Avg	58	Avg 41		
210	Mill-	850 - 8	Transverse	---	.499	.750			4040		110	.153		62	43		
212	Annealed				.499	.751			4190		109	.147		65	44		
211					.499	.751			4620		105	.127		70	45		
213					.499	.751			3300		123	.215		59	42		
214					.499	.751			3620		118	.190		62	43		
													Avg	60	Avg 43		
195	Mill-	900 - 8	Longitudinal	300	.499	.749			3730		122	.212		75	47		
196	Annealed				.499	.750			3860		114	.172		63	43		
197					.499	.750			4610		109	.149		79	48		
198					.499	.751			3660		121	.206		69	45		
199					.499	.749			3980		120	.203		81	49		
													Avg	73	Avg 46		
205	Mill-	900 - 8	Transverse	302	.499	.749			3560		116	.183		57	40		
206	Annealed				.499	.750			3940		110	.154		59	42		
208					.499	.751			3490		115	.179		54	40		
209					.499	.750			3970		116	.183		71	46		
													Avg	60	Avg 42		
223	Re-Solution	850 - 8	Longitudinal	298	.499	.750			4585		108	.139		74	47		
220	Treated				.499	.750			3200		119	.198		51	39		
222					.499	.750			3720		110	.151		52	39		
224					.499	.750			4115		114	.170		71	46		
													Avg	62	Avg 42		
230	Re-Solution	850 - 8	Transverse	---	.499	.750			3825		117	.185		67	44		
232	Treated				.499	.750			4080		110	.153		63	43		
233					.499	.750			4270		118	.190		84	50		
234					.499	.750			3790		115	.177		63	43		
													Avg	69	Avg 45		

Plate

Calibration Constants: Q = 10.75×10^{-6}
R = -35.00×10^{-6}
S = 75.00×10^{-6}

(1) G_{nc} (in.-lb/in.^{2}) and K_{nc} (ksi$\sqrt{in.}$) are based on the proportional-limit load and the effective-crack depth (a) determined from spring-constant-calibration curve G_{Ic} (in.-lb/in.^{2}) and K_{Ic} (ksi$\sqrt{in.}$) are based on the proportional-limit load and the measured crack depth (a) using Bueckner's equation.

(2) Failure occurred within the proportional limit.

(3) Data were not recorded.

TABLE 12 (SHEET 2 of 2 SHEETS)

SLOW-NOTCH-BEND TEST FOR HEAT 07148

Effect of Heat Treatment and Specimen Orientation in Vacuum-Arc-Remelt, Grade 300, 18% Nickel Maraging Steel Plate and Bar Stock

Specimen Number	Material Condition	Aging Cycle °F - hr	Specimen Orientation	.2% Offset Yield (ksi)	Width b (in.)	Depth d (in.)	Proportional Limit Load(L) (lb)	Proportional Limit Deflec.(e) (in.)	Maximum Load (2) Load(L)	Maximum Load (2) Deflec.(e)	eb/L (in.²/lb)x10⁻⁸	Notch+Crack Depth Effective a (in.)	Notch+Crack Depth Measured a (in.)	PLANE-STRAIN FRACTURE TOUGHNESS(1) G_{nc}	K_{nc}	G_{Ic}	K_{Ic}
215	Re-Solution Treated	900 - 8	Longitudinal	302	.499	.750	(3)	(3)	4195	(3)	105	.125	(3)	57	41	(3)	(3)
217					.499	.750			3755		111	.156		55	40		
218					.499	.750			3760		111	.157		55	40		
219					.499	.750			3840		112	.158		58	41		
														Avg 56	Avg 41		
225	Re-Solution Treated	900 - 8	Transverse	299	.499	.750			3920		108	.143		55	40		
226					.499	.750			3900		109	.144		55	40		
227					.499	.750			4095		108	.141		60	42		
228					.499	.750			3945		111	.157		61	43		
229					.499	.750			3870		110	.151		56	41		
														Avg 57	Avg 41		
85	Re-Solution Treated	850 - 8	Longitudinal	---	.499	.751			3950		112	.160		62	43		
86					.499	.751			3600		120	.200		65	44		
87					.499	.751			3960		112	.160		62	43		
89					.499	.751			4460		107	.135		69	45		
														Avg 65	Avg 44		
95	Re-Solution Treated	850 - 8	Transverse	---	.498	.751			5010		103	.115		77	48		
96					.498	.751			3670		124	.220		77	48		
98					.499	.751			4460		106	.130		67	45		
99					.499	.751			4120		110	.150		64	43		
														Avg 71	Avg 46		
91	Re-Solution Treated	900 - 8	Longitudinal	309	.499	.750			4210		113	.167		73	46		
93					.499	.751			4600		109	.148		78	48		
94					.499	.751			4310		120	.201		94	53		
														Avg 82	Avg 49		
100	Re-Solution Treated	900 - 8	Transverse	308	.499	.751			4080		114	.174		71	46		
101					.499	.750			4300		110	.154		71	47		
102					.498	.750			3870		118	.193		72	46		
103					.499	.751			1670		109	.145		75	47		
														Avg 72	Avg 47		

Bar

Calibration Constants: $Q = 10.75 \times 10^{-6}$
$R = -35.00 \times 10^{-6}$
$S = 75.00 \times 10^{-6}$

(1) G_{nc} (in.-lb/in.²) and K_{nc} (ksi$\sqrt{\text{in.}}$) are based on the proportional-limit load and the effective-crack depth (a) determined from spring-constant-calibration curve
G_{Ic} (in.-lb/in.²) and K_{Ic} (ksi$\sqrt{\text{in.}}$) are based on the proportional-limit load and the measured crack depth (a) using Bueckner's equation.

(2) Failure occurred within the proportional limit.

(3) Data were not recorded.

Approved for Public Release

Contrails

TABLE 13

PRECRACK-CHARPY-IMPACT TEST (W/A) FOR HEAT 28889

Effect of Heat Treatment, Test Temperature and Specimen Orientation in Air Melted, Vacuum Degassed, ½-In.-Thick, Grade 200 18% Nickel Maraging Steel

Aging °F-hr	Test Temperature °F	W/A (in.-lb/in.^{2}) Longitudinal	W/A (in.-lb/in.^{2}) Transverse
900 - 4	-100	943-968 Avg 956	616-645 Avg 631
	RT	867-1025 Avg 946	640-661 Avg 650
	200	1070-1130 Avg 1100	673-730 Avg 701
	400	1328-1440 Avg 1384	600-820 Avg 710
900 - 8	-100	660-883 Avg 771	550-598 Avg 574
	RT	832-955 Avg 893	505-605 Avg 555
	200	897-1027 Avg 962	567-650 Avg 609
	400	1140-1230 Avg 1185	572-717 Avg 644

NOTE: This material was mill-annealed plate that was re-solution treated at 1500°F/ for 30 min.

Approved for Public Release

Contrails

TABLE 14

PRECRACK-CHARPY-IMPACT TEST (W/A) FOR HEAT 10675 PLATE

Effect of Heat Treatment, Test Temperature and Specimen Orientation in Air Melted, ½-In.-Thick, Grade 200, 18% Nickel Maraging Steel

Aging °F-hr	Test Temperature °F	W/A (in.-lb/in.^{2}) Longitudinal	W/A (in.-lb/in.^{2}) Transverse
	Mill Annealed		
900 - 4	-100	652-876 Avg 764	828-862 Avg 845
	RT	1346	963-1075 Avg 1019
	200	1415-1493 Avg 1454	1205-1343 Avg 1274
	400	1680-1768 Avg 1724	953-1711 Avg 1332
	Re-Solution Treated*		
900 - 4	-100	892-912 Avg 902	755-760 Avg 757
	RT	1100-1350 Avg 1225	1025-1095 Avg 1060
	200	1133-1450 Avg 1291	1030-1300 Avg 1165
	400	1430-1510 Avg 1470	1160-1163 Avg 1162
900 - 8	-100	478-782 Avg 634	691-715 Avg 703
	RT	935-1070 Avg 1002	830
	200	1228-1320 Avg 1274	890-927 Avg 909
	400	1310	1210

*The material was mill-annealed plate-re-solution treated at 1500°F for 30 min.

Approved for Public Release

Contrails

TABLE 15

PRECRACK-CHARPY-IMPACT TEST (W/A) FOR HEAT 10675 BAR STOCK

Effect of Heat Treatment, Test Temperature and Specimen Orientation in Air Melted, ½-In.-Thick, Grade 200, 18% Nickel Maraging Steel, 4 x 4-In. Bar Stock[1]

Aging °F-hr	Test Temperature °F	W/A (in.-lb/in.^{2}) Longitudinal	W/A (in.-lb/in.^{2}) Transverse
900 - 4	-100	664-963 Avg 814	578[2] - 592
	RT	941[2][4]-1390[2]	848-1100 Avg 974[2]
	200	1054[3]-1208	808-826 Avg 817
	400	1493-1650 Avg 1576	978-1032 Avg 1005[2]
900 - 8	-100	628-663 Avg 645	512-551[2]
	RT	890[4] - 1120	737-825[2] Avg 781
	200	993[4] -1368	630-860[2] Avg 745
	400	1082-1105 Avg 1093	592[3]-855[2]

(1)This material was mill-annealed, cut into specimen blanks, and re-solution treated at 1500°F for 30 min.
(2)Notch parallel to the length of the billet.
(3)Deep fatigue crack
(4)Defect detected in the fracture surfaces by etching.

Approved for Public Release

Contrails

TABLE 16

PRECRACK-CHARPY-IMPACT TEST (W/A) FOR HEAT 13371

Effect of Heat Treatment, Test Temperature and Specimen Orientation in Air Melted ½-In.-Thick, Grade 250, 18% Nickel Maraging Steel

Aging °F-hr	Test Temperature °F	W/A (in.-lb/in.^{2}) Longitudinal	W/A (in.-lb/in.^{2}) Transverse
	As-Rolled		
900 - 8	-100	781-908 Avg 844(1)(2)	177-313(1)
	RT	440-441 Avg 440	436-531 Avg 483(1)
	200	485-494 Avg 489	271-478(1)
	400	2130-4510 Avg 3320(1)(2)	320-576(1)
	Solution-Treated (1500°F-30 min.)		
900 - 4	-100	410-414 Avg 412	273-287 Avg 280
	RT	1500-2280 Avg 1890(3)	336-1234(3)
	200	597-600 Avg 598	357-922(3)
	400	707-3120(3)	412-428 Avg 420
900 - 8	-100	1025-1374 Avg 1199(3)	266-1115(3)
	RT		346-1800(3)
	200	3700(3)	329-364 Avg 346
	400	571-641 Avg 606	370-393 Avg 381

(1) Notch was oriented parallel to the length of the billet.

(2) Specimens split in the fracture face (lamination-like defect).

(3) Notch was oriented parallel to the plate surface.

Approved for Public Release

Contrails

TABLE 17

PRECRACK-CHARPY-IMPACT TEST (W/A) FOR HEAT 120D163

Effect of Test Temperature and Specimen Orientation in Air Melted, Vacuum Degassed, $\frac{1}{2}$-In.-Thick, Grade 250, 18% Nickel Maraging Steel[1]

Aging °F-hr	Test Temperature °F	W/A (in.-lb/in.^{2}) Longitudinal	W/A (in.-lb/in.^{2}) Transverse
900-4	-100	87-95 Avg 90[2]	83-145 Avg 123
	0	293-321 Avg 303	213-271 Avg 238
	RT	329-392 Avg 366	342-364 Avg 353
	200	450-472 Avg 460	394-408 Avg 401
	400	563-605 Avg 584	501-524 Avg 514

(1) Material was as-rolled plate solution-treated at 1500°F for 30 min and aged at 900°F for 4 hr.

(2) Average values are for three tests

Approved for Public Release

Contrails

TABLE 18

PRECRACK-CHARPY-IMPACT TEST (W/A) FOR HEAT 3888472 PLATE

Effect of Heat Treatment, Test Temperature, and Specimen Orientation in Vacuum-Arc-Remelt ½-In.-Thick, Grade 250, 18% Nickel Maraging Steel

Aging °F-hr	Test Temperature °F	W/A (in.-lb/in.^{2}) Longitudinal	W/A (in.-lb/in.^{2}) Transverse
As Rolled			
900 - 8	-100	87	106(1)
	RT	108(1)	137(1)
	200	114-114 Avg 114	160(1)-169
	400	164-172 Avg 168	169
Solution Treated(2)			
850 - 8	-100	90	96
	RT	125-143 Avg 134	125-135(1)
	200	146-146 Avg 146	138
	400	247-323 Avg 285	200-210 Avg 205
900 - 8	-100	111-111(1)	113-122 Avg 117
	RT	136-147 Avg 141	136-143(1)
	200	150-151 Avg 150	145-158 Avg 151
	400	204-220 Avg 212	194-223(1)

(1) These specimens were notched in the as-rolled plate surface.

(2) The as-rolled plate solution was treated at 1500°F for 30 min.

Approved for Public Release

Contrails

TABLE 19

PRECRACK-CHARPY-IMPACT TEST (W/A) FOR HEAT 3888473

Effect of Heat Treatment, Test Temperature, and Specimen Orientation in Vacuum-Arc-Remelt, ½-In.-Thick, Grade 250, 18% Nickel Maraging Steel

Aging °F-hr	Test Temperature °F	W/A (in.-lb/in.) Longitudinal	W/A (in.-lb/in.) Transverse
As-Rolled			
900-8	-100	103-108 Avg 106	155(1)
	RT	160-220(1) Avg 190(1)	136-162(1)
	200	140-204 Avg 172	156-169 Avg 162
	400	238(1)	133-137 Avg 135
Solution Treated(2)			
900-8	-100	109-147 Avg 128	151-172 Avg 161(1)
	RT	214-217(1) Avg 216(1)	204-212(1) Avg 208(1)
	200	185-246(1)	151-210(1)
	400	264-360(1)	247-267 Avg 257
850-8	-100	106-130(1)	122-133(1) Avg 128(1)
	RT	151-175 Avg 163	134-141 Avg 137
	200	175-183 Avg 179	151-232(1)
	400	246-299(1)	193-293(1)

(1) These specimens were notched in the as-rolled plate surface.

(2) Material was as-rolled plate solution treated at 1500°F for 30 min.

Approved for Public Release

Contrails

TABLE 20

PRECRACK-CHARPY-IMPACT TEST (W/A) FOR HEAT 07148 PLATE

Effect of Heat Treatment, Test Temperature, and Specimen Orientation in Vacuum-Arc-Remelt, ½-In.-Thick, Grade 300 18% Nickel Maraging Steel

Aging °F-hr	Test Temperature °F	W/A (in.-lb/in.^{2}) Longitudinal	W/A (in.-lb/in.^{2}) Transverse
Mill Annealed			
900-8	-100	88-92 Avg 90	82-87 Avg 84
	RT	112	130-136(1) Avg 133(1)
	200	146-163(1) Avg 154(1)	124
	400	198-212 Avg 205	208-210(1) Avg 209(1)
Re-Solution Treated(2)			
900-8	-100	96-97(1) Avg 96(1)	95-110(1) Avg 102(1)
	RT	131-141 Avg 136	105-149(1)
	200	169(1)	166-173(1) Avg 169(1)
	400	225-238(1) Avg 231(1)	180-237(1)
850-8	-100	70-85(1)	73-77 Avg 75
	RT	101-130(1)	96-107(1)
	200	150-156(1) Avg 153(1)	157(1)
	400	208-333(1)	219-233(1) Avg 226(1)

(1)These Specimens were notched in the plate surface; all other specimens were notched perpendicular to surface.

(2)Material was Mill-annealed plate re-solution treated at 1500°F for 30 min.

Approved for Public Release

Contrails

TABLE 21

PRECRACK-CHARPY-IMPACT TEST (W/A) FOR HEAT 07148 BAR STOCK

Effect of Heat Treatment, Test Temperature and Specimen Orientation in Vacuum-Arc-Remelt, Grade 300, 18% Nickel Maraging Steel 4 x 4-In. Bar Stock[1]

Aging °F-hr	Test Temperature °F	W/A (in.-lb/in.^{2}) Longitudinal	W/A (in.-lb/in.^{2}) Transverse[2]
850-8	-100	75-82 Avg 78	78-81 Avg (2)79
	RT	102-107 Avg 105	109-115 Avg (2)112
	200	169-183 Avg (2)176	138
	400	270-274 Avg (2)272	179-313
900-8	-100	81-89 Avg (2)85	81-85 Avg (2)83
	RT	123-131 Avg 127	124-129 Avg (2)126
	200	167-170 Avg 168	141-151
	400	223	

(1) Material was a mill-annealed billet cut into specimen blanks and re-solution treated at 1500°F for 30 min.

(2) Specimens were notched parallel to billet axis.

Approved for Public Release

TABLE 22

FILLER WIRE COMPOSITIONS

Weld Wire Heat	Chemical-Analysis Source	Composition, Wt %									
		C	Mn	P	S	Si	Ni	Al	Ti	Mo	Co
7C-091	Mill-Certified	0.03	0.002	0.004	0.006	0.012	18.02	0.015	1.64	4.17	8.02
	Aerojet Analysis	0.035	---	0.005	0.005	0.020	18.5	0.13	1.65	4.0	8.3
7C-092	Mill-Certified	0.027	0.003	0.003	0.008	0.047	18.05	0.016	0.71	5.30	7.03
	Aerojet Analysis	0.032	---	0.006	0.006	0.024	18.3	0.10	0.95	5.1	6.84
7C-094	Mill-Certified	0.024	0.002	0.004	0.007	0.009	17.68	0.017	0.91	4.24	9.93
	Aerojet Analysis	0.032	---	0.004	0.003	0.017	18.4	0.11	1.22	4.6	9.86
7C-093	Mill-Certified	0.030	0.003	0.004	0.006	0.012	18.10	0.016	0.65	4.17	8.07
	Aerojet Analysis	0.033	---	0.004	0.004	0.011	18.5	0.07	0.67	4.7	8.08
7C-090	Mill-Certified	0.022	0.002	0.004	0.007	0.014	18.01	0.016	0.71	4.22	11.90
	Aerojet Analysis	0.035	---	0.006	0.005	0.017	18.1	0.13	0.83	4.0	12.1
34312	Mill-Certified	0.020	0.01	0.005	0.009	0.010	17.90	0.19	0.50	4.45	8.0
	Aerojet Analysis	0.02	---	0.004	0.004	0.017	18.0	0.14	0.59	4.5	7.90
IW450	Mill-Certified	0.003	0.01	0.002	---	---	18.75	---	0.44	4.26	8.16
	Aerojet Analysis	0.003	---	0.04	0.005	0.04	18.37	0.02	0.42	4.40	8.30

Approved for Public Release

Contrails

TABLE 23

COBALT, MOLYBDENUM AND TITANIUM CONTENT OF TIG WELD METAL OBTAINED IN WELDING GRADE 250, 1/2-IN.-THICK, 18% NICKEL MARAGING STEEL PLATE, HEAT 120D163, WITH VARIOUS FILLER WIRES

Weld Wire Heat	Material	Alloy Content, wt %		
		Co	Mo	Ti
7C-092	Wire	6.8	5.1	0.95
	Weld Metal	7.8	4.9	0.80
7C-091	Wire	8.3	4.0	1.65
	Weld Metal	7.2	4.5	.94
7C-094	Wire	9.9	4.6	1.22
	Weld Metal	8.8	4.3	.81
7C-093	Wire	8.0	4.7	0.67
	Weld Metal	8.2	4.6	0.64
7C-090	Wire	12.1	4.0	0.83
	Weld Metal	9.1	4.2	0.65
34312	Wire	7.9	4.5	0.59
	Weld Metal	7.8	4.5	0.57
IW450	Wire	8.3	4.4	0.42
	Weld Metal	8.3	4.3	0.41
--	Base Metal	8.0	4.9	0.48

Approved for Public Release

Contrails

TABLE 24

EFFECTS OF FILLER WIRE COMPOSITION ON THE TRANSVERSE TENSILE PROPERTIES OF TIG-WELDED JOINTS IN GRADE 250, 1/2-IN.-THICK, 18% NICKEL MARAGING STEEL PLATE, HEAT 120D163, AGED 900°F FOR 4 HOURS AFTER WELDING

Weld Wire Heat No.	Calculated[1] Weld Metal Yield Strength ksi	0.2% Offset Yield Strength ksi	Ultimate Tensile Strength ksi	Elongation in 1-in,%	RA %	Fracture[2] Location
7C-092	288	242.0	249.0	5.0	21.0	HAZ
		241.0	252.0	5.6	25.7	HAZ
		240.0	251.0	6.4	36.5	Weld
		239.0	250.0	5.6	23.0	HAZ
	Avg	241.0	250.5	5.6	26.5	
7C-091	286	244.0	254.0	7.5	36.2	Weld
		243.0	254.0	6.5	40.0	HAZ
		244.0	258.0	8.0	43.0	HAZ
		244.0	256.0	6.7	32.5	HAZ
	Avg	244.0	255.5	7.2	37.9	
7C-094	283	243.0	252.0	2.6	4.5	HAZ
		244.0	255.0	6.6	28.0	Weld
		246.0	251.0	1.6	7.5	Weld
		246.0	257.0	1.5	9.5	HAZ
	Avg	244.8	252.8	3.9	12.3	
7C-093	270	240.0	246.0	8.2	38.2	Weld
		239.0	246.0	3.9	25.0	HAZ
		239.0	248.0	6.2	31.5	Weld
	Avg	240.0	247.0	6.1	31.6	
7C-090	270	246.0	258.0	6.0	34.5	HAZ
		246.0	258.0	5.7	26.0	Weld
		248.0	258.0	2.0	8.0	HAZ
		244.0	257.0	4.8	31.7	HAZ
	Avg	246.0	258.0	4.7	25.0	
34312	258	232.0	234.0	7.1	39.5	Weld
		230.0	232.0	9.0	46.0	Weld
		234.0	238.0	7.7	44.2	Weld
		236.0	242.0	9.2	46.5	Weld
	Avg	233.0	236.0	8.2	44.0	
IW-450	244	225	235	9.7	47.0	Weld
		231	240	10.7	44.0	Weld
		—	243	9.9	46.0	Weld
		235	243	10.0	46.0	Weld
	Avg.	230.0	240.0	10.1	46.0	
Base Metal (Longitudinal)		242.9	257.5	9.9	47.8	
		245.4	257.0	8.6	42.6	
		244.4	259.5	9.4	36.5	
	Avg	244.2	258.0	9.3	42.3	
(Transverse)		256.0	268.5	8.1	36.5	
		256.1	268.8	7.2	40.3	
		254.5	270.2	8.3	41.4	
	Avg	255.3	269.2	7.9	39.4	

(1) Chemical Analyses in Tables 22 and 23 ; YS = 38.1 + 22.6 (% Mo) + 8.8 (% Co) + 87.7 (% Ti)

(2) HAZ-Heat-Affected Zone, Weld,-weld Metal.

Approved for Public Release

Contrails

TABLE 25

EFFECTS OF FILLER WIRE COMPOSITION ON THE NOTCHED (K_t 10) TENSILE STRENGTH OF WELD METALS IN GRADE 250, 1/2-IN.-THICK, 18% NICKEL MARAGING STEEL PLATE, HEAT 120D163, AGED 900°F FOR 4 HOURS AFTER WELDING

Weld Wire Heat	Notched Tensile Strength ksi	Ultimate[1] Tensile Strength ksi	Unnotched Ratio
7C-092	268 202 286 226 Avg 245	250.5[2]	0.98
7C-091	218 175 182 166 Avg 185	255.5[2]	0.84
7C-094	230 246 227 222 Avg 231	252.8[3]	0.91
7C-093	340 308 260 284 Avg 298	247.0[4]	1.2
7C-090	169 190 254 304 Avg 229	258.0[2]	0.89
34312	338 322 346 328 Avg 333	236.0[5]	1.4
IW450	385 385 365 385 Avg 380	240[5]	1.6
Base Metal	275 365 342 Avg 360.8	258	1.4

(1) Average value from Table 24
(2) One weld metal failure, three heat-affected zone failures
(3) Two weld metal failures, two heat affected zone failures
(4) Three weld metal failures, one heat affected zone failure
(5) All weld metal failures

Approved for Public Release

Contrails

TABLE 26

LONGITUDINAL TENSILE PROPERTIES OF WELD METALS DEPOSITED WITH THE TIG PROCESS IN GRADE 250, 1/2-IN.-THICK, 18% NICKEL MARAGING STEEL PLATE, HEAT 120D163, AFTER AGING AT 900°F FOR 4 HOURS AFTER WELDING

Weld Wire Heat No.	Potential Yield Strength ksi	0.2% Offset Yield Strength ksi	Ultimate Tensile Strength ksi	Elongation in 1 inch %	RA %
7C-093	270	228	248	9.5	40
		220	241	6.0	14
		222	244	8.6	34
		236	252	6.7	34
		232	250	7.7	40
		234	250	7.6	31
	Avg	229	248	7.7	32
IW-450	244	225	240	10.8	46
		217	232	11.0	44
		226	234	10.4	45
	Avg	222	235	10.7	45

Approved for Public Release

Contrails

TABLE 27

LONGITUDINAL TENSILE PROPERTIES OF WELD METALS DEPOSITED WITH THE TIG PROCESS IN GRADE 200, 1/2-IN.-THICK, 18% NICKEL MARAGING STEEL PLATE, HEAT 10675, AFTER AGING AT 900°F FOR 4 AND 8 HOURS AFTER WELDING

Weld Wire Heat No.	Aging Cycle	0.2% Offset Yield Strength ksi	Ultimate Tensile Strength ksi	Elongation in 1 inch %	RA %
IW-450	900/4 hr	210	222	11.8	59.8
		214	225	12.7	56.4
		213	228	11.7	58.0
		Avg 212	225	12.1	58.1
IW-450	900/8 hr	224	238	10.8	55.4
		222	233	11.7	55.1
		222	233	11.8	57.0
		Avg 223	235	11.4	55.8
Base Metal*					
Longitudinal	900°F/4 hr	218	226	11.0	57.2
Transverse	900°F/4 hr	214	228	10.3	52.3
Longitudinal	900°F/8 hr	226	235	10.7	50.9
Transverse	900°F/8 hr	228	237	11.2	52.8

* As received, average values were obtained from Table 4

Approved for Public Release

Contrails

TABLE 28

COBALT, MOLYBDENUM AND TITANIUM CONTENT OF MIG AND TIG WELD METALS OBTAINED IN WELDING GRADE 250, 1/2-IN.-THICK, 18% NICKEL MARAGING STEEL PLATE, HEAT 120D163 WITH VARIOUS FILLER WIRES

Weld Wire Heat	Material	Alloy Content, Wt %		
		Co	Mo	Ti
	MIG Welded Joints			
7C-094	Wire	9.9	4.6	1.22
	Weld Metal	8.7	4.4	0.60
7C-09	Wire	8.0	4.7	0.67
	Weld Metal	8.0	4.3	0.63
	TIG Welded Joints			
7C-094	Weld Metal	8.8	4.3	0.81
7C-093	Weld Metal	8.2	4.6	0.64
	Base Metal	8.0	4.9	0.48

Approved for Public Release

Contrails

TABLE 29

TRANSVERSE TENSILE PROPERTIES OF MIG AND TIG WELDED JOINTS IN GRADE 250, 1/2-IN.-THICK, 18% NICKEL MARAGING STEEL PLATE, HEAT 120D163, AGED AT 900°F FOR 4 HOURS AFTER WELDING

Weld Wire		Yield Strength 0.2% Offset ksi	Ultimate Tensile Strength ksi	Elongation in 1-in.	RA %	Failure Location
	MIG Welded Joints					
7C-094		251.5	266.2	5.1	17.5	Weld
		259.1	267.7	4.8	27.2	Weld
		252.5	268.2	7.2	30.1	Weld
		252.5	265.8	5.3	29.2	Weld
	Avg	253.9	267.0	5.6	26.0	
7C-093		241.4	250.5	4.1	24.6	Weld
		243.4	249.5	2.8	17.5	Weld
		239.4	247.0	4.5	30.1	Weld
		238.4	248.5	2.2	19.5	Weld
		242.4	251.5	5.5	37.7	Weld
	Avg	241.0	249.4	3.8	25.5	
	TIG Welded Joints					
7C-094	Avg	244.8*	252.8*	3.9*	12.3*	Weld, HAZ*
7C-093	Avg	240.0*	247.0*	6.1*	31.6*	Weld, HAZ*

* These data were obtained from Table 24

Approved for Public Release

Contrails

TABLE 30

COBALT, MOLYBDENUM, SILICON, AND TITANIUM CONTENTS OF SUBMERGED-ARC AND TIG WELD METALS OBTAINED IN WELDING GRADE 250, 1/2-IN.-THICK, 18% NICKEL MARAGING STEEL PLATE WITH 7C-090 FILLER WIRE

Weld Type	Material	Joint Design *	Alloy Content, wt %			
			Co	Mo	Si	Ti
--	Wire	--	12.1	4.0	0.017	0.83
Submerged Arc	Weld Metal	A	10.1	4.4	0.11	0.38
Submerged Arc	Weld Metal	B	10.8	4.4	0.07	0.40
Submerged Arc	Weld Metal	C	10.3	4.4	0.06	0.33
TIG	Weld Metal	D	9.1	4.2	--	0.65

* For specific designs,

A - See Figure 45
B - See Figure 46
C - See Figure 47
D - See Figure 42

Approved for Public Release

TABLE 31

TENSILE PROPERTIES OF SUBMERGED-ARC AND TIG WELDED JOINTS IN GRADE 250, 1/2-IN.-THICK, 18% NICKEL MARAGING STEEL PLATE AGED AT 900° F FOR 4 HOURS AFTER WELDING

Weld Wire Heat	Orientation	Joint[1] Design	0.2% Offset Yield Strength ksi	Ultimate Tensile Strength, ksi	Elongation in 1-In. %	Reduction of Area, %	Location[2] of Failure
			Submerged-Arc Welded Joints				
7C-090	Longitudinal	A	239	251	5.7	21	---
			244	255	7.0	35.4	---
			Avg 232	253	6.4	28.2	
7C-090	Longitudinal	B	243	257	8.8	40.2	---
7C-090	Longitudinal	C	229	241	6.5	32.7	---
			244	257	6.5	26.1	---
			Avg 237	249	6.5	29.4	
7C-090	Transverse	A	248	260	2.6	10.1	WM
			247	259	5.0	24.6	WM
			Avg 248	260	3.8	17.4	
7C-090	Transverse	B	249	260	3.0	12.3	WM
			241	252	5.7	28.7	WM
			Avg 245	256	4.4	20.5	
7C-090	Transverse	C	247	262	3.8	11.7	WM
			248	262	2.5	4.7	WM
			Avg 248	262	3.2	7.7	
			TIG Welded Joints[3]				
7C-090	Transverse	D	246	258	4.7	25	WM, HAZ

(1) For specific designs, A - See Figure 45
B - See Figure 46
C - See Figure 47
D - See Figure 42

(2) WM - Weld Metal
HAZ - Heat-Affected-Zone

(3) Data taken from Table 24

Approved for Public Release

Contrails

TABLE 32

EFFECTS OF AGING TIME AND TEMPERATURE ON THE TENSILE PROPERTIES OF TIG WELD METAL DEPOSITED IN GRADE 250, 1/2-IN.-THICK, 18% NICKEL MARAGING STEEL PLATE, HEAT 120D163, WITH 7C-093 FILLER WIRE

Aging Cycle		0.2% Offset Yield Strength ksi	Ultimate Tensile Strength ksi	Elongation in 1-in. %	Reduction of Area %	Fracture Location
850/4 hr		230	234	6.9	41.5	Weld
		224	235	6.9	41.0	Weld
		224	232	9.9	47.6	Weld
	Avg	226	234	7.9	43.4	
850/8 hr		240	245	6.0	40.4	Weld
		240	246	8.4	40.4	Weld
	Avg	240	246	7.2	43.1	
850/16 hr		245	251	6.0	39.6	Weld
		248	256	7.1	45.0	Weld
		253	256	6.6	34.5	Weld
	Avg	249	254	6.6	39.7	
900/2 hr		242	247	7.8	41.9	Weld
		242	248	9.0	47.2	Weld
		238	244	9.2	49.4	Weld
		242	250	8.0	42.6	Weld
	Avg	241	247	8.5	42.7	
900/4 hr		234	250	8.8	45.4	Weld
		244	250	8.2	49.0	Weld
	Avg	239	250	8.5	47.2	
900/8 hr		240	250	8.2	44.8	Weld
		242	250	7.7	42.5	Weld
		244	252	7.3	41.0	Weld
		244	253	7.6	43.0	Weld
	Avg	243	251	7.7	42.9	
900/16 hr		240	249	6.9	43.8	Weld
		234	252	8.0	43.8	Weld
		240	252	8.0	42.0	Weld
		243	254	7.9	45.8	Weld
	Avg	239	252	7.6	43.8	
950/2 hr		238	246	7.4	45.4	Weld
		241	248	8.4	45.0	Weld
		240	250	8.2	38.9	Weld
		239	249	8.4	47.5	Weld
	Avg	240	248	8.0	44.5	
950/4 hr		222	237	8.2	32.4	Weld
		236	245	6.4	40.5	Weld
	Avg	229	241	7.3	36.5	
950/8 hr		240	246	7.6	36.2	Weld
		236	246	7.0	44.8	Weld
		227	240	7.5	41.0	Weld*
		224	248	8.7	43.8	Weld
	Avg	232	245	7.7	41.2	
950/16 hr		232	242	5.4	34.4	Weld
		228	242	7.9	40.1	Weld
		229	241	7.3	45.6	Weld
	Avg	230	242	6.9	40.0	

Approved for Public Release

Approved for Public Release

TABLE 35

COMPOSITION OF 18% NICKEL MARAGING STEEL, HEAT 24158

		Composition, %											
		C	M	P	S	Si	Ni	Co	Mo	Ti	Al	Zr	B
Grade 200, Nominal		.03 max	.10 max	.01 max	.01 max	-	17.00 19.00	8.00 9.00	3.00 3.50	0.15 0.25	0.05 0.15	0.02	0.003
Specified Analysis		.03 max	.10 max	.025 max	.01 max	0.10 max	17.5 18.5	7.50 8.50	4.00 4.50	0.05 0.25	0.05 0.15	-	-
Heat 24158	Mill Analysis, Slab	.019	0.02	0.001	0.008	0.01	18.29	8.54	3.22	0.16	0.12	0.004	0.004
	Mill Analysis, Plate	.010	0.052	0.001	0.010	0.069	18.20	8.50	3.15	0.17	0.062	-	-
	Check Analysis, 1 x 4 Forging	.013	0.020	0.007	0.012	0.11	17.85	8.33	3.30	0.19	0.08	-	-
	Check Analysis, 4 x 4 Forging	.013	0.03	0.008	0.012	0.13	17.71	8.50	3.30	0.18	0.08	-	-

TABLE 36

AVERAGE TENSILE PROPERTIES OF 18% NICKEL MARAGING STEEL, HEAT 24158

	Aging Condition		Longitudinal Direction				Transverse Direction			
Product	Temperature, °F	Time Hrs	Yield Strength 0.2% Offset Ksi	Tensile Strength, Ksi	Elongation in 1 in., %	RA %	Yield Strength 0.2% Offset, Ksi	Tensile Strength, Ksi	Elongation in 1 in., %	RA %
3/4 In. Plate	850	4	184.3	192.4	12.2	68.3	-	-	-	-
		8	197.5	204.1	10.8	59.9	196.1	205.1	9.9	55.4
		16	200.9	208.9	10.7	60.2	-	-	-	-
	900	2	188.2	198.2	11.2	61.3	-	-	-	-
		4	194.2	203.0	11.1	59.3	195.4	204.4	10.2	52.7
		8	196.8	207.1	11.4	59.2	199.5	208.2	10.3	52.2
		16	197.6	206.6	11.3	59.5	-	-	-	-
	950	2	191.8	201.6	10.9	58.5	-	-	-	-
		4	190.5	200.9	12.4	59.6	-	-	-	-
		8	193.4	203.7	11.4	57.8	196.0	205.1	10.1	53.6
		16	197.2	205.4	11.9	56.7	-	-	-	-
1 x 4 Forging	850	8	187.5	197.6	11.2	54.5	189.4	201.1	10.5	51.1
	900	8	203.6	207.9	9.5	45.9	202.5	213.0	9.6	49.7
	950	8	197.1	202.1	11.6	46.2	199.3	208.0	10.8	46.3
4 x 4 Forging	850	8	182.5	194.0	10.7	47.5	184.6* 182.0	195.7 195.3	10.4 7.7	50.5 33.1
	900	8	199.3	209.4	9.4	47.8	197.5 198.8	208.4 210.0	9.0 6.9	41.0 31.4
	950	8	191.5	203.3	12.1	51.2	192.0 193.5	201.2 206.7	7.2 9.6	29.5 34.7

*Upper values indicate short transverse direction and lower values pertain to transverse direction.

Approved for Public Release

Contrails

TABLE 37

PRECRACK-CHARPY-IMPACT TEST (W/A) FOR OPTIMUM HEAT 24158

Effect of Heat Treatment, Specimen Orientation, and Test Temperature on Toughness in a 4 x 4-In. Mandrel-Forged Section of Grade 200, Vacuum-Arc-Remelt, 18% Nickel Maraging Steel*

Aging °F-hr	Test Temperature °F	W/A (in.-lb/in.^{2}) Longitudinal	Transverse	Short Transverse
850 - 8	-100	692-721 Avg 707	408-418 Avg 413	510-517 Avg 513
	RT	1016-1031 Avg 1024	590-722 Avg 656	685-778 Avg 731
	200	1144-1470 Avg 1307	644-656 Avg 650	817-932 Avg 874
	400	1282-1331 Avg 1306	810-829 Avg 819	909-1063 Avg 986
900 - 8	-100	708-718 Avg 713	359-370 Avg 364	430-448 Avg 439
	RT	848-904 Avg 876	496-505 Avg 500	607-654 Avg 630
	200	1284-1417 Avg 1350	510-564 Avg 537	619-669 Avg 644
	400	1114-1149 Avg 1136	557-604 Avg 580	668-688 Avg 678
950 - 8	-100	851-918 Avg 884	419-420 Avg 420	506-515 Avg 510
	RT	1062-1210 Avg 1136	568-581 Avg 574	698-741 Avg 719
	200	1434-1562 Avg 1498	587-630 Avg 609	769-814 Avg 791
	400	1383-1419 Avg 1401	650-662 Avg 656	921-991 Avg 956

*The mandrel-forged section was mill-annealed at 1500°F for 4 hr.

Approved for Public Release

Contrails

TABLE 38

PRECRACK-CHARPY-IMPACT TEST (W/A) FOR OPTIMUM HEAT 24158

Effect of Heat Treatment, Specimen Orientation, and Test Temperature on Toughness in a 1 x 4-In. Mandrel-Forged Section of Grade 200, Vacuum-Arc-Remelt, 18% Nickel Maraging Steel*

Aging °F-hr	Test Temperature °F	W/A (in.-lb/in.^{2}) Longitudinal	W/A (in.-lb/in.^{2}) Transverse
850 - 8	-100	562-692 Avg 627	
	RT	876-1054 Avg 965	880-885 Avg 882
	200	996-1093 Avg 1044	
	400	1037-1064 Avg 1050	1019-1140 Avg 1079
900 - 8	-100	645-707 Avg 676	
	RT	959-985 Avg 972	
	200	975-1354 Avg 1164	
	400	1105-1431 Avg 1268	
950 - 8	-100	624-814 Avg 759	
	RT	952-1183 Avg 1068	
	200	1120-1185 Avg 1152	
	400	1149-1289 Avg 1219	

*This material was mill-annealed at 1500°F for 2 hr.

Approved for Public Release

Contrails

TABLE 39

PRECRACK-CHARPY-IMPACT TEST (W/A) FOR OPTIMUM HEAT 24158

Effect of Heat Treatment, Specimen Orientation, and Test Temperature on Toughness in 3/4-In.-Thick Plate of Grade 200, Vacuum-Arc-Remelt, 18% Nickel Maraging Steel (1)

Aging °F-hr	Test Temperature °F	W/A (in.-lb/in.^{2})(2) Longitudinal	Transverse
850 - 8	-100	1138-1296 Avg 1218	625-801 Avg 696
	RT	1374-1764 Avg 1566	974-1458 Avg 1134
	200	1802-2028 Avg 1916	1000-1135 Avg 1077
	400	1672-2632 Avg 2017	1266-1300 Avg 1278
900 - 8	-100	798-1063 Avg 910	527-642 Avg 611
	RT	1058-1521 Avg 1273	833-946 Avg 888
	200	1262-1699 Avg 1499	768-1021 Avg 907
	400	951-2003 Avg 1509	996-1158 Avg 1102
950 - 8	-100	1070-1291 Avg 1172	710-811 Avg 749
	RT	1484-1651 Avg 1605	971-1039 Avg 1008
	200	1980-2177 Avg 2094	1031-1266 Avg 1143
	400	1873-2457 Avg 2307	1314-1376 Avg 1346

(1) This material was re-solution treated at 1500°F for 1 hr.

(2) All data are the averages of 3-4 replicate tests.

Approved for Public Release

Contrails

TABLE 40

PRECRACK-CHARPY-IMPACT TEST (W/A) FOR OPTIMUM HEAT 24158

Effect of Heat Treatment, Specimen Orientation, and Test Temperature on Toughness in a 1 x 4-In. Mandrel-Forged Section of Grade 200, Vacuum-Arc-Remelt, 18% Nickel Maraging Steel, 0.75 x 0.394 x 2.1-In. Specimen*

Aging °F-hr	Test Temperature °F	W/A (in.-lb/in.^{2}) Longitudinal	W/A (in.-lb/in.^{2}) Transverse
850 - 8	-100	868	649-685 Avg (2) 667
	RT	1117-1324 Avg (10) 1228	820
	200	1229-1616 Avg (2) 1422	709-938 Avg (2) 823
	400	1311-1790 Avg (2) 1550	779-802 Avg (2) 790
900 - 8	-100	965-1085 Avg (2) 1025	617-640 Avg (2) 628
	RT	1044-1494 Avg (7) 1214	738-849 Avg (6) 800
	200	1436- Avg (2) 1584	743- Avg (2) 854
	400	1266-1443 Avg (2) 1354	678-766 Avg (2) 722
950 - 8	-100		648-743 Avg (2) 695
	RT	1315	713-948 Avg (11) 831
	200		910-912 Avg (2) 911
	400	2199-2510 Avg (2) 2354	871-883 Avg (2) 877

*This material was mill-annealed at 1500°F for 2 hr.

Approved for Public Release

TABLE 41

SLOW-NOTCH-BEND TEST FOR HEAT 24158 MANDREL FORGING

Effect of Heat Treatment and Specimen Orientation in Vacuum-Arc-Remelt, Grade 200, 18% Nickel Maraging Steel, 4 x 4-In. Mandrel Forging

Specimen Number	Material Condition	Aging Cycle °F - hr		Specimen Orientation	.2% Offset Yield (ksi)	Width b (in.)	Depth d (in.)	Proportional Limit Load(L) (lb)	Proportional Limit Deflec.(e) (in.)	Maximum Load Load(L) (lb)	Maximum Load Deflec.(e) (in.)	eb/L (in.²/lb)x10⁻⁸	Notch+Crack Depth Effective a (in.)	Notch+Crack Depth Measured a (in.)	PLANE-STRAIN FRACTURE TOUGHNESS* G_{nc}	K_{nc}	G_{Ic}	K_{Ic}
A592	Re-Solution	850	8	Longitudinal	182.5	.478	.744	5000	.016758	6035	.0229	160.2	.262	.273	320		328	
A593	Treated					.497	.744	5900	.017670	7685	.0240	148.8	.241	.241	314		329	
A594						.497	.744	5010	.017480	7505	.0228	173.5	.282	.232	387		221	
A596						.498	.744	6410	.018012	7860	.0228	139.9	.220	.230	286		354	
														Avg	327	Avg 99	Avg 308	Avg 96
A607	Re-Solution	850	8	Transverse	182	.490	.747	5800	.01615	7070	.0198	136.4	.209	.219	214		269	
A608	Treated					.501	.747	5890	.016872	6540	.0194	143.5	.229	.228	265		285	
A609						.498	.747	6010	.017898	6660	.0200	148.3	.240	.238	320		326	
A610						.499	.747	5700	.016454	6840		144.0	.230	.254	253		331	
A611						.490	.747	5700	.017746	6070	.0207	152.6	.249	.241	334		310	
														Avg	277	Avg 98	Avg 304	Avg 96
A622	Re-Solution	850	8	Short	184.6	.490	.747	5690	.018012	6660	.0221	157.0	.256	.250	365		331	
A623	Treated			Transverse		.496	.749	4500	.015922	5500	.0209	175.5	.285	.282	326		256	
A624						.490	.748	4900	.014136	5905	.0202	141.4	.224	.256	181		256	
A625						.498	.747	4200	.012464	6155	.0194	147.8	.239	.316	154		290	
A626						.496	.749	4800	.016150	5820	.0210	166.9	.273	.277	317		280	
														Avg	269	Avg 90	Avg 283	Avg 95
A597	Re-Solution	900	8	Longitudinal	199.3	.477	.744	6400	.018696	7500	.0232	139.3	.219	.229	307		382	
A598	Treated					.497	.744	6075	.019760	6575	.0226	161.7	.265	.270	455		438	
A599						.498	.745	5820	.018392	6570	.0221	157.4	.257	.255	374		354	
A600						.497	.744	7180	.019456	7950	.0228	134.7	.204	.209	304		376	
A601						.498	.744	6200	.020140	6900	.0238	161.8	.265	.264	472		434	
														Avg	382	Avg 108	Avg 397	Avg 110
A612	Re-Solution	900	8	Transverse	198.8	.499	.748	3210	.011590	4470	.0183	180.2	.292	.324	179		178	
A613	Treated					.498	.749	5250	.016720	5750	.0190	158.6	.260	.256	317		282	
A614						.490	.748	4700	.014598	4980	.0170	152.1	.248	.256	224		236	
A615						.489	.749	4200	.013414	4865	.0170	156.2	.255	.260	197		193	
A616						.499	.749	5080	.016264	5115	.0165	159.8	.261	.253	292		257	
														Avg	243	Avg 86	Avg 229	Avg 83
A627	Solution	900	8	Short	197.5	.496	.746	5275	.016074	6290	.0200	151.1	.246	.237	268		253	
A628	Treated			Transverse		.498	.749	6200	.017822	6860	.0214	143.1	.228	.251	294		379	
A629						.497	.748	4040	.015428	4995	.0209	189.8	.303	.310	329		256	
A630						.498	.746	4830	.015884	5435	.0189	163.8	.268	.280	298		294	
														Avg	297	Avg 99	Avg 295	Avg 95
A602	Re-Solution	950	8	Longitudinal	191.5	.498	.744	6400	.020672	7640	.0258	160.8	.264	.274	496		499	
A603	Treated					.498	.744	6600	.019570	7625	.0243	147.7	.239	.262	370		484	
A604						.501	.749	6600	.019760	8745	.0291	150.0	.244	.257	401		445	
A605						.498	.746	6940	.020406	8230	.0260	146.4	.236	.242	406		451	
A606						.490	.744	6475	.019570	8210	.0272	148.1	.240	.255	384		456	
														Avg	411	Avg 112	Avg 467	Avg 119
A617	Re-Solution	950	8	Transverse	193.5	.497	.749	4100	.013110	5165	.0169	158.9	.260	.254	194		170	
A618	Treated					.490	.745	4930	.015580	5075	.0164	154.9	.253	.262	263		277	
A619						.499	.748	3400	.015694	3550	.0168	230.3	.344	.378	379		302	
A620						.500	.747	4300	.012882	5230	.0163	149.8	.243	.258	169		194	
A621						.500	.747	4915	.014706	5300	.0163	149.6	.243	.252	221		241	
														Avg	245	Avg 87	Avg 237	Avg 85
A632	Re-Solution	950	8	Short	192.0	.498	.748	6680	.017860	7545	.0209	133.1	.199	.227	250		366	
A633	Treated			Transverse		.496	.748	6100	.018848	6670	.0215	153.3	.250	.260	378		399	
A634						.499	.748	6150	.019038	6650	.0216	154.5	.252	.262	390		407	
														Avg	339	Avg 101	Avg 390	Avg 109

Calibration Curve Constants: $Q = 25.0 \times 10^{-6}$, $R = -140 \times 10^{-6}$, $S = 300 \times 10^{-6}$

* G_{nc} (in.-lb/in.^{2}) and K_{nc} (ksi$\sqrt{\text{in.}}$) are based on the proportional-limit load and the effective-crack depth (a) determined from spring-constant-calibration curve

G_{Ic} (in.-lb/in.^{2}) and K_{Ic} (ksi$\sqrt{\text{in.}}$) are based on the proportional-limit load and the measured crack depth (a) using Bueckner's equation.

Approved for Public Release

Confidential

TABLE 42

SLOW-NOTCH-BEND TEST FOR HEAT 24158 MANDREL FORGING

Effect of Heat Treatment and Specimen Orientation in Vacuum-Arc-Remelt, Grade 200, 1 x 4-In. Mandrel Forging, 18% Nickel Maraging Steel

Specimen Number	Material Condition	Aging Cycle °F - hr	Specimen Orientation	.2% Offset Yield (ksi)	Width b (in.)	Depth d (in.)	Proportional Limit Load(L) (lb)	Proportional Limit Deflec.(e) (in.)	Maximum Load Load(L) (lb)	Maximum Load Deflec.(e) (in.)	eb/L $(in.^2/lb)\times10^{-8}$	Notch+Crack Depth Effective a (in.)	Notch+Crack Depth Measured a (in.)	PLANE-STRAIN FRACTURE TOUGHNESS* G_{nc}	K_{nc}	G_{Ic}	K_{Ic}
A721	Re-Solution	850 8	Longitudinal	187.5	.501	.749	5900	.0205	6780	.0253	174	.283	.263	535		372	
A722	Treated				.501	.751	5320	.0190	6210	.0230	179	.302	.289	555		364	
A723					.501	.751	5610	.0178	6640	.0228	159	.276	.248	441		296	
A724					.501	.750	5860	.0186	6585	.0222	159	.276	.236	481		295	
A725					.495	.749	4450	.0171	5670	.0233	190	.304	.301	408		290	
													Avg	484	Avg 122	Avg 324	Avg 99
A736	Re-Solution	850 8	Transverse	189.4	.499	.750	5310	.0140	7760	.0220	132	.195	.208	152		195	
A737	Treated				.499	.750	5400	.0190	5840	.0209	175	.284	.268	457		325	
A738					.499	.751	6050	.0190	7860	.0254	157	.257	.243	403		333	
A739					.499	.750	5810	.0171	8100	.0260	147	.237	.223	287		264	
A740					.499	.752	4380	.0182	5530	.0246	194	.308	.228	409		154	
													Avg	342	Avg 102	Avg 254	Avg 88
A726	Re-Solution	900 8	Longitudinal	204.0	.502	.749	6250	.0209	6600	.0223	168	.274	.257	531		397	
A727	Treated				.501	.750	6250	.0206	6490	.0215	165	.270	.253	506		384	
A729					.502	.749	7100	.0209	7640	.0240	148	.240	.221	440		385	
A730					.501	.749	4300	.0171	5100	.0212	200	.315	.3180	427		301	
													Avg	477	Avg 120	Avg 367	Avg 105
A741	Re-Solution	900 8	Transverse	202.5	.499	.750	5950	.0194	6590	.0222	163	.267	.261	444		373	
A742	Treated				.498	.750	7050	.0213	7330	.0223	151	.256	.241	542		450	
A743					.499	.750	5750	.0197	6130	.0212	171	.279	.281	486		406	
A744					.499	.750	7000	.0217	7390	.0236	155	.253	.253	512		486	
A745					.498	.750	5830	.0186	6000	.0235	159	.276	.286	482		436	
													Avg	493	Avg 121	Avg 430	Avg 114
A746	Re-Solution	950 8	Transverse	199.3	.498	.750	5930	.0194	7040	.0264	163	.267	.268	443		393	
A747	Treated				.498	.749	5630	.0197	6200	.0232	174	.283	.281	493		394	
A749					.499	.750	6600	.0216	7650	.0271	163	.267	.258	547		449	
A750					.499	.750	6470	.0220	7255	.0276	170	.277	.273	599		484	
													Avg	521	Avg 123	Avg 430	Avg 114
A731	Re-Solution	950 8	Longitudinal	197.1	.501	.750	5910	.0205	6630	.0246	173	.282	.281	530		426	
A732	Treated				.501	.751	4930	.0182	5695	.0228	185	.298	.311	453		370	
A733					.501	.751	6900	.0205	7730	.0245	149	.242	.248	428		447	
A734					.501	.749	6620	.0228	6925	.0240	173	.282	.279	664		530	
A735					.500	.751	6550	.0212	7145	.0240	162	.265	.264	522		458	
													Avg	518	Avg 123	Avg 446	Avg 116

Calibration Curve Constants: Q = 25.0×10^{-6}
R = 140×10^{-6}
S = 300×10^{-6}

* G_{nc} (in.-lb/in^2) and K_{nc} (ksi$\sqrt{in.}$) are based on the proportional-limit load and the effective-crack depth (a) determined from spring-constant-calibration curve
G_{Ic} (in.-lb/$in.^2$) and K_{Ic} (ksi$\sqrt{in.}$) are based on the proportional-limit load and the measured crack depth (a) using Bueckner's equation.

Approved for Public Release

TABLE 43

SLOW-NOTCH-BEND TEST FOR HEAT 24153, 3/4 IN. PLATE

Effect of Heat Treatment and Specimen Orientation in Vacuum-Arc-Remelt, Grade 200, 3/4 In. Plate, 18% Nickel Maraging Steel

Specimen Number	Material Condition	Aging Cycle °F - hr	Specimen Orientation	.2% Offset Yield (ksi)	Width b (in.)	Depth d (in.)	Proportional Limit Load(L) (lb)	Proportional Limit Deflec.(e) (in.)	Maximum Load Load(J) (lb)	Maximum Load Deflec.(e) (in.)	eb/L (in.²/lb)x10⁻⁸	Notch+Crack Depth Effective a (in.)	Notch+Crack Depth Measured a (in.)	PLANE-STRAIN FRACTURE TOUGHNESS(1) G_{nc}	K_{nc}	G_{Ic}	K_{Ic}
A1448	Re-Solution	850 8	Longitudinal	197.5	.746	.751	13750	.02240	16650	.0308	121.5	.137	.153	419		325	
A1449	Treated				.746	.751	10500	.02051	11500	.0250	145.8	.219	.229	353		208	
A1450					.746	.751	8500	.0209	9000	.0245	183.3	.298	.304	469		263	
A1451					.745	.751	10850	.02166	12175	.0276	148.5	.226	.217	398		372	
A1452					.746	.752	12250	.02320	12750	.0247	141.3	.206	.227	441		521	
														Avg 415	Avg 112	Avg 338	Avg 101
A1463	Re-Solution	850 8	Transverse	196.1	.747	.752	9800	.02167	10000	.0224(2)	165.2	.264	.264	447		315	
A1465	Treated				.749	.747	8200	.01994	8200	.0201(2)	182.3	.293	.275	412		340	
A1466					.748	.751	8300	.01940	8675	.0201	174.8	.283	.249	383		321	
A1467					.747	.751	8700	.01891	8800	.0192(2)	162.5	.258	.242	333		322	
														Avg 394	Avg 109	Avg 324	Avg 99
A1453	Re-Solution	900 8	Longitudinal	196.8	.746	.750	8800	.02090	9340	.0245	177.2	.284	.287	437		315	
A1455	Treated				.746	.751	9800	.02165	10890	.0248	165.0	.272	.248	483		485	
A1456					.748	.751	8400	.02070	9330	.0252	184.5	.296	.293	446		297	
A1602					.748	.751	8880	.01841	10700	.0240	155.3	.243	.275	303		350	
														Avg 417	Avg 112	Avg 362	Avg 105
A1471	Re-Solution	900 8	Transverse	199.5	.745	.751	8050	.01753	8505	.0191(2)	162.2	.258	.283	287		310	
A1472	Treated				.748	.749	8480	.01808	8760	.0196(2)	159.5	.252	.272	299		341	
														Avg 293	Avg 95	Avg 325	Avg 99
A1458	Re-Solution	950 8	Longitudinal	193.4	.745	.751	9100	.02220	11200	.0293	180.5	.280	.279	451		510	
A1459	Treated				.746	.751	10200	.02166	12850	.0288	158.5	.240	.256	392		440	
A1460					.745	.751	8100	.02166	9720	.0286	199.2	.316	.315	510		313	
A1461					.747	.752	8000	.02128	9160	.0281	198.5	.315	.329	606		448	
A1462					.747	.751	7500	.02186	9150	.0285	217.5	.334	.355	522		441	
														Avg 496	Avg 123	Avg 430	Avg 114
A701	Re-Solution	950 8	Transverse	196.0	.740	.752	9950	.02004	10115	.0207(2)	149.2	.230	.249	350		427	
A702	Treated				.740	.752	8550	.01771	5880	.0199	153.4	.238	.260	279		343	
A703					.737	.751	9400	.01880	10010	.0204	147.5	.224	.243	301		369	
A704					.738	.751	8630	.01980	8720	.0204(2)	169.4	.271	.283	379		422	
A705					.735	.752	16500	.02430	17480	.0266	108.4	.072	.111	484		338	
														Avg 359	Avg 104	Avg 380	Avg 107

Calibration Curve Constants: Q = 21.78 x 10^{-6}
R = -96.67 x 10^{-6}
S = 188.89 x 10^{-6}

(1) G_{nc} (in.-lb/in.²) and K_{nc} (ksi$\sqrt{in.}$) are based on the proportional-limit load and the effective-crack depth (a) determined from spring-constant-calibration curve

G_{Ic} (in.-lb/in.²) and K_{Ic} (ksi$\sqrt{in.}$) are based on the proportional-limit load and the measured crack depth (a) using Bueckner's equation.

(2) Pop-in occurred at the proportional-limit load.

Approved for Public Release

TABLE 44

SLOW-NOTCH-BEND TEST FOR HEAT 24158, 3/4 IN. PLATE

Effect of Heat Treatment and Notch Location in Welded Vacuum-Arc-Remelt, Grade 200, 18% Nickel Maraging Steel, 3/4 In. Plate

Specimen Number	Material Condition	Aging Cycle °F	Aging Cycle hr	Notch Location	.2% Offset Yield (ksi)	Width b (in.)	Depth d (in.)	Proportional Limit Load(L) (lb)	Proportional Limit Deflec.(e) (in.)	Maximum Load Load(L) (lb)	Maximum Load Deflec.(e) (in.)	cb/L (in.²/lb)x10⁻⁸	Notch+Crack Depth Effective a (in.)	Notch+Crack Depth Measured a (in.)	PLANE-STRAIN FRACTURE TOUGHNESS* G_{nc}	K_{nc}	G_{Ic}	K_{Ic}
T1	Welded	900	8	Weld Deposit		.696	.752	6000	.0114	6070	.0123	132	.196	-	102	-	-	-
T21	"			Weld Wire		.696	.750	5100	.0108	5100	.0107	148	.236	-	110	-	-	-
T41				24589		.696	.752	5300	.0125	5350	.0125	164	.268	-	167	-	-	-
T61						.696	.751	4400	.0127	4450	.0134	200	.325	-	210	-	-	-
T80						.690	.751	4000	.0108	4085	.0118	186	.304	-	142	-	-	-
															Avg 146	Avg 66	-	-
T123	Welded	900	8	Weld Deposit		.699	.753	6250	.0215	6820	.0247	240	-	.385	-	-	528	-
T124				Weld Wire		.698	.752	9200	.0208	9880	.0236	158	-	.275	-	-	501	-
T139				34482		.698	.752	9200	.0199	9760	.0225	151	-	.284	-	-	537	-
T140						.699	.752	12850	.0226	13270	.0246	123	-	.203	-	-	551	-
T154						.698	.753	9700	.0224	10265	.0255	161	-	.292	-	-	630	-
T155						.698	.752	9600	.0217	10580	.0255	158	-	.261	-	-	490	-
															-	-	Avg 538	Avg 130
T9	Welded	900	8	Heat-Affected		.696	.752	11750	.0194	15450	.0317	92		.162	-	-	307	-
T29				Zone 1		.696	.752	14050	.0257	15480	.0269	128		.139	-	-	360	-
T49						.695	.752	13000	.0239	13475	.0259	128		.161	-	-	376	-
																	Avg 348	Avg 103
T10	Welded	900	8	Heat-Affected		.696	.751	13000	.0233	15010	.0278	125		.135	-	-	339	-
T30				Zone 2		.695	.752	13375	.0236	15000	.0261	123		.138	-	-	324	-
																	Avg 332	Avg 100
T2	Welded	950	8	Weld Deposit		.696	.751	5400	.0141	5415	.0141	181	.296	-	234	-	-	-
T22				Weld Wire		.696	.751	4700	.0143	4705	.0143	211	.340	-	278	-	-	-
T42				24589		.695	.750	2000	.0111	2575	.0147	386	.575	-	309	-	-	-
T62						.695	.751	7400	.0142	7495	.0144	131	.191	-	149	-	-	-
T81						.696	.749	4600	.0138	5060	.0157	209	.338	-	261	-	-	-
															Avg 246	Avg 84.5		
T125	Welded	950	8	Weld Deposit		.700	.753	6700	.0218	8415	.0321	228	-	.402	-	-	691	-
T126				Weld Wire		.701	.753	13100	.0250	14400	.0267	123	-	.189	-	-	506	-
T141				34482		.700	.752	8630	.0217	8895	.0220	176	-	.319	-	-	616	-
T142						.700	.751	11020	.0217	12880	.0257	138	-	.228	-	-	496	-
T156						.698	.752	11720	.0213	13345	.0261	127	-	.216	-	-	509	-
T157						.699	.753	11560	.0223	12700	.0250	135	-	.240	-	-	571	-
																	Avg 565	Avg 132
T69	Welded	950	8	Heat-Affected		.697	.750	11100	.0215	14380	.0308	135	-	.192			363	-
T88				Zone 1		.696	.751	9880	.0222	11100	.0283	156	-	.271			547	-
T107						.696	.750	9000	.0198	12875	.0312	153	-	.228			320	-
																	Avg 410	Avg 111
T70	Welded	950	8	Heat-Affected		.697	.750	11000	.0225	13250	.0283	142	-	.220			448	-
T89				Zone 2		.696	.751	9900	.0211	11875	.0256	148	-	.254			470	-
T108						.695	.752	11100	.0228	18250	.0353	142	-	.163			282	-
																	Avg 400	Avg 110

* G_{nc} (in.-lb/in.^{2}) and K_{nc} (ksi$\sqrt{\text{in.}}$) are based on the proportional-limit load and the effective-crack depth (a) determined from spring-constant-calibration curve

G_{Ic} (in.-lb/in.^{2}) and K_{Ic} (ksi$\sqrt{\text{in.}}$) are based on the proportional-limit load and the measured crack depth (a) using Bueckner's equation.

Approved for Public Release

TABLE 45

SLOW-NOTCH-BEND TEST FOR HEAT 24158, 3/4 IN. PLATE

Effect of Heat Treatment and Specimen Orientation in Vacuum-Arc-Remelt, Grade 200, 1/2 In.-Thick Plate, 18% Nickel Maraging Steel

Specimen Number	Material Condition	Aging Cycle °F - hr	Specimen Orientation	.2% Offset Yield (ksi)	Width b (in.)	Depth d (in.)	Proportional Limit Load(L) (lb)	Proportional Limit Deflec.(e) (in.)	Maximum Load Load(L) (lb)	Maximum Load Deflec.(e) (in.)	el/L (in.²/lb)x10⁻⁸	Notch+Crack Depth Effective a (in.)	Notch+Crack Depth Measured a (in.)	PLANE-STRAIN FRACTURE TOUGHNESS* G_{nc}	K_{nc}	G_{Ic}	K_{Ic}
A449	Re-Solution Treated	850 - 8	Longitudinal	197.5	.498	.749	6500	.020786	7565	.0252	160.0	.262	.244	498		394	
A450					.499	.749	7900	.021128	9110	.0281	132.9	.198	.210	344		441	
A451					.499	.749	7400	.021622	8570	.0261	145.9	.235	.238	454		486	
A452					.499	.748	7250	.021660	8385	.0265	149.0	.242	.244	476		492	
													Avg	443	Avg 115	Avg 453	Avg 117
A463	Re-Solution Treated	850 - 8	Transverse	196.1	.499	.748	6380	.018544	6380	.0207	145	.233	.227	329		333	
A464					.501	.749	6500	.018734	6600	.0261	144.2	.231	.224	331		332	
A465					.499	.748	7300	.020064	7340	.0202	137.4	.212	.225	330		406	
A466					.501	.750	6400	.018126	6800	.0199	140.6	.222	.234	288		347	
A467					.499	.749	5620	.017252	6380	.0213	151.2	.246	.259	301		330	
													Avg	317	Avg 99	Avg 349	Avg 107
A453	Re-Solution Treated	900 - 8	Longitudinal	196.8	.499	.749	6400	.020672	7315	.0259	160.9	.264	.261	494		435	
A454					.501	.750	6375	.021128	7160	.0281	166.2	.272	.267	540		445	
A455					.501	.748	6600	.020976	7460	.0256	159.0	.260	.260	494		458	
A456					.500	.749	6425	.019874	7110	.0228	154.1	.251	.237	418		362	
A457					.501	.749	5880	.019760	6450	.0236	156.4	.253	.276	358		409	
													Avg	461	Avg 118	Avg 422	Avg 113
A468	Re-Solution Treated	900 - 8	Transverse	199.5	.501	.749	6120	.017860	6445	.0200	147.1	.237	.226	316		299	
A469					.499	.749	5600	.016530	6225	.0207	151.8	.247	.241	303		285	
A470					.499	.748	6000	.017708	6170	.0201	150.6	.245	.231	339		304	
A471					.501	.750	5190	.015960	5860	.0190	154.1	.251	.248	272		252	
A472					.498	.749	5300	.016074	5925	.0185	150.9	.246	.214	269		206	
													Avg	300	Avg 95	Avg 270	Avg 90
A458	Re-Solution Treated	950 - 8	Longitudinal	193.4	.501	.749	5800	.018392	7940	.0285	158.6	.259	.278	377		404	
A459					.499	.749	5900	.017480	8550	.0299	144.1	.230	.261	271		370	
A460					.501	.749	6400	.018240	9040	.0285	140.6	.222	.254	288		408	
A461					.499	.749	6500	.019684	8680	.0293	150.8	.246	.253	403		421	
A462					.498	.750	6550	.020710	8455	.0319	157	.257	.260	474		451	
													Avg	363	Avg 104	Avg 411	Avg 112
A473	Re-Solution Treated	950 - 8	Transverse	196.0	.500	.750	6300	.020520	6990	.0236	162.5	.263	.279	496		479	
A474					.499	.750	7160	.020634	7790	.0228	143.8	.230	.234	400		438	
A475					.500	.748	6900	.019456	7510	.0227	135.9	.198	.238	262		423	
A476					.499	.750	8010	.021318	8450	.0231	132.8	.180	.207	308		440	
													Avg	365	Avg 104	Avg 445	Avg 116

Calibration Curve Constants: Q = 25.0 x 10^{-6}
R = -140 x 10^{-6}
S = 300 x 10^{-6}

* G_{nc} (in.-lb/in.^{2}) and K_{nc} (ksi$\sqrt{in.}$) are based on the proportional-limit load and the effective-crack depth (a) determined from spring-constant-calibration curve

G_{Ic} (in.-lb/in.^{2}) and K_{Ic} (ksi$\sqrt{in.}$) are based on the proportional-limit load and the measured crack depth (a) using Bueckner's equation.

Approved for Public Release

Confidential

TABLE 46

FILLER WIRE COMPOSITIONS

Weld Wire Heat	Chemical Analysis Source	Composition, Wt % C	Mn	P	S	Si	Ni	Al	Ti	Mo	Co
34482	Mill-Certified	0.02	0.01	0.003	0.003	0.007	18.2	0.1	0.24	3.53	7.65
	Aerojet Analyses	0.02	<0.02	0.003	0.005	0.02	18.9	0.1	0.24	4.10	7.80
34428-38Ti	Mill-Certified	0.018	<0.01	<0.01	0.006	0.02	18.1	0.07	0.38	3.90	7.5
	Aerojet Analyses	0.019	<0.2	<0.009	0.008	0.03	18.8	0.09	0.34	4.12	7.4
24589	Mill-Certified	0.02	0.02	-	0.007	-	19.2	0.07	0.60	5.60	9.50
	Aerojet Analysis	-	-	-	-	-	19.3	-	0.65	5.10	9.30

Approved for Public Release

Contrails

TABLE 47

LONGITUDINAL TENSILE PROPERTIES OF TIG WELD METALS IN GRADE 200, 3/4-IN.-THICK, 18% NICKEL MARAGING STEEL PLATE, HEAT 24158

Weld Wire Heat	Aging Cycle °F - hr	0.2% Offset Yield Strength ksi	Ultimate Strength, ksi	Elongation in 1-in. %	Reduction of Area, %
24589	900-8	249	269	8.3	41.3
		240	264	8.3	34.5
		251	273	9.2	37.7
	Avg	247	269	8.6	37.8
24589	950 - 8	231	250	11.3	44.3
		232	250	10.7	43.7
	Avg	232	250	11.0	44.0
34482	900 - 8	214	219	11.0	50.4
		215	218	13.2	61.1
		213	219	12.8	59.5
	Avg	214	219	12.3	57.0
34482	950 - 8	211	217	14.8	60.1
		206	213	14.8	59.5
		210	219	14.0	56.0
	Avg	209	216	14.5	58.5

Approved for Public Release

TABLE 48

TRANSVERSE TENSILE PROPERTIES OF TIG WELDED JOINTS IN GRADE 200, 3/4-IN.-THICK, 18% NICKEL MARAGING STEEL PLATE, HEAT 24153

Weld Wire Heat	Aging Cycle °F-hr	0.2% Offset Yield Strength, ksi	Ultimate Tensile Strength ksi	Elongation in 1-in. %	Reduction of Area %	Location of Failure
24589	900 - 8	214	217	11.9	54.1	HAZ
		212	217	10.7	53.5	HAZ
	Avg	213	217	11.3	53.8	
24589	950 - 8	195	199	14.2	62.8	HAZ
		199	205	13.1	60.7	HAZ
	Avg	197	203	13.7	61.8	
34482	900 - 8	210	214	12.5	54.4	HAZ
		216	218	13.4	57.0	HAZ
		203	206	11.1	55.4	HAZ
	Avg	210	213	12.3	55.0	
34482	950 - 8	210	212	12.3	56.4	HAZ
		209	212	11.5	53.8	HAZ
		299	204	11.6	52.8	HAZ
	Avg	206	207	11.8	54.3	

Approved for Public Release

TABLE 49

COMPOSITION OF TIG WELD METALS DEPOSITED IN
GRADE 200, 3/4-IN.-THICK, 18% NICKEL MARAGING STEEL PLATE,
HEAT 24158

Filler Wire Heat	Material	Alloy Content, wt%									
		C	Mn	P	S	Si	Ni	Al	Co	Mo	Ti
24589	Filler Wire	0.02	0.02	-	0.007	-	19.3	0.07	9.3	5.1	0.65
	Weld Metal	0.014	0.02	-	-	<0.05	18.4	-	9.3	4.5	0.54
34482	Filler Wire	0.02	<0.02	0.003	0.005	0.02	18.9	0.1	7.8	4.1	0.24
	Weld Metal	0.015	0.02	-	-	<0.05	17.4	-	7.8	3.5	0.22

Approved for Public Release

Contrails

TABLE 50

LONGITUDINAL TENSILE PROPERTIES OF MIG WELD METALS IN GRADE 200, 3/4-IN.-THICK, 18% NICKEL MARAGING STEEL PLATE, HEAT 24158

Weld Wire Heat	Aging Cycle % - hr		0.2% Offset Yield Strength ksi	Ultimate Tensile Strength ksi	Elongation in 1-in. %	Reduction of Area, %
24589	900-8		227	247	7.3	31.4
			234	246	7.8	30.8
			223	244	8.1	36.0
		Avg	228	246	7.7	32.7
34428-.38 Ti	900-8		216	225	5.0	21.2
			213	223	8.4	32.2
		Avg	215	224	6.7	26.7
24589	950-8		210	234	6.3	24.1
			222	242	5.3	17.0
			220	240	6.1	16.2
		Avg	217	239	5.9	19.1
34428-.38 Ti	950-8		201	214	9.4	30.8
			202	213	9.5	34.1
		Avg	202	214	9.5	32.5

Approved for Public Release

TABLE 51

TRANSVERSE TENSILE PROPERTIES OF MIG-WELDED JOINTS IN GRADE 200, 3/4-IN.-THICK, 18% NICKEL MARAGING STEEL PLATE, HEAT 24158

Weld Wire Heat	Aging Cycle °F-hr		0.2% Offset Yield Strength ksi	Ultimate Tensile Strength ksi	Elongation in 1-in. %	Reduction of Area %	Location of Failure
24589	900-8		213	215	8.9	40.4	HAZ
			212	213	8.8	43.5	HAZ
			215	216	9.5	44.0	HAZ
		Avg	213	214	9.1	42.6	
34428-.38 Ti	900-8		217	220	10.8	56.1	HAZ
			213*	214*	0.9	2.5*	WM*
24589	950-8		203	210	9.1	51.7	HAZ
			202	211	10.8	53.4	HAZ
			202	208	11.3	54.8	HAZ
		Avg	202	210	10.4	53.3	
34428-.38 Ti	950-8		205	210	10.8	55.7	HAZ
			200	208	10.8	54.8	HAZ
		Avg	203	209	10.8	55.3	

*Lack of fusion defect in specimen.

Approved for Public Release

TABLE 52

COMPOSITION OF MIG WELD METALS DEPOSITED IN
GRADE 200, 3/4-IN.-THICK, 18% NICKEL MARAGING STEEL PLATE,
HEAT 24158

Filler Wire Heat	Material	Alloy Content, wt%									
		C	Mn	P	S	Si	Ni	Al	Co	Mo	Ti
24589	Filler Wire	0.02	0.02	-	0.007	-	19.3	0.07	9.3	5.1	0.65
	Weld Metal	-	<0.02	0.006	-	<0.05	18.3	0.09	9.1	4.5	0.50
34428-.38 Tl	Filler Wire	0.02	<0.02	<0.009	0.008	0.03	18.8	0.09	7.4	4.1	0.34
	Weld Metal	0.013	0.03	-	0.009	<0.05	17.8	0.05	7.8	3.75	0.24

Approved for Public Release

Contrails

TABLE 53
PRECRACKED-CHARPY-IMPACT (W/A) FRACTURE TOUGHNESS OF TIG WELDMENTS IN GRADE 200, 3/4-IN.-THICK, 18% NICKEL MARAGING STEEL PLATE HEAT 24158

Weld Wire Heat	Aging Cycle °F - hr	Notch Location		W/A in.-lb/in.^{2}* -100°F	RT	200°F	400°F
24589	900 - 8	WM		176	495	376	278
				215	259	314	256
					438		
					258		
			Avg	196	388	345	267
34482	900 - 8	WM		633	1252	1164	1581
				837	1269	1270	1507
					920		
					985		
			Avg	735	1157	1217	1544
---	900 - 8	HAZ-1		953	1163	1368	1457
				1255	1050	1150	1411
					1015		
					1426		
			Avg	1104	1164	1259	1434
---	900 - 8	HAZ-2		1004	1280	1169	1181
				930	1277	1372	1126
					1220		
					977		
			Avg	967	1189	1271	1154
---	900 - 8	Base Metal					
		Longitudinal		1025	1214	1584	1354
		Transverse		628	800	854	722
24589	950 - 8	WM		280	267	339	298
				294	296	401	332
					346		
			Avg	287	303	370	315
34482	950 - 8	WM		729	1237	1349	1321
				749	1064	1680	1334
					1041		
					1157		
			Avg	739	1125	1515	1328
---	950 - 8	HAZ-1		1455	1612	1766	1749
				1245	1618	1428	1813
					1799		
					1617		
			Avg	1350	1662	1597	1781
---	950 - 8	HAZ-2		964	1400	1415	1607
					1418	1460	1691
					1779		
					1216		
			Avg		1454	1438	1649
---	950 - 8	Base Metal					
		Longitudinal			1315		2354
		Transverse		695	831	911	877

*These values are based on a specimen size of 0.7 x 0.394-in.

Approved for Public Release

TABLE 54

SLOW-NOTCH-BEND FRACTURE TOUGHNESS OF TIG WELDMENTS IN HEAT 24158, WELDED WITH WELD WIRES 24589 AND 34482

Effect of Heat Treatment and Notch Location in Welded Vacuum-Arc-Remelt, Grade 200, 18% Nickel Maraging Steel, 3/4 In. Plate

Specimen Number	Material Condition	Aging Cycle °F - hr	Notch Location	.2% Offset Yield (ksi)	Width b (in.)	Depth d (in.)	Proportional Limit Load(L)	Proportional Limit Deflec.(e) (in.)	Maximum Load Load(L)	Maximum Load Deflec(e) (in.)	eb/L ($in.^2/lb \times 10^{-8}$)	Notch+Crack Depth Effective a (in.)	Notch+Crack Depth Measured a (in.)	PLANE-STRAIN FRACTURE TOUGHNESS* G_{nc}	K_{nc}	G_{Ic}	K_{Ic}
T1	Welded	900-8	Weld Deposit	247	.696	.752	6,000	.0114	6,070	.0123	132	.196	-	102	-	-	-
T21			Weld Wire		.696	.750	5,100	.0108	5,100	.0107	148	.236	-	110	-	-	-
T41			24589		.696	.752	5,300	.0125	5,350	.0125	164	.268	-	167	-	-	-
T61					.696	.751	4,400	.0127	4,450	.0134	200	.325	-	210	-	-	-
T80					.690	.751	4,000	.0108	4,085	.0118	186	.304	-	142	-	-	-
													Avg	146	Avg 66	-	-
T123	Welded	900-8	Weld Deposit	214	.693	.753	6,250	.0215	6,820	.0247	240	-	.385	-	-	528	-
T124			Weld Wire		.698	.752	9,200	.0208	9,880	.0236	158	-	.275	-	-	501	-
T139			34482		.698	.752	9,200	.0199	9,760	.0225	151	-	.284	-	-	537	-
T140					.699	.752	12,850	.0226	13,270	.0246	123	-	.203	-	-	551	-
T154					.698	.753	9,700	.0224	10,265	.0255	161	-	.292	-	-	630	-
T155					.698	.752	9,600	.0217	10,580	.0255	158	-	.261	-	-	490	-
																Avg 538	Avg 130
T9	Welded	900-8	HAZ-1	-	.696	.752	11,750	.0194	15,450	.0317	92	-	.162	-	-	307	-
T29					.696	.752	14,050	.0257	15,480	.0269	128	-	.139	-	-	360	-
T49					.695	.752	13,000	.0239	13,475	.0259	128	-	.161	-	-	376	-
																Avg 343	Avg 103
T10	Welded		HAZ-2	-	.696	.751	13,000	.0233	15,010	.0278	125	-	.135	-	-	339	-
T30					.695	.752	13,375	.0236	15,000	.0261	123	-	.138	-	-	324	-
																Avg 332	Avg 100
T2	Welded	950-8	Weld Deposit	232	.696	.751	5,400	.0141	5,415	.0141	181	.296	-	234	-	-	-
T22			Weld Wire		.696	.751	4,700	.0143	4,705	.0143	211	.340	-	278	-	-	-
T42			24589		.695	.750	2,000	.0111	2,575	.0147	386	.575	-	309	-	-	-
T62					.695	.751	7,400	.0142	7,495	.0144	131	.191	-	149	-	-	-
T81					.696	.749	4,600	.0138	5,060	.0157	209	.338	-	261	-	-	-
														Avg 246	Avg 84.5		
T125	Welded	950-8	Weld Deposit	209	.700	.753	6,700	.0218	8,415	.0321	228	-	.402	-	-	691	-
T126			Weld Wire		.701	.753	13,100	.0250	14,400	.0267	123	-	.189	-	-	506	-
T141			34482		.700	.752	8,630	.0217	8,895	.0220	176	-	.319	-	-	616	-
T142					.700	.751	11,020	.0217	12,980	.0257	138	-	.228	-	-	496	-
T156					.698	.752	11,720	.0213	13,345	.0261	127	-	.216	-	-	509	-
T157					.699	.753	11,560	.0223	12,700	.0250	135	-	.240	-	-	571	-
																Avg 565	Avg 132
T69	Welded	950-8	HAZ-1	-	.697	.750	11,100	.0215	14,380	.0308	135	-	.192	-	-	363	-
T88					.696	.751	9,380	.0222	11,100	.0283	156	-	.271	-	-	547	-
T107					.696	.750	9,000	.0198	12,875	.0312	153	-	.228	-	-	320	-
																Avg 410	Avg 111
T70	Welded	950-8	HAZ-2	-	.697	.750	11,000	.0225	13,250	.0283	142	-	.220	-	-	448	-
T89					.696	.751	9,900	.0211	11,875	.0256	148	-	.254	-	-	470	-
T108					.695	.752	11,100	.0228	18,250	.0353	142	-	.163	-	-	282	-
																Avg 400	Avg 110

Calibration Curve Constants: $Q = 14.03 \times 10^{-6}$, $R = -66.67 \times 10^{-6}$, $S = 163.89 \times 10^{-6}$

*G_{nc} (in.-lb/in.^{2}) and K_{nc} (ksi $\sqrt{in.}$) are based on the proportional-limit load and the effective-crack depth (a) determined from spring-constant-calibration curve.
G_{Ic} (in.-lb/in.^{2}) and K_{Ic} (ksi $\sqrt{in.}$) are based on the proportional-limit load and the measured crack depth (a) using Bueckner's equation.

Approved for Public Release

Contrails

TABLE 55

PRECRACKED-CHARPY-IMPACT W/A FRACTURE TOUGHNESS OF MIG WELDMENTS IN GRADE 200, 3/4-IN.-THICK, 18% NICKEL MARAGING STEEL PLATE, HEAT 24158

Weld Wire Heat	Aging Cycle °F-hr	Notch Location		W/A (in.-lb/in.^{2})* -100	R+	200	400
24589	900-8	WM		220	221	249	234
					227	264	236
					309		
					320		
			Avg	—	269	257	235
34428-.38 Ti	900-8	WM		332	312	379	452
				273	339	429	465
					423		
					433		
			Avg	303	308	304	459
	900-8	HAZ-1		879	1020	1204	925
				943	1119	1265	1244
					1171		
			Avg	911	1103	1235	1085
	900-8	HAZ-2		756	1226	1103	1475
				985	1353	1156	1904
					1608		
			Avg	871	1395	1130	1690
	900-8	Base Metal Longitudinal		1025	1214	1584	1354
		Transverse		628	800	854	722
24589	950-8	WM		224	294	254	294
				246	324	346	
					420		
			Avg	236	346	300	—
34428-.38 Ti	950-8	WM		-	478	502	469
					447		568
					496		
				—	474	—	519
	950-8	HAZ-1		-	1272	1413	1449
					1286	1444	1552
					1333		
					1379		
			Avg	—	1317	1429	1503
	950-8	HAZ-2		1048	1108	1377	
				1202	1386	1466	
					1510		
					1726		
			Avg	1125	1433	1422	
	950-8	Base Metal Longitudinal		-	1315	-	2354
		Transverse		695	831	911	877

*W/A values are based on a specimen size of 0.7 x 0.394 in.

Approved for Public Release

TABLE 56

SLOW-NOTCH-BEND FRACTURE TOUGHNESS OF MIG WELDMENTS IN HEAT 24158 WELDED WITH WIRES 24589 AND 34428
Effect of Heat Treatment and Notch Location in Vacuum-Arc Remelt, Grade 200, 3/4-In.-Thick, 18% Nickel Maraging Steel

Specimen Number	Material Condition	Aging Cycle °F - hr	Notch Location	.2% Offset Yield (ksi)	Width b (in.)	Depth d (in.)	Proportional Limit Load(L) (lb)	Proportional Limit Deflec.(s) (in.)	Maximum Load (L) (lb)	eb/L (in.²/lb)x10⁻⁸	Notch+Crack Depth Effective a (in.)	Notch+Crack Depth Measured a (in.)	PLANE-STRAIN FRACTURE TOUGHNESS(1) G_{ac}	K_{ac}	G_{Ic}	K_{Ic}
M67	Welded	900 - 8	Weld Metal 24589	226	.704	.753	6980	.01185	6980			.174			124	
M69					.704	.753	7060	.01140	7060			.166			118	
M70					.705	.754	1198	.01350	1198			.211				
M71					.702	.754	2465	.01083	2465			.194				
															Avg 121	Avg 61
M140	Welded	900 - 8	Weld Metal 34428 - .38 Ti	215	.702	.754	5190	.01323	5190	179.0	.267	.389	168		234	
M141					.691	.754	8165	.01482	8165	125.4	.126	.189	178		200	
M142					.701	.751	6980 (2)	.01215	7825	122.0	.112	.206	122		167	
M143					.702	.754	6875	.01243	6875	127.0	.132	.206	125		158	
M144					.700	.750	5650 (2)	.01254	6300	155.4	.222	.272	131		186	
													Avg 145	Avg 67	Avg 189	Avg 76
M6	Welded	900 - 8	HAZ-1	-	.701	.751	13825	.02470	15230			.153			409	
M7					.700	.751	11350	.02072	12645			.203			431	
M8					.695	.751	10375	.01976	12395			.207			378	
M9					.702	.750	10500	.02242	11530			.241			502	
															Avg 409	Avg 111
M2	Welded	900 - 8	HAZ-2	-	.702	.751	15250	.02435	17050			.134			410	
M3					.700	.751	13000	.02204	14450			.157			377	
M4					.700	.750	15825	.02673	16875			.132			438	
M5					.702	.751	17375	.02812	18850			.114			489	
M13					.699	.751	13125	.02407	14185			.178			467	
															Avg 430	
M72	Welded	950 - 8	Weld Metal 24585	217	.704	.753	5495	.01103	5495			.164			70	
M73					.705	.750	3810	.01103	3810			.167			35	
M74					.704	.754	7780	.01197	7780			.121			91	
M75					.702	.753	8020	.01216	8020			.114			90	
M76					.703	.754	3445	.01143	3445			.192			35	
															Avg 64	Avg 44
M151	Welded	950 - 8	Weld Metal 34428 - .38 Ti	202	.701	.751	7990	.01520	7990	133.5	.156	.204	182		215	
M152					.700	.750	7050	.01452	7050	144.5	.192	.248	169		241	
M153					.701	.751	9500	.01732	9500	122.6	.114	.130	246		166	
M154					.705	.750	7850	.01407	7850	126.1	.129	.167	160		179	
M155					.702	.755	7665	.01478	7665	135.3	.164	.208	172		199	
															Avg 186	Avg 75	Avg 200	Avg 78
M10	Welded	950 - 8	HAZ-1	-	.702	.751	11875	.02375	13500			.221			544	
M11					.700	.751	11125	.02195	12910			.231			580	
M12					.701	.750	11650	.02204	15075			.190			408	
M14					.701	.751	10850	.01950	14070			.194			364	
M81					.700	.751	13250	.02420	14750			.209			618	
															Avg 491	Avg 122
M15	Welded	950 8	HAZ-2	-	.701	.751	10825	.02202	13400			.235			507	
M16					.696	.751	16375	.02475	22735			.117			401	
M17					.702	.751	16625	.02584	22700			.103			344	
M79					.704	.753	14750	.02300	19075			.145			438	
M80					.700	.750	14125	.02423	16355			.184			471	
															Avg 452	Avg 117

(1) G_{ac} (in.-lb/in.^{2}) and K_{ac} (ksi $\sqrt{in.}$) are based on the proportional-limit load and the effective-crack-depth (a) determined from spring constant calibration curve.

G_{Ic} (in.-lb/in.^{2}) and K_{Ic} (ksi $\sqrt{in.}$) are based on the proportional-limit load and the measured crack depth (a) using Bueckner's equation.

(2) These are pop-in values.

Approved for Public Release

Contrails

APPENDIX I

SURVEY OF STEEL PRODUCERS

Nine steel mills and the International Nickel Company were visited during August 1962 to discuss melting and mill processing practices and their effect on the properties of the 18% nickel maraging steel. Companies and personnel contacted are listed in Table 57.

A. PRODUCTION HISTORY

Production capacity is adequate to supply the Air Force's foreseeable needs for large rocket chambers, though specific tonnage capacities for each company were difficult to obtain. Such items would depend on demand and how many furnaces would be allocated to procuring the maraging steels. The production history of each company to date (as of August 1962) is described in subsequent paragraphs.

1. Bethlehem Steel Company

The Bethlehem Steel Company has melted one 7-ton, electric-furnace heat, and most of the yield was purchased by Aerojet-General; another heat of the same size and composition is now being poured. The Bethlehem Steel personnel would not estimate a production capacity, because this depends on how many furnaces they would allocate for producing the material, which, in turn, depends on demand. They are confident that their over-all capacity is sufficient to supply the demands of the missile industry. For the present, however, they have allocated only the one 7-ton electric furnace to the production of maraging steel. Plate can be rolled on mills ranging in width to 120 in. Bethlehem's current price is $2.25/lb for plate material; however, they suggested that this may decrease if production increases.

2. Carpenter Steel Company

Carpenter has produced one 1-ton air-induction heat, one 2-1/2-ton air-induction heat, and four 12-1/2-ton electric-furnace heats of materials. All of these were consumable-electrode remelted. Carpenter personnel say that production depends on demand. For the present, they have adequate electric and air-induction furnace capacity to feed two 20 and one 28-in. consumable-electrode remelting furnaces. Carpenter does not have production plate-rolling facilities and would prefer to supply bar and rod or small specialty items such as weld wire. Present price information is based on vacuum-arc-remelted bars, which are $2.50/lb.

3. Allegheny Ludlum Corporation

Allegheny Ludlum has poured 50 induction-melted 5000-lb, 6 electric-furnace 10-ton, and one electric-furnace 12-ton heats of 18% nickel maraging steel. All of these were vacuum-arc remelted to various-size ingots. Their production capacity is 300,000 tons per year of air-melted material and 1,500 tons per year of vacuum-arc-remelted material.

Approved for Public Release

Contrails

Vacuum-arc-remelted ingots can be poured in diameters of 50 in. If orders for vacuum-degassed material are received, their Dunkirk facility has a 15-ton ladle degassing unit and a 25-ton stream degassing unit. Allegheny has contracted with Lukens Steel Company to roll wide (205 in.)plate and has reported that delivery and product quality have been quite satisfactory. Prices are tailored to the producing unit, where the unit used is dictated by the melting technique specified and the size of the order. A price of $3.46/lb for vacuum-arc-remelted, 250-ksi plate has been quoted to Aerojet-General.

4. Special Metals Corporation

The Special Metals Corporation has produced a large number of small vacuum-induction and consumable-electrode-remelted heats. Their activities are concentrated in vacuum melting and remelting. They have no air-melt facilities and no rolling facilities. Their product is considered to be of very high quality because they charge electrolytically pure materials; as a result, the product is quite expensive. Consequently, they have aimed their maraging products toward weld wires and other specialty items.

5. United States Steel Corporation

United States Steel has produced a 20-ton, air-melted heat, which yielded about 11 tons of material. Four slabs were prepared, two going to 3/4-in. plate, one to 1/2-in. plate, and one to 1/4-in. plate, a part of which was sandwich-rolled to sheet. Another 20-ton, air-melted heat is being poured, and this is destined to be processed into 6-, 8-, and 10-in., round-corner, square billets as well as some plate. United States Steel, as do the others, says production capacity is based on demand; and, if warranted, 4000 tons per month could be produced. This corporation and Bethlehem are the only two that have integrated facilities beginning with melting and ending with a possible 160-in.-wide plate. United States Steel is currrently making pilot tests on their vacuum degassing facility, and this, together with a rolling mill capable of rolling plate more than 200 in. wide, will be available early next year. United States Steel has quoted a price of $1.40/lb for plate, based on melting costs and considering a projected heat loss estimated from previous experience with other steels.

6. Republic Steel Company

The Republic Steel Company is aggressively attempting to supply the needs of the missiles industry. 18% nickel maraging steels have been produced for evaluations aimed at supplying optimum materials for landing gears, submarine hulls, and large rocket-motor chambers. In all cases, material was consumable-electrode-remelted. Production capacities and prices were not specifically quoted because of the complexity of demand and capacity.

7. Latrobe Steel Company

Latrobe Steel has poured six production heats of vacuum consumable-electrode-remelted material. Of these, five were 5000 lb and one was 30,000 lb. Latrobe has one of the country's largest vacuum consumable-electrode melting facilities consisting of one 36-in.-dia, one 30-in.-dia, and two 20-in.-dia vacuum consumable-electrode melting furnaces. They rate

Approved for Public Release

Contrails

their total production capacity at 535,000 lb of vacuum-remelted material per week. Products made have been billets, bars, plate, and sheet. If an order is received for plate more than about 1 ft wide, Latrobe has negotiated an agreement with Lukens to have their material rolled. Officials at the company are reticent to state opinions concerning projected prices; however, an estimate of around $2.00/lb was stated for air-melted plate and $2.50/lb for consumable-electrode vacuum-melted plate.

8. Vanadium Alloys Steel Corporation

Vanadium Alloys has poured more production heats of 18% nickel material than any other. Approximately 125 vacuum-arc-remelted heats ranging from 1000 lb to one at 30,000 lb have been poured. Vanadium Alloys' production capacity is now 3.5 to 4 million lb/year, with a 9- to 10-million-lb/year capacity projected to November 1962. Their consumable-electrode-melted ingots are 24 in. in diameter and weigh 9,000 lb, and, by the end of the year, they expect to produce material 33 in. in diameter and weighing about 15,000 lb. Personnel at Vanadium Alloys have stated that they do not expect to roll wide plate through Lukens or other companies with large rolling mills but, instead, will concentrate on the smaller specialty items, such as sheet and bar. In this regard, they have a wide variation of furnace capacities, allowing them to supply quantities from less than 100 lb to 15 tons. One of their specialties is vacuum-arc-remelted weld wires.

B. MELTING AND CONVERSION PRACTICE

1. Basic Electric Furnace Practice

The International Nickel Company has established a basic electric furnace procedure and has offered consultation services to any company intending to produce the maraging steels. Although each producer may vary somewhat from International Nickel's recommended practice, depending on his plant layout and experience, maraging steels are generally melted in three basic stages, as follows:

a. A high-quality charge is fed into the furnace. This charge contains scrap iron having 0.20 to 0.40% carbon with low sulphur, phosphorous, and other impurities; molybdenum as ferromolybdenum; electrolytic nickel and cobalt; and slag ingredients totalling approximately 2% by volume of the melt. The slag ingredients are CaO and SiO_2 in amounts that produce a basicity ratio of approximately 2:1, based on scrap quality. Variations of slag ingredients involving the use of CaO alone or CaO plus fluorspar (CaF_2) have been used with good results. When the heat becomes molten, it is blown with oxygen. The carbon reacts with the oxygen, causing considerable boiling and turbulence, which provides the mixing action required to maximize removal of phosphorus, manganese, silicon, hydrogen and nitrogen. CaO then acts as a catalyst to stabalize P_2O_5.

b. The oxidizing slag is raked out of the furnace and the refining slag is added (1-1/2 to 2% by volume). This slag is composed of six parts CaO, three parts CaF_2, and one part granular aluminum. After oxygen and sulphur have been removed, adjustments are made to balance the composition.

Approved for Public Release

Contrails

c. The refining slag is removed, leaving enough to protect the melt. CaO and aluminum in the proportion of 3 parts CaO to 1 part aluminum are added to bring the slag volume to approximately 2%. The aluminum is pushed down into the melt and acts as a final deoxidizer and possibly as a grain refiner. The required amount of titanium metal is then added in the same manner. Previous work at International Nickel indicates that zirconium and boron contribute to stress-corrosion resistance and, for this reason, are added to maraging steel as NiZr and ferroboron, respectively. The last addition is metallic calcium. A maximum of 0.06 wt % calcium is added in 0.02% increments to combine with any residual sulphur (0.005%) as CaS_2. The sulphides thus formed are globular and not concentrated in the grain boundaries. This calcium addition is made to prevent the formation of titanium sulphide stringers at the grain boundaries, which would cause embrittlement. Finally, the melt is teemed into an ingot.

It is generally considered desirable to degas at this time, if the heat is not to be vacuum-arc remelted. Degassing is conducted either by having both the crucible and ingot mold under vacuum during teeming (stream degassing) or by having only the mold enclosed in a vacuum (ladle degassing). Of the companies interviewed, only Bethlehem and Allegheny Ludlum are producing air-melted and vacuum-degassed material.

2. Consumable-Electrode Vacuum Remelting

Vacuum remelting by use of consumable electrodes is done by all companies visited except Bethlehem and United States Steel. The advantage cited for the process is that the resultant material is superior from the standpoint of segregation and cleanliness.

Primary-arc-melted or induction-melted material is poured into an elongated cylindrical mold to produce an electrode for vacuum-arc remelting.

The electrode is top- and bottom-trimmed, and the total surface is ground, wire-brushed, and wiped with acetone. These precautions are necessary to produce the necessary cleanliness in the subsequent remelted ingot. The electrode is then placed in the water-cooled, copper crucible of a consumable-electrode vacuum furnace. A vacuum of 1 to 5 microns mercury is introduced to the system, and the power input and electrode travel rate are carefully controlled to produce the required pool configuration. Improper control results in oxygen entrapment and a phenomenon referred to as "freckling." "Freckles" appear to be high-alloy areas and area containing low-melting carbides.

3. Vacuum Induction Melting

For small quantities (5000 lb or less), vacuum-induction-melting is sometimes used. In this system, an ultrapure charge is put in the melting crucible. A current is induced in the charge, thus generating the heat necessary for melting. The crucible and ingot mold are both contained in a vacuum, in which the heat is poured. Because there can be no slagging action in this process, the only refinement taking place is removal of gaseous interstitials. Carpenter Steel and Special Metals use this process for preparing ingots to be used in the manufacture of weld wire.

Approved for Public Release

Contrails

4. Breakdown Practice

Normal precautions are taken to avoid hydrogen flaking during primary conversion. The ingot is stripped as hot as possible. The ingot is heated twice at 2300°F during primary breakdown to promote homogenization. The major reduction is effected at 1900°F, with finishing temperatures between 1400 and 1500°F. International Nickel Company recommends a slow (furnace) cool period from rolling temperatures through the Martensite transformation (Ms) to room temperature, to avoid any possible hydrogen-flaking damage.

The following is a Latrobe Steel rolling schedule, which is representative of the processing procedure for producing plate.

a. Material was charged to the furnace at 1880°F, and the control temperature was raised to 1930°F.

b. After 45 min, the system reached 1930°F; then the 16 x 16 x 1-3/4-in. bar was reduced seven times at 20% reduction per pass.

c. The material was reheated to 1930°F, and the thickness was reduced to 0.245 in. in three 20%-reduction passes. From there, the material was sent to the finishing mill and reduced to 0.150 in., beginning at 1900°F and finishing below 1700°F.

d. Immediately after the first piece was processed prior to reheating (approximately 5 min lapsed time), the 24-in.-square slab was rolled, beginning at 1930°F.

e. With twelve 20%-reduction passes, this material was reduced to 0.380 in. The piece was then reheated at 1800°F for 20 min.

f. The piece was then rolled to the finish size, 0.265 in. thick, in four passes (approximately 8% reduction per pass). The finishing temperature was described as being well below 1700°F.

5. Miscellaneous Items

Some problems have been encountered by certain mills in their initial attempts to produce maraging steels. On the basis of their past experience with high-temperature alloys such as A-286 Carpenter Steel Company poured a heat that exhibited gross segregates in 12-in.- and 9-in.-long bars cogged from 20-in.-long vacuum-arc-remelted ingots. They did not offer information as to the nature of the segregates or what measures they took to remedy the problem. However, succeeding heats have apparently been clean. Personnel at the International Nickel Company have examined samples of Carpenter material that was described by the producer as being defective and have noted a segregate they have identified as titanium sulphide. As a result of these observations, the importance of imposing requirements for ASTM E45 J&K chart indications of inclusion content in a material specification has been emphasized. Unfortunately, a similar specification does not exist for controlling carbides and nitrides, and this problem remains to be resolved.

Approved for Public Release

Contrails

The United States Steel Company has adopted the melting procedure recommended by International Nickel, but, because they do not vacuum-degas, they repeat their oxidizing and refining slag operations. This, they maintain, is sufficient to reduce the hydrogen content to a level where it does not cause flaking during primary conversion.

Approved for Public Release

Contrails

TABLE 57

PERSONNEL CONTACTED AND STEEL COMPANIES VISITED
TO ESTABLISH MILL PRACTICES

1. Latrobe Steel Company, Latrobe, Pennsylvania

   Mr. Berger Johnson, Sales
   Dr. Edward Becht, Research

2. Vanadium Alloys Steel Company, Latrobe, Pennsylvania

   Mr. Allen Johnson, Research
   Mr. Dan Yates, Research

3. Allegheny-Ludlum Steel Company, Brackenridge, Pennsylvania and Watervliet

   Mr. A. Graae (Watervliet)
   Mr. Ray Lula, Research
   Mr. Ralph DeVreis, Special Products Development
   Mr. A. Fulton (Westwood Plant)

4. Bethlehem Steel Company, Bethlehem, Pennsylvania

   Mr. R. Metzger, Missile Products Sales
   Mr. J. Clark, Assistant Mill Metallurgist

5. Carpenter Steel Company, Reading, Pennsylvania

   Mr. J. Lynch, Special Products Sales
   Mr. M. Sullivan, Metallurgist

6. Special Metals Corporation, New Hartford, New York

   Mr. W. Boesch, Manager, Technical Services
   Mr. C. Freer, Customer Services

7. United States Steel Corporation, Pittsburgh, Pennsylvania

   Mr. E. VanMeter, Metallurgical Engineer, Alloy Steels Metallurgy, Steel Operating Division

8. Republic Steel Corporation, Massilon, Ohio

   Mr. R. J. Place, Sales Engineer
   Mr. D. Whitney, Special Products Sales
   Mr. W. Barcle, Supervisor, Research and Development

9. International Nickel Company, New York, New York

   Mr. C. C. Clark, Technical Services, Development and Research Div.
   Mr. L. Diran, Metallurgical Services

Approved for Public Release

Contrails

APPENDIX II

ULTRASONIC INSPECTION PROCEDURES

Heat 120D163, 1/2 In. Plate Material

Ultrasonic inspection was used to determine the cleanliness of air-melted and vacuum-degassed heat 120D163. A plate, 18 x 24-in., was contact-inspected by means of a 5-megacycle, 1/2-in. transducer and the longitudinal-mode and pulse-echo technique. The instrument (Sonoray Model 5)was calibrated so that the signal representing the first back-reflection reached the top grid line on the instrument's scale. Figure 107 depicts the initial pulse and the first two reflections from the back of the plate. It is significant to note that the attenuation losses are negligible, as evidenced by the very minor difference in the first and second back-reflection signal amplitudes, and permit the direct measurement of flaw indications without compensating for attenuation losses.

The sensitivity used for the inspection was dictated primarily by the predominance of strong signal reflections from discontinuities present in the plate. At the settings used, reflections from a 13/64-in.-dia, flat-bottomed hole that was located 3/8 in. from the transducer had a signal amplitude of 60% of full scale. Signals from many discontinuities found in the plate exceeded this amplitude. Since the second back-reflection was not needed for the inspection, the oscilloscope presentation was adjusted so that only the initial pulse and the first back-reflection would be seen (Figure 107). The instrument was calibrated in such a manner that a full-scale back-reflection signal from the back surface of the plate was located three grid spaces to the right of the initial pulse representing the front surface (Figure 107). The plate was slowly scanned with the transducer restricted to a straight-line movement parallel to the edge of the plate. This was repeated at 1/4-in. intervals until the entire plate was inspected. The area and signal intensity associated with each discontinuity were recorded on the plate and on a map of the plate (Figure 108). A typical oscilloscope track of an internal defect is shown in Figure 107. In this instance, the signal amplitude is in excess of the 60% of full scale associated with a 13/64 in., flat-bottomed hole, and the defect is located about 1-1/2 grid spaces to the right of the initial (contact surface) pulse. The latter observation positions the defect approximately half way through the thickness of the plate. Because the initial impulse obscured information concerning the quality of the plate near the transducer to a depth of approximately 3/16 in., the plate was scanned from both sides.

Three intense ultrasonic indications were checked by metallographic inspection at locations P, R, and S shown on the ultrasonic map in Figure 108. During mounting of these specimens, subsurface cracks were observed. Figure 109 shows the defect at Location R at two magnifications (100 and 500X) It appears to be a stringer of aluminates that probably derived from the remnants of some slag that was not cropped from the ingot. The same defect was also noted in sections P and S.

Approved for Public Release

Contrails

Attempts to detect these defects by means of a shear mode of vibration were unsuccessful. Several angles of incidence, transducers of different frequencies, and various sensitivity levels were used without success. In view of this, it was assumed that the defects were oriented in the plane of the plate surface and that they were not thick enough to observe considering the sensitivity of the shear-wave inspection.

Although the contact method was used in this investigation, either the immersion or the contact-immersion technique is superior and is recommended for ultrasonic inspection of plates and forgings used in the fabrication of large-diameter booster motors. Furthermore, no surface defects have been found on any of the plate materials inspected by use of dye-penetrant or magnetic-particle techniques. However, surface-quality inspection by means of these tests is also recommended for plate and forgings used in the fabrication of large booster motors.

Heat 24158, 3/4 In. Plate Material

The plate material from heat 24158 was inspected by use of the same procedures that were followed in inspecting the plate from heat 120D163 as described above. The inspection indicated that the plate was free of flaws that can normally be detected ultrasonically.

Heat 24158, Ring Forgings

Prior to inspection, the two ring forgings from heat 24158 were surface-machined to provide a surface (RMS 125) suitable to the use of the ultrasonic wave technique. A minimum amount of material was removed in the process in order that the cross-section be altered as little as possible.

A Branson Sonoray, Model 50 unit was used to inspect the material. To inspect the 4-in.-thick forging, the machine was calibrated so that the signal response of the echo from an 8/64-in.-dia, flat-bottomed hole covered 50% of the full screen amplitude. The calibration hole was drilled half way through a 2-1/2-in.-thick test block. An additional gain correction was required for inspecting from the outside diameter of the forging's wall because the response from a convex surface is inherently less than that from a flat surface. At the calibrated gain setting, the third back-reflection from a sound portion of the 2-1/2-in.-thick test block produced a signal response equal to 25% of the full screen amplitude. With the transducer on the convex portion of the forging, the gain was similarly adjusted so that the third back-reflection yielded a signal equal to 25% of full screen. No flaws of any signal amplification were encountered during the regular scan-type inspection.

The same approach was used to inspect the 1-in.-thick ring forging. The 8/64-in.-dia, flat-bottomed hole calibration was performed in a 1/2-in.-thick test bar. The inspection of this forging did not show any significant flaw indications. A 3-1/2 megacycle transducer, 1/2-in.-dia was used for these inspections.

The two forgings were also inspected by use of the shear wave mode. The calibration was accomplished by adjusting the signal response from an 0.015-in.-deep milled slot, one inch wide in a 1/2-in.-thick plate, such that the amplitude was 50% of full-screen with the transducer located 8 in. from the

Approved for Public Release

Contrails

slot. A 3/4 in. by 1/2 in. 2-1/4 megacycle transducer mounted on a 45-deg shoe was used for this inspection. After recording the calibrated gain setting (D 1:39), the gain was increased to D 1:300. The ultrasonic inspection performed at this setting did not detect the presence of any flaw indications.

Approved for Public Release

Contrails

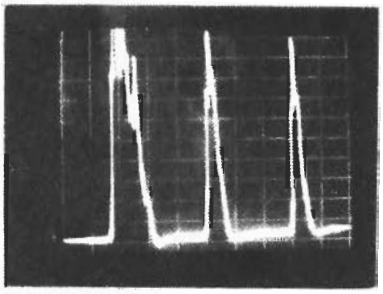

A
Initial Pulse and First and Second Back Reflection from the Plate Surface

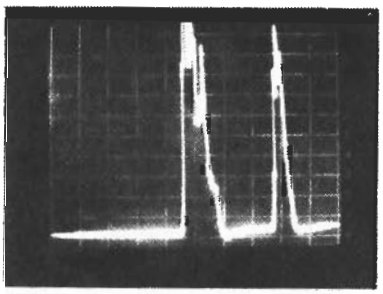

B
Initial Pulse and First Back Reflection from the Plate Surface

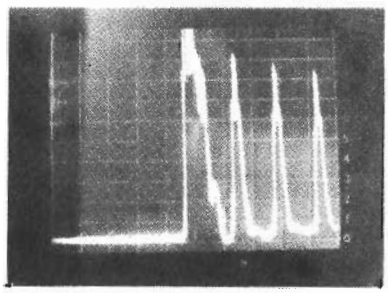

C
Initial Pulse and Three Back Reflections from an Internal Discontinuity

Figure 107. Typical Oscilloscope Traces Obtained During Ultrasonic Inspection of 1/2-In.-Thick, Grade 250, 18% Nickel Maraging Steel Plate, Heat 120D163

Approved for Public Release

Contrails

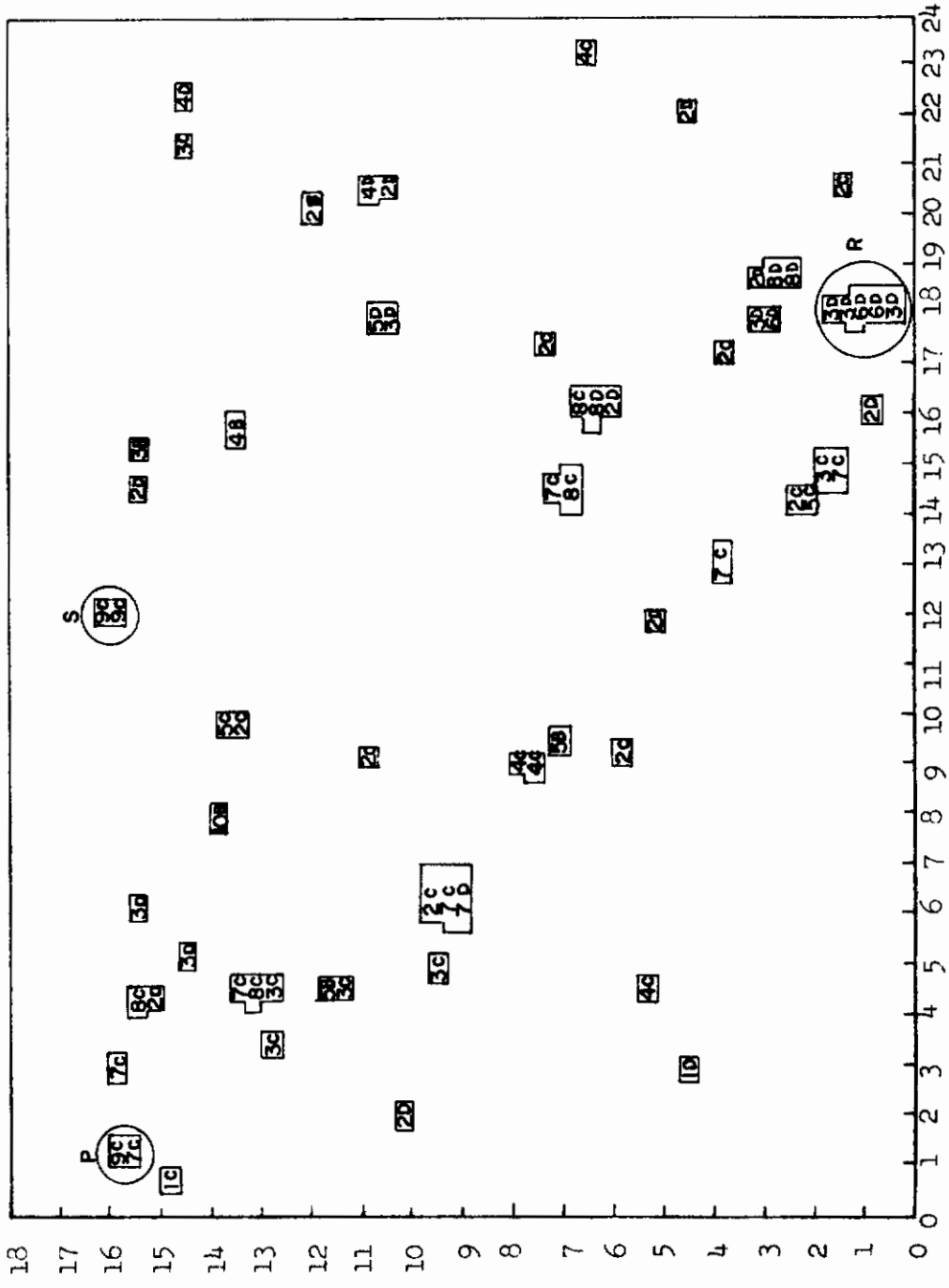

Figure 108. Contact Ultrasonic Test Results from 1/2-In.-Thick, Grade 250, 18% Nickel Maraging Steel Plate, Heat 120D163, Side 1

Approved for Public Release

Contrails

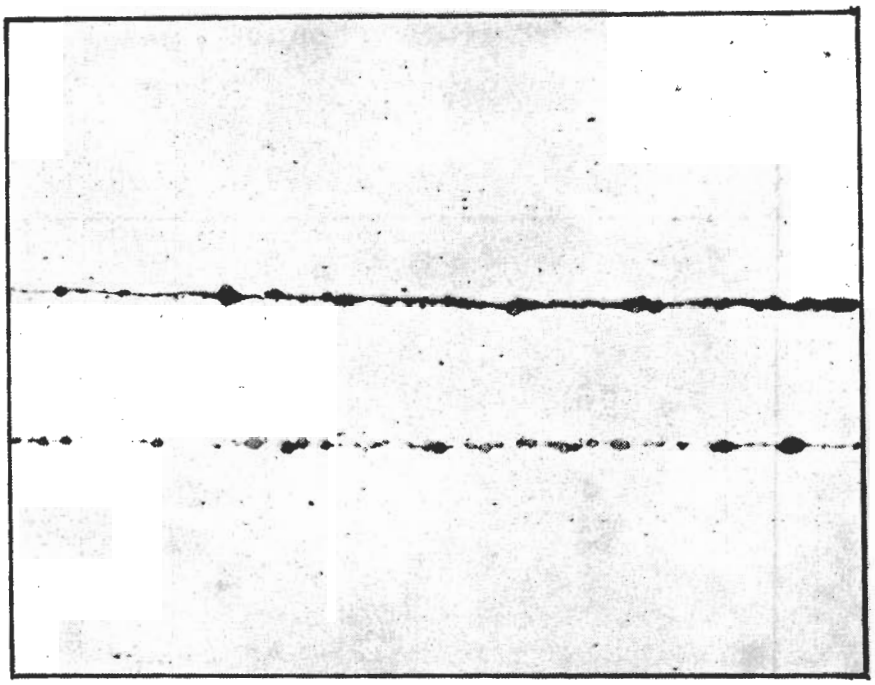

As Polished Magnification: 100X

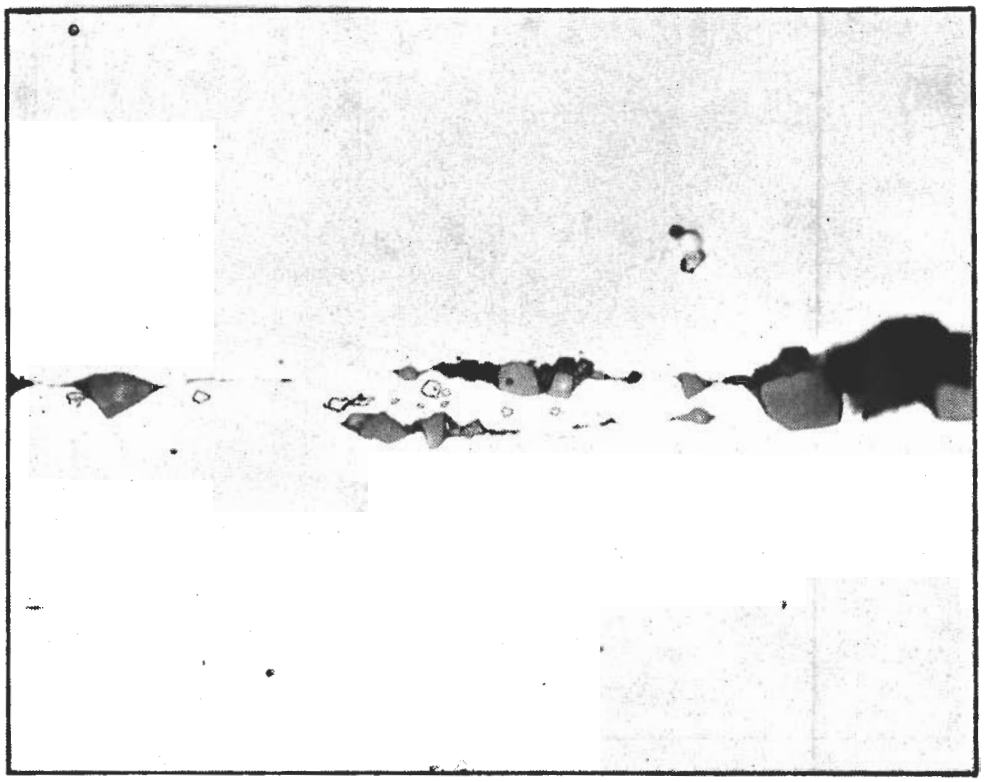

As Polished Magnification: 500X

Figure 109. Inclusions in 1/2-In.-Thick, Grade 250, 18% Nickel Maraging Steel Plate, Heat 120D163, Indicated to be Worst Condition by Ultrasonic Inspection

Approved for Public Release

Contrails

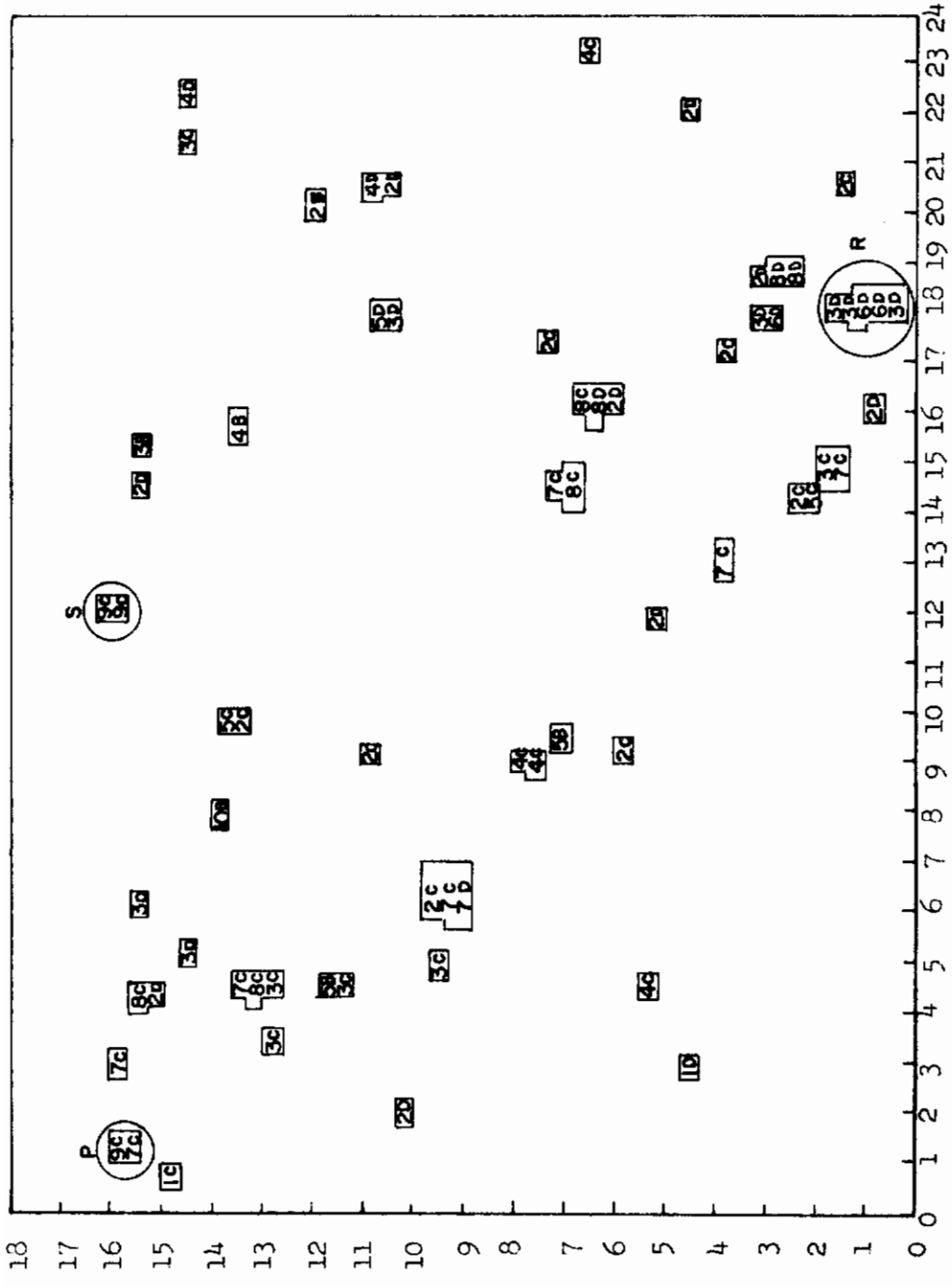

Figure 108. Contact Ultrasonic Test Results from 1/2-In.-Thick, Grade 250, 18% Nickel Maraging Steel Plate, Heat 120D163, Side 1

Approved for Public Release

Contrails

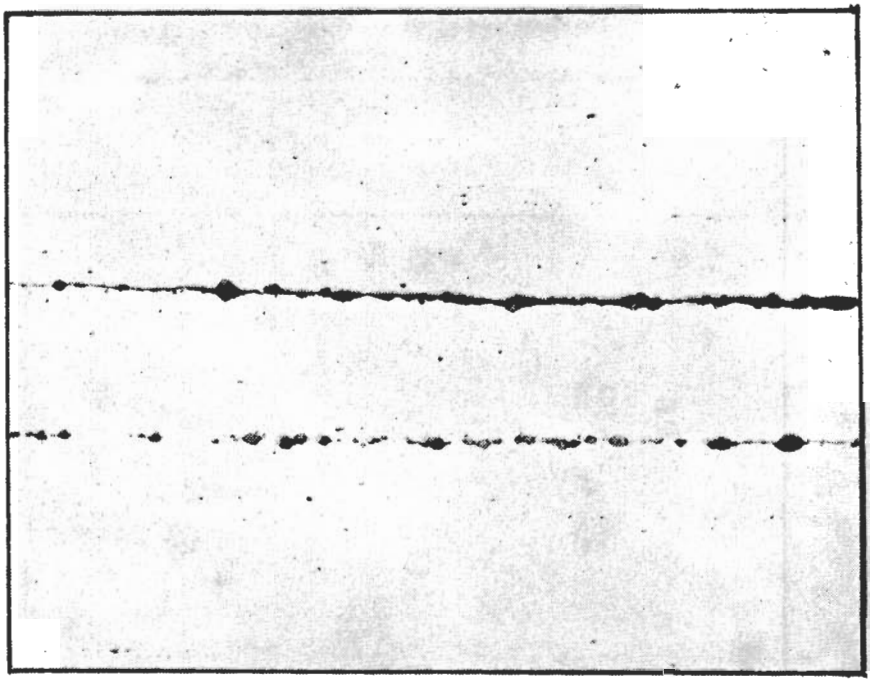

As Polished Magnification: 100X

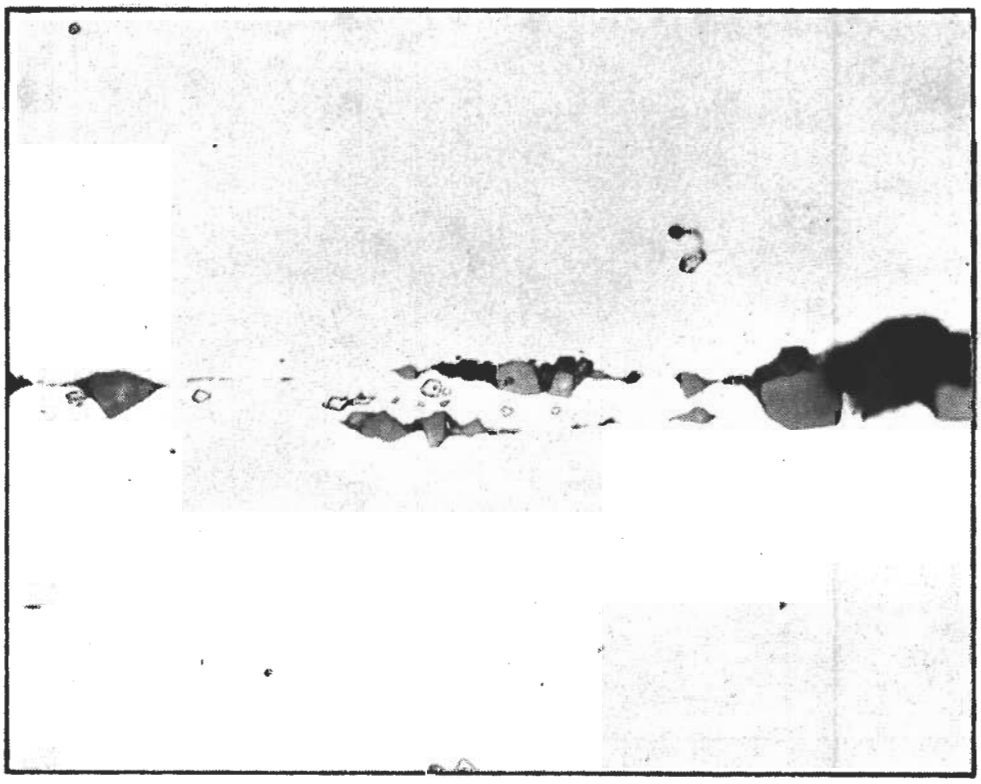

As Polished Magnification: 500X

Figure 109. Inclusions in 1/2-In.-Thick, Grade 250, 18% Nickel Maraging Steel Plate, Heat 120D163, Indicated to be Worst Condition by Ultrasonic Inspection

Approved for Public Release

Contrails

APPENDIX III

TENSION TEST RESULTS

Approved for Public Release

Contrails

TABLE 58
TENSILE PROPERTIES OF GRADE 200, AIR MELTED, VACUUM DEGASSED, 1/2-IN.-THICK, 18% NICKEL MARAGING STEEL PLATE, HEAT 28889
Mill-Annealed at 1500°F for 1 Hour and Aged

Aging Treatment Temp °F	Aging Treatment Time, Hrs	Orientation	Yield Strength at 0.2% Offset, ksi	Ultimate Tensile Strength	Elongation % in 1 inch	Reduction of Area, %	Notch Tensile Strength, ksi
850	2	Longitudinal	183.8	185.0	13.2	56.8	306.9
			185.4	186.3	13.3	64.5	309.5
			186.7	188.2	13.0	59.4	309.6
		Average	185.3	186.5	13.2	60.2	308.7
850	4	Longitudinal	193.7	195.1	13.0	64.6	314.9
			193.8	194.6	12.2	58.7	314.9
			193.5	195.1	14.4	61.5	316.2
		Average	193.7	194.9	13.2	61.6	315.3
850	8	Longitudinal	204.5	205.3	11.5	63.5	321.5
			204.6	205.7	11.9	56.8	328.0
			203.7	204.3	11.8	64.0	327.0
		Average	204.3	205.1	11.7	61.4	325.6
		Transverse	203.8	204.8	11.6	56.4	322.9
			208.2	209.7	11.2	54.5	323.7
			209.1	211.2	11.4	54.7	317.1
		Average	207.0	208.6	11.4	55.2	321.2
850	16	Longitudinal	213.8	214.7	11.2	58.0	333.1
			211.2	211.8	12.0	54.3	333.8
			213.0	214.2	11.3	56.4	364.4
		Average	212.7	213.6	11.5	56.2	343.8
900	2	Longitudinal	200.0	200.8	12.4	63.4	317.8
			197.6	198.2	12.1	54.9	317.1
			197.8	198.2	11.2	62.1	315.2
		Average	198.5	199.1	11.9	60.1	316.7
900	4	Longitudinal	195.5	204.0	10.0	52.7	322.2
			198.0	203.5	9.6	60.4	321.2
			196.5	204.0	9.7	53.3	317.5
		Average	196.7	203.8	9.8	55.5	320.3
		Transverse	202.0	210.0	9.9	53.3	314.5
			201.5	211.5	9.8	53.2	319.7
			201.0	210.5	9.7	53.3	321.9
		Average	201.5	210.7	9.8	53.3	318.7
900	8	Longitudinal	210.7	211.8	11.4	54.9	328.6
			210.1	211.3	12.8	58.4	329.4
			210.8	211.8	11.8	51.1	329.5
		Average	210.5	211.6	12.0	54.8	329.2
		Transverse	216.1	218.1	10.8	48.6	317.1
			217.5	218.3	9.7	51.1	326.5
			216.4	218.0	11.5	50.1	307.4
		Average	216.7	218.1	10.7	50.0	317.0
950	2	Longitudinal	204.7	205.5	11.7	56.0	321.5
			204.8	205.5	11.3	53.5	312.7
			203.6	204.8	12.5	56.7	320.9
		Average	204.4	205.3	11.8	55.4	318.4
		Transverse	210.9	212.0	11.5	51.1	320.8
			209.0	209.7	11.0	48.8	305.7
			208.0	209.2	11.6	49.6	323.3
		Average	209.3	210.3	11.4	49.8	316.6
950	4	Longitudinal	204.0	206.0	12.6	57.0	320.1
			205.2	207.5	13.5	62.1	315.2
			205.4	208.1	13.0	55.7	310.4
		Average	204.9	207.5	13.0	58.3	315.2

Approved for Public Release

Contrails

TABLE 59

TENSILE PROPERTIES OF GRADE 200, AIR MELTED, 1/2-IN.-THICK, 18% MARAGING STEEL PLATE, HEAT 10675
Mill-Annealed at 1500°F for 30 Minutes and Aged

Aging Treatment Temp °F	Time, hrs	Orientation		Yield Strength at 0.2% Offset, ksi	Ultimate Tensile Strength, ksi	Elongation in 1 inch, %	Reduction of Area, %
850	4	Longitudinal		208.4	219.9	12.1	59.4
				217.9	221.0	11.2	58.4
				215.6	219.2	12.0	57.7
			Average	214.0	220.0	11.8	58.5
	8	Longitudinal		217.2	225.2	11.8	56.3
				216.9	225.1	11.9	58.0
				217.2	224.2	10.8	54.1
			Average	217.1	224.8	11.5	56.1
		Transverse		216.4	227.1	10.6	53.7
				218.4	226.1	10.9	52.7
				216.7	227.3	11.3	55.1
			Average	217.2	226.8	10.9	53.8
	16	Longitudinal		229.3	238.4	12.3	51.9
				226.3	235.3	10.8	53.1
				227.3	237.4	11.8	56.3
			Average	227.8	237.0	11.6	53.8
900	2	Longitudinal		204.5	217.2	12.4	58.7
				203.7	217.9	12.5	54.7
				206.1	217.2	12.8	58.3
			Average	204.8	217.4	12.6	57.2
	4	Longitudinal		217.2	227.3	11.0	58.3
				217.2	225.2	11.2	55.7
				218.2	225.9	10.8	57.7
			Average	217.5	226.1	11.0	57.2
		Transverse		215.4	228.5	10.5	53.5
				217.2	229.3	11.0	52.5
				210.3	227.1	9.5	50.9
			Average	214.3	228.3	10.3	52.3
	8	Longitudinal		224.4	235.5	11.3	52.9
				225.5	234.5	10.1	49.6
				226.9	234.5	10.6	50.0
			Average	225.6	234.8	10.7	50.9
		Transverse		227.9	235.5	11.5	51.7
				230.1	230.3	11.1	52.7
				226.5	237.5	11.0	53.9
			Average	228.2	237.4	11.2	52.8
900	16	Longitudinal		238.3	245.4	9.0	50.5
				232.3	242.4	9.4	46.8
				233.3	242.4	9.1	50.9
			Average	234.6	243.4	9.2	49.4
950	2	Longitudinal		220.5	228.1	12.1	55.3
				220.7	226.3	11.0	56.7
				219.2	226.3	10.5	57.7
			Average	220.1	226.9	11.2	56.6
	4	Longitudinal		223.7	230.3	10.3	57.3
				222.2	230.3	10.0	55.7
				223.0	232.3	10.7	56.3
			Average	222.9	231.0	10.3	56.4

Approved for Public Release

Contrails

TABLE 60

TENSILE PROPERTIES OF GRADE 200, AIR MELTED, 1/2-IN.-THICK, 18% NICKEL MARAGING STEEL PLATE, HEAT 10675
Re-Solution Annealed at 1500°F for 30 Minutes and Aged

Treatment Time, hrs	Orientation		Yield Strength at 0.2% Offset, ksi	Ultimate Tensile Strength, ksi	Elongation in 1 in., %	Reduction of Area, %
4	Longitudinal		228.3	235.3	10.5	58.7
			230.7	235.2	11.5	60.0
			219.2	224.4	10.8	58.1
		Average	225.6	231.6	10.9	58.9
8	Longitudinal		224.2	232.3	12.0	58.3
			215.6	238.4	11.9	59.3
			226.1	235.2	15.7	57.0
		Average	222.0	235.3	12.9	58.2
	Transverse		230.2	234.5	11.5	53.5
			225.6	234.1	10.8	56.0
			217.2	227.3	12.0	53.5
		Average	224.3	231.9	11.4	54.3
16	Longitudinal		227.5	235.5	9.5	56.7
			246.9	249.5	11.5	54.3
			231.3	240.4	10.8	55.1
		Average	235.2	241.8	10.6	55.4
2	Longitudinal		228.6	232.2	11.9	58.0
			221.5	227.1	12.6	58.0
			227.3	232.3	12.5	57.3
		Average	225.8	230.5	12.3	57.6
4	Longitudinal		228.1	234.2	10.6	54.3
			231.7	238.3	10.6	58.4
			237.4	242.4	11.1	58.7
		Average	232.4	238.3	10.8	57.1
	Transverse		222.1	234.5	12.6	55.6
			227.9	233.5	12.7	55.1
			225.4	237.5	11.2	55.5
		Average	225.1	235.5	12.2	55.4
8	Longitudinal		237.0	246.5	12.1	54.5
			229.8	236.4	10.7	53.1
			237.3	243.4	11.3	55.3
		Average	234.7	242.1	11.4	54.3
	Transverse		245.9	252.5	11.3	54.7
			246.9	251.5	11.1	56.4
			242.9	248.5	12.0	55.1
		Average	245.2	250.8	11.5	55.4
16	Longitudinal		239.9	247.5	10.0	51.3
			241.5	248.5	9.1	52.9
			237.4	245.4	8.6	53.5
		Average	239.6	247.1	9.2	52.6
2	Longitudinal		222.8	229.0	9.9	57.7
			237.4	240.4	11.8	55.7
			238.8	240.8	10.3	54.7
		Average	233.0	236.7	10.6	56.0
4	Longitudinal		233.2	238.3	12.0	57.4
			227.9	236.4	11.5	54.1
			226.3	237.4	11.5	55.7
		Average	229.1	237.4	11.7	55.7

Approved for Public Release

Contrails

TABLE 61

TENSILE PROPERTIES OF GRADE 200, AIR MELTED, 18% NICKEL MARAGING STEEL 4 x 4-IN. BAR, HEAT 10675
Mill-Annealed at 1500°F for 7-10 Hours and Aged

Aging Treatment Temp, °F	Time, hr		Yield Strength at 0.2% Offset, ksi	Ultimate Tensile Strength, ksi	Elongation in 1 in., %	Reduction in Area, %	Notch Tensile Strength, ksi
850	2		251.5	252.5	9.7	40.6	
			245.3	255.1	8.3	40.0	
			247.4	256.5	7.5	33.9	
		Average	248.1	254.7	8.5	38.2	
850	4		248.5	259.0	8.4	41.4	
			245.5	258.0	8.4	40.5	
			244.0	257.5	8.7	42.0	
		Average	246.0	258.2	8.5	41.3	
850	8		254.0	265.5	9.0	41.0	
			252.0	263.5	8.3	35.9	
			254.5	268.0	9.2	37.7	
		Average	253.5	265.7	8.8	38.2	
850	16		260.6	273.7	8.6	45.6	
			259.5	269.5	8.8	40.6	
			262.1	274.7	7.5	33.3	
		Average	260.7	272.6	8.3	39.8	
900	2		255.8	263.5	9.3	45.4	358.0
			259.3	266.6	9.3	49.6	363.0
		Average	257.6	265.1	9.3	47.5	360.5
900	4		258.7	268.8	8.5	45.2	275.0
			259.7	269.9	9.6	46.4	365.0
			254.9	270.0	10.3	46.1	342.0
		Average	257.8	269.6	9.5	45.9	360.8
900	8		266.9	277.0	10.2	48.1	334.0
			266.3	276.1	8.5	41.0	354.0
			269.1	278.9	9.4	45.5	359.0
		Average	267.4	277.3	9.3	44.8	349.0
900	16		251.4	258.8	10.2	46.3	352.0
			258.3	268.2	8.2	45.1	349.0
			258.7	268.5	8.4	44.5	355.0
		Average	256.1	265.2	8.9	45.3	352.0
950	4		251.5	262.6	11.9	51.3	
			253.0	264.2	8.3	45.2	
			253.0	264.5	8.3	43.0	
		Average	252.5	263.8	9.5	46.5	
950	16		244.3	254.5	7.4	37.2	
			247.4	258.2	9.8	41.8	
			241.4	255.4	8.6	41.7	
		Average	244.4	255.4	8.6	41.7	

Approved for Public Release

TABLE 62

TENSILE PROPERTIES OF GRADE 200, AIR MELTED
18% NICKEL MARAGING STEEL 4 x 4-IN. BAR, HEAT 10675
Re-Solution Annealed at 1500°F for 30 Minutes and Aged

Aging Treatment						
Temp °F	Time, hrs	Rolling Direction	Yield Strength at 0.2% Offset, ksi	Ultimate Tensile Strength, ksi	Elongation in 1 in., %	Reduction of Area, %
850	8	Transverse	223.0	234.2	10.4	50.6
			222.0	232.5	11.2	52.2
			221.8	232.5	10.4	48.0
		Average	222.3	233.1	10.6	50.3
		Short Transverse	222.0	233.0	10.0	48.6
			221.0	234.0	10.0	47.8
			222.0	233.0	9.8	45.6
		Average	221.7	233.3	9.9	47.3
		Longitudinal	221.0	232.0	11.7	59.2
			220.0	230.0	12.2	59.5
			220.1	230.0	12.7	59.5
		Average	220.3	230.7	12.2	59.4
900	8	Transverse	229.0	239.0	11.6	51.0
			229.0	238.0	8.5	36.8
				182.0		
		Average	229.0	238.5	10.0	43.9
		Short Transverse	230.5	238.0	9.8	49.0
			230.5	238.0	12.3	58.3
			230.0	237.0	11.9	57.7
		Average	230.4	237.8	11.3	55.0
		Longitudinal	226.0	237.0	12.5	58.2
			229.0	237.2	10.0	50.0
		Average	227.5	237.1	11.7	54.1

Approved for Public Release

Contrails

TABLE 63

TENSILE PROPERTIES OF GRADE 250, AIR MELTED, 1/2-IN.-THICK, 18% NICKEL MARAGING STEEL PLATE, HEAT 13371
As Rolled and Aged

Aging Treatment Temp °F	Time, hr	Orientation	Yield Strength at 0.2% Offset, ksi	Ultimate Tensile Strength, ksi	Elongation in 1 in., %	Reduction in Area, %
850	4	Transverse	251.0	262.0	8.4	38.8
			253.5	263.6	9.1	39.5
			250.5	263.0	9.5	40.6
		Average	251.7	262.9	9.0	39.6
850	8	Transverse	260.6	272.2	8.2	38.3
			259.5	271.0	8.8	40.6
			260.1	271.7	8.9	37.7
		Average	260.1	271.6	8.6	38.9
900	4	Transverse	264.1	272.7	6.6	33.3
			264.5	272.0	8.0	38.2
			265.5	273.0	8.2	40.0
		Average	264.7	272.6	7.6	37.2
		Longitudinal	244.4	257.0	-	38.9
			243.4	255.5	9.4	40.8
			241.9	253.5	9.6	42.4
		Average	243.2	255.3	9.5	40.7
900	8	Transverse	282.0	286.0	7.5	40.7
			284.0	292.5	7.4	36.7
			283.0	289.0	6.4	38.4
		Average	283.0	289.2	7.1	38.6
		Longitudinal	261.9	269.3	7.9	41.7
			263.7	272.9	7.6	43.3
			263.0	274.0	8.4	43.7
		Average	262.9	272.1	8.0	42.9
950	2	Transverse	266.0	273.0	8.4	41.8
			264.5	271.5	8.6	40.6
			262.5	271.5	6.0	33.2
		Average	264.3	272.0	7.7	38.5
950	4	Transverse	266.0	277.5	8.1	40.0
			266.5	276.0	7.7	39.4
			266.0	275.5	7.1	38.2
		Average	266.2	276.3	7.6	39.2

Approved for Public Release

Contrails

TABLE 64

TENSILE PROPERTIES OF GRADE 250, AIR MELTED, 1/2-IN.-THICK, 18% NICKEL MARAGING STEEL PLATE, HEAT 13371

Solution-Annealed at 1500°F for 30 Minutes and Aged

Aging Treatment Temp °F	Time, hr	Rolling Direction		Yield Strength at 0.2% Offset, ksi	Ultimate Tensile Strength, ksi	Elongation in 1 in., %	Reduction in Area %
850	4	Transverse		263.2	267.8	8.3	45.1
				256.7	265.1	9.7	48.6
				255.0	265.1	9.2	47.3
			Average	258.3	266.0	9.1	47.0
850	8	Transverse		268.0	276.3	8.6	45.5
				270.1	277.4	8.8	47.2
				265.9	274.2	9.0	46.8
			Average	268.0	276.0	8.8	46.5
850	16	Transverse		284.4	290.8	7.7	41.9
				282.3	290.6	7.0	40.2
				284.3	291.4	8.2	44.3
			Average	283.7	290.9	7.7	42.1
		Longitudinal		252.1	275.7	7.6	42.6
				272.7	280.3	7.9	41.6
				268.2	273.3	8.8	43.0
			Average	264.3	276.4	8.1	42.4
900	4	Transverse		275.5	281.0	8.0	43.2
				274.5	281.0	8.3	46.0
				274.1	280.5	7.6	41.2
			Average	274.7	280.8	7.9	43.5
		Longitudinal		260.0	270.5	9.5	47.9
				260.0	266.5	8.2	45.5
				258.0	266.0	8.8	46.7
			Average	259.3	267.7	8.8	46.7
900	8	Transverse		288.0	293.5	7.1	36.7
				285.0	291.0	8.2	40.5
				284.5	292.0	7.6	43.6
			Average	285.8	292.2	7.6	40.3
		Longitudinal		273.3	279.4	7.1	43.1
				273.5	279.4	7.0	41.4
				273.0	279.0	8.3	44.2
			Average	273.3	279.3	7.5	42.9
950	2	Transverse		260.6	267.5	9.2	46.8
				265.3	270.3	8.4	44.8
				256.6	263.6	9.3	47.8
			Average	260.8	267.1	8.9	46.5
950	4	Transverse		271.9	279.0	8.1	42.7
				271.3	280.4	7.6	39.9
				264.5	274.4	8.0	42.2
			Average	269.3	277.9	7.9	41.6

Approved for Public Release

Contrails

TABLE 65

LONGITUDINAL TENSILE PROPERTIES OF GRADE 250, AIR MELTED, VACUUM DEGASSED, 1/2-IN.-THICK, 18% NICKEL MARAGING STEEL PLATE, HEAT 120D163

As Rolled and Aged

Temp, °F	Time, hr		Yield Strength at 0.2% Offset, ksi	Ultimate Tensile Strength, ksi	Elongation in 1 in., %	Reduction in Area, %	Notch Tensile Strength, ksi
850	4						288.9
							322.8
			240.5	255.5	8.7	45.6	351.6
			239.9	255.0	9.6	44.8	336.3
			241.8	256.6	9.0	43.9	329.1
		Average	240.7	255.7	9.1	44.8	327.7
850	8						335.4
							318.2
			248.5	264.5	8.5	46.0	334.5
			249.0	266.0	9.0	47.4	346.4
			247.4	262.1	9.4	45.6	321.1
		Average	248.3	264.2	9.0	46.3	331.1
850	16						357.9
							325.8
			258.5	271.7	8.0	43.4	351.4
			259.5	274.2	7.1	26.6	331.7
			259.0	272.7	8.7	36.5	349.0
		Average	259.0	272.8	7.9	35.5	334.6
900	2		243.4	255.5	9.6	49.6	
			243.4	255.0	9.6	44.2	
			240.9	255.0	9.9	47.4	
		Average	242.5	255.1	9.7	47.1	
900	4						346.7
							343.7
			242.9	257.5	9.9	47.8	360.6
			245.4	257.0	8.6	42.6	369.3
			244.4	259.5	9.4	36.5	300.0
		Average	244.2	258.0	9.3	42.3	344.1
900	8						309.5
			257.5	268.6	7.6	40.2	310.3
			259.8	270.3	9.0	45.8	338.2
			255.0	266.6	8.2	42.6	368.5
		Average	257.4	268.5	8.3	43.9	331.6
900	16		247.9	270.2	6.7	35.9	
			254.5	269.6	7.7	42.6	
			258.5	269.6	7.3	43.2	
		Average	253.6	269.8	7.2	40.6	
950	2		253.5	264.7	5.8	28.1	
			252.5	263.0	5.5	24.6	
			252.5	265.6	7.2	35.3	
		Average	252.8	264.4	6.2	31.1	
950	4		252.5	265.6	7.3	45.6	
			253.0	264.6	8.0	45.6	
			255.6	266.8	9.0	40.3	
		Average	253.7	265.7	8.1	43.8	
950	8		239.4	253.5	8.3	29.8	
			241.4	254.5	9.0	41.2	
			242.4	257.0	9.6	43.0	
		Average	241.1	255.0	9.0	38.0	
950	16		238.9	252.5	11.5	47.2	
			242.4	257.0	9.3	38.9	
			240.4	254.5	10.6	40.8	
		Average	240.6	254.7	10.5	42.3	

Approved for Public Release

TABLE 66

TRANSVERSE TENSILE PROPERTIES OF GRADE 250, AIR MELTED
VACUUM DEGASSED, 1/2-IN.-THICK, 18% NICKEL MARAGING STEEL PLATE, HEAT 120D163
As Rolled and Aged

Aging Treatment		Yield Strength	Ultimate Tensile	Elongation in	Reduction in	Notch
Temp °F	Time, hrs	at 0.2% Offset, ksi	Strength, ksi	1 in., %	Area, %	Tensile Strength, ksi
850	16	264.5	282.0	7.4	35.0	
		265.1	281.3	7.3	34.5	
		269.6	282.8	7.0	38.3	
	Average	266.4	282.0	7.2	35.9	
900	2	251.5	262.1	7.6	42.0	
		253.5	265.2	8.3	41.5	
		251.5	265.7	8.8	39.1	
	Average	252.1	264.3	8.2	40.9	
900	4	256.0	268.6	8.1	36.5	309.5
		256.1	268.8	7.2	40.3	269.0
		254.5	270.2	8.3	41.4	355.0
	Average	255.3	269.2	7.9	39.4	311.2
900	8	264.5	277.5	7.6	40.0	
		266.6	277.7	8.0	33.3	
	Average	265.5	277.6	7.8	36.6	
950	2	260.1	273.7	6.5	35.6	296.0
		259.5	271.7	7.5	40.8	319.0
		260.1	272.7	6.5	38.9	285.0
	Average	259.9	272.7	6.8	38.4	300.0

Approved for Public Release

Confidential

TABLE 67

LONGITUDINAL TENSILE PROPERTIES OF GRADE 250, AIR MELTED, VACUUM DEGASSED, 1/2-IN.-THICK, 18% NICKEL MARAGING STEEL PLATE, HEAT 120D163

Solution-Annealed at 1500°F for 30 Minutes

Aging Treatment						
Temp °F	Time, hrs	Orientation	Yield Strength at 0.2% Offset, ksi	Ultimate Tensile Strength, ksi	Elongation in 1 in., %	Reduction of Area, %
900	8	Longitudinal	237.2	242.6	10.2	55.4
			232.9	239.8	10.2	51.5
		Average	235.1	241.2	10.2	53.4
		Transverse		151.0		
			231.0	241.5	7.9	41.3
		Average	231.0	241.5	7.9	41.3
		Short Transverse	235.0	244.3	8.8	42.5
			232.5	240.6	9.1	47.3
		Average	233.7	242.5	9.0	44.9

Approved for Public Release

Confidential

Contrails

TABLE 68

TRANSVERSE TENSILE PROPERTIES OF GRADE 250, AIR MELTED, VACUUM DEGASSED, 1/2-IN.-THICK, 18% NICKEL MARAGING STEEL PLATE, HEAT 120D163

Solution-Annealed at 1500°F for 30 Minutes

Aging Treatment Temp, °F	Time, hr		Yield Strength at 0.2% Offset, ksi	Ultimate Tensile Strength, ksi	Elongation in 1 in., %	Reduction in Area, %	Notch Tensile Strength, ksi
850	4		254.5	265.0	7.3	32.1	
			253.5	267.5	5.5	28.7	
			254.5	267.5	6.0	26.0	
		Average	254.2	266.6	6.3	28.9	
850	8		262.5	272.5	6.7	26.6	
			263.5	275.5	6.8	30.7	
			263.5	276.0	7.3	40.4	
		Average	263.2	274.7	6.9	32.6	
850	16	269	269.5	281.5	7.4	31.2	
			271.7	281.8	8.3	41.4	
			269.6	283.3	6.6	29.2	
		Average	270.3	282.2	7.4	33.9	
900	2		263.6	270.5	10.0	47.3	264.0
			266.7	274.6.	8.7	46.3	366.5
			263.9	273.6	10.9	45.8	352.0
		Average	264.7	272.9	9.9	46.5	360.8
900	4		271.3	280.6	7.7	37.0	353.0
			271.4	278.9	10.0	45.9	353.0
		Average	271.4	279.7	8.8	41.4	353.0
900	8		274.2	284.0	9.0	46.3	334.0
			274.9	284.7	8.4	45.0	342.0
		Average	274.6	284.3	8.7	45.7	338.0
900	16		265.2	274.1	8.3	43.3	334.0
			257.8	267.1	11.1	50.2	330.0
			258.1	268.5	8.4	44.4	329.0
		Average	260.4	269.9	9.3	46.0	334.3
950	4		259.5	271.2	7.6	42.0	
			259.0	272.7	7.5	41.4	
			260.1	271.2	7.4	38.3	
		Average	259.5	271.7	7.5	40.6	
950	16		250.5	262.6	8.7	37.7	
			250.0	264.6	9.7	38.3	
			252.5	263.6	10.1	40.8	
		Average	251.0	263.6	9.5	39.0	

Approved for Public Release

Contrails

TABLE 69

TENSILE PROPERTIES OF GRADE 250, VACUUM-ARC REMELTED, 1/2-IN.-THICK, 18% NICKEL MARAGING STEEL PLATE, HEAT 3888472
Solution-Annealed at 1500°F for 30 Minutes and Aged

Aging Treatment Temp, F	Aging Treatment Time, hrs	Rolling Direction		Yield Strength at 0.2% Offset, ksi	Ultimate Tensile Strength, ksi	Elongation in 1 in., %	Reduction in Area, %
850	4	Longitudinal		278.0	287.0	9.3	41.4
				278.0	288.2	8.1	34.6
				280.0	287.0	9.7	44.2
			Average	278.7	287.4	9.0	40.1
850	8	Longitudinal		272.5	285.5	9.7	43.5
				274.5	288.0	9.7	44.0
				275.0	288.0	9.4	41.5
			Average	274.0	287.2	9.6	43.0
		Transverse		272.5	283.0	9.0	40.0
				274.0	285.6	6.8	42.0
				271.0	285.5	10.0	43.6
			Average	272.5	284.7	8.6	41.9
850	16	Longitudinal		287.0	292.5	8.7	40.5
				282.5	292.0	9.7	42.0
				282.0	293.5	9.4	40.4
			Average	283.8	292.7	9.3	41.0
900	4	Longitudinal		276.0	285.0	10.2	43.4
				274.0	284.0	9.3	40.4
				282.5	294.0	9.7	42.2
			Average	277.5	287.7	9.7	42.0
		Transverse		275.0	284.0	7.9	36.8
				272.8	282.5	9.9	42.2
				273.2	282.5	9.1	42.6
			Average	273.7	283.0	9.0	40.5
900	8	Longitudinal		272.0	284.0	8.2	41.2
				280.5	293.0	7.6	36.9
				283.8	293.7	9.7	41.7
			Average	278.8	290.2	8.5	39.9
		Transverse		287.5	293.6	8.4	41.7
				284.5	292.5	8.6	40.8
				286.0	294.0	8.7	37.1
			Average	286.0	293.4	8.6	39.9
900	16	Longitudinal		279.0	289.5	8.4	40.0
				279.0	289.0	8.1	38.0
				279.0	290.0	8.6	37.6
			Average	279.0	289.5	8.4	38.5
950	2	Longitudinal		274.0	282.5	9.7	42.2
				274.0	282.5	7.8	33.2
				277.0	282.0	8.9	38.6
			Average	275.0	282.4	8.8	38.0
		Transverse		272.0	293.0	7.5	31.8
				270.0	283.5	8.3	41.5
				271.0	283.0	8.5	37.5
			Average	271.0	286.5	8.1	36.9
950	4	Longitudinal		271.5	282.5	9.0	41.7
				271.5	283.0	10.4	46.0
				269.5	282.5	9.3	42.4
			Average	270.8	282.7	9.6	43.4
950	8	Longitudinal		268.5	282.0	9.3	41.5
				268.5	281.0	9.3	43.7
				268.0	281.0	8.9	42.1
			Average	268.4	281.7	9.1	42.4

Approved for Public Release

Contrails

TABLE 70
TENSILE PROPERTIES OF GRADE 250, VACUUM-ARC REMELTED, 1/2-IN.-THICK, 18% NICKEL MARAGING STEEL PLATE, HEAT 3888473
Solution-Annealed at 1500°F for 30 Minutes and Aged

Aging Treatment Temp °F	Aging Treatment Time, hrs	Rolling Direction		Yield Strength at 0.2% Offset, ksi	Ultimate Tensile Strength, ksi	Elongation in 1 in., %	Reduction in Area, %
850	4	Longitudinal		284.2	291.5	9.3	45.0
				284.0	294.0	9.0	38.4
				280.0	289.0	8.4	36.2
			Average	282.7	291.5	8.9	40.5
850	8	Longitudinal		281.5	292.0	9.2	42.3
				279.0	291.8	8.6	39.9
				279.4	290.5	9.0	39.8
			Average	280.0	291.4	8.9	40.7
		Transverse		283.0	295.0	8.9	37.6
				284.0	296.0	8.2	35.8
				277.0	290.0	7.6	35.8
			Average	281.3	293.6	8.2	36.6
850	16	Longitudinal		289.0	298.0	9.1	42.5
				290.0	300.0	8.2	39.2
				286.0	297.5	8.4	36.1
			Average	283.3	298.5	8.6	39.3
900	4	Longitudinal		278.1	289.0	8.5	38.4
				276.0	285.5	8.6	39.8
				278.0	285.0	7.5	37.6
			Average	277.4	286.5	8.2	38.6
		Transverse		282.4	293.5	8.8	40.0
				280.0	293.6	9.3	40.4
				284.0	293.0	8.2	37.6
			Average	282.1	293.4	8.8	39.3
900	8	Longitudinal		285.0	296.0	8.5	39.2
				290.0	296.0	8.5	39.8
				292.0	298.0	8.9	42.2
			Average	289.0	296.7	8.6	40.4
		Transverse		294.4	302.0	7.9	37.6
				294.0	301.5	8.5	36.3
				295.2	301.6	7.9	36.6
			Average	294.5	301.7	8.1	36.8
900	16	Longitudinal		280.5	292.5	7.9	38.4
				279.8	291.0	8.4	42.0
				276.0	290.5	8.8	40.2
			Average	278.8	291.3	8.4	40.2
950	2	Longitudinal		273.0	284.0	9.2	44.5
				278.0	286.0	8.5	43.0
				273.6	283.6	9.1	43.5
			Average	274.9	284.5	8.9	43.7
		Transverse		280.0	290.0	8.8	41.0
				280.0	289.5	8.4	39.2
				278.0	289.0	8.2	37.8
			Average	279.3	289.5	8.5	39.3
950	4	Longitudinal		274.5	286.8	9.4	41.1
				275.0	286.0	9.5	43.8
				270.5	282.0	8.7	40.2
			Average	273.3	284.9	9.2	41.7
950	8	Longitudinal		267.5	281.0	9.0	39.4
				270.5	283.0	8.1	36.6
				267.0	281.5	9.0	42.3
			Average	268.3	281.8	8.7	39.4

Approved for Public Release

Contrails

TABLE 71

TENSILE PROPERTIES OF GRADE 300, VACUUM-ARC REMELTED, 1/2-IN.-THICK, 18% NICKEL MARAGING STEEL PLATE, HEAT 07148
Mill-Annealed at 1500°F for 30 Minutes and Aged

Aging Treatment Temp °F	Aging Treatment Time, hrs	Orientation		Yield Strength at 0.2% Offset, ksi	Ultimate Tensile Strength, ksi	Elongation in 1 in., %	Reduction of Area, %
850	8	Longitudinal		295.6	304.1	8.2	43.2
				293.6	302.6	8.0	42.4
				293.9	307.6	9.0	41.0
			Average	294.4	304.8	8.4	42.2
	16	Longitudinal		-	-	-	-
				300.1	313.7	8.8	39.0
				304.0	313.1	7.0	36.0
			Average	302.0	313.4	7.9	37.5
900	2	Longitudinal		286.5	292.9	8.5	41.6
				285.6	291.6	9.4	38.8
				283.6	294.5	8.4	43.0
			Average	285.2	293.0	8.8	41.1
		Transverse		280.6	296.6	8.5	43.6
				285.8	297.2	8.6	38.7
				279.6	294.4	8.6	39.2
			Average	282.0	296.1	8.6	40.5
	4	Longitudinal		293.4	301.3	9.4	42.8
				291.9	299.7	9.3	43.6
				291.7	303.2	9.4	40.5
			Average	292.2	302.9	9.4	42.3
		Transverse		295.2	302.7	8.0	36.7
				293.2	303.2	7.8	37.5
				292.4	302.8	8.5	36.6
			Average	293.6	302.9	8.1	36.9
	8	Longitudinal		301.5	310.1	8.9	42.8
				300.0	309.6	9.5	40.2
				299.7	310.6	8.6	43.7
			Average	300.4	310.1	9.0	42.2
		Transverse		-	-	-	-
				302.1	310.1	8.2	37.0
				301.8	310.1	8.0	39.2
			Average	301.9	310.1	8.1	38.0
	16	Longitudinal		306.2	315.6	8.4	38.0
				308.7	315.1	8.6	38.6
				304.0	315.2	8.5	37.2
			Average	306.3	315.3	8.5	37.9
950	2	Longitudinal		290.9	302.9	8.5	41.7
				288.2	299.6	9.6	43.2
				290.6	301.1	9.8	44.8
			Average	289.9	301.2	9.3	43.2
	4	Longitudinal		297.2	306.7	7.9	40.0
				294.6	305.6	8.4	37.7
				298.0	306.6	8.2	43.2
			Average	296.6	306.6	8.2	38.8

Approved for Public Release

Contrails

TABLE 72

TENSILE PROPERTIES OF GRADE 300, VACUUM-ARC REMELTED, 1/2-IN.-THICK, 18% NICKEL MARAGING STEEL PLATE, HEAT 07148 Re-Solution Annealed at 1500°F for 30 Minutes and Aged

Aging Treatment Temp °F	Aging Treatment Time, hrs	Rolling Direction		Yield Strength at 0.2% Offset, ksi	Ultimate Tensile Strength, ksi	Elongation in 1 in., %	Reduction of Area, %
850	4	Longitudinal		287.9	302.0	8.2	41.4
				289.2	298.4	7.2	40.3
				287.9	305.1	7.0	42.0
			Average	288.3	301.8	7.5	41.2
	8	Longitudinal		297.0	306.0	7.3	37.7
				298.0	305.5	6.7	38.3
				298.0	307.1	6.7	38.9
			Average	297.7	306.2	6.9	38.3
	16	Longitudinal		304.1	312.1	6.7	38.3
				303.5	310.1	6.1	37.1
				305.5	312.6	6.7	38.4
			Average	304.4	311.6	6.5	37.9
900	2	Longitudinal		285.3	293.9	7.4	37.7
				287.9	295.9	7.6	38.9
				283.8	294.9	7.7	40.2
			Average	285.7	294.9	7.5	38.9
	4	Longitudinal		292.9	301.5	7.6	41.0
				290.4	300.5	7.6	39.5
				291.9	300.5	7.4	38.3
			Average	291.7	300.8	7.5	39.6
		Transverse		292.9	301.5	7.1	37.1
				292.8	301.9	7.4	36.0
				288.9	299.5	7.0	37.1
			Average	291.5	301.0	7.2	36.7
900	8	Longitudinal		303.0	311.1	7.1	40.2
				302.0	310.1	7.2	38.3
				300.5	310.1	7.2	38.9
			Average	301.8	310.4	7.2	39.1
		Transverse		298.5	310.1	6.7	34.5
				300.1	309.6	5.4	30.7
				298.5	308.1	6.7	35.1
			Average	299.1	309.3	6.3	33.4
900	16	Longitudinal		301.4	315.2	7.0	38.4
				305.5	314.2	7.2	40.3
				304.0	313.1	7.1	38.3
			Average	303.6	314.2	7.1	39.0
950	2	Longitudinal		292.9	302.0	8.0	41.5
				291.9	303.0	8.1	40.2
				297.9	304.0	7.5	38.4
			Average	294.2	303.0	7.9	40.0
		Transverse		295.2	302.0	6.8	34.9
				292.9	303.0	7.2	34.5
				292.9	302.5	6.8	32.7
			Average	293.7	302.5	6.9	34.0
950	4	Longitudinal		300.4	305.5	8.1	41.5
				298.0	305.0	7.9	43.0
				291.3	303.0	7.6	42.3
			Average	296.7	304.5	7.9	42.4
		Transverse		290.9	304.0	6.7	[illegible]
				292.8	304.5	6.4	[illegible]
				297.0	305.1	6.2	35.3
			Average	294.0	304.5	[illegible]	[illegible]
950	8	Longitudinal		299.4	304.4	7.5	39.5
				295.3	306.0	7.2	39.1
				297.1	303.5	7.2	[illegible]
			Average	[illegible]	304.6	7.3	39.2

Approved for Public Release

Contrails

TABLE 73

TENSILE PROPERTIES OF GRADE 300, VACUUM-ARC REMELTED, 18% NICKEL MARAGING STEEL, 4 x 4-IN. BAR, HEAT 07148
Mill-Annealed at 1500°F for 4 Hours and Aged

Aging Treatment		Orientation		Yield Strength at 0.2% Offset, ksi	Ultimate Tensile Strength, ksi	Elongation in 1 in., %	Reduction of Area, %
Temp - °F	Time, hrs						
900	8	Longitudinal		300.4	311.6	6.7	35.4
				297.0	310.1	7.4	33.3
				297.5	311.1	5.5	30.1
			Average	298.3	310.9	6.5	32.9
		Transverse		297.4	310.6	2.5	10.1
				298.0	312.7	3.6	14.5
				298.0	311.1	4.6	13.9
			Average	297.8	311.5	3.6	12.8
		Short Transverse		295.2	311.1	4.5	27.4
				299.4	310.6	3.9	13.8
				300.4	311.6	4.8	26.0
			Average	298.3	311.1	4.4	22.4

Approved for Public Release

TABLE 74

TENSILE PROPERTIES OF GRADE 300, VACUUM-ARC REMELTED, 18% NICKEL MARAGING STEEL, 4 x 4-IN. BAR, HEAT 07148
Re-Solution Annealed at 1500°F for 30 Minutes and Aged

Aging Treatment				Yield Strength at 0.2% Offset, ksi	Ultimate Tensile Strength, ksi	Elongation in 1 in., %	Reduction of Area, %
Temp °F	Time, hrs	Orientation					
900	4	Longitudinal		300.0	307.0	3.2	14.5
				300.5	308.5	8.0	42.1
			Average	300.3	307.0	5.6	28.3
		Transverse		295.0	305.0	3.9	18.4
				295.5	306.5	3.4	15.0
			Average	295.3	305.7	3.6	16.7
		Short Transverse		300.5	307.5	3.6	17.4
				300.5	307.0	3.5	16.1
			Average	300.5	307.3	3.5	16.7
900	8	Longitudinal		308.7	315.3	8.0	43.7
				309.0	317.0	7.6	40.6
				310.5	316.0	7.6	43.1
			Average	309.4	316.1	7.7	42.5
		Transverse		303.5	312.9	3.6	15.8
				307.9	317.5	7.6	41.9
				311.0	315.0	2.8	12.8
			Average	307.5	315.1	4.7	23.5
		Short Transverse		311.5	318.0	3.7	20.5
				304.5	312.1	3.6	18.3
				307.0	316.5	2.4	11.8
			Average	307.7	315.5	3.2	16.9

Approved for Public Release

Contrails

TABLE 75

TENSILE PROPERTIES OF 3/4-IN.-THICK, 18% NICKEL MARAGING STEEL PLATE, HEAT 24158
Re-Solution Annealed at 1500°F for 30 Minutes and Aged

Aging Condition Temp. °F	Time, hrs.	Orientation	Yield Strength at 0.2% Offset, ksi	Ultimate Tensile Strength ksi	Elong. in 1-in. %	Reduction of Area, %
850	4	Longitudinal	185.8	193.5	12.3	63.1
			183.8	192.4	11.4	79.3
			184.4	191.4	13.0	62.6
			184.3	192.4	12.2	68.3
850	8	Longitudinal	200.1	202.6	11.0	60.0
			196.0	205.1	10.5	60.4
			196.5	204.7	10.8	59.4
			197.5	204.1	10.8	59.9
		Transverse	194.9	203.5	11.0	59.7
			197.0	205.9	10.3	53.1
			196.5	206.0	8.5	53.5
			196.1	205.1	9.9	55.4
850	16	Longitudinal	200.5	208.1	10.7	59.7
			201.6	208.2	11.0	60.4
			200.6	210.3	10.4	60.4
			200.9	208.9	10.7	60.2
900	2	Longitudinal	187.9	197.5	11.3	61.4
			187.4	198.6	11.3	60.4
			189.4	198.6	11.1	62.1
			188.2	198.2	11.2	61.3
900	4	Longitudinal	194.6	203.3	10.5	59.7
			194.4	203.0	10.7	59.3
			193.5	202.6	12.0	59.0
			194.2	203.0	11.1	59.3
		Transverse	196.5	204.7	9.5	53.1
			195.4	204.5	10.5	52.5
			194.4	204.0	10.6	52.5
			195.4	204.4	10.2	52.7
900	8	Longitudinal	198.4	208.3	11.2	59.1
			197.0	206.6	10.7	58.8
			195.1	206.4	12.2	59.7
			196.8	207.1	11.4	59.2
900	8	Transverse	199.5	207.6	10.1	51.3
			199.1	208.3	10.4	52.1
			200.0	208.6	10.5	53.1
			199.5	208.2	10.3	52.2
900	16	Longitudinal	198.8	207.7	11.2	60.1
			196.0	205.6	12.2	59.8
			198.1	206.4	10.5	58.7
			197.6	206.6	11.3	59.5
950	2	Longitudinal	190.9	200.6	10.6	59.1
			190.9	201.6	11.2	58.0
			193.5	202.6	10.8	58.4
			191.8	201.6	10.9	58.5
950	4	Longitudinal	189.4	200.5	13.0	59.8
			191.5	201.7	12.0	59.7
			190.5	200.8	12.1	59.4
			190.5	200.9	12.4	59.6
950	8	Longitudinal	192.2	202.6	10.4	59.5
			194.5	204.7	11.3	55.4
			193.5	203.7	12.5	58.4
			193.4	203.7	11.4	57.8
		Transverse	197.0	205.7	10.9	53.1
			196.0	205.0	10.4	53.1
			194.9	204.5	11.3	54.7
			196.0	205.1	10.9	53.6
950	16	Longitudinal	196.3	204.7	10.1	60.5
			196.6	204.3	11.8	58.7
			198.6	207.2	9.8	50.8
			197.2	205.4	11.9	56.7

Approved for Public Release

Contrails

TABLE 76

TENSILE PROPERTIES OF 18% NICKEL MARAGING STEEL, 4 x 4-IN. FORGING, HEAT 24158

Re-Solution Annealed at 1500°F for 30 Minutes and Aged

Aging Cycle Temp °F	Aging Cycle Time, Hrs.	Orientation	0.2% Offset Yield Strength, ksi	Ultimate Tensile Strength, ksi	Elongation in 1-inch %	Reduction of Area, %
850	8	Longitudinal	181.8	193.5	10.5	47.0
			183.3	194.5	10.8	48.0
		Average	182.5	194.0	10.7	47.5
		Transverse	181.7	195.1	6.2	29.5
			182.3	195.5	9.3	36.6
		Average	182.0	195.3	7.7	33.1
		Short Transverse	183.3	195.5	10.3	48.6
			185.9	196.0	10.6	52.5
		Average	184.6	195.7	10.4	50.5
900	8	Longitudinal	200.0	209.6	9.7	48.0
			198.6	209.3	9.2	47.6
		Average	199.3	209.4	9.4	47.8
		Transverse	196.5	208.3	7.4	32.1
			201.1	211.8	6.3	30.7
		Average	198.8	210.0	6.9	31.4
		Short Transverse	198.1	208.8	9.0	41.5
			196.9	208.1	9.0	40.6
		Average	197.5	208.4	9.0	41.0

Approved for Public Release

Contrails

TABLE 77

TENSILE PROPERTIES OF 18% NICKEL MARAGING STEEL, 1 x 4-IN. FORGING, HEAT 24158

Re-Solution Annealed at 1500°F for 30 Minutes and Aged

Aging Cycle Temp °F	Aging Cycle Time, Hrs.	Orientation	0.2% Offset Yield Strength, ksi	Ultimate Tensile Strength, ksi	Elongation in 1-inch %	Reduction of Area, %
850	8	Longitudinal	188.1	198.2	11.1	54.3
			186.9	197.0	11.3	54.7
		Average	187.5	197.6	11.2	54.5
		Transverse	188.0	199.8	10.8	53.3
			190.9	202.5	10.3	49.0
		Average	189.4	201.1	10.5	51.1
900	8	Longitudinal	203.7	212.2	10.3	48.6
			203.5	211.1	8.7	43.2
		Average	203.6	211.5	9.5	45.9
		Transverse	203.0	213.6	9.3	50.5
			202.0	212.5	9.8	49.0
		Average	202.5	213.0	9.6	49.7
950	8	Longitudinal	197.4	206.9	11.3	44.4
			197.0	206.6	11.8	48.0
		Average	197.1	202.1	11.6	46.2
		Transverse	199.0	207.5	11.1	44.4
			199.6	208.6	10.5	48.2
		Average	199.3	208.0	10.8	46.3

Approved for Public Release

Contrails

APPENDIX IV

AN EVALUATION OF SLOW-NOTCH-BEND TEST PROCEDURES

A. FATIGUE CRACKING AND BEND TESTING PROCEDURES IN THE SLOW-NOTCH-BEND TEST

1. Fatigue Cracking

Slow-notch-bend (SNB) bars were fatigue-cracked on the electrodynamic vibration system shown in Figure 110. Special components added to this machine for cracking the SNB specimens included a fixture to hold the specimen in place during vibration and a weight that could be attached to one end of the bars to be cracked (weights used in this program were 1-1/4 and 2 lb for 1/2 and 3/4-in.-wide by 3/4-in.-deep specimens, respectively). One end of a bar was inserted in the vise so that the notch was close to the holding fixture, thus inducing a maximum bending moment in the notched section. The weight was installed on the other end of the bar. The specimen was then subjected to vibration at resonant frequency (approximately 600 to 700 cps for a 1/2-in.-wide bar) until a crack approximately 0.100 in. deep appeared below the vertex of the machined notch. The input intensity level during vibration was 45 to 50 g-pk. The length of cycle required to produce a desired crack was 2 to 3 min. The stress level for fatigue cracking 1/2 x 3/4-in. bars was calculated to be approximately 80 ksi at the midsection of the bar. Penetrant ink was used to facilitate detection of the crack growth.

2. Slow Bending

Slow-notch-bend tests were made on a 60,000-lb, hydraulically operated, Baldwin testing machine. The rate of loading was 2500 lb per min (manually controlled with a pacer). The load range was either 0 to 1200 or 0 to 30,000 lb, depending on the maximum load required for the material condition being tested.

Test-bar deflection was measured with a microformer-type deflectometer in conjunction with a stress-strain recorder. The deflection of the test specimen was measured from the movement of the load-applying mandrel.

The three-point-loading apparatus is shown in Figure 111. The supporting rollers were made from alloy steel with the surfaces ground to a 16 RMS finish. All critical dimensions were held to close tolerances. To permit accurate location of the machined V-notch at mid-span, the distance between one end of each test specimen and the V-notch was machined to 2 in. + 0.003 in. Before the test was conducted, the specimen was centered between the upper rollers and the load-applying mandrel by a micrometer (attached to the bend fixture) that was in contact with the indexing end of the test piece. A load of 500 to 1000 lb was then applied and released to eliminate any backlash that might be encountered in the gears of the microformer recorder. This practice ensured a straight line within the proportional limit on the load-deflection curve.

Approved for Public Release

Contrails

B. BASIS OF SLOW-NOTCH-BEND TEST FRACTURE TOUGHNESS CALCULATIONS

1. Irwin's Expression for G and the Modification by Rawe

Irwin and his coworkers have shown that the strain-energy release rate (G) in a slow-notch-bend test bar of the configuration shown in Figure 112 can be expressed in terms of the load and the change in spring constant with respect to crack depth.* If the applied load per unit thickness is 2P and the elastic displacement of load application is e, then

$$2P = Me \tag{1}$$

where M is the spring constant per unit thickness. Irwin has shown that

$$G = \frac{1}{2}(2P)^2 \frac{d(1/M)}{da} \tag{2}$$

For the general case of beam-width, b, Equation 2 can be written as:

$$G = \frac{1}{2}(L/b)^2 \frac{d(b/M)}{da} \tag{3}$$

where: L = 2P, maximum failure load,

M = L/e, spring constant per unit width of specimen,

e = deflection at maximum load,

b = beam width,

$\frac{b}{M}$ = reciprocal of the spring constant for a given width, and

a = crack depth.

Thus, the spring constant of a bar in bending is defined as the load divided by the deflection of the load. For a given specimen width, the spring constant varies as the depth beneath the notch, or inversely, as the notch depth.

In notched bars containing a fatigue crack at the apex of the machined notch, the crack effectively increases the notch depth and, therefore, influences the spring constant. If the variation of spring constant as a function of crack depth is accurately known, then measurement of the spring constant in a given test specimen provides the crack depth at any load.

To determine the relationship between spring constant and notch depth, a series of calibration bars containing varying notch depths (from 0 to approximately 0.400 in. deep) are tested. The spring constant for each bar is determined by loading the bar elastically and autographically

*G. R. Irwin, J. A. Kies, and H. L. Smith, Fracture Strength Relative to Onset and Arrest of Crack Propagation, ASTM, Volume 58, p. 640 (1958).

Approved for Public Release

Contrails

recording the load-deflection curve. The spring constant of a bar is determined from the slope of the load-deflection curve as

$$M = L/e$$

where: L = applied load, and

e = deflection caused by the load.

Three or four loadings and unloadings per bar increase the accuracy of the slope measurement when the deflections are averaged. When the reciprocal of the spring constant, b/M, is plotted against effective crack depth, a curve such as that shown in Figure 113 results.

The equation of the curve relating spring constant to notch or crack depth, a, was found by Rawe* to be of the form

$$b/M = M_o + Qa^2 + Ra^3 + Sa^4 \qquad (4)$$

where: M_o is the intercept on the b/M axis (or the reciprocal of the spring constant of an unnotched bar), and Q, R, S are the constants defining the position of the curve with respect to b/M and a. The values of the constants are determined by computer solution of three simultaneous equations involving three unknowns (Q, R, and S) by substituting three values for b/M and corresponding values of a as determined from the calibration curve, in Equation 4.

The fracture toughness of a material is a function of the first derivative of the reciprocal of the spring constant with respect to the crack depth, a. Differentiating Equation 4 with respect to a:

$$\frac{d(b/M)}{da} = 2Qa + 3Ra^2 + 4Sa^3. \qquad (5)$$

Substituting this in Irwin's equation (Equation 3) results in the relationship

$$G = \frac{1}{2}(L/b)^2 (2Qa + 3Ra^2 + 4Sa^3). \qquad (6)$$

Values of G are obtained from Equation 6 by use of a computer, using the previously determined coefficients Q, R, and S, and values of load, L, specimen width, b, and crack depth, a, determined from individual SNB test specimens.

---

*R. A. Rawe, Slot Notch Bend Test Procedure, Aerojet-General Report M2085, August (1960).

Approved for Public Release

Contrails

2. Calculation of the Plane-Strain Fracture Toughness

In determining plane-stress fracture toughness, the load and crack length at the onset of instability are the basis for calculation. In determining plane-strain fracture toughness, the load and crack depth corresponding to initial crack growth are the basis for calculation. To determine the plane-strain fracture toughness of a given heat of material, slow-notch-bend test specimens are loaded to failure, and load-deflection curves are autographically recorded. The spring constant is determined by measuring the specimen width, and by reading from the load-deflection diagrams the values of load and deflection, e, corresponding to initial crack growth. Reference is then made to the previously constructed calibration curve to determine the effective crack depth as a function of the reciprocal of the spring constant, eb/L.

Autographically recorded load-deflection diagrams of slow-notch-bend tests consist of two general types. The first of these is the type-1 diagram, in which failure of the test specimen occurs before the proportional-limit load is reached. The second is the type-2 diagram, in which failure of the test specimen occurs after plastic-deformation work is done in bending; that is, failure beyond the proportional limit. These diagram types are illustrated in Figure 114. When a material fails and a type-1 load-deflection diagram is recorded, maximum load is used to calculate fracture toughness without problem. On the other hand, when a material failure produces a type-2 load-deflection diagram, initial deviation from the straight-line portion of the load-deflection diagram may be attributed either to the formation of a plastic zone at the tip of the fatigue crack or to initial crack extension. Preliminary ink-staining experiments indicate that pop-in occurs at or just beyond the proportional limit. These results are illustrated in Figure 115, which show a typical type-2 load-deflection curve obtained for a Grade 200 18% nickel maraging steel and the extent of crack growth associated with various points along the curve.

The extent of crack growth associated with this point and at other locations along the load-deflection curve, were determined by means of a series of 0.5-in. thick 18% nickel maraging steel bend-test-specimens that were loaded to various points along this curve. Then, ink was introduced in the crack and the specimen unloaded and allowed to dry. Next, the specimens were fractured and photographs were taken of the fracture surface to show the extent of crack propagation that occurred during the loading.

In calculating the plane-strain fracture toughness, the load associated with the initial deviation from a straight line is used (point X). From the fracture surfaces shown in Figure 115, the crack propagation, as outlined by the ink staining, that occurred at point X on the load-deflection curve apparently was associated entirely with the flat fracture surface. Consequently, fracture-toughness values calculated by using the load and deflection associated with the first deviation from linearity in the load-deflection curve should provide an accurate measurement of plane-strain fracture toughness.

Whenever the load-deflection diagram indicates that pop-in occurs, it may be associated with secondary rather than initial crack

Approved for Public Release

Contrails

extension. Thus, for a type-2 load-deflection diagram, the calculation of plane-strain fracture toughness based on pop-in indications from the load-deflection diagram generally involves loads above the proportional limit, which, result in higher values of G_{nc} than the calculation based on proportional-limit load. Thus, use of the proportional-limit load is a conservative approach. For example, in connection with the type-two load-deflection diagram for heat 24158, the G_{Ic} (Bueckner) value corresponding to the proportional-limit load of 5889 lb was 409 in.-lb/in.^{2} and the value of corresponding to the pop-in load of 6220 lb was 435 in.-lb/in.^{2}

C. DISCUSSION OF THE SLOW-NOTCH-BEND TEST

As a rough check on the accuracy of the spring-constant method for determining the crack depth, the measured (optically) and effective (spring-constant) crack depths in heat 24158 were compared. Figure 116 indicates good agreement between the measured and effective crack depths and shows the consistency of the fatigue-crack depths. In theory, the crack depth as determined from the spring-constant calibration curve should reflect the depth of the notch-plus-crack as well as the plastic zone formed at the tip of the crack - this is called the "effective" crack depth. Thus, the effective crack depth should be somewhat larger than the optically measured crack depth. Slow-notch-bend data have provided numerous examples of measured crack depths that were found to be greater than the effective crack depths; this has raised a question as to the source and magnitude of experimental error in the SNB test. Obviously, there is a practical limit to the accuracy of the experimental procedure used in determining the calibration curve and the loads and deflections in the individual SNB tests. The following paragraphs discuss various sources of error in the SNB test.

1. Effect of Errors in the Measurement of Load and Crack Depth

The scatter in SNB test data may be partly the result of experimental errors in determining the proportional-limit load and the effective crack depth. Although the load-deflection diagrams of 18% nickel maraging steel generally gave straight lines up to the proportional limit, occasionally the straight-line portion of the diagram involved some curvature which made accurate selection of the proportional-limit load uncertain. Likewise, errors in the effective crack depth may result from errors in the original calibration or in reading the calibration curve.

The effect of such experimental error on the calculated value of G_{nc} is illustrated in Table 78. This table shows the effect of 5 and 10% errors in the proportional-limit load on the fracture toughness G_{nc} at three crack-depth levels. The sample calculations indicated that a 5% error in effective crack depth can cause a greater change in the fracture toughness value (G_{nc}) than a 5% error in estimating the proportional-limit load. It should be noted in this connection that an error in estimating the proportional-limit load has little effect on eb/L (the reciprocal of the spring constant) and, thus, has little influence on the effective crack depth. The experimental error in reading the effective crack depth from the calibration curve is of the order of 2% (see the appended sample calculations); however, the calibration curve itself may be somewhat inaccurate.

Approved for Public Release

Contrails

2. Reproducibility of the Calibration Curves

To determine the reproducibility of the calibration curves, calibrations were made for each grade of maraging steel and for each specimen size. Figure 117 shows the scatter in 11 calibration curves, involving eight heats of 18% nickel maraging steel (two of which were Grade 250, three were Grade 200, three were re-run calibration curves). At $eb/L = 160$ in.^{2}/lb x 10^{-8}, the re-run calibration curve for heat 24158 (see Figure 118) fell mid-way in the scatter band at a = 0.250 in. (from Figure 116 this is a typical notch-plus-crack depth). To illustrate the magnitude of the error that would be introduced by using a "representative" plot of 1/M versus a for all heats and grades of 18% nickel maraging steel, the following values compare the G_{nc} values calculated from: 1) the re-run calibration curve for heat 24158 at the center of the scatter band, 2) the calibration and coefficients curve for heat 120D163 (see Figure 113) at the low side of the scatter band ($eb/L = 160 \times 10^{-8}$ and a = .236) and the first-run calibration curve and coefficients for heat 24158 at the high side of the scatter band ($eb/L = 160 \times 10^{-8}$ and a = 0.270).

Calibration Curve	eb/L (in.^{2}/lb)	Effective Crack Depth, a (in.)	G_{nc}* (in.-lb/in.^{2})
1st-run 24158	160×10^{-8}	0.270	422
re-run 24158	160×10^{-8}	0.250	329
1st-run 120D163	160×10^{-8}	0.236	355

*Assuming a 9000 lb proportional-limit load.

Thus, if a representative curve were used, the G_{nc} toughness value would be 329 in.-lb/in.^{2}, whereas the actual G_{nc} values calculated from curves on either extreme of the band would be 422 in.-lb/in.^{2} and 355 in.-lb/in.^{2} (calculated from the b/M versus a curve at the low side of the band). Based on a comparison between the toughness calculated from the representative curve and the toughness computed from actual curves falling at either extreme of the band, the percent (calculated from the b/M versus a curve on the high side of the band) difference was indicated to be as much as (422-329)/422 or 22%. Thus, comparisons between calibration curves from grade-to-grade and heat-to-heat indicated that the use of a single curve for all grades might introduce a significant error in calculating the fracture toughness. Consequently, the fracture toughness calculations in this investigation were based on individual calibration curves for each heat and grade.

To provide further information on the reproducibility of calibration curves, each of two sets of calibration bars (one set 1/2 x 3/4 x 4-in. and the other set 3/4 x 3/4 x 4-in.) from the same 3/4-in.-thick plate material (heat 24158) was tested twice, using the calibration procedure described earlier in this appendix. In other words, calibration curves were established with each of the two sets of bars by using the standard procedure. Then, each set of bars was re-run to establish a second set of calibration curves. Comparisons were made between the calibration curves

Approved for Public Release

Contrails

for the two sizes of test specimens and between the re-run calibration curves for a given size of test specimen. The results in terms of G_{nc} are presented in Tables 79 and 80, and the calibration curves are shown in Figures 118 and 119.

Table 79 indicates that the re-run calibration curve generally resulted in lower G_{nc} values. The decrease in fracture toughness values resulted from lower effective crack-depth values and a change in the calibration-curve coefficients. The largest difference in G_{nc} values were obtained where the effective crack-depth values were larger than 0.3 in. The fracture toughness values differed in some instances by over 150 in.-lb/in.^{2}, suggesting that one of the two calibration-curve equations does not accurately fit the experimental results for large values of effective crack depth.

The possibility of strain-hardening at the tip of the crack from run-to-run was discounted because there did not appear to be any systematic change in slope from one loading to the next in testing the calibration bars (three or four loadings and unloadings of each calibration bar was standard in determining the spring constant). However, the fact that the slope subsequently changed on re-running the calibration experiment suggest the possibility of strain-aging in the plastic zone at the tip of the crack. This hypothesis is supported by the fact that the effective crack depth, a, consistently decreased as the result of a re-run (compare effective crack depths a_1 and a_2 in Tables 79 and 80). If such a phenomenon does in fact occur in laboratory testing of the 18% nickel maraging steel alloys, it would also be expected in connection with a defect in service. Therefore, the use of re-run calibration curves may better represent service conditions and, in any case, constitutes a conservative approach.

A comparison of the scatter in G_{nc} values as calculated from the two calibration curves showed that a reduction of scatter in the order of 20% or more was obtained by using the re-run calibration curves. However, some scatter within any one group of replicate test specimens was still present, regardless of which calibration curve was used, indicating that an inherent scatter in G_{nc} values can be expected due to material variations.

Table 81 and Figure 120 compare the calibration curves and G_{nc} values obtained from two specimen sizes using re-run calibration curves. The average G_{nc} values (generally based on five replicate test specimens) determined from the two widths of specimen check well except in the group involving large effective a values where the difference was in excess of 100 in.-lb/in.^{2} However, differences between individual 1/2- and 3/4-in.-wide test specimens were as great as 300 in.-lb/in.^{2} (for a given specimen orientation and heat treatment).

On the basis of differences in average G_{nc} values as obtained from replicate test specimens, variations in G_{nc} of the order of 100 in.-lb/in.^{2} can be expected as a result of experimental procedure in the SNB test.

Approved for Public Release

Contrails

3. Increased Accuracy in G_{nc} by Fitting a Least-Squares Polynomial to Bend-Test Calibration Data

Irwin's equation* shows that the fracture toughness of a material as measured by slow-notch-bend test is a function of the first derivative of the reciprocal of the spring constant (b/M) with respect to crack depth, a:

$$G = 1/2(L/B)^2 \frac{d(b/M)}{da} . \qquad (8)$$

As an alternative method for computing the plane-strain fracture toughness, the experimental data obtained from a set of calibration bars (first run of 3/4 x 3/4 x 4-in. specimens from heat 24158) were put into a computer to determine the lowest-degree least-squares polynomial equation that adequately fitted the plot of 1/M versus a. The computer-drawn curve relating reciprocal of the spring constant to crack depth together with the experimental calibration data are shown in Figure 121. Deviations from the experimental points were considered to be "experimental error" in the calibration experiment. The computer then plotted the first derivative of b/M with respect to a against crack depth (Figure 122). These curves were then used to calculate fracture toughness from Equation 8. For example, by using the deflection and proportional-limit load measured in the SNB tests, eb/L was computed and used to obtain an effective crack depth, a, from Figure 121. The a value was then used to obtain a value of d(b/M)/da from Figure 121. This value substituted in Equation 8 together with appropriate values of load, L, and beam width, b, gave the plane-strain fracture toughness value G_{nc}.

Table 82 provides a comparison between G_{nc} values calculated by using 1) the method described earlier in this appendix for computer solution of three simultaneous equations to obtain Q, R, and S based on values of a and b/M read from a hand-drawn calibration curve, followed by solution of Equation 6, and 2) the d(b/M)da values obtained from the computer-drawn curve (Figure 122). The table shows that generally lower G_{nc} values were obtained by using the least-squares method. The difference between the two methods was most striking in specimen-group A1458 to 1462, which involved large effective a values. In this group, use of the least-squares method resulted in an average G_{nc} value 260 in.-lb/in.^{2} smaller than that obtained using coefficients from the run-1 calibration curve. In addition to the least-squares method giving lower G_{nc} values, the scatter in the test results in any given group of replicate test specimens was appreciably less with the least-squares method.

From the above test results, it is concluded that use of the computer-drawn curves of 1/M versus a, and d(b/M)da versus a, provides a more general fit of the experimental data, which in turn minimizes scatter in the test results. Moreover, it appears that the least-squares method gives somewhat lower and, therefore, more conservative values of plane-strain fracture toughness.

*H. I. Bueckner, On the 3-Point Bar Bending Test, Large Steam Turbine Generator Department, General Electric Data Folder, June 1957.

Approved for Public Release

Contrails

D. SLOW-NOTCH-BEND TEST ANALYSIS BY BUECKNER

1. Bueckner's Analytical Solution for the Energy Release Rate G

Winne and Wundt,* based on the work of Bueckner derived the following expression for the strain-energy-release rate in a notched beam under 3-point loading:

$$K_{Ic}^2 = \sigma_n^2 \; h \; f\,(a/d) \tag{9}$$

or

$$G_{Ic} = \frac{(1-\nu^2)}{E} \sigma_n^2 \; h \; f\,(a/d), \tag{10}$$

where σ_n is the nominal bending stress at the notched section of net depth, h,

$$\sigma_n = 6M/h^2,$$

M is the bending moment at the notched section, v is Poisson's ratio, E is the modulus of elasticity, h, a, and d are the dimensions shown in Figure 112, and f(a/d) is the strain-energy-release rate as calculated by Bueckner.** Bueckner's calculated values of f(a/d) were adapted for use in Equation 10, where f(a/d) has the values

a/d	0.1	0.2	0.5
f(a/d)	0.204	0.317	0.488

where a is the notch-plus-crack depth and d is the over-all depth of the beam. Figure 124 is a reproduction of the computer-drawn, least-squares curve relating the above data graphically.

---

*D. H. Winne and B. M. Wundt, "Application of the Griffith-Irwin Theory of Crack Propagation to the Bursting Behavior of Disks, Including Analytical and Experimental Studies," Trans. ASME, Vol. 80, pp. 1643-1658 (1958); also, B. M. Wundt, A Unified Interpretation of Room-Temperature Strength of Notched Specimens as Influenced by Their Size, ASME Paper 59-MET-9, 1959.

**H. F. Bueckner, The Stress Concentration of a Notched Bar in Bending, Large Steam Turbine-Generator Department, General Electric Company, Data Folder, 28 June 1957; also, H. F. Bueckner, On the 3-Point Bar Bending Test, Large Steam Turbine-Generator Department, General Electric, Data Folder, 14 June 1957.

Approved for Public Release

Contrails

2. The Influence of Errors in Proportional-Limit Load and Measured Crack Depth on Fracture Toughness Calculated from Bueckner's Equation

The effect of an experimental error in measuring crack depth a or proportional-limit load on the G_{Ic} values calculated by Bueckner's equation is illustrated in Table 83 by using the same specimens as in Table 78. A comparison of the effect of a 5% error in crack length as computed by the spring-constant method (see Table 78), and by Bueckner's method indicated the latter to be appreciably less affected. For example, based on 1/M, a +5% error at a crack length of 0.261 in. (specimen A468) resulted in a G_{nc} value 18% too high, whereas, by using Bueckner's method, a +5% error at a crack length of 0.237 in. (specimen A468) resulted in a G_{nc} value 7% too high.

E. CONCLUSIONS

1. Bueckner's solution for use in the slow-notch-bend test generally resulted in a more conservative and a more accurate measurement of plane-strain fracture toughness than Rawe's solution which uses the spring-constant technique.

2. If the spring-constant solution is used in the slow-notch-bend test, a computer should be employed in each step to eliminate the need for determining the coefficients to the equation relating b/M to the variable a. Thus, the computer would be used to:

a. obtain a least-squares best fit of the calibration data, plotting b/M versus a,

b. obtain the first derivative with respect to crack depth at any given experimental value of b/M and a, and

c. Solve Irwin's equation

$$G_{Ic} = \frac{1}{2}\left(\frac{L}{b}\right)^2 d(b/M)/da \qquad (3)$$

by a direct substitution of d(b/M)/da (obtained by computer during step 2b), proportional-limit load and specimen width. Thus, the input to the computer would be the data from the initial calibration experiment, and the proportional-limit load, deflection at the proportional-limit load and specimen width from the individual SNB tests.

F. SAMPLE CALCULATIONS BASED ON THE SPRING CONSTANT EQUATION AND BUECKNER'S EQUATION

1. Objective

The objective of these calculations is to illustrate the details of the G calculation using both the spring-constant and Bueckner's equation, and to compare the effect of a small error in crack depth on the G calculation using both the spring-constant and Bueckner's equation. For

Approved for Public Release

Contrails

purposes of the calculation, the experimental data from SNB specimen A473 (Table 80) and the first run calibration curve for heat 24158 (Figure 119) were used.

2. Spring-Constant Equation

$$G_{nc} = \frac{1}{2}\left(\frac{L}{b}\right)^2 \left[2Qa + 3Ra^2 + 4Sa^3\right]$$

where: a = notch-plus-crack depth, in.,

b = specimen width, in.,

L = proportional-limit load, lb, and

Q, R and S are constants determined from calibration specimens.

ASSUMPTION

Assume an experimental accuracy of $\pm$ .002 in. for the crack depth, a. Let a = 0.273, 0.275, and 0.277 in.

CALCULATION

Let: L = 6300 lb, b = 0.500 in., Q = 23.5×10^{-6}, R = -135×10^{-6}, S = 300×10^{-6}

$$G_{nc} = \frac{1}{2}\left(\frac{L}{b}\right)^2 \left[2Qa + 3Ra^2 + 4Sa^3\right]$$

$$= \frac{1}{2}\left(\frac{6300}{.500}\right)^2 \left[2(23.5\times10^{-6})a + 3(-135\times10^{-6})a^2 + 4(300\times10^{-6})a^3\right]$$

$$= 79.4\left[47a - 405a^2 + 1200a^3\right]$$

for a = 0.277 in.

$$G_{nc} = 79.4\left[47(.277) - 405(.0767) + 1200(.0212)\right]$$

$$= 79.4\left[13.03 - 31.10 + 25.50\right]$$

$$= 79.4\left[7.43\right]$$

$$= \underline{\underline{590}}$$

for a = 0.275 in.

$$G_{nc} = 79.4\left[47(.275) - 405(.0756) + 1200(.0208)\right]$$

$$= 79.4\left[12.93 - 30.62 + 24.97\right]$$

$$= 79.4\left[7.28\right]$$

$$= \underline{\underline{578}}$$

Approved for Public Release

Contrails

for a = 0.273 in.

G_{nc} = 79.4 47(.273) - 405(.0745) + 1200(.0203)

= 79.4 12.83 - 30.20 + 24.40

= 79.4 7.03

= 558

3. Bueckner's Equation

$$G_{Ic} = \frac{(1-\gamma^2)}{E} (\sigma^2) (h) \quad f\left(\frac{a}{d}\right) \quad \text{and } \sigma = \frac{4.5}{b} \left(\frac{L}{h^2}\right)$$

where: a = notch-plus-crack depth, in. E = Young's modulus

d = specimen depth, in. b = specimen width, in.

σ = nominal bending stress, psi L = proportional-limit load, lb

γ = Poisson's ratio h = d - a

f(a/d) = Function a/d determined graphically from Figure 124.

ASSUMPTION

Assume an experimental accuracy of + .002 in. for the crack depth a, calculate G_{Ic} for a = 0.273, 0.275, and 0.277.

CALCULATION

Let: d = 0.750, σ = 0.31, E = 27 x 10^{-6}, b = 0.500 and L = 6300.

a	d-a = h	h^2	a/d	$f\left(\frac{a}{d}\right)$
.277	.750-.277 = .473	.2237	$\frac{.277}{.750}$ = 0.369	0.443
.275	.750-.275 = .475	.2256	$\frac{.275}{.750}$ = 0.367	0.442
.273	.750-.273 = .477	.2275	$\frac{.273}{.750}$ = 0.364	0.440

and $\sigma = \frac{4.5}{b} \left(\frac{L}{h^2}\right) = \frac{4.5}{.500} \left(\frac{6300}{h^2}\right)$

$= \frac{56700}{h^2}$

Approved for Public Release

Contrails

a	
.277	$\sigma^2 = \frac{56700}{.224} = (2.53 \times 10^5)^2 = 6.40 \times 10^{10}$
.275	$\sigma^2 = \frac{56700}{.226} = (2.51 \times 10^5)^2 = 6.30 \times 10^{10}$
.273	$\sigma^2 = \frac{56700}{.227} = (2.49 \times 10^5)^2 = 6.20 \times 10^{10}$

a	
	$G_{Ic} = \left(\frac{1-\nu^2}{E}\right) \quad (\sigma^2) \quad (h) \quad f \quad \left(\frac{a}{d}\right)$
.277	$= (3.35 \times 10^{-8}) (6.40 \times 10^{10}) (.473) (.443)$
	$= \underline{\underline{447}}$
.275	$= (3.35 \times 10^{-8}) (6.30 \times 10^{10}) (.475) (.442)$
	$= \underline{\underline{443}}$
.273	$= (3.35 \times 10^{-8}) (6.20 \times 10^{10}) (.477) (.440)$
	$= \underline{\underline{436}}$

Approved for Public Release

Contrails

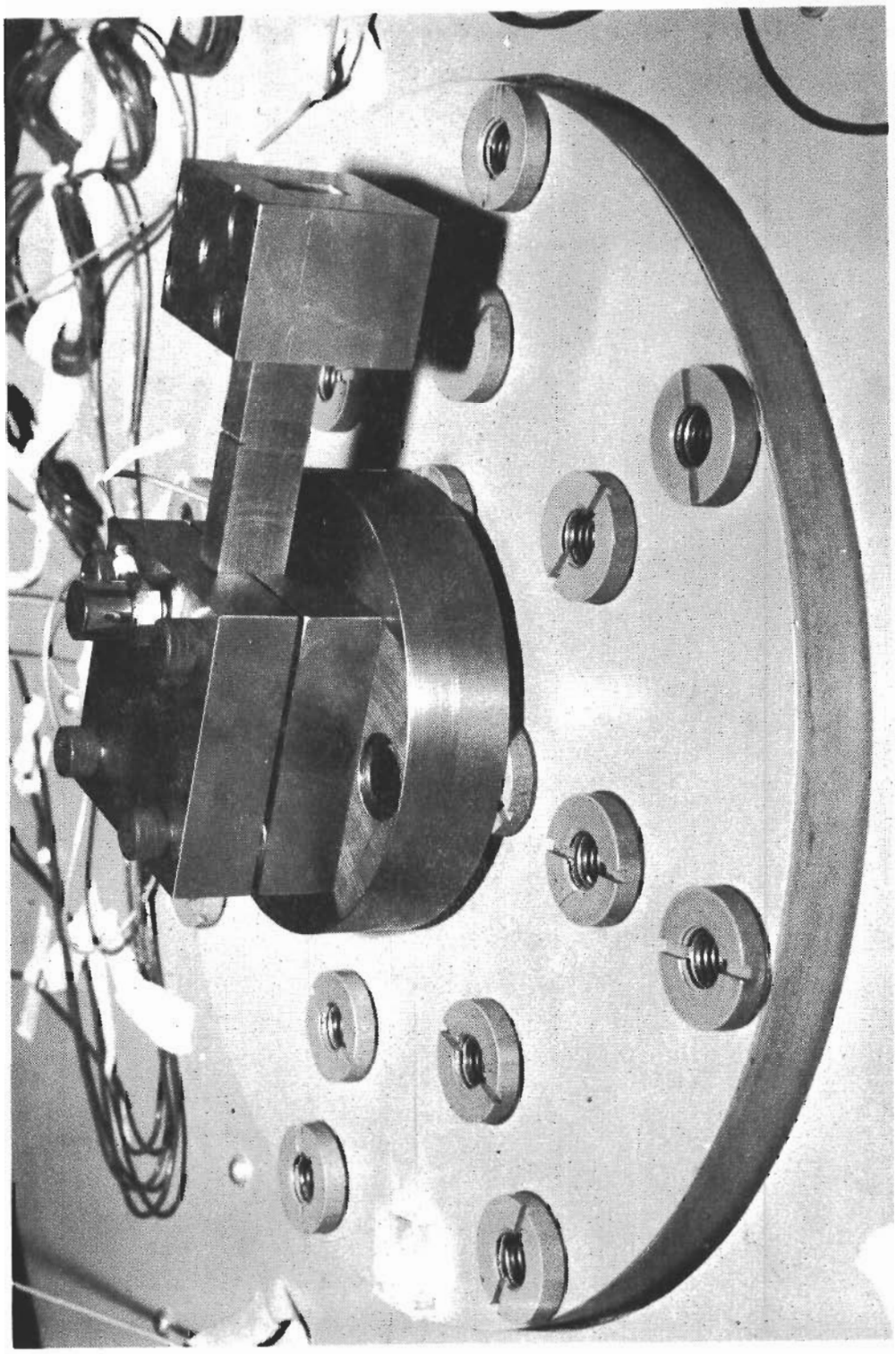

Figure 110. Vibration Setup Used for Fatigue Cracking Slow-Notch-Bend Specimens

Approved for Public Release

Contrails

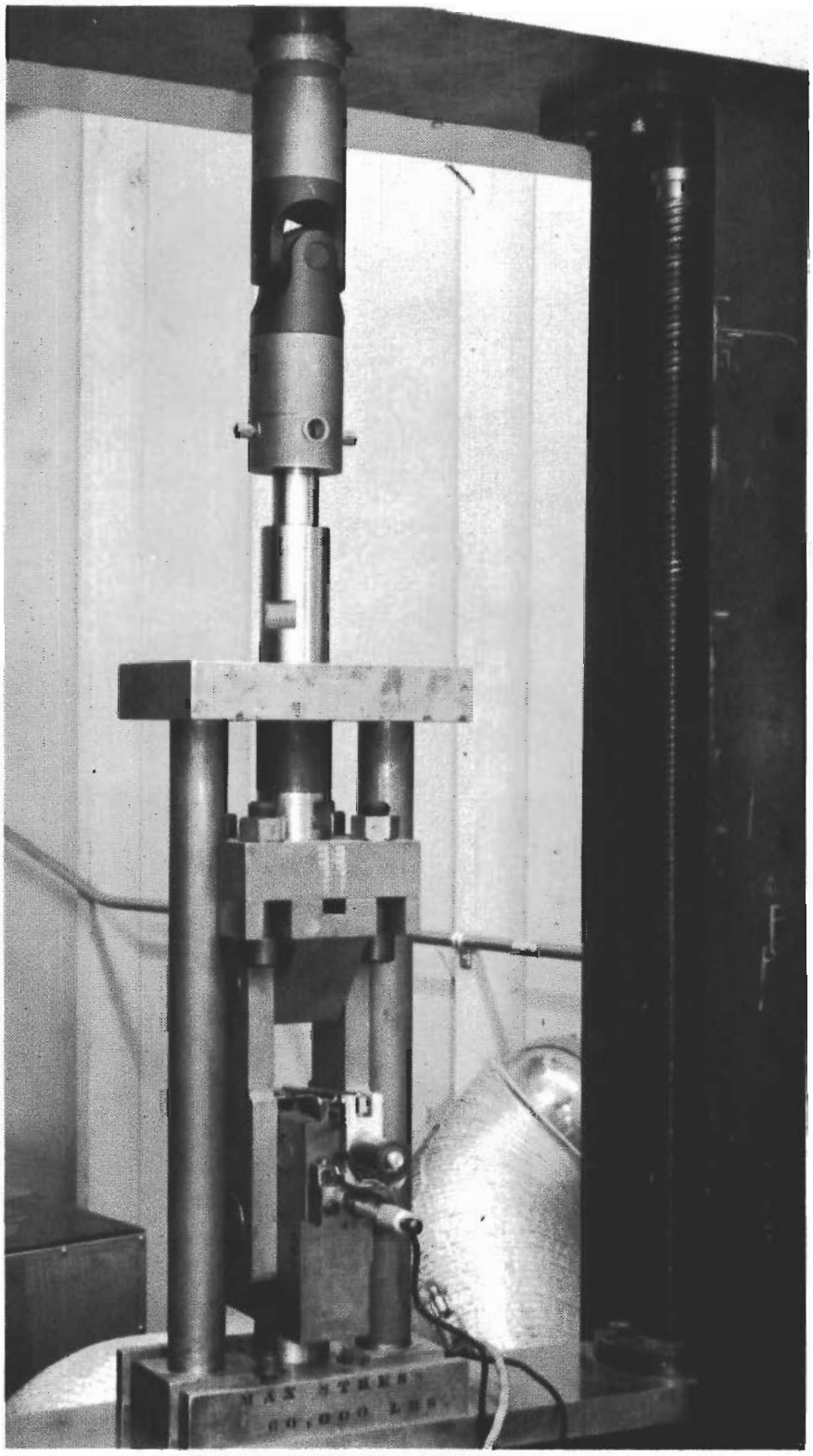

Figure 111. Three-Point Loading Apparatus for Slow Bending

Approved for Public Release

Contrails

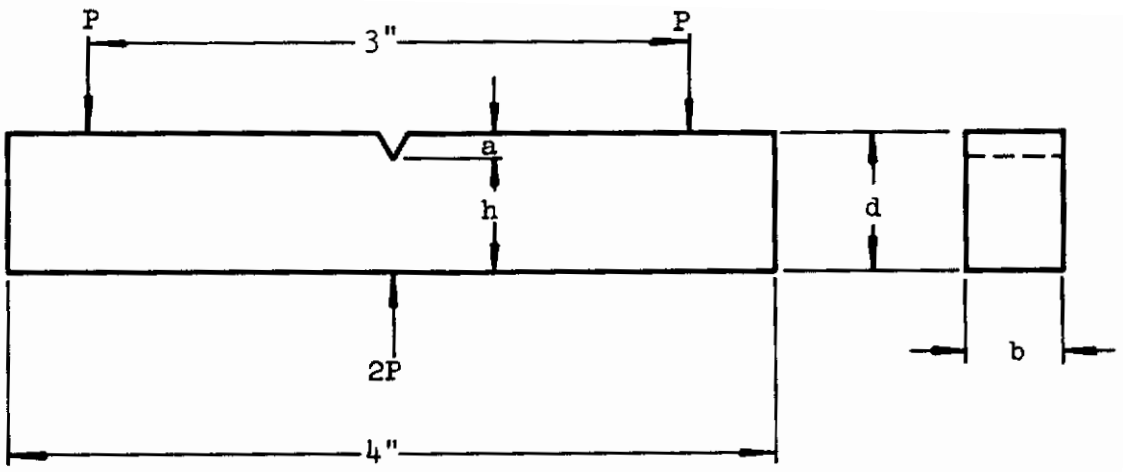

Figure 112. Slow-Notch-Bend Test Specimen

Approved for Public Release

Contrails

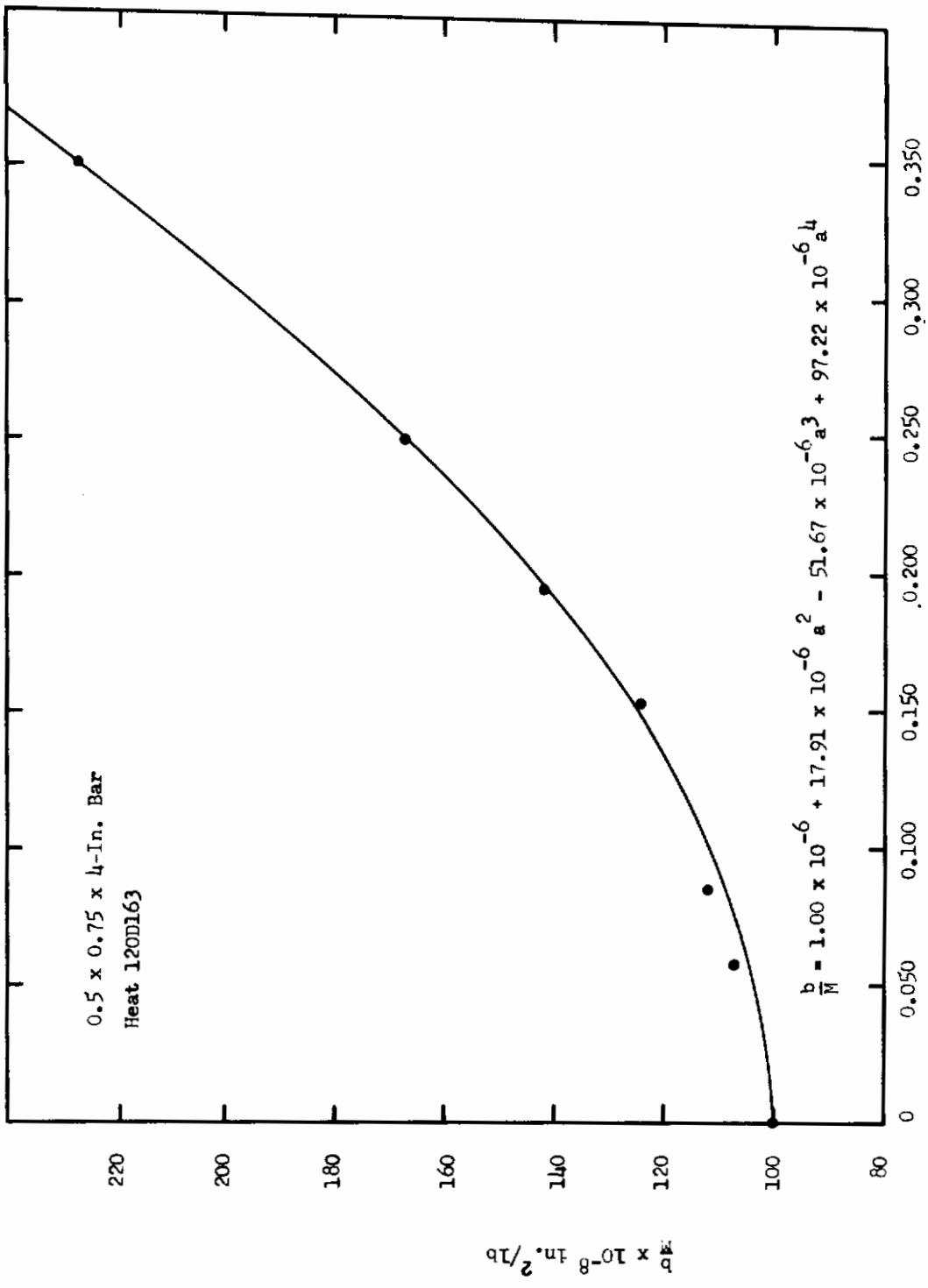

Figure 113. Typical Calibration Curve Relating the Reciprocal of the Spring Constant and Notch-Plus-Fatigue Crack Depth

Approved for Public Release

Contrails

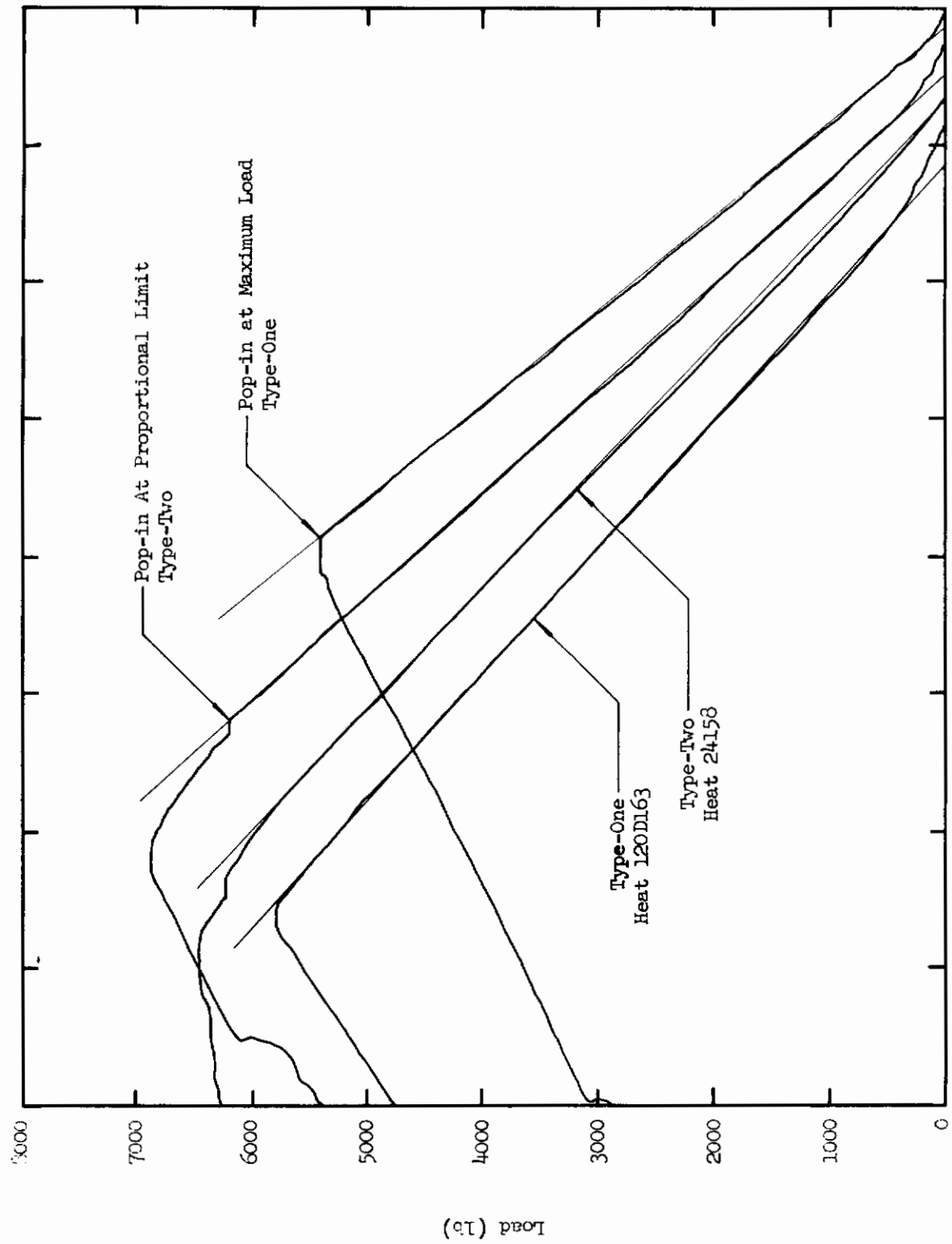

Figure 114. Typical Load-Deflection Diagrams in the Slow-Notch-Bend Test

Approved for Public Release

Contrails

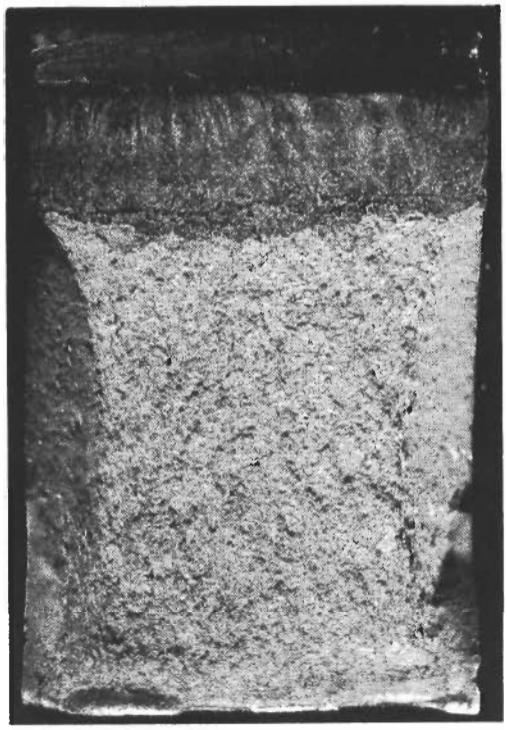

Point A

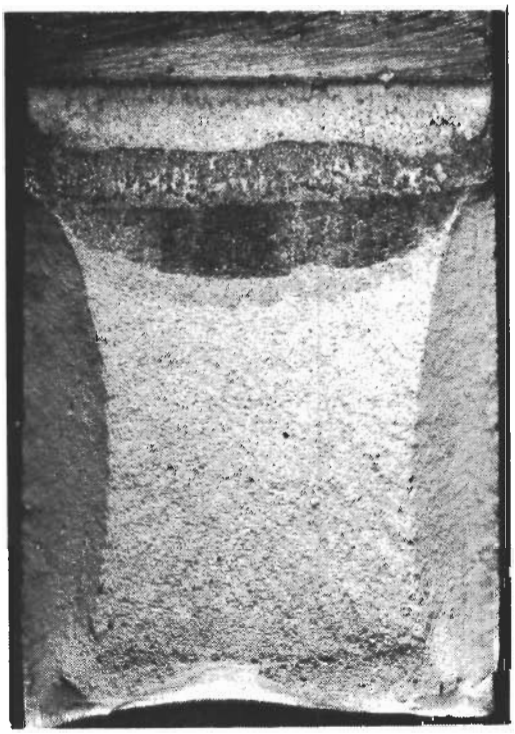

Point B

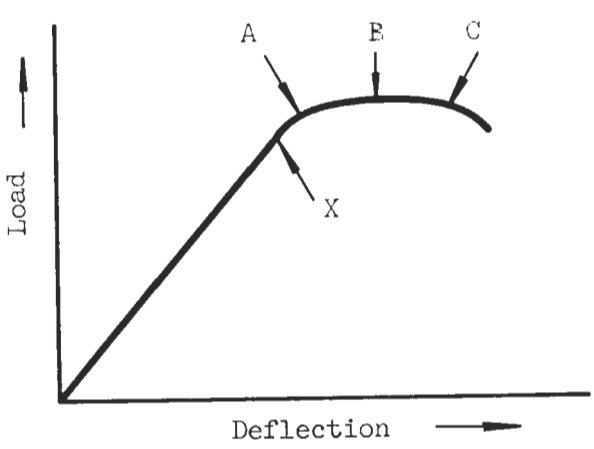

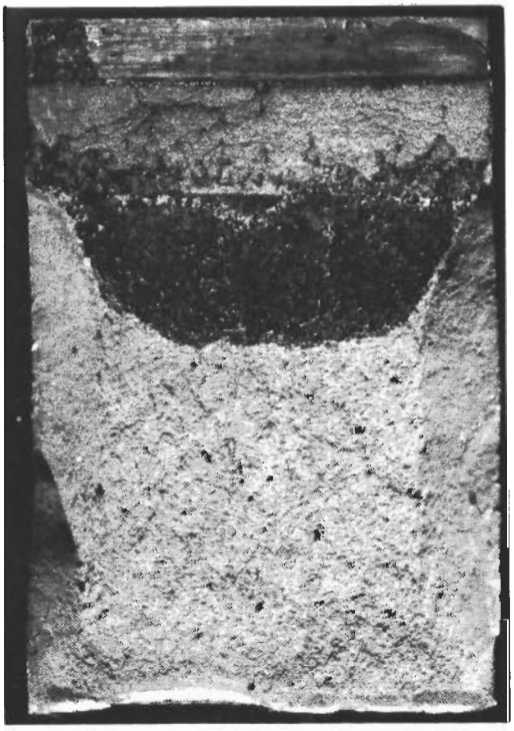

Point C

Figure 115. Relationship Between Crack Growth and Load-Deflection Point X (Proportional-Limit Load) Indicates Load and Deflection Values Used in Calculating Fracture Toughness

Approved for Public Release

Contrails

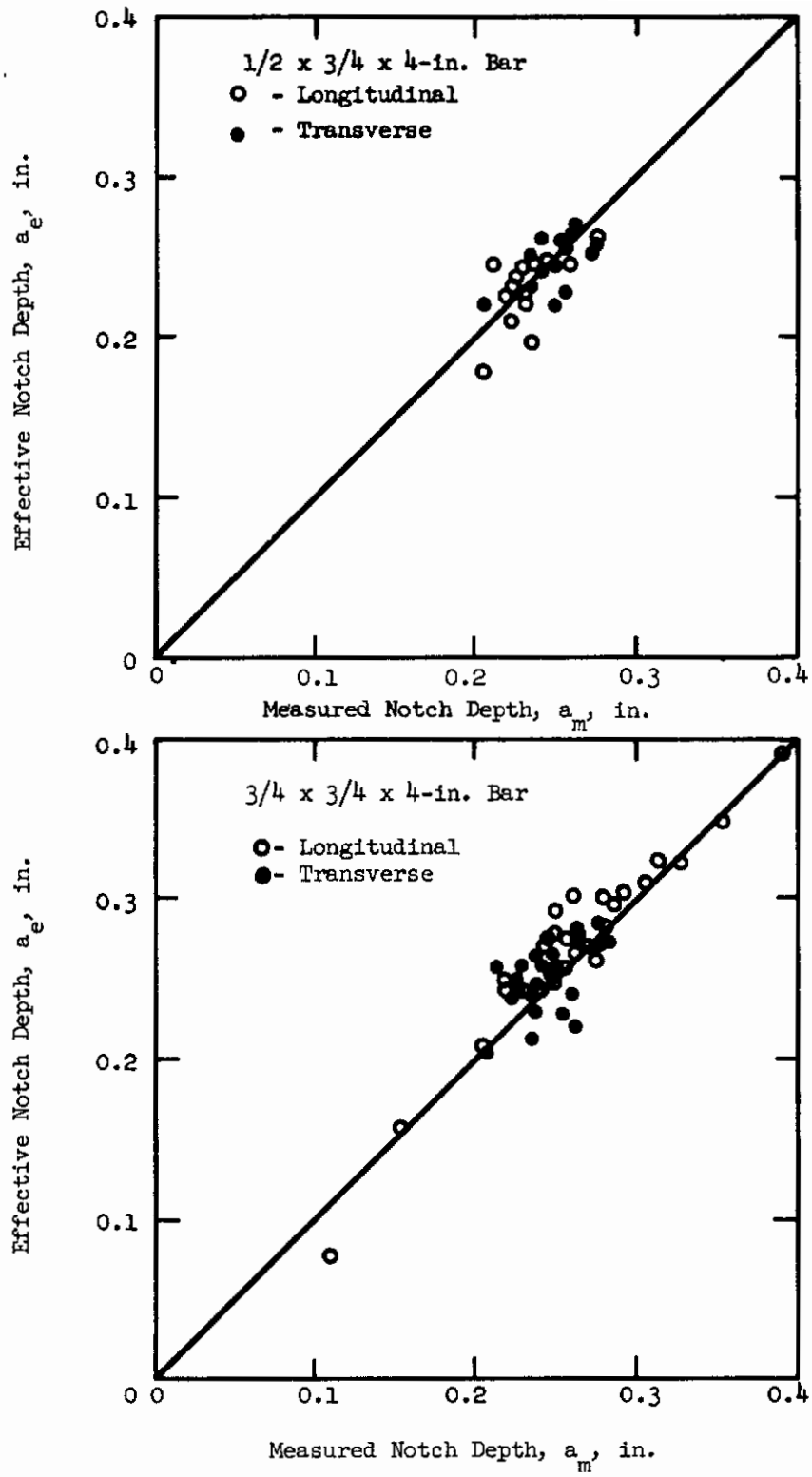

Figure 116. Plot of Effective Crack Depth, a_e, vs Measured Crack Depth, a_m, for 1/2- and 3/4-In.-Wide Specimens, Heat 24158

Approved for Public Release

Contrails

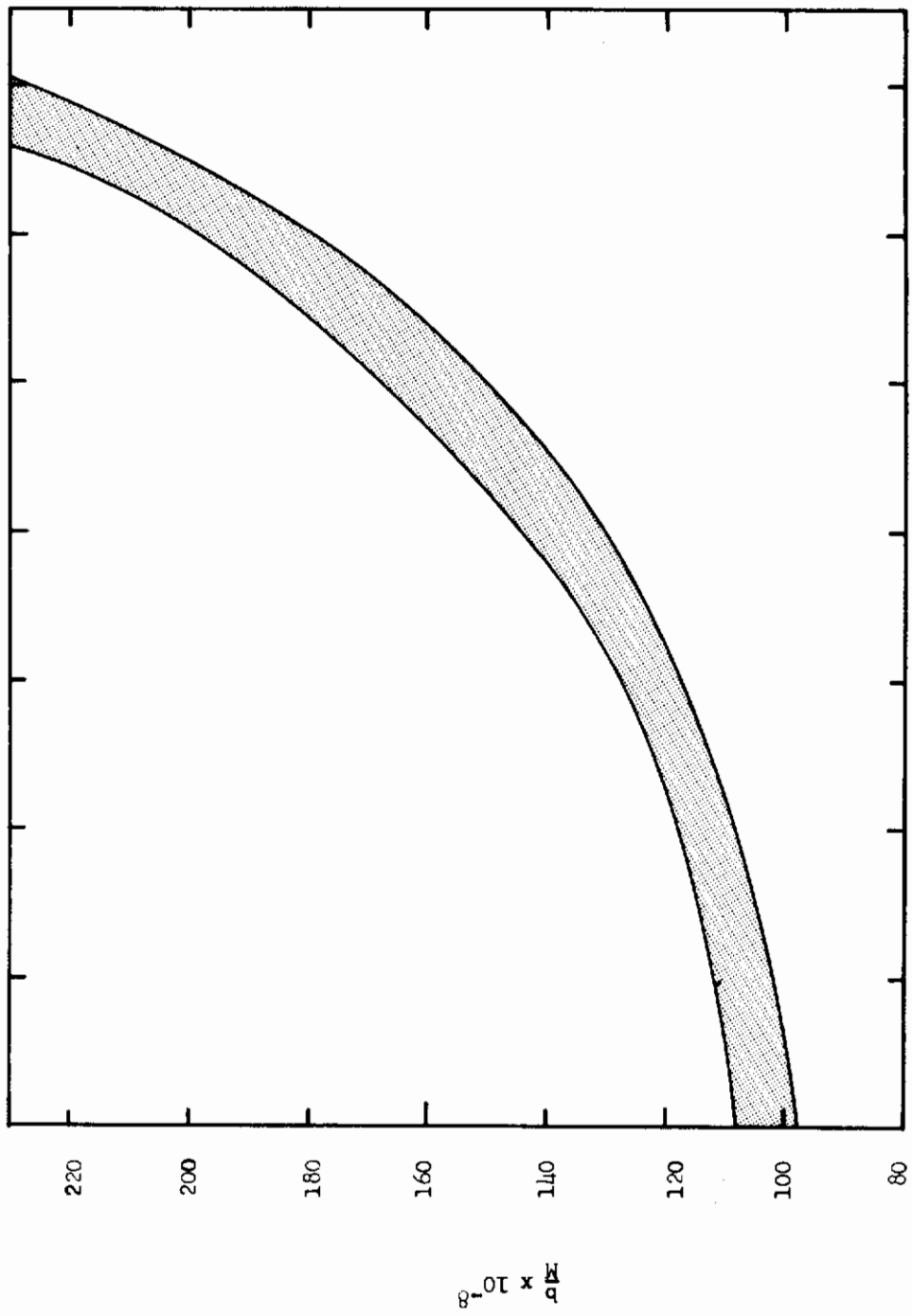

Figure 117. Composite of Eleven Calibration Curves for 18% Nickel Maraging Steel

Approved for Public Release

Contrails

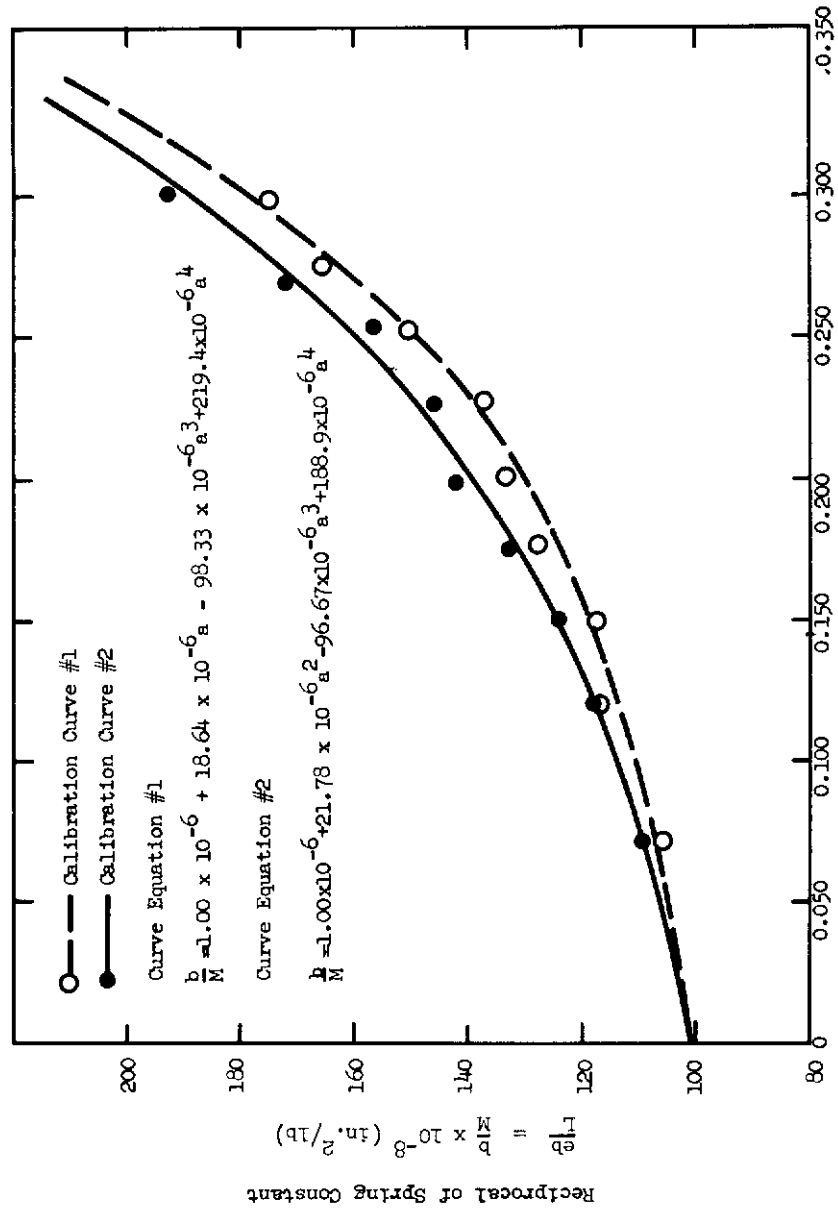

Figure 118. Composition of Calibration Curves for the Same Calibration Specimens Tested at Different Times

Approved for Public Release

Contrails

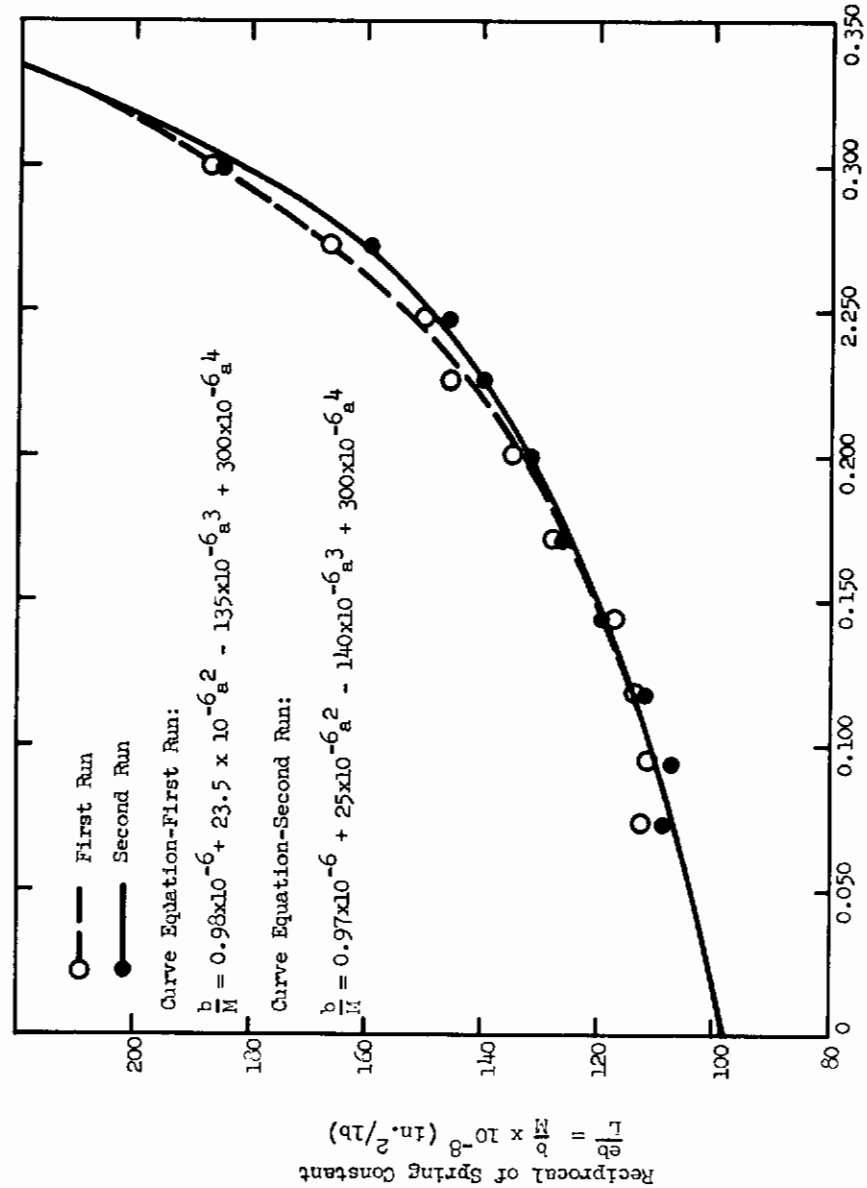

Figure 119. Comparison of Calibration Curves for the Same Calibration Specimens Tested at Different Times

Approved for Public Release

Contrails

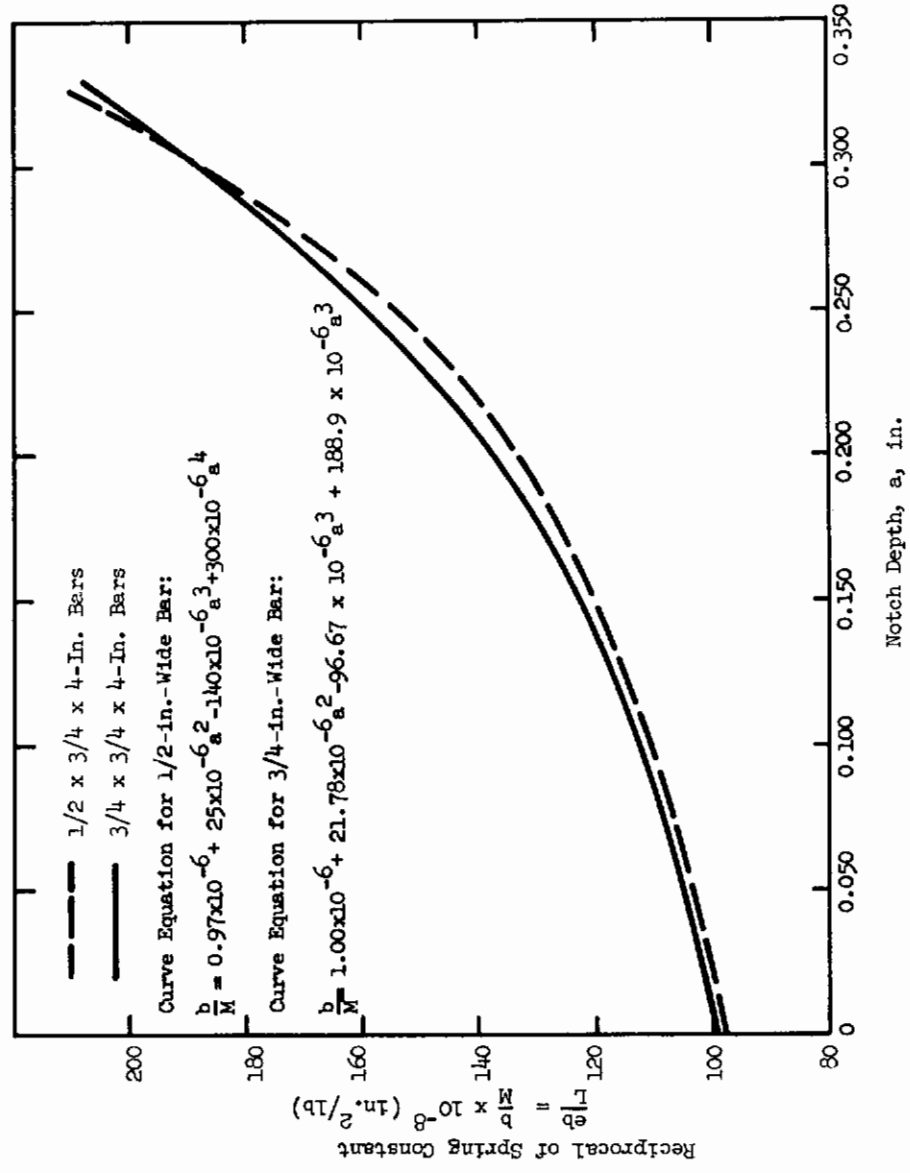

Figure 120. Comparison of Calibration Curves from 1/2- and 3/4-In.-Wide Bars

Approved for Public Release

Contrails

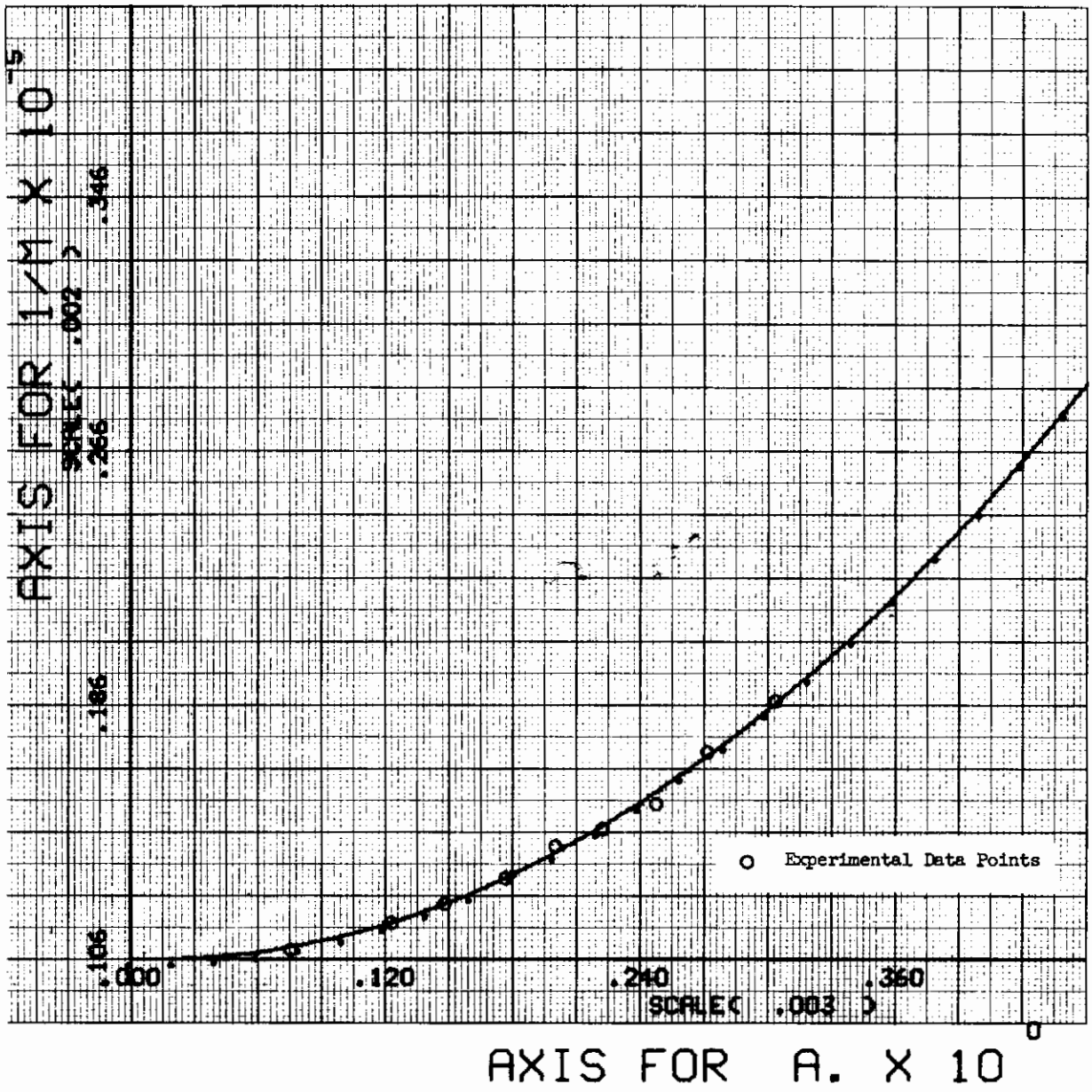

Figure 121. Calibration Curve for Heat 24158, 3/4 x 3/4-In. Bar, Reciprocal of Spring Constant, b/M, vs Notch Depth, a

Approved for Public Release

Contrails

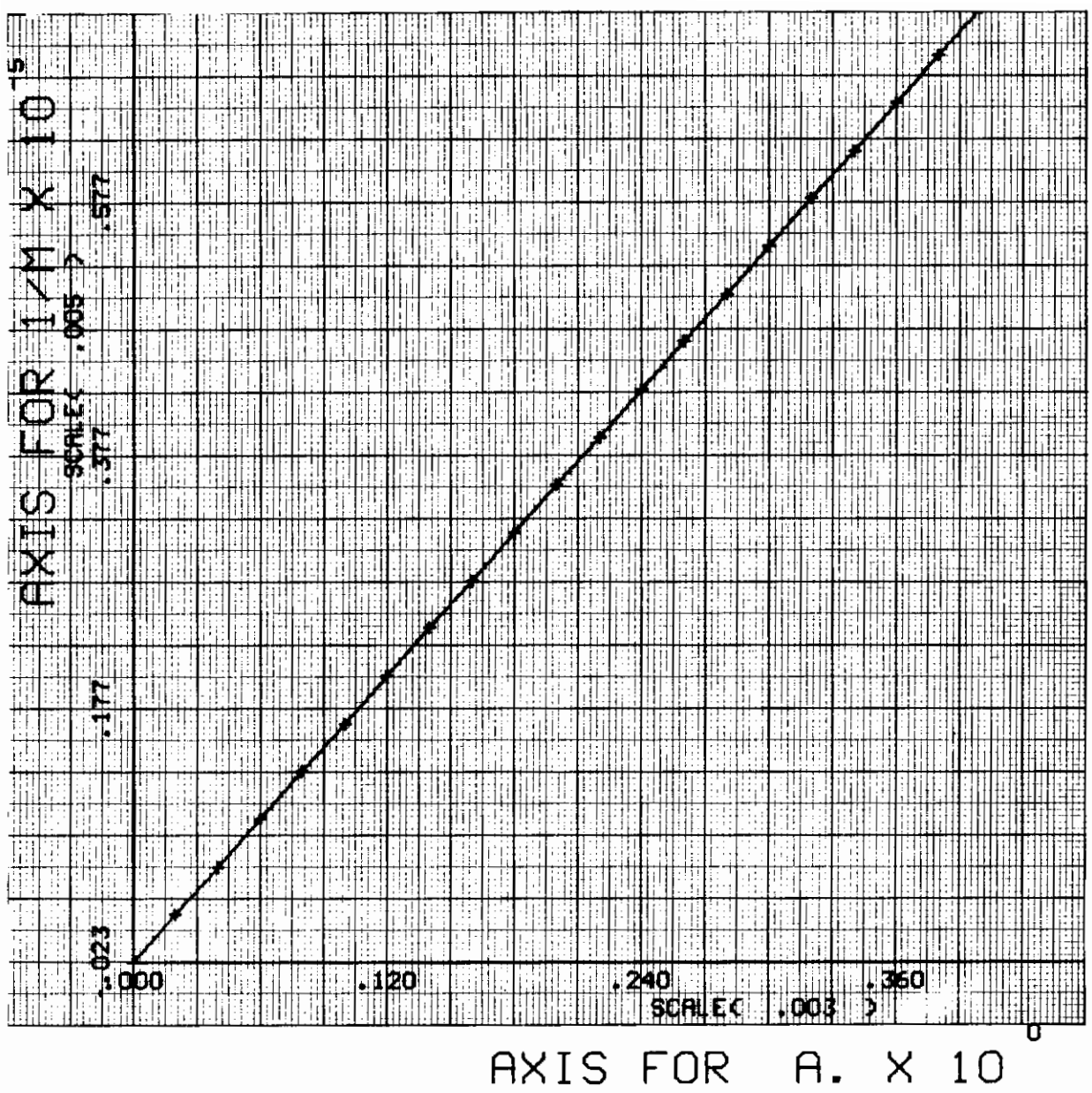

Figure 122. Plot of the Derivative of b/M vs Notch Depth, a

Approved for Public Release

Contrails

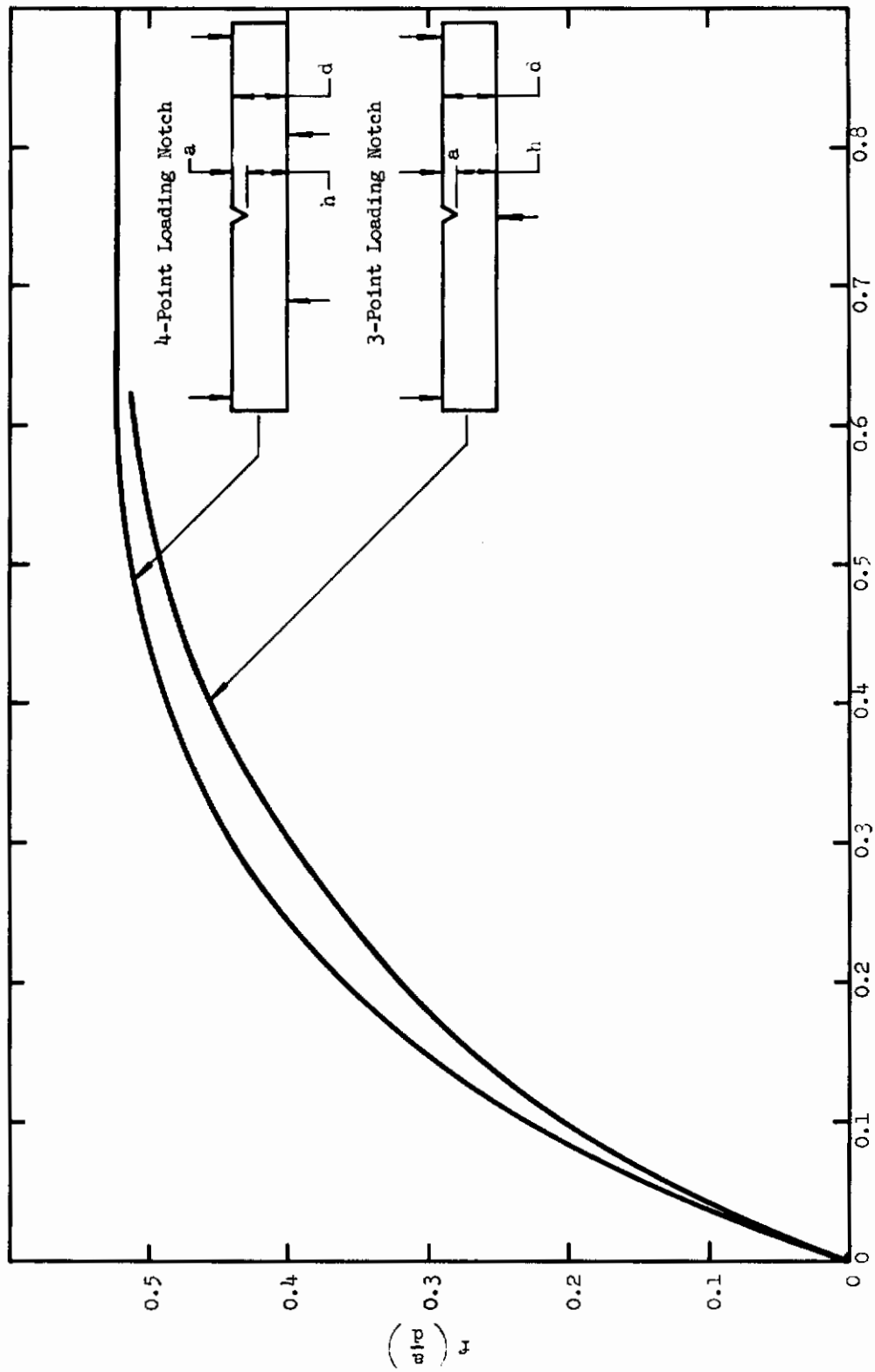

Figure 123. Function of $f(\frac{a}{d})$ vs the Crack Depth to Beam Depth Ratio, $\frac{a}{d}$

Approved for Public Release

Contrails

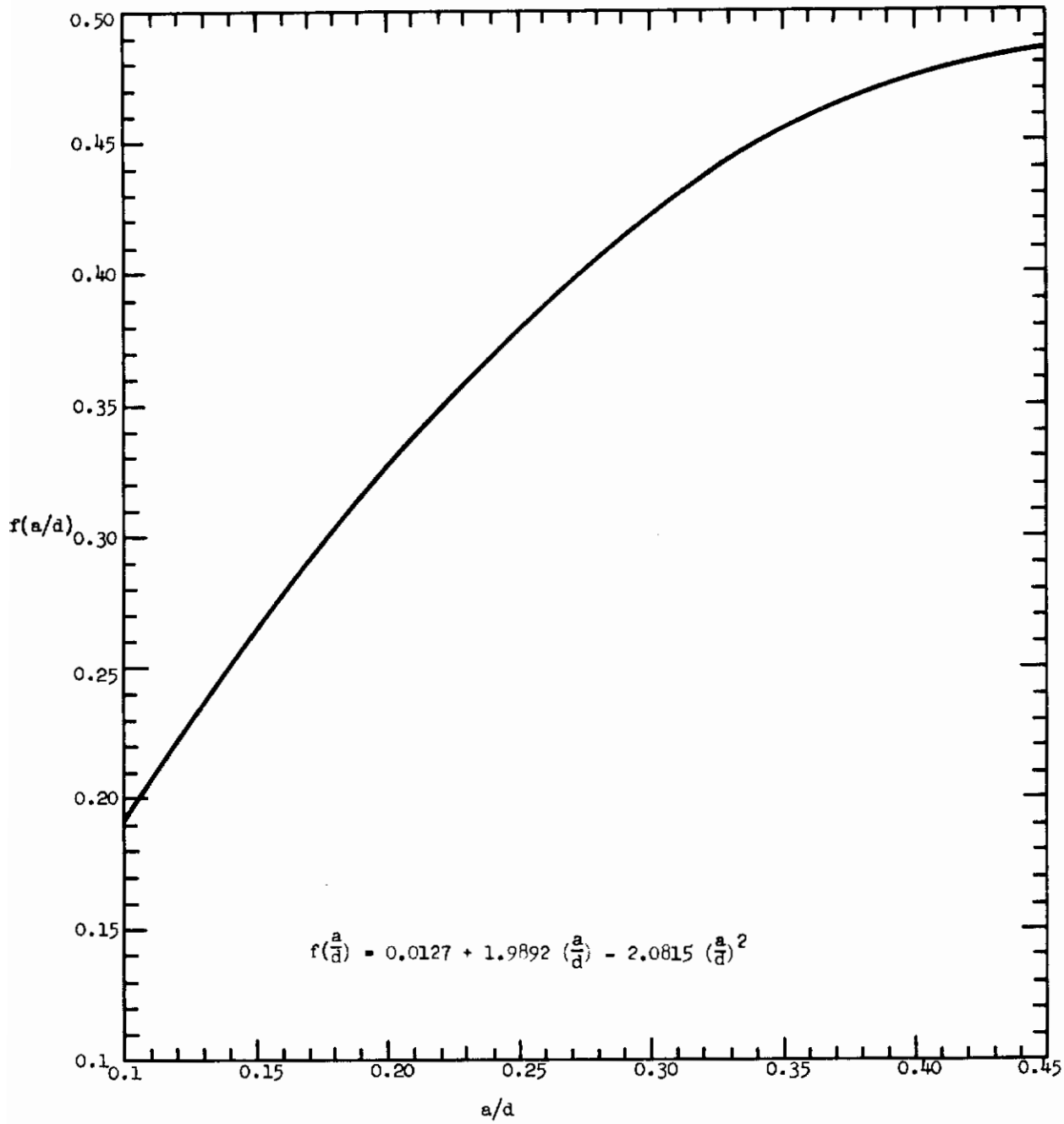

Figure 124. Strain-Energy Release Rate for Notch Beams in Three-Point Loading (after Bueckner)

Approved for Public Release

Contrails

TABLE 78

EFFECT OF 5% AND 10% CHANGES IN VALUES OF EFFECTIVE a AND PROPORTIONAL LIMIT LOAD ON G_{nc} VALUES FOR THREE GRADE 200 TEST SPECIMENS, HEAT 24158

Specimen	Proportional Limit Load	% Error in Proportional Limit Load	Notch Depth, Effective, a, in.	% Error in Effective, a, in.	Fracture Toughness G_{nc} (in.lb/in.^{2})	G_{nc} % Change
A450	7900 lbs		.201		354*	
"	"		.211	(5%)	396	11.9
"	"		.221	(10%)	446	26
"	8295 lbs	(5%)	.201		390	10.2
"	8690 lbs	(10%)	.201		428	20.9
A468	6160 lbs		.249		382*	
"	"		.261	(5%)	452	18.3
"	"		.274	(10%)	550	44.0
"	6468 lbs	(5%)	.249		421	10.2
"	6776 lbs	(10%)	.249		461	20.7
A473	6300 lbs		.284		648*	--
"	"		.298	(5%)	778	20.1
"	"		.312	(10%)	934	44.1
"	6615 lbs	(5%)	.284		716	10.5
"	6930 lbs	(10%)	.284		785	21.2

*Computer Calculated Values

Approved for Public Release

Contrails

TABLE 79

FRACTURE TOUGHNESS RESULTS OF HEAT 24158 USING TWO EXPERIMENTAL CALIBRATION CURVES OF FIGURE 114 3/4 x 3/4x 4-IN. BAR

Specimen Number	Rolling Direction	Prop. Limit Load lbs	Width b	$\frac{eb}{L}$ in.^{2}/lb x 10^{-8}	Effective a_1 in.	Effective a_2 in.	Fracture Toughness in. lb/in.^{2} G_{nc_1}	G_{nc_2}
A1448	Long	13750	.746	121.5	.159	.137	339	419
A1449		10500	.746	145.8	.242	.219	415	353
A1450		8500	.746	185.4	.307	.298	587	469
A1451		10850	.745	148.5	.247	.226	471	398
A1452		12250	.746	141.3	.221	.206	408	441
						Ave.	444	415
A1463	Transv.	9800	.747	165.2	.278	.264	553	447
A1465		8200	.749	182.3	.302	.293	510	412
A1466		8300	.748	174.8	.292	.283	467	383
A1467		8700	.747	162.5	.273	.258	409	333
						Ave.	484	394
A1453		8800	.746	177.2	.296	.284	553	437
A1455	Long	9800	.746	165.0	.277	.272	548	483
A1456		8400	.748	184.5	.306	.296	563	446
A1602		8880	.748	155.3	.261	.243	369	303
						Ave.	508	417
A1470		8050	.745	162.2	.272	.258	349	287
A1471	Transv.	8480	.748	159.5	.268	.252	366	299
						Ave.	358	293
A1458		9100	.745	180.5	.300	.280	629	451
A1459		10200	.746	158.5	.266	.240	520	392
A1460	Long	8100	.745	199.2	.326	.316	655	510
A1461		8000	.747	198.5	.325	.315	629	606
A1462		7500	.747	217.5	.347	.334	710	522
						Ave.	628	496
A701		9950	.740	149.2	.249	.230	406	350
A702	Transv.	8550	.740	153.4	.257	.238	333	279
A703		9400	.737	147.5	.245	.224	353	301
A704		8630	.738	169.4	.284	.271	472	379
A705		16500	.735	108.4	.078	.072	385	484
						Ave.	390	359

Approved for Public Release

Contrails

TABLE 80

FRACTURE TOUGHNESS RESULTS OF HEAT 24158
USING TWO EXPERIMENTAL CALIBRATION CURVES OF FIGURE 119
1/2 x 3/4 x 4-IN. BAR

Specimen Number	Rolling Direc-tions	Prop. Limit Load lbs	Width b, in.	$\frac{eb}{L}$, $in.^2/lb \times 10^{-8}$	Effective a_1 in.	Effective a_2 in.	Fracture Toughness in. lb/$in.^2$ G_{nc_1}	G_{nc_2}
A449	Long.	6500	.498	160.0	.275	.262	618	498
A450		7900	.499	133.0	.201	.198	354	344
A451		7400	.499	146.0	.246	.235	541	454
A452		7250	.499	149.0	.254	.242	578	476
						Ave.	523	443
A463		6380	.499	145.0	.242	.233	447	329
A464	Transv.	6500	.501	144.2	.238	.231	419	331
A465		7300	.499	137.4	.219	.212	363	338
A466		6400	.501	140.6	.228	.222	317	288
A467		5620	.499	151.2	.257	.246	361	301
						Ave.	381	317
A453		6400	.499	161.0	.276	.264	604	494
A454	Long.	6375	.501	166.2	.283	.272	653	540
A455		6600	.501	159.0	.274	.260	621	494
A456		6425	.500	154.0	.265	.251	524	418
A451		5880	.501	156.4	.269	.253	461	358
						Ave.	573	461
A468		6120	.501	147.0	.249	.237	382	316
A469	Transv.	5600	.499	151.8	.261	.247	379	303
A470		6000	.499	150.6	.258	.245	418	339
A471		5190	.501	154.0	.266	.251	345	272
A472		5300	.498	151.0	.257	.246	323	269
						Ave.	369	300
A458		5800	.501	158.6	.273	.259	473	377
A459	Long.	5900	.499	144.0	.240	.230	317	271
A460		6400	.501	140.6	.228	.222	317	288
A461		6500	.499	150.8	.257	.246	483	403
A462		6550	.498	157.0	.265	.257	541	474
						Ave.	426	363
A473		6300	.500	163	.275	.267	566	496
A474	Transv.	7160	.499	143.8	.240	.230	467	400
A475		6900	.500	136.0	.213	.198	308	262
A476		8010	.499	132.8	.201	.180	364	308
						Ave.	426	365

Approved for Public Release

Contrails

TABLE 81

COMPARISON OF FRACTURE TOUGHNESS RESULTS FOR HEAT 24158 USING 1/2 AND 3/4-IN.-WIDE BARS

Spec. No. 1/2"	Spec. No. 3/4"	Aging Cycle Temp. °F-Hrs.	Rolling Direction		Fracture Toughness G_{nc}, in-lb/in.^{2} b = 1/2 in.	b = 3/4 in.
A449	A1448	850-8	Longitudinal		498	419
A450	A1449				344	353
A451	A1450				454	469
A452	A1451				476	398
	A1452					441
				Ave.	443	415
A463	A1463	850-8	Transverse		329	447
A464	A1465				331	412
A465	A1466				338	383
A466	A1467				288	333
A467					301	
				Ave.	317	394
A453	A1453	900-8	Longitudinal		494	437
A454	A1455				540	483
A455	A1456				494	446
A456	A1602				418	303
A457					358	
				Ave.	461	417
A468	A1470	900-8	Transverse		316	287
A469	A1471				303	299
A470					339	
A471					272	
A472					269	
				Ave.	300	293
A458	A1458	950-8	Longitudinal		377	451
A459	A1459				271	392
A460	A1460				288	510
A461	A1461				403	606
A462	A1462				474	522
				Ave.	363	496
A473	A701	950-8	Transverse		471	350
A474	A702				400	279
A475	A703				262	301
A476	A704				308	379
	A705					484
				Ave.	360	359

Approved for Public Release

Contrails

TABLE 82

COMPARISON OF FRACTURE TOUGHNESS RESULTS OF HEAT 24158 USING THE PROCEDURE DESCRIBED BY RAWE AND THE LEAST SQUARES FIT METHOD, 3/4 x 3/4 x 4-In. BAR

Spec No	Aging Temp °F	Cycle Time Hrs	Rolling Direction	Prop. Limit Load, lbs	Width b, in.	$\frac{eb}{L} \times 10^{-8}$ in.2/16	Effective a_1 (1)	Effective a_2 (2)	Fracture Toughness C_{nc_1} (1) in.	Fracture Toughness G_{nc_1} (2) lb/in.^{2}
A1448	850	8	Longit.	13,750	.746	121.5	.159	.159	338	428
A1449				10,500	.746	145.8	.242	.230	415	392
A1450				8,500	.746	185.4	.307	.314	587	370
A1451				10,850	.745	148.5	.247	.240	471	447
A1452				12,250	.746	141.3	.221	.223	408	513
								Ave.	444	430
A1463	850	8	Transv.	9,800	.747	165.2	.278	.276	553	422
A1465				8,200	.749	182.3	.302	.309	510	334
A1466				8,300	.748	174.8	.292	.294	467	325
A1467				8,700	.747	162.5	.273	.271	409	325
								Ave.	484	352
A1453	900	8	Longit.	8,800	.746	177.2	.296	.298	553	372
A1455				9,800	.746	165.0	.277	.276	543	418
A1456				8,400	.748	184.5	.306	.312	563	372
A1602				8,880	.748	155.3	.261	.256	369	316
								Ave.	508	370
A1470	900	8	Transv.	8,050	.745	162.2	.272	.270	349	278
A1471				8,480	.748	159.5	.268	.265	366	300
								Ave.	358	289
A1458	950	8	Longit.	9,100	.745	180.5	.300	.306	629	336
A1459				10,200	.746	158.5	.266	.263	520	432
A1460				8,100	.745	199.2	.326	.339	655	365
A1461				8,000	.747	198.5	.325	.336	629	362
A1462				7,500	.747	217.5	.347	.366	710	338
								Ave.	628	367
A701	950	8	Transv.	9,950	.740	149.2	.249	.240	406	375
A702				8,550	.740	153.4	.257	.251	333	291
A703				9,400	.737	147.5	.245	.239	353	337
A704				8,630	.738	169.2	.284	.285	472	335
A705				16,500	.735	108.4	.078	.088	385	264
								Ave.	390	322

(1) Rawe's Method

(2) Least Square Method

Approved for Public Release

Contrails

TABLE 83

EFFECT OF 5% AND 10% ERROR IN MEASURED a AND PROPORTIONAL LIMIT LOAD ON G_{Ic} VALUE FOR HEAT 24158 (GRADE 200)

Specimen	Proportional Limit Load	% Error in Prop. Limit Load	Notch Depth, Measured a	% Error In Measured a	G_{Ic}	% Change in G_{Ic}
A450	7900 lbs		.210		416	--
A450	7900 lbs		.220	(5%)	453	8.9%
A450	7900 lbs		.231	(10%)	494	18.8%
A450	8295 lbs	(5%)	.210		458	10.1%
A450	8690 lbs	(10%)	.210		504	21.2%
A468	6160 lbs		.226		281	--
A468	6160 lbs		.237	(5%)	300	6.8%
A468	6160 lbs		.249	(10%)	337	16.6%
A468	6468 lbs	(5%)	.226		311	10.7%
A468	6776 lbs	(10%)	.226		340	21.0%
A473	6300 lbs		.279		461	--
A473	6300 lbs		.293	(5%)	510	10.6%
A473	6300 lbs		.307	(10%)	571	23.9%
A473	6615 lbs	(5%)	.279		507	10.0%
A473	6930 lbs	(10%)	.279		558	21.0%

Approved for Public Release

Contrails

APPENDIX V

PART-THROUGH-CRACK, CENTER-NOTCH TENSILE, AND PRECRACK-CHARPY-IMPACT TEST DESCRIPTIONS

A. PART-THROUGH-CRACK (PTC) TENSILE TEST

Plate-size, surface-flawed, fracture-toughness specimens (Figure 125) were used to determine the fracture-toughness parameter K_{Ic} in 1/2-in.-thick, Grade 250 18% nickel maraging steel, heat 120D163. The configuration of this specimen is shown in Figure 125. In addition to these specimens, subscale PTC specimens (0.125 x 8 in.) were later obtained from the broken halves of the plate-size specimens.

The initial surface notch in these specimens was produced by using electrical-discharge machining (EDM). The notch obtained was semicircular, with the terminating radius being less than 0.005 in. In both the plate-size and subscale specimens, the initiating fatigue crack was induced from the starter notch by cyclic bending, using a maximum bending stress of approximately 70% of the 0.2% offset yield strength of the material. Penetrant dye was used for detecting and measuring the initial flaw extension. The desired length of fatigue cracks was induced in about 5 to 20 min. The large PTC specimens were tested to ultimate load in tension in a 4-million-lb Southwark Emery Testing Machine located at the Engineering Materials Laboratory of the University of California at Berkeley. The rate of loading used in the tensile testing of the plate-size PTC specimens was approximately 100,000 lb-min. The subscale PTC specimens were tensile tested to failure on a conventional testing machine, on which a grip-type loading device was used. Care was taken in properly aligning the specimens. The subscale PTC specimens were tested to failure at a loading rate of 5,000 lb/min.

Analysis of test results was made by using the following equation by Irwin for the stress-intensity factor around the edge of a flat, semi-elliptical crack that penetrates through not more than half the thickness of a wide, plane plate that caries a tensile stress, σ, normal to the crack:

$$K_{Ic}^2 = 1.21\pi\sigma^2 a/(\phi^2 - 0.212\sigma^2/\sigma_{ys}^2) \qquad (1)$$

$$\phi = \int_0^{\pi/2} \sqrt{1-\left(\frac{c^2 - a^2}{c^2}\right) \sin^2\theta}\, d\theta$$

where σ_{ys} is the tensile yield strength, and ϕ is the elliptic integral function of the ratio of crack depth to half-length, a/c. ϕ^2 was obtained from a plot of ϕ^2 versus a/c.* A more recent approach simplifies Equation 1 as:

$$K_{Ic}^2 = 1.21\pi\,(a/Q)\,\sigma^2,$$

*"The Slow Growth and Rapid Propagation of Cracks, Second Report of a Special ASTM Committee," ASTM Bulletin, May 1961, p. 390.

Approved for Public Release

Contrails

where a is the depth of the surface flaw and Q is a flaw-shape parameter obtained through a graphical solution shown in Figure 126.

B. CENTER-NOTCH TENSILE TEST

The center-notch tensile test was employed to determine plane-stress fracture toughness, G_c and also the value of G at crack initiation. A complete description of the test is contained in the report from the ASTM Special Committee on Fracture Testing of High Strength Materials.*

The center-notch tensile specimen conditions required for a meaningful test, the ratios of specimen width-to-thickness and length-to-width must be maintained at approximately 16:1 and 4:1, respectively. Thus, to evaluate a 1/2-in.-thick plate, a specimen 8 in. wide and 32 in. long was required. Holes were placed in the ends of the specimen to allow pin loading. The slot in the center of the specimen was produced by electrical-discharge machining. The notches in the edge of the slot were also produced by this technique. The root-radius of the notch was held at 0.001 in. or smaller, to facilitate fatigue cracking.

Center-notch tensile specimens were fatigue-cracked in the machine shown in Figure 127. A cyclical bending-load was used in this machine to induce a crack in the notches on one surface of the specimen. The specimen was then turned over to induce cracks in the opposite surface. A maximum bending stress of approximately 70% of the 0.2% offset yield strength of the material was used to initiate wing-type fatigue cracks approximately 0.08 in. long on each side of the machined notch. An illustration of the shape of the fatigue cracks is shown in Figure 128.

The fatigue-cracked, center-notch, tensile specimens were tested to failure in a 4-million-lb Southwark Emery Testing Machine shown in Figure 129. Load was applied to the specimen at a rate of approximately 100,000 lb/min. Liquid-dye staining was used to indicate the extent of slow crack growth.

The fracture toughness, G_c, of the specimens was computed from the following equation:

$$G_c = \frac{\sigma_o^2 B}{E} \tan \frac{(\pi a)}{w}, \qquad (2)$$

where G_c is the critical crack extension force, uncorrected for plastic zone straining; σ_o is the gross section stress; a is the crack half-length; E is Young's modulus; and B is the specimen width.

Approximate values for load at crack initiation were obtained by noting the load at the first audible crack signal. This load and the initial slot length (2a), plus the fatigue crack depth, were used in the G_c formula (equation 2) to calculate G_{Ic}.

*"Fracture Testing of High Strength Sheet Materials: A Report of a Special ASTM Committee," ASTM Bulletin,

Approved for Public Release

Contrails

B. PRECRACK-CHARPY-IMPACT TEST

Precracked-Charpy-impact tests were made on a subsize Charpy machine designed by ManLabs with a capacity of 24 ft-lb. Energy readings on this machine were made with an accuracy of ± 0.005 ft-lb in the low energy range (1 to 5 ft-lb). A ManLabs fatigue-cracking machine was used to automatically precrack Charpy-impact specimens to a desired depth. Precracking was accomplished in 1 to 2 min producing a fatigue-crack depth of 0.005 to 0.030-in. The precracking apparatus is shown in Figure 130. The ManLabs Charpy I pact Testing Machine is shown in Figure 132, together with the slow-notch-bend specimen for size comparison.

The energy (W/A) required to propagate a crack per unit area of fracture surface was determined for impact rates of loading. W/A values were calculated by dividing the impact energy by the cross-sectional fracture area. Expressed in units of in.-lb/in.^{2}, W/A values are directly comparable to, although not necessarily identical with, the plane-stress fracture toughness (G_c).

Approved for Public Release

Contrails

Approved for Public Release

Contrails

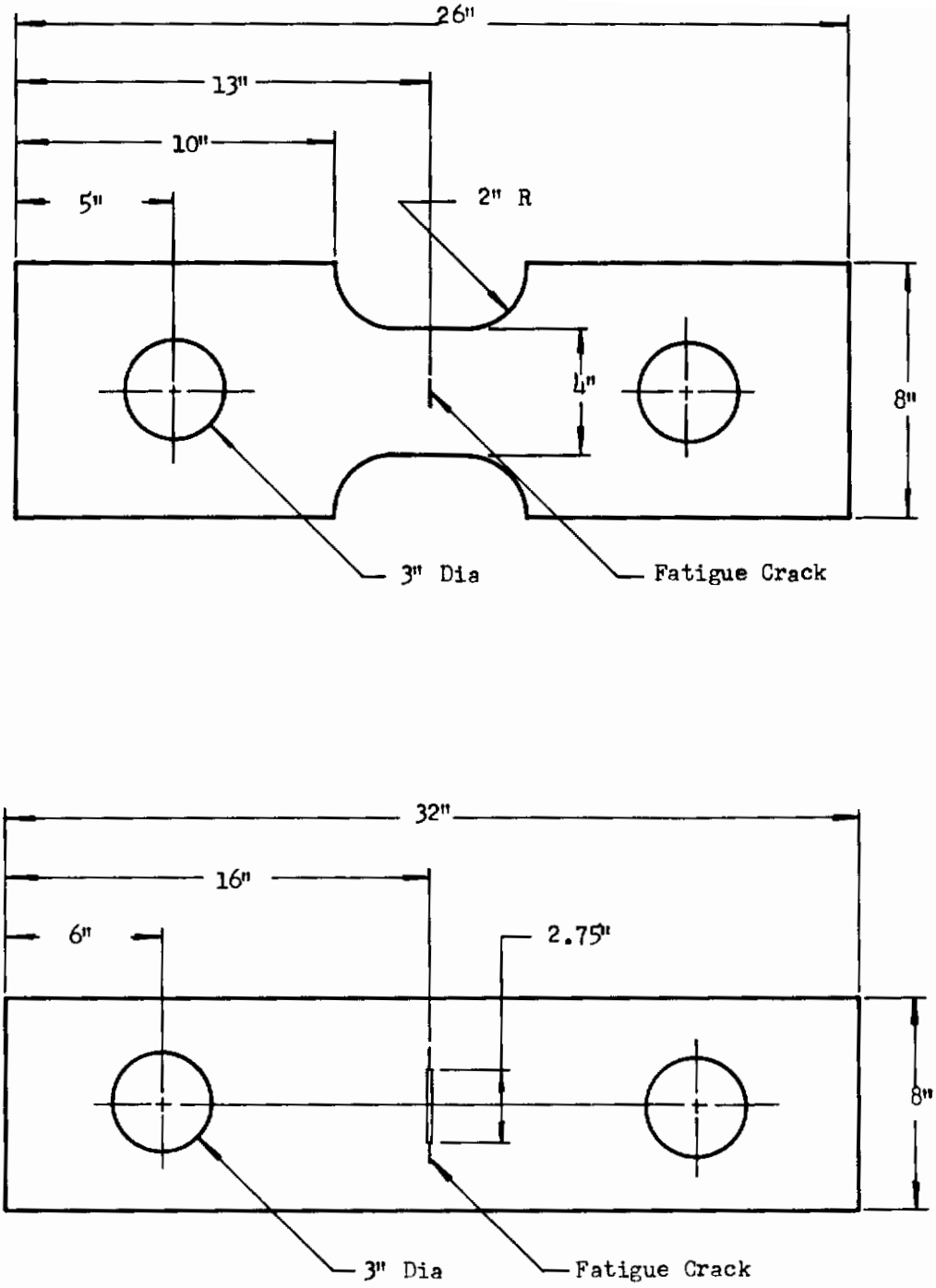

Figure 125. Fatigue-Cracked Part-Through-Crack and Center-Notch Tensile Specimen Configuration for Testing 1/2-In.-Thick Plates

Approved for Public Release

Contrails

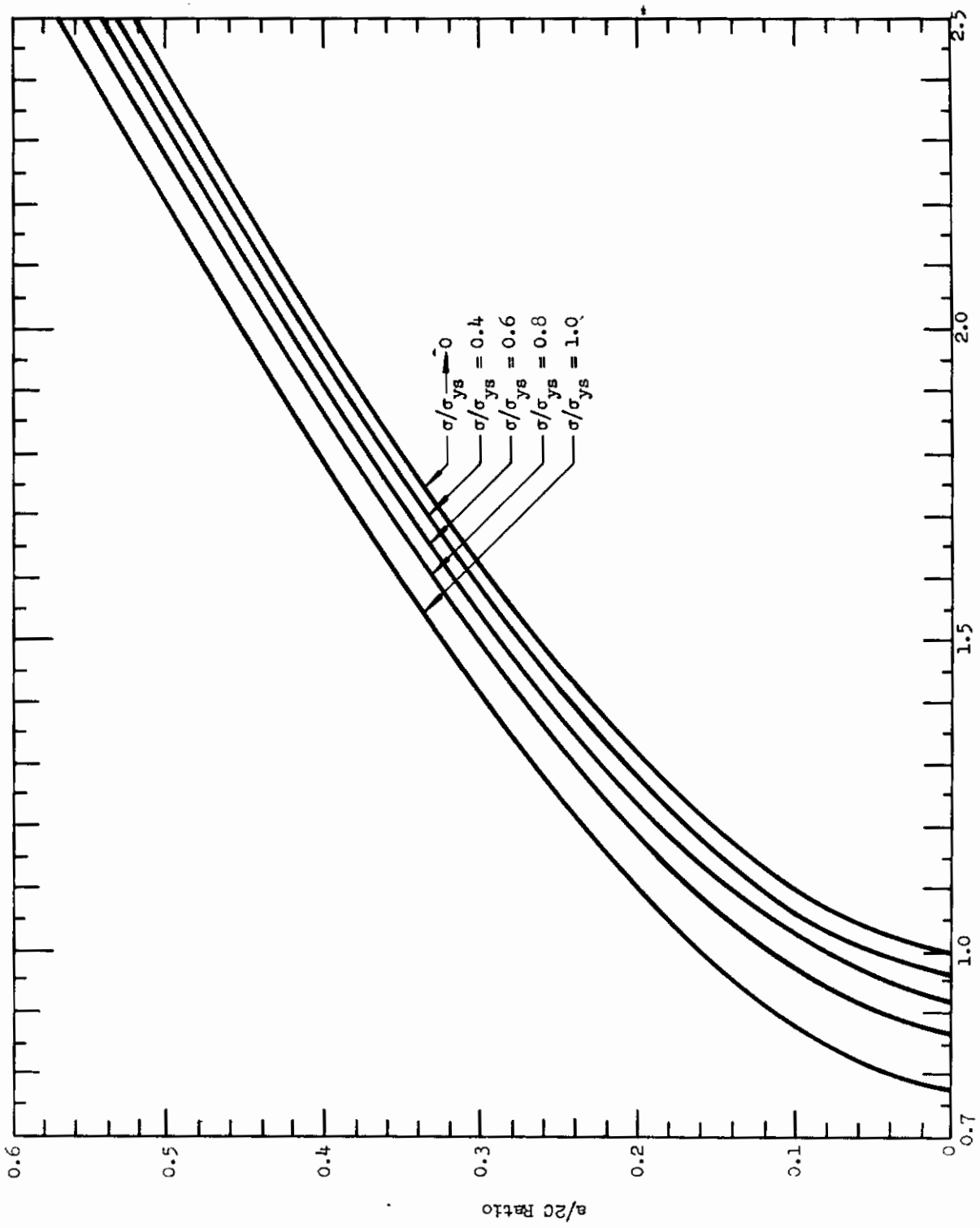

Figure 126. Flaw-Shape Parameter for Surface and Embedded Flaws

Approved for Public Release

Contrails

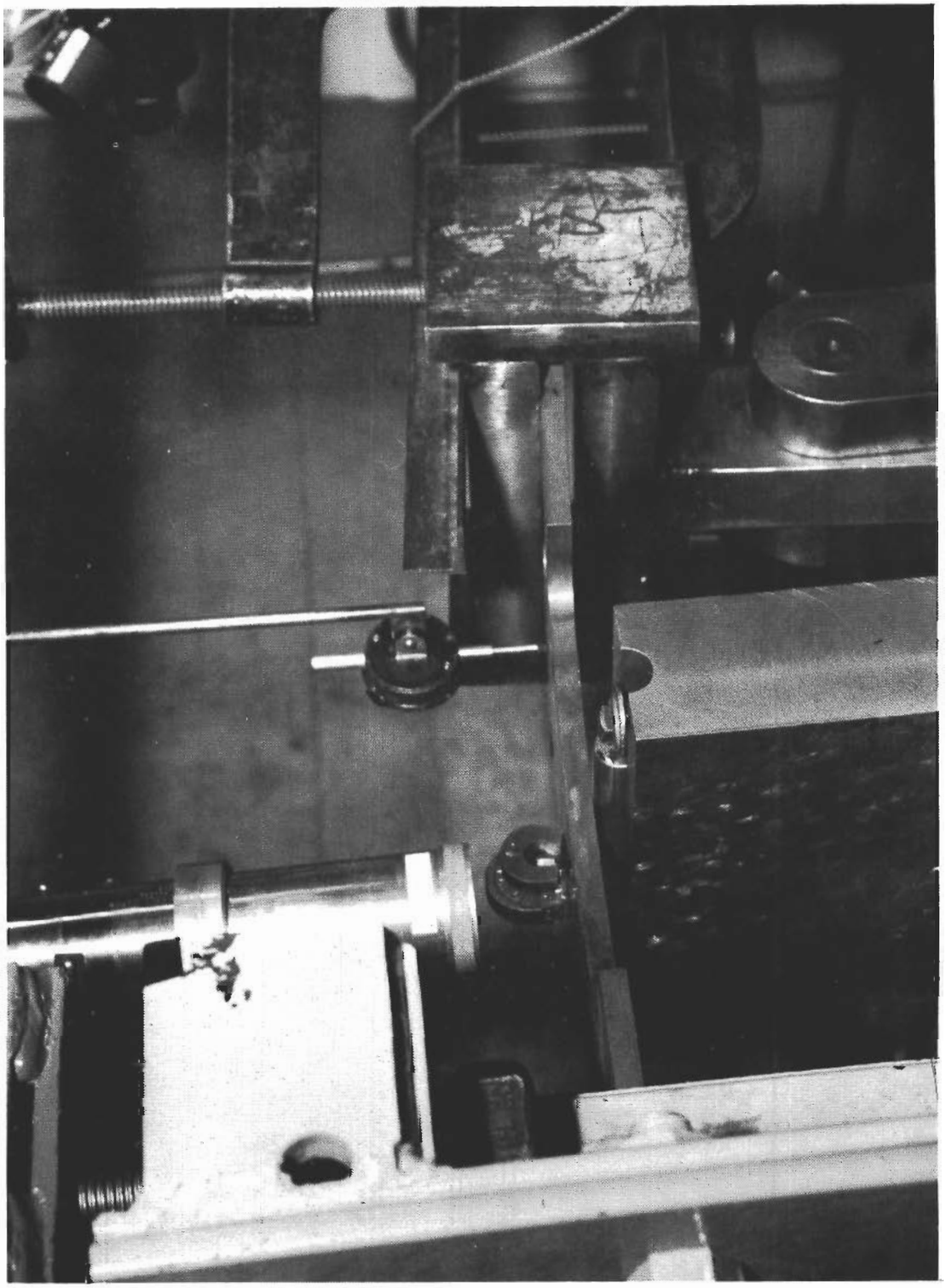

Figure 127. Hydraulically Operated Fatigue-Machine Used to Induce Starter Cracks in Plate Sized Part-Through-Crack and Center-Notch-Tensile Specimens

Approved for Public Release

Contrails

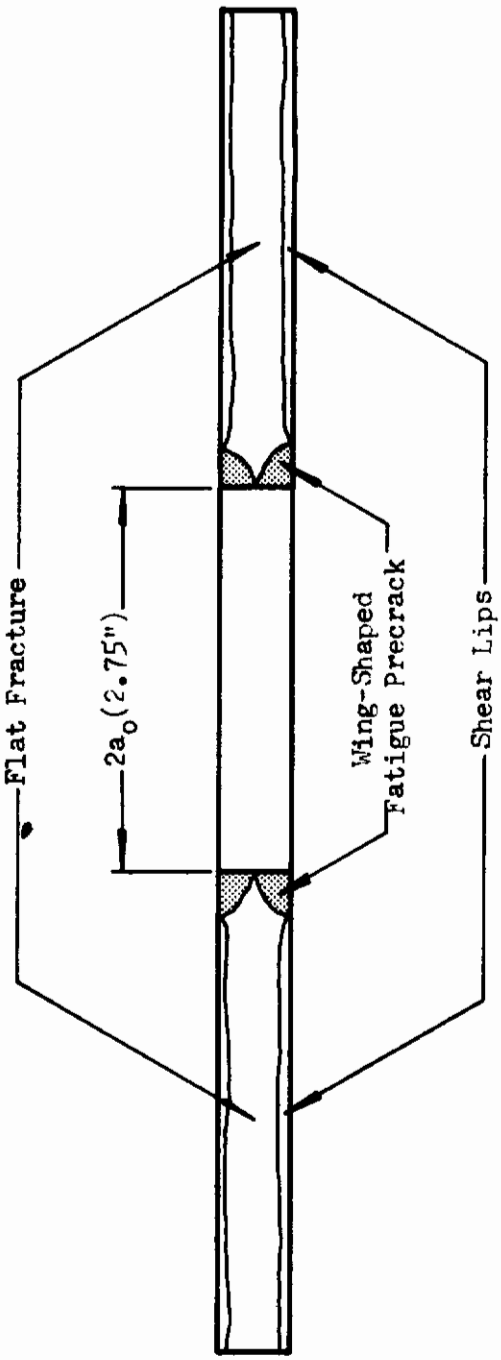

Figure 128. Sketch Showing the Central Area of a Fractured Half of a 1/2-In.-Thick, 18% Nickel Maraging Steel Center-Notch Tensile Specimen.

Approved for Public Release

Contrails

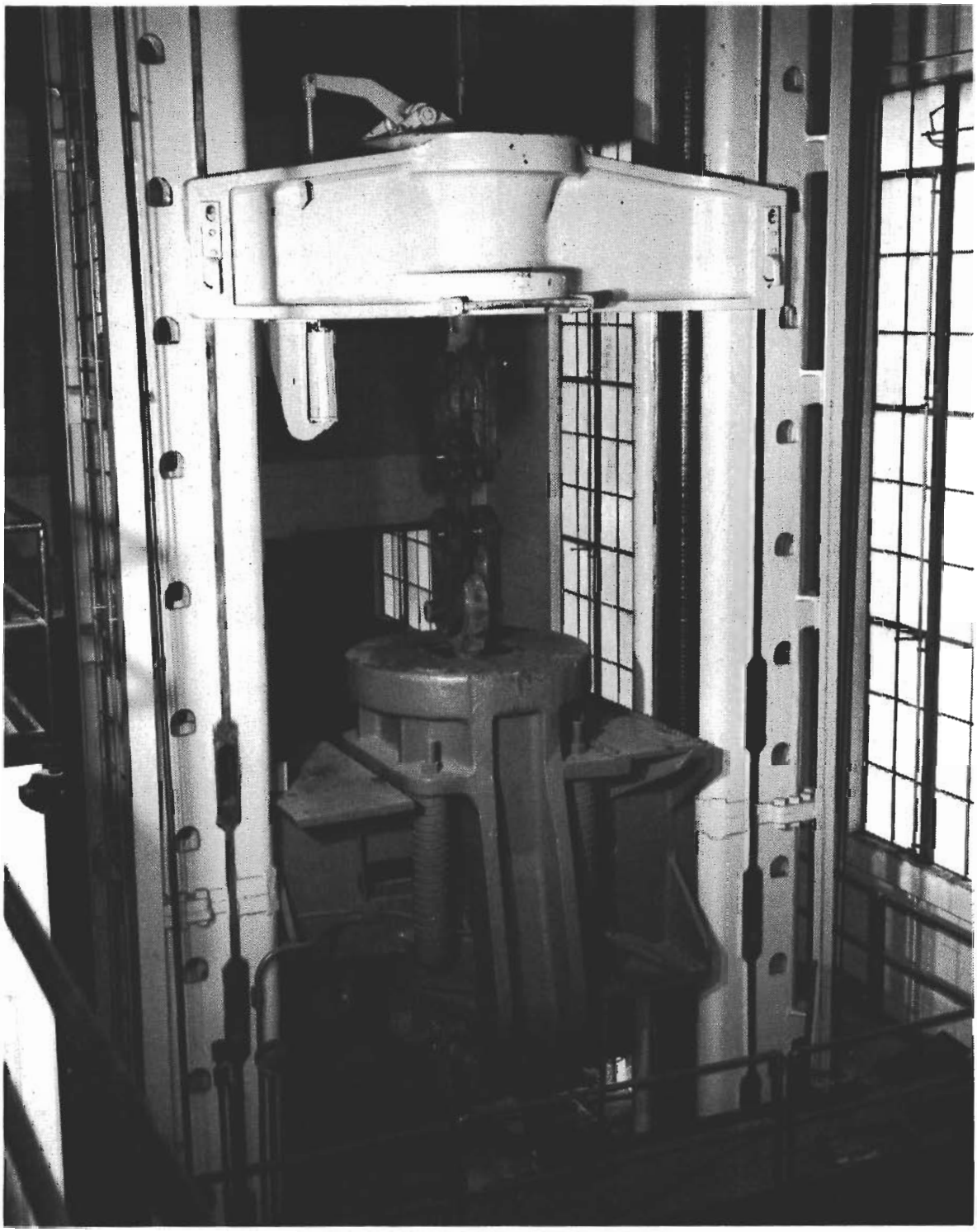

Figure 129. Four-Million lb Tensile-Testing Machine with Test Specimen in Place

Approved for Public Release

Contrails

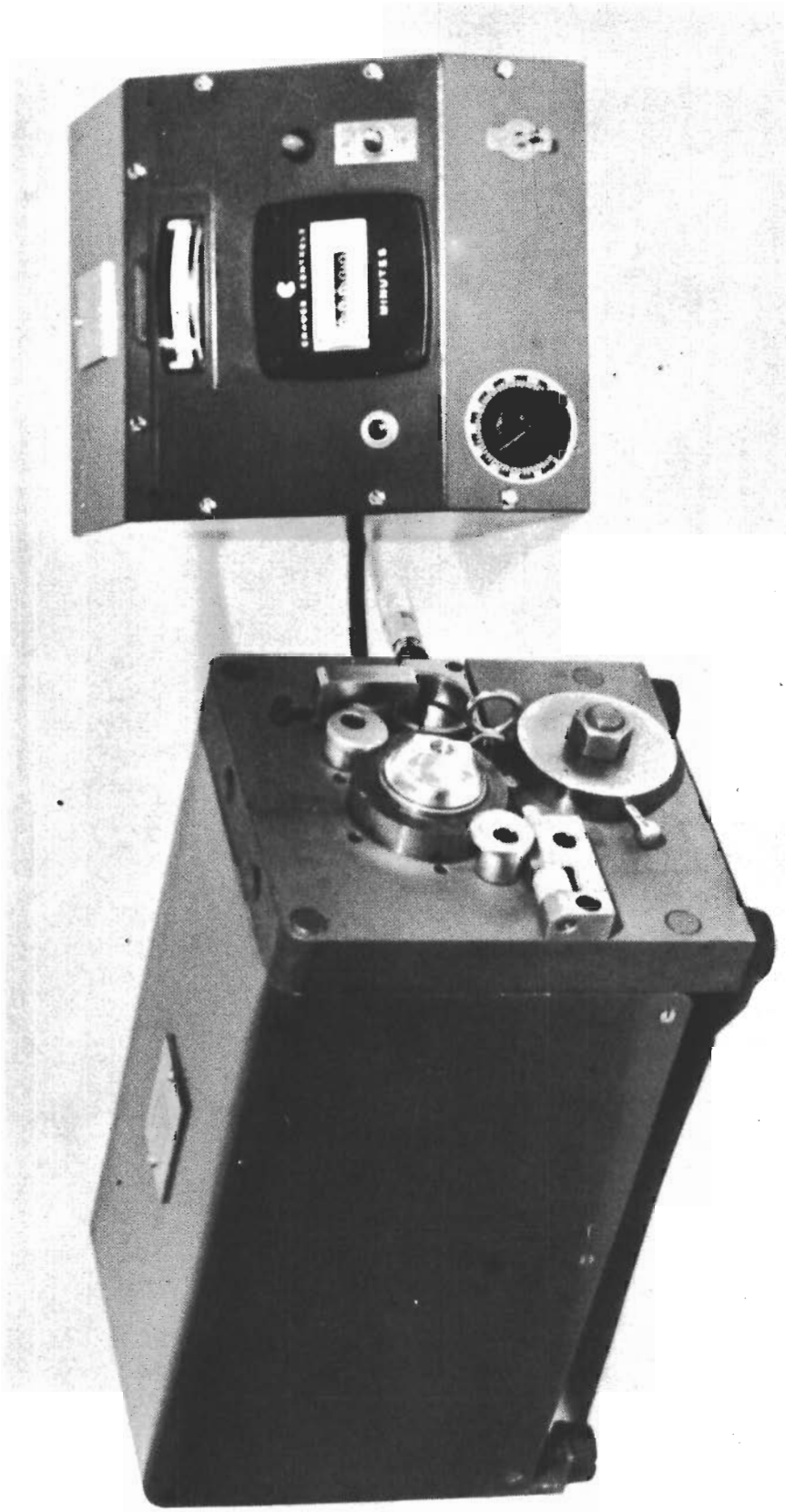

Figure 130. Precrack Apparatus Used to Fatigue-Crack Charpy-Impact Specimens

Approved for Public Release

Contrails

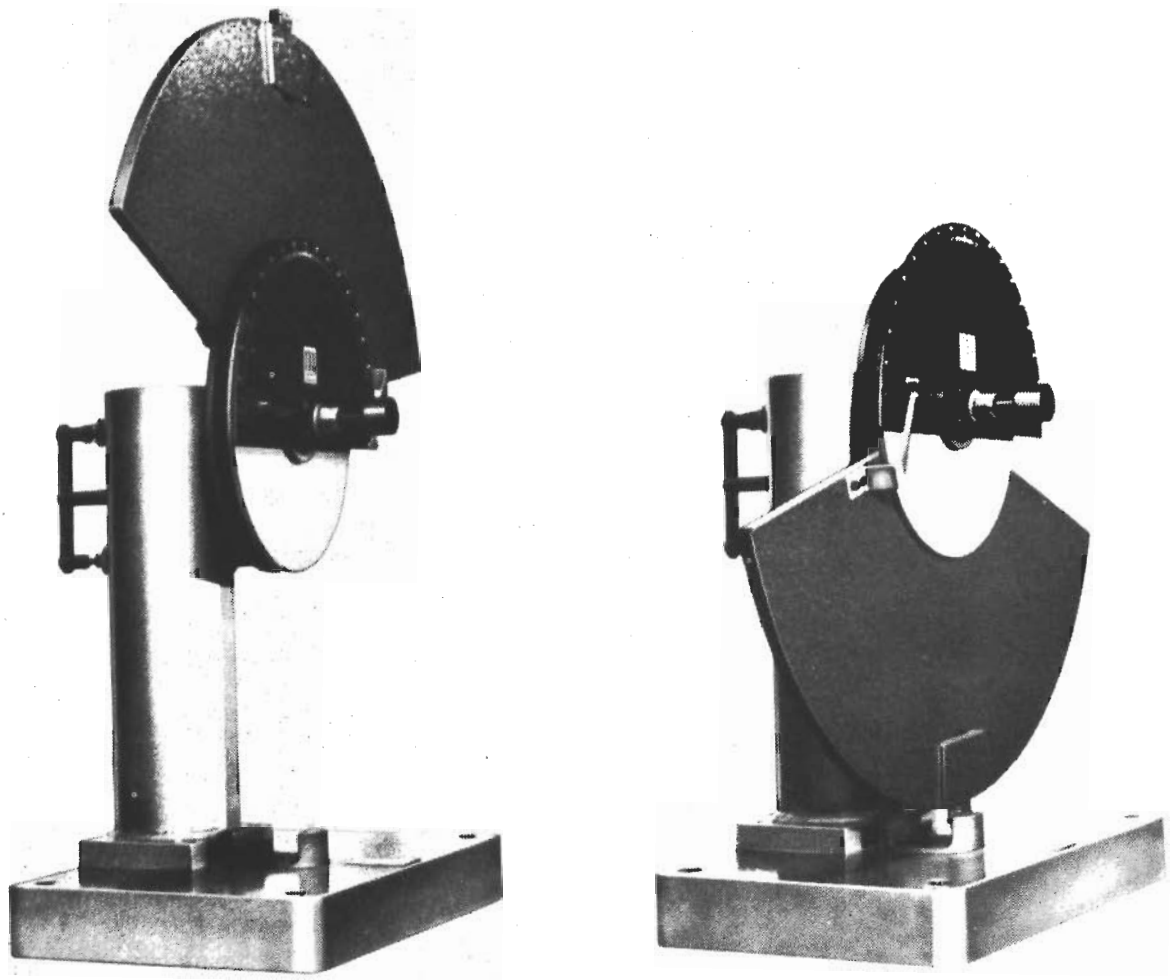

Figure 131. Precrack-Charpy-Impact Testing Machine

Approved for Public Release

Contrails

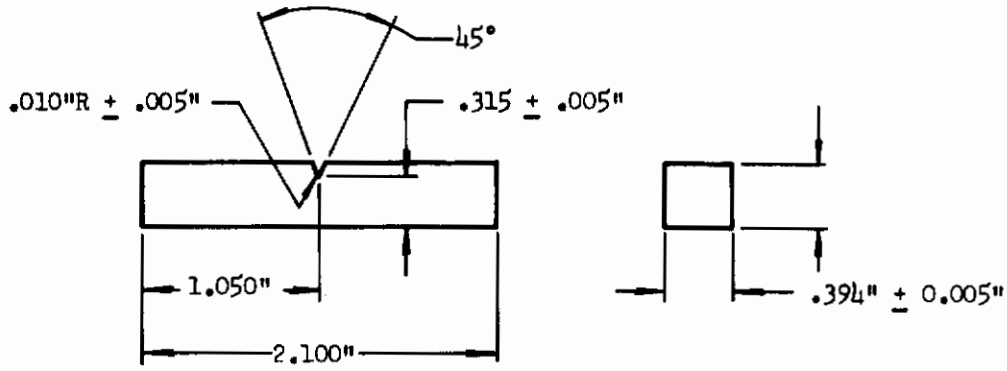

Fatigue-Precrack Charpy Specimen

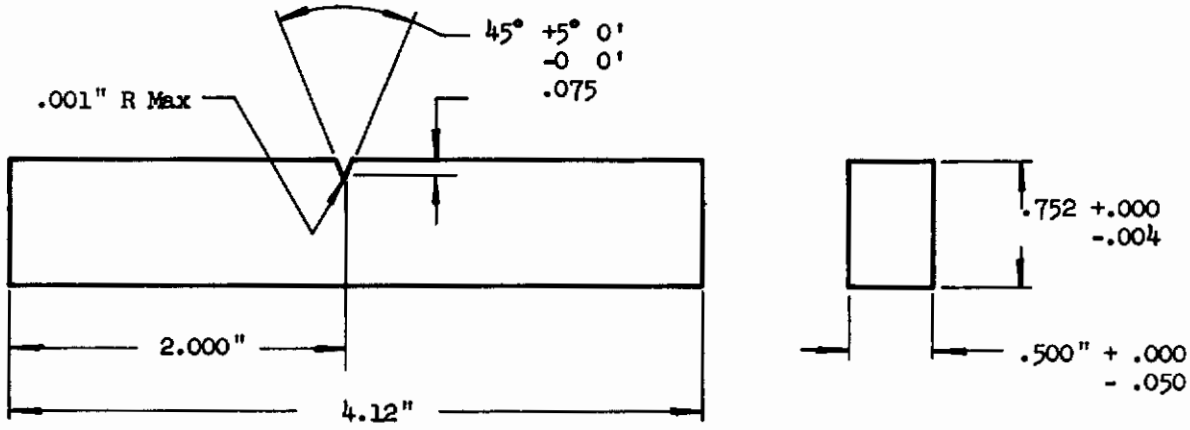

Figure 132. Fracture Toughness Specimens Used to Determine G_{nc} ans W/A Values

Approved for Public Release

Contrails

APPENDIX VI

DEVELOPMENT SPECIFICATIONS

Approved for Public Release

Contrails

APPENDIX VI

DEVELOPMENT SPECIFICATION

STEEL PLATES, MARAGING, 18% NICKEL

Approved for Public Release

Contrails

APPENDIX VI

STEEL PLATES, MARAGING, 18% NICKEL

1. SCOPE

1.1 Scope. - This specification covers three classes of maraging 18% nickel steel plate, 200 to 235 ksi yield strength.

1.2 Classification. - Maraging steel plates shall be classified in accordance with the melting practice used in manufacture as follows:

Grade	Melting Practice
A	Vacuum-arc remelted
B	Vacuum degassed
C	Air melted

2. APPLICABLE DOCUMENTS

2.1 Department of Defense documents. - Unless otherwise specified, the following documents, listed in the issue of the Department of Defense Index of Specifications and Standards in effect on the date of invitation for bids, shall form a part of this specification to the extent specified herein.

SPECIFICATION

Military

MIL-C-16173 Corrosion Preventive Compound, Solvent Cutback, Cold-Applications

STANDARDS

Federal

Fed. Test Method Std. No. 151 Metals: Test Methods

Fed. Std. No. 183 Continuous Identification Marking of Iron and Steel Products

(Copies of documents required by contractors in connection with specific procurement functions should be obtained as indicated in the Department of Defense Index of Specifications and Standards.)

Approved for Public Release

Contrails

2.2 Other documents. - Unless otherwise specified, the following documents, of the issue in effect on the date of invitation for bids, shall form a part of this specification to the extent specified herein.

SPECIFICATION

Society of Automotive Engineers

AMS-2252	Tolerances, Alloy Steel Sheet, Strip and Plate

(Copies may be obtained from the Society of Automotive Engineers, Inc., 485 Lexington Avenue, New York 17, New York.)

PUBLICATION

American Society for Testing and Materials

ASTM E 45	Recommended Practice for Determining the Inclusion Content of Steel
ASTM E 112-61	Methods for Estimating the Average Grain Size of Metals

(Copies may be obtained from the American Society for Testing and Materials, 1916 Race Street, Philadelphia 3, Pennsylvania.)

3. REQUIREMENTS

3.1 Chemical composition. - The steel shall contain the following elements within the limits as indicated:

	Element	Percent Min	Percent Max
(a)	Carbon	---	0.03
(b)	Manganese	---	0.10
(c)	Silicon	---	0.10
(d)	Phosphorus	---	0.025
(e)	Sulfur	---	0.01
(f)	Nickel	17.5	19.0
(g)	Titanium	0.05	0.25
(h)	Aluminum	0.05	0.15
(i)	Cobalt	7.0	8.0
(j)	Molybdenum	4.0	4.5

Approved for Public Release

Contrails

3.2 Melting practice. - The melting practice used in the manufacture of the steel shall be in accordance with the following:

Grade	Melting Practice
A	Vacuum-arc remelted
B	Vacuum degassed
C	Air melted

3.2.1 Additives. - The following materials shall be added to the steel during melting:

Material	Amount, Percent
(a) Boron	0.003
(b) Zirconium	0.02
(c) Calcium	0.06 in increments of 0.02

3.3 Solution treatment. - Steel plates shall be solution-treated after rolling at 1500 + 25°F for not less than one hour. Plates greater than one inch (in.) thick shall be held at temperature for time of one hour per inch of thickness.

3.4 Mechanical properties. - The steel plates shall have a yield strength of 200,000 to 235,000 psi at 0.2% offset after treatment in accordance with 4.4.3.

3.5 Grain size. - The steel plates shall have a grain size of five or finer; however, occasional grains as large as three shall be acceptable.

3.6 Inclusion rating. - The inclusion rating shall be determined by comparison of the worst area of inclusions found in the test specimens with Plate I of Publication ASTM E 45. The inclusion rating of each type of thin or heavy series of inclusions shall not exceed the following ASTM E 45 numerical designations:

Type Inclusion	Numerical Designation of Maximum Permissible Inclusion Rating	
	Thin Series	Heavy Series
A	2	1-1/2
B	2-1/2	1-1/2
C	2	1-1/2
D	2-1/2	2

(Titanium nitrides shall be rated as type B inclusions.)

Approved for Public Release

Contrails

3.7 Tolerances. - Tolerances shall be in accordance with Specification AMS-2252. Maximum rate of change for any variation from flatness (waviness, kinks, etc.) to be 0.25 in. per foot. Maximum variation from flatness (buckles, kinks, oil canning, etc.) shall be 2 in. in any 12 feet in any direction.

3.8 Identification. - Steel plates shall be marked in accordance with Standard Fed. Std. No. 183. Marking shall not be accomplished with sulfur or lead base inks, or with any other material capable of degrading the physical or mechanical properties of the steel. Each steel plate shall be identified with the following information:

(a) Number of this specification

(b) Supplier identification

(c) Supplier heat number

(d) Nominal thickness

3.9 Workmanship. - Steel plates furnished under this specification shall be uniform in quality and contain no tears, cracks, seams, laps, internal ruptures, imbedded scale, or segregation. Material surface shall have a finish suitable for magnetic particle and ultrasonic inspection. Plates may be conditioned by the supplier for the removal of surface imperfections or depressions on either surface by grinding or other suitable methods, provided the area is well flared or blended and the grinding does not exceed the flatness variation or thickness tolerances. All conditioning shall be completed before magnetic-particle and ultrasonic inspection.

4. QUALITY ASSURANCE PROVISIONS

4.1 Supplier responsibility.

4.1.1 Inspection. - Unless otherwise specified, the supplier is responsible for the performance of all inspection requirements specified herein and may use any facilities acceptable to the procuring activity.

4.1.2 Processing changes. - The supplier shall make no changes in processing techniques or other factors affecting the quality of the product without prior approval of the procuring activity.

4.1.3 Reports. - The supplier shall submit with each shipment four copies of test results verifying that the requirements of section 3 have been met. In addition, this report shall include:

(a) Melting-practice report

(b) Additives report

(c) Solution-treatment report

(d) Name of the supplier

(e) Testing laboratory

Approved for Public Release

Contrails

(f) Purchase order number

(g) Number of this specification

(h) Physical dimensions or referenced engineering document

(i) Quantity from each heat

4.2 Lot size. - Each heat shall constitute a lot.

4.3 Sampling. - Preparation of samples shall be in accordance with Standard Fed. Test Method Std. No. 151. Selection of samples shall be as follows:

4.3.1 Chemical composition grain size and inclusion rating. - At least one sample shall be taken from the center and edge of both ends of each plate for the analysis of chemical composition, for determination of grain size and for determination of inclusion rating. Samples shall be selected from each as-rolled plate. An as-rolled plate is the product of one slab.

4.3.2 Mechanical properties. - At least three longitudinal test specimens and three transverse test specimens for determination of mechanical properties shall be prepared from samples obtained from each as-rolled plate.

4.3.3 Tolerances and workmanship. - The determination of tolerances, ultrasonic inspection, and magnetic particle inspection shall be performed on each finished and solution-treated plate.

4.4 Test methods. - The following test methods shall be used to determine compliance with requirements of section 3.

	Requirement	Test Method
(a)	Chemical composition	4.4.1
(b)	Melting practice	4.4.2
(c)	Additives	4.4.2
(d)	Solution treatment	4.4.2
(e)	Mechanical properties	4.4.3
(f)	Grain size	ASTM E 112-61
(g)	Inclusion rating	ASTM E 45
(h)	Tolerances	4.4.2
(i)	Identification	4.4.2
(j)	Defects	4.4.4
(k)	Workmanship	4.4.2

Approved for Public Release

Contrails

4.4.1 Chemical composition. - Chemical composition shall be determined as specified in Standard Fed. Test Method Std. No. 151, method 111 or 112, or other approved method. In the event of variation of composition, analysis shall be by method 111, except for carbon which shall be by the combustion method.

4.4.2 Visual examination. - Compliance with the requirements for melting practice, additives, and solution treatment, shall be verified by surveillance by the procuring activity and inspection of supplier certifications. Compliance with the requirements for tolerances, identification, workmanship, and the requirements of section 5 shall be verified by visual inspection of the steel plates presented for acceptance.

4.4.3 Mechanical properties. - Mechanical properties shall be determined as specified in Standard Fed. Test Method Std. No. 151, method 211. Test results shall be identified by item, serial number, heat number, etc. Test specimens shall be solution treated at 1500 ± 25°F for 30 minutes, air cooled to room temperature, and aged at 890 ± 10°F for four to eight hours.

4.4.4 Defects. - Steel plates shall be inspected for defects by using longitudinal and shear-wave ultrasonic inspection and magnetic-particle inspection shall be used employing the yoke method. Sufficient current shall be used to reveal any detrimental discontinuities. Distance between poles shall be 18 in. or greater. The inspection media will be fluorescent particles. Any controversial indication that cannot be resolved will be investigated further by polishing and etching, and viewed by employing magnification of 10X or higher. Demagnetization shall be accomplished by using alternating current to reduce the residual magnetic field to a level of intensity which will not be detrimental during subsequent machining, forming, and welding operations.

4.5 Retest. - Rejected parts shall not be resubmitted for inspection without furnishing full particulars concerning previous rejection and measures taken to overcome the defects.

5. PREPARATION FOR DELIVERY

5.1 Preservation. - Unless otherwise specified, all material shall be prepared for storage by coating with corrosion preventive compound that conforms to the requirements of Specification MIL-C-16173, grade 2.

6. NOTES

6.1 Ordering data. - Procurement documents should specify the following:

(a) Number of this specification
(b) Place of inspection
(c) Lot size
(d) Place of delivery
(e) Marking location (if applicable)

Approved for Public Release

Contrails

(f) Forming process (if applicable)

(g) Tensile coupon specimen location (if applicable)

Approved for Public Release

Contrails

DEVELOPMENT SPECIFICATION

STEEL FORGING, MARAGING, 18% NICKEL

Approved for Public Release

Contrails

APPENDIX VI

STEEL FORGING, MARAGING, 18% NICKEL

1. SCOPE

1.1 This specification covers 200 to 235 ksi yield strength, vacuum-arc remelted, 18% nickel maraging steel alloy forgings.

2. APPLICABLE DOCUMENTS

2.1 Department of Defense documents. - Unless otherwise specified, the following documents, listed in the issue of the Department of Defense Index of Specifications and Standards in effect on the date of invitation for bids, shall form a part of this specification to the extent specified herein.

SPECIFICATION

Military

MIL-C-16173	Corrosion Preventive Compound Solvent Cutback, Cold-Applications

STANDARD

Federal

Fed. Test Method Std. No. 151	Metals: Test Method

(Copies of documents required by contractors in connection with specific procurement functions should be obtained as indicated in the Department of Defense Index of Specifications and Standards.)

2.2 Other documents. - Unless otherwise specified, the following document, of the issue in effect on the date of invitation for bids, shall form a part of this specification to the extent specified herein.

SPECIFICATION

Society of Automotive Engineers, Inc.

AMS - 2808	Identification, Forgings

(Copies may be obtained from the Society of Automotive Engineers, Inc., 845 Lexington Avenue, New York 17, New York.)

Approved for Public Release

Contrails

STANDARD

American Society for Testing and Materials

ASTM E 45	Recommended Practice for Determining the Inclusion Content of Steel
ASTM E 112-61	Methods for Estimating the Average Grain Size of Metals

(Copies may be obtained from the American Society for Testing and Materials, 1916 Race Street, Philadelphia 3, Pennsylvania.)

3. REQUIREMENTS

3.1 Chemical composition. - The steel shall contain the following elements:

Element	Percentage Min.	Max.
(a) Carbon	---	0.03
(b) Manganese	---	0.10
(c) Silicon	---	0.10
(d) Phosphorus	---	0.025
(e) Sulfur	---	0.01
(f) Nickel	17.5	19.0
(g) Titanium	0.05	0.25
(h) Aluminum	0.05	0.15
(i) Cobalt	7.0	8.0
(j) Molybdenum	4.0	4.5

3.2 Melting practice. - The melting practice used in the manufacture of the steel shall be vacuum-arc remelt.

3.3 Additives. - The following materials shall be added to the steel during melting:

Material	Amount, Percent
(a) Boron	0.003
(b) Zirconium	0.02
(c) Calcium	0.06 in increments of 0.02

Approved for Public Release

Contrails

3.4 Solution treatment. - The steel shall be solution-treated at a temperature of 1500 + 25°F. After forgings reach furnace equilibrium, they shall be held at temperature for one hour, minimum, or one hour for each inch of thickness, whichever is greater.

3.5 Mechanical properties. - The steel shall have a yield strength of 200,000 to 235,000 pounds per square inch at 0.2% offset after treatment in accordance with 4.4.4.1.

3.6 Grain size. - The steel shall have a grain size of five or finer, except that occasional grains as large as three shall be acceptable. Forging stock shall be of such size and dimensions that the work accomplished in forming to finished shape shall result in approximately uniform grain size throughout.

3.7 Grain flow. - The grain flow pattern in highly stressed areas shall be parallel to the principal stresses specified in applicable drawings. The grain flow pattern shall be free from re-entrant lines and from sharply folded lines.

3.8 Inclusion rating. - The inclusion rating shall be determined by comparison of the worst area of inclusions found in the test specimens with Plate I of ASTM E 45. The inclusion rating of each type of thin and heavy series of inclusions shall not exceed the following ASTM E 45 numerical designations:

Maximum Permissible Numerical Designation of Inclusion Rating

Type of Inclusion	Thin Series	Heavy Series
A	2	1-1/2
B	2-1/2	1-1/2
C	2	1-1/2
D	2-1/2	2

(Titanium nitrides shall be rated as Type B inclusions.)

3.9 Tolerances. - Forging tolerances shall be specified on Applicable drawings.

3.10 Cleaning. - Forgings shall be cleaned by tumbling, machining, shot or sand blasting, pickling, or other process approved by the procuring activity.

3.11 Identification. - Forgings shall be marked in accordance with Specification ASM-2808. Ink or other substance used in marking shall be free of sulfur, lead, or other materials capable of degrading the physical or mechanical properties of the steel. Each forging shall be marked with the following information:

Approved for Public Release

Contrails

(a) Number and revision letter of this specification

(b) Supplier identification

(c) Supplier heat number

(d) Drawing number of machined forging (if applicable)

(e) Serial number of forging (if applicable)

3.12 Defects. - The steel shall be free from injurious defects and shall have a finish suitable for magnetic-particle and ultrasonic inspection. All conditioning shall be completed before magnetic-particle and ultrasonic inspection.

4. QUALITY ASSURANCE PROVISIONS

4.1 Supplier responsibility.

4.1.1 Inspection. - Unless otherwise specified, the supplier is responsible for the performance of all inspection requirements specified herein and may use any facilities acceptable to the procuring activity.

4.1.2 Processing changes. - The supplier shall not make changes in processing techniques or other factors affecting the quality of the product without prior approval of the procuring activity.

4.1.3 Reports. - The supplier shall submit with each shipment four copies of test results verifying the requirements of section 3 have been met. In addition, this report shall include

(a) Melting-practice report

(b) Additives report

(c) Solution-treatment report

(d) Name of the supplier

(e) Testing laboratory

(f) Purchase order number

(g) Number and revision letter of this specification

(h) Physical dimensions or referenced engineering document

(i) Quality from each heat

(j) Size of stock used to make the forgings

4.2 Lot. - Each heat shall constitute a lot.

4.3 Sampling. - Samples shall be made from each lot. When more than one forging is made from a lot, samples shall be made from each forging. No further forging or hot reductions shall be performed on the samples after they have been separated from the parent material. If made separately from the forging, samples shall be heat-treated with the forging they represent.

Approved for Public Release

Contrails

When multiple parts are made by machining from a single forging, samples from the original forging shall apply to the individual parts.

4.3.1 Chemical composition, inclusion rating, and grain size. - At least one sample each shall be taken for analysis of chemical composition for determination of inclusion rating and for determination of inclusion rating and for determination of grain size. Samples shall be taken from excess forged material at a point mid-way between the surface and center of solid forgings, or at any point mid-way between the inner and outer surfaces of the wall of hollow forgings. Samples may be taken from broken tensile specimens with procuring activity approval.

4.3.2 Grain flow. - After the forging technique has been established, one forging shall be selected to represent grain flow. If the forging practice is altered, one additional forging shall be submitted.

4.3.3 Mechanical properties. - At least three tensile-test specimens shall be selected for testing.

4.3.3.1 Location of tensile specimens. - Test specimens shall be made from a full-size prolongation sample of the material in the direction of maximum reduction. When this is not practical, a separate test specimen shall be prepared from the same bar, billet, or bloom as the forging it represents. The reduction given this specimen shall be equal to or less than the minimum reduction given the forging.

4.4 Test methods. - The following test methods shall be used to determine compliance with the requirements of section 3.

	Requirement	Test Method
(a)	Chemical composition	4.4.1
(b)	Melting practice	4.4.2
(c)	Additives	4.4.2
(d)	Solution treatment	4.4.2
(e)	Mechanical properties	4.4.4
(f)	Grain size	ASTM E 112-61
(g)	Grain flow	4.4.3
(h)	Inclusion rating	ASTM E 45
(i)	Tolerances	4.4.2
(j)	Cleaning	4.4.2
(k)	Identification	4.4.2
(l)	Defects	Ultrasonic Inspection Longitudinal and shear-wave techniques Magnetic-particle inspection

Approved for Public Release

Contrails

4.4.1 Chemical composition. - Chemical composition shall be determined as specified in Federal Test Method Standard Number 151, method 111 or 112, or other approved analytical method. In the event of variation in composition, analysis shall be by method 111, except for carbon, which shall be by the combustion method.

4.4.2 Visual examination. - Compliance with the requirements for melting practice additives, and solution treatment, shall be verified by surveillance by the procuring activity and by inspection of supplier certifications. Compliance with the requirements for tolerances, cleaning, and identification shall be verified by visual inspection of the steel presented for acceptance.

4.4.3 Grain flow. - Grain flow shall be determined as specified in Federal Test Method Standard Number 151, method 321. The sample shall be sectioned and etched. Macrophotographs shall be prepared. This test may be waived at the discretion of the procuring activity when size of the forging is too large to make sectioning practical.

4.4.4 Mechanical properties. - Mechanical properties shall be determined as specified in Federal Test Method Standard Number 151, method 211. The test results shall be identified by item, serial number, heat number, etc. Test specimens prepared as follows:

4.4.4.1 Preparation of test specimens. - Test specimens shall be solution treated at 1500 ± 25°F for 30 min, minimum, air-cooled to room temperature, and aged at a temperature of 890 ± 10°F for a time period between 4 and 8 hr. Three additional specimens shall be prepared, solution-treated, and shipped with each forging.

4.5 Retest. - Rejected parts shall not be resubmitted for acceptance without full particulars having been furnished concerning previous rejection and measures taken to overcome the defects.

5. PREPARATION FOR DELIVERY

5.1 Preservation. - Unless otherwise specified, all material shall be prepared for storage by coating with corrosion-preventive compound conforming to Specification MIL-C-16173, grade 2.

6. NOTES

6.1 Ordering data. - Procurement documents should specify the following:

(a) Material type
(b) Number and revision letter of this specification
(c) Place of inspection
(d) Lot size
(e) Place of delivery
(f) Marking location (if applicable)

Approved for Public Release

Contrails

(g) Forming process (if applicable)

(h) Tensile coupon specimen location (if applicable)

Approved for Public Release

Contrails

DEVELOPMENT SPECIFICATION

WIRE FILLER: 200 TO 235 KSI, 18% NICKEL
MARAGING STEEL, FOR FUSION WELDING

Approved for Public Release

Contrails

APPENDIX VI

DEVELOPMENT SPECIFICATION

WIRE-FILLER: 200 to 235 KSI, 18% NICKEL
MARAGING STEEL, FOR FUSION WELDING

1. SCOPE

1.1 This specification covers the requirements for one grade of vacuum-arc-remelted 18% nickel maraging steel filler wire.

2. APPLICABLE DOCUMENTS

2.1 Department of Defense documents. - Unless otherwise specified, the following documents, listed in the issue of the Department of Defense Index of Specifications and Standards in effect on the date of invitation for bids, shall form a part of this specification to the extent specified herein.

STANDARDS

Federal

Fed. Test Method Std. No. 151	Metals; Test Methods
Fed. Std. No. 102	Preservation, Packaging and Packing Levels

Military

MIL-STD-129	Marking for Shipment and Storage

(Copies of documents required by contractors in connection with specific procurement functions should be obtained as indicated in the Department of Defense Index of Specifications and Standards.)

3. REQUIREMENTS

3.1 Chemical composition. - The filler wire shall be manufactured from vacuum-melted steels and shall have the following end-product chemical analysis:

Element		Wt%
(a)	Carbon	0.03 max
(b)	Manganese	0.10 max
(c)	Silicon	0.01 max
(d)	Sulfur	0.01 max

Approved for Public Release

Contrails

	Element	Wt%
(e)	Phosphorus	0.01 max
(f)	Aluminum	0.1 added
(g)	Nickel	17.5/18.5
(h)	Cobalt	7.5/8.0
(i)	Molybdenum	3.6/3.8
(j)	Titanium	0.26/0.30
(k)	Metallic calcium	0.05 (optional)

3.1.1 Gas impurities. - Gas impurities in the material shall not exceed the following:

	Element	Parts per Million
(a)	Oxygen	40
(b)	Hydrogen	5
(c)	Nitrogen	40

3.2 Dimensions and weights. - Wire shall be wound on standard spools for use on automatic welding equipment, or furnished in packages of straight lengths. The wire shall have the following dimensions.

3.2.1 Spooled wire. - Spooled wire shall have a diameter from 0.020 to 0.093 in. with a tolerance of ± 0.001 in. The approximate coil weight shall be as follows:

(a) 0.062 in. diameter and larger: 25 lb

(b) Less than 0.062 in. diameter: 10 lb

3.2.2 Straight lengths. - Straight lengths shall be 36 ± 0.25 in. long and shall have a diameter from 0.062 to 0.093 in. with a tolerance of plus 0.002, minus 0.003. A package shall weigh 2 to 5 lb.

3.3 Uniformity. - The wire shall meet the following requirements:

3.3.1 Spooled wire. - The wire on any single spool shall be one continuous length from one heat of material.

3.3.2 Straight wire. - The wire in a single package shall represent one heat of material.

3.4 Workmanship. - The wire surfaces shall be uniform in quality and shall show no pits, die marks, corrosion, scale, scrapes, splits, cracks, seams, or other defects; and, in addition, the material shall contain no internal foreign material or gas pockets. The wire shall be manufactured so as not to be wavy or kinked, and shall melt and flow smoothly during a welding process.

Approved for Public Release

Contrails

4. QUALITY ASSURANCE PROVISIONS

4.1 Supplier responsibility.

4.1.1 Inspection. - Unless otherwise specified, the supplier is responsible for the performance of all inspection requirements specified herein and may use any facilities acceptable to the procuring activity.

4.1.2 Processing changes. - The supplier shall make no changes in processing techniques or other factors affecting the quality of the product without prior approval of the procuring activity.

4.2 Sampling. - A sample of filler wire shall be randomly selected from each heat of wire.

4.3 Acceptance tests. - Acceptance tests for individual heats shall be performed on each sample for all requirements in Section 3.

4.4 Test methods. - Tests to determine compliance with the requirements of Section 3 shall be in accordance with the following:

Requirement		Test
(a)	Composition	Method 111, Fed. Test Method Std. No. 151
(b)	Gas impurities	Method 111, Fed. Test Method Std. No. 151
(c)	Dimensions and weights	4.4.1
(d)	Uniformity	4.4.1
(e)	Workmanship	4.4.1

4.4.1 Visual examination. - Each weld wire sample shall be examined to determine compliance with the requirement of Section 3 for dimensions, weight, and workmanship. The supplier shall furnish certification that the material meets the requirements of Section 3 for uniformity.

4.5 Test. - The material shall be chemically analyzed in accordance with method 111 of Standard Fed. Test Method Std. No. 151.

5. PREPARATION FOR DELIVERY

5.1 Preservation, packaging, and packing. - Except as specified herein, preservation, packaging, and packing methods shall conform to level C of Standard Fed. Std. No. 102.

5.1.1 Containers. - Coils and rods shall be packaged in clean, hermetically sealed containers with a dry internal atmosphere. The material shall be packaged in such a manner as to ensure freedom of the wire from deterioration, due to environmental conditions, for a minimum period of one year after sealing.

Approved for Public Release

Contrails

5.1.2 Spools. - The materials and construction of the spools shall furnish protection for the wire against damage and shall electrically insulate the wire from the welding-machine spindle.

5.2 Layer winding. - Wire shall be closely wound in layers, but adjacent turns within a layer need not be touching. The winding shall not produce kinks, waves, or sharp bends. Unwinding of the coil shall be restricted, without overlapping or wedging. The terminal end of the coiled wire shall be marked and shall be readily accessible.

5.3 Marking. - Each spool package and shipping container shall be marked in conformance with Standard MIL-STD-129 and shall include, but not be limited to, the following information:

(a) Wire size
(b) Wire quantity
(c) Material heat number
(d) Purchase order number
(e) Manufacturer's identification
(f) Number of this specification
(g) Do not open for receiving inspection
Verify accountability only

6. NOTES

6.1 Intended use. - Material conforming to the requirements of this specification is intended for use on material that develops a yield strength of 200 to 235 ksi, in the following processes:

(a) Inert-gas, metal-arc, nonconsumable electrode
(b) Inert-gas, metal-arc, consumable electrode

Approved for Public Release